VOLUME 64
NUMBER 2 / NUMÉRO 2
FEBRUARY / FÉVRIER
2007

Canadian Journal of FISHERIES AND AQUATIC SCIENCES

cjfas.nrc.ca

Journal canadien des SCIENCES HALIEUTIQUES ET AQUATIQUES

jcsha.cnrc.ca

An NRC Research Press
JOURNAL
Une REVUE des
Presses scientifiques du CNRC

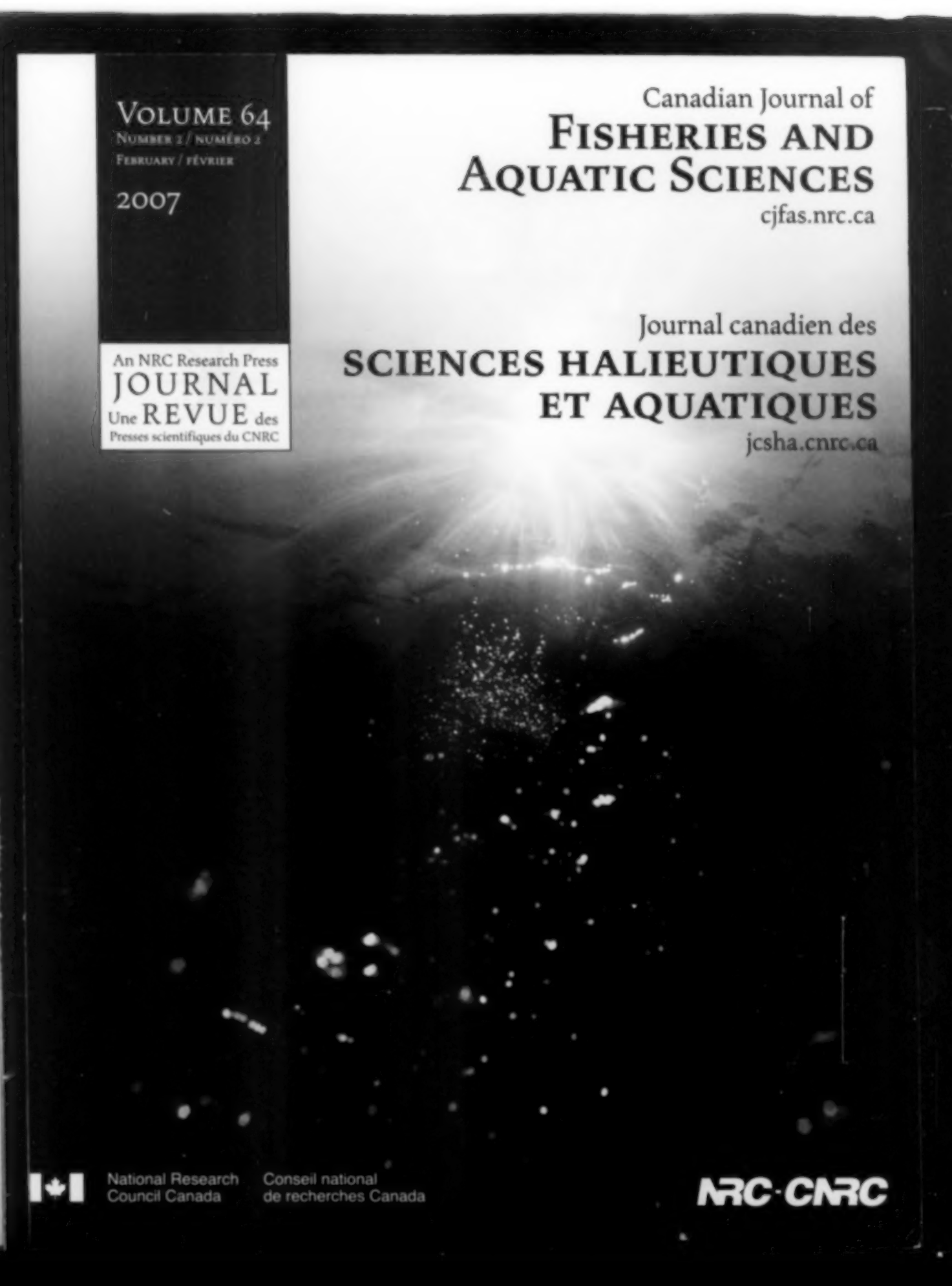

National Research Council Canada
Conseil national de recherches Canada
NRC·CNRC

ISSN 0706-652X / CJFSDX 64(2) 181–386 (2007)

The *Canadian Journal of Fisheries and Aquatic Sciences*, previously published as *Contributions to Canadian Biology* 1901–1925, *Contributions to Canadian Biology and Fisheries* 1926–1934, *Journal of the Biological Board of Canada* 1934–1937, and *Journal of the Fisheries Research Board of Canada* 1938–1979, is issued monthly to form annual volumes of 12 numbers plus supplements.

Editorial policy. The Journal publishes original research articles, perspectives (syntheses, critiques, reevaluations), discussions (comment and reply), and rapid communications. Manuscripts may concern cells, organisms, populations, communities, ecosystems, or processes that affect aquatic systems. They may cover a range of disciplines including biology and ecology of marine and freshwater organisms, limnology, oceanography, physiology, toxicology, genetics, economics, disease, and management. Preference will be given to manuscripts that emphasize understanding of observed phenomena and interpretation of experimental results. The Journal encourages papers that lead from clearly stated purpose or rationale and from testable hypotheses, concepts, or questions to identifiable conclusions or syntheses. Such papers may amplify, modify, question, or redirect accumulated knowledge embodied in contemporary perceptions of a particular state of aquatic sciences. The Journal discourages papers that are essentially descriptive, except in emerging disciplines; have only site-specific or local applications (a certain year, place, taxon, chemical compound, etc.); only confirm previously established principles; or apply standard techniques without breaking new methodological ground.

Manuscripts for publication should be submitted to the Editorial Office via NRC Research Press' online submission and peer review system (**OSPREY**) at http://pubs.nrc-cnrc.gc.ca/cjfas/osprey. Alternatively, manuscripts may be submitted to the Senior Editor, *Canadian Journal of Fisheries and Aquatic Sciences*, Department of Integrative Biology, Building #006, Room 118, University of Guelph, Guelph, ON N1G 2W1, Canada (519-824-4120 ext. 52646; fax: 519-767-9798; e-mail: cjfas@uoguelph.ca).

Submissions in either English or French are acceptable. The information must be original, that is, not copyrighted, published, or submitted elsewhere except in abstract form or unless by written consent of the Editor.

Correspondence concerning accepted manuscripts and corrected proofs should be sent to NRC Research Press, National Research Council of Canada, Ottawa, ON K1A 0R6, Canada (fax: 613-952-7656; e-mail: pubs@nrc-cnrc.gc.ca).

Instructions to Authors are published once a year in the first issue of each volume. Copies are available from NRC Research Press or at cjfas.nrc.ca. The **Publication Policy** of NRC Research Press is available at pubs.nrc-cnrc.gc.ca.

Microfilm. Issues from 1934 through the current volume can be purchased on 16- or 35-mm microfilm. Photocopies of individual articles or issues can be purchased from University Microfilms International, 330 North Zeeb Road, Ann Arbor, MI 48106, USA.

The *Canadian Journal of Fisheries and Aquatic Sciences*, ISSN 0706-652X, is published monthly, 12 times per year, by NRC Research Press, c/o USACAN Media Dist. Srv. Corp. at 26 Power Dam Way, Suite S1-S3, Plattsburgh, NY 12901, USA. Periodicals postage paid at Plattsburgh, NY. POSTMASTER: Send address changes to *Canadian Journal of Fisheries and Aquatic Sciences*, c/o NRC, P.O. Box 2888, Plattsburgh, NY 12901, USA.

Publié sans interruption depuis 1901, le *Journal canadien des sciences halieutiques et aquatiques* a paru sous plusieurs titres : *Contributions to Canadian Biology* 1901–1925, *Contributions to Canadian Biology and Fisheries* 1926–1934, *Journal of the Biological Board of Canada* 1934–1937, et *Journal of the Fisheries Research Board of Canada* 1938–1979. Le Journal paraît tous les mois, formant ainsi un volume de 12 numéros, et offre en plus jusqu'à deux suppléments par année.

Politique éditoriale. On publie, dans le Journal, des articles rendant compte de recherche originale, des perspectives (synthèses, critiques et réévaluations), des discussions (commentaires et réponses) et des communications rapides. Les documents peuvent porter sur les cellules, organismes, populations, communautés, écosystèmes ou processus qui affectent les systèmes aquatiques. Ils peuvent relever de divers domaines y compris la biologie et l'écologie des organismes marins et d'eau douce, la limnologie, l'océanographie, la physiologie, la toxicologie, la génétique, l'économie, la pathologie et la gestion. On accorde la préséance aux articles qui contribuent à la compréhension de phénomènes observés et à l'interprétation de résultats expérimentaux. On invite les auteurs à soumettre des articles ayant des objectifs précis ou relevant d'hypothèses, de concepts ou de questions vérifiables et se terminant par de solides conclusions ou d'utiles synthèses. Ces articles enrichissent, changent, mettent en question ou réorientent les connaissances acquises sur divers aspects des sciences aquatiques. On décourage toutefois la soumission d'articles simplement descriptifs (à moins qu'il ne s'agisse de nouvelles disciplines), d'application très limitée (applicables à une seule année, une seule région ou un seul taxon, portant sur un unique composé chimique, etc.); d'articles qui ne font que reprendre les principes énoncés dans des articles précédents; et d'articles rendant compte de l'application de normes sans gain de méthodologie.

Les auteurs sont invités à soumettre leur **manuscrit** au Bureau de la rédaction par le truchement du Système de soumission et d'examen en direct des articles (**OSPREY**) des Presses scientifique du CNRC à http://pubs.nrc-cnrc.gc.ca/jcsha/osprey. Sinon, ils peuvent transmettre leur manuscrit par la poste à la directrice scientifique principale, *Journal canadien des sciences halieutiques et aquatiques*, Département de biologie intégrative, édifice 006, bureau 118, University of Guelph, Guelph, ON N1G 2W1, Canada (519-824-4120 poste 52646; télécopieur : 519-767-9798; courriel : cjfas@uoguelph.ca).

Les contributions peuvent être en anglais ou en français. Elles doivent être originales, c.-à.-d. qu'elles ne doivent pas avoir fait l'objet d'un copyright, avoir été publiées ou soumises ailleurs, sauf sous forme abrégée ou avec le consentement du rédacteur. Le CNRC ne se tient en aucune façon responsable des opinions exprimées par un collaborateur ou des déclarations qui pourrait faire ce dernier.

La correspondance ayant trait aux manuscrits acceptés et les **épreuves corrigés** doivent être envoyées aux Presses scientifiques du CNRC, Conseil national de recherches du Canada, Ottawa, ON K1A 0R6, Canada (télécopieur : 613-952-7656; courriel : pubs@nrc-cnrc.gc.ca).

Les Recommandations aux auteurs sont publiées une fois par année dans le premier numéro de chaque volume. Des copies sont disponibles auprès du Bureau de la rédaction aux Presses scientifiques du CNRC ou au jcsha.cnrc.ca. **La Politique de publication** est disponible auprès des Presses scientifiques du CNRC ou au pubs.nrc-cnrc.gc.ca.

Microfilms. On peut acheter sur microfilms de 16 ou 35 mm tous les numéros depuis 1934. Des photocopies d'articles ou de numéros individuels sont aussi en vente auprès de University Microfilms International, 330 North Zeeb Road, Ann Arbor, MI 48106, É.-U.

This Journal is indexed or abstracted in / Cette revue est signalée ou résumée dans

ABSEARCH; Applied Science and Technology Index and Abstracts; Aquatic Sciences and Fisheries Abstracts; Biological Abstracts; Biological and Agricultural Abstracts; CAB Abstracts; Chemical Abstracts; Current Contents; Elsevier BIOBASE; Environmental Abstracts; ETDE Energy Database; General Science Index and Abstracts; GEOBASE; GeoRef; Life Sciences Collection; Meteorological and Geoastrophysical Abstracts; Oceanic Abstracts; PASCAL Database; Science Citation Index.

Volume 64, Number 2, February 2007

Canadian Journal of Fisheries and Aquatic Sciences

Published by the National Research Council of Canada

Volume 64, numéro 2, février 2007

Journal canadien des sciences halieutiques et aquatiques

Publié par le Conseil national de recherches du Canada

Senior Editor / Directrice scientifique principale **Moira M. Ferguson**

Editors / Directeurs

Jeffrey A. Hutchings, *Dalhousie University, Halifax*
Pierre Pepin, *Northwest Atlantic Fisheries Centre, DFO/MPO, St. John's, Newfoundland*
W. Gary Sprules, *University of Toronto at Mississauga*
Assistant to the Editors / Adjointe aux directeurs scientifiques **Holly Foster**

Associate Editors / Directeurs scientifiques associés

D. Boisclair, *Université de Montréal*
U. Borgmann, *Environment Canada, Burlington*
M.J. Bradford, *DFO/MPO and Simon Fraser University*
S.E. Campana, *DFO/MPO, Dartmouth*
R. Carignan, *Université de Montréal*
K.T. Frank, *DFO/MPO, Dartmouth*
J.W.A. Grant, *Concordia University*
M.M. Hansen, *Danish Institute for Fisheries Research, Silkeborg, Denmark*
R. Hilborn, *University of Washington*
D.F. Houlihan, *University of Aberdeen*
F.A. Huntingford, *University of Glasgow*
J.M. Jech, *NFSC/NOAA, Woods Hole, Mass.*
B. Jonsson, *Norwegian Institute for Nature Research, Oslo, Norway*
K.A. Kidd, *University of New Brunswick*
D.L. MacLatchy, *University of New Brunswick, Saint John*
P. Magnan, *Université du Québec à Trois Rivières*
C.T. Marshall, *University of Aberdeen*
R.B. Millar, *University of Auckland, New Zealand*
W.P. Patterson, *University of Saskatchewan*
Y.T. Prairie, *Université du Québec à Montréal*
T.J. Quinn II, *University of Alaska–Fairbanks, Juneau, Alaska*
T.P. Quinn, *University of Washington*
C.W. Ramcharan, *Laurentian University*
J.S. Richardson, *The University of British Columbia*
B. Sainte-Marie, *DFO/MPO, Mont-Joli*
R.E.H. Smith, *University of Waterloo*
S.J. Smith, *DFO/MPO, Dartmouth*
E.B. Taylor, *The University of British Columbia*
W.F. Vincent, *Université Laval*
R.D. Vinebrooke, *University of Alberta*
C.J. Walters, *The University of British Columbia*
B. de Young, *Memorial University of Newfoundland*

NRC Research Press / Presses scientifiques du CNRC

Fax / Télécopieur : 613-952-7656; e-mail / courriel : pubs@nrc-cnrc.gc.ca; URL / URL : pubs.nrc-cnrc.gc.ca

Editor-in-Chief / Directeur scientifique en chef **Bruce P. Dancik**
Assistant Editor-in-Chief / Adjoint au directeur scientifique en chef **Donald S. Mavinic**
Director / Directeur **Cameron D. Macdonald**

Acting Business Manager / Gestionnaire des affaires commerciales par intérim **Mike Boruczki**
Advertising and reprints / Annonces publicitaires et tirés à part **Roxanne Landriault** (613-990-2254)
Subscriptions / Abonnements **Eileen Evans-Nantais** (613-990-7873), **André Séguin** (613-993-9084)

Manager, Journals Program / Gestionnaire du Programme des revues **Carolyn Brown**
Managing Editor / Rédactrice administrative **Cecily M. Pearson** (613-993-9099)
Publication Officers / Agents de publication **Jennifer McColl, Thad Costigan**
Editorial Publication Assistant / Adjointe à la publication **Diana Leck**

Production Manager / Gestionnaire de la production **Brad Stoppa**
Production Application Support Technician / Technicienne au soutien de la production **Judy Hum**
Desktop Publishing Technician / Technicienne en éditique **Lisette Séguin**
Graphics Technician / Technicien en graphisme **Jeff Wisking**
Web Technician / Technicien Web **Dennis Cafferty**

The National Research Council of Canada accepts no responsibility for statements or opinions expressed by a contributor. Acceptance of an advertisement, announcement, or other material does not imply endorsement by either the Journal's Senior Editor or the National Research Council.

© National Research Council of Canada 2007. All rights reserved.

No part of this publication may be reproduced, stored, or transmitted in any form or by any means, without the written permission of the publisher, except as stated below.

The National Research Council of Canada grants **permission*** to individuals to make single copies of articles for personal use. Any person may reproduce short excerpts from articles in the journal for any purpose that respects the moral rights of authors, provided that the source is fully acknowledged. As a courtesy, the consent of authors of such material should be obtained directly from the author.

Authorization to reproduce items for other than personal use, as stated above, is granted by the National Research Council of Canada provided that the copyright fee of $7.00 per copy is paid directly to Access Copyright, The Canadian Copyright Licensing Agency, One Yonge Street, Suite 800, Toronto, ON M5E 1E5, Canada.

*The above permission does not extend to other kinds of copying, such as copying for general distribution, for advertising, or promotional purposes, for creating new collective works, or for resale. For such copying, arrangements must be made with the publisher, National Research Council of Canada, Ottawa, ON K1A 0R6, Canada.

Subscription information

The *Canadian Journal of Fisheries and Aquatic Sciences* (ISSN 0706-652X) is published monthly by the National Research Council of Canada. The 2007 annual subscription rates (second class postage) for Canada are $1051CAN institutional and $325CAN personal, for US & foreign $1051US institutional and $325US personal. For air mail add $150US to foreign rate. Canadian customers please include 6% GST (business no. 12149 1807 RT 0275). Subscriptions are entered for the calendar year. Remittances should be made payable to the Receiver General for Canada, credit NRC. Price for regular single issues: institutional, $110.00; personal, $35.00. Supplements will be priced separately. Special rates apply to members of Canadian scientific and engineering societies if they subscribe through their respective societies.

There are no refunds on cancelled subscriptions once delivery has begun. Claims for missing issues should be made within four months (North America) or six months (outside North America) following the date of publication. The publisher expects to supply missing issues only when losses have occurred in transit and when the reserve stock will permit. For change of address and subscription enquiries: Subscription Office, NRC Research Press, National Research Council of Canada, Ottawa, ON K1A 0R6, Canada; tel.: 613-993-9084; fax: 613-952-7656; e-mail: pubs@nrc-cnrc.gc.ca.

Microform backfiles are available from UMI, P.O. Box 1346, Ann Arbor, MI 48106-1346, USA, and Micromedia Ltd., 20 Victoria St., Toronto, ON M5C 2N8, Canada.

All issues of the *Canadian Journal of Fisheries and Aquatic Sciences* since 1996 are available on the Web. Pricing information can be found at pubs.nrc-cnrc.gc.ca.

Le Conseil national de recherches du Canada ne se tient en aucune façon responsable des opinions exprimées par un collaborateur ou des déclarations que pourrait faire ce dernier. La publication d'annonces publicitaires, d'avis et autres n'implique pas l'endossement de leur contenu par la directrice principale de la Revue ou le CNRC.

© Conseil national de recherches du Canada 2007. Tous droits réservés.

Il est interdit de reproduire, de sauvegarder ou de transmettre quelque partie de la présente publication dans quelque format ou de quelque façon sans le consentement écrit de l'éditeur, à l'exception des conditions suivantes.

Le Conseil national de recherches du Canada accorde aux particuliers le droit de faire des copies individuelles pour leur usage personnel. Toute personne peut reproduire de courts extraits des articles de la Revue pour autant que les droits moraux de l'auteur soient respectés et que la mention de provenance soit clairement indiquée. Il est de convenance de demander le consentement de l'auteur avant de faire mention de son travail.

On obtiendra l'autorisation de reproduire des articles à d'autres fins que l'usage personnel (tel qu'on l'a décrit ci-dessus) auprès du Conseil national de recherches du Canada pour autant que des redevances de droits d'auteurs de 7,00 $/copie soient versées au Access Copyright, The Canadian Copyright Licensing Agency, 1, rue Yonge, bureau 800, Toronto, ON M5E 1E5, Canada.

*La permission ci-dessus ne s'applique pas à la reproduction à grande échelle, telle que la reproduction aux fins de distribution générale, publicitaire ou promotionnelle, de compilation de nouveaux ouvrages collectifs ou de revente. Dans de tels cas, il faudra ratifier une entente particulière avec l'éditeur, le Conseil national de recherches du Canada, Ottawa, ON K1A 0R6, Canada.

Renseignements sur l'abonnement

Journal canadien des sciences halieutiques et aquatiques (ISSN 0706-652X) est une publication mensuelle du Conseil national de recherches du Canada. Le prix de l'abonnement annuel en 2007 au Canada (courrier de deuxième classe) est de 1051 $CAN pour les organismes et de 325 $CAN pour les particuliers. À l'étranger (y compris les É.-U.), le prix de l'abonnement est de 1051 $US pour les organismes et de 325 $US pour les particuliers. L'expédition par avion exige des frais de 150 $US en sus du prix d'abonnement à l'étranger. Les clients du Canada doivent ajouter la TPS de 6 % (numéro d'entreprise 12149 1807 RT 0275). Les abonnements sont pour l'année civile. Tout paiement doit être adressé au Receveur général du Canada, crédit du CNRC. Le prix par numéro est de 110 $ pour les organismes et de 35 $ pour les particuliers. Le prix des hors-série varie. Les membres des sociétés canadiennes de sciences et de génie bénéficient de taux préférentiels en s'abonnant via leurs sociétés respectives.

Aucun remboursement ne sera accordé ni aucune annulation acceptée une fois que les livraisons auront commencé. Les réclamations de numéros manquants devront être soumises dans les quatre mois (Amérique du Nord) ou dans les six mois (à l'extérieur de l'Amérique du Nord) suivant la date de publication. L'éditeur ne fournira de numéros manquants que si le document a été perdu pendant l'expédition et que si le stock le permet. Adressez tout changement d'adresse ou toute question quant à l'abonnement au : Bureau des abonnements, Presses scientifiques du CNRC, Conseil national de recherches Canada, Ottawa, ON K1A 0R6, Canada; téléphone : 613-993-9084; télécopieur : 613-952-7656; courriel : pubs@nrc-cnrc.gc.ca.

On peut obtenir les fichiers rétrospectifs sur **microforme** auprès de UMI, P.O. Box 1346, Ann Arbor, MI 48106-1346, É.-U., et auprès de Micromedia Ltée, 20, rue Victoria, Toronto, ON M5C 2N8, Canada.

À partir de 1996, tous les numéros de *Journal canadien des sciences halieutiques et aquatiques* sont accessibles sur le Web. On trouvera des renseignements sur les tarifs à pubs.nrc-cnrc.gc.ca.

RAPID COMMUNICATION / COMMUNICATION RAPIDE

Logging-induced variations in dissolved organic carbon affect yellow perch (*Perca flavescens*) recruitment in Canadian Shield lakes

Andrea Bertolo and Pierre Magnan

Abstract: There is increasing interest in the effects of allochthonous carbon on lake food webs. By temporarily increasing levels of dissolved organic carbon (DOC) in lakes, logging can help us understand how carbon from the watershed could affect lake biota. The goals of this study were to determine whether (*i*) logging has a significant effect on the abundance of young-of-the-year (YOY) yellow perch (*Perca flavescens*) in Canadian Shield lakes and (*ii*) any changes in yellow perch recruitment could be related to increases in nutrients (N and P) and (or) DOC following logging. To do this, we examined 22 Canadian Shield lakes: the watersheds of 13 were not impacted, while 9 underwent logging (1%–78% of the watershed area). We found that the relative abundance of YOY yellow perch increased after logging in proportion to the ratio between the area of the logged watershed and the lake volume. We show that this effect is likely explained by an increase in DOC following logging. This might be related to (*i*) an increase in secondary productivity due to a positive effect of terrestrial carbon on the microbial loop and (or) (*ii*) an increased hatching success and (or) larval survival due to a greater protection from UV radiation by DOC.

Résumé : Les effets du carbone allochtone sur les réseaux trophiques lacustres font l'objet d'un intérêt grandissant. En augmentant les niveaux du carbone organique dissous (COD) dans les lacs, les coupes forestières peuvent servir de modèle pour comprendre comment le carbone provenant du bassin versant peut affecter le compartiment biotique des lacs. Les objectifs de cette étude étaient de déterminer (*i*) si les coupes forestières ont un effet significatif sur l'abondance des jeunes perchaudes (*Perca flavescens*) de l'année (YOY) dans les lacs du bouclier canadien et (*ii*) si d'éventuels changements dans le recrutement de la perchaude peuvent être mis en relation avec l'augmentation des éléments nutritifs (N et P) et (ou) de COD suite aux coupes forestières. Nous avons échantillonné 22 lacs du bouclier canadien, dont 13 n'avaient subi aucune perturbation et 9 avaient subi des coupes forestières dans leur bassin versant (1–78 % de la superficie du bassin). L'abondance relative des jeunes perchaudes a augmenté suite aux coupes forestières, proportionnellement au rapport entre la superficie du bassin affecté par les coupes et le volume du lac. Nous montrons que cet effet est probablement expliqué par une augmentation du COD suite aux coupes forestières. Ceci pourrait être en relation avec (*i*) une augmentation de la productivité secondaire due à un effet positif du carbone d'origine terrestre dans la boucle microbienne et (ou) (*ii*) à une augmentation du succès de l'éclosion et (ou) de la survie larvaire due à une protection accrue contre les rayons UV par le COD.

Introduction

While there is an increasing interest on the effects of allochthonous carbon on lake food webs, its effects on higher trophic levels are still not fully understood (Steinberg et al. 2006). Carignan et al. (2000) found that logging increased ion (i.e., K^+, Cl^-, and Ca^{2+}), nutrient (i.e., N and P) and dissolved organic carbon (DOC) loads. Even though clear effects of logging were found on lake water chemistry, relatively small effects have been observed on phytoplankton biomass after deforestation (Planas et al. 2000). The reduced penetration of solar radiation in the water column, caused by the increased DOC, might explain such a result. Thus, it is not straightforward to predict to what degree the nutrient (P and N) and carbon enrichment caused by forest exploitation will be transferred to higher trophic levels.

Received 19 October 2006. Accepted 9 January 2007. Published on the NRC Research Press Web site at http://cjfas.nrc.ca on 5 February 2007.
J19611

A. Bertolo[1] and P. Magnan. Département de Chimie-Biologie, Université du Québec à Trois-Rivières, C.P. 500, Trois-Rivières, QC G9A 5H7, Canada.

[1]Corresponding author (e-mail: andrea.bertolo@uqtr.ca).

 doi:10.1139/F07-004 © 2007 NRC Canada

In fact, it is still largely unknown if allochthonous organic carbon might be efficiently transferred, directly or indirectly, via the microbial loop to zooplanktonic consumers and from these to fish (Steinberg et al. 2006). As fish yield is strongly correlated to lake productivity (Godbout and Peters 1988), forest clearance may increase fish productivity only if it induces an increase in the productivity of primary producers and (or) bacteria.

In a study comparing control vs. impacted lakes, St-Onge and Magnan (2000) showed that logging was associated with a reduction in the numbers of small size classes of both yellow perch (*Perca flavescens*) and white sucker (*Catostomus commersonii*) (<75 and <160 mm, respectively) 1–2 years following the perturbation. While these results suggest that logging could affect fish communities by reducing the survival of juvenile fish, they do not support the hypothesis of a positive effect of logging through an increase in fish productivity. The sampling device (i.e., gill nets) used by St-Onge and Magnan (2000) did not allow the sampling of small-bodied and young-of-the-year (YOY) fish, which are probably the most sensitive to watershed perturbations and variations in lake productivity. The objectives of our study were to determine whether (*i*) logging has a significant effect on the abundance of YOY yellow perch in Canadian Shield lakes and (*ii*) any changes in yellow perch recruitment could be related to increases in nutrients (N and P) and (or) DOC following logging. We used a before–after control–impact (BACI) experimental design to address these objectives. Lakes were sampled once (1–2 years) before and once (1–2 years) after the perturbation (i.e., logging).

Materials and methods

Study area

Twenty-two thermally stratified headwater lakes were selected on the basis of comparable size (fetch greater than 1 km), basin morphometry (maximum depth exceeding 5 m), and catchment properties (<6% of catchment covered by wetlands). The lakes were accessible only by plane and are located within a 50 000 km^2 area surrounding the Gouin Reservoir, Quebec, Canada (48°50′N, 75°00′W). The forest is primarily composed of black spruce (*Picea mariana*), balsam fir (*Abies balsamea*), jack pine (*Pinus divaricata*), white birch (*Betula papyrifera*) and trembling aspen (*Populus tremuloides*). Only minor logging occurred in the watersheds of these lakes prior to 2000, while clearcuts occurred between 2000 and 2002 in nine of them (Table 1). Because of their remoteness, the fish communities of these lakes are generally unexploited or only lightly exploited. This should reduce any bias related to potential increases in fishing pressure due to the presence of better access roads following logging. The most common fish species in the study lakes were yellow perch (n = 22), northern pike (*Esox lucius*) (n = 21), white sucker (n = 16), walleye (*Sander vitreus*) (n = 14), lake whitefish (*Coregonus clupeaformis*) (n = 14), and fallfish (*Semotilus corporalis*) (n = 12). On average, yellow perch represented 74.6% ± 31.6% (mean ± standard deviation, SD) of the total catches by seine.

Fish sampling

We used a beach seine to estimate the catch per unit of effort (CPUE) of YOY yellow perch; this technique is well suited to sampling juvenile fish. For logistic reasons, 7 lakes were sampled in 2000 and 15 in 2001 (before perturbation), while all lakes were resampled in 2002 (1–2 years after perturbation). Each lake was seined once between June and August. On average, 34 ± 10 samples (mean ± SD) were taken in each lake at randomly selected littoral stations.

Plankton and water chemistry analyses

Water for the analyses of chemical variables, chlorophyll *a* (Chl), and zooplankton was sampled in June and August 2000, 2001, and 2002 (the same years as the seine fishing). We used average summer values in statistical analyses. Sampling for chemical variables and phytoplankton took place in the euphotic zone, while zooplankton samples were taken over the entire water column with a 53 µm mesh cantilevering net. Total phosphorus (TP) was measured using the molybdenum blue method, whereas total nitrogen (TN) was measured as NO_3 after alkaline persulfate digestion. Chl was extracted using hot 90% ethanol, and absorbance was measured spectrophotometrically. DOC was measured within 72 h by infrared gas analysis after sample acidification and He sparging followed by Pt-catalyzed oxidation at 700 °C. Zooplankton samples were fractionated into two size classes (smaller or larger than 500 µm) before estimating dry weight. Each zooplankton size class was filtered separately onto precombusted GF/A (Whatman) glass fiber filters, dried at 40 °C for 18 h, weighed, ashed at 500 °C for 18 h, and weighed again to estimate dry weight. See Carignan et al. (2000), Patoine et al. (2000), and Planas et al. (2000) for details on the analytical methods.

Statistical analysis

Analyses of variance (ANOVA) were used to compare physico-chemical and plankton variables between unperturbed lakes and lakes that experienced logging in their watershed. Multiple linear regressions were used to determine environmental factors that best explained variations in CPUE (i.e., ΔCPUE) of both YOY yellow perch and older individuals following logging. We also analyzed the before–after logging variations in the CPUE of other fish species (yellow perch excluded) and in the total fish CPUE (including yellow perch) caught in seines. To take into account the BACI protocol, the dependent and independent variables used in analyses were represented by their variation between the period preceding and the period following deforestation: changes in dissolved organic carbon (ΔDOC); total phosphorus (ΔTP); total nitrogen (ΔTN); chlorophyll *a* (ΔChl); and the biomass of total zooplankton (ΔZOO), small zooplankton (<500 µm) ($\Delta ZOO_{<500}$), and large zooplankton (>500 µm) ($\Delta ZOO_{>500}$). To examine differences in seining dates before and after logging (Table 1), we used the difference in the day of the year between the two samplings (Δday) as a covariable. The ratio between the watershed area logged and the lake volume (hereafter CUT/VOL) was used as a measure of the potential impact of logging on lake physico-chemistry (Carignan et al. 2000).

Independent variables included in the models were selected by a stepwise selection procedure in multiple regres-

© 2007 NRC Canada

Table 1. General characteristics of study lakes.

Lake	Area (km^2)	Max depth (m)	Watershed area (km^2)	Seining date (dd-mm-yy) BF	Seining date (dd-mm-yy) AF	Logging year*	TP (µg·L^{-1}) BF	TP (µg·L^{-1}) AF	TN (µg·L^{-1}) BF	TN (µg·L^{-1}) AF	Chl (µg·L^{-1}) BF	Chl (µg·L^{-1}) AF	DOC (mg·L^{-1}) BF	DOC (mg·L^{-1}) AF	CUT* (%)	CUT/VOL* (m^{-1})
AB220	0.359	18.3	2.52	24-06-01	11-06-02	—	6.4	7.3	187.0	242.0	1.9	2.3	4.1	4.4	0.0	0.00
AB35	0.873	21.7	2.63	17-06-01	14-06-02	—	6.9	9.0	241.0	301.5	2.8	2.9	5.4	5.6	0.0	0.00
CSL2	0.850	10.2	2.83	09-07-01	21-07-02	—	7.0	6.8	200.5	238.7	1.6	2.6	5.7	6.3	0.0	0.00
CSL5	0.153	9.2	2.42	04-07-01	19-07-02	—	9.3	9.7	294.8	311.9	2.4	3.1	10.5	10.6	0.0	0.00
DA4	0.258	6.7	3.90	02-08-01	01-07-02	—	9.4	8.7	254.5	264.5	2.3	1.7	8.5	9.0	0.0	0.00
DA9	0.160	9.2	5.92	28-07-01	28-06-02	—	10.0	10.9	326.3	365.0	2.3	3.6	9.7	10.4	0.0	0.00
DF2	0.294	6.7	1.15	09-08-00	01-08-02	2000–2002	9.1	10.2	222.0	285.3	2.2	3.3	7.2	8.3	50.1	0.51
DF4	0.303	6.4	1.97	13-08-01	04-08-02	—	8.9	9.1	283.3	274.0	2.1	2.3	9.2	9.4	0.0	0.00
DF5	0.446	13.7	4.39	14-08-01	06-08-02	2001–2002	6.1	6.6	242.0	232.5	1.5	1.7	8.0	8.1	0.6	0.01
DF7	0.318	10.8	3.06	11-08-01	30-07-02	2001–2002	9.1	11.0	245.7	284.7	2.8	1.8	11.0	12.5	63.4	1.80
DF9	0.421	10.5	2.23	25-06-00	18-07-02	2000–2001	15.7	14.9	395.0	458.0	3.6	2.8	12.7	14.9	62.9	0.81
K1	0.324	9.1	2.32	25-07-01	05-07-02	2001–2002	11.0	11.2	245.5	282.0	2.6	3.0	6.5	6.7	9.6	0.21
K2	1.421	12.2	9.14	22-07-01	07-07-02	—	9.3	8.7	302.8	331.0	2.1	1.9	8.4	9.2	0.0	0.00
K3	0.829	7.2	3.27	06-07-00	12-07-02	2000–2001	10.8	9.6	242.0	278.8	2.6	2.7	6.1	6.6	25.5	0.27
K4	0.192	8.0	1.05	28-06-00	14-07-02	2000–2001	11.1	11.9	265.5	301.0	3.4	3.5	7.3	8.2	41.8	0.64
K8	0.756	8.6	5.66	02-07-00	09-07-02	2000–2002	15.0	15.4	318.5	356.2	3.2	3.5	9.9	11.1	47.8	1.30
N35	0.212	9.1	1.36	20-07-00	19-06-02	—	7.8	8.1	239.0	245.3	2.3	3.0	4.4	4.1	0.0	0.00
N43	0.297	9.5	5.39	16-07-01	27-07-02	—	8.1	9.5	269.0	277.0	1.9	2.2	9.5	9.4	0.0	0.00
N55	0.261	7.8	1.36	29-06-01	23-06-02	—	11.6	10.9	253.3	306.8	3.6	4.2	5.0	5.2	0.0	0.00
N70	0.654	20.4	2.35	12-07-00	26-06-02	—	8.2	5.5	257.0	249.0	2.1	2.2	5.8	5.5	0.0	0.00
N89	0.670	14.0	2.67	14-07-01	28-07-02	—	5.1	4.1	153.3	181.0	1.4	1.8	3.7	4.1	0.0	0.00
P109	0.505	10.7	2.74	04-08-01	03-07-02	2001–2002	6.9	7.3	235.4	245.8	1.4	2.4	6.1	7.0	60.6	0.77

Note: Total phosphorus (TP), total nitrogen (TN), chlorophyll *a* (Chl), and dissolved organic carbon (DOC) are summer averages (from samplings in June and August) measured before (BF; 2000 or 2001) or after (AF; 2002) logging. CUT, percent watershed area logged between the two seining dates; CUT/VOL, ratio between the watershed area logged (m^2) and the lake volume (m^3).

*Logging that occurred before seining was not taken into account.

© 2007 NRC Canada

Fig. 1. Relationship between the before–after impact variation in dissolved organic carbon (ΔDOC) and the before–after impact variation in catch per unit effort (ΔCPUE) of (*a*) young-of-the-year (YOY) yellow perch (*Perca flavescens*), (*b*) yellow perch >0+, (*c*) other fish species, and (*d*) total fish in seines. Results of linear regressions are shown when significant. Open circles indicate lakes with unperturbed watersheds; solid circles indicate lakes with logged watersheds. The sizes of the solid circles are proportional to the watershed perturbation (CUT/VOL). The arrow in panel *a* indicates lake AB35, which was excluded from the analysis (see text).

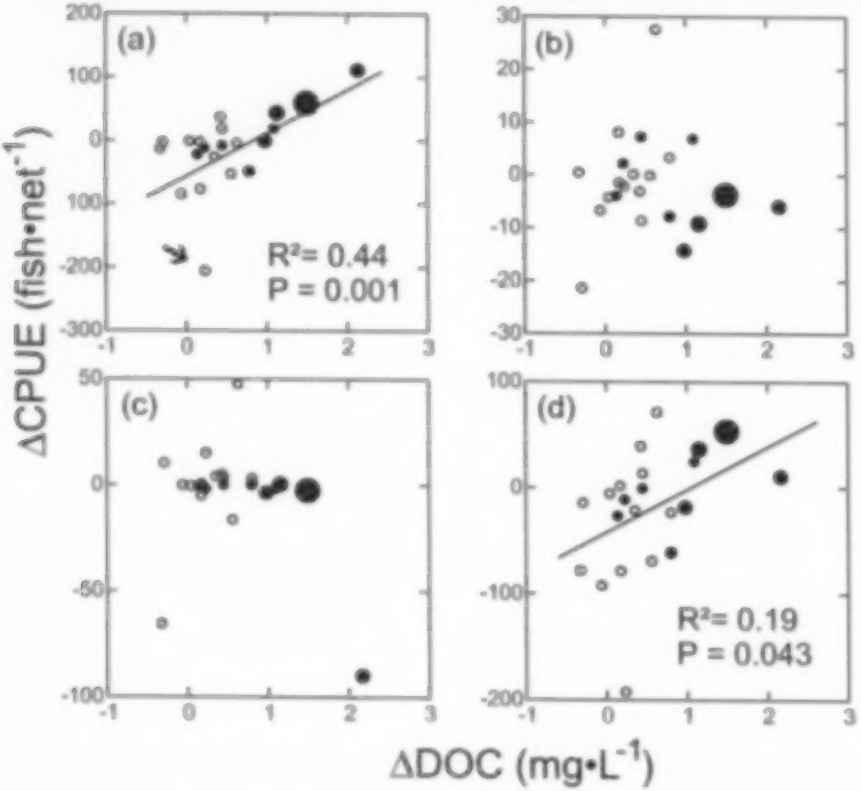

sion analysis (α to enter = 0.10; α to stay = 0.05). Analyses were performed both including and excluding zooplankton data because these data were available only for 20 out of 22 lakes.

Results and discussion

CUT/VOL was significantly correlated with ΔDOC (Spearman's $r = 0.67$, $P = 0.0006$), but not with nutrients (ΔTP and ΔTN), phytoplankton biomass (ΔChl), or zooplankton biomass (ΔZOO, $\Delta ZOO_{<500}$, $\Delta ZOO_{>500}$). ANOVA confirmed that ΔDOC differed significantly between unperturbed and logged lakes ($F_{[1,20]} = 11.2$, $P = 0.0033$), but also showed that both $\Delta ZOO_{<500}$ and ΔZOO were significantly higher in logged lakes than in unperturbed lakes ($F_{[1,18]} = 4.8$, $P = 0.0419$ and $F_{[1,18]} = 5.6$, $P = 0.0299$, respectively).

CUT/VOL was significantly correlated with ΔCPUE of YOY yellow perch (Spearman's $r = 0.51$, $P = 0.015$). No significant correlations were found between CUT/VOL and the before–after variation in the CPUE of older yellow perch, other fish species caught in seines, and total fish ΔCPUE ($P = 0.24$, $P = 0.07$, and $P = 0.10$, respectively). ANOVA showed that YOY yellow perch ΔCPUE tended to differ between unperturbed and logged lakes ($F_{[1,20]} = 4.0$, $P = 0.060$). No significant differences were found in ΔCPUE for >0+ yellow perch, other fish species, and total fish.

ΔDOC was significantly correlated with ΔCPUE of YOY yellow perch (Spearman's $r = 0.49$, $P = 0.0218$; Fig. 1*a*) and ΔCPUE of total fish (Spearman's $r = 0.51$, $P = 0.0153$; Fig. 1*d*). No correlation was found between ΔDOC and the ΔCPUE of yellow perch >0+ or other fish species (Figs. 1*b*–1*c*). ΔTP, ΔChl, and variations in zooplankton biomass (ΔZOO, $\Delta ZOO_{<500}$, $\Delta ZOO_{>500}$) were not correlated to any of the ΔCPUE variations. ΔTN was only significantly correlated to the ΔCPUE of yellow perch >0+ ($r = 0.46$, $P = 0.030$).

The stepwise selection procedure selected ΔDOC (+) and ΔTP (–) to explain the ΔCPUE of YOY yellow perch. This model explained 52% of the variation in the dependent variable. However, the model was sensitive to lake AB35 (an unperturbed lake), which experienced the highest reduction in the CPUE of both YOY yellow perch as well as a relatively large increase in TP. Besides improving the normality of the data, excluding this point improved the relationship with ΔDOC, whereas no relationship was found with ΔTP (Fig. 1). A similar result was obtained for total ΔCPUE, with only

© 2007 NRC Canada

ΔDOC (+) selected in the model (R^2 = 0.19, P = 0.0430). The best model to explain the ΔCPUE yellow perch >0+ included ΔTN (+) and ΔChl (+) (R^2 = 0.37, P = 0.0118). No variable was selected to explain the ΔCPUE of other fish species.

No significant relationship between Δday and any of the dependent variables described above was found, suggesting that our results are not biased by the seining date. Within-lake variability in total CPUE was significantly higher before logging (CV = 84.7) than after (CV = 14.1) (χ^2 = 25.9, P < 0.0001), but no correlation was found between the CV of total CPUE and CUT/VOL in 2002 (Spearman's r = –0.06, P = 0.78).

Our study indicates that logging, by increasing DOC, is an important factor affecting the abundance of YOY yellow perch (Fig. 1*a*). This result refutes the hypothesis suggested by St-Onge and Magnan (2000) that post-emergence mortality increased after logging. Because yellow perch prefers to spawn on submerged vegetation or fallen trees rather than on gravel substrata, it is unlikely that perch suffered from siltation caused by logging. This result rather suggests a potential pathway linking the watershed perturbations to an increase in secondary production. This is apparently at odds with the observed changes in nutrients and Chl and with the results of a previous study on the impact of logging conducted in the same area by Planas et al. (2000). These authors showed that a relatively small increase in nutrients caused by logging did not initiate an increase in primary production because of the concomitant increase in light limitation caused by an increase of water colour; based on this result, only weak effects on secondary production might be expected after logging. In contrast, our results suggest that an increase in secondary production (YOY yellow perch and zooplankton) is possible despite a lack of effect on primary producers. To our knowledge, an important contribution of carbon subsidies from the watershed to fish production has been observed only in very small lakes (Cole et al. 2006), which are likely to receive proportionally larger supplies of allochthonous carbon. Even though the variation in zooplankton biomass was not correlated to CUT/VOL and the ΔCPUE of YOY yellow perch, both total and small zooplankton increased in logged lakes. Zooplankton may have benefited from an increase in the flow of energy and matter transmitted by the microbial loop, which was boosted by the increased DOC after logging, or they may have benefited directly from DOC by consuming colloidal or aggregated carbon particles (Kerner et al. 2003; Steinberg et al. 2006).

It is also possible that logging reduced ultraviolet (UV)-induced damage to yellow perch eggs and (or) larvae by increasing the DOC concentration and thus reducing the penetration of UV in the water column (Huff et al. 2004). Exposure to UV can dramatically reduce yellow perch egg survival to hatching in lakes with low DOC contents (Huff et al. 2004). The fact that the ΔCPUE of YOY yellow perch was strongly correlated with ΔDOC, but not with the variation in zooplankton biomass, lends additional support to the UV-protection hypothesis over the productivity one. However, average DOC concentrations in the study lakes before logging were relatively high (Table 1), and changes in UV penetration should have been biologically meaningful only in the shallower layers of the water column. Considering that yellow perch tend to spawn in shallow waters in such lakes (Huff et al. 2004) and that yellow perch larvae are positively phototropic (see references in Huff et al. 2004), we cannot exclude a DOC-mediated effect of UV on yellow perch recruitment in our lakes.

Yellow perch older than 0+ did not show any response to logging or to variations in DOC. This is not in contradiction with the UV-protection hypothesis, since these individuals can easily reduce their exposure to UV by regulating their depth.

St-Onge and Magnan (2000) observed, as with logging activities, that fires in watershed areas were associated with lower numbers of small-sized (<75 mm) yellow perch, even though this perturbation was not associated with an increase in DOC. It is thus possible that another mechanism explained their results. St-Onge and Magnan (2000) excluded any direct effect of the watershed perturbation on fish survival but hypothesized that the perturbation might have indirectly affected this size class by reducing the biomass of benthic invertebrates. Assuming that fine sediment can reach the lakeshore in perturbed watersheds, macroinvertebrate habitats and survival could have been negatively affected (Miller et al. 1997), reducing the abundance of food for older yellow perch. This would also explain why >0+ yellow perch did not respond positively to DOC in our study. Some studies have reported a reduction in macroinvertebrate density following timber harvesting (e.g., Vuori and Joensuu 1996). The increase in yellow perch recruitment following logging might have increased the intraspecific competition with other cohorts, with a negative effect on larger individuals. It has been shown that YOY have a competitive advantage over larger individuals and that the occurrence of a strong year class may lead to a drastic reduction of older cohorts in yellow perch populations (Sanderson et al. 1999).

Our study showed that yellow perch recruitment increases following logging and that this increase is correlated with the related DOC increase. Future work will be needed to elucidate the mechanisms by which logging and increased DOC induce changes in yellow perch recruitment.

Acknowledgements

We thank R. Proulx, D. Boula, E. Garcia, W. Giroux, F. Guillemette, P. Lafrance, D. Monté, Y. Paquette, A. Patoine, P. St-Onge, and L. Duhaime for their field and laboratory assistance. We are also grateful to P. East and M. Lapointe for their invaluable assistance at many stages of this research and to P. D'Arcy for his logistical support. L. Devine and F. Darchambeau provided helpful comments on earlier versions of this paper. We thank Richard Carignan for nutrient and DOC data and Dolors Planas and Bernadette Pinel-Alloul for Chl and zooplankton data. A.B. was supported by the Canada Research Chair in Freshwater Ecology. This project was supported by grants from the Sustainable Forest Management Network Center of Excellence and the Natural Sciences and Engineering Research Council of Canada to P.M. This study is a contribution of the Groupe de recherche interuniversitaire en limnologie et en environnement aquatique (GRIL).

© 2007 NRC Canada

References

Carignan, R., D'Arcy, P., and Lamontagne, S. 2000. Comparative impacts of fire and forest harvesting on water quality in Boreal Shield lakes. Can. J. Fish. Aquat. Sci. **57**: 105–117.

Cole, J.J., Carpenter, S.R., Pace, M.L., Van de Bogert, M.C., Kitchell, J.L., and Hodgson, J.R. 2006. Differential support of lake food webs by three types of terrestrial organic carbon. Ecol. Lett. **9**: 558–568.

Godbout, L., and Peters, R.H. 1988. Potential determinants of stable catch in the brook trout (*Salvelinus fontinalis*) sport fishery in Quebec. Can. J. Fish. Aquat. Sci. **45**: 1771–1778.

Huff, D.D., Grad, G., and Williamson, C.E. 2004. Environmental constraints on spawning depth of yellow perch: the roles of low temperatures and high solar ultraviolet radiation. Trans. Am. Fish. Soc. **1333**: 718–726.

Kerner, M., Hohenberg, H., Ertl, S., Reckermann, M., and Spitzy, A. 2003. Self-organization of dissolved organic matter to micelle-like microparticles in river water. Nature (London), **422**: 150–154.

Miller, L.B., McQueen, D.J., and Chapman, L. 1997. Impacts of forest harvesting on lake ecosystems: a preliminary literature review. B.C. Ministry of the Environment, Lands and Park Wildlife Branch, Victoria. Wildl. Bull. No. B-84.

Patoine, A., Pinel-Alloul, B., Prepas, E.E., and Carignan, R. 2000. Do logging and forest fires influence zooplankton biomass in Canadian Boreal Shield lakes? Can. J. Fish. Aquat. Sci. **57**: 155–164.

Planas, D., Desrosiers, M., Groulx, S.R., Paquet, S., and Carignan, R. 2000. Pelagic and benthic algal responses in eastern Canadian Boreal Shield lakes following harvesting and wildfires. Can. J. Fish. Aquat. Sci. **57**: 136–145.

Sanderson, B.L., Hrabik, T.R., Magnuson, J.J., and Post, D.M. 1999. Cyclic dynamics of a yellow perch (*Perca flavescens*) population in an oligotrophic lake: evidence for the role of intraspecific interactions. Can. J. Fish. Aquat. Sci. **59**: 1534–1542.

Steinberg, C.E.W., Kamara, S., Prokhotskaya, V.Y., Manusadzianas, L., Karasyova, T.A., Timofeyev, M.A., Jie, Z., Paul, A., Meinelt, T., Farjalla, V.F., Matsuo, A.Y.O., Kent Burnison, B., and Menzel, R. 2006. Dissolved humic substances — ecological driving forces from the individual to the ecosystem level? Freshw. Biol. **51**: 1189–1210.

St-Onge, I., and Magnan, P. 2000. Impact of logging and natural fires on fish communities of Laurentian Shield lakes. Can. J. Fish. Aquat. Sci. **57**: 165–174.

Vuori, K.-M., and Joensuu, I. 1996. Impact of forest drainage on the macroinvertebrates of a small boreal headwater stream: do buffer zones protect lotic biodiversity? Biol. Conserv. **77**: 87–95.

© 2007 NRC Canada

Variance estimation in integrated assessment models and its importance for hypothesis testing

Richard B. Deriso, Mark N. Maunder, and John R. Skalski

Abstract: Variance in likelihood functions for multiple normally distributed data sets can be reliably estimated in integrated assessment models, and their values are important for accurate hypothesis tests. Commonly, assessment models are fitted to multiple types of observations by constructing a joint likelihood function that is then maximized. When a model contains no random effects and all random variables in the likelihood function represent errors in the prediction of measurements, then variances for each of the error distributions are estimable provided that no likelihood component has zero degrees of freedom. Theory for estimation of variances is reviewed. We show the relationship between concentrated likelihood based on the normal distribution and weighted least squares. Concentrated likelihood and weighted least squares are equivalent when the likelihood is made of normally distributed errors with constant variances, and the least squares weights are inversely proportional to the maximum likelihood estimates of the variances. A simulation study was made to show that variances and several output quantities are reasonably estimated for a herring-like population with moderate amounts of data. The simulation analysis and a case study with application to a herring population show that the choice of variances can strongly affect results of hypothesis tests.

Résumé : Les modèles intégrés d'évaluation permettent d'estimer de manière fiable la variance dans les fonctions de vraisemblance pour des ensembles multiples de données à distribution normale; ces valeurs sont importantes pour tester les hypothèses avec précision. Généralement, on ajuste des modèles d'évaluation à de multiples types d'observations en construisant une fonction de vraisemblance commune que l'on maximise ensuite. Lorsqu'un modèle ne contient pas d'effets aléatoires et que toutes les variables aléatoires dans la fonction de vraisemblance représentent des erreurs dans la prédiction des mesures, il est alors possible d'estimer les variances pour chacune des distributions d'erreurs à la condition qu'aucune composante de la vraisemblance ne possède zéro degré de liberté. Nous passons en revue la théorie de l'estimation des variances. Nous montrons la relation qui existe entre la vraisemblance concentrée basée sur la distribution normale et les moindres carrés pondérés. La vraisemblance concentrée et les moindres carrés pondérés sont équivalents lorsque la vraisemblance se compose d'erreurs à distribution normale avec une variance constante ou lorsque les poids des moindres carrés sont inversement proportionnels aux estimations de leur vraisemblance maximale. Une simulation permet de montrer que les variances et plusieurs autres valeurs générées sont raisonnablement estimées dans le cas d'une population de type hareng pour laquelle on possède des quantités moyennes de données. La simulation et une étude de cas avec application à une population de harengs indiquent que le choix des variances peut fortement affecter les résultats des tests d'hypothèses.

[Traduit par la Rédaction]

Introduction

In modern fisheries stock assessment, it is common to use multiple types of data in a single integrated assessment model (e.g., Fournier and Archibald 1982). However, each data type, and even each data point, may be of a different quality, and its weight in the objective function used to fit the assessment model to observations should reflect this quality. This can be achieved through weighted least squares (LS) or by modifying a variance-related quantity in the likelihood function (e.g., the standard deviation in a likelihood function based on the normal distribution). A variety of choices have been made by different authors for choices for these weights (or equivalently, the variances for each data type). For example, Deriso et al. (1985) use relative weights chosen by examination of retrospective performance. In recent years, estimation of the weights to some data types have been based partly or wholly on maximum likelihood

Received 18 January 2006. Accepted 9 October 2006. Published on the NRC Research Press Web site at http://cjfas.nrc.ca on 1 February 2007.
J19113

R.B. Deriso.[1] Scripps Institution of Oceanography, La Jolla, CA 92093-0203, USA; Inter-American Tropical Tuna Commission, 8604 La Jolla Shores Drive, La Jolla, CA 92037-1508, USA.
M.N. Maunder. Quantitative Resource Assessment LLC, San Diego, CA USA; Inter-American Tropical Tuna Commission, 8604 La Jolla Shores Drive, La Jolla, CA 92037-1508, USA.
J.R. Skalski. School of Aquatic and Fishery Sciences, University of Washington, 1325 Fourth Avenue, Suite 1820, Seattle, WA 98101-2509, USA.

[1]Corresponding author (e-mail: rderiso@iattc.org).

 doi:10.1139/F06-178 © 2007 NRC Canada

estimates (MLEs) (McAllister and Ianelli 1997; Maunder and Starr 2003; Francis 2005). In other cases, all variances are chosen by judgment often supplemented by estimates of sample variances (Sullivan et al. 1999). Rarely have weights for all data types in an integrated assessment model been estimated by maximum likelihood methods. When a model contains no random effects and all random variables in the likelihood function represent errors in the prediction of measurements, the models can be regarded as multiresponse models, in the sense of Seber and Wild (1989). The theory for multiresponse models (Seber and Wild 1989) shows that maximum likelihood methods are applicable to that class of models, which include several integrated assessment models. Variances for each of the error distributions in the likelihood function are estimable in such models provided that no likelihood component has zero degrees of freedom (such as occurs, for example, when fishing mortality is an estimated parameter for every fishing effort datum point).

The prespecified weighting factors developed from characteristics of the data can often be inappropriate. For example, catch-at-age data are often more overdispersed than the standard multinomial sampling model used to represent the data. This can be caused when fish school by age. Therefore, it is suggested that the sample size used in the likelihood function should be reduced from the actual sample size (Fournier and Archibald 1982). Similarly, the variance estimates for indices of abundance from catch-per-unit-of-effort (CPUE) standardization are often too small (Maunder and Punt 2004). This is because the variances estimated in these analyses are for the CPUE year effects and not the abundance, and there may be a factor that causes annual variation in catch rates not included in the analysis. There may also be additional process error not included in the stock assessment model that can be accommodated by the variance in the likelihood function (Francis et al. 2003).

Conclusions drawn from application of integrated models can be strongly influenced by the choice of weightings used to determine the importance of a particular data set on the fitting of the model. The choice of weights also determines the total uncertainty in the estimates for calculating confidence intervals and performing hypothesis tests. Therefore, the appropriate weighting of data sets is important in the quantitative analysis of fisheries data.

One such application where the weightings used for different data sets may influence results is the evaluation of a disease (viral hemorrhagic septicemia) effect on adult survival of Prince William Sound Pacific herring (*Clupea pallasii*). Hypothesis tests, using prespecified weights for survey and age composition data in an age-structured stock assessment model, rejected the null hypothesis of no disease effect (Marty et al. 2003). These results have substantial impact on the interpretation of disease as a contributing factor in the decline of this stock in 1993 (Pearson et al. 1999), and results using alternative weightings (e.g., those based on MLEs) for the different data sets may change the conclusions of the hypothesis testing.

First, we outline the theory for estimation of variances and show the relationship between likelihood and weighted LS. Then we describe a simulation analysis based on a herring-like population that investigates the sensitivity of parameter estimates and hypothesis tests to the weighting of data sets and the estimation variances in the likelihood function. Finally, we illustrate the importance of appropriate weighting of data sets by analyzing data for the Prince William Sound herring population to determine the influence of disease on survival.

Theory on choice of optimum weights

We review and derive some basic results on the types of objective functions suitable for estimation of parameters in integrated assessment models. We focus on LS and normal-distribution-based likelihood functions, how they are used to weight different data sets and data points, and the differences and similarities between the two methods.

The weighting of each data set or data point determines the relative influence of each data point on the model estimates. Therefore, for parameter estimation, it is important that the relative weights are appropriately determined. Weighted LS can be used to put relative weights on the different data sets or data points. In the normal-distribution-based likelihood approach, the variance can be used to implement the relative weighting. The relative weighting is also important for estimating confidence intervals and hypothesis testing. However, for confidence intervals and hypothesis testing, the absolute weighting is also important.

Least squares

The simple LS objective function is just the sum of the squared difference between the observed (O_i) and predicted (P_i) data. The sum of squared difference is minimized to estimate the model parameters.

$$(1) \qquad \mathrm{LS} = \sum_i (O_i - P_i)^2$$

Likelihood

The likelihood based on the normal distribution is, assuming independence, simply the product of the likelihood for each data point. The likelihood is maximized to estimate the model parameters. The likelihood of each data point is proportional to the normal probability density function of the data given the parameter values.

$$(2) \qquad L(\theta|\mathrm{data}) = \prod_i \frac{1}{\sigma\sqrt{2\pi}} \exp\left[-\frac{(O_i - P_i)^2}{2\sigma^2}\right]$$

It is often convenient to work with the negative of the natural logarithm of the likelihood, and this also simplifies the comparison with LS. The negative log-likelihood is minimized, as with LS, to estimate the model parameters.

$$(3) \qquad -\ln L(\theta|\mathrm{data}) = \sum_i \left[\ln(\sigma) + 0.5\ln(2\pi) + \frac{(O_i - P_i)^2}{2\sigma^2}\right]$$

The term $0.5\ln(2\pi)$ is an additive constant independent of the parameters and for most purposes can be left out of the equation. If the standard deviation is fixed, the term $\ln(\sigma)$ is independent of the estimated parameters and can also be left out of the equation.

The standard deviation in the likelihood function can be estimated as a free parameter. However, there is an analyti-

© 2007 NRC Canada

cal formula for the MLE of the standard deviation. This can be obtained by setting the derivative of the negative log-likelihood to zero and solving for the standard deviation.

$$\hat{\sigma} = \sqrt{\frac{\sum_i (O_i - P_i)^2}{n}} \quad (4)$$

Inserting the analytical formula for the MLE of the standard deviation (eq. 4) into the negative log-likelihood (eq. 3) gives the concentrated likelihood (ignoring additive constants)

$$-\ln L(\theta|\text{data}) = 0.5n \ln\left[\sum_i (O_i - P_i)^2\right] \quad (5)$$

where n is the number of observations, which is simply half the product of the number of data points and the natural logarithm of the sums of squares. Because the natural logarithm is a monotonic function, the MLE and LS will give the same parameter estimates for constant variance.

Weighted data

It is common to use multiple types of data in a single analysis. Multiple data points are summed together in the LS approach. Similarly, in the likelihood approach, the product of the likelihood for each data point is used, which corresponds to summation for the negative log-likelihood. However, each data type, and even each data point, may be of a different quality, and its weight in the objective function should reflect this quality. This can be achieved through weighted LS or by modifying the standard deviation of the likelihood function.

For a single data set with different standard deviations for each data point, the negative log-likelihood is

$$-\ln L(\theta|\text{data}) = \sum_i \left[\ln(w_i\sigma) + 0.5\ln(2\pi) + \frac{(O_i - P_i)^2}{2w_i^2\sigma^2}\right] \quad (6)$$

We have separated the standard deviation into a relative component (w_i), which is prespecified, and an over all scalar (σ), which allows estimation of the overall scalar if desired:

$$\hat{\sigma} = \sqrt{\frac{\sum_i \frac{(O_i - P_i)^2}{w_i^2}}{n}} \quad (7)$$

An example of a normal likelihood function with a weighted variance is given by the Fournier et al. (1990) normal approximation to the multinomial likelihood function used for age or length frequency data. This likelihood uses the binomial variance $p(1 - p)$ as a weighting factor for the variance in the normal likelihood function. A constant (k) is added so that the variance will not be zero if the proportion is zero or one. In this case, $w_i^2 = p_i(1 - p_i) + k$ and the negative log-likelihood is

$$-\ln L(\theta|\text{data}) = \sum_i \left[\ln\left\{\sigma\sqrt{[p_i(1-p_i)+k]}\right\} + 0.5\ln(2\pi) + \frac{(O_i - P_i)^2}{2[p_i(1-p_i)+k]\sigma^2}\right] \quad (8)$$

and the analytical formula for the standard deviation scalar is

$$\hat{\sigma} = \sqrt{\frac{\sum_i \frac{(O_i - P_i)^2}{p_i(1-p_i)+k}}{n}} \quad (9)$$

In an analogous approach, the simple LS is modified by weighting factors to model differences in reliability in individual data points

$$\text{LS} = \sum_{\text{all } i} v_i (O_i - P_i)^2 \quad (10)$$

which gives the same estimates as the concentrated likelihood with weighted variance

$$-\ln L(\theta|\text{data}) = 0.5n \ln\left[\sum_i \frac{(O_i - P_i)^2}{w_i^2}\right] \quad (11)$$

provided the weights are chosen as

$$v_i \propto \frac{1}{w_i^2} \quad (12)$$

Multiple data sets

For multiple data sets with a common standard deviation for data within a data set, the negative log-likelihood is

$$-\ln L(\theta|\text{data}) = \sum_j \sum_{\text{all } i} \left[\ln(\sigma_j) + \frac{(O_i - P_i)^2}{2\sigma_j^2}\right] \quad (13)$$

The analytical formula for the variance could be calculated separately for each data set using the formula above. However, in this case the concentrated likelihood

$$-\ln L(\theta|\text{data}) = \sum_j 0.5n_j \ln\left[\sum_{\text{all } i} (O_i - P_i)^2\right] \quad (14)$$

where n_j is the number of observations in data set j, no longer gives the same estimates as a simple LS (eq. 1), as it is equal to the sum of the natural logarithm of the sums of squares for each data set.

Different weighting of data sets is often carried out by weighting the sum of squares from each data set by a constant (λ_j), representing the amount of emphasis placed on that data set, where

$$\text{LS} = \sum_j \lambda_j \sum_{\text{all } i} (O_i - P_i)^2 \quad (15)$$

This produces the same estimates as MLEs from the concentrated likelihood provided the weights (λ_j) are set proportional to the inverse of the MLE variance for the jth data set (as shown in Appendix A). However, the relative weights cannot be automatically calculated as they are for the concentrated likelihood of multiple data sets. The derivation in

© 2007 NRC Canada

Appendix A shows that if the proportionality constant is set to one (that is, $\lambda_i = 1/\hat{\sigma}_i^2$), then the sum of squares has an expected value of N, the number of data points in LS. Therefore, if the weights are set based on assumptions about the variance, comparing the sum of squares with N would seem to be a good check to assess whether the weights chosen are consistent with MLE estimates for the variances.

Alternative likelihood functions

Up until now, we have focused on the normal likelihood function. However, depending on the assumed error structure, other likelihood functions may be appropriate. The multinomial likelihood function is often used for catch-at-age or catch-at-length data.

The multinomial likelihood function is given by

$$(16) \quad L(\theta|\text{data}) = \binom{n}{n_1 \quad n_2 \quad \dots \quad n_A} p_1^{n_1} p_2^{n_2} \dots p_A^{n_A}$$

The negative of the natural logarithm of the likelihood assuming known effective sample size and ignoring additive constants is

$$(17) \quad -\ln L(\theta|\text{data}) = -\sum_a n_a \ln(p_a)$$

No simple and computationally efficient algebraic formula is available for the effective sample size, and iterative procedures are required (McAllister and Ianelli 1997). Alternatively, approximations based on other likelihood functions that allow the estimation of variance parameters can be used (e.g., the normal likelihood function with variance based on the binomial distribution; see above).

Hypothesis testing

A standard approach to hypothesis testing is the likelihood ratio test for nested models. Two times the difference between the negative log likelihood of the two models is asymptotically χ^2-distributed with the degrees of freedom (df) equal to the difference in the number of parameters between the two models.

$$(18) \quad 2[-\ln L(M_A|\Theta) + \ln L(M_B|\Theta)] \sim \chi^2_{df}$$

where M_A is the reduced model nested within model M_B. To compare two models that differ by a single parameter, 2 times the difference in the negative log likelihoods is compared with 3.84 based on $\Pr(\chi^2_1 < 3.84) = 0.95$.

To use LS to do hypothesis testing based on the χ^2 distribution, the sums of squares is converted into the concentrated likelihood (see above) and the likelihood ratio test is applied.

$$(19) \quad -\ln L(\theta|\text{data}) = 0.5n \ln(\text{LS})$$

Simulation design

A simulation study was carried out based roughly on the dynamics of the Prince William Sound Pacific herring population model, as described in Marty et al. (2003); their model is a modification of the assessment model given in Quinn and Deriso (1999, section 8.2.5) and Quinn et al. (2001). Equations for the simulation model are given in Appendix B. Random variability is incorporated into the annual recruitment and in the simulated observed data. We used a systematic approach and based the simulated data on the typical data available for many stock assessments. We generated five scenarios of simulated data, with each scenario containing 500 randomly generated data sets. Each data set spanned 20 years and seven age classes.

Five scenarios were investigated. (1) Catch-at-age data is based on multinomial sampling (sample size = 50); additionally, an index of log-transformed, exploitable abundance with normally distributed error (0.2 standard deviation) is available for all 20 simulated years. (2) This scenario is the same as (1) except a second age frequency data set is available from sampling of spawners (sample size = 50); additionally, an index of log-transformed egg production with normal error (0.5 standard deviation) is available for the stock for all years. (3) This scenario is crafted more closely to follow the Prince William Sound herring in the number of data points of each data type and effective variances for each year of age data, as given in the spreadsheet model used by Marty et al. (2003). (4) and (5) are the same as (2) and (3), respectively, except that natural mortality was deterministically related to a environmental index as described in Marty et al. (2003). Scenarios 3 and 5 were used only in the simulation testing of hypothesis Type I and II errors, as described later.

Simulation testing was made with scenarios 1, 2, and 4, and variations on scenarios 2 and 4 where a disease parameter is either estimated or assumed to equal 0.0 and not estimated. We investigated four alternative objective functions for parameter estimation and (or) hypothesis testing: (*a*) LS. (*b*) A normal likelihood function with a constant variance for the catch-at-age data and a lognormal likelihood function with constant variance for each of the abundance indices. The variances in all likelihood functions were estimated using the analytical MLE formula. (*c*) The same as (*b*) but with a binomial-based variance for the catch-at-age data. (*d*) The same as (*b*) but with a multinomial likelihood for the catch-at-age data with known sample size used in generating the simulations and known standard deviations for the abundance index likelihoods. This likelihood function is expected to perform best and can be considered the best case reference.

The parameters of the model estimated were the numbers at ages 2 and 3 in the first year, recruitment for every year, and the two parameters of the selectivity curve (the mean and the left-hand variance of the double normal selectivity curve; the right-hand variance was fixed at a large number to implement asymptotic selectivity with age). When the catch-at-age data and the index of egg production for the population was included, the two parameters of the logistic partial recruitment proportion curve were also estimated. Partial recruitment proportion quantifies the proportion by age of a year class that joins the spawning population. The coefficients of proportionality between abundance and the relative index of abundance were calculated using the analytical maximum likelihood formula. Two types of analyses were carried out: one estimating the slope of the relationship and one with no relationship (slope = 0). These two analyses were used to carry out hypothesis tests on the slope of the relationship between the environmental index and natural mortality. (Appendix C contains a list of parameters and

© 2007 NRC Canada

Table 1. Relative root mean squared error (RMSE) and relative bias for estimates of (*i*) average recruitment and (*ii*) depletion from the simulation analysis.

	Simulation setting		Objective function used			
	Scenario	Estimate β?	*a*	*b*	*c*	*d*
Average recruitment						
Relative RMSE	1	No	0.36	0.26	0.23	0.28
	2	No	0.65	0.16	0.14	0.14
	4	Yes	19.11	0.28	0.25	0.31
	4	No	10.03	0.39	0.37	0.36
	2	Yes	207.26	0.34	0.23	0.25
Relative bias	1	No	0.068	0.037	0.002	0.04
	2	No	0.105	0.006	–0.024	0.007
	4	Yes	1.671	0.046	0.015	0.06
	4	No	0.349	–0.166	–0.194	–0.18
	2	Yes	12.147	0.057	0.021	0.054
Depletion from the simulation analysis						
Relative RMSE	1	No	0.218	0.187	0.185	0.177
	2	No	0.297	0.165	0.163	0.157
	4	Yes	0.306	0.184	0.181	0.175
	4	No	0.316	0.304	0.298	0.276
	2	Yes	0.301	0.178	0.175	0.167
Relative bias	1	No	0.025	0.011	0.016	0.01
	2	No	0.051	0.008	0.012	0.006
	4	Yes	0.052	0.009	0.012	0.009
	4	No	0.05	0.041	0.042	0.022
	2	Yes	0.053	0.012	0.017	0.009

variables with details about them.) Parameter estimation was implemented in the software ADMB© (Otter Research Ltd., Sidney, British Columbia) by generating each simulated data set and objective function combination one at a time and then combining outputs as described below. Common random seeds were used to make results more comparable across different objective functions.

The output from the simulation analysis included the relative root mean squared error (eq. 20) and relative bias (eq. 21) for the average recruitment, the depletion level (the abundance in the last year of the simulation divided by the abundance in the first year of the simulation), and the standard deviations of the indices of abundance, where

$$\text{(20)}\quad \text{relative RMSE} = \frac{\sqrt{\dfrac{\sum_i (\hat{\theta}_i - \theta_i^{\text{sim}})^2}{N_{\text{sims}}}}}{\dfrac{\sum_i \theta_i^{\text{sim}}}{N_{\text{sims}}}}$$

$$\text{(21)}\quad \text{relative Bias} = \frac{1}{N_{\text{sims}}} \sum_i \frac{(\hat{\theta}_i - \theta_i^{\text{sim}})}{\theta_i^{\text{sim}}}$$

where i indexes the simulation and N_{sims} is the total number of simulations. A positive bias indicates on average that the estimate exceeds the true value for a parameter; a negative bias indicates just the opposite.

Hypothesis testing with the asymptotic χ^2 statistic ($p = 0.05$) was made for each combination of the data sets 2–5 and objective functions. The four data sets in the testing represented two simulation scenarios either with an environmental factor or without an environmental factor. This allowed us to examine both Type I and Type II errors.

Results

In general, the LS method (*a*) performs worse than the likelihood methods (*b*, *c*, and *d*). The LS approach has higher variance in estimates of all quantities, generally more bias, and in some cases it can have substantial bias for average recruitment (as shown in Table 1). Estimation assuming either the constant variance or the binomial objective functions (functions *b* and *c*) perform similar to one another and nearly as good as the best-case reference (*d*) in which all variances and sampling model structure are known in advance. The likelihood methods (*b* and *c*) are able to estimate the standard deviation of the likelihood functions for the indices of abundance (Table 2). However, they are moderately negatively biased.

The results from the hypothesis testing (Table 3) show the Type II error for the LS method is similar to that for the likelihood methods; both fail to reject the null hypothesis about 7%–10% of the time when the null hypothesis was false. However, the Type I error is far worse for the weighted LS method (35%–89% of the time, the null hypothesis was rejected for a range of weights when the null hypothesis was true), as compared with the likelihood methods (10%–11%, excluding the multinomial function (*d*)), which are about twice the $p = 0.05$ value assumed for the χ^2 statistic. In all simulations performed for this paper, numerical convergence occurred in the maximum likelihood computations.

© 2007 NRC Canada

Table 2. Relative root mean squared error (RMSE) and relative bias for the estimates of standard deviations of the likelihood functions for the indices of abundance from the simulation analysis.

	Simulation setting		Abundance index		Egg production index	
	Scenario	Estimate β^2	Objective function (*b*)	Objective function (*c*)	Objective function (*b*)	Objective function (*c*)
Relative RMSE	1	No	0.19	0.19	—	—
	2	No	0.18	0.18	0.17	0.17
	4	Yes	0.2	0.2	0.17	0.17
	4	No	0.39	0.39	0.18	0.18
	2	Yes	0.19	0.19	0.17	0.17
Relative bias	1	No	–0.08	–0.09	—	—
	2	No	–0.08	–0.08	–0.06	–0.06
	4	Yes	–0.09	–0.1	–0.07	–0.07
	4	No	0.25	0.25	0.02	0.02
	2	Yes	–0.09	–0.1	–0.07	–0.07

Table 3. The proportion of simulations in which the environmental relationship with natural mortality was selected as the best model (i.e., the null hypothesis was rejected).

Simulation scenario and objective function used	Simulated data has environmental relationship (1 – Type II error)	Simulated data does not have environmental relationship (Type I error)
Scenarios 2 and 4, constant variance function (*b*)	0.912	0.106
Scenarios 2 and 4, binomial function (*c*); $k = 0.01$ in eq. 8	0.902	0.112
Scenarios 2 and 4, binomial function (*c*); $k = 0.1$ in eq. 8	0.914	0.104
Scenarios 2 and 4, multinomial function (*d*)	0.908	0.058
Scenarios 2 and 4, weighted least squares with various λ values as defined in eq. 15		
λ for age frequency in both data sets is 0.2	0.92	0.89
λ for age frequency in both data sets is 1.0	0.92	0.52
λ for age frequency in both data sets is 5.0	0.93	0.41
λ for age frequency in both data sets is 10.0	0.93	0.35
Scenarios 3 and 5		
λ for age frequency in both data sets is 1.0	0.872	0.564
Constant variance function (*b*)	0.884	0.1

Table 4. Applications to Prince William Sound Pacific herring (*Clupea pallasii*) to test statistical significance ($p = 0.05$) for disease as a factor affecting adult herring survival.

	No. of parameters		2 × log-likelihood			
Method	Without covariate	With covariate	Without covariate	With covariate	Likelihood ratio test statistic	Significant
(A) Weighted least squares	31	32	438.053	432.554	5.499	Yes
(B) Concentrated likelihood	35	36	299.036	299.032	0.004	No

Case study of application to Prince William Sound herring

We repeated some of the analyses reported in Marty et al. (2003) with some small modifications of their spreadsheet model. We confirm their results of hypothesis testing with the weights they assumed in the model. With those weights, we can statistically reject the null hypothesis of no disease affect for the years 1994–2000 (as shown in Table 4, method A).

The spreadsheet model was then modified by writing the objective function as a concentrated likelihood. As shown earlier, this amounts to replacing the residual sum of squares for each data type by the number of observations times the logarithm of the residual sum of squares for each data type and corresponds to the objective function (*b*) from the simulation tests. The null hypothesis of no disease effect is not rejected (as shown in Table 4, method B); indeed the test statistic is very far away from the 0.05 significance level (χ^2 of 3.84 versus test statistic of 0.0). These results were con-

© 2007 NRC Canada

Table 5. Weights for the different data types for methods A and B.

Data type	No. of observations	Method A	Method B
Seine age frequency	88	1.0	1.000
Spawner age frequency	130	10.0	1.092
Egg survey index	10	1.0	0.008
Mile-days of milt index	21	0.50	0.022

Note: Weights are those that would be applied in a weighted least squares objective function. The weights for method B are calculated from the variance estimates in the likelihood function. Data types are more fully described in Marty et al. (2003).

firmed by an independent programming of the assessment model in ADMB© to insure the spreadsheet model was providing accurate results.

The primary reason that conclusions about the significance of disease are so affected by the use of a concentrated likelihood is that the estimated relative weights of the different data types are much different than those weights assumed in Marty et al. (2003) (as seen in Table 5). The relative weights for the concentrated likelihood vary only slightly between the model with the disease parameter versus the model without the disease parameter.

Discussion

The weighting of data sets (or data points) in quantitative analysis of fisheries data is important. Relative weighting of data influences the parameter estimates. The relative weighting also influences confidence intervals and hypothesis tests, but in these cases absolute weighting is also important. Weighting of data can be achieved by weighted LS or by modifying a variance-related quantity in the likelihood function (e.g., the standard deviation in a likelihood function based on the normal distribution). Weighted LS is equivalent to normal-distribution-based maximum likelihood if the weights are proportional to the inverse of the variance in the likelihood function (Appendix A). The MLE variance estimates provide an objective choice for weights, as opposed to the subjective choices often made in weighted LS.

The theory for estimation of variances (or equivalently relative weights) for different data types depends on the structure of the assessment model. For multiresponse models, MLEs can be made for the variances. However, favorable properties of the MLEs are generally an asymptotic property not easily discerned for complex models such as those often employed in stock assessments. Simulation studies, such as those presented here, which are crafted around a particular number of data types and years of data, are likely a necessity to establish the reliability of MLEs for variances. The MLEs of variances in the likelihood functions were negatively biased. This is a well-known property of MLEs under small sample sizes and is due to not adjusting for the degrees of freedom lost from estimating other model parameters (Shaw 1987). The negative bias may be corrected by using restricted maximum likelihood (Shaw 1987).

There are several reasons why the MLE of the variance or sample size can be substantively different from the prespecified value. The prespecified variance could simply be wrong or the model may be mis-specified. Model mis-specification could be due to using the wrong distribution for the likelihood function (e.g., using a normal distribution with constant variance instead of a multinomial), incorrect assumptions in the model of the system (e.g., assuming a Beverton–Holt stock recruitment relationship instead of a Ricker), incorrect assumptions in the observation model that relates the likelihood function to the model of the system (assuming that CPUE is proportional to effort when there is hyperstability in the CPUE), or unmodeled stochastic processes (e.g., annual variation in growth). For example, the effective sample size for catch-at-age data is often much smaller than the actual sample size because of fish schooling by age. Therefore, a likelihood function based on the multinomial distribution using the observed sample size is inappropriate. However, a likelihood function that accounts for the schooling by age using the observed sample size may be appropriate.

Both maximum likelihood and LS are based on the existence of a global optimum and that this optimum has been found. However, there are often multiple global optima, and the estimation procedure may result in one of these rather than in the global optima. In addition to best estimates, measures of uncertainty and hypothesis tests will be biased if based on local rather than global optima. As models get more complex and the number of parameters increase, the possibility of local optima usually increases.

Some of the results were surprising to us. Simple likelihood functions, like one in which each data type is assumed to be normally distributed with constant variance, performed in our study only slightly less precise than the performance when all likelihood variances and structure were known in advance. Weighted LS performs poorer than the likelihood methods, but not too poorly except for particular quantities.

Of particular concern from our simulations is the substantially worse Type I error (rejecting the null hypothesis when it is true) of weighted LS. In some applications, the analyst has valid reason for assigning weights, based perhaps on statistical prior probabilities of certain choices. In the simulation analyses, the Type I errors were reduced by putting more relative weight on the catch-at-age data, and if the weights were set proportional to the inverse of the variance from the maximum likelihood analyses, the Type I error would be the same as those for the likelihood analyses. Our case study with Prince William Sound herring shows that there is no statistical basis for disease as a factor affecting their survival if objective MLE-based weights are chosen for the analysis. This study illustrates that it is likely a wise choice to also apply MLE theory to identify situations where prior assumptions about relative variances determine the statistical significance of any conclusion.

We have shown using a simple deterministic relationship between a model parameter, survival, and a covariate that hypothesis tests are influenced by the relative weighting of different data sets. However, the relationship is probably not deterministic, and there is additional temporal variation in survival around the relationship. This additional variation can be modeled as a random effect. Maunder and Watters (2003) showed that hypothesis tests that assumed a deterministic relationship when a random effect was present had high Type I error, but when a random effect was included in the model the Type I error was greatly reduced. The Maun-

© 2007 NRC Canada

der and Watters (2003) analysis assumed that the variance of the random effect was known. MLEs of the random effect variance are not statistically consistent (Seber and Wild 1989), and integrating the likelihood functions across the domain of the random effect is more appropriate (Maunder and Deriso 2003). However, this integration is computationally intensive. It may be possible in some applications to constrain the range of the unknown variance for the random effect and utilize a local maximum that sometimes occurs for the likelihood function (Maunder and Deriso 2003). If estimation is not practical, a value for the variance could be assumed and the robustness of the conclusions determined by varying the assumed variance. Alternatively, analysis of deviance could be used for hypothesis testing to compensate for the additional unexplained variation (Skalski 1996). In our model, this would consist of calculating (*i*) the full model with a natural mortality parameter for each year, (*ii*) the grand mean model with a constant natural mortality over time, and (*iii*) the model being tested with the environmental relationship for natural mortality and applying the methods described in Skalski (1996).

Acknowledgements

Funding for this project was provided by Exxon Mobil. T.J. Quinn II provided the Excel spreadsheet model for Prince William Sound herring. Two anonymous reviewers and an associate editor provided comments that improved the manuscript.

References

Deriso, R.B., Quinn, T.J., II, and Neal, P.R. 1985. Catch-age analysis with auxiliary information. Can. J. Fish. Aquat. Sci. **42**: 815–824.

Fournier, D., and Archibald, C.P. 1982. A general theory for analyzing catch at age data. Can. J. Fish. Aquat. Sci. **39**: 1195–1207.

Fournier, D.A., Sibert, J.R., Majkowski, J., and Hampton, J. 1990. MULTIFAN a likelihood-based method for estimating growth parameters and age composition from multiple length frequency data sets illustrated using data for southern bluefin tuna (*Thunnus maccoyii*). Can. J. Fish. Aquat. Sci. **47**: 301–317.

Francis, R.I.C.C. 2005. Assessment of hoki (*Macruronus novaezelandiae*) in 2004. N.Z. Fish. Assess. Rep. No. 2005/35.

Francis, R.I.C.C., Hurst, R.J., and Renwick, J.A. 2003. Quantifying annual variation in catchability for commercial and research fishing. Fish. Bull. **101**: 293–304.

Marty, G.D., Quinn, T.J., II, Carpenter, G., Meyers, T.R., and Willits, N.H. 2003. Role of disease in abundance of a Pacific herring (*Clupea pallasi*) population. Can. J. Fish. Aquat. Sci. **60**: 1258–1265.

Maunder, M.N., and Deriso, R.B. 2003. Estimation of recruitment in catch-at-age models. Can. J. Fish. Aquat. Sci. **60**: 1204–1216.

Maunder, M.N., and Punt, A.E. 2004. Standardizing catch and effort data: a review of recent approaches. Fish. Res. **70**: 141–159.

Maunder, M.N., and Starr, P.J. 2003. Fitting fisheries models to standardised CPUE abundance indices. Fish. Res. **63**: 43–50.

Maunder, M.N., and Watters, G.M. 2003. A general framework for integrating environmental time series into stock assessment models: model description, simulation testing, and examples. Fish. Bull. **101**: 89–99.

McAllister, M.K., and Ianelli, J.N. 1997. Bayesian stock assessment using catch-age data and the sampling – importance resampling algorithm. Can. J. Fish. Aquat. Sci. **54**: 284–300.

Pearson, W.H., Elston, R.A., Bienert, R.W., Drum, A.S., and Antrim, L.D. 1999. Why did the Prince William Sound, Alaska Pacific herring (*Clupea pallasi*) fisheries collapse in 1993 and 1994? Review of hypotheses. Can. J. Fish. Aquat. Sci. **56**: 711–737.

Quinn, T.J., II, and Deriso, R.B. 1999. Quantitative fish dynamics. Oxford University Press, New York.

Quinn, T.J., II, Marty, G.D., Wilcock, J., and Willette, M. 2001. Disease and population assessment of Pacific herring in Prince William Sound, Alaska. *In* Herring: expectations for a new millennium. *Edited by* F. Funk, J. Blackburn, D. Hay, A.J. Paul, R. Stephensen, R. Toreson, and D. Witherell. Alaska Sea Grant College Program, AK-SG-01-04. pp. 363–379.

Seber, G.A., and Wild, C.J. 1989. Nonlinear regression. John Wiley and Sons, New York.

Shaw, R.G. 1987. Maximum-likelihood approaches applied to quantitative genetics of natural populations. Evolution, **41**: 812–826.

Skalski, J.R. 1996. Regression of abundance estimates from mark–recapture surveys against environmental covariates. Can. J. Fish. Aquat. Sci. **53**: 196–204.

Sullivan, P.J., Parma, A.M., and Clark, W.J. 1999. The Pacific halibut stock assessment of 1997. I.P.H.C. Sci. Rep. No. 79.

Appendix A. Derivation of condition for equivalence between concentrated likelihood and weighted least squares (LS)

We show that weighted LS is equivalent to normal-distribution-based maximum likelihood if the LS weighting factors are proportional to the inverse of the likelihood variance.

With multiple data sets, it may be desirable to use a likelihood with weighted variances. If we assume that the error on each observation in data set j has variance σ_j^2, then we can use weights w_j that express the variance of each data set in terms of a common variance of all data points from all data sets (i.e., $\sigma_j^2 = w_j^2\sigma^2$).

The overall likelihood is then (for d data sets)

$$\text{(A.1)}\quad L(\theta|\text{data}) = \prod_{j=1}^{d}\prod_{i=1}^{n_j}\left\{\frac{1}{\sqrt{2\pi}\sigma w_j}\exp\left[\frac{-(O_{ij}-P_{ij})^2}{2\sigma^2 w_j^2}\right]\right\}$$

The MLE of σ^2 is

$$\text{(A.2)}\quad \hat{\sigma}^2 = \frac{1}{N}\sum_{j=1}^{d}\sum_{i=1}^{n_j}\frac{(O_{ij}-P_{ij})^2}{w_j^2}$$

where $N = \sum_{j=1}^{d} n_j$ is the total number of observations from all data sets. Substituting eq. A.2 into eq. A.1 gives the concentrated negative log-likelihood with weighted variance as follows (with additive constants removed):

$$\text{(A.3)}\quad -\ln L(\theta|\text{data}) = \frac{N}{2}\ln\left[\sum_{j=1}^{d}\sum_{i=1}^{n_j}\frac{(O_{ij}-P_{ij})^2}{w_j^2}\right]$$

For a given set of weights w_j, eq. A.3 should be minimized to find estimates (MLEs) of the predicted values P_{ij}.

Using weighted LS, the function to minimize is

© 2007 NRC Canada

$$\text{(A.4)}\quad \text{LS} = \sum_{j=1}^{d} \lambda_j \sum_{i=1}^{n_j} (O_{ij} - P_{ij})^2$$

where the weights or emphasis factors λ_j weight each data set separately. For the appropriate choice of emphasis factors λ_j, the predicted values P_{ij} found from eq. A.4 should equal the MLEs of P_{ij} found from eq. A.3. Thus, at the MLE of P_{ij}

$$\text{(A.5)}\quad \frac{\partial(-\ln L)}{\lambda P_{ij}} = \frac{\lambda \text{LS}}{\lambda P_{ij}}$$

or

$$\text{(A.6)}\quad \frac{-N(O_{ij} - P_{ij})/w_j^2}{\sum_{j=1}^{d}\sum_{i=1}^{n_j}[(O_{ij} - P_{ij})^2/w_j^2]} = -2\lambda_j(O_{ij} - P_{ij})$$

giving

$$\text{(A.7)}\quad \lambda_j = \frac{\frac{1}{2w_j^2}}{\frac{1}{N}\sum_{j=1}^{d}\sum_{i=1}^{n_j}[(O_{ij} - P_{ij})^2/w_j^2]} = \frac{1}{2\hat{\sigma}^2 w_j^2} = \frac{1}{2\hat{\sigma}_j^2}$$

Thus, the proper values of λ_j are proportional to $1/\hat{\sigma}_j^2$, where $\hat{\sigma}_j^2$ is the MLE of the variance for data set j:

$$\text{(A.8)}\quad \hat{\sigma}_j^2 = \frac{1}{n_j}\sum_{i=1}^{n_j}(O_{ij} - P_{ij})^2$$

Using $\lambda_j = 1/\hat{\sigma}_j^2$, eq. A.4 becomes

$$\text{(A.9)}\quad \text{LS} = \sum_{j=1}^{d}\frac{1}{\hat{\sigma}_j^2}\sum_{i=1}^{n_j}(O_{ij} - P_{ij})^2$$

Substituting equation A.8 into eq. A.9 gives

$$\text{(A.10)}\quad \text{LS} = \sum_{j=1}^{d} n_j = N$$

Thus, if the optimal emphasis factors λ_j are used, then the observed LS should be approximately equal to the total number of observations from all data sets (N).

Appendix B. Population dynamics

The following equations describe the population dynamics model used in both the simulator and estimator.

The population dynamics are modeled using a difference equation that removes the catch halfway through the year and uses a plus group to accumulate old individuals.

$$N_{t,1} = R_t$$

$$N_{t+1,a+1} = [N_{t,a}\exp(-0.5M_a) - C_{t,a}]\exp(-0.5M_a) \qquad 1 < a < A-1$$

$$N_{t+1,A} = [N_{t,A-1}\exp(-0.5M_{A-1}) - C_{t,A-1}]\exp(-0.5M_{A-1}) + [N_{t,A}\exp(-0.5M_A) - C_{t,A}]\exp(-0.5M_A)$$

Initial conditions are estimated for the first few ages and assumed in equilibrium for the older ages.

$$N_{1,a} = N_{\text{init},a} \qquad 1 < a \le a_{\text{init}}$$

$$N_{1,a} = N_{1,a-1}\exp(-M_{\text{init},a-1}) \qquad a_{\text{init}} < a < A$$

$$N_{1,A} = \frac{N_{1,A-1}\exp(-M_{\text{init},A-1})}{1 - \exp(-M_{\text{init},A})}$$

Exploitation rate is calculated as the catch divided by the vulnerable biomass in the middle of the year:

$$u_t = \frac{C_t^{\text{obs}}}{B_t}$$

$$B_t = \sum_a N_{t,a}\exp(-0.5M_{t,a})s_a w_a$$

$$C_{t,a} = u_t s_a N_{t,a}\exp(-0.5M_{t,a})$$

Selectivity is modeled using a double normal distribution:

$$s_a = \begin{cases} \exp\left[-\dfrac{(a-\mu_s)^2}{V_L}\right] & \text{if } a \le \mu_s \\ \exp\left[-\dfrac{(a-\mu_s)^2}{V_R}\right] & \text{if } a > \mu_s \end{cases}$$

Natural mortality is correlated with an environmental covariate and modeled using an offset for the oldest age:

$$M_{t,a} = M_0\exp(\beta_M I_{M,t}) \qquad 1 \le a < A$$

where the simulated environmental data is generated normally distributed, $N(0,1)$.

$$M_{t,A} = M_{t,A-1} + \delta_M$$

The number of eggs is

$$E_t = \text{sex}_t\sum_a N_{t,a} f_a m_a$$

Partial recruitment proportion is modeled using a logistic curve:

$$m_a = \frac{\exp(\alpha + \beta a)}{1 + \exp(\alpha + \beta a)}$$

Appendix C. Variables, parameters, and data used in the simulation trials

Appendix appears on the following pages.

© 2007 NRC Canada

Table C.1. Variable and parameter definitions.

Variable–parameter	Description (simulated value)	Estimate
a	Age	NA
t	Year	NA
A	Maximum age in the model used as a plus group (7)	NA
$N_{t,a}$	Numbers at age a in year t	NA
M_a	Natural mortality at age a	NA
$C_{t,a}$	Catch in numbers of age a in year t	NA
u_t	Exploitation rate in year t	NA
C_t^{obs}	Catch in biomass in year t	Data
B_t	Midyear vulnerable biomass in year t	NA
s_a	Selectivity to the fishing gear at age a	NA
w_a	Average weight of an individual of age a	Data
$I_{M,t}$	Environmental covariate for natural mortality in year t	Data
E_t	Total number of eggs in the population in year t	NA
sex_t	Proportion females in year t	Data
f_a	Fecundity at age a	Data
R_t	Annual recruitment for simulations, $R_t = \bar{R}\exp(\varepsilon_t - 0.5\sigma_R^2)$ where $\varepsilon_t \sim N(0, \sigma_R^2)$ and ($\sigma_R = 0.6$, $\bar{R} = 272$)	Yes
$N_{\text{init},a}$	Initial numbers at age for ages 2 (657) and 3 (92), older ones at equilibrium	Yes
M_0	Average natural mortality for young ages (0.33)	Fixed
β_M	Slope of relationship between natural mortality and the covariate (–0.5 or 0)	Only if investigating relationship, otherwise fixed at 0
δ_M	Difference between old and young natural mortality (0.27)	Fixed
q_{abdt}	Proportionality constant for the exploitable abundance index (1)	Analytical formula
q_E	Proportionality constant for the egg index (1)	Analytical formula for scenarios 2–5
σ_C	Standard deviation (or scalar) of the likelihood function for the catch-at-age data (not used in simulator, data generated using multinomial)	Analytical formula for objective functions *b* and *c*
σ_t	Standard deviation (or scalar) of the likelihood function for the spawner age-frequency data (not used in simulator, data generated using multinomial)	Analytical formula for objective functions *b* and *c* for scenarios 2–5
σ_{abdt}	Standard deviation of the likelihood function for the exploitable abundance index (0.2)	Analytical formula for objective functions *b* and *c*
σ_E	Standard deviation of the likelihood function for the egg index (0.5)	Analytical formula for objective functions *b* and *c* for scenarios 2–5
μ_s	Mean of the double normal selectivity curve (4)	Yes
V_L	Left-hand variance of the double normal selectivity curve (5)	Yes
V_R	Right-hand variance of the double normal selectivity curve (1 000 000)	Fixed
α and β	Parameters for the logistic partial recruitment proportion curve (–1.4 and 1.0, respectively)	Scenarios 2–5

© 2007 NRC Canada

Table C.2. Exploitation rates used in the simulation trials.

Year	Exploitation rate
1	0.155
2	0.206
3	0.131
4	0.046
5	0.103
6	0.093
7	0.157
8	0.106
9	0.111
10	0.020
11	0.103
12	0.217
13	0.286
14	0.082
15	0.020
16	0.020
17	0.025
18	0.212
19	0.187
20	0.020
21	0.020

© 2007 NRC Canada

Frequency of multiple paternity in an unexploited tropical population of sandbar sharks (*Carcharhinus plumbeus*)

Toby S. Daly-Engel, R. Dean Grubbs, Brian W. Bowen, and Robert J. Toonen

Abstract: Elasmobranch mating systems have received growing attention in the past few years because of worldwide overexploitation of shark populations. Few studies to date have examined mating systems in sharks because of difficulty in sampling. The sandbar shark (*Carcharhinus plumbeus*) is heavily harvested around the world and is the dominant species in the main commercial fishery for large coastal sharks in the United States. In contrast, Hawaii hosts one of the few unexploited populations of sandbar sharks and represents an opportunity to gather data on the reproductive biology of a vulnerable shark species without the confounding effects of fishing mortality. We examined the frequency of multiple paternity in Hawaiian sandbar sharks using 130 individuals (20 gravid females with three–eight pups each per litter) surveyed with six polymorphic microsatellite loci and determined that 8 of the 20 litters (40%) were multiple-sired. A Bayesian approach estimated the frequency of multiple mating in this population at 43.8%, with a 95% confidence interval of 23%–63%. We conclude that multiple paternity and genetic monogamy occur with roughly equal frequency in the Hawaiian sandbar shark population. This study may serve as groundwork for understanding the impact of commercial fishing pressure on elasmobranch mating systems.

Résumé : Les systèmes de reproduction des élasmobranches suscitent de plus en plus d'intérêt depuis quelques années à cause de la surexploitation des populations de requins à l'échelle du globe. Jusqu'à présent, peu d'études ont examiné les systèmes de reproduction des requins à cause des difficultés d'échantillonnage. Le requin gris (*Carcharhinus plumbeus*) est intensément pêché à l'échelle mondiale et constitue l'espèce dominante dans la principale pêche commerciale de grands requins côtiers aux États-Unis. En revanche, il existe à Hawaii l'une des rares populations inexploitées de requins gris; c'est donc une occasion de recueillir des données sur la biologie reproductive de cette espèce de requin vulnérable sans avoir les effets confondants de la mortalité due à la pêche. Nous avons étudié la fréquence des paternités multiples chez les requins gris d'Hawaii d'après l'analyse de 6 locus microsatellites polymorphes chez 130 individus (20 femelles gravides possédant trois–huit petits par portée); 8 (40 %) des 20 portées comportaient des paternités multiples. Une méthodologie bayésienne permet d'estimer la fréquence des accouplements multiples à 43,8 %, avec un intervalle de confiance de 95 % de 23–63 %. Nous concluons que la paternité multiple et la monogamie génétique existent à peu près en parts égales dans la population de requins gris d'Hawaii. Notre étude peut servir de travail de base pour comprendre l'impact de la pression de la pêche commerciale sur les systèmes de reproduction des élasmobranches

[Traduit par la Rédaction]

Introduction

Polyandry (females mating with more than one male) and multiple paternity (the siring of a single brood of offspring by multiple males) have been recognized as common strategies in diverse taxa, including sharks (reviewed by Zeh and Zeh 2003). While the evolutionary relevance of polyandry and multiple paternity is debated (Jennions and Petrie 2000; Tregenza and Wedell 2002), the number of studies documenting multiple mating in wild populations continues to grow (reviewed by Neff and Pitcher 2005). These now include members of such varied groups as salamanders, fishes, crickets, and turtles (Hoekert et al. 2002; Adams et al. 2005; Bretman and Tregenza 2005), as well as marine fishes (DeWoody and Avise 2001). Many of these studies are motivated by conservation concerns because understanding

Received 12 May 2006. Accepted 26 October 2006. Published on the NRC Research Press Web site at http://cjfas.nrc.ca on 8 February 2007.
J19322

T.S. Daly-Engel.[1] University of Hawai'i at Mānoa, Department of Zoology, 2538 McCarthy Mall, Edmonson 152, Honolulu, HI 96822, USA.
R.D. Grubbs,[2] **B.W. Bowen, and R.J. Toonen.** Hawai'i Institute of Marine Biology, P.O. Box 1346, Kane'ohe, HI 96744, USA.

[1]Corresponding author (e-mail: tengel@hawaii.edu).
[2]Present address: Department of Fisheries Science, Virginia Institute of Marine Science, P.O. Box 1346, Gloucester Point, VA 23062, USA.

 doi:10.1139/F07-005 © 2007 NRC Canada

these and other reproductive strategies is necessary for effective management of populations that are at risk of overexploitation (Rowe and Hutchings 2003).

Elasmobranch population collapse as a result of directed fisheries has been well documented (Olsen 1959; Ketchen 1969; Anderson 1990), and the sustainability of large-scale fisheries for sharks has been questioned (Holden 1973; Walker et al. 1998). Most shark species exhibit slow growth, late sexual maturation, and low fecundity (Branstetter 1990; Hoenig and Gruber 1990), and intrinsic rates of increase in elasmobranches are more comparable with those of cetaceans and chelonians than to bony fishes (Musick 1999). Sharks are therefore particularly slow to rebound from population depletion (Smith et al. 1998).

The sandbar shark (*Carcharhinus plumbeus*) is prized in the soup fin trade because of the large size and high quality of dorsal and pectoral fins. This coastal species has a circumglobal distribution in tropical and warm temperate seas, and it is targeted by large-scale fisheries throughout much of this range. This species accounts for ~60% of the annual catch of large coastal sharks from the directed longline fishery in the northwestern Atlantic (NMFS 2003), where it was severely depleted during the 1980s (Musick et al. 1993). Sandbar sharks have estimated population doubling times of 14–25 years (Smith et al. 1998). Despite known vulnerability to depletion, worldwide harvests of sandbar sharks and other elasmobranches continue to increase (IUCN 2005).

Reproductive strategies can impact genetic diversity, which in turn effects the ability of populations to respond to selection pressure and adapt to changing environmental conditions (evolutionary potential, Rowe and Hutchings 2003; Frankham 2005). For these reasons, loss of genetic diversity has been associated with increased vulnerability to population depletion and extinction risk (reviewed by Lande and Shannon 1996; Rowe and Hutchings 2003; Neff and Pitcher 2005). The reproductive strategies of vulnerable marine species are therefore of interest to conservation biologists.

Because direct observation is difficult, little is known about the mating systems of wild sharks. In some shark species, females can mate with multiple males over the course of a single breeding season (Carrier et al. 1994) and are capable of storing viable sperm for long periods of time in the oviducal gland (Pratt 1993), which may result in temporal polyandry (Moon et al. 2006). All elasmobranches have internal fertilization, but shark reproductive modes range from lecithotrophic oviparity (where an egg capsule is deposited externally and the embryo feeds off the yolk) through many forms of aplacental viviparity (e.g., strict lecithotrophy, oophagy, matrotrophy through trophonemata) to viviparity using yolk sac placentae. Placental viviparity is the most advanced form of development, where embryos feed initially on yolk and then the empty yolk sac interdigitates with the mother's uterine wall, forming a highly vascularized placenta where nutrients are transferred directly to the embryo from the mother's bloodstream (Musick and Ellis 2005; Hamlett et al. 2005). Placental viviparous sharks, including all members of the genus *Carcharhinus*, give birth to small numbers of fully developed young. In Hawaii, sandbar shark size at birth is approximately 45–50 cm precaudal length (PCL), and young receive no parental care following parturition (Carrier et al. 2004).

Polyandry can have individual fitness benefits such as increasing the number of viable offspring in a clutch (e.g., Newcomer et al. 1999). Polyandry as a reproductive strategy may also have advantages at the population level (reviewed by Reynolds 1996; Jennions and Petrie 2000; Neff and Pitcher 2005), such as the maintenance of genetic diversity and an increased effective population size (Zane et al. 1999; Hoekert et al. 2002). Although the development of highly variable genetic markers is making parentage analyses more feasible (Sunnucks 2000; Heist 2004), studies of sharks are impeded by pragmatic difficulties associated with finding and catching gravid females, especially in populations with high seasonality and low site fidelity. A few recent studies have documented the occurrence of multiple paternity in single litters of sharks (Feldheim et al. 2001; Saville et al. 2002; Daly-Engel et al. 2006), but only two studies to date have measured the frequency of multiple paternity (*Sphyrna tiburo*, Chapman et al. 2004; and *Negaprion brevirostris*, Feldheim et al. 2004). These studies found that 19%–86% of litters were multiple-sired.

Temperate populations of sandbar sharks undergo strong seasonal migrations over hundreds of miles along coastlines and continental shelves (Grubbs et al. 2007), while tropical populations are more sedentary (Joung et al. 2004). Sandbar sharks in Hawaii can be obtained from the same sampling location throughout the year (T.S. Daly-Engel and R.D. Grubbs, unpublished data). While the sandbar shark is the most common shark species in Hawaii and is occasional bycatch in the Hawaiian bottomfish fishery, this population is not targeted commercially because of a ban on longline fishing in the nearshore waters and recognition of the shark as an ʻAumakua or traditional Hawaiian spirit guardian. The Hawaiian population of sandbar sharks, therefore, offers a rare opportunity to measure multiple paternity and other population parameters without the confounding effect of fishing mortality.

Previously, we detected multiple paternity in a single litter of sandbar sharks from Hawaii (Daly-Engel et al. 2006). Here we examine 20 litters in a near-pristine population of sandbar sharks to estimate the frequency of multiple paternity using six microsatellite loci developed by Keeney and Heist (2003). These data may serve as a foundation for future studies examining the effect of fishing pressure on elasmobranch mating systems.

Materials and methods

We collected 18 gravid females ~5 km outside Kaneohe Bay on the eastern coast of Oahu, Hawaii, at ~80 m depth between September 2003 and December 2005. Two litters were also obtained from the Kona Coast of the Island of Hawaii during the same time period. We used experimental monofilament longlines (~0.8–1.2 km) that were anchored at each end and marked with buoys. Gangions, 4 m in length, were made from stainless steel tuna clips attached to 2.5 m of 250–400 kg monofilament line. The line was attached to 1.5 m of 1.6 or 2.2 mm stainless steel aircraft cable using a 9/0 stainless steel swivel. The gangions were terminated by

© 2007 NRC Canada

either 14/0 or 18/0 baited circle hooks. Each line consisted of 50–80 gangions spaced ~15 m apart.

We collected small samples of fin or muscle tissue from mothers and pups using scissors or a hole punch and stored them in 20% dimethylsulfoxide salt buffer (Seutin et al. 1991) or 75% ethanol (EtOH). DNA was extracted from tissue using a salting-out protocol adapted from Sunnucks and Hales (1996). Samples stored in EtOH were squeezed with a dry paper towel and dried in a speed vacuum for 1 h at 55 °C before extraction.

Polymerase chain reaction (PCR) was used to amplify six previously developed microsatellite loci (Keeney and Heist 2003; Daly-Engel et al. 2006). These six microsatellite primer pairs (Cli-110, Cli-108, Cli-106, Cli-102, Cli-12, and Cli-7; see table 1 in Daly-Engel et al. 2006) were originally developed for the blacktip shark, *Carcharhinus limbatus*, by Keeney and Heist (2003). Unlabeled forward primers were obtained from Integrated DNA Technologies, Inc. (Coralville, Indiana). Reverse primers were labeled with 6-FAM, VIC, NED, and PET proprietary dyes (see table 1 in Daly-Engel et al. 2006) (Applied Biosystems, Foster City, California). PCR consisted of 0.1 U (1 U = 16.67 nkat) Biolase *Taq* DNA polymerase (Bioline, Randolph, Massachusetts), 1× PCR buffer, 0.25–0.0625 µm of each primer (table 1, Daly-Engel et al. 2006), 200 µm each dNTP, and 2.0 mmol·L^{-1} $MgCl_2$. PCR conditions and optimal annealing temperatures for all loci followed Daly-Engel et al. (2006). PCR products were resolved with an ABI 3100 automated sequencer and visualized using ABI PRISM GeneMapper software version 3.0 (Applied Biosystems).

We initially tested for heritability and quantified allelic variation at nine loci developed by Keeney and Heist (2003), but three were subsequently rejected because of null alleles (Cli-112), lack of allelic variation (Cli-107), or presence of more than two alleles per individual (Cli-103, after Selkoe and Toonen 2006). We estimated heterozygosity and tested for deviation from Hardy–Weinberg equilibrium using GENEPOP v.3.4 (Raymond and Rousset 1995) and detected null alleles using MICRO-CHECKER v.1 (van Oosterhout et al. 2004). MICRO-CHECKER was used to identify genotyping errors due to null alleles, short PCR dominance (large allele dropout), the scoring of stutter peaks, and typographic errors. GIMLET v.1.3.2 (Genetic Identification with MultiLocus Tags) was used to construct consensus genotypes of all individuals included in this study and to estimate error rate associated with genotyping (Valiere 2002).

We inferred the minimum number of sires from the number of nonmaternal alleles detected among the pups following the methods of Toonen (2004) and Neff et al. (2002). For each litter, we removed the maternal alleles and counted the number of unique nonmaternal alleles. Since the genotypes of the sires are unknown in these field-collected animals, we used the conservative assumption that every female mated with only heterozygous males. Given this assumption, the minimum number of sires per litter is one-half the number of nonmaternal alleles. If an odd number of nonmaternal alleles were detected among the pups, the minimum number of males was rounded up. For example, if three nonmaternal alleles were detected, the minimum estimated number of sires was rounded up from 1.5 to 2 males. Mendelian inheritance of maternal alleles was tested in each litter using a χ^2 goodness-of-fit test against an expected 1:1 inheritance ratio.

We used the program PrDM v.1 (Neff and Pitcher 2002) to calculate the probability of detecting multiple mating (PrDM) in a sample of offspring based on (*i*) the number of loci, (*ii*) the number of alleles per locus, (*iii*) allele frequencies in the natural population (obtained by sampling 69 unrelated individuals over the course of this study), (*iv*) the conservative estimate of number of sires contributing to each brood, and (*v*) reproductive skew of each sire (Vieites et al. 2004). The model assumes single-sex multiple mating (polygyny or polyandry), where all offspring in a brood were either full siblings or half siblings. We used a model of only two sires, each with the probability of mating equal to 0.5, because this is the most conservative estimate. Adding sires to the model would increase the statistical power to detect multiple paternity, but could lead to false overestimation of multiple matings. We performed six replicates of the analysis for the range observed in our samples (three–eight pups).

We used a Bayesian approach developed by Neff et al. (2002) to estimate frequency of multiple paternity in this population. Since not all of the males in the population are heterozygous for alleles other than those carried by the mother, an estimate based solely on the observed number of nonmaternal alleles will underestimate the true frequency of multiple paternity (Neff et al. 2002; Toonen 2004). The Bayesian approach used in the F(mm) v.1 program (Neff et al. 2002) takes the allele frequency distribution of the population into consideration when calculating the most likely frequency of multiple paternity and assigns a 95% confidence interval on that estimate. Statistical correlations among the total length of the mother, number of pups per litter, and number of paternal alleles detected were tested with JMP v.4.1 (SAS Institute Inc., Cary, North Carolina).

Results

We found evidence of multiple paternity (three or four paternal alleles at each of one–three loci) in 40% of the litters sampled (8 of 20 litters; Table 1). Each pup had at least one maternal allele, and χ^2 tests confirmed that inheritance of these alleles did not vary from predicted 1:1 Mendelian inheritance ratios within each litter ($df = 1$, $P > 0.05$). The Bayesian maximum likelihood estimate of frequency of multiple paternity was 43.8%, which closely matched our estimate of 40% based on direct count of nonmaternal alleles. The 95% confidence interval is 23%–63% mixed paternity. Mean litter size was 5.5 pups (Table 1). PrDM assigned a 75% probability of detecting multiple paternity in litters of this size (Neff and Pitcher 2002); hence we were constrained by litter size in our ability to detect multiple paternity in sandbar sharks. If we conservatively adjusted our calculation of multiple paternity to assume that it occurred in the 25% of cases where we lacked statistical power to detect it, then the frequency of multiple paternity in this population is approximately 50%, well within the 95% confidence interval calculated by F(mm).

The genotyping error rate calculated by GIMLET (Valiere 2002) was 3%. MICRO-CHECKER (van Oosterhout et al. 2004) was used to calculate error rate due to DNA degradation, low DNA concentrations, and primer-site mutations,

© 2007 NRC Canada

Table 1. Date of capture and precaudal length (PCL) of the mother is shown for each of 20 litters, as well as the number of pups per litter, the maximum number of paternal alleles detected across six microsatellite loci, and the minimum number of sires indicated by the presence of these alleles in each litter.

Litter ID	Date of capture	Size of mother (PCL in cm)	No. of pups in litter	Max. no. of paternal alleles	Min. no. of sires
A	Sept. 2003	135	5	3	2
B	Sept. 2003	134	4	3	2
C	Aug. 2004	140	5	2	1
D	Aug. 2004	147	7	3	2
E	Sept. 2004	121	7	2	1
G	Oct. 2004	124	6	3	2
H	Oct. 2004	130	6	2	1
I	Nov. 2004	128	4	2	1
J[a]	Dec. 2004	—[b]	4	3	2
K[a]	Dec. 2004	—[b]	3	2	1
M	Aug. 2005	128	6	2	1
N	Sept. 2005	147	8	2	1
O	Sept. 2005	137	7	3	2
P	Sept. 2005	139	5	2	1
Q	Sept. 2005	137	5	2	1
R	Sept. 2005	138	4	2	1
S	Sept. 2005	130	5	3	2
T	Sept. 2005	135	5	2	1
U	Oct. 2005	146	6	2	1
V	Dec. 2005	~140[b]	8	4	2

[a]Sharks were caught in Kona, Hawaii. All others were caught in Kaneohe, Oahu.
[b]Caudal peduncle and fin were bitten off; PCL is not given or is an estimate based on morphometrics.

and no errors of these types were detected. There was no evidence of deviation from Hardy–Weinberg equilibrium for any locus except Cli-7, which showed moderate heterozygote deficiency in the sample of 69 unrelated individuals (Table 2). Because maternal alleles at this locus were inherited in expected 50:50 ratios in all offspring in 20 litters and because this locus provided substantial statistical power to detect multiple paternity, we retained it in our analysis. MICRO-CHECKER was used to verify these results, and no null alleles were inferred at Cli-7. Across all six loci, we detected two nonmaternal alleles in 12 litters, three nonmaternal alleles in seven litters, and four nonmaternal alleles in one litter that had eight pups (see Table 2).

Among these 20 litters, we found no significant correlation (Pearson correlation, df = 1, $\alpha = 0.05$) between the size of the mothers and the number of pups per litter ($r^2 = 0.059$, $P = 0.33$), the size of the mother and the number of paternal alleles found in the litter ($r^2 = 0.003$, $P = 0.83$), or the number of pups in each litter and the number of paternal alleles ($r^2 = 0.076$, $P = 0.23$). For those females with pups larger than 40 cm PCL, there was no correlation between the size of the mothers and mean pup size ($r^2 = 0.141$, $P = 0.138$).

Discussion

Multiple paternity occurs in ~40% of sandbar shark litters in Hawaii. This suggests that multiple paternity and genetic monogamy are occurring with roughly equal frequency in this population. The average litter size (5.5 pups) was smaller than that in other populations of sandbar sharks (Springer 1960; Joung and Chen 1995; Sminkey and Musick 1996), which may be a function of the smaller size at maturity and smaller maximum size of individuals in the Hawaiian population (Romine et al. 2006).

Table 2. Allelic diversity (k), observed and expected heterozygosities (H_{obs} and H_{exp}, respectively), and probabilities (P values) from Hardy–Weinberg equilibrium (HWE) tests for homozygote excess at six microsatellite loci based on multilocus genotypes from 69 individual sandbar sharks.

Locus	k	H_{obs}	H_{exp}	HWE
Cli-7	5	0.647	0.727	$P = 0.01$*
Cli-12	3	0.561	0.565	$P = 1.00$
Cli-102	2	0.529	0.514	$P = 0.63$
Cli-106	8	0.735	0.817	$P = 0.82$
Cli-108	13	0.636	0.684	$P = 0.51$
Cli-110	3	0.119	0.128	$P = 1.00$

*Statistically significant at $P < 0.05$.

Reproductive strategies can have significant implications for the conservation and management of exploited marine species (Rowe and Hutchings 2003). Although multiple paternity has now been detected in a number of shark species (e.g., Saville et al. 2002; Chapman et al. 2004; Daly-Engel et al. 2006), only two studies to date have examined the frequency of this strategy, with strikingly different findings. Feldheim et al. (2004) examined 45 litters of lemon sharks (*Negaprion brevirostris*) in Bimini, Bahamas, and estimated that 86.6% of the litters were sired by more than one male. In contrast, Chapman et al. (2004) examined 22 litters of bonnethead sharks (*Sphyrna tiburo*) and found ~19% of litters were multiple-sired and these were usually from the larger females. This study is the third to investigate fre-

© 2007 NRC Canada

quency of multiple mating in sharks, and the 40% frequency falls between the two previous estimates. Taken together, these studies suggest that polyandry is common in sharks but the frequency of multiple paternity likely varies widely among species.

Polyandrous mating is favored when females incur the bulk of the energetic investment of reproduction and receive no postcopulatory investment from males (Jennions and Petrie 2000; Zeh and Zeh 2001; Tregenza and Wedell 2002). If polyandry is a function of encounter rate between conspecifics, and females mate with every male they encounter, then the simplest explanation for the multiple paternity observed in the Hawaiian population of sandbar sharks is that approximately half the female sharks encountered more than one male over the course of the breeding season. This hypothesis is unlikely, however, given high population density, relative stability, and habitat limitations; sandbar sharks in Hawaii are primarily restricted to the narrow slope habitat around the islands (T.S. Daly-Engel and R.D. Grubbs, unpublished data). Polyandry can also arise through parent–offspring conflict over prenatal investment (Crespi and Semeniuk 2004) or during group courtship behavior when several males attempt to copulate with one female during a mating aggregation (Carrier et al. 1994; Whitney et al. 2004). This behavior has been observed in several shark species, but no mating events have yet been observed in sandbar sharks (Pratt and Carrier 2001).

Polyandry and multiple paternity may enhance reproductive success (Newcomer et al. 1999; Madsen et al. 2005; Neff and Pitcher 2005). If there is little or no opportunity to evaluate males prior to copulation, a female may hedge her bets by mating multiply and increase her chances that one of these matings may lead to higher survivorship of some of her offspring (Watson 1991; Madsen et al. 2005). Likewise if there is an opportunity to evaluate male fitness but encounter rates are low, a female may mate with the first male she encounters but trade up given the opportunity to mate with successive males (Watson 1991; Jennions and Petrie 2000). In cases when females are able to evaluate males, multiple paternity may be a response to environmental variability (Yasui 1998). In a stable environment, the characters needed to succeed are more predictable, and a female should use the strategy most likely to duplicate her own success. If the environment is unstable or unpredictable, then multiple mating is usually advantageous for reasons of genetic bet-hedging (Watson 1991; Yasui 1998). Given the low seasonal variation in Hawaii (e.g., water temperature varies by only 4 °C, Levitus 1987), we would expect bet-hedging to be less advantageous here than in a location with high seasonality. Multiple paternity may also function to limit sibling competition. A litter with lower genetic relatedness will reduce the competition for resources among full sibling offspring (Barton and Post 1983; Ridley 1993; Yasui 1998). Competition avoidance may be particularly relevant in shark populations that exhibit high site fidelity, mating aggregations, or philopatry.

Alternatively, a female shark may mate multiply to avoid inbreeding or increase the likelihood that her offspring will be sired by a male whose genes are compatible with hers (genetic compatibility hypothesis, Zeh and Zeh 2001; Feldheim et al. 2004; Neff and Pitcher 2005). Feldheim et al. (2004) tested predictions of this hypothesis in the Bimini population of lemon sharks, where adult females show high biennial philopatry. The authors did not find any correlation between relatedness of mates and the number of offspring produced (Feldheim et al. 2004), indicating that inbreeding avoidance is not driving polyandrous mating behavior in the lemon shark population at Bimini.

Given the advantages outlined above, it might be expected that multiple paternity should be the rule among sexually reproducing species (reviewed by Zeh and Zeh 2001; Crespi and Semeniuk 2004); however, sharks examined to date cover the entire spectrum from high multiple paternity to genetic monogamy. Why is multiple paternity not the dominant mating strategy in sharks? Multiple mating may be disadvantageous because of risk of injury to female sharks during mating events. Mating in wild sharks is difficult to observe, and copulation conditions are largely unknown. Nonetheless, female sharks are often wounded during mating (Pratt and Carrier 2001), and many females in this study had visible scars that were likely incurred during copulation. Injuries from multiple mating events also may increase vulnerability to predation and infection; therefore, hypothesized benefits to offspring may not outweigh the risk to the mother.

Furthermore, there is an ongoing debate over whether multiple paternity maintains or decreases the genetic diversity of populations (Zeh and Zeh 2003). One hypothesis states that multiple paternity may buffer against the loss of allelic diversity by increasing the effective population size (Newcomer et al. 1999; Martinez et al. 2000; Hoekert et al. 2002). This is countered, however, by theoretical results indicating that by increasing the variance in male reproductive success, multiple paternity may reduce the effective population size and the genetic diversity of the next generation (Nunney 1993; Ramakrishnan et al. 2004; Hedrick 2005). If the latter hypothesis holds true, then a population with a high frequency of multiple paternity may be more susceptible to loss of genetic diversity from overfishing and the resulting loss of evolutionary potential and increased extinction risk (reviewed by Frankham 2005).

The conditions that determine the frequency of multiple paternity are largely unknown and untested. As the current study and others show, the frequency of multiple paternity appears to be highly variable among shark species. If polyandry and multiple paternity depend on the rate at which female sharks encounter male conspecifics over the course of the breeding season, then such factors as high population density, site fidelity, and aggregate mating could all increase the average number of sires in a litter. The next step is to survey multiple paternity in additional species and populations of the same species that differ in their growth, habitat use, and movement patterns to understand how these factors influence multiple mating in sharks. It will also be informative to survey populations of sandbar sharks that have been heavily fished to investigate how frequency of multiple paternity varies with exploitation.

Acknowledgements

The authors extend special thanks to Kim Holland, with whose support this project was made possible. Thanks go to John Musick, Jason Romine, Amanda Southwood, Yannis

© 2007 NRC Canada

Papastamatiou, David Itano, Amy Long, Austin Stankus, Lenore Litherland, Thomas Tinhan, and Jeff Eble for help with sample collection. Marc Crepeau, Kimberly Andrews, Jonathan Puritz, Sarah Daley, and Iliana Baums helped with genetic analysis, and Stephen Karl, Iliana Baums, Matthew Craig, and Gregory Concepcion gave valuable input that greatly improved this manuscript. Thanks also go to all the lab mates and volunteers who helped with fieldwork. Genetic analyses were made possible by the EPSCoR Evolutionary Genetics Facility at the Hawaii Institute of Marine Biology, and funding came from the Ecology, Evolution and Conservation Biology (EECB) Program at the University of Hawaii, the National Science Foundation (NSF Graduate K-12 program grant No. 0232016 to EECB, OCE-0453167 to B.W.B. and R.J.T., and EPS-0554657 to the University of Hawaii), and Sigma Xi. We also thank reviewers and editors Moira Ferguson and Jeffrey Hutchings for helpful comments and improvements to the manuscript. This is contribution No. 1240 from the Hawaii Institute of Marine Biology and contribution No. 6836 from the School of Ocean and Earth Science and Technology at the University of Hawaii.

References

Adams, E.M., Jones, A.G., and Arnold, S.J. 2005. Multiple paternity in a natural population of a salamander with long-term sperm storage. Mol. Ecol. **14**: 1803–1810.

Anderson, E.D. 1990. Fishery models as applied to elasmobranch fisheries. National Oceanic and Atmospheric Administration, National Marine Fisheries Service, US Department of Commerce, National Technical Information Service, Springfield, Va. NOAA/NMFS Rep. 90.

Barton, N.H., and Post, R.J. 1983. Competition between siblings and advantage of mixed families. J. Theor. Biol. **120**: 381–387.

Branstetter, S. 1990. Early life-history implications of selected carcharhinoid and lamnoid sharks of the northwest Atlantic. National Oceanic and Atmospheric Administration, National Marine Fisheries Service, US Department of Commerce, National Technical Information Service, Springfield, Va. NOAA/NMFS Rep. 90.

Bretman, A., and Tregenza, T. 2005. Measuring polyandry in wild populations: a case study using promiscuous crickets. Mol. Ecol. **14**: 2169–2179.

Carrier, J.C., Pratt, H.L.J., and Martin, L.K. 1994. Group reproductive behaviors in free-living nurse sharks, *Ginglymostoma cirratum*. Copeia, 1994: 646–656.

Carrier, J.C., Pratt, H.L., and Castro, J.I. 2004. Reproductive biology of Elasmobranchs. *In* Biology of sharks and their relatives. *Edited by* J.C. Carrier, J.A. Musick, and M.R. Heithaus. CRC Press, Boca Raton, Fla. pp. 269–286.

Chapman, D.D., Prodohl, P.A., Gelsleicher, J., Manire, C.A., and Mahmood, S.S. 2004. Predominance of genetic monogamy by females in a hammerhead shark, *Sphyrna tiburo*: implications for shark conservation. Mol. Ecol. **13**: 1965–1974.

Crespi, B., and Semeniuk, C. 2004. Parent–offspring conflict in the evolution of vertebrate reproductive mode. Am. Nat. **163**: 635–653.

Daly-Engel, T.S., Grubbs, R.D., Holland, K.N., Toonen, R.J., and Bowen, B.W. 2006. Assessment of multiple paternity in single litters from three species of carcharhinid sharks in Hawaii. Environ. Biol. Fishes, **76**: 419–424.

DeWoody, J.A., and Avise, J.C. 2001. Genetic perspectives on the natural history of fish mating systems. J. Hered. **92**: 167–172.

Feldheim, K.A., Gruber, S.H., and Ashley, M.V. 2001. Multiple paternity of a lemon shark litter (Chondrichthyes: Carcharhinidae). Copeia, 2001: 781–786.

Feldheim, K.A., Gruber, S.H., and Ashley, M.V. 2004. Reconstruction of parental microsatellite genotypes reveals female polyandry and philopatry in the lemon shark, *Negaprion brevirostris*. Evolution, **58**: 2332–2342.

Frankham, R. 2005. Genetics and extinction. Biol. Conserv. **126**: 131–140.

Grubbs, R.D., Musick, J.A., Conrath, C.L., and Romine, J.G. 2007. Migratory movements, philopatry, and temporal delineation of summer nurseries for juvenile sandbar sharks, *Carcharhinus plumbeus*, in the Chesapeake Bay region. Am. Fish. Soc. In press.

Hamlett, W.C., Jones, C.J.P., and Paulesu, L.R. 2005. Placentatrophy in sharks. *In* Reproductive biology and phylogeny of Chondrichthyes: sharks, batoids, and chimaeras. *Edited by* W.C. Hamlett. Science Publishers, Inc., Plymouth, UK. pp. 463–502.

Hedrick, P. 2005. Large variance in reproductive success and N_e/N ratio. Evolution, **59**: 1596–1599.

Heist, E.J. 2004. Genetics of sharks, skates, and rays. *In* Biology of sharks and their relatives. *Edited by* J.C. Carrier, J.A. Musick, and M.R. Heithaus. CRC Press, Boca Raton, Fla. pp. 471–486.

Hoekert, W.E.J., Neufeglise, H., Schouten, A.D., and Menken, S.B.J. 2002. Multiple paternity and female-biased mutation at a microsatellite locus in the olive ridley sea turtle (*Lepidochelys olivacea*). Heredity, **89**: 107–113.

Hoenig, J.M., and Gruber, S.H. 1990. Life-history patterns in elasmobranchs: implications for fisheries management. National Oceanic and Atmospheric Administration, National Marine Fisheries Service, US Department of Commerce, National Technical Information Service, Springfield, Va. NOAA/NMFS Rep. 90.

Holden, M.J. 1973. Are long-term sustainable fisheries for elasmobranchs possible? Rapp. P.-V. Réun. Cons. Int. Explor. Mer, **64**: 360–367.

IUCN. 2005. The IUCN red list of threatened species: habitats authority file. *In* Authority files for habitats, threats, conservation actions and utilization of species [online]. Available from http://www.iucn.org/themes/ssc/sis/authority.htm [accessed January 2006].

Jennions, M.D., and Petrie, M. 2000. Why do females mate multiply? A review of the genetic benefits. Biol. Rev. Camb. Philos. Soc. **75**: 21–64.

Joung, S.-J., and Chen, C.-T. 1995. Reproduction in the sandbar shark, *Carcharhinus plumbeus*, in the waters off northeastern Taiwan. Copeia, 1995: 659–665.

Joung, S.-J., Liao, Y.-Y., and Chen, C.-T. 2004. Age and growth of sandbar shark, *Carcharhinus plumbeus*, in northeastern Taiwanese waters. Fish. Res. **70**: 83–96.

Keeney, D.B., and Heist, E.J. 2003. Characterization of microsatellite loci isolated from the blacktip shark and their utility in requiem and hammerhead sharks. Mol. Ecol. Notes, **3**: 501–504.

Ketchen, K.S. 1969. A review of the dogfish problem off the western coast of Canada. Fish. Res. Board Can. MS. Rep. Ser. 1048.

Lande, R., and Shannon, S. 1996. The role of genetic variation in adaptation and population persistence in a changing environment. Evolution, **50**: 434–437.

Levitus, S. 1987. A comparison of the annual cycle of two sea surface temperature climatologies of the world ocean. J. Phys. Oceanogr. **17**: 197–214.

Madsen, T., Ujvari, B., Olsson, M., and Shine, R. 2005. Paternal alleles enhance female reproductive success in tropical pythons. Mol. Ecol. **14**: 1783–1787.

Martinez, J.L., Moran, P., Perez, J., De Gaudemar, B., Beall, E., and Garcia-Vazquez, E. 2000. Multiple paternity increases effec-

© 2007 NRC Canada

tive size of southern Atlantic salmon populations. Mol. Ecol. **9**: 293–298.

Moore, J.C., McCoy, E.D., Mushinsky, H.R., and Karl, S.A. 2006. Multiple paternity and breeding system in the gopher tortoise, *Gopherus polyphemus*. J. Hered. **97**: 150–157.

Musick, J.A. 1999. Ecology and conservation of long-lived marine animals. *In* Life in the Slow Lane: Ecology and Conservation of Long-Lived Marine Animals, American Fisheries Society Symposium 23, Bethesda, Md. *Edited by* J. Musick. American Fisheries Society, Bethesda, Md. pp. 1–10.

Musick, J.A., Branstetter, S., and Colvocoresses, J.A. 1993. Trends in shark abundance from 1974 to 1991 for the Chesapeake Bight region of the U.S. mid-Atlantic coast. National Oceanic and Atmospheric Administration, National Marine Fisheries Service, US Department of Commerce, National Technical Information Service, Springfield, Va. NOAA/NMFS Rep. 115.

Musick, J.A., and Ellis, J.K. 2005. Reproductive evolution of Chondrichthyes. *In* Reproductive biology and phylogeny of Chondrichthyes: sharks, batoids, and chimaeras. *Edited by* W.C. Hamlett. Science Publishers, Inc., Plymouth, UK. pp. 45–79.

Neff, B.D., and Pitcher, T.E. 2002. Assessing the statistical power of genetic analyses to detect multiple mating in fish. J. Fish Biol. **61**: 739–750.

Neff, B.D., and Pitcher, T.E. 2005. Genetic quality and sexual selection: an integrated framework for good genes and compatible genes. Mol. Ecol. **14**: 19–38.

Neff, B.D., Pitcher, T.E., and Repka, J. 2002. A Bayesian model for assessing the frequency of multiple mating in nature. J. Hered. **93**: 406–414.

Newcomer, S.D., Zeh, J.A., and Zeh, D.W. 1999. Genetic benefits enhance the reproductive success of polyandrous females. Proc. Natl. Acad. Sci. U.S.A. **96**: 10236–10241.

NMFS. 2003. Final amendment 1 to the fishery management plan for Atlantic tunas, swordfish, and sharks. National Oceanic and Atmospheric Administration, National Marine Fisheries Service, US Department of Commerce, Highly Migratory Species Management Division, Silver Spring, Md.

Nunney, L. 1993. The influence of mating system and overlapping generations on effective population size. Evolution, **47**: 1329–1341.

Olsen, A.M. 1959. The status of the school shark fishery in south-eastern Australia waters. Aust. J. Mar. Freshw. Res. **10**: 150–176.

Pratt, H.L. 1993. The storage of spermatozoa in the oviducal glands of western North Atlantic sharks. Environ. Biol. Fishes, **38**: 139–149.

Pratt, H.L., and Carrier, J.C. 2001. A review of elasmobranch reproductive behavior with a case study on the nurse shark, *Ginglymostoma cirratum*. Environ. Biol. Fishes, **60**: 157–188.

Ramakrishnan, U., Storz, J.F., Taylor, B.L., and Lande, R. 2004. Estimation of genetically effective breeding numbers using a rejection algorithm approach. Mol. Ecol. **13**: 3283–3292.

Raymond, M., and Rousset, F. 1995. GENEPOP Version 1.2. Population genetics software for exact tests and ecumenicism. J. Hered. **86**: 248–249.

Reynolds, J.D. 1996. Animal breeding systems. Trends Ecol. Evol. **11**: 68–72.

Ridley, M. 1993. Clutch size and mating frequency in parasitic Hymenoptera. Am. Nat. **142**: 893–910.

Romine, J.G., Grubbs, R.D., and Musick, J.A. 2006. Age and growth of the sandbar shark, *Carcharhinus plumbeus*, in Hawaiian waters through vertebral analysis. Environ. Biol. Fishes, **77**(3–4): 229–239.

Rowe, S., and Hutchings, J.A. 2003. Mating systems and the conservation of commercially exploited marine fish. Trends Ecol. Evol. **18**: 567–572.

Saville, K.J., Lindley, A.M., Maries, E.G., Carrier, J.C., and Pratt, H.L.J. 2002. Multiple paternity in the nurse shark, *Ginglymostoma cirratum*. Environ. Biol. Fishes, **63**: 347–352.

Selkoe, K.A., and Toonen, R.J. 2006. Microsatellites for ecologists: a practical guide for using and evaluating microsatellite markers. Ecol. Lett. **9**: 615–629.

Seutin, G., White, B.N., and Boag, P.T. 1991. Preservation of avian blood and tissue samples for DNA analyses. Can. J. Zool. **69**(1): 82–90.

Sminkey, T.R., and Musick, J.A. 1996. Demographic analysis of the sandbar shark, *Carcharhinus plumbeus*, in the western North Atlantic. Fish. Bull. **94**: 341–347.

Smith, S.E., Au, D.W., and Show, C. 1998. Intrinsic rebound potentials of 26 species of Pacific sharks. Mar. Freshw. Res. **49**: 663–678.

Springer, S. 1960. Natural history of the sandbar shark *Eulamia milberti*. Fish. Bull. **61**: 1–36.

Sunnucks, P. 2000. Efficient genetic markers for population biology. Trends Ecol. Evol. **15**: 199–203.

Sunnucks, P., and Hales, D.F. 1996. Numerous transposed sequences of mitochondrial cytochrome oxidase I-II in aphids of the genus *Sitobion* (Hemiptera: Aphididae). Mol. Biol. Evol. **13**: 510–524.

Toonen, R.J. 2004. Genetic evidence of multiple paternity of broods in the intertidal crab, *Petrolisthes cinctipes*. Mar. Ecol. Prog. Ser. **270**: 259–263.

Tregenza, T., and Wedell, N. 2002. Polyandrous females avoid cost of inbreeding. Nature (London), **6837**: 71–73.

Valiere, N. 2002. GIMLET: a computer program for analysing genetic individual identification data. Mol. Ecol. Notes, **2**: 377–379.

van Oosterhout, C.V., Hutchinson, W., Wills, D., and Shipley, P. 2004. MICRO-CHECKER: software for identifying and correcting genotype errors in microsatellite data. Mol. Ecol. Notes, **4**: 535–538.

Vieites, D.R., Nieto-Roman, S., Barluenga, M., Palanca, A., Vences, M., and Meyer, A. 2004. Post-mating clutch piracy in an amphibian. Nature (London), **431**: 305–308.

Walker, T.I., Taylor, B.L., Hudson, R.J., and Cottier, J.P. 1998. The phenomenon of apparent change of growth rate in gummy shark (*Mustelus antarcticus*) harvested off southern Australia. Fish. Res. **39**: 139–163.

Watson, P.J. 1991. Multiple paternity as genetic bet hedging in female sierra dome spiders, *Linyphia litigiosa* (Linyphiidae). Anim. Behav. **41**: 343–360.

Whitney, N.M., Pratt, H.L., and Carrier, J.C. 2004. Group courtship, mating behaviour and siphon sac function in the whitetip reef shark, *Triaenodon obesus*. Anim. Behav. **68**: 1435–1442.

Yasui, Y. 1998. The 'genetic benefits' of female multiple mating reconsidered. Trends Ecol. Evol. **13**: 246–250.

Zane, L., Nelson, W.S., Jones, A.G., and Avise, J.C. 1999. Microsatellite assessment of multiple paternity in natural populations of a live-bearing fish, *Gambusia holbrooki*. J. Evol. Biol. **12**: 61–69.

Zeh, J.A., and Zeh, D.W. 2001. Reproductive mode and the genetic benefits of polyandry. Anim. Behav. **61**: 1051–1063.

Zeh, J.A., and Zeh, D.W. 2003. Toward a new sexual selection paradigm: polyandry, conflict, and incompatibility. Ethology, **109**: 929–950.

© 2007 NRC Canada

Admitting ageing error when fitting growth curves: an example using the von Bertalanffy growth function with random effects

Jason M. Cope and André E. Punt

Abstract: A way to explicitly incorporate ageing error into the estimation of von Bertalanffy growth function (VBGF) parameters using a random effects (RE) modeling framework is presented. This RE framework also accounts for the effects of selectivity on growth curve estimation by characterizing the distribution of true ages derived from multiple age reads using either an exponential or gamma distribution. Simulation testing across four life histories is used to compare the RE approach with standard nonlinear (SNL) approaches that use the primary, average, or median ages in growth estimation. Sensitivity tests compare the effects of assumed length and ageing error, selectivity, and recruitment variability on the estimation of growth curve parameters. Results support the use of the RE method using a gamma distribution over the SNL methods because RE method estimates of VBGF growth parameters were more precise across life histories and sensitivity trials. This general approach can be applied and expanded to other growth models. Applications demonstrate that the results from RE methods may differ in biologically important ways to those obtained from SNL approaches.

Résumé : Nous présentons une méthode pour incorporer de façon explicite l'erreur de détermination de l'âge dans l'estimation des paramètres de la fonction de croissance de von Bertalanffy (VBGF) dans le cadre de la modélisation à effets aléatoires (RE). Ce cadre RE tient aussi compte des effets de la sélectivité sur l'estimation de la courbe de Hcroissance en caractérisant la distribution des âges réels dérivée de lectures multiples des âges à l'aide des distributions exponentielle ou gamma. Nous effectuons une vérification par simulation sur quatre cycles biologiques afin de comparer la méthodologie RE avec les méthodes standard non linéaires (SNL) qui utilisent les âges primaires, moyens ou médians dans l'estimation de la croissance. Des tests de sensibilité servent à comparer les effets des erreurs présumées de longueur et d'âge, de la sélectivité et de la variabilité du recrutement sur l'estimation des paramètres de la courbe de croissance. Nos résultats appuient le choix de la méthode RE avec une distribution gamma plutôt que les méthodologies SNL parce que la méthode RE génère des estimations plus précises des paramètres de croissance de VBGF au cours des cycles biologiques et dans les tests de sensibilité. Cette méthodologie générale peut être étendue et s'appliquer à d'autres modèles de croissance. Les applications des méthodes RE révèlent que les résultats peuvent différer de ceux des méthodologies SNL de différentes manières qui ont des conséquences biologiques importantes.

[Traduit par la Rédaction]

Introduction

The biological relationship between age and length is fundamental to many fisheries population dynamics models. Estimates of growth drive size- and age-structured stock assessment models (Quinn and Deriso 1999), scale yield calculations (Beverton and Holt 1957; Gulland 1983; Haddon 2001), and are related to life history traits such as natural mortality (M) and age or length at maturity (Charnov 1993; Jensen 1998). Besides pure application, age and growth studies are also important in describing the basic biology and ecology of fishes (Weatherley and Gill 1987; Cailliet and Goldman 2004).

Although many growth curves are available, the von Bertalanffy growth function (VBGF; von Bertalanffy 1938) is the most widely used in fisheries, and its parameters are particularly useful in describing general fish growth (Chen et al. 1992; Quinn and Deriso 1999), deriving fisheries reference points (Clark 1991; Williams and Shertzer 2003) and estimating life history parameters (Beverton and Holt 1959; Beverton 1992). Most commonly, data will consist of one age and length measure per individual collected from many individuals, although data from length frequencies (Wang and Ellis 1998, 2005) or multiple measures of the same individual through tag–recapture (Fabens 1965; Wang 1998) and repeated-measures studies (Palmer et al. 1991) are also used.

Current VBGF estimation techniques use nonlinear regression or likelihood methods to fit deterministic relationships, assuming that all variance between the model and the data is due to heterogeneity in length at age (Quinn and Deriso 1999). This variance describes natural variation in the length at age attributable to individual growth processes and is commonly termed process error. This estimation ap-

Received 25 April 2006. Accepted 17 October 2006. Published on the NRC Research Press Web site at http://cjfas.nrc.ca on 10 February 2007.
J19291

J.M. Cope[1] and A.E. Punt. School of Aquatic and Fishery Sciences, University of Washington, Box 355020, Seattle, WA 98195-5020, USA.

[1]Corresponding author (e-mail: jcope@u.washington.edu).

 doi:10.1139/F06-179 © 2007 NRC Canada

Fig. 1. Illustration of the data generation and subsequent fit to the random effects (RE) method. This example shows how the true age of individual i (T_i) is drawn from a population (shaded bars) and results in an observed length l_i (resulting from an expected length L_i and derived via the von Bertalanffy growth function (VBGF) from T_i with process error ε_L) and r age reads t_{ir} (T_i with ageing error $\varepsilon_{T,ij}$). Sources of stochasticity (with likelihood components $\mathcal{L}_x$) are noted at the arrows between the observed and expected values. Exponential (broken line) and gamma (solid line) fits to the true sample age population are also shown.

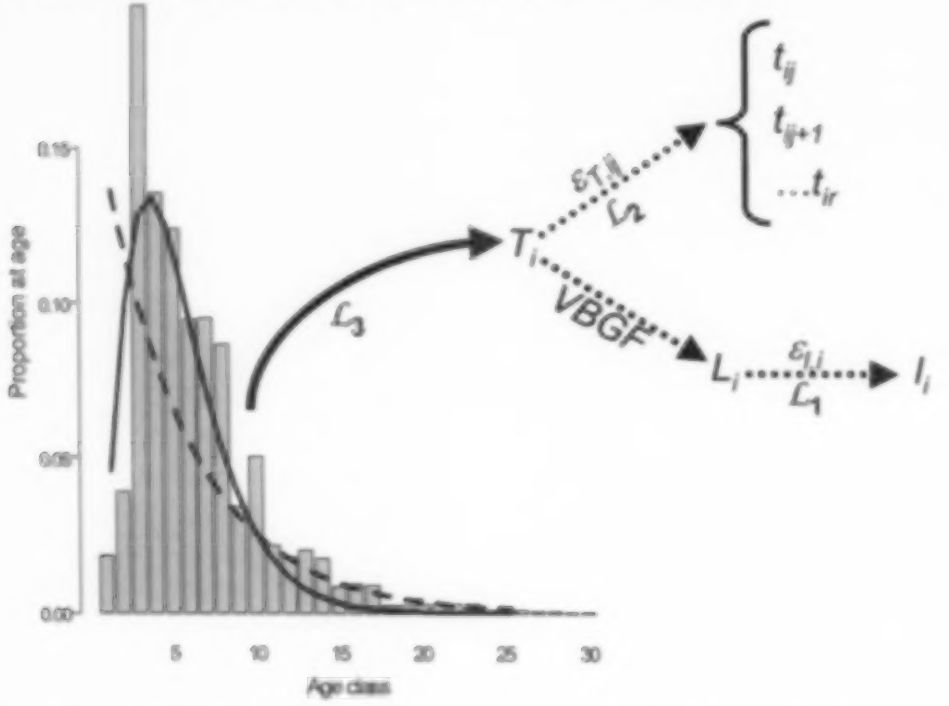

proach is referred to in this paper as the standard nonlinear (SNL) method.

Also frequent (especially in temperate fishes), but often overlooked, is measurement error in reading ageing structures. The formation of ageing structures (e.g., otoliths) and the subsequent interpretation of the growth record is not always consistent, leading to observation error in the assignment of age (Evans and Hoenig 1998; Campana 2001). Such error can greatly affect estimates of growth, mortality, recruitment, and yield (Tyler et al. 1989; Bradford 1991; Reeves 2003). Ageing error should therefore be considered when fitting growth curves.

To address this issue, multiple age reads of fish are often taken, and the precision of the reads is quantified (Beamish and Fournier 1981; Chang 1982; Campana 2001). Kimura and Anderl (2005) present a way to compare different measures of ageing precision, and Campana et al. (1995) and Cailliet et al. (1990) present graphical ways to summarize inter-read variation, bias, and precision. However, none of these studies accounted for ageing error when fitting growth curves.

Advances have been made to incorporate different types of error when fitting the VBGF. For example, individual variation in VBGF growth parameters (Sainsbury 1980; Wang and Thomas 1995; Pilling et al. 2002), seasonal variation in growth (Pitcher and MacDonald 1973; Cloern and Nichols 1978; Appledoorn 1982), autocorrelated error (Venugopalan and Prajneshu 1997), and stochastic environmental fluctuations (Prajneshu and Venugopalan 1999) have all been investigated, though none of these studies considered ageing error. Nummi (2000) presents a general method to incorporate error in the dependent variable for repeated-measures studies, though this does not apply to typical fisheries age and growth data (i.e., one length measurement per

Table 1. Estimated parameters of the standard nonlinear (SNL) and two random effects (RE_Exp, RE_Gamma) methods compared in this study.

	Method		
Parameters	SNL	RE_Exp	RE_Gamma
L_∞	×	×	×
k	×	×	×
t_0	×	×	×
CV_L	×	×	×
CV_T	NA	●	●
λ	NA	×	NA
γ	NA	NA	×
β	NA	NA	×

Note: RE_Exp, uses the exponential distribution to describe the sample population; RE_Gamma, uses the gamma distribution to describe the sampled population; ×, estimated within the model; ●, estimated external to the model; NA, not applicable or estimated. See Materials and methods for definitions of parameters.

© 2007 NRC Canada

Table 2. Values used to parameterize the operating model for (*i*) each life history and (*ii*) each sensitivity.

	Parameter									
	M (year^{-1})	L_∞ (mm)	k (year^{-1})	t_0 (year)	ω (year)	CV_L	CV_T	ϕ_1 (year)	ϕ_2 (year)	σ_R
Life history base-case values										
1	0.075	500	0.05	0	100	0.1	0.1	5	5	0.6
2	0.15	500	0.09	0	50	0.1	0.1	4	4	0.6
3	0.25	500	0.152	0	30	0.1	0.1	3	2	0.6
4	0.5	500	0.303	0	10	0.1	0.1	2	1	0.6
Life history 3: base case and sensitivities										
Base case	0.25	500	0.152	0	30	0.1	0.1	3	2	0.6
Sensitivities										
Low CV_L	0.25	500	0.152	0	30	0.05[a]	0.1	3	2	0.6
High CV_L	0.25	500	0.152	0	30	0.2[a]	0.1	3	2	0.6
Low CV_T	0.25	500	0.152	0	30	0.1	0.05[a]	3	2	0.6
High CV_T	0.25	500	0.152	0	30	0.1	0.2[a]	3	2	0.6
ΔCV_T low	0.25	500	0.152	0	30	0.1	0.05–0.20[a]	3	2	0.6
ΔCV_T high	0.25	500	0.152	0	30	0.1	0.1–0.20[a,b]	3	2	0.6
Low σ_R	0.25	500	0.152	0	30	0.1	0.1	3	2	0.3[a]
High σ_R	0.25	500	0.152	0	30	0.10	0.1	3	2	1.0[a]
Low selectivity	0.25	500	0.152	0	30	0.1	0.1	0	0	0.6
High selectivity	0.25	500	0.152	0	30	0.1	0.1	0.4	0.3	0.6
ΔCV_T, selectivity high	0.25	500	0.152	0	30	0.1	0.10–0.20[a,b]	0.1	0.2	0.6

[a]Values that differ from the base case.
[b]The linear increase in CV_T is applied to ages 10–30 only.

Fig. 2. Simplified illustration of creating the sampled population of true ages given (*a*) natural mortality (M), (*b*) M and recruitment variability (σ_R), and (*c*) M, σ_R, and logistic selectivity (ϕ_1, ϕ_2; see eq. 8): (*a*) stable age distribution given a specified M; (*b*) the same age structure with added σ_R; (*c*) how the age structure in (*b*) is impacted by ϕ and is the age-structures sampled for simulation purposes.

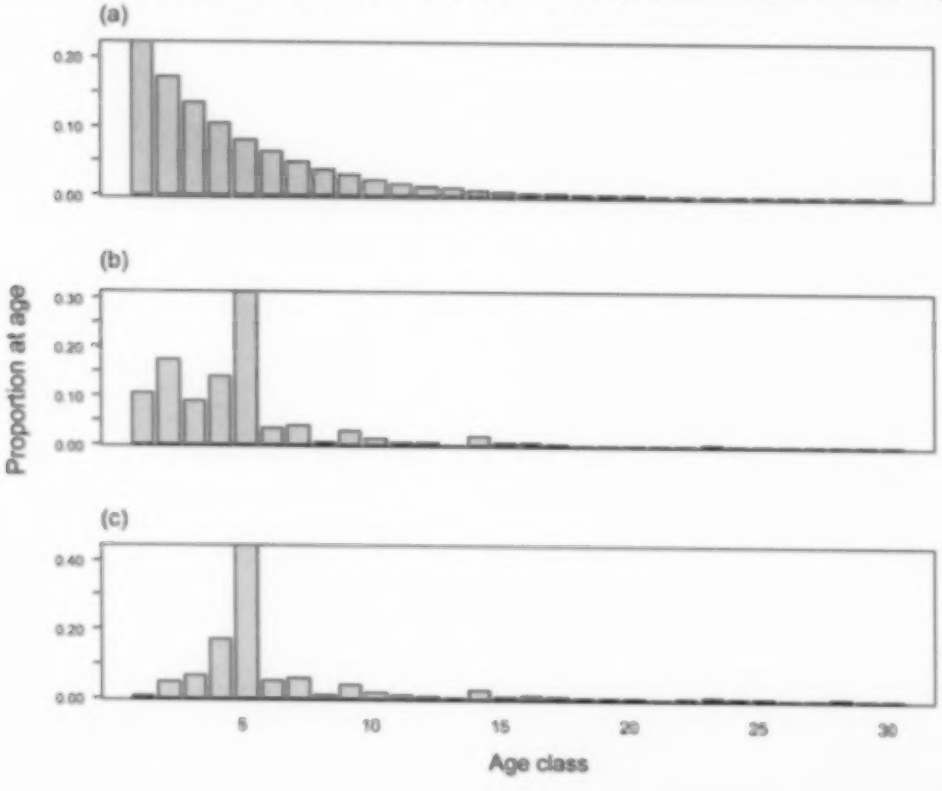

© 2007 NRC Canada

sampled individual). Richards et al. (1992) present a way to account for ageing error from multiple age reads when developing age compositions, but not when fitting age and growth models.

Kimura (2000) addresses the problem of measurement error in age estimates when fitting growth models using an errors-in-variables approach based on functional regression. However, Kimura's approach requires the specification of a variance ratio term that is unknown. Although Kimura (2000) gives guidance in choosing this ratio, uncertainty associated with its value may greatly influence the resulting growth curve estimation.

This study presents an approach to explicitly incorporate ageing error into the estimation of the VBGF parameters using a random effects (RE) modeling framework. (A Microsoft Excel®-based application to implement the estimation approaches used in this paper is available from the corresponding author.) An RE approach is powerful in three main ways: (*i*) it allows for explicit incorporation of ageing error for multiple reads when estimating VBGF parameters, (*ii*) the only internally inestimable parameter can be derived from the age-at-length data, and (*iii*) an estimate of the sampled population from which the true ages is produced "corrects" the VBGF parameters for selectivity and may lead to an independent estimate of total mortality (Z; estimating mortality rates from this approach will be covered in a subsequent study). Simulation testing across four different life histories is used to compare the RE approach with three variants of the SNL approach based on using (*i*) the primary read only, (*ii*) the average age of multiple reads, and (*iii*) the median age of multiple reads. Each method is then applied to age and length data of four species (sand sole (*Psettichthys melanostictus*), cabezon (*Scorpaenichthys marmoratus*), greenspotted rockfish (*Sebastes chlorostictus*), and blackgill rockfish (*Sebastes melanostomus*)) to demonstrate the use of the RE approach.

Materials and methods

Model formulation

The models presented presume that the data set consists of one length and one or multiple age reads (r is the total number of age reads) per individual for n individuals. The methods presented can be extended straightforwardly to cases when the number of reads for each individual varies.

Standard von Bertalanffy growth function

The observed length at age (l_i) for the ith individual in the sample can be formulated as follows:

$$(1) \qquad l_i = L_i + \varepsilon_{L,i} \qquad \varepsilon_{L,i} \sim N(0, \sigma^2_{L,i})$$

where L_i is calculated from the traditional three-parameter VBGF (Beverton and Holt 1957):

$$(2) \qquad L_i = L_\infty\{1 - \exp[-k(T_i - t_0)]\}$$

where L_i is the expected length at age for the ith individual, L_∞ is theoretical maximum length, k is the Brody growth coefficient, t_0 is theoretical age at length 0, and T_i is the true age of the ith individual.

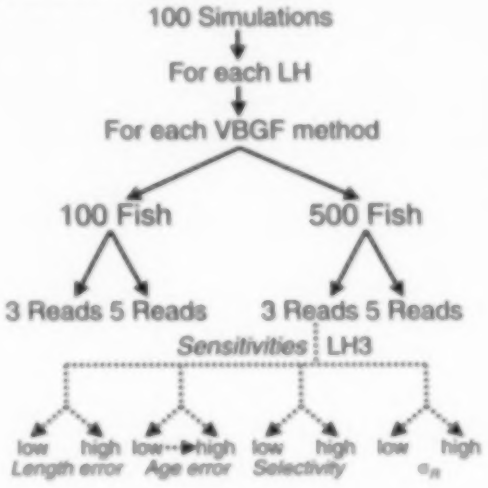

Fig. 3. Schematic of the simulation testing process. Solid lines are simulation pathways for each life history base case. Broken lines are simulations exploring sensitivity to different parameter values. The sensitivities are only examined for life history 3 (LH3) with 500 individuals and 3 reads.

The coefficient of variation of the normally distributed process error, CV_L, is assumed to be the same for all individuals in the population. The standard deviation of the process error in length for individual i, $\sigma_{L,i}$, is therefore given by $\sigma_{L,i} = CV_L L_i$. All variance in the data is therefore associated with estimated length process error, and L_∞, k, and t_0 are estimable parameters (Table 1). The likelihood function (L_1, Fig. 1) maximized to estimate the values of these parameters (coded in AD Model Builder; Otter Research Ltd. 2005*a*) is

$$(3) \qquad L = \prod_i \frac{1}{\sqrt{2\pi}\,\sigma_{L,i}} \exp\left[-\frac{(l_i - L_i)^2}{2\sigma^2_{L,i}}\right]$$

Traditionally, only one age per individual is used to fit the VBGF. When multiple reads (t_{ij}: $j = 1, 2, \ldots, r$) are available for each individual i, three approaches are typically used to obtain the one age read per individual: (*i*) a primary age reader is established and only their read is used to fit the model, (*ii*) multiple reads are averaged, and (*iii*) the median value of the multiple reads is taken to decrease the influence of outliers.

Growth curve models with random effects

RE models allow one to fit nonGaussian, nonlinear models with additional variance components (e.g., error in the independent variable) by specifying an additional likelihood component based on (in the case of growth curves) the fit of the observed age reads to the expected true age (L_2, Fig. 1) and a distribution for the ages of the sampled individuals (L_3, Fig. 1). In this approach, one can envision sampling a true age T_i from the population (Fig. 1, bars), of which a length is measured — with process error — from the growth curve (e.g., VBGF). Likewise, multiple reads of the true age are obtained with observation error (Fig. 1). All three components (length (L_1), age (L_2), and sampled population (L_3)) comprise the statistical model for the data.

© 2007 NRC Canada

Fig. 4. Proportional error ((estimated – true)/true) among four life histories in the estimates of the von Bertalanffy growth function (VBGF) parameter L_∞ for the two random effects (RE_Exp, random effects with exponential distribution; RE_Gamma, random effects with gamma distribution) and three standard nonlinear (SNL_A, averages of multiple reads; SNL_M, medians of multiple reads; SNL_P, primary reads only) methods when the number of individuals (i) sampled is either 100 or 500 and 3 or 5 age reads (j) are made. Box plot description: median, bold solid line; 1st and 3rd interquartile range, box; 1.5 times the interquartile range, whiskers; outliners, circles. The horizontal line denotes zero error. (*a*) Life history 1; (*b*) life history 2; (*c*) life history 3; (*d*) life history 4.

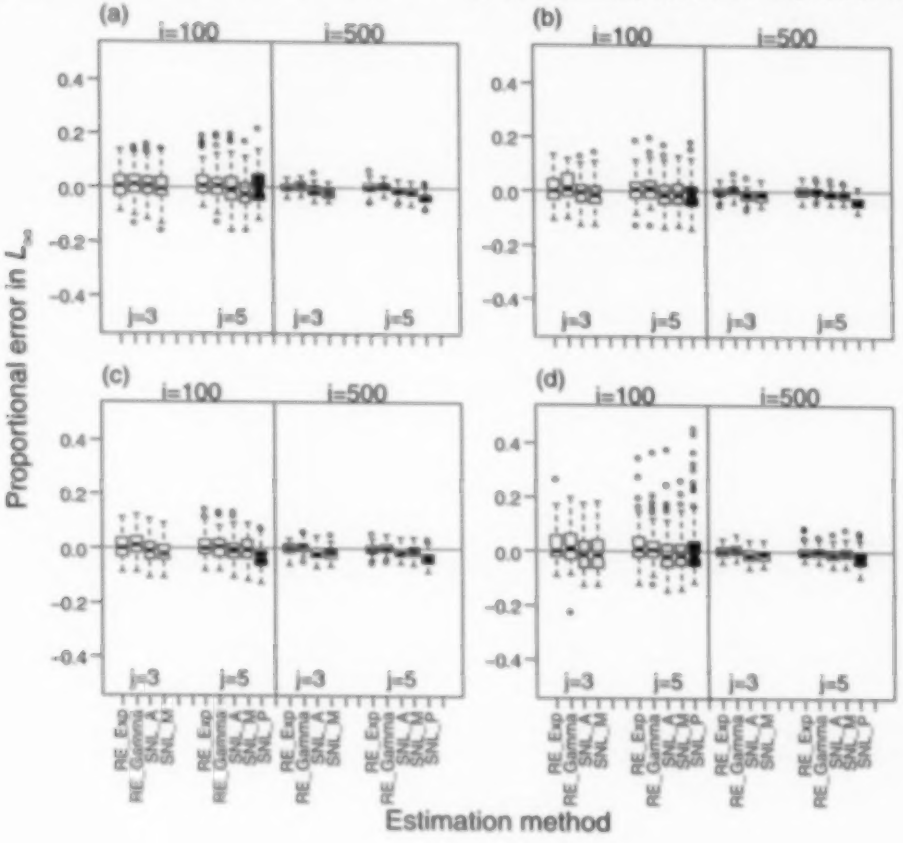

VBGF with random effects

A relationship between the observed and true ages can be formulated. For example

$$t_{ij} = T_i + \varepsilon_{T,ij} \qquad \varepsilon_{T,ij} \sim N(0, \sigma^2_{T,i}) \tag{4}$$

where the standard deviation of the age-reading error for individual i, $\sigma_{T,i}$, is based on that assumption that the CV of the ageing error is constant (i.e., $\sigma_{T,i} = \mathrm{CV}_T T_i$ (Kimura and Lyons 1991; Piner et al. 2005, 2006), where CV_T is the coefficient of variation of ageing error).

The value of CV_T cannot be estimated within the model because of lack of degrees of freedom (Otter Research Ltd. 2005*b*), although it can be estimated from the multiple age reads assuming that ageing is unbiased:

$$\widehat{\mathrm{CV}}_T = \sqrt{\frac{\sum_{i=1}^{n} \mathrm{CV}_{T,i}^2}{n}} \tag{5}$$

where $\mathrm{CV}_{T,i}$ is the age coefficient of variation for each individual i.

Given the models for the errors in observed lengths (eqs. 1–2) and estimated ages (eq. 4), the RE model lastly requires characterizing the distribution of the true ages. This distribution has biological meaning, as it is the true age composition of the sampled population. For the purposes of this paper, either the exponential (Fig. 1, broken line) or gamma distribution (Fig. 1, solid line) is used to describe the sampled population. These two distributions were chosen because the exponential distribution is a simplistic, continuous representation of an age structure decaying over time and is a special case of the gamma distribution (Casella and Berger 2002), which contains one more parameter, but is flexible enough to characterize vagaries in the sampled age composition attributable to trends in recruitment and (or) sampling selectivity.

The complete likelihood function for the RE model is given by

© 2007 NRC Canada

Fig. 5. Proportional error ((estimated – true)/true) among four life histories in the estimates of the von Bertalanffy growth function (VBGF) parameter k for the two random effects (RE_Exp, random effects with exponential distribution; RE_Gamma, random effects with gamma distribution) and three standard nonlinear (SNL_A, averages of multiple reads; SNL_M, medians of multiple reads; SNL_P, primary reads only) methods when the number of individuals (i) sampled is either 100 or 500 and 3 or 5 age reads (j) are made. Box plot description: median, bold solid line; 1st and 3rd interquartile range, box; 1.5 times the interquartile range, whiskers; outliers, circles. The horizontal line denotes zero error. (*a*) Life history 1; (*b*) life history 2; (*c*) life history 3; (*d*) life history 4.

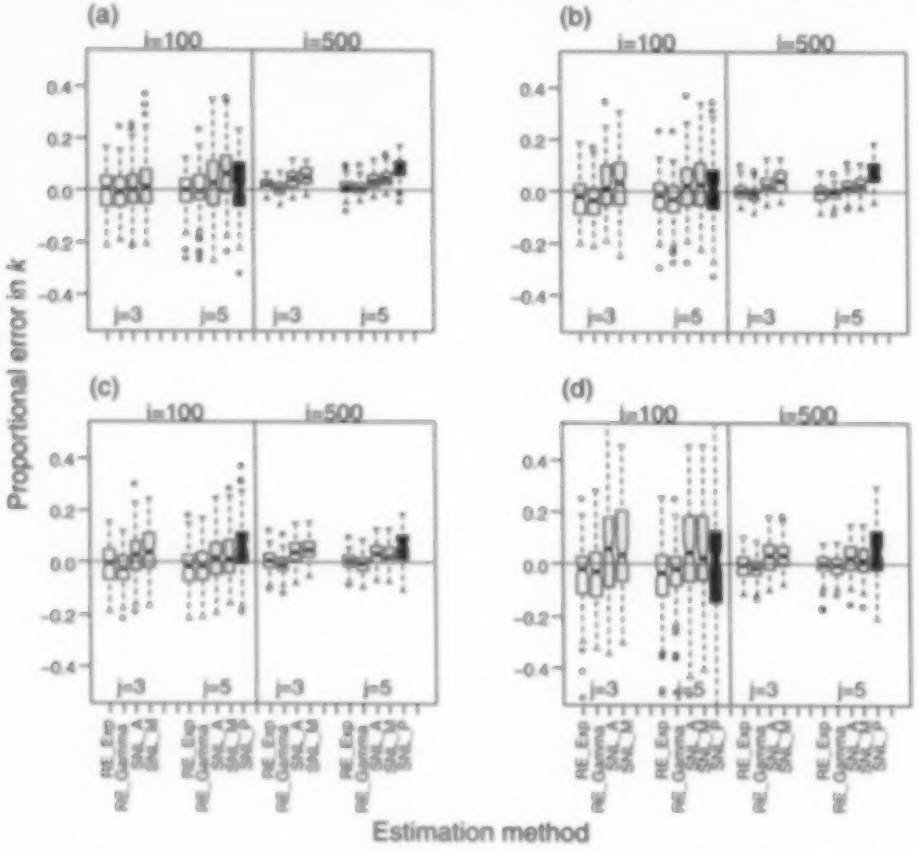

(*i*) Exponential model:

$$L = \prod_i \int \frac{1}{\sqrt{2\pi}\,\sigma_{L,i}} \exp\left[-\frac{(l_i - L_T)^2}{2\sigma_{L,i}^2}\right] \prod_j \frac{1}{\sqrt{2\pi}\,\sigma_{T,i}} \times \exp\left[-\frac{(l_{ij} - T_i)^2}{2\sigma_{T,i}^2}\right] \lambda \exp(-\lambda T)\,dT \quad (6)$$

(*ii*) Gamma model:

$$L = \prod_i \int \frac{1}{\sqrt{2\pi}\,\sigma_{L,i}} \exp\left[-\frac{(l_i - L_T)^2}{2\sigma_{L,i}^2}\right] \prod_j \frac{1}{\sqrt{2\pi}\,\sigma_{T,i}} \times \exp\left[-\frac{(l_{ij} - T_i)^2}{2\sigma_{T,i}^2}\right] \frac{(T/\beta)^{(\gamma-1)} \exp[-(T/\beta)]}{\beta\Gamma(\gamma)}\,dT \quad (7)$$

The RE model was implemented using the AD Model Builder RE module (ADMB-RE; Otter Research Ltd. 2005*b*), which is based on using the Laplace approximation to integrate over the random effects (Skaug and Fournier 2006) and partial separability of the objective function to increase computational efficiency and speed when handling hundreds to thousands of random effects (Gay 1996). Table 1 lists all the parameters for each method and indicates which are estimated either internal or external to the model.

Simulation testing

Base case

Lengths with multiple age reads were generated to evaluate the ability of the three SNL and two RE methods to estimate the values for the VBGF parameters. An (operating) model that captures relevant processes and dynamics with known relationships and produces data with acceptable error structures was created and used to generate artificial data sets. These data sets were then used by each of the estimation methods, and the resulting estimated parameter values were compared with true values.

© 2007 NRC Canada

Fig. 6. Box plots of the asymptotic standard deviations (solid lines within box) for the von Bertalanffy growth function (VBGF) growth parameter k for 100 simulations compared with the root mean square error (RMSE, broken lines).

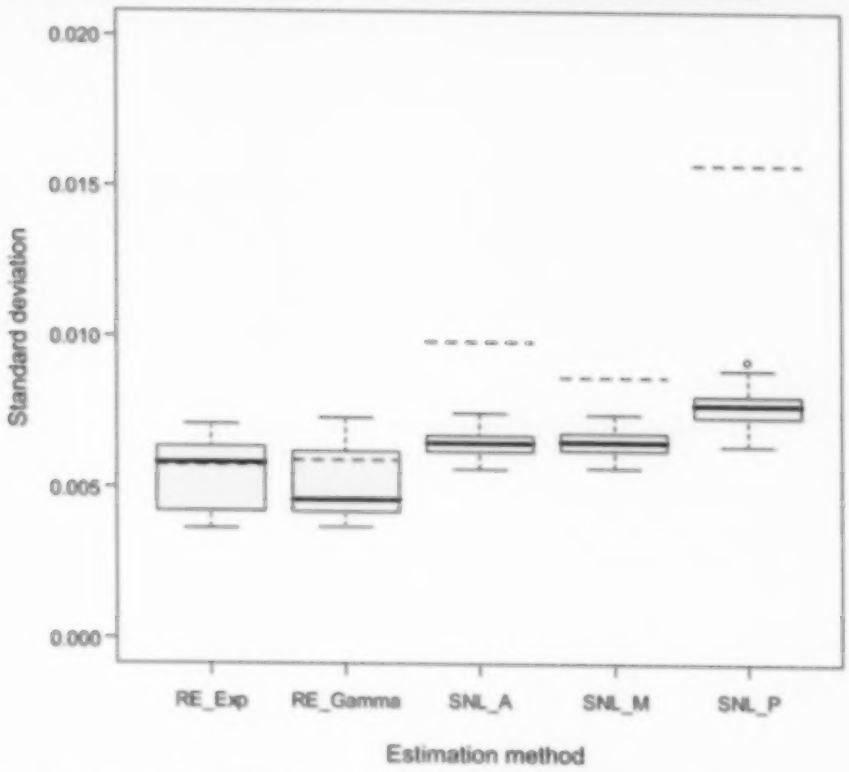

Data generation began by first simulating an age-structured population from which to sample the true ages. Four life histories were considered, corresponding roughly to the blackgill (*Sebastes melanostomus*), blue (*Sebastes mystinus*), olive (*Sebastes serranoides*), and calico (*Sebastes dalli*) rockfishes and differing in longevity (ω), natural mortality (M), and age-specific selectivity (Table 2). Sampled populations of true ages (Fig. 2) were created through the interaction of M, lognormal recruitment variability (σ_R), and a two-parameter (ϕ_1, ϕ_2) model of logistic selectivity interact to create a sampled population of true ages

$$\phi_l = [1 + \exp[-\log(19)(L_s - \phi_1)/\phi_2]]^{-1} \quad (8)$$

where ϕ_l is selectivity at length l, ϕ_1 is the length at 50% selectivity (determined by age), and ϕ_2 is the difference between the length at 95% selectivity and that at 50% selectivity. A specified number (either 100 or 500) of true-aged individuals was then sampled from this population. Length at age was then calculated using eqs. 1 and 2 with process error based on a CV_L set to 0.1 (Bowker 1995). The ratio M/k was set to 1.65 (Charnov 1993), so specifying M also specified the VBGF k value. Multiple age reads (either 3 or 5) were generated from each true age assuming a constant ageing observation error CV_T of 0.1 (Campana 2001; Dunn et al. 2002). The base case parameter values for each life history are listed (Table 2). After generating the length-at-age data, each of the five methods was then applied and the resulting parameter estimates were stored. This data-generation – model fit procedure was repeated for a total of 100 simulations for each life history, estimation method, and individual–read combination (Fig. 3).

Sensitivities

The sensitivity of the simulation results to the specifications of the base case operating model was explored by changing the values assumed for the extent of length error, ageing error, selectivity, and recruitment variation. High and low values for each of these processes were specified for life history 3 (Table 2) to capture a realistic range of values. In addition, the impact of violating the assumption that the ageing error CV is independent of age was explored in three ways: (*i*) CV_T increasing from 0.05 to 0.20 across all ages (trial: ΔCV_T low), (*ii*) CV_T increasing from 0.10 to 0.20 from ages 10 to 30 (trial: ΔCV_T high), and (*iii*) CV_T increasing from 0.10 to 0.20 from ages 10 to 30 with selectivity modified to include the sampling of more older ages (trial: ΔCV_T, selectivity high; Table 2).

Results

Base case

Performance of the various estimation methods is consistent across the four life histories (Figs. 4 and 5). Little gain in accuracy (no error in median estimation) or precision (spread of the box plot) is evident when the number of reads

© 2007 NRC Canada

Fig. 7. Proportional error in the estimate of the von Bertalanffy growth function (VBGF) growth parameter k for sensitivities based on varying the extent of (*a*) length and (*b*) ageing error; (*c*) sampling selectivity; and (*d*) recruitment variability.

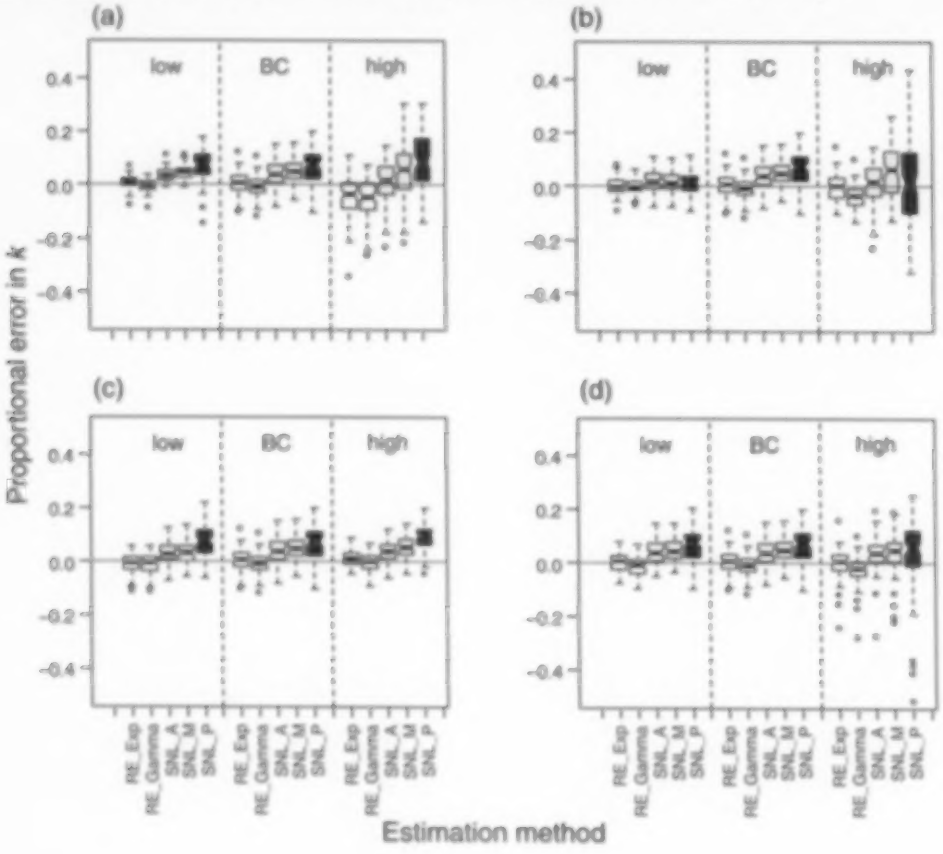

was increased from 3 to 5 (a subset of trials using only 2 reads also showed little difference from those using 3), but both accuracy and precision increased when the number of individuals sampled increased from 100 to 500 (i.e., improved estimates of the VBGF parameters k and L_∞ occur with increased sampling, rather than with the number of times an individual is aged).

The estimates of L_∞ and k showed less proportional error when derived from the RE methods (Figs. 4 and 5). Both RE and SNL methods demonstrated bias when sample size was low, but precision was always greatest with the RE approaches. When the number of individuals sampled increased, the RE approaches were both more accurate and precise. This is particularly apparent when estimating k; SNL methods tended to overestimate the value of this parameter (Fig. 5). The estimates of k were the most biased and least precise when only the primary read was used. Imprecision tended to also increase as M increased (e.g., compare the results for life history 1 with those for life history 4 in Fig. 5). Precision is an important consideration when evaluating the overall usefulness of each method, because one will not usually have the luxury of 100 samples of 500 individuals, so a method with poor precision may result in estimates that differ substantially from the true values. The high precision of the RE methods compared with the SNL methods may translate into important differences when applied to typical age and growth data (see forthcoming applied examples).

Proportional error was lower for L_∞ (Fig. 4) than for k (Fig. 5) and was negatively correlated between these two parameters (e.g., positive proportional error in L_∞ meant negative proportional error in the k). This correlation is as expected given the known correlation between these parameters (Quinn and Deriso 1999).

The asymptotic standard deviations (based on inverting the Hessian matrix) for the estimates of k are lowest for the RE methods (Fig. 6), although all of the methods had relatively low standard deviations. The asymptotic standard deviations for the RE methods provide a better reflection of the true error associated with estimating k than is the case for the SNL methods (Fig. 6).

Sensitivities: life history 3 (500 individuals, 3 reads)

Sensitivity results are shown only for k and life history 3 when 500 individuals are sampled and when 3 age reads are made. We chose this subset because there was very little qualitative difference in the results among the four life histo-

© 2007 NRC Canada

Fig. 8. Proportional error in the estimate of the von Bertalanffy growth function (VBGF) growth parameter k for sensitivity trials based on changing CV_T with age. BC refers to the base case for life history 3. The specifications of the other trials can be found in Table 2.

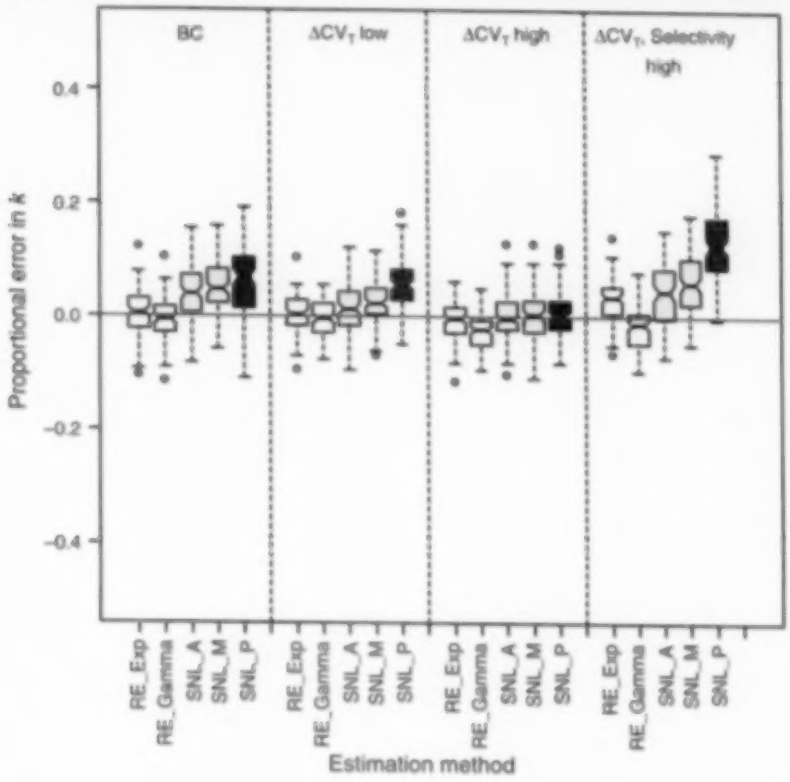

ries, between L_∞ and k, and between 3 and 5 age reads when 500 individuals were sampled.

Both RE methods are robust to the factors considered in the sensitivity analysis. Specifically, the RE methods always exhibited the greatest precision and often the highest accuracy (Fig. 7). Increasing length error and recruitment variability led to the greatest overall decrease in precision. High length error also led to a negative bias in the estimate of k for the RE methods, whereas all levels of length and ageing error, selectivity, and recruitment variability led to positive biases for the SNL methods. The SNL method based on the primary read only (SNL_P in Fig. 7) was particularly sensitive to factors considered in the sensitivity analyses. Precision in the SNL methods was also sensitive to high ageing error. Increasing recruitment variation generally led to poorer precision, but had little effect on accuracy, whereas all methods were relatively insensitive to changes in selectivity.

The RE approaches remain the most accurate and precise even when CV_T changes linearly with age (Fig. 8). There is little difference between the base case and the ΔCV_T low trial because overall, the amount of ageing error is similar. The differences between the methods are less apparent in the ΔCV_T high trial, but this is attributable to fewer ages with ageing error being sampled. When the number of ages with ageing error being sampled is increased (trial ΔCV_T, high selectivity), the advantages of using the RE approaches are again apparent, particularly when the gamma distribution is assumed. Low selectivity across much of the younger ages causes the exponential distribution to be a poor approximation to the sampled population, whereas the gamma distribution captures this selectivity, providing more accurate and precise estimates of k than the other methods.

Varying the specifications of the operating model had little influence on the estimates of CV_L among the RE methods, and these estimates were generally precise and accurate (Fig. 9*a*). However, the estimates of CV_L among the SNL methods were biased for most of the trials. The greatest inaccuracy and imprecision in SNL methods resulted from low length error and high ageing error. This bias is attributable to ageing error increasing the estimate of process error. Only when ageing error was low did the SNL methods estimate the extent of process error with low bias. Estimates of CV_L were generally insensitive to selectivity and recruitment variability.

The estimates of CV_T do not depend on the choice of how the age structure of the sampled population is modeled (gamma or exponential), because they are based on eq. 5. These estimates are generally positively biased (a product of estimating the CV from few age reads), but the extent of bias is generally insensitive to the specifications of the oper-

© 2007 NRC Canada

Fig. 9. Proportional error in the estimates of (*a*) length error (CV_L) and (*b*) ageing error (CV_T) for the base case (BC) and the sensitivity trials. For the length error plot, each trial grouping reads, from left to right, RE_Exp, RE_Gamma, SNL_A, SNL_M, and SNL_P. For the ageing error plot, the proportional error shown is for the random effects methods.

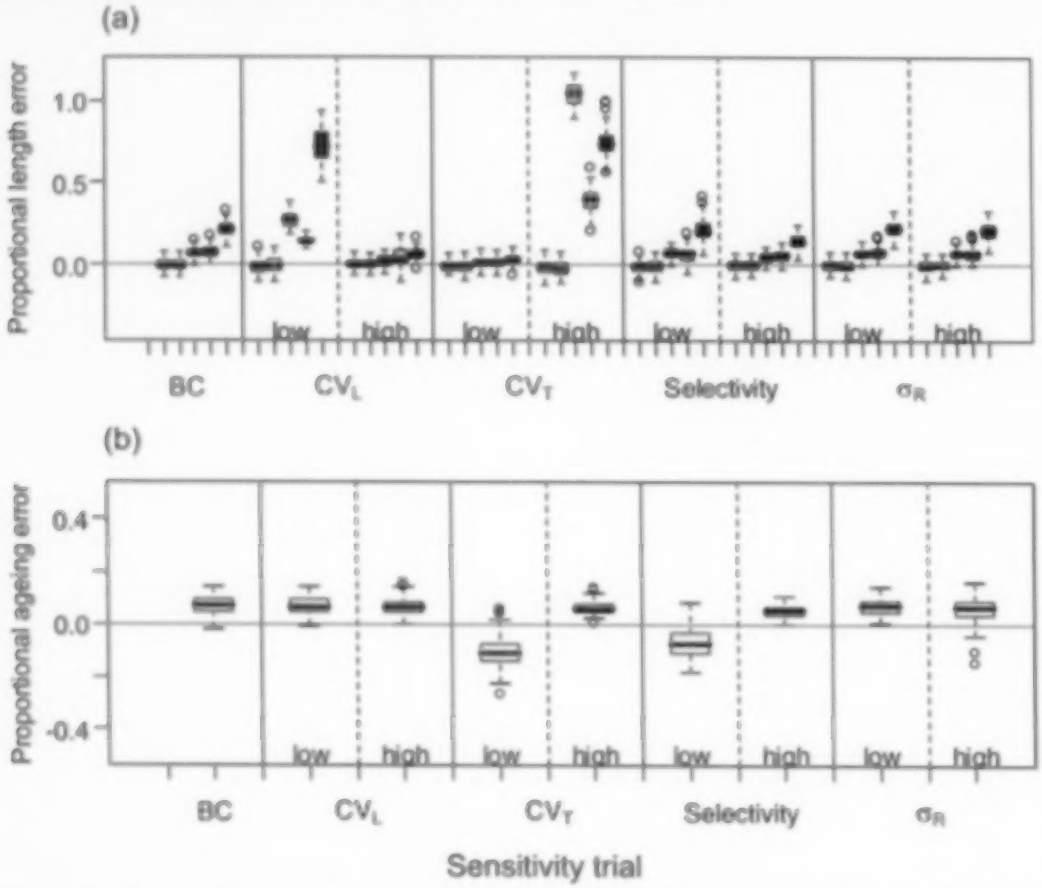

ating model (Fig. 9*b*). However, the extent of overestimation was relatively low and had no impact on the estimation of the VBGF parameters, thus perhaps explaining the negligible difference in parameter estimation when 5 age reads were used (Fig 5).

Applying the RE methods: examples

Four examples of applying the VBGF estimation methods are given in Table 3. This table proceeds from relatively faster to slower life histories, and the examples differ in gender, number of individuals aged, and number of age reads available. The differences in the estimates of k between the exponential and gamma RE models for female sand sole, female greenspotted rockfish, and male cabezon are indicative of strong selection for older individuals in the sampled population. This strong selection also biases the estimates from the SNL methods (illustrated in Table 3). Additionally, differences in results between the RE and SNL methods for sand sole and cabezon can be attributed to the relatively large amount of ageing error. The results for male greenspotted rockfish and blackgill rockfish differ little among the RE and average and (or) median SNL approaches. It is noteworthy that except for blackgill rockfish, the estimates of k from the SNL_P approach differs the most from the other methods.

Discussion

Since the inception of the VBGF (von Bertalanffy 1934, 1938), there has been a steady evolution in its use and estimation. Beverton and Holt (1957) popularized the current form of the VBGF by changing the original three-parameter formulation to include t_0 rather than L_0. Several estimation techniques, ranging from linear fitting (Walford 1946; Stamatopoulos and Caddy 1989) to nonlinear least squares (Tomlinson and Abramson 1961; Marquardt 1963), iterative fitting (Rafail 1973), and likelihood (Kimura 1980) methods have subsequently been proposed. Kimura (2000) then suggested a functional regression approach to explicitly incorporate ageing error. The RE approach developed here is a natural step in the evolution of fitting growth curves, as it makes maximum use of information contained in multiple-aged individuals. The RE approach performs better than traditional methods across a wide range of life histories and under different rates of process and observation error, sam-

© 2007 NRC Canada

Table 3. Results of fitting the von Bertalanffy growth function to age and length data with multiple reads for four species based on the five estimation methods.

				Sample size		L_∞ (mm)		k (year^{-1})		t_0 (year)		Error	
Species	Gender	Method	No. of reads	N	n	Mean	SD	Mean	SD	Mean	SD	Length	Age
Sand sole (*Psettichthys melanostictus*)[a]	F	RE_Exp	2	426	269	388	7	0.688	0.065	–0.01	0.10	0.10	0.24
		RE_Gamma	2	426	269	410	8	0.566	0.031	0.00	0.00	0.09	0.24
		SNL_A/M	2	426	269	385	6	0.652	0.064	–0.29	0.12	0.10	—
		SNL_P	1	426	—	375	5	0.780	0.074	–0.26	0.11	0.10	—
	M	RE_Exp	2	178	121	348	38	0.414	0.156	–0.84	0.44	0.13	0.25
		RE_Gamma	2	178	121	359	45	0.432	0.168	–0.57	0.38	0.13	0.25
		SNL_A/M	2	178	121	331	20	0.468	0.113	–0.92	0.30	0.10	—
		SNL_P	1	178	—	311	12	0.604	0.123	–0.72	0.26	0.10	—
Cabezon (*Scorpaenichthys marmoratus*)[b]	F	RE_Exp	3	379	379	612	18	0.203	0.014	–1.27	0.08	0.11	0.17
		RE_Gamma	3	379	379	615	19	0.200	0.014	–1.27	0.08	0.11	0.17
		SNL_A	3	379	379	593	14	0.222	0.013	–1.22	0.07	0.10	—
		SNL_M	3	379	379	584	13	0.232	0.014	–1.19	0.07	0.10	—
		SNL_P	1	379	—	546	10	0.284	0.018	–1.16	0.09	0.10	—
	M	RE_Exp	3	238	238	424	7	0.478	0.038	–0.74	0.09	0.10	0.20
		RE_Gamma	3	238	238	426	7	0.465	0.038	–0.76	0.09	0.10	0.20
		SNL_A	3	238	238	420	6	0.508	0.037	–0.71	0.09	0.10	—
		SNL_M	3	238	238	422	6	0.485	0.038	–0.83	0.10	0.10	—
		SNL_P	1	238	—	409	5	0.582	0.051	–0.74	0.10	0.10	—
Greenspotted rockfish (*Sebastes chlorostictus*)[a]	F	RE_Exp	2	180	80	380	10	0.087	0.005	0.00	0.00	0.07	0.12
		RE_Gamma	2	180	80	402	14	0.077	0.005	0.00	0.00	0.07	0.12
		SNL_A/M	2	180	80	373	17	0.092	0.100	0.40	1.03	0.10	—
		SNL_P	1	180	—	383	25	0.072	0.100	–2.44	2.01	0.10	—
	M	RE_Exp	2	150	50	404	16	0.074	0.009	–0.50	0.72	0.07	0.09
		RE_Gamma	2	150	50	412	19	0.072	0.009	–0.29	0.75	0.07	0.09
		SNL_A/M	2	150	50	401	21	0.074	0.100	–0.62	0.87	0.10	—
		SNL_P	1	150	—	410	23	0.069	0.100	–0.86	0.91	0.10	—
Blackgill rockfish (*Sebastes melanostomus*)[c]	C	RE_Exp	2,3	112	108, 94	495	27	0.057	0.012	–0.50	2.01	0.16	0.13
		RE_Gamma	2,3	113	108, 95	499	28	0.056	0.012	–0.35	2.01	0.16	0.13
		SNL_A	2,3	114	108, 96	500	18	0.057	0.008	–0.87	1.39	0.10	—
		SNL_M	2,3	115	108, 97	503	19	0.054	0.008	–1.91	1.44	0.10	—
		SNL_P	1	116	—	492	19	0.057	0.009	–2.54	1.80	0.10	—

Note: When there are only two reads, the average and median age methods are the same (denoted here as SNL_A/M). Gender designations are as follows: F, female; M, male; C, combined gender data. The number of reads includes the primary read and may be a mixture of one to two additional reads (e.g., blackgill rockfish). N, total number of primary reads; n, total number of additional reads (not all ageing structures were read more than once).

[a]Don Pearson, NOAA Fisheries, Southwest Fisheries Science Center, Fisheries Ecology Division, 110 Shaffer Road, Santa Cruz, CA 95060, USA, unpublished data.

[b]Grebel 2003.

[c]Stevens et al. 2004.

© 2007 NRC Canada

pling conditions, and assumed population dynamics. Beyond benefits to model fitting, the RE approach may also provide information on the underlying population the samples are taken from and thus be informative of other population parameters, such as mortality rate. The general RE framework is also flexible enough to be extended to other growth models (e.g., the Gompertz or Schnute growth models; Schnute 1981).

The need for proper age estimates and subsequent growth models that incorporate uncertainty in ageing has been recognized for years (Lai and Gunderson 1987; Campana 2001). The general method presented here addresses this need and offers two main advantages over traditional growth curve estimation methods.

Including ageing error

First and most obviously, the RE method explicitly accounts for ageing error. The RE method is advantageous compared with functional regression approaches because it does not require the specification of an error ratio that is usually only roughly estimated. The only unknown parameter in the RE method not estimated by maximizing the likelihood function (σ_r) can be estimated directly from the multiple age reads and showed little influence on growth curve estimation even when estimated with some bias. Even when the extent of ageing error changes with age, the assumption of a constant ageing error CV is robust, although a simple modification to the likelihood functions (eqs. 6 and 7) could explicitly account for the ageing error CV changing with age.

There are still issues concerning ageing error that need further consideration. The simulations used here ignore bias in age reading. Although nonrandom errors between readers can be corrected with further training, systematic nonrandom errors in the growth structure itself can be harder to resolve (Campana 2001). In addition, ageing error may become skewed for older individuals (e.g., underageing of older individuals). Exploring the impact of alternative formulations of ageing error (i.e., log-normal) in the RE method using simulations may help address this issue.

Likewise, alternative assumptions regarding process error can also be explored with alternative model formulations. Bowker (1995) demonstrated that the CV of length in many fish decreases with age. A simple modification to the present model is to allow the CV in length to change with age, though the qualitative results presented here are not expected to change.

Accounting for selectivity

Second, the RE method treats the ages represented in the sample as random. This is a key reason for improved performance when different portions of the population are sampled and for the overall stability–precision of the RE method. Besides the exponential and gamma models, other distributions may more appropriately describe the sampling of ages. These can easily be accounted for by modifying the likelihood for the true age distribution in eqs. 6 or 7. Based on the current results, the gamma is recommended over the exponential distribution given that it is more flexible, has only one additional parameter, and contains the exponential distribution as a special case. This advantage is most apparent when selectivity for the younger ages is low.

One caveat of the current model formulation is that it does not correct for selectivity of individuals with varying growth rates (k) or maximum sizes (L_∞). Overall, selectivity can be visualized in two dimensions, of which the current method only corrects for the first: (*i*) selectivity across size and age classes and (*ii*) selectivity across variability of growth within a given size or age class. Therefore, younger, faster-growing and older, slower-growing individuals may be disproportionately represented in a given sample, leading to biased estimation of growth parameters (Parma and Deriso 1990; Vaughan and Burton 1994; Sinclair et al. 2002). One way to approach this problem may be to reformulate selectivity as a function of length rather than of age, a more realistic representation of selectivity. Troynikov (1999) and Taylor et al. (2005) introduce ways to account for size-selective mortality when estimating the standard process error formulation of the VBGF. Further investigation is needed to determine how these or other ideas may be incorporated into the RE method to account for size-selective mortality.

General recommendations

The inclusion of ageing error and the use of an RE framework in the estimation of the VBGF is an improvement over other standard, nonlinear estimation approaches. This highlights the importance of recording ageing error when undertaking age and growth studies. Typically only 20%, if any, of the ageing structures are reread (Kimura and Lyons 1991; Kimura and Anderl 2005). This number is sufficient for characterizing general ageing imprecision and bias, as well as assessing quality control among readers, but reduces the ability to account for the influence of ageing error in age and growth fits. Often the decision is made to allocate finite resources to ageing more individuals only once rather than ageing fewer individuals more times. This study demonstrates consistent bias in parameter estimates when using only one age read regardless of the sample size and method used to incorporate the information obtained from multiple reads. This study also demonstrates that two or three reads is generally sufficient to adequately characterize the ageing error, and we recommend more effort be allocated to collecting and ageing more fish once this minimum number of reads is acquired. Although the RE approach works with a mixed data set of singly and multiply aged individuals, increasing the number of multiple-aged fish within a study may lead to substantial and biologically relevant improvements to growth fits.

Acknowledgements

A self-standing, executable program that interacts with Microsoft® Excel to perform the RE methods described in this paper is available from JMC for general use. Thanks go to A. MacCall for the initial brainstorming session that lead to this investigation. Thanks go to D. Fournier and H. Skaug for their assistance regarding ADMB-RE. B. Horness, D. Pearson, and M. Schirripa were generous in providing ageing samples from NOAA Fisheries surveys for use in testing these methods. Thanks also go to J. Grebel, B. Matta, and M. Stevens for providing age and growth data sets to ex-

© 2007 NRC Canada

plore. Z.T. A'mar, G. Fay, M. Haltuch, and D. Kinzey provided considerable discussion during this work, and two anonymous reviewers offered valuable suggestions that greatly improved the presentation and readability of this paper. Support for JMC and AEP was provided by National Marine Fisheries Service (NMFS) grant NA07FE0473.

References

Appledoorn, R.S. 1982. Variation in the growth rate of *Mya arenaria* and its relationship to the environment as analyzed through principle component analysis and the omega parameter of the von Bertalanffy equation. Fish. Bull. **81**: 75–84.

Beamish, R.J., and Fournier, D.A. 1981. A method for comparing the precision of a set of age determinations. Can. J. Fish. Aquat. Sci. **38**: 982–983.

Beverton, R.J.H. 1992. Patterns of reproductive strategy parameters in some marine teleost fishes. J. Fish Biol. **41**(Suppl. B): 137–160.

Beverton, R.J.H., and Holt, S.J. 1957. On the dynamics of exploited fish populations. Chapman and Hall, London, UK.

Beverton, R.J.H., and Holt, S.J. 1959. A review of the life-spans and mortality rates of fish in nature, and their relationship on growth and other physiological characteristics. *In* Ciba Foundation Colloquia on Ageing. Vol. 5. The lifespan of animals. J. & A. Churchill Ltd., London, UK.

Bowker, D.W. 1995. Modeling the patterns of dispersion of length at age in teleost fishes. J. Fish Biol. **46**(3): 469–484.

Bradford, M.J. 1991. Effects of ageing errors on recruitment time series estimated from sequential population analysis. Can. J. Fish. Aquat. Sci. **48**: 555–558.

Cailliet, G.M., and Goldman, K.J. 2004. Age determination and validation in chondrichthyan fishes. *In* Biology of sharks and their relatives. *Edited by* J. Carrier, J.A. Musick, and M.R. Heithaus. CRC Press LLC, Boca Raton, Fla. pp. 399–447.

Cailliet, G.M., Yudin, K.G., Tanaka, S., and Taniuchi, T. 1990. Growth characteristics of two populations of *Mustelus manazo* from Japan based upon cross-readings of vertebral bands. NOAA Tech. Rep. No. 90.

Campana, S.E. 2001. Accuracy, precision and quality control in age determination, including a review of the use and abuse of age validation methods. J. Fish Biol. **59**(2): 197–242.

Campana, S.E., Annand, M.C., and McMillan, J.I. 1995. Graphical and statistical methods for determining the consistency of age determination. Trans. Am. Fish. Soc. **124**: 131–138.

Casella, G., and Berger, R.L. 2002. Statistical inference. Duxbury, Pacific Grove, Calif.

Chang, W.Y.B. 1982. A statistical method for evaluating the reproducibility of age determination. Can. J. Fish. Aquat. Sci. **39**: 1208–1210.

Charnov, E.L. 1993. Life history invariants: some explorations of symmetry in evolutionary ecology. Oxford University Press, Oxford, UK.

Chen, Y., Jackson, D.A., and Harvey, H.H. 1992. A comparison of von Bertalanffy and polynomial functions in modeling fish growth data. Can. J. Fish. Aquat. Sci. **49**: 1228–1235.

Clark, W.G. 1991. Groundfish exploitation rates based on life history parameters. Can. J. Fish. Aquat. Sci. **48**: 734–750.

Closs, J.E., and Nichols, F.H. 1978. A von Bertalanffy growth model with a seasonally varying coefficient. J. Fish. Res. Board Can. **35**: 1479–1482.

Dunn, A., Francis, R.I.C.C., and Doonan, I.J. 2002. Comparison of the Chapman–Robson and regression estimators of *Z* from catch-curve data when non-sampling stochastic error is present. Fish. Res. **59**(1–2): 149–159.

Evans, G.T., and Hoenig, J.M. 1998. Testing and viewing symmetry in contingency tables, with application to readers of fish ages. Biometrics, **54**: 620–629.

Fabens, A.J. 1965. Properties and fitting of the von Bertalanffy growth curve. Growth, **29**: 265–289.

Gay, D. 1996. More AD of nonlinear AMPL models: computing Hessian information and exploiting partial separability. *In* Computational differentiation: techniques, applications, and tools. *Edited by* M. Berz, C. Bischof, G. Corliss, and A. Griewank. Society for Industrial and Applied Mathematics (SIAM), Philadelphia, Pa. pp. 173–184.

Grebel, J.M. 2003. Age, growth, and maturity of cabezon, *Scorpaenichthys marmoratus*, in California. M.S. thesis, Moss Landing Marine Laboratories, San Jose State University, Calif.

Gulland, J.A. 1983. Fish stock assessment: a manual of basic methods. John Wiley & Sons, Chichester, UK.

Haddon, M. 2001. Modelling and quantitative methods in fisheries. Chapman and Hall, London, UK.

Jensen, A.L. 1998. Simulation of relations among fish life history parameters with a bioenergetics-based population model. Can. J. Fish. Aquat. Sci. **55**(2): 353–357.

Kimura, D.K. 1980. Likelihood estimates for the von Bertalanffy growth curve. Fish. Bull. **77**: 765–776.

Kimura, D.K. 2000. Using nonlinear functional relationship regression to fit fisheries models. Can. J. Fish. Aquat. Sci. **57**(1): 160–170.

Kimura, D.K., and Anderl, D.M. 2005. Quality control of age data at the Alaska Fisheries Science Center. Mar. Freshw. Res. **56**(5): 783–789.

Kimura, D.K., and Lyons, J.J. 1991. Between-reader bias and variability in the age-determination process. Fish. Bull. **89**(1): 53–60.

Lai, H.L., and Gunderson, D. 1987. Effects of ageing error on estimates of growth, mortality and yield per recruit for walleye pollock (*Theragra chalcogramma*). Fish. Res. **5**: 287–302.

Marquardt, D.W. 1963. An algorithm for least-squares estimation of nonlinear parameters. J. Soc. Indust. Appl. Math. **11**(2): 431–441.

Nummi, T. 2000. Analysis of growth curves under measurement errors. J. Appl. Stat. **27**(2): 235–243.

Otter Research Ltd. 2005*a*. An introduction to AD Model Builder. Version 7.0.1. For use in non-linear modeling and statistics. Otter Research Ltd., Sydney, B.C.

Otter Research Ltd. 2005*b*. Random effects in AD Model Builder: ADMB-RE user guide. Otter Research Ltd., Sydney, B.C.

Palmer, M.J., Phillips, B.F., and Smith, G.T. 1991. Application of nonlinear models with random coefficients to growth data. Biometrics, **47**: 623–635.

Parma, A.M., and Deriso, R.B. 1990. Dynamics of age and size composition in a population subject to size-selectivity mortality: effects of phenotypic variability in growth. Can. J. Fish. Aquat. Sci. **47**: 274–289.

Pilling, G.M., Kirkwood, G.P., and Walker, S.G. 2002. An improved method for estimating individual growth variability in fish, and the correlation between von Bertalanffy growth parameters. Can. J. Fish. Aquat. Sci. **59**(3): 424–432.

Piner, K.R., Hamel, O.S., Menkel, J.L., Wallace, J.R., and Hutchinson, C.E. 2005. Age validation of canary rockfish (*Sebastes pinniger*) from off the Oregon coast (USA) using the bomb radiocarbon method. Can. J. Fish. Aquat. Sci. **62**(5): 1060–1066.

Piner, K.R., Wallace, J.R., Hamel, O.S., and Mikus, R. 2006. Evaluation of ageing accuracy of bocaccio (*Sebastes paucispinis*) rockfish using bomb radiocarbon. Fish. Res. **77**(2): 200–206.

© 2007 NRC Canada

Pitcher, T.J., and MacDonald, P.D.M. 1973. Two models for seasonal growth in fishes. J. Appl. Ecol. **10**(2): 599–606.

Prajneshu, and Venugopalan, R. 1999. von Bertalanffy growth model in a random environment. Can. J. Fish. Aquat. Sci. **56**: 1026–1030.

Quinn, T.J., and Deriso, R.B. 1999. Quantitative fish dynamics. Oxford University Press, New York.

Rafail, S.Z. 1973. A simple and precise method for fitting a von Bertalanffy growth curve. Mar. Biol. **19**: 354–358.

Reeves, S.A. 2003. A simulation study of the implications of age-reading errors for stock assessment and management advice. ICES J. Mar. Sci. **60**(2): 314–328.

Richards, L.J., Schnute, J.T., Kronlund, A.R., and Beamish, R.J. 1992. Statistical models for the analysis of ageing errors. Can. J. Fish. Aquat. Sci. **49**(9): 1801–1815.

Sainsbury, K.J. 1980. Effect of individual variability on the von Bertalanffy growth equation. Can. J. Fish. Aquat. Sci. **37**: 241–247.

Schnute, J.T. 1981. A versatile growth model with statistically stable parameters. Can. J. Fish. Aquat. Sci. **38**: 1128–1140.

Sinclair, A.F., Swain, D.P., and Hanson, J.M. 2002. Disentangling the effects of size-selective mortality, density, and temperature on length-at-age. Can. J. Fish. Aquat. Sci. **59**(2): 372–382.

Skaug, H., and Fournier, D. 2006. Automatic approximation of the marginal likelihood in non-Gaussian hierarchical models. Computational Statistics & Data Analysis, **51**: 699–709.

Stamatopoulos, C., and Caddy, J.F. 1989. Estimation of von Bertalanffy growth parameters: a versatile linear regression approach. J. Cons. Int. Explor. Mer, **45**: 200–208.

Stevens, M.M., Andrews, A.H., Cailliet, G.M., Coale, K.H., and Lundstrom, C.C. 2004. Radiometric validation of age, growth, and longevity for the blackgill rockfish (*Sebastes melanostomus*). Fish. Bull. **102**(4): 711–722.

Taylor, N.G., Walters, C.J., and Martell, S.J.D. 2005. A new likelihood for simultaneously estimating von Bertalanffy growth parameters, gear selectivity, and natural and fishing mortality. Can. J. Fish. Aquat. Sci. **62**(1): 215–223.

Tomlinson, P.K., and Abramson, N.J. 1961. Fitting a von Bertalanffy growth curve by least squares. California Department of Fish and Game, Sacramento, Calif. Fish. Bull. No. 116.

Troynikov, V.S. 1999. Use of Bayes theorem to correct size-specific sampling bias in growth data. Bull. Math. Biol. **61**: 355–363.

Tyler, A.V., Beamish, R.J., and McFarlane, G.A. 1989. Implications of age determination errors to yield estimates. *In* Effects of ocean variability on recruitment and an evaluation of parameters used in stock assessment models. *Edited by* R.J. Beamish and G.A. McFarlane. Can. Spec. Publ. Fish. Aquat. Sci. No. 108. pp. 27–35.

Vaughan, D.S., and Burton, M.L. 1994. Estimation of von Bertalanffy growth parameters in the presence of size-selected mortality: a simulated example with red grouper. Trans. Am. Fish. Soc. **123**(1): 1–8.

Venugopalan, R., and Prajneshu. 1997. von Bertalanffy growth model with autocorrelated errors. Indian J. Fish. **44**: 63–67.

von Bertalanffy, L. 1934. Untersuchungen uber die Gestzlichkeit des Wachstums. I. Teil. Allgemeine Grundlagen der Theorie; mathematische and physiologische Gesetzlichkeiten des Wachstums bei Wassertieren. Arch. Entwicklungsmech. Org. (Wilhelm Roux), **131**: 613–652.

von Bertalanffy, L. 1938. A quantitative theory of organic growth. Hum. Biol. **10**: 181–213.

Walford, L. 1946. A new graphical method of describing the growth of animals. Biol. Bull. **90**: 141–147.

Wang, Y.-G. 1998. An improved Fabens method for estimation of growth parameters in the von Bertalanffy model with individual asymptotes. Can. J. Fish. Aquat. Sci. **55**: 397–400.

Wang, Y.-G., and Ellis, N. 1998. Effect of individual variability on estimation of population parameters from length–frequency data. Can. J. Fish. Aquat. Sci. **55**: 2393–2401.

Wang, Y.-G., and Ellis, N. 2005. Maximum likelihood estimation of mortality and growth with individual variability from multiple length–frequency data. Fish. Bull. **103**: 380–391.

Wang, Y.-G., and Thomas, M.R. 1995. Accounting for individual variability in the von Bertalanffy growth model. Can. J. Fish. Aquat. Sci. **52**: 1368–1375.

Weatherley, A.H., and Gill, H.S. 1987. The biology of fish growth. Academic Press, London, UK.

Williams, E.H., and Shertzer, K.W. 2003. Implications of life-history invariants for biological reference points used in fishery management. Can. J. Fish. Aquat. Sci. **60**(6): 710–720.

© 2007 NRC Canada

Nonrandom mating in a broadcast spawner: mate size influences reproductive success in Atlantic cod (*Gadus morhua*)

Sherrylynn Rowe, Jeffrey A. Hutchings, and Jon Egil Skjæraasen

Abstract: We tested the hypothesis that reproductive success in Atlantic cod (*Gadus morhua*) is random with respect to similarity in body size between mates. Immediately prior to their natural breeding periods, groups of 52–93 cod from three Northwest Atlantic populations were transported to a large (15 m diameter, 4 m deep) tank where they spawned undisturbed at densities similar to those in nature. Based on microsatellite DNA-parentage assignment of 8913 offspring from four spawning groups, females and males achieved their highest reproductive success when breeding with mates that were larger than themselves. Our observations are consistent with the hypothesis that some form of intrasexual competition or mate choice is a constituent of the mating system of this species and that this can have an important influence on individual fitness. Our results further suggest that reductions in the mean and variance in body size of commercially exploited marine fishes concomitant with size-selective harvesting may have greater negative consequences for population recovery than previously thought.

Résumé : Nous éprouvons l'hypothèse qui veut que le succès reproductif chez la morue franche (*Gadus morhua*) soit aléatoire en ce qui a trait à la similarité de taille corporelle des partenaires. Immédiatement avant leur période de reproduction naturelle, nous avons placé des groupes de 52–93 morues provenant de trois populations du nord-ouest de l'Atlantique dans de grands bassins (diamètre de 15 m, profondeur de 4 m) dans lesquels ils ont frayé à loisir à des densités semblables à celles trouvées en nature. D'après la détermination de la filiation de 8913 rejetons de quatre groupes de fraye par l'analyse des microsatellites de l'ADN, les femelles et les mâles atteignent leur succès reproductif maximal lorsqu'ils s'accouplent avec des partenaires qui leur sont supérieurs en taille. Nos observations s'accordent avec l'hypothèse selon laquelle le système de reproduction de l'espèce inclut une forme quelconque de compétition intrasexuelle ou de choix de partenaire et que cela peut avoir un effet important sur la fitness individuelle. Nos résultats laissent croire, de plus, que les réductions de la moyenne et de la variance de la taille corporelle chez les poissons marins exploités commercialement qui coïncident avec les récoltes sélectives en fonction de la taille peuvent avoir des conséquences négatives plus importantes sur la récupération des populations qu'on ne le croyait jusqu'ici.

[Traduit par la Rédaction]

Introduction

It has been hypothesized that the resistance and resilience of a species to environmental perturbation can be affected by that species' mating system (Møller and Legendre 2001; Rowe and Hutchings 2003; Quader 2005). The link between population dynamics and components of mating systems may be particularly important among severely depleted species (Kokko and Rankin 2006), such as many marine fishes, subject to past and present exploitation. Fishing, for example, by preferentially harvesting individuals by size, age, growth rate, behaviour, or some combination thereof has the potential to impose strong differential mortality, and selection among heritable characteristics, within exploited populations (Stokes et al. 1993; Law 2000; Conover and Munch 2002). If this differential mortality should negatively affect mate choice, the structure of dominance hierarchies, or other constituents of a species' mating system, then rates of population decline attributable to exploitation may increase, and subsequent rates of recovery may decrease, with increased mating system complexity.

Reproduction in commercially exploited marine fishes is often portrayed as a behaviourally vacuous process in which individuals mate with one another largely at random (Breder and Rosen 1966; Nordeide and Folstad 2000). Support for this depiction is usually derived from the observation that these species are often broadcast spawners, releasing large numbers (typically hundreds of thousands and often millions) of very small (typically less than 1.5 mm diameter) eggs directly into the water column, often in several batches

Received 8 March 2006. Accepted 17 October 2006. Published on the NRC Research Press Web site at http://cjfas.nrc.ca on 14 February 2007.
J19212

S. Rowe.[1] Fisheries and Oceans Canada, Bedford Institute of Oceanography, P.O. Box 1006, Dartmouth, NS B2Y 4A2, Canada.
J.A. Hutchings. Department of Biology, Dalhousie University, Halifax, NS B3H 4J1, Canada.
J.E. Skjæraasen. Department of Biology, University of Bergen, N-5020 Bergen, Norway.

[1]Corresponding author (e-mail: RoweS@mar.dfo-mpo.gc.ca).

 doi:10.1139/F06-182 © 2007 NRC Canada

throughout a breeding season, and providing them with no parental care (Hutchings 2002; Rowe and Hutchings 2003). Because energetic investment per gamete is likely to be extremely low for both sexes, and the probability of survival to maturity for each egg is typically less than 1×10^{-6} (Chambers 1997), the fitness benefits of aggressively competing for mates or exerting mate choice may be negligible. Consequently, it might not be unreasonable to predict that breeding groups of marine fishes lack the behavioural complexity seen in bird and mammal mating systems and, instead, reproduce in an unstructured manner.

An emerging view is that the mating systems of marine fishes might be considerably more complex. For example, based on studies of spawning behaviour, it has been hypothesized that mate choice may be integral to the mating systems of marine fishes such as Atlantic cod (*Gadus morhua*) (Engen and Folstad 1999; Hutchings et al. 1999; Rowe and Hutchings 2006). In this species, release of gametes occurs during a ventral mount, in which the male positions himself directly beneath the female while grasping her with his pelvic fins and matching her swimming speed (Brawn 1961). Under these circumstances, it may be beneficial for mates to be similar in body size, such that their urogenital openings are aligned directly opposite one another during gamete release and that high fertilization success is achieved, a benefit that might be expected to favour size-based, positive assortative mating (Hutchings and Myers 1993; Rakitin et al. 2001; Bekkevold et al. 2002). Alternatively, it could also be argued that this pattern of assortative mating, commonly observed in salmonids (Foote 1988), could arise if individuals of both sexes prefer large individuals as mates. Given that fecundity and sperm volume increase with body size in fishes (Trippel and Morgan 1994; Wootton 1998; McIntyre and Hutchings 2003), selection might be expected to favour individuals that mate with larger fish than themselves if male and female reproductive success is limited primarily by the number of gametes with which individuals come into contact during spawning. This prediction is based on the analogy that the probability that a fertilized egg produced by a broadcast-spawning marine fish will survive to attain maturity is akin to winning a lottery; the greater the number of gametes, the greater the number of "lottery tickets", and the greater the probability of success. Surprisingly, notwithstanding its intuitive nature, the prediction that reproductive success increases with body size has rarely been empirically tested for broadcast-spawning marine fishes.

The potential for mating system complexity to influence the degree to which intense exploitation affects population growth rate led Rowe and Hutchings (2003) to articulate two predictions. Firstly, the probability that exploitation negatively affects reproductive success is predicted to increase with the prevalence of dominance hierarchies, territorial behaviour, and mate choice in mating systems. Secondly, rate of population decline and time to population recovery is predicted to increase with (*i*) intensity of mate competition, (*ii*) importance of mate choice to fitness, and (*iii*) the magnitude of sex bias and differential mortality with respect to phenotype in commercial harvests. Irrespective of the precise mechanism(s) resulting in individual variation in reproductive success, these predictions centre ultimately on the question of whether reproduction is random or biased with respect to phenotype, a question that has received little attention in broadcast-spawning, commercially exploited marine fishes such as Atlantic cod, haddock (*Melanogrammus aeglefinus*), and European plaice (*Pleuronectes platessa*).

We established experimental spawning groups to examine whether reproduction in Atlantic cod is random with respect to phenotype. In contrast with previous work (Hutchings et al. 1999; Rakitin et al. 2001; Bekkevold et al. 2002), our experimental facilities provided an unprecedented opportunity to study the breeding dynamics of a broadcast-spawning marine fish within large groups of individuals and, thus, at a scale that potentially allowed for more biologically meaningful behavioural interactions. Immediately prior to their natural spawning periods, Northwest Atlantic cod from geographically distinct regions were transferred to a large aquarium where they were allowed to spawn undisturbed in breeding groups of more than 50 individuals. Based on information obtained from four such groups, we partitioned data on individual body size and reproductive success by sex to test several hypotheses. Firstly, we tested the null hypothesis that individual reproductive success is independent of the body size similarity of potential mates. Upon rejection of this hypothesis, we then examined whether reproductive success was greatest when cod spawned with individuals smaller than, similar to, or larger than themselves. We tested this hypothesis separately for both sexes. Lastly, we examined the degree to which variability in a prominent mating behaviour of Atlantic cod is a reliable metric of individual reproductive success.

Materials and methods

Examination of parental fish and sampling of offspring

We examined fish from three spatially distinct areas in the Northwest Atlantic: Western Scotian Shelf, Southern Gulf of St. Lawrence, and Eastern Scotian Shelf, identified by the Northwest Atlantic Fishery Organization (NAFO) as divisions 4X, 4T, and 4W, respectively. Fish from each NAFO area were captured approximately 2–3 weeks prior to their annual spawning periods, individually tagged (using unique combinations of 7.5 cm long coloured T-bar anchor tags) and taken to the 684 m^3 Pool Tank at Dalhousie University (Halifax, Nova Scotia), where they were allowed to spawn undisturbed. Cod experienced water temperatures of ~8 °C, ambient photoperiods, and were fed Shurgain® 8 mm fish feed daily.

We quantified reproductive success of four groups of spawning cod (Table 1). Groups 1 and 3 were composed of cod from Western Scotian Shelf that spawned in 2001 and 2002, respectively. The spawning period for Western Scotian Shelf cod encompassed December through March. Group 2 comprised Southern Gulf of St. Lawrence cod that spawned from May through July 2001. Group 4 comprised cod from Eastern Scotian Shelf that spawned in November and December 2002.

Seawater was continuously pumped into the tank, and spawned eggs were collected by a plankton net covering the single tank outflow located at the surface. The plankton net was checked daily at ~1600 h, and any eggs present were extracted. Examination of the developmental stage of random

© 2007 NRC Canada

Table 1. Average body sizes (±1 standard error, SE) and sex ratios within four experimental groups of spawning Atlantic cod (*Gadus morhua*).

Group	Geographical location (year)	Sex	Mean length (cm)	SE	Length range (cm)	*N*
1	Western Scotian Shelf (2001)	Female	56.7	2.0	42.0–77.8	25
		Male	53.7	1.6	44.0–76.8	27
2	Southern Gulf of St. Laurence (2001)	Female	57.9	0.7	50.0–69.7	41
		Male	58.0	0.8	53.5–65.9	18
3	Western Scotian Shelf (2002)	Female	74.9	2.2	54.0–105.0	25
		Male	72.7	1.4	62.0–92.0	29
4	Eastern Scotian Shelf (2002)	Female	49.9	1.2	35.0–84.0	56
		Male	44.9	1.2	34.0–62.0	37

samples of eggs collected indicated that almost all had been freshly spawned and fertilized within the previous 24 h. Each batch of eggs was incubated at ~8 °C in 20 L containers with circulating seawater and aeration. When eggs were within ~24 h from hatching (groups 1–3) or larvae were within 7 days after hatching (group 4), a random sample of several thousand offspring from each batch was collected and stored in ethanol for subsequent genetic analysis.

Experiments were terminated and fish sacrificed when no eggs had been collected for at least 5 days. Blood samples were obtained from each individual and preserved in ethanol for pedigree analysis. We recorded total length of each individual to the nearest millimetre. We also determined sex and stage of maturity by observation of gross morphology of the gonad (Morrison 1990).

The behaviour of Southern Gulf of St. Lawrence cod in group 2 was recorded daily during the last 8 h of daylight (1200–2000 h) from 15 May 2001 through 14 July 2001 by four video cameras mounted above the tank and by a colour videotape recorder. Subsequent to the spawning season, all videotapes were reviewed (totaling 488 h of video coverage) to document the incidence of courtship behaviour, particularly ventral mounts, in the group and identities of the fish involved (whenever possible).

Genetic analysis

DNA was extracted from blood of parental fish, using a Qiagen genomic extraction kit according to the manufacturer's protocol, and from whole offspring, following the extraction method described by Jones and Hutchings (2002). The number of daily samples for which incubated offspring were available for analysis ranged between 20 (Eastern Scotian Shelf) and 38 (Western Scotian Shelf in 2001). Given time and financial constraints and to maximize the number of samples across the spawning periods, our objective was to genotype 75 to 100 of the several thousand offspring that were usually available from each daily batch of collected eggs. On a few occasions, low egg–larval survival led to fewer than 75 offspring being available for genotyping. The number of genotyped offspring from each daily batch averaged 80.3 ± 20.3 standard deviation (SD) (range: 11–171), resulting in totals of 2931, 1633, 2652, and 1697 offspring genotyped for the full spawning period from Western Scotian Shelf in 2001, Southern Gulf of St. Lawrence, Western Scotian Shelf in 2002, and Eastern Scotian Shelf, respectively.

From a variety of available cod microsatellite DNA loci, three tetranucleotide repeat loci, *Gmo8*, *Gmo19*, and *Gmo37*, and one trinucleotide repeat locus, *Gmo35*, were chosen to be run on all samples (with the exception of those from the Western Scotian Shelf in 2002), based on their high levels of heterozygosity and genotyping reliability (Miller et al. 2000). In cases where these loci proved insufficient in determining parentage, two tetranucleotide repeat loci, *Gmo34* (Miller et al. 2000) and *Mae9* (a haddock microsatellite DNA locus; O'Reilly et al. 2002), were also examined. For cod from the Western Scotian Shelf in 2002, the following loci were run on each sample: *Gmo8*, *Gmo19*, *Gmo34*, *Gmo35*, and *Tch5* (a walleye pollock (*Theragra chalcogramma*) microsatellite DNA locus; O'Reilly et al. 2000). Loci were amplified using polymerase chain reaction conditions specified by Miller et al. (2000) and O'Reilly et al. (2000, 2002), samples were run on 6% denaturing acrylamide gels, and microsatellite alleles or bands were visualized using an FMBIO II (Hitachi, Tokyo, Japan). For parental fish, all loci were amplified and run three times to ensure correct genotyping. Standard individuals were run on all gels to check consistency in fragment lengths. Allelic data for offspring and their putative parents were analysed with PAPA 2.0 (Duchesne et al. 2002) to determine parentage assignments for fish from each of the four groups. More than 95% of the offspring were assigned parentage to both a mother and father in each group. Offspring for which full parentage could not be unambiguously established were excluded from our analyses.

Data analyses

We quantified two metrics of size similarity between mates. The first reflected the proportional difference in body size between mates and was calculated as L_M/L_F, i.e., the length of the male divided by the length of the female. The second metric, $L_M - L_F$, reflected the absolute difference in body length (cm) between mates. To test the null hypothesis that reproduction was random with respect to body size similarity between mates, we compared observed frequency distributions of size similarity for both metrics with those expected by chance, using *G* tests. The latter null distributions represented the frequencies in size similarity between all possible breeding pairs. Observed distributions represented the size similarities between successfully reproducing individuals (as determined by the parentage analyses) of those breeding pairs for which each individual had its greatest reproductive success.

© 2007 NRC Canada

We also examined the degree to which ventral mounts of females by males reflected reproductive success. Firstly, we compared the frequency distribution of size similarity among those pairs for which ventral mounts were observed with that expected by chance, weighting the size similarity for each pair by the number of ventral mounts observed for that pair. Secondly, we compared this observed distribution of size similarities for pairs in which mounts were observed with the distribution of size similarities between pairs that produced offspring, weighting the size similarity for each pair by the number of offspring produced.

Results

Average body size ranged between 45 and 75 cm among the four spawning groups of Atlantic cod (Table 1). There were substantive differences (≥28 cm) in body length among individuals within sexes in all groups, with the exception of Southern Gulf of St. Lawrence cod in group 2, for which the range in body size was less than 20 cm for both sexes. The number of individuals per group ranged between 52 and 93, which corresponds to spawning densities between 0.08 and 0.14 fish·m^{-3}, densities which fall within the range of estimates of cod spawning density in the wild (Rose 1993; Morgan et al. 1997). Based on G tests, sex ratio did not differ among spawning groups 1, 3, and 4 ($p > 0.05$); cod in group 2 were significantly biased towards females ($p < 0.05$). Pooling data from all four groups, thus including all possible pair combinations of mates within each group ($n = 4210$), males were found to be, on average, 4% smaller (3.3 ± 0.2 cm standard error (SE) in absolute terms) than females (Table 2). However, based on the results of a two-way analysis of variance (ANOVA), neither this difference in body size nor those between the sexes within each spawning group were statistically significant ($p > 0.05$). Based on linear regression analyses, there was no association between body size and the dates on which individuals initiated and terminated spawning ($p > 0.05$).

Reproductive success was not random with respect to size similarity between mates. The frequency distribution of size similarity at which individual reproductive success was maximal differed significantly from that expected by chance for both females ($p < 0.001$) and males ($p < 0.01$) (Fig. 1), irrespective of the metric of size similarity used in the analysis. For both sexes, reproductive success was highest when an individual's mate was, on average, larger than themselves (Fig. 1). Pooling data from all four experimental groups, female reproductive success was highest when individuals mated with males that were an average 5% greater in length (ranging from 1% to 20% larger at the level of spawning group) (Table 2). In absolute terms, females achieved their highest reproductive success when they spawned with males similar to (group 2) or as much as 9.9 ± 3.7 cm longer (group 1) than themselves (Table 2). By contrast, males achieved their highest reproductive success when spawning with females that were, on average, 14% larger than they were, a proportional difference that corresponded to 10.5 cm in length (Table 2).

Our observation that reproductive success was highest when individuals mated with fish larger than themselves was evident within three of the four experimental spawning groups (Fig. 2). For Southern Gulf of St. Lawrence cod (group 2), there were no discernible differences when comparing the size similarity of individuals that reproduced successfully with the size similarity of those individuals with whom they could have reproduced. Interestingly, however, the variability in body size within this group was the smallest among the four groups, the coefficient of variation (CV) in size similarity (9.3) being considerably less than the CV in size similarity in the other groups (ranging between 17.3 and 22.9). Although sample sizes were relatively small within groups, the size similarity between mates during their most successful breeding events differed statistically from that expected by chance for females in group 1 ($p < 0.05$) and males in group 3 ($p < 0.0001$).

Egg release by individual female Atlantic cod typically occurs during a ventral mount in which the male, while

Table 2. A comparison of two metrics of body size similarity within and among four experimental groups of spawning Atlantic cod (*Gadus morhua*): relative length of male to female (L_M/L_F) and absolute difference (in cm) between length of male and length of female ($L_M - L_F$).

Metric of size similarity	Group	Sex	Mean	SE	n
L_M/L_F	All	Both	0.96	0.01	4210
		Female	1.05	0.02	98
		Male	0.88	0.02	80
	1	Both	0.97	0.01	675
		Female	1.20	0.07	10
		Male	0.89	0.05	19
	2	Both	1.01	0.01	738
		Female	1.01	0.02	37
		Male	0.99	0.02	16
	3	Both	0.99	0.01	725
		Female	1.07	0.04	25
		Male	0.80	0.02	28
	4	Both	0.93	0.01	2072
		Female	1.03	0.04	26
		Male	0.89	0.03	17
$L_M - L_F$	All	Both	−3.3	0.2	4210
		Female	2.4	1.1	98
		Male	−10.5	1.6	80
	1	Both	−3.0	0.5	675
		Female	9.9	3.7	10
		Male	−8.9	3.5	19
	2	Both	0.1	0.2	738
		Female	0.3	1.1	37
		Male	−1.1	1.3	16
	3	Both	−2.2	0.5	725
		Female	3.4	2.8	25
		Male	−19.2	2.9	28
	4	Both	−5.0	0.2	2072
		Female	1.5	2.0	26
		Male	−6.6	2.1	17

Note: For each group, the size similarity data for both sexes represent the average for all possible pairs in that group. When reported for each sex separately, the metrics represent the average similarity in body sizes between successfully reproducing individuals of those breeding pairs for which each individual had its greatest reproductive success, i.e., greatest number of offspring produced for both females and males.

© 2007 NRC Canada

Fig. 1. Comparisons between observed (solid bars) frequency distributions of mate size similarity at which individual reproductive success was maximal and those expected by chance (open bars). Data on proportional size similarity (length of male divided by length of female, L_M/L_F) are presented for females and males in panels (*a*) and (*b*), respectively. Data on absolute size similarity ($L_M - L_F$) are presented for females and males in panels (*c*) and (*d*), respectively.

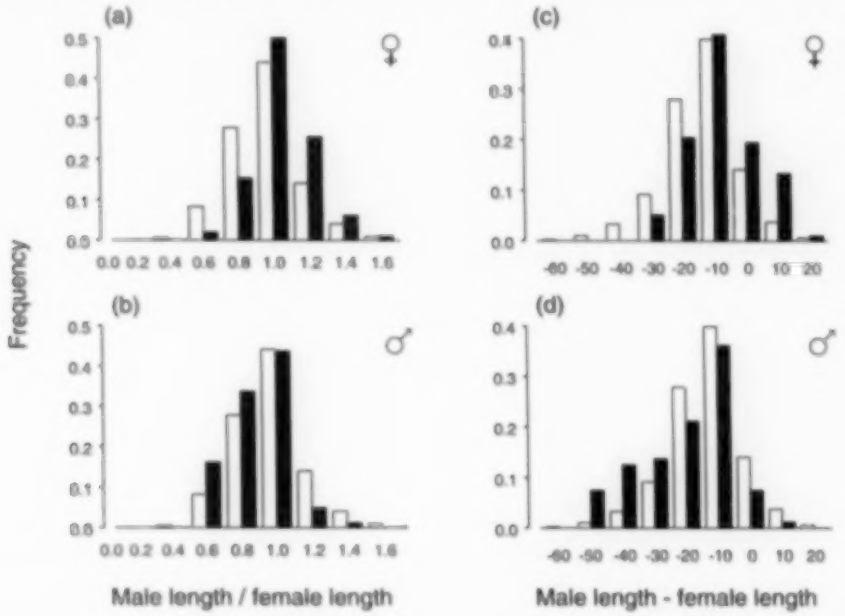

grasping the female with his pelvic fins and matching her swimming speed, positions himself directly beneath the female, such that their urogenital openings are approximately aligned with one another (Brawn 1961). Among the Southern Gulf of St. Lawrence cod in spawning group 2, males did tend to mount females that were most similar in body size, but the frequency with which they did so did not differ from that expected by chance ($p > 0.05$; Fig. 3*a*). There was, however, a highly significant ($p < 0.0001$) difference between the relative sizes of females with whom males mounted and the relative sizes of mating pairs that produced offspring (Fig. 3*b*). Although the average size similarity did not differ between pairs in which mounts were observed (0.99 ± 0.07 SD) and pairs that produced offspring (0.97 ± 0.12 SD), the variation in size similarity was significantly greater (Bartlett's test for homogeneity of variances; $p < 0.01$) among the latter pairs than it was among the former.

Discussion

We established experimental spawning groups of Atlantic cod to examine whether reproductive success is random or biased with respect to the similarity in body size between potential mates. Our data suggest that reproductive success in cod depends on the relative sizes of spawning individuals. Both females and males achieved their highest success when breeding with mates that were, on average, larger in body size than themselves. To our knowledge, this is the first empirical support for the prediction that both female and male reproductive success increase with body size in broadcast-spawning marine fishes. These observations are consistent with the hypothesis that some form of intrasexual competition or mate choice is a constituent of the mating system of this species and that this can have an important influence on individual fitness. Experimental data also suggest that estimates of mating success (based solely on behavioural observations, such as ventral mounts) may underestimate variability in individual reproductive success, one of the key parameters that influence effective population size. The existence of nonrandom mating in Atlantic cod has conservation implications for commercial fisheries that selectively harvest individuals on the basis of size, growth rate, and sex.

The scale of our analysis, in terms of the size of experimental spawning groups and the number of offspring examined for parentage assignment, is unprecedented among studies of marine fishes. Comparing our work with other studies of Atlantic cod, the only species that has been examined previously, each of our spawning groups was composed of at least 50 individuals, whereas those studied by Rakitin et al. (2001) and Bekkevold et al. (2002) consisted of 3 and 8 individuals (on average), respectively. Our parentage analyses were based on the genotyping of almost 9000 offspring, compared with the 1340 and ~4100 offspring genotyped by Bekkevold et al. (2002) and Rakitin et al. (2001), respectively. One particular strength of our analysis was that we were able to compare our results among three geographically distinct populations, including a comparison of two separate years for one population. The fact that the relationships between body size and reproductive success reported here were temporally replicated for one population and spatially replicated among three populations suggests that these patterns may be general ones for this species.

However, notwithstanding these experimental differences, our finding that reproductive success in Atlantic cod is not

© 2007 NRC Canada

Fig. 2. Comparisons between observed (solid bars) frequency distributions of mate size similarity at which individual reproductive success was maximal and those expected by chance (open bars). Each of the four rows of figures depicts the distributions for females (left panels) and males (right panels) in a single spawning group: (*a* and *b*) group 1 (Western Scotian Shelf cod, 2001); (*c* and *d*) group 2 (Southern Gulf of St. Lawrence cod, 2001); (*e* and *f*) group 3 (Western Scotian Shelf cod, 2002); (*g* and *h*) group 4 (Eastern Scotian Shelf cod, 2002).

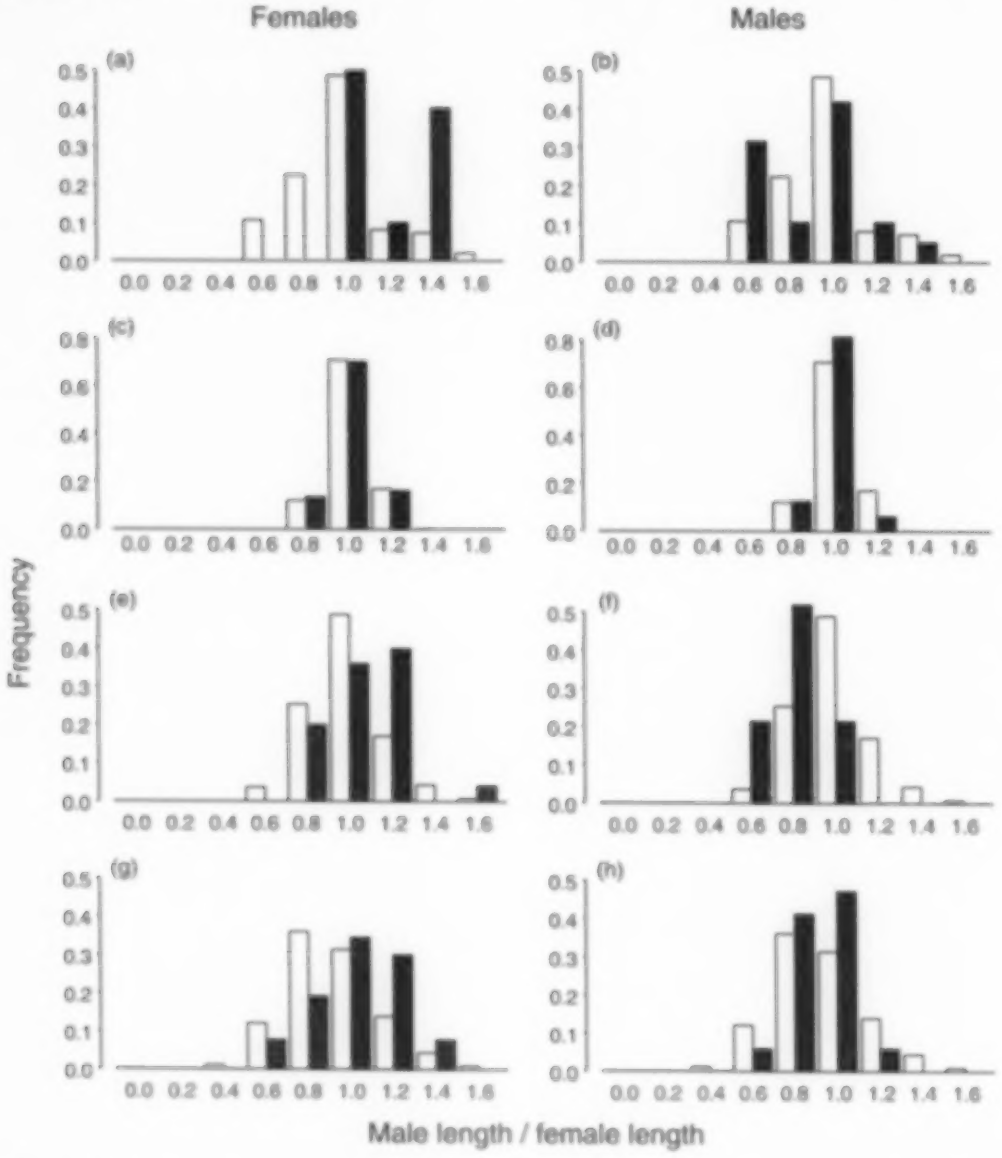

random with respect to body size is consistent with previous work. Rakitin et al. (2001) reported that the greater the similarity in body length between mates, the higher male reproductive success, suggesting that there might be size-based assortative mating in this species. However, as the authors noted, the number of individuals in their eight experimental groups (each of which comprised two males competing for a single female) was too small to allow for one sex to choose another within a behavioural and phenotypic milieu somewhat similar to that which exists in the wild. Bekkevold et al. (2002) examined how the proportion of offspring fertilized by males during single spawning events varied with the male's size relative to that of the female. Their data indicated that male reproductive success tended to be highest when males were similar to or larger than the female with whom they spawned, although they did not compare the observed frequency distribution of size similarity between mates with that expected by chance.

© 2007 NRC Canada

Fig. 3. Comparisons of size similarity among female–male pairs for which ventral mounts were observed (solid bars) with (*a*) the frequency distribution of all potential female–male pairs (open bars) and (*b*) female–male pairs that produced offspring, irrespective of whether mounts were observed between the pair (hatched bars), for Southern Gulf of St. Lawrence cod in spawning group 2.

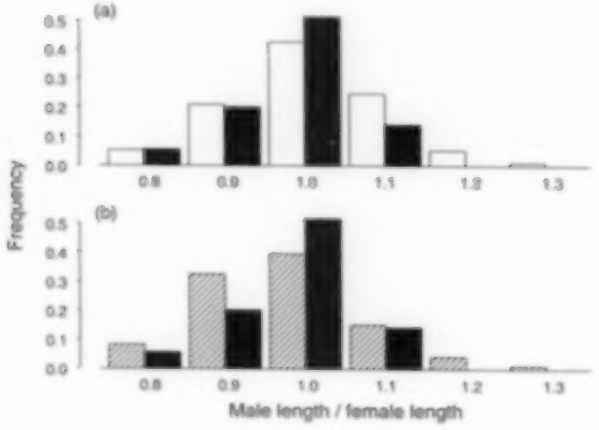

Although nonrandom mating in Atlantic cod could be attributable to a number of mechanisms (Andersson 1994), mate competition, mate choice, or some combination thereof may be among the most probable. Studies have shown that successful reproduction in Atlantic cod involves complex behaviour within and between sexes (Brawn 1961; Hutchings et al. 1999). Before ventral mounting attempts, agonistic interactions (especially chases) are often seen among males and are believed to influence access to females (Brawn 1961; Hutchings et al. 1999). In some species, such as Atlantic salmon (*Salmo salar*), where males compete aggressively for access to females, body size has been found to be an important determinant of male reproductive success (Hutchings and Myers 1988).

As argued previously, there may be important fitness benefits for broadcast-spawning fish that provide no parental care to mate with larger individuals because of the increased number of gametes with which they come into contact during spawning (Trippel and Morgan 1994; McIntyre and Hutchings 2003). These advantages may lead to mate choice by both females and males for larger individuals of the opposite sex.

Both sexes are afforded various opportunities to exert choice during the spawning period. Females can do so by controlling the timing of their spawning. Although egg release is preceded by the ventral mount of a single female by a single male (Brawn 1961), not every mount is followed by egg release (Rowe and Hutchings 2006), suggesting that females are capable of selecting the mounting male with whom they choose to mate. Males can exert choice in one of two ways. Behaviourally dominant males can potentially select their mates by deciding which females to court and mount ventrally. Other males, rather than engaging in courtship, may adopt a satellite-spawning strategy, releasing sperm near a spawning couple and successfully fertilizing eggs in competition with the dominant male (Hutchings et al. 1999; Rakitin et al. 2001; Bekkevold et al. 2002). Each satellite male can potentially exert choice by selecting the spawning events in which he will participate. If smaller individuals are more likely to fertilize eggs as satellite males than larger individuals and if the majority of males achieve fertilizations by adopting the satellite spawning tactic, this type of choice could generate a frequency distribution of mate size similarity in which male reproductive success is highest when males are small relative to the size of the spawning female, a pattern documented in three of the four spawning groups that we studied. Sperm competition might also affect a male's reproductive success, although it is not clear that this would necessarily lead to the bias in size similarity between mates observed here. On the other hand, sperm competition might account, in part, for the higher variance in reproductive success relative to mating success, which we observed among Southern Gulf of St. Lawrence cod in group 2.

Most commercial fisheries are size-selective, with larger individuals more likely to be caught than smaller individuals (Law 2000). Persistent removal of larger individuals will ultimately lead to a reduction in the average size of spawners and, thus, a reduction in the total number of eggs released during the spawning period, among other negative consequences for population growth (Walsh et al. 2006). From a mate-choice perspective, regular removal of the largest individuals will also lead to a reduction in body size variability (Rowe and Hutchings 2003). Within the context of the present study, we would predict that reduced variability in body size would reduce the scope for and the effectiveness of choice, negatively affecting individual reproductive success, recruitment to the fished population, and recovery following population collapse. This prediction is consistent with the results of a modeling analysis undertaken by Bessa-Gomes et al. (2003) who describe how either acceptance or refusal of unattractive mates, two potential consequences of a reduced breadth of choice, can negatively affect population growth rate and increase the probability of extinction. If reduced variability in body size narrows the scope for mate choice in Atlantic cod, we would predict that this would be reflected by a reduction in the variance in individual reproductive success, a prediction borne out by recent experimental work (Bekkevold 2006).

Our work provides strong evidence that reproductive success in Atlantic cod, a broadcast spawner, is not random with respect to the phenotype of potential mates. The observation that reproductive success was highest when both sexes reproduced with individuals larger than themselves is consistent with the hypothesis that mate choice is exerted by both sexes in this species, although we also draw attention to the potential importance of mate competition, particularly among males. If variability in body size enhances choice and the fitness benefits derived therefrom, then the severe truncations in the size-frequency distributions of reproductive individuals typically associated with population collapse may have greater negative consequences for recovery than previously thought. Research focused on the causal basis for nonrandom mating in Atlantic cod and the incidence of such a mating pattern in other commercially exploited marine fishes is warranted.

© 2007 NRC Canada

Acknowledgements

We are grateful to Paty Avendaño, Jim Eddington, and Steve Thompson for providing support and technical assistance in the lab. Parentage analysis would not have been possible without the help of Louise Bezanson, Roxanne Gillett, Matt Jones, and Cheryl Smith. Logistic support for fish collections was provided by Fisheries and Oceans Canada and by Inshore Fisheries Limited. We thank Dorte Bekkevold and an anonymous reviewer for their insightful comments on a previous version of the manuscript. Financial support was provided by the Natural Sciences and Engineering Research Council of Canada and by the Norwegian Research Council.

References

Andersson, M. 1994. Sexual selection. Princeton University Press, Princeton, N.J.

Bekkevold, D. 2006. Male size composition affects male reproductive variance in Atlantic cod *Gadus morhua* L. spawning aggregations. J. Fish Biol. **69**: 945–950.

Bekkevold, D., Hansen, M.M., and Loeschcke, V. 2002. Male reproductive competition in spawning aggregations of cod (*Gadus morhua* L.). Mol. Ecol. **11**: 91–102.

Bessa-Gomes, C., Danek-Gontard, M., Cassey, P., Møller, A.P., Legendre, S., and Clobert, J. 2003. Mating behaviour influences extinction risk: insights from demographic modeling and comparative analysis of avian extinction risk. Ann. Zool. Fenn. **40**: 231–245.

Brawn, V.M. 1961. Reproductive behaviour of the cod (*Gadus callarias* L.). Behaviour, **18**: 177–198.

Breder, C.M., Jr., and Rosen, D.E. 1966. Modes of reproduction in fishes. Natural History Press, Garden City, N.Y.

Chambers, R.C. 1997. Environmental influences on egg and propagule sizes in marine fishes. *In* Early life history and recruitment in fish populations. *Edited by* R.C. Chambers and E.A. Trippel. Chapman & Hall, London. pp. 63–102.

Conover, D.O., and Munch, S.B. 2002. Sustaining fisheries yields over evolutionary time scales. Science (Washington, D.C.), **297**: 94–96.

Duchesne, P., Godbout, M.-H., and Bernatchez, L. 2002. PAPA (package for the analysis of parental allocation): a computer program for simulated and real parental allocation. Mol. Ecol. Notes, **2**: 191–193.

Engen, F., and Folstad, I. 1999. Cod courtship song: a song at the expense of dance? Can. J. Zool. **77**: 542–550.

Foote, C.J. 1988. Male mate choice dependent on male size in salmon. Behaviour, **106**: 63–80.

Hutchings, J.A. 2002. Life histories of fish. *In* Handbook of fish biology and fisheries. Vol. 1. Fish biology. *Edited by* P.J.B. Hart and J.D. Reynolds. Blackwell Science, Oxford. pp. 149–174.

Hutchings, J.A., and Myers, R.A. 1988. Mating success of alternative maturation phenotypes in male Atlantic salmon, *Salmo salar*. Oecologia, **75**: 169–174.

Hutchings, J.A., and Myers, R.A. 1993. Effect of age on the seasonality of maturation and spawning of Atlantic cod, *Gadus morhua*, in the Northwest Atlantic. Can. J. Fish. Aquat. Sci. **50**: 2468–2474.

Hutchings, J.A., Bishop, T.D., and McGregor-Shaw, C.R. 1999. Spawning behaviour of Atlantic cod, *Gadus morhua*: evidence of mate competition and mate choice in a broadcast spawner. Can. J. Fish. Aquat. Sci. **56**: 97–104.

Jones, M.W., and Hutchings, J.A. 2002. Individual variation in Atlantic salmon fertilization success: implications for effective population size. Ecol. Appl. **12**: 184–193.

Kokko, H., and Rankin, D.J. 2006. Lonely hearts or sex in the city? Density-dependent effects in mating systems. Philos. Trans. R. Soc. Lond. B Biol. Sci. **361**: 319–334.

Law, R. 2000. Fishing, selection, and phenotypic evolution. ICES J. Mar. Sci. **57**: 659–668.

McIntyre, T.M., and Hutchings, J.A. 2003. Small-scale temporal and spatial variation in Atlantic cod (*Gadus morhua*) life history. Can. J. Fish. Aquat. Sci. **60**: 1111–1121.

Miller, K.M., Le, K.D., and Beacham, T.D. 2000. Development of tri- and tetranucleotide repeat microsatellite loci in Atlantic cod (*Gadus morhua*). Mol. Ecol. **9**: 238–239.

Møller, A.P., and Legendre, S. 2001. Allee effect, sexual selection and demographic stochasticity. Oikos, **92**: 27–34.

Morgan, M.J., DeBlois, E.M., and Rose, G.A. 1997. An observation on the reaction of Atlantic cod (*Gadus morhua*) in a spawning shoal to bottom trawling. Can. J. Fish. Aquat. Sci. **54**(Suppl. 1): 217–223.

Morrison, C.M. 1990. Histology of the Atlantic cod, *Gadus morhua*: an atlas. Part three. Reproductive tract. Can. Spec. Publ. Fish. Aquat. Sci. 110.

Nordeide, J.T., and Folstad, I. 2000. Is cod lekking or a promiscuous group spawner? Fish Fish. **1**: 90–93.

O'Reilly, P.T., Canino, M.F., Bailey, K.M., and Bentzen, P. 2000. Isolation of twenty low stutter di- and tetranucleotide microsatellites for population analyses of walleye pollock and other gadoids. J. Fish Biol. **56**: 1074–1086.

O'Reilly, P.T., McPherson, A.A., Kenchington, E., Taggart, C., Jones, M.W., and Bentzen, P. 2002. Isolation and characterization of tetranucleotide microsatellites from Atlantic haddock (*Melanogrammus aeglefinus*). Mar. Biotechnol. **4**: 418–422.

Quader, S. 2005. Mate choice and its implications for conservation and management. Curr. Sci. **89**: 1220–1229.

Rakitin, A., Ferguson, M.M., and Trippel, E.A. 2001. Male reproductive success and body size in Atlantic cod *Gadus morhua* L. Mar. Biol. **138**: 1077–1085.

Rose, G.A. 1993. Cod spawning on a migration highway in the north-west Atlantic. Nature (London), **366**: 458–461.

Rowe, S., and Hutchings, J.A. 2003. Mating systems and the conservation of commercially exploited marine fish. Trends Ecol. Evol. **18**: 567–572.

Rowe, S., and Hutchings, J.A. 2006. Sound production by Atlantic cod during spawning. Trans. Am. Fish. Soc. **135**: 529–538.

Stokes, T.K., McGlade, J.M., and Law, R. 1993. The exploitation of evolving resources. Springer-Verlag, Berlin.

Trippel, E.A., and Morgan, M.J. 1994. Age-specific paternal influences on reproductive success of Atlantic cod (*Gadus morhua* L.) of the Grand Banks, Newfoundland. ICES Mar. Sci. Symp. **198**: 414–422.

Walsh, M.R., Munch, S.B., Chiba, S., and Conover, D.O. 2006. Maladaptive changes in multiple traits caused by fishing: impediments to population recovery. Ecol. Lett. **9**: 142–148.

Wootton, R.J. 1998. Ecology of teleost fishes. 2nd ed. Kluwer Academic Publishers, London.

© 2007 NRC Canada

Periphyton biomass response to changing phosphorus concentrations in a nutrient-impacted river: a new methodology for phosphorus target setting

Michael J. Bowes, Jim T. Smith, John Hilton, Michael M. Sturt, and Patrick D. Armitage

Abstract: Nutrient modification experiments were conducted in streamside flumes to determine the concentration at which P limits algal growth in the mesotrophic River Frome, Dorset, UK. The soluble reactive P (SRP) concentration in each flume was either increased (by P addition), decreased (by precipitating P with iron(II) sulphate solution), or left unaltered (control), producing SRP concentrations ranging from 32 to 420 $\mu g \cdot L^{-1}$. Increasing the ambient SRP concentration did not increase epilithic algal growth, showing that the River Frome was not P limited at 109 μg SRP$\cdot L^{-1}$. In the P-stripped flumes, algal biomass declined as the SRP concentration fell below ~90 $\mu g \cdot L^{-1}$, with a 60% biomass reduction at <40 μg SRP$\cdot L^{-1}$. Phosphorus-diffusing periphytometers deployed in the P-stripped flumes confirmed that reduced rates of algal growth were due to P limitation rather than a physical effect of $FeSO_4$ addition. The ~90 $\mu g \cdot L^{-1}$ maximum P-limiting concentration is likely to be similar for comparable nutrient-impacted rivers. This iron-stripping approach expands the existing river nutrient-enrichment methodology so that it can be used in nutrient-impacted rivers and should allow catchment managers to produce knowledge-based P reduction targets prior to introducing remediation.

Résumé : Nous avons mené des expériences de modification des nutriments dans des canalisations en bordure du cours d'eau afin de déterminer la concentration à laquelle le P limite la croissance des algues dans une rivière mésotrophe, la Frome, Dorset, R.-U. Nous avons augmenté (par addition de P), diminué (par précipitation du P avec une solution de sulfate de fer(II)) ou maintenue inchangée (témoin) la concentration de P réactif soluble (SRP) dans chaque canalisation, ce qui a produit des concentrations variant de 32 à 420 $\mu g \cdot L^{-1}$. L'accroissement de la concentration de SRP ambiant ne fait pas augmenter la croissance des algues épilithiques, ce qui montre que la Frome n'est pas limitée par P à 109 μg SRP$\cdot L^{-1}$. Dans les canalisations à P réduit, la biomasse des algues décline lorsque les concentrations de SRP baissent sous ~90 $\mu g \cdot L^{-1}$; la réduction de biomasse est de 60 % lorsque les concentrations de SRP sont <40 μg SRP$\cdot L^{-1}$. L'utilisation de périphytomètres diffuseurs de P dans les canalisations à P réduit confirme que la diminution des taux de la croissance des algues est due à une pénurie de P plutôt qu'à un effet physique de l'addition de $FeSO_4$. La concentration limite maximale de P de ~90 $\mu g \cdot L^{-1}$ est vraisemblablement similaire dans des rivières comparables affectées par les nutriments. Notre méthode de réduction du P à l'aide du fer vient s'ajouter aux méthodologies existantes pour l'étude de l'enrichissement des rivières en nutriments; elle peut être utilisée dans les rivières affectées par les nutriments et elle devrait permettre aux gestionnaires des bassins versants de fixer des objectifs de réduction de P qui soient basés sur des études avant de mettre en place des mesures de mitigation.

[Traduit par la Rédaction]

Introduction

Much effort is currently being focused on reducing P and N loadings in nutrient-impacted freshwaters to improve environmental status and reduce the risk of eutrophication. Initiatives such as the Urban Wastewater Treatment Directive (European Economic Community 1991) were designed to produce significant reductions in P concentrations in the mainly urbanized lowland catchments across the European Union. However, the resulting step-changes in P loading following P removal from sewage treatment works often have no effect on algal community structure (Kelly and Wilson 2004), suggesting that P concentrations are not limiting (or colimiting) algal growth in many of these rivers. Catchment

Received 19 June 2006. Accepted 13 October 2006. Published on the NRC Research Press Web site at http://cjfas.nrc.ca on 14 February 2007.
J19373

M.J. Bowes,[1] **J.T. Smith, J. Hilton, and P.D. Armitage.** Centre for Ecology and Hydrology-Dorset, Winfrith Technology Centre, Dorchester, Dorset, DT2 8ZD, England, UK.
M.M. Sturt. School of Biological Sciences, University of Wales, Bangor, Gwynedd, LL57 2UW, Wales, UK.

[1]Corresponding author (e-mail: mibo@ceh.ac.uk).

 doi:10.1139/F06-180 © 2007 NRC Canada

managers and policy makers need to focus their resources on implementing nutrient load reductions to rivers that would produce an observable environmental improvement and a reduction in nuisance algal biomass. However, the information that they require to make such decisions (such as what is the river's limiting nutrient and what target nutrient concentration should be set) is extremely limited.

One approach commonly used to determine which nutrient is potentially limiting algal growth is molar ratios of N to P in river water (Redfield 1958). However, many recent studies have questioned the effectiveness of this approach (Allen and Hershey 1996; Francoeur et al. 1999; Stelzer and Lamberti 2001). At the elevated nutrient concentrations present in many urbanized lowland rivers across Europe, algal biomass is likely to be light or temperature limited (Hilton et al. 2006), and so nutrient ratios may be of little value.

Nutrient-diffusing substrata have been used to determine which nutrient, if any, is limiting periphyton growth (Chessman et al. 1992; Francoeur et al. 1999; Matlock et al. 1999). These studies are purely quantitative, as the amount of nutrient enrichment cannot be quantified (owing to varying nutrient diffusion rates from the substrate (Scrimgeour and Chambers 1997) combined with changing river flow velocities). They are therefore unable to show how a specific change in nutrient concentration will affect the quantity of periphyton in a river. Other researchers have studied the effects of direct nutrient enrichment of streams (Elwood et al. 1981; Peterson et al. 1993; Sabater et al. 2005) and within-stream/streamside flumes (Bothwell 1985; Lohman et al. 1991; Stelzer and Lamberti 2001). Most of these studies have been based on predominantly rural catchments with low initial nutrient concentrations. This approach allows algal biomass response to be determined following specific increases in nutrient concentration. However, such experiments can only simulate the effect of nutrient concentration increases and not decreases.

To determine the actual concentration at which P no longer limits algal growth (the maximum P-limiting concentration), the initial river P concentration already needs to be below this concentration (i.e., P must be limiting for P enrichment to be an effective approach). As most lowland rivers in urbanized catchments already have high P loadings (Bowes et al. 2005*a*), nutrient-enrichment approaches often cannot be used to determine this P-limiting concentration. Rier et al. (2006) have addressed this weakness by decreasing stream nutrient concentrations using algal uptake in partially recirculating flumes, but this nutrient reduction approach is unlikely to be suitable for use in highly nutrient-impacted systems.

This study aims to develop a P-stripping technique to expand the existing methods of studying nutrient limitation in rivers, which can be used to simultaneously assess the effects of increasing and decreasing soluble reactive P (SRP) concentration on algal biomass. The ability to decrease SRP concentrations means that P limitation can, for the first time, be studied in highly nutrient-impacted rivers, where ambient P concentrations are in excess of algal growth limiting concentrations. This approach will allow the effects of specific P mitigation strategies to be quantified in terms of a direct impact on algal biomass. This study applies this new methodology to determine the SRP concentration at which P begins to limit epilithic algal growth for a mesotrophic river, the River Frome, Dorset, UK.

Materials and methods

Study area

The River Frome drains a predominantly chalk catchment of 414 km^2 area (Casey and Newton 1973) (Fig. 1). The land use within the catchment is primarily agricultural, mainly grassland and cereals (Casey et al. 1993). The town of Dorchester is the only significant urban area within the study reach. Ten sewage treatment works discharge treated effluent into the River Frome and its tributaries (Fig. 1). The largest of these serve the towns of Dorchester (population equivalent = 27 600), Wool (population equivalent = 8000), and Warmwell (population equivalent = 3900). The mean annual discharge of the river at East Stoke was 5.13 $m^3 \cdot s^{-1}$ in 1999 (Bowes et al. 2005*b*).

This research was conducted using experimental flumes located at the Freshwater Biological Association's Dorset River Centre in East Stoke, Dorset, UK (formally the Institute of Freshwater Ecology's River Laboratory). The research facility is located alongside the Mill Stream, which is a branch of the lower River Frome.

This study was conducted using a series of 11 identical flow-through flumes (12.5 m long × 0.3 m wide). They were constructed from stainless steel and filled with 3 cm of cleaned river substrate consisting mainly of course gravels with some interstitial sands and silts. They were located immediately adjacent to the Mill Stream below the water level of the river. The flumes were supplied with river water, by gravity, directly from the Mill Stream via pipes through the riverbank. The location was unshaded, and all flumes received similar light levels.

Flume experiments

This study consisted of two experiments: the first was conducted between 29 June and 4 July 2005 and the second between 8 and 17 August 2005. Before the commencement of each experiment, the water velocity through each flume was standardized to 0.12 $m \cdot s^{-1}$ by adjusting valves on the water inlet pipe of each flume. The water velocities were measured using a SENSA RC-2 ultrasonic flowmeter. The depth of the water was standardized at 4 cm above the gravel substrate in the middle of each flume by adjusting the height of a weir at the end of the flumes. This gave a water through-flow rate of ~1.4 $L \cdot s^{-1}$. Stone dams were then constructed 2 m downstream from the inlet pipe to produce a deeper (12 cm) section at the front of each flume to increase the residence time of the river water to over 1 min in this impounded upper section. This improved the mixing of the different nutrient treatments before entering the main flume section and allowed time for chemical precipitation reactions to occur for the iron(II) sulphate ($FeSO_4$) treatments described below.

One of three treatments was randomly assigned to each flume. Some flumes had the SRP concentrations of their river water increased by the continuous addition of a concentrated potassium dihydrogen orthophosphate (KH_2PO_4) solution in deionized water dripped directly into the water inflow using a peristaltic pump. A range of SRP concentra-

© 2007 NRC Canada

Fig. 1. Map of the River Frome catchment in Dorset, UK (inset).

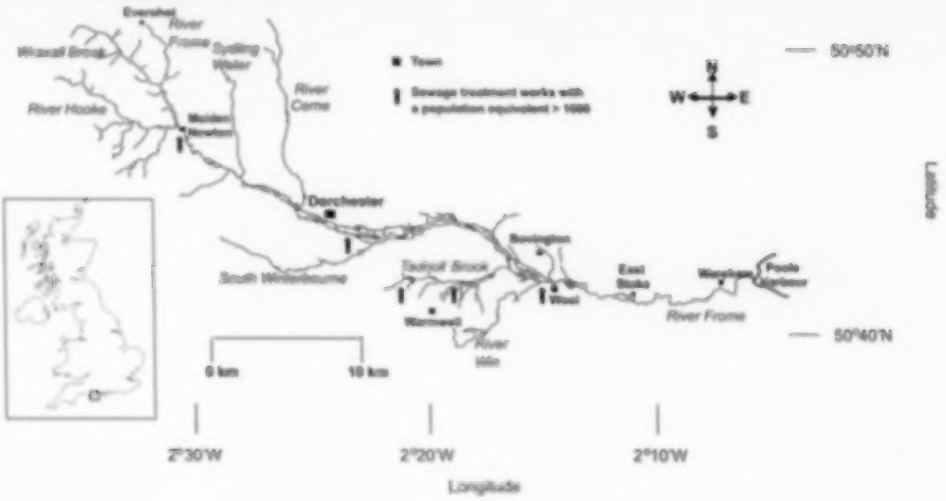

tions was achieved by using varying drip rates, with the maximum rate quadrupling the mean SRP concentration observed in the Mill Stream during the experimental period. The mean SRP concentration in the river between June and August 2005 was 120 $\mu g \cdot L^{-1}$, which is classified as mesoeutrophic in the United Kingdom (Mainstone et al. 2000) and exceeds the UK government's 60 μg SRP$\cdot L^{-1}$ target for chalk rivers (Environment Agency 2000). Therefore, a doubling of SRP concentration will exceed the interim target for heavily enriched rivers of 200 $\mu g \cdot L^{-1}$, and an SRP concentration in excess of 400 $\mu g \cdot L^{-1}$ should produce hypereutrophic conditions (Mainstone and Parr 2002).

The SRP concentrations in other flumes were decreased by the addition of a concentrated $FeSO_4$ solution in deionized water dripped directly into the flume inflow. The $FeSO_4$ solution was added either by using a peristaltic pump (for low addition rates) or by siphoning the iron solution from a constant-head stock tank into the flumes and controlling the addition rate using tube clamps (for flumes requiring higher addition rates). The added $FeSO_4$ reacts with dissolved phosphate ions present in the incoming river water, rapidly forming insoluble (and therefore nonbioavailable) $Fe_3(PO_4)_2$ (Reynolds and Davies 2001; Suschka et al. 2001). Dosing with iron salts has been routinely used by the water industry across Europe to decrease soluble phosphate concentrations in wastewater effluents and water inputs to reservoirs (Bernhardt and Clasen 1982; Perkins and Underwood 2001). The dammed front section of the flumes increased the water residence time, allowing the P-stripping reaction to occur before reaching the main algal monitoring section of the flume. The dam also prevented much of the resulting $Fe_3(PO_4)_2$ precipitate from entering the main flume channel. Target SRP concentrations were produced by using different rates of $FeSO_4$ addition, determined during previous pilot studies. The remaining flumes received no additions of KH_2PO_4 or $FeSO_4$ and acted as experimental controls.

Immediately before the start of the experiments, the gravel substrates in all of the flumes were agitated to release any fine sediment and filamentous algae that had accumulated prior to the start of the experiment. Algae that had grown along the sides of the flumes were removed by scrubbing. The flumes were searched for invertebrates and any found were removed. After all of the flumes were cleaned and appeared identical, the planned treatments (P addition, $FeSO_4$ addition, and control) were randomly assigned to the flumes and the additions of KH_2PO_4 and $FeSO_4$ commenced.

Three flumes were used during Experiment 1. One flume received SRP additions (which aimed to double the River Frome SRP concentration from 120 to 240 $\mu g \cdot L^{-1}$), one flume was dosed with $FeSO_4$ (aiming to reduce the River Frome SRP concentration by 80% to between 20 and 30 $\mu g \cdot L^{-1}$), and the remaining flume received no treatment and acted as an experimental control. Experiment 2 used 11 flumes. Two flumes received SRP additions (targeting a doubling and quadrupling of the River Frome SRP concentration), five flumes received a range of $FeSO_4$ dosing, and the remaining four flumes received no additions and acted as experimental controls. After 90 min of P and $FeSO_4$ addition, water samples were taken from the middle of each flume, filtered through a 0.45 µm membrane filter (WCN grade; Whatman, UK), and analysed for SRP concentration (see Water chemistry analysis section below), which confirmed that the range of SRP concentrations was satisfactory and the P stripping was working. A rectangular slate tile (0.52 m × 0.26 m) (previously thoroughly scrubbed and washed in deionized water) was then placed in each flume, 2 m downstream of the dam, to act as clean growth substrates for epilithic algae to colonize.

The SRP concentrations of the flumes were monitored between four and six times per day throughout the course of each experiment. Water samples were taken from the downstream end of the dammed sections to give time for the KH_2PO_4 and $FeSO_4$ treatments to mix and react and to avoid any disturbance of the algae and sediment around the slate tiles during water sampling. A 50 mL sample was taken using a syringe and then immediately filtered through a 0.45 µm membrane filter. Samples were stored at 4 °C in the dark

© 2007 NRC Canada

and analysed for SRP within 12 h to avoid errors associated with sample instability (Haygarth et al. 1995; House and Warwick 1998).

Water flow rates and depths and treatment drip rates were monitored and adjusted at 2 h intervals throughout the day. Plant debris and invertebrates that had been washed into the flumes from the Mill Stream were regularly removed so that they did not disturb or consume the algae growing on the slate tiles.

Water samples (500 mL) were also taken from the Mill Stream upstream of the flume facility during the two experiments to allow the nutrient concentration of the incoming flume water to be monitored. The average sampling frequency was five per day, taken using an automatic water sampler (model 1011; Montec Epic, Manchester, UK). The water sampler inlet pipe was positioned to face downstream at a fixed height above the bed of the river (approximately at the midpoint of the water column) within the main flow of the river. Aliquots of these Mill Stream samples were filtered through a 0.45 µm membrane filter (WCN grade; Whatman, UK) and analysed for SRP and total oxidizable N (TON). The remaining unfiltered samples were analysed for total P (TP) concentration.

The two experiments were run until a strong, visible algal growth had developed on some of the slates. In Experiment 1, slates were immersed for 4 days, and in Experiment 2, the slates were left for a longer period (9 days). At the end of each experiment, the slates were carefully removed and the algal–sediment layer from each slate was transferred into an airtight sampling jar. This was immediately returned to the laboratory, stored in the dark at 4 °C (so as to avoid degradation of the chlorophyll), and analysed for chlorophyll *a* concentration within 24 h (HMSO 1986). Bulk samples of water were then taken from the downstream end of each flume and analysed for pH and suspended solids concentration.

Water chemistry analysis

The filtered water samples were analysed for SRP, TON, and dissolved reactive Si concentration using a SEAL AQ2 discrete multichemistry analyser (Synermed Analytical and Environmental Ltd., Burgess Hill, UK). Each batch of samples was analysed alongside quality control nutrient standards.

SRP concentration was determined using a spectrophotometric method (Murphy and Riley 1962). SRP present in the water sample was reacted with an acid molybdate reagent, in the presence of antimony, to form a yellow-coloured phosphomolydate complex. This was then reduced by the addition of ascorbic acid to form the intensely coloured phosphomolybdenum blue, which was quantified spectrophotometrically at a wavelength of 880 nm. TON was quantified by reducing all nitrate ions present in the sample to nitrite by reaction with hydrazine in alkaline conditions using cupric ions as a catalyst. This reduced nitrate, plus any nitrite present in the original sample, was then reacted with sulphanilamide and *N*-(1-naphthyl)-ethylenediamene dihydrochloride to form red-coloured azo dye, which was quantified spectrophotometrically at a wavelength of 546 nm (SEAL 2004). Dissolved reactive Si concentration was determined by reaction with ammonium molybdate to form molybdosilicic acid, which was then reduced by the addition of ascorbic acid to form a silicomolybdenum blue complex. This was quantified spectrophotometrically at a wavelength of 880 nm (Mullin and Riley 1955).

TP concentration was determined by digesting unfiltered samples with acidified potassium persulphate in an autoclave (121 °C, 40 min). The digest was then reacted with acidified ammonium molybdate to form an intensively blue-coloured molybdenum–P complex, which was quantified spectrophotometrically at a wavelength of 880 nm (Eisenreich et al. 1975).

Suspended solid concentrations were determined by filtering a known weight of previously unfiltered sample through preweighed GF/C-grade glass microfibre filter paper (Whatman, UK) and then oven drying the filter and sediment overnight at 105 °C.

Chlorophyll *a* analysis

The algae biomass on each slate was quantified by chlorophyll *a* analysis. The algae–sediment samples from each slate were diluted to 1 L with deionized water. The jar was shaken vigorously to homogenize the sample and then subsampled in triplicate (20 mL). Each subsample was filtered through a 0.45 µm membrane filter. The chlorophyll *a* on each filter was quantified spectrophotometrically following overnight methanol extraction (Marker 1972; HMSO 1986; Gainswin et al. 2006) using a Beckman DU520 spectrophotometer.

Nutrient-diffusing periphytometers

Nutrient-diffusing periphytometers (Matlock et al. 1998) were used to determine whether high $FeSO_4$ additions to the flumes had a detrimental effect on algal growth. The periphytometers consisted of a 100 mL polyethylene bottle with a 20 mm diameter hole drilled through the cap. The bottles were filled with either deionized water (control) or a concentrated P solution (20 mmol $Na_2HPO_4 \cdot L^{-1}$ in deionized water). A diffusion membrane with a 12 000 to 14 000 Da pore size (Medicell; London, UK) and a glass fibre filter paper (grade MF300; Fisher Scientific, UK) were placed over the neck of the bottle and held in place by the bottlecap. The membrane allowed nutrient to diffuse out of the periphytometer but prevented algae from colonizing the inside of the bottle and thereby depleting the excess nutrient. The filter paper served as a substrate for algal growth.

The periphytometers were deployed during Experiment 1. Five control and five P-enriched periphytometers were placed (in a randomized order) in the downstream end of Flume 1, which was receiving a maximum dose rate of $FeSO_4$. The periphytometers were left in the flume until the end of the experiment (5 days). They were then carefully removed, dismantled, and the mass of algae on each filter quantified by chlorophyll *a* analysis (HMSO 1986).

Nutrient-diffusing periphytometers were also deployed in the River Frome on 16 June 2005. The periphytometers were filled with one of eight nutrient-enrichment treatments: P, Si, N, deionized water (control), P + N, P + Si, N + Si, and all three nutrients. Each nutrient treatment had three replicates. The array of periphytometers was placed inside a floating mesh cage (to decrease the influence of fish and invertebrate grazing and to prevent plant debris covering the bottles) at a depth of 4 cm below the river surface. After 6 days,

© 2007 NRC Canada

the periphytometers were removed, dismantled, and the filter paper substrates analysed for chlorophyll *a* concentration.

Mill Stream monitoring

Mill Stream water samples were taken between February and December 2005 at a minimum frequency of two per day using an Epic water sampler. The sampling rate was increased to as many as eight per day during storm events. All samples were analysed for SRP, TON, and TP concentration. This 10-month data set was gathered to monitor changes in concentration and nutrient ratio throughout the year and allowed the nutrient concentrations observed during the flume experiments to be put in the context of an annual pattern.

Statistical analysis

For all statistical analyses, Ryan–Joiner tests were performed to confirm that the data were normally distributed, and homogeneity of variances was tested using Bartlett's test. Analysis of variance (ANOVA) was used to assess differences in chlorophyll *a* concentration in the P addition, control and $FeSO_4$ addition flumes in Experiment 1 and to determine the effect of different periphytometers nutrient treatments. When ANOVA was significant, differences between treatments were tested using the Tukey multiple comparison test. Coefficients of variance of the SRP concentrations produced in each flume in Experiment 2 were calculated to confirm that the variation in P concentration was relatively similar for each treatment. Data were analysed using Minitab statistical software, release 14 (Minitab Inc., State College, Pennsylvania).

Results and discussion

Experiment 1

Nutrient concentrations

The P addition and precipitation treatments resulted in actual mean SRP concentrations that were within 8% of the target concentrations. The SRP concentrations observed in each flume over the course of Experiment 1 are shown in Fig. 2. Flume 2 received no treatment, and this unaltered River Frome water had an initial SRP concentration of 16 $\mu g \cdot L^{-1}$, gradually decreasing to 118 $\mu g \cdot L^{-1}$ by the end of the experiment (mean concentration = 132 $\mu g \cdot L^{-1}$). These SRP concentrations are similar to the mean values observed in the River Frome in July 1999 and 2000 (143 and 152 $\mu g \cdot L^{-1}$, respectively) (Bowes et al. 2005*b*). The addition of P solution to Flume 3 increased the SRP concentration of the river water to between 213 and 289 $\mu g \cdot L^{-1}$ (mean SRP concentration = 246 $\mu g \cdot L^{-1}$), which was equivalent to a 90% increase in SRP concentration. The addition of $FeSO_4$ to Flume 1 decreased the SRP concentration of the river water to between 21 and 42 $\mu g \cdot L^{-1}$ (mean concentration = 32 $\mu g \cdot L^{-1}$), a reduction in mean SRP concentration of 75%. Analysis of flume water samples confirmed that TON and Si concentrations were the same as those measured in the River Frome, thereby confirming that the $FeSO_4$ additions had no effect on N and Si. The mean TON concentration in the River Frome during this period was 6.0 $mg \cdot L^{-1}$ (Fig. 3), which meant that the three flumes had a mean N:P molar ratio of 415, 101, and 54 for the $FeSO_4$ addition, control, and P addition treatments, respectively. These ratios are much higher than the 16:1 N:P Redfield ratio (Redfield 1958) and so imply that P could be limiting to algal growth owing to the excess of bioavailable N. However, concentrations of both nutrients were relatively high in all flumes, and so the Redfield ratio may not be an effective means of determining nutrient limitation.

Periphyton biomass

After 4 days of immersion, the slate tiles in all three flumes had been colonized by filamentous algae of up to 5 mm thickness. The experiment was terminated and the slates were removed at this point, as some small-scale sloughing of the biofilm had been observed in the control and P addition flumes. Periphyton biomass was estimated by quantifying the density of chlorophyll *a* on each slate (Fig. 4).

There was no significant difference between the control and P addition flumes, whereas the flume that received the $FeSO_4$ addition had significantly lower chlorophyll *a* concentration (Tukey's test, ANOVA, $F = 50.3$, $p < 0.001$). The mean chlorophyll *a* concentrations of the control and P addition flumes were 9.1 and 9.3 $\mu g \cdot cm^{-2}$, respectively, despite the P addition flume having a mean SRP concentration of 246 $\mu g \cdot L^{-1}$. This result implies that P was not limiting algal growth at concentrations above 130 $\mu g \cdot L^{-1}$. Almost doubling the SRP concentration in the River Frome during the critical summer growing period would therefore be unlikely to have any effect on the rate of periphyton growth or biomass in the lower River Frome; consequently, increases in SRP concentration would not lead to an increase in eutrophication and a decline in environmental water quality. Studies by Jarvie et al. (2002*b*) have observed a similar lack of ecological response to a sustained increase in SRP concentration (up to 160 $\mu g \cdot L^{-1}$) in the River Kennet, UK.

The flume that received the $FeSO_4$ addition had significantly lower chlorophyll *a* concentration (5.2 $\mu g \cdot cm^{-2}$) (Fig. 4). This 44% decrease in chlorophyll *a* density on the slate substrates implies that the reduced concentration of bioavailable P in the overlying water is either reducing the growth rate of the periphyton or reducing the biomass of algae that can be sustained under these potentially P-limited conditions. Therefore, a similar reduction in SRP concentration in the River Frome to 32 $\mu g \cdot L^{-1}$ during this monitoring period would cause a significant reduction in periphyton growth rate and would result in a significant improvement in water quality of the river. These results agree with the eutrophication classification system devised by Mainstone and Parr (2002) derived from SRP concentrations and N:P ratios of 5000 river monitoring sites across England and Wales. They identified 50 μg SRP$\cdot L^{-1}$ as being the concentration below which P is likely to become limiting throughout the year. Based on this classification, the control and P addition flumes were only deemed to be possibly P limited for part of the growing season, whereas the P-stripped flume would be classified as being likely to be P limited.

However, the reduced periphyton colonization in the P-stripped flume could also be due to high Fe concentrations somehow inhibiting algal growth or other physical effects of $FeSO_4$ addition, such as changes in river water pH (Perkins and Underwood 2001). The pH values of the flumes were all

© 2007 NRC Canada

Fig. 2. SRP concentrations during Experiment 1. ◇, $FeSO_4$ addition (Flume 1); □, control (Flume 2); ▲, P addition (Flume 3). SRP concentrations measured in the River Frome are represented by the thick solid line.

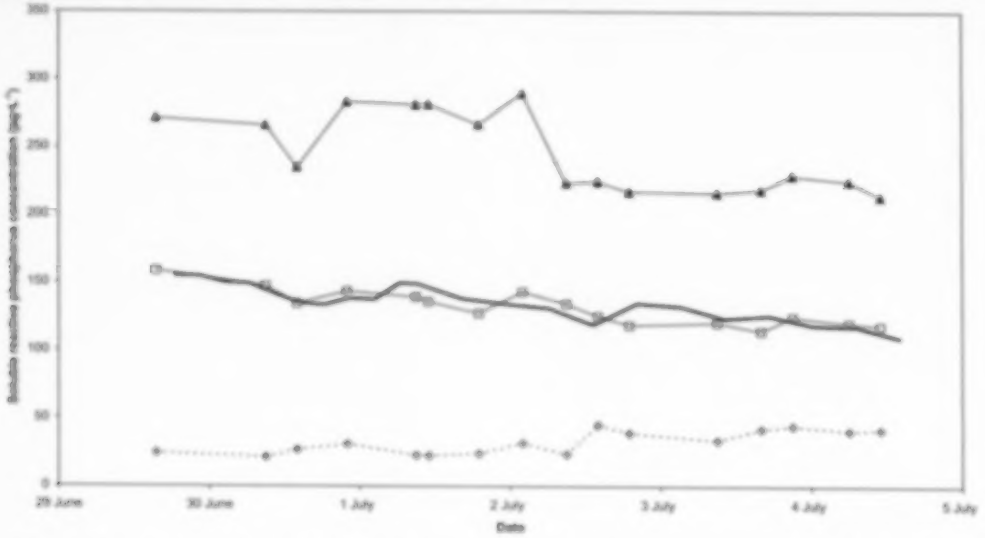

7.7 (measured just before the end of Experiment 1), and so the reduced algal growth on the slates was not due to changes in pH caused by $FeSO_4$ addition. The reaction of $FeSO_4$ with dissolved P results in the formation of a precipitate, and this may increase the turbidity of the overlying river water (although most of the precipitate was retained in the upper section of the flume upstream of the dam). Analysis of bulk water samples taken at the end of Experiment 1 were analysed for suspended solid concentration and confirmed that Flume 1 ($FeSO_4$ addition) had a higher suspended solids concentration (13 mg·L^{-1}) than the control (5.3 mg·L^{-1}) and P addition flumes (5.9 mg·L^{-1}). Therefore, the $FeSO_4$ addition could be "shading out" the periphyton, resulting in less chlorophyll *a* concentration on the Flume 1 slate substrate.

Periphytometers

Control and P-diffusing periphytometers were deployed in Flume 1 to investigate the effects of $FeSO_4$ additions on algal growth. The periphytometer chlorophyll *a* concentration results from this $FeSO_4$-treated flume are provided in Fig. 5*a*. The control periphytometers (no nutrient addition) had a mean chlorophyll *a* concentration of 3.0 µg·cm^{-2}. The P-diffusing periphytometers had significantly higher chlorophyll *a* concentrations (5.3 µg·cm^{-2}) (ANOVA, $F = 36.8$, $p < 0.001$), demonstrating that the periphyton was clearly P limited at an ambient SRP concentration of 32 µg·L^{-1}. These results suggest that the reduced chlorophyll *a* concentration on the slate substrate in Flume 1 was due to the decreased concentration of SRP in the overlying water and not due to elevated $FeSO_4$ concentration inhibiting algal growth,. This conclusion would have been strengthened if periphytometers had also been deployed in the control and P addition flumes. The authors plan to do this in future studies.

The periphytometer deployment in the River Frome itself, prior to the start of Experiment 1, demonstrated that there was no significant difference in chlorophyll *a* concentration between any of the treatments (Tukey's test, ANOVA, $F = 0.18$, $p = 0.986$) (Fig. 5*b*). These results confirm that algal growth was not P, N, or Si limited (or colimited) during the 16–22 June 2005 deployment period (mean TP, SRP, TON, and Si concentrations = 167 µg·L^{-1}, 114 µg·L^{-1}, 5.6 mg·L^{-1}, and 2.3 mg·L^{-1}, respectively).

Experiment 2

Experiment 1 demonstrated that a wide range of SRP concentrations could be produced and maintained in the flumes over a period of days and that the P-stripping methodology was capable of reducing SRP concentrations to 21 µg·L^{-1}. The results from the periphytometers deployed in the P-stripped flume confirmed that P concentration was limiting periphyton growth in the River Frome at 32 µg·L^{-1}. The chlorophyll *a* concentration results in Experiment 1 implied that increases in River Frome P concentration would not produce enhanced periphyton growth, but this was only based on a single observation. Therefore, Experiment 2 aimed to verify this by investigating the effect that a doubling and quadrupling of the SRP concentration in the River Frome would have on epilithic algal growth.

The chlorophyll *a* results from the control and P-stripped flumes in Experiment 1 indicated that SRP concentration begins to limit periphyton growth between 32 and 132 µg·L^{-1}, but there were clearly not enough data points to determine where the "breakpoint" was (i.e., the P-limiting concentration, where increases in SRP do not lead to increased periphyton growth and reductions in P concentration lead to reductions in growth). To determine this P-limiting concentration, five flumes received different rates of $FeSO_4$ additions so that a wide range of SRP concentrations were produced between the ambient River Frome P concentration and 30 µg·L^{-1}.

Nutrient concentrations

The SRP concentrations observed over the course of Experiment 2 (8–17 August 2005) are shown in Fig. 6. The SRP concentration in the four control flumes (receiving unaltered

© 2007 NRC Canada

Fig. 3. Nutrient concentrations in the River Frome at East Stoke, Dorset, 2005 (shaded areas denote the periods of the flume experiments).

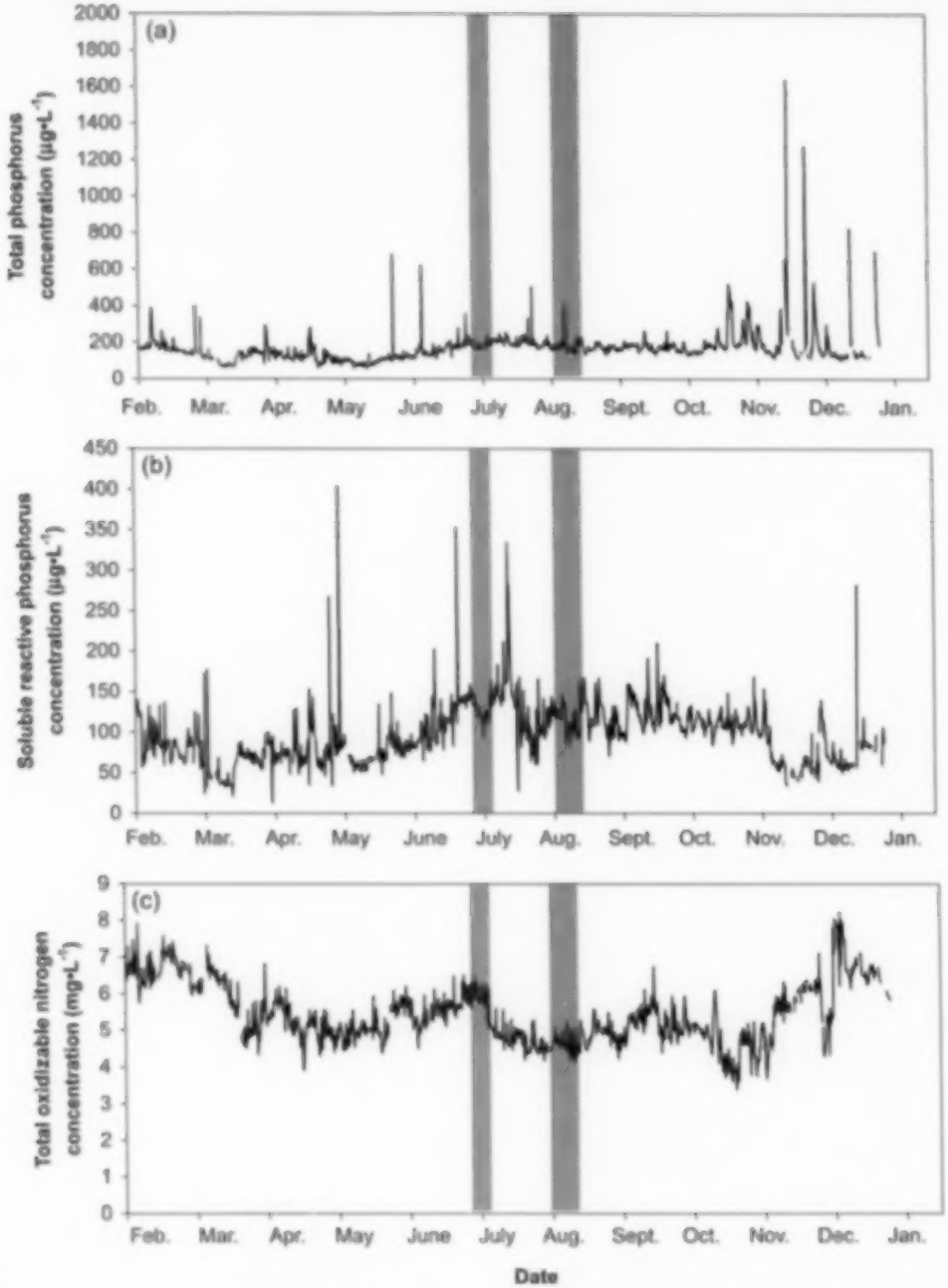

River Frome water) varied between 80 and 150 µg·L^{-1} over the course of the experiment, with a mean SRP concentration of 109 µg·L^{-1}. The mean SRP concentration measured in the River Frome during this period was 111 µg·L^{-1}. These SRP concentrations and fluctuations were typical of the River Frome nutrient chemistry over the July–October 2005 period (Fig. 3), although they were much lower than observed in previous studies (mean SRP concentrations in August 1999 and August 2000 of 176 and 218 µg·L^{-1}, respectively) (Bowes et al. 2005*b*). The two flumes receiving P additions (Flumes 3 and 10) had their mean SRP concentrations increased to 196 µg·L^{-1} (80% increase) and 423 µg·L^{-1} (290% increase), respectively. The coefficients of variance in the P addition flumes (Flume 3 = 17%, Flume 10 = 14%) were very similar to those of the four control flumes (coefficients of variation of between 11% and 14%). The remain-

© 2007 NRC Canada

Fig. 4. Chlorophyll *a* concentrations on slate substrates at the end of Experiment 1. ×, $FeSO_4$ addition (Flume 1); △, control (Flume 2); ■, P addition (Flume 3). Error bars are ±2 SD derived from the three subsamples analysed from each slate. The curve represents the best fit of the data to Michaelis–Menten hyperbolic regression analysis (Dawes 1972).

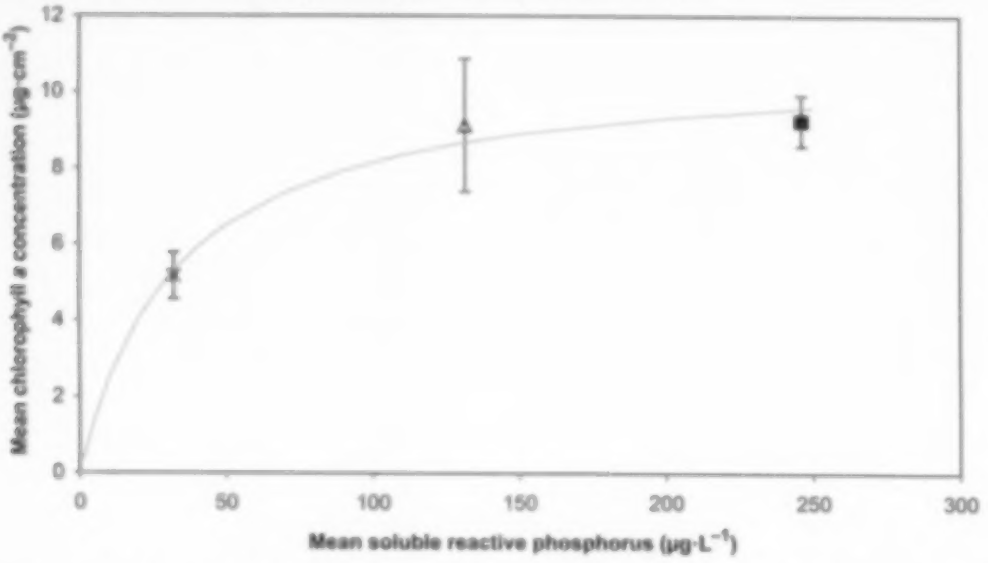

ing five flumes received a range of $FeSO_4$ addition rates, resulting in mean SRP concentrations from 88 $\mu g \cdot L^{-1}$ (equivalent to a 20% reduction in ambient concentration) to 36 $\mu g \cdot L^{-1}$ (a 67% reduction). The mean TON concentration in the River Frome during this period was 4.6 $mg \cdot L^{-1}$ (Fig. 3), which meant that the flumes in Experiment 2 had mean N:P molar ratios ranging from 285:1 (for the flume with the highest P-stripping rate) to 24:1 for Flume 10 (receiving the maximum P addition).

Periphyton biomass

After 9 days of the experiment, all slates had been colonized by significant quantities of epilithic algae. Algal sloughing was observed on the P-addition and control slates, indicating that periphyton biomass was approaching its maximum, and so the experiment was terminated. Periphyton biomass was estimated by quantifying the density of chlorophyll *a* on each slate (Fig. 7). Algal biomass showed the same response to increasing SRP concentration that was suggested by the results from Experiment 1. The highest mean chlorophyll *a* concentrations were observed in the four control flumes (between 35.6 and 36.6 $\mu g \cdot cm^{-2}$). There was very little variation in the chlorophyll *a* concentrations in these four control flumes, which indicates that there is minimal physical variation between the flumes and that the precision of the sampling and analytical technique is high. The chlorophyll *a* concentrations in the control and P addition flumes were much higher than those observed in other longer-duration studies (Mundie et al. 1991; Tank and Dodds 2003; Sabater et al. 2005), showing that algal growth rates were higher in this nutrient-rich river. Chlorophyll *a* concentrations were higher than those observed in Experiment 1 owing to the 5-day extra duration of Experiment 2, allowing for greater algal accrual. An 80% increase in SRP concentration produced the next highest algal biomass with a mean concentration of 34 $\mu g \cdot cm^{-2}$. A further increase in SRP concentration to 423 $\mu g \cdot L^{-1}$ resulted in a reduction in chlorophyll *a* concentration to 28.4 $\mu g \cdot cm^{-2}$. This reduction in algal biomass at elevated SRP concentration may be due to the colonizing algae being increasingly filamentous and friable, which appeared to result in a higher sloughing rate. These results imply that a significant increase in SRP concentration in the River Frome would not have increased the epilithic algal biomass during this study period and indicate that the river was not P-limited.

The five flumes receiving $FeSO_4$ additions all had reduced epilithic algal biomass compared with the control flumes. The flumes with SRP concentrations of 88 and 55 $\mu g \cdot L^{-1}$ had mean chlorophyll *a* concentrations of 27.3 and 29.8 $\mu g \cdot cm^{-2}$, respectively. The three flumes with the lowest SRP concentrations (35.8, 36.2, and 38.9 $\mu g \cdot L^{-1}$) had the lowest observed mean chlorophyll *a* concentrations (19.6, 21.4, and 12.2, respectively). This step-change in algal biomass under 50 µg $SRP \cdot L^{-1}$ concentration supports findings from other UK river studies (Mainstone and Parr 2002). Similar patterns of increasing algal biomass with increasing P concentration followed by a leveling off as the P concentration exceeds the maximum P-limiting concentration) have been observed in previous studies (Dodds et al. 1997; Scrimgeour and Chambers 1997; Rier and Stevenson 2006). This pattern is likely to be observed in all rivers, although the breakpoint in the graph will vary depending on the concentration of N and other plant nutrients. In the River Frome, periphytometer studies showed that P, N, and Si were not limiting (or colimiting) algal growth, and therefore, when P concentrations are above the maximum P-limiting concentration of ~90 $\mu g \cdot L^{-1}$ observed in Experiment 2, epilithic algal growth is likely to be either light limited or growing at its maximum possible rate. This 90 µg $SRP \cdot L^{-1}$ target value is likely to be similar for other comparable nutrient-impacted rivers, but

© 2007 NRC Canada

Fig. 5. Chlorophyll *a* concentrations on nutrient-diffusing periphytometers (*a*) after 5 days of immersion in Flume 1 ($FeSO_4$ addition, mean SRP concentration = 32 $\mu g \cdot L^{-1}$) ($n = 5$) and (*b*) after immersion in the River Frome, 16–22 June 2005 ($n = 3$). Error bars are ±1 SE). C, control; P, P addition; N, N addition; Si, Si addition.

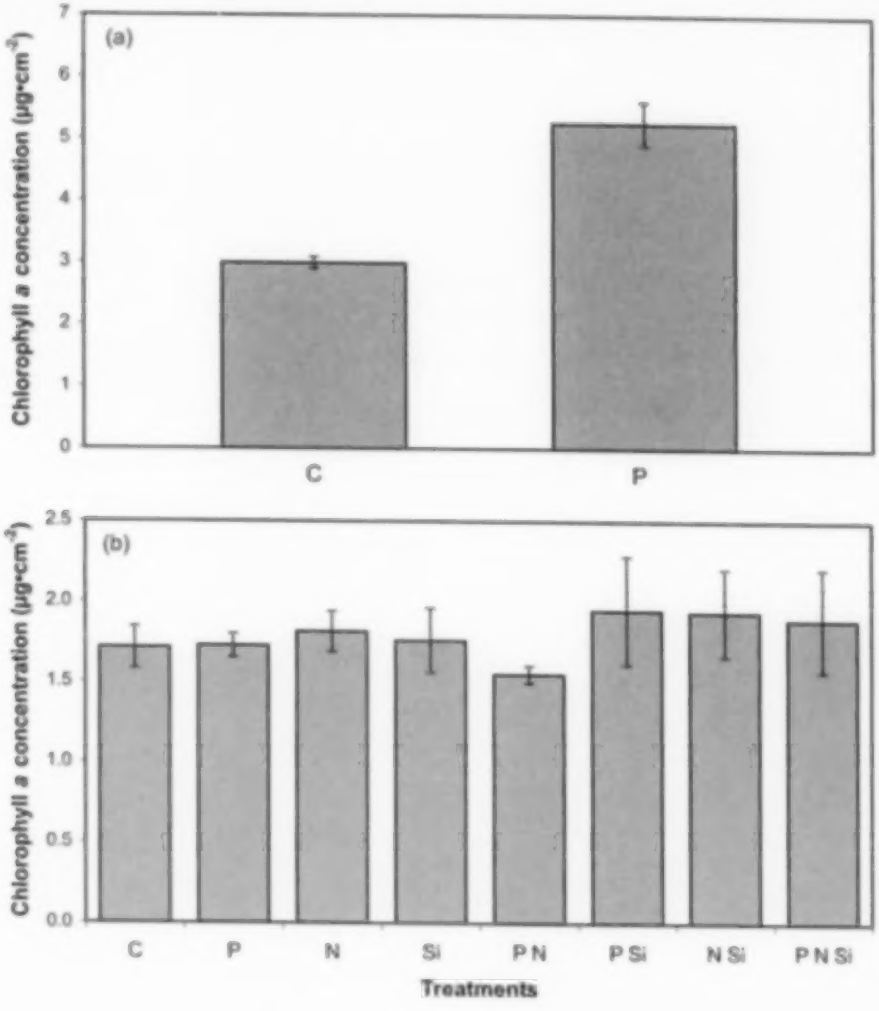

this needs to be confirmed by applying this methodology to other catchments.

The pattern shown in Fig. 7 explains why step-reductions in P loading often produce no ecological response in many urbanized lowland rivers (Jarvie et al. 2002*a*), as they have SRP concentrations far in excess of the maximum P-limiting concentration. The P concentration of the river, following remediation, remains above the maximum P-limiting concentration, and so the river remains on the horizontal part of the curve. There is therefore no algal biomass response to changing SRP concentrations.

Phosphorus limitation in the River Frome

The results from both flume experiments show that epilithic algal growth in the River Frome was not P limited throughout the summer of 2005. An increase in SRP concentration during this period would not produce increased algal biomass in the river and so would not lead to an increased level of eutrophication or a decline in environmental water quality. The highest measured SRP concentration in the River Frome in 2005 was a sharp peak of 404 $\mu g \cdot L^{-1}$ (Fig. 3), associated with a rainfall event in May 2005, but Experiment 2 has shown that even an increase in mean SRP concentration to over 420 $\mu g \cdot L^{-1}$ for a sustained period of 9 days did not result in an increase in epilithic algal biomass. These findings are supported by the results from the nutrient-diffusing periphytometers deployed in the River Frome in June 2005, which showed that algae were not limited (or colimited) by SRP, TON, or Si concentration.

The results from the P-stripping flumes indicate that below ~90 $\mu g \cdot L^{-1}$ SRP, algal biomass in the River Frome would decline with decreasing SRP concentration. An SRP concentration of 60–80 $\mu g \cdot L^{-1}$ may cause the epilithic algal biomass to fall by 20%–25%. An SRP concentration of

© 2007 NRC Canada

Fig. 6. SRP concentrations during Experiment 2. Solid lines and symbols, flumes receiving P additions; solid lines and open symbols, control flumes; broken lines and open symbols, flumes receiving $FeSO_4$ additions; thick solid line, SRP concentrations measured in the River Frome.

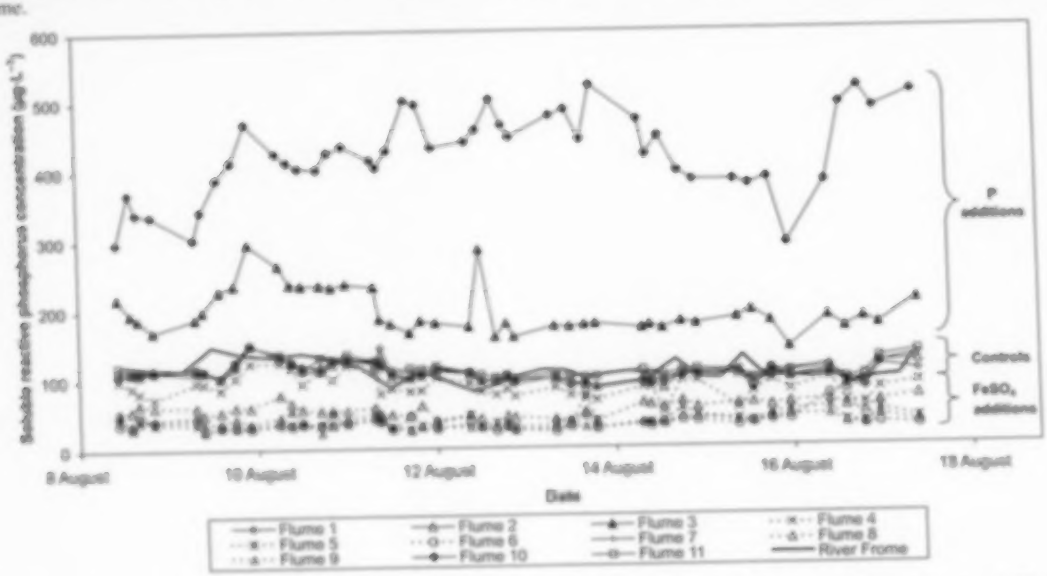

Fig. 7. Mean chlorophyll *a* concentrations on slate substrates at the end of Experiment 2. ×, $FeSO_4$ addition; △, control; ■, P addition. Error bars are ±2 SD derived from the three subsamples analysed from each slate. The curve represents the best fit of the data to Michaelis–Menten hyperbolic regression analysis (Dowes 1972).

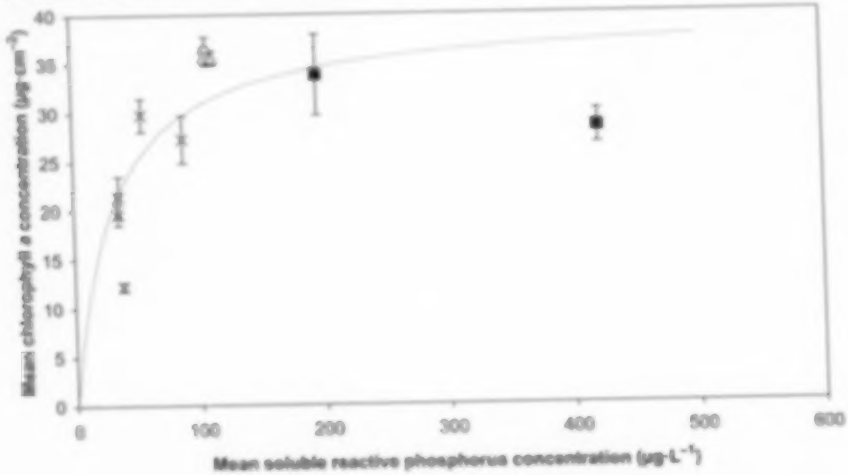

<40 µg·L^{-1} may result in a significant (up to 60%) reduction in algal biomass to between 12 and 24 µg chlorophyll *a*·cm^{-2}. The use of nutrient-diffusing periphytometers in Experiment 1 confirmed that this was caused by P limitation at these low SRP concentrations. A desk study by Dodds et al. (1997) suggested a similar target P concentration (30 µg·L^{-1}) to keep epiphytic chlorophyll *a* concentrations below 10 µg·cm^{-2}.

The River Frome intensive monitoring data for 2005 (Fig. 3) shows that the SRP concentration rarely fell below 40 µg·L^{-1} for a sustained period (>12 h), occurring only in March and November. These periods account for only 3% of the monitoring period and occur outside the spring–summer algal growing season typical of rivers in southern England. Therefore, they are likely to have little effect on controlling the total algal biomass in the River Frome over an annual cycle. However, the SRP concentration of the River Frome is between 60 and 90 µg·L^{-1} for much of the annual cycle (Fig. 3), particularly during long periods in March, May, and November 2005, and algal growth would be expected to be suppressed during these periods owing to P limitation. During the critical June–September summer period, when eutrophic events are most likely to occur, the River Frome SRP concentration is at its highest owing to the lack of dilu-

© 2007 NRC Canada

tion of sewage effluent inputs during this low river flow period. The mean SRP concentration in the River Frome at this time is 120 $\mu g \cdot L^{-1}$ and rarely falls below 90 $\mu g \cdot L^{-1}$, and so, algal biomass is likely to be at its maximum. Summer P concentrations need to be reduced until the maximum SRP concentration is below the ~90 $\mu g \cdot L^{-1}$ maximum P-limiting concentration before significant improvements in the environmental status of the River Frome would be observed. This maximum target SRP concentration agrees closely with the UK Environment Agency's mean P concentration target of 60 $\mu g \cdot L^{-1}$ for chalk rivers (Mainstone and Parr 2002).

The use of $FeSO_4$ to reduce bioavailable P concentration in river water provides a convenient method to greatly extend the scope of nutrient-enrichment experiments. Such experiments have previously only been able to simulate the effect of nutrient increases on an aquatic ecosystem. The use of streamside flumes, receiving either P or $FeSO_4$ additions, allows the effects of increasing and decreasing bioavailable P concentration to be simultaneously studied for the first time. $FeSO_4$ P stripping also allows such experiments to be used on rivers that already have P concentrations in excess of that needed for maximum algal growth. It is these highly nutrient-impacted rivers, common across most of the urbanized lowland catchments of the European Union and elsewhere, that are currently the focus of nutrient mitigation.

Determining the SRP concentration at which algae become growth limited is vital for effective eutrophication management, as this provides the basis for nutrient target setting within a catchment. Previous studies have shown that this target SRP concentration varies greatly between study areas, ranging from 3 $\mu g \cdot L^{-1}$ (Scrimgeour and Chambers 1997) to >110 $\mu g \cdot L^{-1}$ (Matlock et al. 1999). As the cost of introducing nutrient remediation measures to a catchment is closely dependent on the P target concentration that is set, it is vital that target setting is "knowledge based" for individual catchments. The new methodology presented in this paper could greatly assist catchment managers and policy makers in setting realistic P targets for individual nutrient-impacted rivers, allow them to identify what specific P load reduction is required before an environmental improvement will be observed, and should quantify reductions in algal biomass that would result from various levels of remediation.

Acknowledgements

The authors would like to thank Brian Godfrey (Freshwater Biological Association) for his technical assistance with the flume experiments and Ceri Davies and Phillip Sellick for their help with fieldwork and chemical analysis. We would also like to thank the two referees who provided constructive reviews that greatly improved the final manuscript.

References

Allen, N.S., and Hershey, A.E. 1996. Seasonal changes in chlorophyll alpha response to nutrient amendments in a North Shore tributary of Lake Superior. J. North Am. Benthol. Soc. **15**: 170–178.

Bernhardt, H., and Clasen, J. 1982. Limnological effects of the elimination of phosphorus from the Wahnbach Reservoir. Water Sci. Technol. **14**(4–5): 397–406.

Bothwell, M.L. 1985. Phosphorus limitation of lotic periphyton growth-rates — an intersite comparison using continuous-flow troughs (Thompson River system, British-Columbia). Limnol. Oceanogr. **30**: 527–542.

Bowes, M.J., Hilton, J., Irons, G.P., and Hornby, D.D. 2005*a*. The relative contribution of sewage and diffuse phosphorus sources in the River Avon catchment, southern England: implications for nutrient management. Sci. Total Environ. **344**(1–3): 67–81.

Bowes, M.J., Leach, D.V., and House, W.A. 2005*b*. Seasonal nutrient dynamics in a chalk stream: the River Frome, Dorset, UK. Sci. Total Environ. **336**(1–3): 225–241.

Casey, H., and Newton, P.V.R. 1973. The chemical composition and flow of the River Frome and its main tributaries. Freshw. Biol. **3**: 317–333.

Casey, H., Clarke, R.T., and Smith, S.M. 1993. Increases in nitrate concentrations in the River Frome (Dorset) catchment related to changes in land use, fertiliser applications and sewage input. Chem. Ecol. **8**: 105–117.

Chessman, B.C., Hutton, P.E., and Burch, J.M. 1992. Limiting nutrients for periphyton growth in sub-alpine, forest, agricultural and urban streams. Freshw. Biol. **28**: 349–361.

Dawes, E.A. 1972. Quantitative problems in biochemistry. Churchill Livingstone, Edinburgh, U.K.

Dodds, W.K., Smith, V.H., and Zander, B. 1997. Developing nutrient targets to control benthic chlorophyll levels in streams: a case study of the Clark Fork River. Water Res. **31**: 1738–1750.

Eisenreich, S.J., Bannerman, R.T., and Armstrong, D.E. 1975. A simplified phosphorus analytical technique. Environ. Lett. **9**: 45–53.

Elwood, J.W., Newbold, J.D., Trimble, A.F., and Stark, R.W. 1981. The limiting role of phosphorus in a woodland stream ecosystem — effects of P-enrichment on leaf decomposition and primary producers. Ecology, **62**: 146–158.

Environment Agency. 2000. Aquatic eutrophication in England and Wales: a management strategy. Environment Agency, Bristol, U.K.

European Economic Community. 1991. Urban waste water treatment. Directive 91/271/EEC. European Economic Community, Brussels, Belgium.

Francoeur, S.N., Biggs, B.J.F., Smith, R.A., and Lowe, R.L. 1999. Nutrient limitation of algal biomass accrual in streams: seasonal patterns and a comparison of methods. J. North Am. Benthol. Soc. **18**: 242–260.

Gainswin, B.E., House, W.A., Leadbeater, B.S.C., Armitage, P.D., and Patten, J. 2006. The effects of sediment size fraction and associated algal biofilms on the kinetics of phosphorus release. Sci. Total. Environ. **360**: 142–157.

Haygarth, P.M., Ashby, C.D., and Jarvis, S.C. 1995. Short-term changes in the molybdate reactive phosphorus of stored soil waters. J. Environ. Qual. **24**: 1133–1140.

Hilton, J., O'Hare, M., Bowes, M.J., and Jones, J.I. 2006. How green is my river? A new paradigm of eutrophication in rivers. Sci. Total Environ. **365**(1–3): 66–83.

HMSO. 1986. The determination of chlorophyll-*a* in aquatic environments. HMSO, London, U.K.

House, W.A., and Warwick, M.S. 1998. Intensive measurements of nutrient dynamics in the River Swale. Sci. Total Environ. **210**(1–6): 111–137.

Jarvie, H.P., Lycett, E., Neal, C., and Love, A. 2002*a*. Patterns in nutrient concentrations and biological quality indices across the upper Thames River basin, U.K. Sci. Total Environ. **282**: 263–294.

Jarvie, H.P., Neal, C., Warwick, A., White, J., Neal, M., Wickham, H.D., Hill, L.K., and Andrews, M.C. 2002*b*. Phosphorus uptake into algal biofilms in a lowland chalk river. Sci. Total Environ. **282**: 353–373.

© 2007 NRC Canada

Kelly, M.G., and Wilson, S. 2004. Effect of phosphorus stripping on water chemistry and diatom ecology in an eastern lowland river. Water Res. **38**: 1559–1567.

Lohman, K., Jones, J.R., and Baysingerdaniel, C. 1991. Experimental evidence for nitrogen limitation in a northern Ozark stream. J. North Am Benthol. Soc. **10**: 14–23.

Mainstone, C.P., and Parr, W. 2002. Phosphorus in rivers — ecology and management. Sci. Total Environ. **282**: 25–47.

Mainstone, C.P., Parr, W., and Day, M. 2000. Phosphorus and river ecology. Tackling sewage inputs. English Nature and Environment Agency, Peterborough, U.K.

Marker, A.F.H. 1972. The use of acetone and methanol in the estimation of chlorophyll in the presence of phaeophytin. Freshw. Biol. **2**: 361–385.

Matlock, M.D., Matlock, M.E., Storm, D.E., Smolen, M.D., and Henley, W.J. 1998. Limiting nutrient determination in lotic ecosystems using a quantitative nutrient enrichment periphytometer. J. Am. Water Resour. Assoc. **34**: 1141–1147.

Matlock, M.D., Storm, D.E., Smolen, M.D., and Matlock, M.E. 1999. Determining the lotic ecosystem nutrient and trophic status of three streams in eastern Oklahoma over two seasons. Aquat. Ecosyst. Health Manag. **2**: 115–127.

Mullin, J.B., and Riley, J.P. 1955. The colourometric determination of silicate with special reference to sea and natural waters. Anal. Chim. Acta, **12**: 31–36.

Mundie, J.H., Simpson, K.S., and Perrin, C.J. 1991. Responses of stream periphyton and benthic insects to increases in dissolved inorganic phosphorus in a mesocosm. Can. J. Fish. Aquat. Sci. **48**: 2061–2072.

Murphy, J., and Riley, J.P. 1962. A modified single solution method for the determination of phosphorus in natural waters. Anal. Chim. Acta, **12**: 31–36.

Perkins, R.G., and Underwood, G.J.C. 2001. The potential for phosphorus release across the sediment–water interface in an eutrophic reservoir dosed with ferric sulphate. Water Res. **35**: 1399–1406.

Peterson, B.J., Deegan, L., Helfrich, J., Hobbie, J.E., Hullar, M., Moller, B., Ford, T.E., Hershey, A., Hiltner, A., Kipphut, G., Lock, M.A., Fiebig, D.M., McKinley, V., Miller, M.C., Vestal, J.R., Ventullo, R., and Volk, G. 1993. Biological responses of a tundra river to fertilization. Ecology, **74**: 653–672.

Redfield, A.C. 1958. The biological control of chemical factors in the environment. Am. Sci. **46**: 205–221.

Reynolds, C.S., and Davies, P.S. 2001. Sources and bioavailability of phosphorus fractions in freshwaters: a British perspective. Biol. Rev. **76**: 27–64.

Rier, S.T., and Stevenson, R.J. 2006. Response of periphytic algae to gradients in nitrogen and phosphorus in streamside mesocosms. Hydrobiologia, **561**: 131–147.

Sabater, S., Acuna, V., Giorgi, A., Guerra, E., Munoz, I., and Romani, A.M. 2005. Effects of nutrient inputs in a forested Mediterranean stream under moderate light availability. Arch. Hydrobiol. **163**: 479–496.

Scrimgeour, G.J., and Chambers, P.A. 1997. Development and application of a nutrient-diffusing bioassay for large rivers. Freshw. Biol. **38**: 221–231.

SEAL. 2004. Total oxidized nitrogen in drinking and surface waters, and domestic and industrial wastes. SEAL Analytical Ltd., Burgess Hill, Sussex, U.K. p. 11.

Stelzer, R.S., and Lamberti, G.A. 2001. Effects of N:P ratio and total nutrient concentration on stream periphyton community structure, biomass, and elemental composition. Limnol. Oceanogr. **46**: 356–367.

Suschka, J., Machnicka, A., and Poplawski, S. 2001. Phosphates recovery from iron phosphates sludge. Environ. Technol. **22**: 1295–1301.

Tank, J.L., and Dodds, W.K. 2003. Nutrient limitation of epilithic and epixylic biofilms in ten North American streams. Freshw. Biol. **48**: 1031–1049.

© 2007 NRC Canada

Interaction between temperature and photoperiod on growth and feeding of Atlantic cod (*Gadus morhua*): possible secondary effects

Albert Kjartansson Imsland, Atle Foss, Thomas Alvseike, Arild Folkvord, Sigurd Olav Stefansson, and Thor Magne Jonassen

Abstract: Interactions between temperature and photoperiod on growth of Atlantic cod (*Gadus morhua*) juveniles (initial weight 9.1 g) were studied by rearing juvenile cod 3 months under simulated natural photoperiod (LDN) and continuous light (LD24:0) at 7, 10, and 13 °C. Juvenile Atlantic cod exposed to LD24:0 had higher growth rate and better feed conversion efficiency compared with cod reared under LDN. Optimal temperature for growth of juvenile Atlantic cod in the size range 5–50 g was influenced by photoperiod and was estimated to be 12.3 °C under LD24:0 and 15.7 °C under LDN. After termination of the laboratory study, the fish were reared in sea pens at ambient conditions for 17 months. The growth-enhancing effect of LD24:0 could be traced far beyond the duration of the laboratory trial, as the final mean weights in June 2005 of the fish reared at LD24:0 and 13 and 10 °C in the laboratory trial were 8% and 13% higher than those of the respective LDN groups. Our study indicates a physiological mechanism that might be linked to cod migrations, as maximal growth and feeding efficiency will be attained in areas during a season with extended day length or continuous light.

Résumé : L'élevage de jeunes morues franches (*Gadus morhua*) (masse initiale de 9,1 g) durant 3 mois sous une photopériode naturelle simulée (LDN) ou en lumière continue (LD24:0) et à des températures de 7, 10 et 13 °C a permis d'étudier les effets des interactions entre la température et la photopériode sur la croissance. Les jeunes morues franches exposées à LD24:0 ont un taux de croissance plus élevé et une meilleure efficacité de conversion de leur nourriture que les morues gardées à LDN. La température optimale pour la croissance des jeunes morues franches dans l'intervalle de tailles de 5–50 g est influencée par la photopériode et est estimée à 12,3 °C à LD24:0 et à 15,7 °C à LDN. Après la fin de l'étude de laboratoire, les poissons ont été gardés dans des enclos marins aux conditions ambiantes pendant 17 mois. L'effet de stimulation de la croissance par LD24:0 se manifeste bien au-delà des expériences de laboratoire, puisque les masses moyennes finales en juin 2005 des poissons élevés en laboratoire à LD24:0 et aux températures de 13 et de 10 °C étaient respectivement de 8 % et de 13 % plus élevées que celles des groupes LDN correspondants. Notre étude indique l'existence d'un mécanisme physiologique qui pourrait être relié aux migrations des morues, puisque les maximums de croissance et d'efficacité alimentaire sont atteints dans des zones où il y a une saison de lumière continuelle ou de photophase étendue.

[Traduit par la Rédaction]

Introduction

Information about the effect of photoperiod on growth dynamics in early juvenile Atlantic cod (*Gadus morhua*) is limited. In wild populations of Atlantic cod, seasonal variations in growth rate have been demonstrated (e.g., Schwalme and Chouinard 1999), although the changes caused by photoperiods per se are difficult to isolate from other concurrent changes in environmental factors such as temperature. Under altered photoperiods, fish are expected to adjust gradually to a new photoperiod regime by regulating feeding activity, growth, and food utilization (Boehlert 1981; Woiwode and Adelman 1991; Bromage et al. 2001). Photoperiod manipulation has been shown to enhance growth in several species. A growth-promoting effect of extended photoperiods has been demonstrated in juvenile Atlantic salmon (*Salmo salar*) (e.g., Stefansson et al. 1989; Solbakken et al. 1994) and

Received 24 May 2006. Accepted 26 October 2006. Published on the NRC Research Press Web site at http://cjfas.nrc.ca on 15 February 2007.
J19335

A.K. Imsland.[1] Akvaplan-niva Iceland Office, Akralind 4, 201 Kópavogur, Iceland, and Department of Biology, University of Bergen, High Technology Centre, 5020 Bergen, Norway.
A. Foss. Akvaplan-niva Bergen, Nordnesboder 5, 5005 Bergen, Norway.
T. Alvseike, A. Folkvord, and S.O. Stefansson. Department of Biology, University of Bergen, High Technology Centre, 5020 Bergen, Norway.
T.M. Jonassen. Marine Harvest Norway AS, Sandviksboder 78A, 5835 Bergen, Norway.

[1]Corresponding author (e-mail: albert.imsland@akvaplan.niva.no).

 doi:10.1139/F07-006 © 2007 NRC Canada

Pacific salmonids (*Oncorhynchus* spp.) (e.g., Clarke et al. 1981). This also seems to be the case for splitnose rockfish (*Sebastes diploproa*) (Boehlert 1981), turbot (*Scophthalmus maximus*) (Imsland et al. 1995, 1997, 2003), Atlantic halibut (*Hippoglossus hippoglossus*) (Simensen et al. 2000; Imsland and Jonassen 2005), and early Atlantic cod juveniles (Folkvord and Otterå 1993), although the response does not appear to be as pronounced as that observed in salmonids. A delayed response to photoperiod at low temperature has been shown in Atlantic salmon (Solbakken et al. 1994), and Clarke et al. (1978) concluded that changes in growth rate resulting from photoperiod were apparent sooner at higher temperatures owing to the rate-controlling effect of temperature. In contrast, Imsland et al. (1995) found that the relative response and duration of the growth enhancement of continuous light were longer at suboptimal temperature in turbot. Similarly, Jonassen et al. (2000*a*) found a significant interaction between temperature and light, suggesting a relatively stronger growth-enhancing effect of continuous light at lower temperature.

Many of the world's most commercially important cod populations perform extended seasonal migrations (up to 1000 km; Comeau et al. 2002*a*). In spring, migratory cod generally move from offshore to inshore areas (Lear and Green 1984; Comeau et al. 2002*a*, 2002*b*) where prey is abundant (e.g., Lambert and Dutil 1997). To ensure that the evolutionary benefits of migration outweigh the risks, a safe and reliable control mechanism must be in place so that migratory movements are initiated at the appropriate times within the physiological and environmental cycles (Comeau et al. 2002*a*). Off the Norwegian coast, coastal cod live their whole life close to the coast, while northeast Arctic cod spawn in Norwegian coastal areas in spring but feed in the Barents Sea – Svalbard region. Northeast Arctic cod perform yearly migrations of several thousand kilometres and it is unclear whether this is driven by photoperiod conditions (Stensholt 2001). However, such photoperiod-related migration has been indicated off the eastern coast of Canada (Comeau et al. 2002*a*, 2002*b*).

The purpose of this study was to investigate the possible interactive effect of photoperiod and temperature on both short- and long-term growth in juvenile Atlantic cod. By quantifying the possible gain in terms of increased growth, feed intake, and improved feed efficiency of cod reared at continuous light, we hope to gain more understanding of the underlying mechanism behind life history and migration strategies.

Materials and methods

Fish material and rearing conditions

The eggs were obtained from two commercial cod juvenile producers. The first group was attained from a cod hatchery in western Norway (59°50′N) and transported to the facilities of the University of Bergen where they were incubated. The broodfish were wild caught in the area around Bømlo (western Norway) in 2003 and reared in 40 m^3 tanks at simulated natural photoperiod and temperature of 6–8 °C (seawater pumped from 160 m depth). The mean weight of the broodfish was approximately 7 kg (range 5–18 kg). The eggs hatched on 28 March and the larvae were subsequently transferred to a 500 L tank with a constant temperature of 7.8 °C. The larvae were reared under continuous light, fed fresh filtered natural zooplankton (gradually increasing size fraction from 80 to 1000 µm), and weaned on a commercial formulated feed (Marin 030 and 050; Ewos A/S, Bergen, Norway) containing 60% protein, 12% fat, and 12% carbohydrates. On 20 June 2003, the juveniles were brought to the Industrial and Aquatic Laboratory (ILAB) at the Bergen High Technology Centre and reared at 10 °C and under a simulated natural photoperiod (LDN, 60°N) until the start of the study. This group of fish was mixed with an equal number of fish originating from another cod hatchery from western Norway (61°40′N). The broodfish were wild caught in the area around Møre (western Norway) in 2003 and reared in 70 m^3 tanks under LDN and temperature of 6–8 °C (seawater pumped from 100 m depth). The mean weight of the broodfish was approximately 15 kg (range 7–22 kg). The eggs were incubated at 7.0 °C, hatched on 25 March, and kept at 8–10 °C (gradual increase) during the first weeks of development. The larvae were reared under constant 16 h light : 8 h darkness (LD16:8), fed (size at start-feeding approximately 5 mm) enriched (Nannochloropsis Instant Algae®) rotifers for 35 days (prey density 2000 rotifers·L^{-1} for the first 10 days and then 4000 rotifers·L^{-1}), and then cofed for 10 days with commercial dry feed (Ewos Marin 030 and 050). On 22 June, the fish were transported to the ILAB and reared under the same conditions as described above. A more detailed description of the larvae and early juvenile protocol is given in Imsland et al. (2006).

After arrival at ILAB, the juveniles from the different producers were tagged with visible implant fluorescent elastomer tags (Northwest Marine Technology, Shaw Island, Washington), and thereafter, the fish (n = 1347) from the two groups were mixed and distributed randomly into 12 experimental tanks. Equal numbers of fish from the two producers were placed in each tank. The 1 m^2 square, grey, covered fiberglass experimental tanks had a rearing volume of 400 L and a bottom outlet. Seawater with a salinity of 33.5‰ (±0.2‰) was pumped from 90 m depth. Water flow was set to 10 L·min^{-1} for all experimental tanks. Oxygen saturation was measured weekly in the effluent (i.e., bottom outlet) water of all tanks and was higher than 80% at all times. A 36 W fluorescent daylight tube (Osram L36 W/12 Lumilux Deluxe Daylight; Osram GmbH, München, Germany) integrated in the tank cover provided light. Photon irradiation measured at the bottom of the tanks was approximately 5 µmol·m^{-2}·s^{-1}. During both the acclimation period and the experiment, the juveniles were fed a commercial dry diet (Marin 10 and 20, Ewos AS; 55% protein, 12% fat, 11% carbohydrate, gross digestible energy 20.4 MJ·kg^{-1}). Feed was provided in excess for 2 h daily (0800–0900 and 1400–1500). Pellet size (2 and 3 mm) was adjusted during the experiment, depending on fish size, with an introduction of 3 mm pellets beginning 14 October. Uneaten pellets were collected after each feeding (no later than 30 min after each feeding pulse) by filtering the outlet water with a fine mesh and counted to estimate feed intake and feed conversion efficiency. Our observations showed that the amount of feed broken down was negligible in the short time from feeding to sampling and that this sampling method gave an accurate estimate of the amount of feed eaten.

© 2007 NRC Canada

Experimental design

The growth study was carried out from 8 September until 12 December 2003. On 25 August 2003, in preparation for the study, a subgroup within each tank (n = 44–46 in each tank, total n = 538) were tagged intraperitoneally with Trovan® passive transponder tags and gradually acclimated over 1 day to 7 and 13 °C (eight tanks) or kept at 10 °C (four tanks). At each temperature, one group was exposed to LDN for Bergen (60°25′N) generated by a computer program (Lysstyr v. 2.0; Hansen 1990), including twilight periods, whereas the other group was exposed to continuous light (LD24:0). Each photoperiod–temperature regime consisted of two replicate tanks, so our setup is a three-way nested design where temperatures and photoperiods are crossed and replicates nested within temperatures and photoperiods. The temperature in all groups was measured twice daily and remained within ±0.2 °C (SD) of that prescribed. All fish were anaesthetized (0.05 g metacain·L^{-1}) and weighed individually (0.1 g) at 22–28 day intervals during the experiment.

After termination of the laboratory trial, all individually tagged fish (n = 597) were acclimated to 10 °C and transported by truck on 15 January 2004 to the production site of Marine Harvest at Tustna (North Trøndelag County, western Norway). Here, the fish were held in a land-based tank (8 m in diameter, 85 m^3 volume) until 25 May 2004 when they were transferred to a sea site at Smøla (western Norway, 63°31′N). The fish were reared at ambient temperatures (range mean temperatures 15 °C in August to 5 °C in March) together with 7500 other (untagged) cod in one sea pen (40 m in diameter, 7 m deep, 1000 m^3 volume). Mean weight at the start (all fish) was 172 g and the total biomass in the sea pen was approximately 9000 kg at the start. The fish were hand-fed five times a week using a commercial formulated feed from Dana Feed (Dan-Ex 1562 containing 15% fat and 58% protein). On 29 June 2005, the weight of 105 tagged fish from the laboratory study was measured. The total number of fish in June 2005 was 7700 with an average weight (all fish) of 1200 g.

Data analysis and statistical methods

Total feed consumption (C_T) was calculated as total feed supplied minus the total remaining feed. The C_T was calculated on a daily basis and then summarized for each of the four growth periods. Daily feeding rate ($F\%$) was calculated as

$$F\% = 100[C/((B_1 + B_2)/2)](t_2 - t_1)^{-1} \quad (1)$$

where C is feed consumption (g) in the period and B_1 and B_2 are fish biomass (g) on days t_1 and t_2, respectively. Feed conversion efficiency (FCE) was calculated as biomass gain per unit weight of feed consumed:

$$\text{FCE} = (B_2 - B_1)/C \quad (2)$$

Specific growth rate (G) was calculated according to the formula of Houde and Schekter (1981):

$$G = (e^g - 1)100 \quad (3)$$

where the instantaneous growth coefficient g is

$$g = (\ln W_2 - \ln W_1)(t_2 - t_1)^{-1} \quad (4)$$

where W_2 and W_1 are wet weight (g) on days t_2 and t_1, respectively.

All statistical analyses were performed with STATISTICA™ 6.1 (StatSoft Inc., Tulsa, Oklahoma). To assess normality of distributions, a Kolmogorov–Smirnov test was used and homogeneity of variances was tested using the Levene F test. A three-way ANOVA (Zar 1984) was applied to calculate the effect of different photoperiods and temperatures on mean weights, specific growth, feed consumption, daily feeding rate, and feed conversion efficiency, where the replicates are nested within the photoperiods and temperatures. The model equation of the nested ANOVA has the form

$$X_{ijkl} = \mu + \alpha_i + \beta_j + \gamma_{ij} + C_{ijk} + \varepsilon_{ijkl} \quad (5)$$

where μ is the general level, α_i is the treatment effect of temperature i, β_j is the treatment effect of photoperiod j, γ_{ij} is the effect of interactions between temperature α_i and photoperiod β_j, C_{ijk} is the contribution caused by replicate (here, tank) k in group ij, and ε_{ijkl} is the error term. Significant ANOVAs were followed by a Student–Newman–Keuls multiple comparison test to locate differences among treatments (Zar 1984). For weight data of fish in sea pens, we used a Tukey honestly significant difference (HSD) unequal N test to locate differences, as the number of fish was unequal between the groups.

Individual growth trajectories were analysed using a growth curve analysis (GCM) multivariate analysis of variance (MANOVA) model (Timm 1980; Chambers and Miller 1995). The model equation of the GCM has the form

$$\mathbf{Y}(n \times p) = \mathbf{X}(n \times q)\,\mathbf{B}(q \times p) + \mathbf{E}(n \times p) \quad (6)$$

where $\mathbf{Y}(n \times p)$ are the growth at age vectors

$$\mathbf{y} = (y_1, y_2, \ldots, y_p) \quad (7)$$

for each p (age) measurement on n individual fish, $\mathbf{X}(n \times q)$ is the design matrix or the set of extraneous variables measured for each individual, i.e., q = age p+ temperature i + photoperiod j + replicate k (i = 7, 10, 13 °C; j = LDN, LD24:0; k = replicate a, replicate b), $\mathbf{B}(q \times p)$ is the matrix of parameters estimated by the model, and $\mathbf{E}(n \times p)$ is the matrix of deviations for each individual from the expected value of $\mathbf{Y} = \mathbf{XB}$.

Specific growth in relation to photoperiods was analysed with a parabolic regression (Zar 1984) where growth was regressed against temperature for the two photoperiod groups. The regression was made using the combined growth rates of all tagged fish at each temperature for the photoperiod groups. Optimal temperatures for growth ($T_{opt}G$) were calculated as the zero solution to the first derivative of the parabolic regression equations, i.e., the solution of

$$G = aT^2 + bT + c \text{ or } dG/dT = 0 \rightarrow T_{opt}G = -b/2c \quad (8)$$

where G is specific growth rate, T is temperature (°C), and a, b, and c are constants determined by the regression. The asymptotic SE of the mean for $T_{opt}G$ was calculated based on individual growth data. As we were limited to only three temperatures when calculating $T_{opt}G$, a jackknife procedure (Shao and Tu 1996) was applied to generate new data sets so

© 2007 NRC Canada

that that bias of the estimator ($T_{opt}G$) could be reduced by calculating several jackknife estimators.

Results

Mortality

Total mortality during the tank study was 2.0% (11 fish). No systematic trend was found, as mortality occurred in all rearing units, except the 7 °C-LD24:0 group. Although not significantly different, overall mortality was higher under LDN, as eight of the dead fish were from the LDN groups and three from the LD24:0 group ($\chi^2_1 = 3.2$, $p > 0.07$). At 7 °C, mortality was higher in the LDN group ($\chi^2_1 = 5.4$, $p < 0.05$). A size-dependent mortality was found in the LDN group, as the dead fish were significantly smaller than the surviving fish (one-way ANOVA, $p < 0.05$). No size-dependent mortality was seen for the LD24:0 groups (one-way ANOVA, $p > 0.70$).

Short-term effect of photoperiod on growth

The overall initial mean weight (SD) was 9.1 (2.7) g and did not differ (three-way nested ANOVA, power $(1 - \beta) > 0.7$) (Fig. 1) between the photoperiod groups. From October onwards, the 13 °C-LD24:0 group had the highest mean weight (three-way nested ANOVA, $p < 0.05$) (Fig. 1), whereas no differences were found between the photoperiod groups at 7 °C. Accordingly, a significant interaction between temperature and photoperiods (three-way nested ANOVA, $p < 0.05$) was found from October until December. The final mean weights in December 2003 of the LD24:0 groups at 13 and 10 °C were 15% and 11% higher, respectively, than those of the LDN group.

The fish reared under the different photoperiod regimes differed in their growth patterns and the GCM analyses revealed differences between the individual growth trajectories of the photoperiod regimes ($MANOVA_{(PHOTOPERIOD)}$, Wilk's $\Lambda_{4,570} = 0.88$, $p < 0.001$) and between the temperatures ($MANOVA_{(TEMPERATURE)}$, Wilk's $\Lambda_{8,1050} = 0.38$, $p < 0.001$). Growth in the different time periods varied highly (Fig. 2), but in general, significant differences were seen between the LDN and LD24:0 groups at each temperature from late October onwards (Student–Newman–Keuls, $p < 0.05$) (Fig. 2). Accordingly, the LD24:0 groups had higher overall specific growth rate compared with the respective LDN groups at all temperatures (Fig. 2). The relative difference between the overall growth rates under LDN and LD24:0 varied between the temperatures and was highest at 10 °C (11% difference), and consequently, an interaction between temperature and photoperiod was seen ($MANOVA_{PHOTOPERIOD \times TEMPERATURE}$, Wilk's $\Lambda_{8,1050} = 0.95$, $p < 0.01$). A significant interaction effect between temperature and photoperiod on growth was found in the first and third experimental periods (Fig. 2).

When growth rates were plotted against temperature for the two photoperiod groups, the resulting parabolic regressions (Fig. 3) indicated that the temperature optimum for maximum growth in juvenile cod ($T_{opt}G \pm$ SE) varied between photoperiods and was estimated to be 15.7 ± 0.5 °C for the LDN group and 12.3 ± 0.2 °C for the LD24:0 group.

Feed intake, feeding rate, and feed conversion efficiency

The overall mean feed consumption (C_T) and daily feeding rate ($F\%$) did not differ between the photoperiod groups at each temperature (three-way nested ANOVA, $p > 0.3$) (Table 1). However, the LD24:0 groups had higher feed conversion efficiencies compared with the LDN groups at all temperatures (Student–Newman–Keuls test, $p < 0.05$). Feed consumption and daily feeding rate differed between temperature regimes (Table 1). The 13 °C group had the highest feed consumption and the 7 °C group the lowest consumption. Across temperatures, the 7 °C group had the lowest $F\%$, whereas the 10 and 13 °C groups showed similar daily feeding rates.

Long-term effect of photoperiod on growth

The mean weight of fish reared at different temperatures and photoperiods during the early juvenile stages differed following the 17-month commercial rearing period (Tukey HSD unequal N test, $p < 0.05$) (Fig. 4). On 29 June 2005, the mean weights (±SE) of the fish previously reared under LD24:0 at 10 and 13 °C were highest (1.70 ± 0.04 kg, n = 18 and 1.69 ± 0.08 kg, n = 22, respectively) followed by the 13 °C-LDN fish (1.56 ± 0.05 kg, n = 21). The fish reared at 7 °C (both groups: 1.50 ± 0.06 kg, n = 11 and 15 for former LD24:0 and LDN groups, respectively) in the laboratory trial and the fish reared under LDN and at 10 °C were significantly smaller (1.48 ± 0.08 kg, n = 18) than the fish reared under LD24:0 at 10 and 13 °C in the laboratory trial.

Discussion

Our data show that juvenile Atlantic cod exposed to continuous light have higher growth and better feed conversion efficiency than cod reared on simulated natural photoperiod during autumn. Earlier studies have addressed the effect of continuous light on survival and growth of Atlantic cod larvae (Puvanendran and Brown 2002), short-term effects on 1–2 g juveniles (Folkvord and Otterå 1993), and effects on sexual maturation and growth of adult cod (Hansen et al. 2001; Karlsen et al. 2006; Taranger et al. 2006). However, studies on the effects of photoperiod on survival, growth, and feed conversion efficiency in early juvenile (3–100 g) Atlantic cod have been absent until now. Puvanendran and Brown (2002) found that cod larvae grew and survived better under continuous light compared with LD18:6 and LD12:12 regimes. The combination of rearing the larvae at high light intensities (2400 lx) and continuous light increased encounter rate and improved capture success of the larvae towards its prey. For adult cod, continuous light could, theoretically, have a dual effect on growth: a direct growth-enhancing effect and a secondary effect by arresting gonad development and inhibiting spawning. Earlier studies with adult cod were unable to differentiate whether the growth gain is due to direct photostimulation of growth or inhibition of sexual maturation allowing continued growth (e.g., Hansen et al. 2001; Karlsen et al. 2006; Taranger et al. 2006). In the present study with immature juvenile cod, a direct growth-enhancing effect was demonstrated. Such a direct growth-promoting effect of long days or continuous light has been found in Atlantic salmon (Kråkenes et al. 1991; Hansen et al. 1992),

© 2007 NRC Canada

Fig. 1. Mean (±SE) weight for individually tagged Atlantic cod (*Gadus morhua*) reared at different photoperiods and temperatures. The vertical line indicating SE may be obscured by the symbol. Different letters indicate statistical differences (three-way nested ANOVA, $p < 0.05$) between the experimental groups, with *a* as the highest value. The values for two replicates are combined, $n = 80–82$ for each mean value. ns, not significant;an asterisk indicates a significant interaction between temperature and photoperiod regime. Squares, 7 °C; triangles, 10 °C; circles, 13 °C; open symbols and broken line, LDN; solid symbols and solid line, LD24:0.

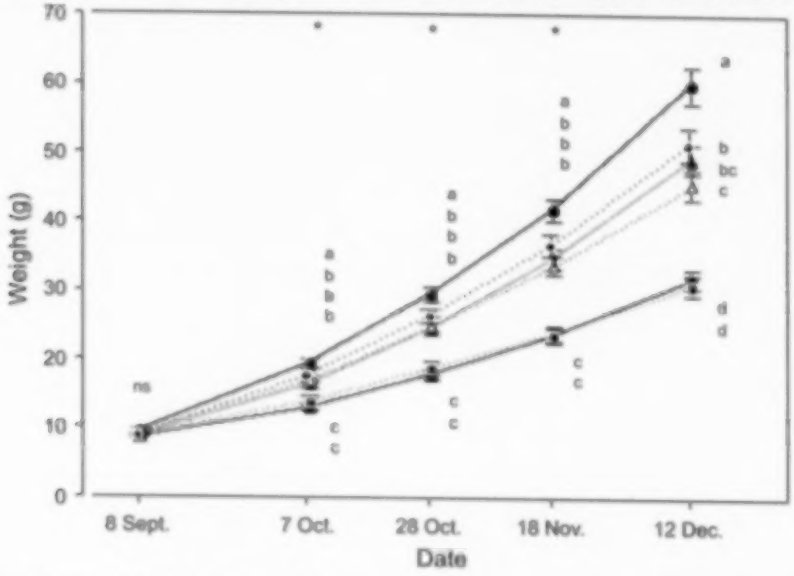

Fig. 2. Mean specific growth rates of individually tagged Atlantic cod (*Gadus morhua*) reared at different photoperiods and temperature during the experimental period. Vertical whiskers indicate SE. Different letters denote significant differences (Student–Newman–Keuls test, $p < 0.05$) between the experimental groups, with *a* as the highest value. The values for two replicates are combined, $n = 80–82$ for each mean value. ns, not significant; an asterisk indicates a significant interaction between temperature and photoperiod regime. Solid bars, 7 °C-LD24:0; open bars, 7 °C-LDN; grey bars, 10 °C-LD24:0; hatched bars, 10 °C-LDN; vertical lined bars, 13 °C-LDN24:0; horizontal lined bars, 13 °C-LDN.

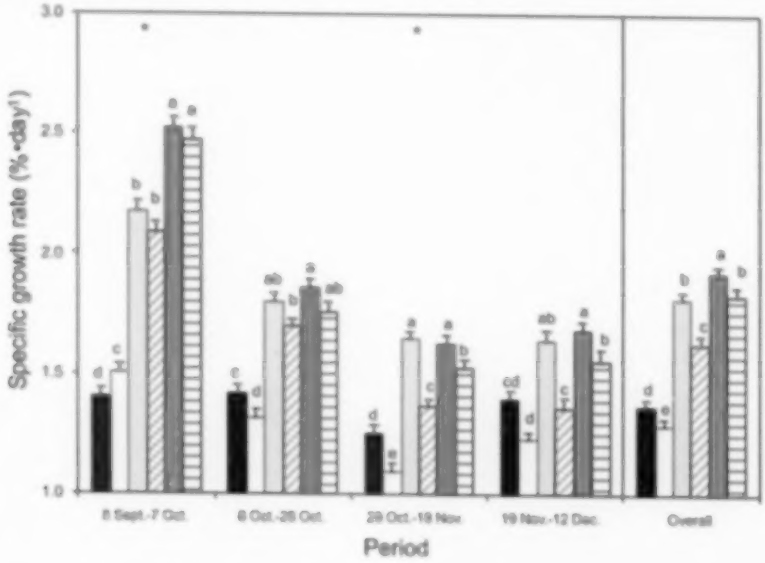

Atlantic halibut (Simensen et al. 2000; Imsland and Jonassen 2005), and turbot (Imsland et al. 1995, 1997, 2003). The present study is the first to verify this effect in the early juvenile stages of cod. Taken together, the data from studies with larval (Puvanendran and Brown 2002), juvenile (this study), and adult cod (Davie et al. 2003; Karlsen et al. 2006;

© 2007 NRC Canada

Fig. 3. Changes in specific growth rate (SGR) of juvenile Atlantic cod (*Gadus morhua*) with temperature for two different photoperiod regimes. The lines represent the least squares second-order polynomial fit to the data: $SGR = aT^2 + bT + c$, where T is temperature and a, b, and c are constants determined by the regression. Solid line, LD24:0; broken line, LDN. Vertical lines indicate SE of the mean, $n = 83$–90 for each data point. For the two photoperiod groups, optimum temperature for growth ($T_{opt}G$) indicated by the solid line (LD24:0) and broken line (LDN) line was calculated from the first-order derivative of the parabolic regressions (i.e., when $dG/dT = 0$). Equations for the two photoperiods: LD24:0, $SGR = -0.019T^2 + 0.477T - 1.035$; LDN, $SGR = -0.008T^2 + 0.248T - 0.069$.

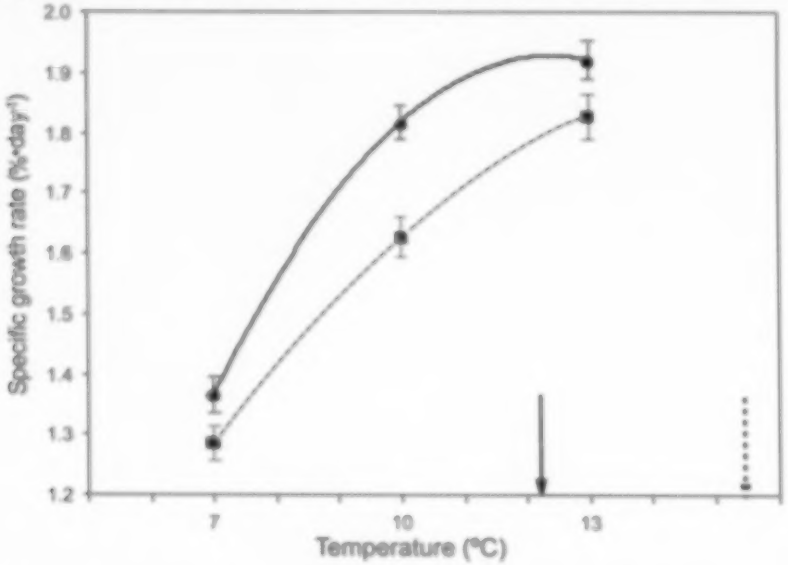

Table 1. Feed consumption (C_T), daily feeding rate ($F\%$), and feed conversion efficiency (FCE) of juvenile Atlantic cod (*Gadus morhua*) reared under three temperature regimes and two photoperiods.

Temperature (°C)	Photoperiod	C_T (g wet weight)	$F\%$	FCE
7	LDN	428.3 (41.4)*c*	1.01 (0.15)*b*	1.10 (0.13)*b*
	LD24:0	485.9 (102.6)*c*	1.12 (0.11)*b*	1.22 (0.04)*a*
10	LDN	655.3 (76.8)*b*	1.31 (0.22)*a*	1.14 (0.09)*b*
	LD24:0	752.4 (130.4)*b*	1.41 (0.25)*a*	1.22 (0.07)*a*
13	LDN	883.7 (149.8)*a*	1.46 (0.27)*a*	1.14 (0.06)*b*
	LD24:0	926.3 (207.1)*a*	1.48 (0.25)*a*	1.24 (0.05)*a*

Note: Results are given as mean (SD) ($n = 8$) for each factor combination. Different letters denote significant differences (three-way nested ANOVA, $p < 0.05$) between temperature and photoperiod treatments.

Taranger et al. 2006) all highlight the positive short- and long-term effect of continuous light on growth.

Interacting effects of light and temperature are often caused by a shift in the optimum temperature for growth with a changing photoperiod. A positive relationship between day length and optimum temperature for growth is evident in most investigations of freshwater fish (Kilambi et al. 1970; Woiwode and Adelman 1991; Solbakken et al. 1994). Most reports on temperate marine species, however, differ from this pattern. No seasonal differences have been found in the final temperature preference of European plaice (*Pleuronectes platessa*) (Zahn 1963) or the estuarine goby (longjaw mudsucker) (*Gillichthys mirabilis*) (DeVlaming 1971). The same was evident for optimum temperature for growth in Atlantic halibut (*Hippoglossus hippoglossus*) (Hallaråker et al. 1995) and splitnose rockfish (*Sebastes diplopora*) (Boehlert 1981). A possible reason for the apparent lack of a seasonal temperature acclimation in marine species could be the relatively stable seasonal temperature regime in the sea compared with fresh water, thus reducing the selection pressure for such adaptations. Moreover, in Atlantic halibut (Jonassen et al. 2000*b*), turbot (Imsland et al. 2000), and Atlantic silverside (*Menidia menidia*) (Conover 1990; Conover and Present 1990), countergradient growth compensation, rather than temperature acclimation, has been suggested as an adaptation to a temperature-restricted growing season at higher latitudes. Our data point out the possibility of a changed optimum temperature during rearing under continuous light as an explanation of the relatively stronger growth-enhancing effect of continuous light at high temperatures (although it should be noted that our model is derived from three data points from each photoperiod and hence requires confirmation). Our calculated optimal temperature for growth is higher (15.7 °C) for the LDN group compared

© 2007 NRC Canada

Fig. 4. Mean weight of Atlantic cod (*Gadus morhua*) reared under different temperature and photoperiod regimes during the early juvenile stage and then reared in sea pens at ambient conditions for 17 months. Different letters indicate statistical differences (Tukey's HSD unequal N test, $p < 0.05$), with *a* as the highest value, $n = 11–22$ for each mean value.

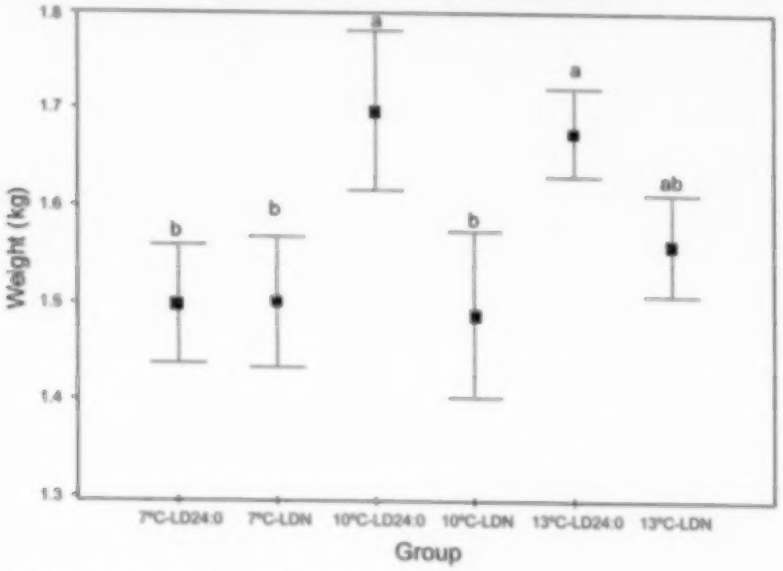

with the LD24:0 group (12.3 °C). It is possible that this temperature–photoperiod growth model may vary in relation to genotype. In a parallel study, Imsland et al. (2005) found significant interaction between haemoglobin genotypes and photoperiods, demonstrated by the variation in genotype response towards photoperiod treatment. At both temperatures investigated (10 and 13 °C), the highest growth rates were found for the *Hb-I(2/2)* genotype at LD24:0, whereas the lowest overall mean growth rates were found for the same genotype reared under LDN. Conversely, the *Hb-I(1/1)* genotype displayed the fastest specific growth rates in the LDN groups at both temperatures. The data of Imsland et al. (2005) clearly suggest that the genetic composition must be considered in order to increase the effect of photoperiod treatment in Atlantic cod.

It has been shown that bigger size-at-age found in the northeast Arctic cod when compared with Nova Scotian cod in Canada is linked with photoperiod, indicating a possible light-limited feeding opportunity in southern cod stocks (Suthers and Sundby 1996). Our data indicate a more direct effect, as continuous light was found to both enhance growth and improve feed conversion under conditions where feed was not limiting. The data of Suthers and Sundby (1996) together with our findings suggest that photoperiod could be a powerful driving force behind cod migrations, where fish could maximize their size-at-age by northbound migration during summertime in the Northern Hemisphere. Such photoperiod-related migration has been indicated off the eastern coast of Canada (Comeau et al. 2002*a*, 2002*b*). Clearly, there are other proximal cues that govern the migratory behaviour of cod (Stensholt 2001; Comeau et al. 2002*a*, 2002*b*), but our data point to an interesting secondary effect of seeking out high-latitude areas during summer. Foraging in such areas (where light is continuous during summer) will have a direct growth-enhancing effect, thus shortening the time the fish needs to achieve a critical size to survive the first winter (Shuter and Post 1990; Conover 1992 and references therein).

Based on our data, it seems that continuous light has similar effect in Atlantic cod as found for salmonids, where the growth-enhancing effect of extended photoperiods and continuous light is more prominent at near-optimal temperatures (Clarke et al. 1978; Solbakken et al. 1994). Earlier findings in other marine species, e.g., Atlantic halibut and turbot, contrast our findings on Atlantic cod. The findings of Jonassen et al. (2000*a*) suggest that the magnitude of the effect of continuous light on growth is inversely related to temperature in Atlantic halibut. Further support for this is found in studies on juvenile turbot (Imsland et al. 1995, 1997) demonstrating that the growth-promoting effect of continuous light can be stronger at low temperatures than at the near-optimum temperature for the species. These findings on Atlantic halibut and turbot contrast our data where the growth-enhancing effect of continuous light increased with increasing temperature.

Photostimulation may affect fish growth through better food conversion efficiency and not just through stimulated food intake (see review by Boeuf and Le Bail 1999). In a recent study of Atlantic salmon, Handeland et al. (2003) showed that constant light stimulated growth through increased food consumption (but not improved food conversion efficiency) in both wild and selected strains, concurrent with an increase in growth hormone, while the selected strains showed better food conversion than the wild strains under both LD24:0 and LDN. In contrast, Jonassen et al. (2000*a*) reported improved food conversion efficiency (but no difference in food consumption) in juvenile halibut subjected to continuous light at two temperatures. Accordingly, it appears that nonsalmonids adjust to extended photoperiods by displaying higher feeding activity, growth, and food utilization (Boehlert 1981;

© 2007 NRC Canada

Woiwode and Adelman 1991). Boehlert (1981) found positive effects of photoperiod on growth in splitnose rockfish, where constant LD16:8 resulted in enhanced growth compared with LD12:12 and was probably related to a greater scope for growth owing to a lower standard metabolic rate. In the current trial, Atlantic cod reared at continuous light had higher growth in conjunction with higher feed conversion. In contrast, food consumption and feeding rate followed the increase in temperature and were independent of photoperiod.

The observed growth response following a sudden increase in photoperiod was delayed by at least 21 days after the exposure of the fish to continuous light, and in fact, an initial negative effect of continuous light was seen at 7 °C in this period. The same pattern has been reported in Atlantic salmon subjected to continuous additional light superimposed on natural photoperiod in seawater (Hansen et al. 1992; Endal et al. 2000) and in Atlantic halibut (Simensen et al. 2000), suggesting that the fish in seawater require some time to adapt to changes in photoperiod. Moreover, the previous photoperiod history of the fish may have an important influence on the growth response to a change in light regime (Hoar 1988; Clarke et al. 1989), with a decrease in photoperiod having a growth-depressing effect in several species (e.g., Skilbrei et al. 1997). This could explain some of the differences seen between the two light regimes, as the LDN group experienced diminishing light as the daylight period was reduced from approximately 12 h in September to 7 h in December.

A finding in this study that could have an important implication for the aquaculture sector is the advantage of rearing the fish at optimal temperatures and under continuous light during the juvenile period, as size differences established at this stage may be maintained in the adult fish (Imsland et al. 2006). Similar findings have been observed for wild juvenile northeast Arctic cod where significant size correlations are documented between year-classes and the basis for these relative size differences are formed during the first half year of life (Ottersen et al. 2002). In contrast, recent findings (Sæther 2005) have indicated that moving juvenile cod from different rearing temperatures (between 8 and 15 °C) to low temperature (3 °C) will lead to growth reduction in all groups that will obliterate the short-term gain of rearing juvenile cod at elevated temperatures. In our study, the tagged fish were acclimatized to 10 °C before transport to commercial ongrowing in northwestern Norway and moved to sea pens when sea temperature was approximately 7 °C. Size differences after 17 months in sea pens were slightly reduced, but the general picture was that differences in the juvenile stage could be traced throughout the adult stage. This long-term growth effect could have a positive effect on the commercial aquaculture of Atlantic cod. By applying optimal combinations of temperatures and photoperiods during the juvenile phase in land-based farms, the farmer may be able to produce more biomass on a given time scale of a commercial-sized fish.

Earlier studies have shown that increased light intensity and (or) photoperiod may decrease the incidence of early cannibalism (Baras et al. 1999, 2000). In vindu (*Heterobranchus longifilis*), cannibalism was found to be essentially nocturnal (Baras et al. 1999) and decreased with increased day length, with the lowest cannibalism seen in groups reared under continuous light. Whether this is the case in early juvenile Atlantic cod is unknown. The present data show that total mortality (cannibalism and other causes) was slightly higher in the LDN group compared with the continuous light group. A more detailed study of the interplay between light and cannibalism is needed to verify, or falsify, whether continuous light may reduce the incidence of cannibalism in early juvenile cod.

In conclusion, the present study shows that Atlantic cod exposed to continuous light had higher growth and better feed conversion efficiency and were significantly larger than cod reared under a simulated natural photoperiod. The effect is more profound at near-optimal temperatures, and these differences in size as result of previous temperature and light regime are maintained at later stages. These findings may have important consequences for optimization of the commercial production of Atlantic cod and may increase our knowledge of proximal cues for migrations in Atlantic cod.

Acknowledgements

We thank Sagafjord Seafarm, Stord, Norway, and Havlandet Marin Yngel, Florø, Norway, for supplying the biological material. This study was financed by the Norwegian Research Council (No. 156204/120).

References

Baras, E., Tissier, F., Philippart, and Melard, C. 1999. Sibling cannibalism among juvenile vundu under controlled conditions: Part II. Effect of body weight and environmental variables on the periodicity and intensity of type II cannibalism. J. Fish Biol. **54**: 106–118.

Baras, E., Maxi, M.Y., Ndao, M., and Melard, C. 2000. Sibling cannibalism in dorada under experimental conditions. Part II. Effect of initial size heterogeneity, diet and light regime on early cannibalism. J. Fish Biol. **57**: 1021–1036.

Boehlert, G.W. 1981. The effects of photoperiod and temperature on laboratory growth of juvenile *Sebastes diploproa* and a comparison with growth in the field. Fish. Bull. **79**: 789–794.

Boeuf, G., and Le Bail, P.Y. 1999. Does light have an influence on fish growth? Aquaculture, **177**: 129–152.

Bromage, N., Porter, M., and Randall, C. 2001. The environmental regulation of maturation in farmed finfish with special reference to the role of photoperiod and melatonin. Aquaculture, **197**: 63–98.

Chambers, R.C., and Miller, T.J. 1995. Evaluating fish growth by means of otolith increment analysis: special properties of individual-level longitudinal data. *In* Recent developments in fish otolith research. *Edited by* D.H. Secor, J.M. Dean, and S.E. Campana. University of South Carolina Press, Colombia, S.C. pp. 155–175.

Clarke, W.C., Shelbourn, J.E., and Brett, J.R. 1978. Growth and adaptation to sea water in 'underyearling' sockeye (*Oncorhynchus nerka*) and coho (*O. kisutch*) salmon subjected to regimes of constant or changing temperature and day length. Can. J. Zool. **56**: 2413–2421.

Clarke, W.C., Shelbourn, J.E., and Brett, J.R. 1981. Effect of artificial photoperiod cycles, temperature, and salinity on growth and smolting in underyearling coho (*Oncorhynchus kisutch*) and chi-

© 2007 NRC Canada

nook (*O. tshawytscha*), and sockeye (*O. nerka*) salmon. Aquaculture, **22**: 105–116.

Clarke, W.C., Shelbourn, J.E., Ogasawara, T., and Hirano, T. 1989. Effect of initial daylength on growth, seawater adaptability and plasma growth hormone levels in underyearling coho, chinook, and chum salmon. Aquaculture, **82**: 51–62.

Comeau, L.A., Campana, S.E., and Chouinard, G.A. 2002*a*. Timing of Atlantic cod (*Gadus morhua* L.) seasonal migrations in the southern Gulf of St. Lawrence: interannual variability and proximate control. ICES J. Mar. Sci. **59**: 333–351.

Comeau, L.A., Campana, S.E., and Castonguay, M. 2002*b*. Automated monitoring of a large-scale cod (*Gadus morhua*) migration in the open sea. Can. J. Fish. Aquat. Sci. **59**: 1845–1850.

Conover, D.O. 1990. The relation between capacity for growth and length of growing season: evidence for and implications of countergradient variation. Trans. Am. Fish. Soc. **119**: 416–430.

Conover, D.O. 1992. Seasonality and the scheduling of life history at different latitudes. J. Fish Biol. **41**(Suppl. B): 161–178.

Conover, D.O., and Present, T.M.C. 1990. Countergradient variation in growth rate: compensation for length of the growing season among Atlantic silversides from different latitudes. Oecologia, **83**: 316–324.

Davie, A., Porter, M.J.R., and Bromage, N. 2003. Photoperiod manipulation of maturation and growth of Atlantic cod (*Gadus morhua*). Fish Physiol. Biochem. **28**: 399–401.

DeVlaming, V.L. 1971. Thermal selection in the estuarine goby *Gillichthys mirabilis* Cooper. J. Fish Biol. **3**: 277–286.

Endal, H.P., Taranger, G.L., Stefansson, S.O., and Hansen, T. 2000. Effects of continuous additional light on growth and sexual maturity in Atlantic salmon, *Salmo salar*, reared in sea cages. Aquaculture, **191**: 205–214.

Folkvord, A., and Otterå, H. 1993. Effects of initial size distribution, day length and feeding frequency on growth, survival and cannibalism in juvenile Atlantic cod (*Gadus morhua* L.). Aquaculture, **114**: 243–260.

Hallaråker, H., Folkvord, A., and Stefansson, S.O. 1995. Growth of juvenile halibut (*Hippoglossus hippoglossus*) related to temperature, day length and feeding regime Neth. J. Sea Res. **34**: 139–147.

Handeland, S.O., Porter, M., Björnsson, B.T., and Stefansson, S.O. 2003. Osmoregulation and growth in a wild and a selected strain of Atlantic salmon smolts on two photoperiod regimes. Aquaculture, **222**: 29–43.

Hansen, E.H. 1990. The use of artificial light and light manipulation for controlled production of salmonids. Dr. Ing. thesis, Norwegian Institute of Technology, University of Trondheim. (In Norwegian with summary in English)

Hansen, T., Stefansson, S., and Taranger, G.L. 1992. Growth and sexual maturation in Atlantic salmon, *Salmo salar* L., reared in sea cages at two different light regimes. Aquac. Fish. Manag. **23**: 135–140.

Hansen, T., Karlsen, Ø., Taranger, G.L., Hemre, G.I., Holm, J.C., and Kjesbu, O.S. 2001. Growth, gonadal development and spawning time of Atlantic cod (*Gadus morhua*) reared under different photoperiods. Aquaculture, **203**: 51–67.

Hoar, W.S. 1988. The physiology of smolting salmonids. *In* Fish physiology. Vol. XIB. *Edited by* W.S. Hoar and D.J. Randall. Academic Press, New York. pp. 275–343.

Houde, E.D., and Schekter, R.C. 1981. Growth rates, rations and cohort consumption of marine fish larvae in relation to prey concentrations. Rapp. P.-v. Réun. Cons. Int. Explor. Mer, **178**: 441–453.

Imsland, A.K., and Jonassen, T.M. 2005. The relation between age at first maturity and growth of Atlantic halibut (*Hippoglossus hippoglossus* L.) reared under four different light regimes. Aquac. Res. **36**: 1–7.

Imsland, A.K., Folkvord, A., and Stefansson, S.O. 1995. Growth, oxygen consumption and activity of juvenile turbot (*Scophthalmus maximus* L.) reared under different temperatures and photoperiods. Neth. J. Sea Res. **34**: 149–159.

Imsland, A.K., Folkvord, A., Jónsdóttir, Ó.D.B., and Stefansson, S.O. 1997. Effects of exposure to extended photoperiods during the first winter on long-term growth and age at first maturity in turbot (*Scophthalmus maximus*). Aquaculture, **159**: 125–141.

Imsland, A.K., Foss, A., Nævdal, G., Cross, T., Bonga, S.W., van Ham, E.H., and Stefansson, S.O. 2000. Countergradient variation in growth and food conversion efficiency of juvenile turbot. J. Fish Biol. **57**: 1216–1226.

Imsland, A.K., Dragsnes, M., and Stefansson, S.O. 2003. Exposure to continuous light inhibits maturation in turbot (*Scophthalmus maximus*). Aquaculture, **219**: 911–919.

Imsland, A.K., Foss, A., Folkvord, A., Stefansson, S.O., and Jonassen, T.M. 2005. Genotypic response to photoperiod treatment in Atlantic cod (*Gadus morhua*). Aquaculture, **250**: 525–532.

Imsland, A.K., Foss, A., Koedijk, R., Folkvord, A., Stefansson, S.O., and Jonassen, T.M. 2006. Short and long term differences in growth, feed conversion efficiency and deformities of juvenile Atlantic cod (*Gadus morhua*) startfed on rotifers or zooplankton. Aquac. Res. **37**: 1015–1027.

Jonassen, T.M., Imsland, A.K., Kadowaki, S., and Stefansson, S.O. 2000*a*. Interaction of temperature and photoperiod on growth of Atlantic halibut *Hippoglossus hippoglossus* L. Aquac. Res. **31**: 219–227.

Jonassen, T.M., Imsland, A.K., FitzGerald, R., Stefánsson, M.Ö., Bonga, S.W., van Ham, E., Nævdal, G., and Stefansson, S.O. 2000*b*. Geographic variation in growth and food conversion efficiency of juvenile Atlantic halibut related to latitude. J. Fish Biol. **56**: 279–294.

Karlsen, Ø., Norberg, B., Kjesbu, O.S., and Taranger, G.L. 2006. Effects of photoperiod and exercise on growth, liver size, and age at puberty in farmed Atlantic cod (*Gadus morhua* L.). ICES J. Mar. Sci. **63**: 355–364.

Kilambi, R.V., Noble, J., and Hoffman, J.E. 1970. Influence of temperature and photoperiod on growth, food consumption, and food conversion efficiency of channel catfish. Proc. Annu. Conf. Southeast. Assoc. Game Fish Comm. **24**: 519–531.

Kråkenes, R., Hansen, T., Stefansson, S.O., and Taranger, G.L. 1991. Continuous light increases growth rate of Atlantic salmon (*Salmo salar* L.) postsmolts in sea cages. Aquaculture, **95**: 281–287.

Lambert, Y., and Dutil, J.-D. 1997. Condition and energy reserves of Atlantic cod (*Gadus morhua*) during the collapse of the northern Gulf of St. Lawrence stock. Can. J. Fish. Aquat. Sci. **54**: 2388–2400.

Lear, W.H., and Green, J.M. 1984. Migration of the "northern" Atlantic cod and the mechanisms involved. *In* Mechanisms of migration in fishes. *Edited by* J.D. McCleave, G.P. Arnold, J.J. Dodson, and W.H. Neill. Plenum Press, New York. pp. 309–316.

Ottersen, G., Helle, K., and Bogstad, B. 2002. Do abiotic mechanisms determine interannual variability in length-at-age of juvenile Arcto-Norwegian cod? Can. J. Fish Aquat. Sci. **59**: 57–65.

Puvanendran, V., and Brown, J.A. 2002. Foraging, growth and survival of Atlantic cod larvae. Aquaculture, **214**: 131–151.

Schwalme, K., and Chouinard, G.A. 1999. Seasonal dynamics in feeding, organ weights, and reproductive maturation of Atlantic cod (*Gadus morhua*) in the southern Gulf of St. Lawrence. ICES J. Mar. Sci. **56**: 303–319.

© 2007 NRC Canada

Shao, J., and Tu, D. 1996. The jackknife and bootstrap. Springer series in statistics. SpringerVerlag, New York.

Shuter, B.J., and Post, J.R. 1990. Climate, population viability, and the zoogeography of temperate fishes. Trans. Am. Fish. Soc. **119**: 314–336.

Simensen, L.M., Jonassen, T.M., Imsland, A.K., and Stefansson, S.O. 2000. Photoperiod regulation of growth of juvenile halibut (*Hippoglossus hippoglossus* L.) reared at different photoperiods. Aquaculture, **119**: 119–128.

Skilbrei, O.T., Hansen, T., and Stefansson, S.O. 1997. Effects of decreases in photoperiod on growth and bimodality in Atlantic salmon *Salmo salar* L. Aquac. Res. **28**: 43–49.

Solbakken, V.A., Hansen, T., and Stefansson S.O. 1994. Effects of photoperiod and temperature on growth and parr–smolt transformation in Atlantic salmon (*Salmo salar*) and subsequent performance in seawater. Aquaculture, **121**: 13–27.

Stefansson, S.O., Nævdal, G., and Hansen, T. 1989. The influence of three unchanging photoperiods on growth and parr–smolt transformation in Atlantic salmon, *Salmo salar* L. J. Fish Biol. **35**: 237–247.

Stensholt, B.K. 2001. Cod migration patterns in relation to temperature: analysis of storage tag data. ICES J. Mar. Sci. **58**: 770–793.

Suthers, I.M., and Sundby, S. 1996. Role of the midnight sun: comparative growth of pelagic juvenile cod (*Gadus morhua*) from the Arcto-Norwegian and a Nova Scotian stock. ICES J. Mar. Sci. **53**: 827–836.

Sæther, B.S. 2005. Toleranse for temperaturfall hos torsk i settefiskfasen. Potensiell flaskehals i intensiv sesonguavhengig produksjon. Rep. 14/2005. ISBN-10 82-7251-564-4. Norwegian Institute of Fisheries and Aquaculture Research, Tromsø, Norway. (In Norwegian with English abstract)

Taranger, G.L., Aardal, L., Hansen, T., and Kjesbu, O.S. 2006. Continuous light delays sexual maturation and increases growth of Atlantic cod (*Gadus morhua* L.) in sea cages. ICES J. Mar. Sci. **63**: 365–375.

Timm, N.H. 1980. Multivariate analysis of variance of repeated measurements. *In* Handbook of statistics. Vol. 1. Analysis of variance. *Edited by* P.R. Krishnaiah. North-Holland Publishing Company, Amsterdam, Netherlands. pp. 41–87.

Woiwode, J.G., and Adelman, I.R. 1991. Effects of temperature, photoperiod, and ration size on growth of hybrid striped bass × white bass. Trans. Am. Fish. Soc. **120**: 217–229.

Zahn, M. 1963. Jahrzitliche veränderungen der vorzugstemperaturen von scholle (*Pleuronectes platessa* Linne.) und bitterling (*Rhodeus sericeus* Linne.). Verhandlungen der Deutschen zoologischen Gesellschaft, Muenchen. pp. 562–580.

Zar, J.H. 1984. Biostatistical analysis. 2nd ed. Prentice-Hall, Englewood Cliffs, N.J.

© 2007 NRC Canada

Natural mortality, growth parameters, and environmental temperature in fishes revisited

David Griffiths and Chris Harrod

Abstract: Pauly (1980. J. Cons. Int. Explor. Mer, **39**: 175–192) showed that natural mortality rates in fish could be predicted from body growth parameters and environmental temperature but found no evidence for ecological or taxonomic influences. Using an updated database and techniques that avoid some of the earlier analytical problems, we confirm Pauly's conclusion that mortality is correlated with growth and temperature. A path model supports the role of ecological effects on mortality. A phylogenetic effect is also apparent: perciform fishes occupy warmer environments than other species, but in the predator-rich reef habitat they suffer much lower mortality rates. Species that are cryptic or hide in burrows or have morphological defences against predators show the lowest mortality rates.

Résumé : Pauly (1980. J. Cons. Int. Explor. Mer, **39**: 175–192) a montré que les taux de mortalité naturelle chez les poissons pouvaient être prédits à partir des paramètres de croissance corporels et de la température du milieu, mais il n'a trouvé aucun indice de l'influence des caractères écologiques et taxonomiques. À l'aide d'une banque de données renouvelée et de techniques qui permettent d'éviter quelques-uns des problèmes analytiques antérieurs, nous confirmons la conclusion de Pauly qu'il y a une corrélation entre la mortalité, d'une part, et la croissance et la température, d'autre part. Un modèle de trajectoire laisse croire à l'existence d'effets écologiques sur la mortalité. Un effet phylogénétique est aussi apparent: les poissons perciformes vivent dans des milieux plus chauds que les autres espèces; cependant, dans l'habitat de récif qui est riche en prédateurs, ils subissent des taux de mortalité beaucoup moindres. Les espèces qui sont camouflées, qui se cachent dans des gîtes ou qui possèdent des structures morphologiques de défense contre les prédateurs ont les taux de mortalité les plus bas.

[Traduit par la Rédaction]

Introduction

Mortality rates are affected by intrinsic and extrinsic tradeoffs. For example, the asymptotic size (W) and growth coefficient (K) of the von Bertalanffy growth equation are negatively correlated because of tradeoffs among energy allocation to growth, maintenance, and reproduction (Roff 1992). There are a number of possible extrinsic mortality agents, both abiotic and biotic. In many aquatic environments, physical and chemical factors are relatively constant (Cyr and Cyr 2003), but biotic factors, particularly predation, are potentially important and variable. Aquatic animals at all trophic levels experience predation risk – food reward tradeoffs (Werner and Gilliam 1984; Werner and Anholt 1993) because food-rich habitats are usually riskier. These intrinsic and extrinsic tradeoffs are at least partially linked. For example, an increased allocation to reproduction will reduce growth rates and, because aquatic mortality rates are strongly size dependent (Peterson and Wroblewski 1984; McGurk 1986), increase mortality rates.

In a widely cited paper, Pauly (1980) analysed the relationships among (adult) natural mortality, growth parameters, and mean water temperature for 175 fish stocks belonging to 113 species (not 84 as stated in the abstract to that paper). He showed that the instantaneous natural mortality rate (M) was well predicted from W and K and water temperature (T). Jensen (2001) reanalysed Pauly's data and suggested that stocks could be divided into two groups, from temperate and warmer waters. Pauly considered various explanations, both direct and indirect, for the surprising role of temperature on mortality rates. He favoured a causal (physiological) effect whereby fishes in warmer waters, because of their higher metabolic rates, need to feed more frequently. Consequently, prey species are exposed more frequently to predators, which in turn impose greater mortality. He noted that with two possible exceptions, mortality rates did not vary with taxonomy or ecology. Since Pauly's paper, additional data have accumulated (available in FishBase 2004), but there has been no subsequent attempt to explore further the roles of environmental temperature, taxonomy, and ecology in affecting mortality

Received 8 June 2006. Accepted 30 October 2006. Published on the NRC Research Press Web site at http://cjfas.nrc.ca on 22 February 2007.
J19354

D. Griffiths.[1] School of Environmental Sciences, University of Ulster, Coleraine, BT52 1SA, United Kingdom.
C. Harrod.[2] Department of Physiological Ecology, Max Planck Institute for Limnology, Postfach 165, 24302 Plön, Germany.

[1]Corresponding author (e-mail: d.griffiths@ulster.ac.uk).
[2]Present address (as of March 2007): School of Biology and Biochemistry, Queen's University of Belfast, Quercus, Lisburn Road, Belfast BT9 7BL, United Kingdom.

 doi:10.1139/F07-002 © 2007 NRC Canada

Table 1. Multiple regression results for natural mortality (M) as a function of size (W), growth coefficient (K), and water temperature (T) for (*a*) stocks and species treated as independent data points and (*b*) phylogenetically independent contrasts.

(*a*) Stocks and species treated independently.

	Stocks (n = 458, R^2 = 0.706)				Species (n = 173, R^2 = 0.771)			
Effect	Coefficient±SE	Standardized coefficient	t	P	Coefficient±SE	Standardized coefficient	t	P
Intercept	0.034±0.054	—	0.64	0.53	0.102±0.086	—	1.19	0.24
log W	−0.043±0.014	−0.12	3.06	0.002	−0.066±0.020	−0.18	3.25	0.001
log K	0.833±0.045	0.72	18.43	<0.001	0.814±0.067	0.70	12.09	<0.001
log T	0.189±0.040	0.13	4.68	<0.001	0.190±0.065	0.12	2.95	0.004

(*b*) Phylogenetically independent (n = 68, R^2 = 0.639).

Effect	Coefficient±SE	Standardized coefficient	t	P
log W	−0.084±0.035	−0.25	2.38	0.002
log K	0.625±0.119	0.59	5.23	<0.001
log T	0.150±0.159	0.08	0.94	0.349

rates. Fish exhibit diverse morphological (e.g., spines) and behavioural (e.g., schooling) adaptations to reduce the risk of being eaten, and one would expect these to be reflected in variation in mortality rates. Similarly some environments (e.g., pelagic habitats, tropical reefs) are potentially more hazardous than others (Moyle and Cech 2000). Here we explore the roles of temperature, taxonomy, and ecology on mortality rates using the more extensive data in FishBase (2004).

Central to Pauly's analysis is the assumption that the data points and variables analysed are independent. Jensen (2001) reanalysed Pauly's data because potentially high levels of multicollinearity rendered multiple linear regression suspect, but he came to similar conclusions. However, his reanalysis made no allowance for phylogenetic or multistock non-independence; some species were represented by multiple measurements (e.g., nine for *Gadus morhua*), thereby inflating the number of degrees of freedom, while no allowance was made for phylogenetic relatedness (e.g., 1–11 species/family). Consequently it is not clear to what extent the published relationships are supported statistically, a situation that we attempt to remedy.

Materials and methods

Data

Information from FishBase 2004 on the mortality rates of 458 fish stocks belonging to 173 species was compiled, along with relevant growth and environmental information (Binohlan and Pauly 2000; Froese 2000; Froese et al. 2000; Palomares 2000; Palomares and Pauly 2000; Preikshot et al. 2000). FishBase provides estimates of M derived in a variety of ways. We used only independently estimated values obtained from, for example, plots of total mortality against effort in exploited populations or catch curves in unexploited populations, and not those predicted from empirical relationships for other species, such as was done in Hoenig (1983). Mean values were used whenever there was more than one stock per species.

The Brody growth coefficient K is sometimes referred to as a growth rate but it has dimensions of time^{-1}. Pauly (1994) has argued that the growth performance index ($\Phi = \log K + 2/3 \log W$ (Froese and Pauly 2000)), derived from body growth within stocks, with the more usual dimensions of mass-time^{-1} and with a clearer biological meaning (it is the intercept in $\log K$, $\log W$ regressions), is a more appropriate measure. Φ values were not available in FishBase so we substituted mean K and W values in the above equation to estimate Φ for each species.

Table 2. Comparison of regression models for predicting instantaneous natural mortality rates (M) for species data using Akaike's information criterion (AIC).

Model	AIC_c	ΔAIC_c	Akaike weights	R^2
WKT	−543.46	0	0.946	0.771
WK	−536.89	6.6	0.035	0.759
KT	−535.10	8.4	0.014	0.757
WT	−437.71	105.8	1.028×10^{-23}	0.573
W	−404.44	139.0	6.137×10^{-31}	0.476
K	−532.63	10.8	0.004	0.750
T	−315.90	227.6	3.657×10^{-50}	0.125

Note: All variables were log-transformed, and all regressions were statistically significant ($P < 0.001$). *W*, size; *K*, growth coefficient; *T*, water temperature.

Growth rates vary with food supply, which in turn will vary with trophic level and availability. Primary production is largely restricted to surface waters, and one would expect food availability to decline with increasing depth (Moyle and Cech 2000). FishBase reports the upper, lower, and "common" depths at which many species occur. All three measures are correlated, but most data were available for the lower depth limit, and we used this (log-transformed) as an indicator of food availability. Water temperature is also a function of depth. The Foodtroph index in FishBase was used as an measure of trophic level; Foodtroph is defined as (1 + mean trophic level of the food items), with autotrophs, for example, being assigned to trophic level 1.

Information on the habitats occupied by each species was also obtained from FishBase 2004. Demersal species live and (or) feed on or near the bottom, benthopelagic species occupy a similar zone to demersal species but also occur in midwater, while pelagic species occur mainly in the water

© 2007 NRC Canada

Fig. 1. Path diagrams for the effect of size (W), growth coefficient (K), and environmental temperature (T) on natural mortality rates (M) and significant coefficients for (*a*) species and (*b*) phylogenetic data.

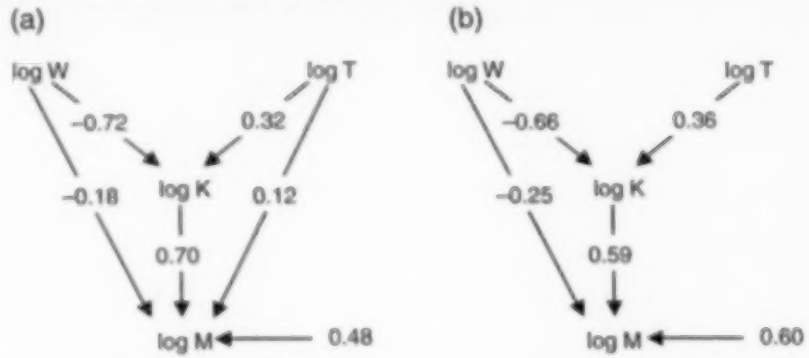

Fig. 2. Path analysis of a model of the effect of size (W), growth performance ($\emptyset$), untransformed temperature (T), trophic level, and maximum depth of occurrence on mortality rates (M). The model tested is shown by arrows; nonsignificant path is shown in gray. The path coefficients were estimated by RAMONA (Browne 2004). For clarity of presentation, the path from the residual variable is shown only for M. To aid interpretation, the width of the lines is approximately proportional to the size of the path coefficients.

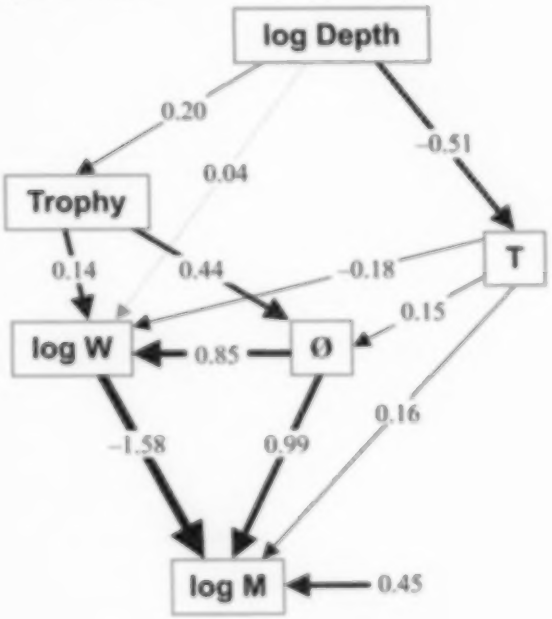

Table 3. A summary of the direct and indirect effects of the predictor variables on mortality rates, as estimated by multiple regression and correlation (n = 131).

Variable	Direct	Indirect	Total
W	−1.59	0.88	−0.71
Ø	1.00	−1.41	−0.40
T	0.15	0.28	0.43
Trophic level	−0.00	−0.40	−0.41
Depth	−0.02	−0.37	−0.39

Note: W, size; Ø, growth performance; T, untransformed temperature.

column and do not feed on benthic organisms. Reef-associated species live and (or) feed on reefs. All these species normally occupy the top 200 m of water. Two other habitat categories, occupying deeper water, were infrequently represented in the data (n = 1, 6) and were omitted when investigating habitat effects.

Statistical analyses

To estimate the direct and indirect effects of W, K, and T on mortality rates, we calculated path coefficients (i.e., the strengths of the direct and indirect linkages between any two variables) from standardized regression coefficients (Sokal and Rohlf 1995). In a similar but more complicated analysis, we fitted a path model using the RAMONA procedure in SYSTAT 11.0 (Browne 2004). Each dependent variable has a path coefficient representing the unexplained variation and is referred to here as the residual variable.

We checked if collinearity was a problem with the data by examination of condition indices and tolerance statistics in multiple linear regression and by ridge regression. Since weight and length are expected to be and are strongly correlated (r = 0.975, n = 173, P < 0.001), we, unlike Jensen (2001), used only one size measure per analysis and only present results where W was used. All variables were $\log_{10}$-transformed to be consistent with Pauly's analysis and to normalize or improve the normality and linearity of the data; all errors are standard errors. Lowercase t in the tables refers to the t statistic.

The "best" model (i.e., the one that provides the best fit for the fewest predictor variables) was determined using Akaike's information criterion (AIC) (Burnham and Anderson 1998). The small sample variant (AIC_c) was used because the ratio of number of observations to number of estimated parameters was appreciably below 40. Model fits were then compared with ΔAIC_c and Akaike weights (the relative likelihood of the models) (Burnham and Anderson 1998).

To examine the effects of relatedness (i.e., nonindependence of species values (Harvey and Pagel 1991)), we performed a comparative analysis by independent contrasts

© 2007 NRC Canada

Fig. 3. The habitat temperatures experienced by perciform (shaded) and nonperciform (open) marine fishes.

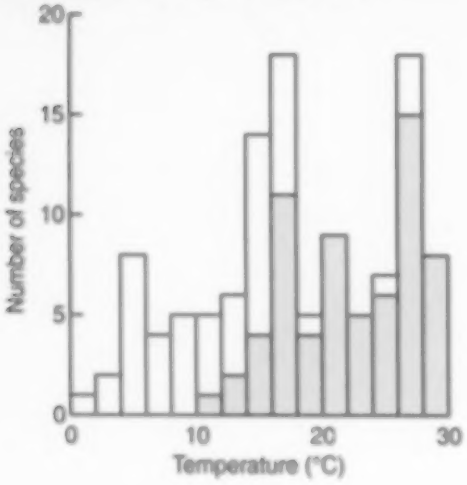

Fig. 4. Mean environmental temperatures (±1 SE) experienced by perciform (●) and nonperciform (△) species in different habitats: bp, benthopelagic; d, demersal; p, pelagic; r, reef-associated.

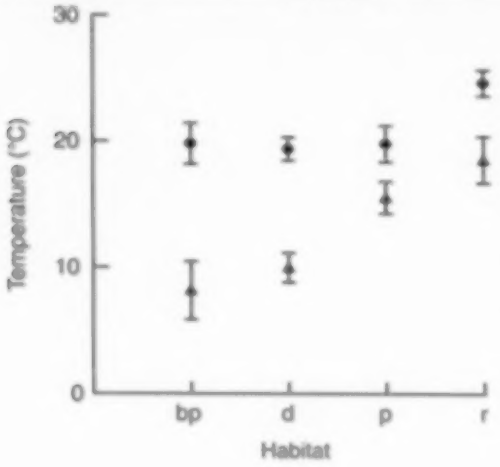

using the CAIC software (Purvis and Rambaut 1995) and the continuous variable (Crunch) option. Contrasts in the dependent variable were regressed, through the origin, against contrasts in the independent variables. There is no well-established phylogeny for fish, so we used the taxonomy in Froese and Pauly (2000); given the wide range of taxa in the data set and the relatively small numbers of species per genus for most genera, we believe that this procedure will not bias the results appreciably.

Results

T, *W*, and *K* all contributed significantly to predicting *M*. The standardized coefficients are similar for stock and species data (Table 1*a*) and show *K* to be the dominant predictor variable. Despite significant correlations between *K* and *W* (stocks: –0.706, $n = 485$, $P < 0.001$; species: –0.717, $n = 175$, $P < 0.001$), condition indices and tolerance statistics provided no indication of collinearity in the regressions. Similarly, ridge regression provided no evidence that inclusion of both *K* and *W* affected the regression coefficients to any appreciable degree.

Comparison of the full suite of models using AIC shows that the full (*WKT*) model was better than any of the others in predicting *M* (Table 2); it was 0.946/0.035 = 27 times more likely to be better than the next best fitting (*WK*) model.

Path analysis of species data (Fig. 1*a*) showed that the direct effects of *W* and of *T* on *M* were much less than the indirect effects (path coefficients *W*: –0.18, –0.50; *T*: 0.12, 0.22, respectively). The phylogenetically independent data strengthened the role of *W* as a significant predictor of mortality rates (Table 1*b*; Fig. 1*b*), and the direct and indirect effects are similar (–0.25, –0.39). However, the indirect effect of *T* was much stronger than the direct effect (0.21, 0.08, respectively), and the total temperature effect was not significant. The total effects for the species and phylogenetic data are 0.68 and 0.64 for *W* and 0.34 and 0.29 for *T*, respectively.

Food supply was assumed to affect size and growth rates and consequently influence mortality rates. In turn, food supply should vary with trophic level and with water depth. Water depth should also influence mortality rates by its effect on water temperature. We tested a model incorporating these effects and using untransformed temperature (*T*, since this was closer to normality in its distribution) by path analysis (Fig. 2). Although the direct effect of depth on *W* was not significant, the model provided an excellent fit to the data (root mean square error of approximation = 0.03). Size and *T* had large effects on *M*, but the indirect effects of Ø, trophic level, *T*, and depth were stronger than the direct effects (Table 3). Similar results were obtained when the analysis was restricted to marine species.

The conflicting temperature effects in the species and phylogenetically independent contrast analyses could reflect heterogeneity in the thermal preferences of different lineages. Bimodality is apparent in the habitat temperatures experienced (Fig. 3). Some of this bimodality is because of differences between taxa (perciform vs. nonperciform fishes), but note that bimodality is still apparent within perciform fishes, the taxon that contributes most to the overall bimodality. *W*, *K*, and *T* contributed significantly to predicting *M* in perciform fishes ($R^2 = 0.80$, $n = 95$), but in nonperciforms ($R^2 = 0.76$, $n = 78$), *T* was not a significant predictor. The mean temperatures that these taxa occupy are significantly different (least squares adjusted means all salinities: perciforms, 21.1 ± 0.62 °C, $n = 132$; nonperciforms, 13.7 ± 0.66 °C, $n = 115$ ($F_{[1,245]} = 67.71$, $P < 0.001$); marine species: 21.1 ± 0.63 °C, $n = 111$; 12.0 ± 0.76 °C, $n = 75$, respectively ($F_{[1,184]} = 73.01$, $P < 0.001$)).

The environmental temperatures experienced by marine species (i.e., excluding freshwater and estuarine species) varied across taxonomic group and habitat, and there was a marginally significant interaction term ($F_{[3,171]} = 2.38$, $P = 0.07$). In each habitat, perciforms occupied warmer environ-

© 2007 NRC Canada

Table 4. (*a*) General linear model showing the contributions of size (W), growth performance (Φ), temperature (T), habitat, and taxon to mortality rate and (*b*) a summary of the mortality regression results for perciform and nonperciform fishes.

(*a*) General linear model.

Source	df	Mean square	F	P
W	1	8.105	219.345	<0.001
Φ	1	2.633	71.246	<0.001
T	1	0.244	6.593	0.011
Habitat	3	0.117	3.16	0.027
Taxon	1	0.265	7.162	0.008
Habitat × Taxon	3	0.105	2.841	0.041
T × Taxon	1	0.264	7.146	0.009
Error	124	0.037	—	—

(*b*) Mortality regression.

Taxon	Habitat	Intercept	W	Φ	t	n	R^2
Perciforms	All	0.148	–0.616	0.780	0.014	83	0.81
Nonperciforms*	Benthic–deep	0.230	–0.499	0.567	—	57	0.80
Nonperciforms*	Pelagic	0.367	–0.499	0.567	—	57	0.80
Nonperciforms*	Reef	0.586	–0.499	0.567	—	57	0.80

*The equations for nonperciforms are for three habitat categories, which were coded as dummy variables.

ments than nonperciform fishes ($F_{[1,171]} = 54.17$, $P < 0.001$) (Fig. 4). The temperatures decreased with increasing depth (pelagic, p; demersal, d; benthopelagic, bp) for nonperciform fishes but were independent of depth for perciforms ($F_{[1,64]} = 3.90$, $P = 0.05$; $F_{[1,107]} = 0.01$, $P = 0.93$); reef-associated (r) fish in each taxon lived in warmer waters than in the other habitats ($F_{[1,64]} = 9.74$, $P < 0.01$; $F_{[1,107]} = 17.85$, $P < 0.001$).

An a priori model of mortality rates using W, Φ, untransformed T, and the taxonomic and habitat categories (Table 4*a*) explained 81% of the variance (marine species only, $n = 136$). The inclusion of taxonomic and habitat variables resulted in only a small increase in the variation explained (0.78 to 0.81). However, random sorting of the taxonomic variable supported the conclusion that this was a significant contributor to mortality rates. Mortality rates differed across habitats in nonperciform fishes ($F_{[3,86]} = 3.53$, $P < 0.05$) but not in perciforms ($F_{[3,76]} = 0.30$) (Fig. 5; Table 4*b*). Perciforms suffered higher mortality rates when living in demersal habitats, but nonperciforms had higher mortality rates when associated with reefs ($F_{[1,124]} = 3.79$, $P = 0.05$; $F_{[1,124]} = 4.81$, $P < 0.05$, respectively).

These species belonged to 48 families. Least squares adjusted means were calculated for families, with W, Φ, and untransformed T as covariates. 15 of the 18 species belonging to the 11 families with the lowest mortality rates showed adaptations that would be expected to reduce their vulnerability to predators; 11 species are flatfish (pleuronectiforms), which are cryptic and lie at least partly buried in the substrate, two occupy burrows (cheilodactylid, malacanthid), one is heavily armoured (gasterosteid), and one is armed with poisonous spines (sebastid). There was no obvious reason why the remaining three species (acipenserid, lethrinid, triakid) should have low mortality rates. Pauly (1980) noted that 25 clupeid stocks (belonging to 14 species) tended to have M values less than those predicted by his equation (using W, K, T as predictor variables), whereas engraulids, which also strongly school, did not. We found no significant difference in M among the 14 clupeid and 8 engraulid species ($F_{[1,17]} = 0.27$; W, K, T as covariates).

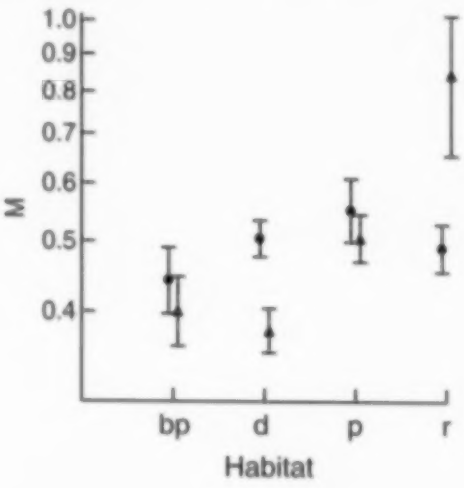

Fig. 5. Least squares adjusted instantaneous mean mortality rates (M) (±1 SE) of perciform (●) and nonperciform (△) species in different habitats: bp, benthopelagic; d, demersal; p, pelagic; r, reef-associated.

Discussion

Stock and species data regressions using W, K, and T to predict mortality rates showed good agreement. Our standardized coefficients for stocks were also similar to those obtained by Pauly (1980, his table 6), although the temperature effect was stronger for his smaller data set. There was agreement also in the importance of W and K for phylogen-

© 2007 NRC Canada

etically independent contrasts, but the direct effect of temperature was no longer significant.

Savage et al. (2004) tested the metabolic theory of ecology with Pauly's (1980) data and found broad agreement; the slope of the size-corrected mortality rate and temperature gave an activation energy somewhat below the predicted value (–0.45 eV vs. 0.6–0.7 eV), but the slope of the temperature-corrected mortality rate as a function of body mass (–0.23) was very close to the predicted value of –0.25. Using species rather than stock data gives the expected slope (–0.26), but the activation energy of 0.33 eV is only half that expected. Charnov and Gillooly (2004), using a model in which temperature is assumed to affect only growth, argue that the temperature effect on mortality could be indirect, via life history optimization, in line with the analysis presented here.

Depth in the path model is a surrogate for both temperature and food supply. We expected mean trophic level to increase with depth if only because of the loss of herbivorous species. In deep waters, productivity is limited, and coupled with the low temperatures, this should favour large, slowly growing species (Moyle and Cech 2000). We also expected positive correlations between trophic level and body size (because piscivorous fish are usually larger than their prey) and between trophic level and growth performance (because piscivores are nutritionally more similar to their prey than lower trophic levels). All, except the direct size–depth relationship, were found.

Pauly (1980) considered various direct and indirect effects of T on M. He favoured the notion that fish in warm waters are more likely to encounter predators that are hungry because of higher metabolic rates at higher temperatures. The results presented here are at least partly consistent with this possibility. Mean mortality rates decline from 0.76 (T = 21.6 °C) in reef to 0.59 (T = 17.7 °C) in pelagic to 0.42 in demersal (T = 14.7 °C) and benthopelagic habitats (T = 14.0 °C). However, the significant effect of taxonomic group on mortality rates suggests that indirect effects are also important. We expected predation risk to differ across habitats, dependent on the number of predators and the availability of hiding places. The high productivity relative to surrounding waters, the large number of predatory species, and the many defensive mechanisms found suggest that piscivory is intense on tropical reefs (Hixon 1991; Moyle and Cech 2000), despite there being many potential refuges from predators. In contrast, pelagic species live in an environment lacking hiding places, but the frequency of schooling in these species suggests that predation is also an important factor there. Excluding temperature and its interaction with taxon from the model in Table 4 significantly reduced the variance explained (R^2 = 0.79, ΔAIC_c = 9.94 for the reduced model), suggesting that both habitat and temperature effects are important. This analysis shows that mortality rates are correlated with taxon and habitat in a way that reflects a more direct role for ecology than implied by the physiological effects of temperature. The low mortality rates for species that are hidden or morphologically protected from predators supports this interpretation.

Perciforms occupy substantially warmer habitats than nonperciform species, and with the exception of reef species, they tend to suffer higher mortality rates, consistent with Pauly's explanation. Moyle and Cech (2000) attribute the success of perciforms as a group to a number of factors, including the presence of spines and high manoeuvrability. They suggest that these features enable the fish to occupy riskier, more exposed, habitats (e.g., shallow or surface waters) than other taxa; these will be warmer than deeper or more offshore waters. However, if such defences were highly effective, one would expect lower mortality rates in this group than in nonperciforms. Perciforms suffer higher mortality rates than other fishes in demersal habitats, but the markedly higher temperatures they experience suggest that they occupy rather different demersal habitats from the nonperciforms analysed. The much higher mortality rates experienced by nonperciforms in what is probably the most dangerous habitat (i.e., tropical reef) is consistent with an effective defensive role for perciform spines.

While Pauly (1980) and the equations generated here explain much of the variance in mortality rates, they are poor predictors; for example, the median and 90th percentile jackknife prediction errors for perciform fish, calculated using the procedure in Pascual and Iribarne (1993), were 20% and 76%, respectively. Pauly's stock-based equation explains almost as much of the variance as the species versions generated here; the original conclusions were not affected by the nonindependence of many of the data points. However, both ecology and taxonomy do influence fish mortality rates, although taxonomy does not necessarily closely map to phylogeny (Harvey and Pagel 1991). While phylogeny has been taken into account in some comparative analyses of marine fish biology (e.g., Block and Finnerty 1994), in many others it has not, with the possibility that valuable insights will be lost. Such analyses require a well-established phylogeny, something that is lacking for many fish groups.

Acknowledgements

Our thanks go to Jyrki Lappalainen, Christophe Eizaguirre, and two referees for helpful comments on earlier versions of the manuscript and to Nick Isaac for help in using the CAIC program.

References

Binohlan, C., and Pauly, D. 2000. The POPGROWTH table. *In* FishBase 2000: concepts, design and data sources. ICLARM, Los Baños, Laguna, Philippines. pp. 138–145.

Block, B.A., and Finnerty, J.R. 1994. Endothermy in fishes: a phylogenetic analysis of constraints, predispositions, and selective pressures. Environ. Biol. Fishes, **40**: 283–302.

Browne, M.W. 2004. Path analysis (RAMONA). *In* SYSTAT 11. SYSTAT Software, Inc., Richmond, Calif. pp. 1–61.

Burnham, K.P., and Anderson, D.R. 1998. Model selection and inference: a practical information–theoretic approach. Springer-Verlag, New York.

Charnov, E.L., and Gillooly, J.F. 2004. Size and temperature in the evolution of fish life histories. Integr. Comp. Biol. **44**: 494–497.

Cyr, H., and Cyr, I. 2003. Temporal scaling of temperature variability from land to oceans. Evol. Ecol. Res. **5**: 1183–1197.

FishBase. 2004. FishBase 2004 [CD-ROM]. ICLARM, Manila.

Froese, R. 2000. The FAMILIES table. *In* FishBase 2000: concepts, design and data sources. *Edited by* R. Froese and D. Pauly. ICLARM, Los Baños, Laguna, Philippines. pp. 60–61.

© 2007 NRC Canada

Froese, R., and Pauly, D. (*Editors*) 2000. FishBase 2000: concepts, design and data sources. ICLARM, Los Baños, Laguna, Philippines.

Froese, R., Capuli, E., Garilao, C., and Pauly, D. 2000. The SPECIES table. *In* FishBase 2000: concepts, design and data sources. *Edited by* R. Froese and D. Pauly. ICLARM, Los Baños, Laguna, Philippines. pp. 76–85.

Harvey, P.H., and Pagel, M.D. 1991. The comparative method in evolutionary biology. Oxford University Press, Oxford, UK.

Hixon, M.A. 1991. Predation as a process structuring coral reef fish communities. *In* The ecology of fishes on coral reefs. *Edited by* P.F. Sale. Academic Press, San Diego. pp. 475–508.

Hoenig, J.M. 1983. Empirical use of longevity data to estimate mortality rates. Fish. Bull. **82**: 898–903.

Jensen, A.L. 2001. Comparison of theoretical derivations, simple linear regressions, multiple linear regression and principal components for analysis of fish mortality, growth and environmental temperature data. Environmetrics, **12**: 591–598.

McGurk, M.D. 1986. Natural mortality of marine pelagic fish eggs and larvae: role of spatial patchiness. Mar. Ecol. Prog. Ser. **34**: 227–242.

Moyle, P.B., and Cech, J.J. 2000. Fishes: an introduction to ichthyology. Prentice-Hall, Upper Saddle River, N.J.

Palomares, M.L.D. 2000. The ECOLOGY table. *In* FishBase 2000: concepts, design and data sources. *Edited by* R. Froese and D. Pauly. ICLARM, Los Baños, Laguna, Philippines. pp. 178–182.

Palomares, M.L.D., and Pauly, D. 2000. The POPQB table. *In* FishBase 2000: concepts, design and data sources. *Edited by* R. Froese and D. Pauly. ICLARM, Los Baños, Laguna, Philippines. pp. 197–199.

Pascual, M.A., and Iribarne, O.O. 1993. How good are empirical predictions of natural mortality? Fish. Res. **16**: 17–24.

Pauly, D. 1980. On the interrelationships between natural mortality, growth parameters, and mean environmental temperature in 175 fish stocks. J. Cons. Int. Explor. Mer, **39**: 175–192.

Pauly, D. 1994. On the sex of fish and the gender of scientists. Chapman & Hall, London, UK.

Peterson, I., and Wroblewski, J.S. 1984. Mortality rate of fishes in the pelagic ecosystem. Can. J. Fish. Aquat. Sci. **41**: 1117–1120.

Preikshot, D., Froese, R., and Pauly, D. 2000. The ORDERS table. *In* FishBase 2000: concepts, design and data sources. *Edited by* R. Froese and D. Pauly. ICLARM, Los Baños, Laguna, Philippines. pp. 55–59.

Purvis, A., and Rambaut, A. 1995. Comparative analysis by independent contrasts (CAIC): an Apple Macintosh application for analysing comparative data. Comput. Appl. Biosci. **11**: 247–251.

Roff, D.A. 1992. The evolution of life histories; theory and analysis. Chapman and Hall, London, UK.

Savage, V.M., Gillooly, J.F., Brown, J.H., West, G.B., and Charnov, E.L. 2004. Effects of body size and temperature on population growth. Am. Nat. **163**: 429–441.

Sokal, R.R., and Rohlf, F.J. 1995. Biometry. 3rd ed. W.H. Freeman and Company, New York.

Werner, E.E., and Anholt, B.R. 1993. Ecological consequences of the trade-off between growth and mortality rates mediated by foraging activity. Am. Nat. **142**: 242–272.

Werner, E.E., and Gilliam, J.F. 1984. The ontogenetic niche and species interactions in size-structured populations. Annu. Rev. Ecol. Syst. **15**: 393–425.

© 2007 NRC Canada

State-dependent life history plasticity in Sacramento River winter-run chinook salmon (*Oncorhynchus tshawytscha*): interactions among photoperiod and growth modulate smolting and early male maturation

Brian R. Beckman, Brad Gadberry, Paul Parkins, Kathleen A. Cooper, and Kristen D. Arkush

Abstract: An experiment was performed to determine the relative effects of photoperiod at emergence and growth rate on smolting pattern and early male maturation rate in Sacramento River (California, USA) winter-run chinook salmon (*Oncorhynchus tshawytscha*) (listed as endangered under the US Endangered Species Act). Fry were ponded on the same day but at three different points in the seasonal photoperiod cycle (using artificial lighting) spanning the natural range of emergence timing in this population. Significant increases in gill Na^+,K^+-ATPase activity and seawater survival were found during March and April in all treatments, similar to yearling smolting patterns found in many salmonids. Fish that emerged early and grew at a relatively high rate also demonstrated signs of smolting in August–November. Male maturation was growth dependent, with HiFeed groups maturing at a rate double that found in LoFeed groups. Male maturation was also photoperiod dependent with a linear relation found between emergence date and rate of male maturation. These results demonstrate that individual life history pattern was variable and dependent on emergence timing and growth rate.

Résumé : Nous avons procédé à des expériences afin de déterminer les effets relatifs de la photopériode au moment de l'émergence et du taux de croissance sur les patterns de transformation en saumoneaux et le taux de maturation précoce des mâles chez les saumons chinook (*Oncorhynchus tshawytscha*) de la montaison d'hiver du Sacramento (Californie, É.-U.), une espèce menacée d'après la loi américaine sur les espèces menacées. Nous avons placé des alevins dans des étangs le même jour, mais soumis à trois régimes différents du cycle photopériodique saisonnier (à l'aide de lumière artificielle) qui couvrent l'étendue naturelle des périodes d'émergence chez cette espèce. Dans toutes les conditions expérimentales, il y a en mars et avril des augmentations significatives de l'activité de la Na^+,K^+-ATPase des branchies ainsi que de la survie en eau de mer, semblables à celles observées chez de nombreux salmonidés lors de la transformation annuelle des poissons d'un an en saumoneaux. Les poissons qui émergent tôt et qui croissent à un taux relativement élevé montrent aussi des signes de transformation en saumoneaux en août–novembre. La maturation des mâles est dépendante de la croissance et les groupes nourris abondamment atteignent la maturité à une fréquence double de celle des groupes moins bien nourris. La maturation des mâles est aussi reliée à la photopériode et il existe une relation linéaire entre la date de l'émergence et le taux de maturation des mâles. Ces résultats démontrent que les patrons des cycles biologiques individuels sont variables et qu'ils dépendent du moment de l'émergence et du taux de croissance.

[Traduit par la Rédaction]

Introduction

The life history of chinook salmon (*Oncorhynchus tshawytscha*) is structured by migrations between freshwater and oceanic habitats that are coupled to life stage specific developmental events (smolting and sexual maturation). Intra- and inter-population variability in age, size, and seasonal timing at which these developmental events occur are a mark of the species (Healey 1991). Smolting is a physiological process that both allows and stimulates juvenile salmonids to under-

Received 18 April 2006. Accepted 22 December 2006. Published on the NRC Research Press Web site at http://cjfas.nrc.ca on 22 February 2007.
J19277

B.R. Beckman[1] and B. Gadberry. Northwest Fisheries Science Center, NOAA Fisheries, 2725 Montlake Boulevard E., Seattle, WA 98112, USA.
P. Parkins and K.A. Cooper. School of Aquatic and Fishery Sciences, University of Washington, Seattle, WA 98195, USA.
K.D. Arkush. Bodega Marine Laboratory, University of California at Davis, P.O. Box 247, Bodega Bay, CA 94923, USA.

[1]Corresponding author (e-mail: Brian.Beckman@NOAA.gov).

 doi:10.1139/F07-001 © 2007 NRC Canada

take the initial freshwater to seawater migration (Hoar 1976). Smolting is thus a key life history transition fundamental to the nature of salmon, as it allows juvenile fish to leave relatively unproductive riverine or lacustrine freshwater habitats to take advantage of relatively richer ocean feeding grounds (Gross 1987).

There are four life history groups of chinook salmon in California's Central Valley: spring, fall, late fall, and winter defined by adult migration and spawn timing (Myers et al. 1998; Yoshiyama et al. 1998; Lindley et al. 2004). Each of these groups is distinct genetically (Bartley et al. 1992; Banks et al. 2000) and they were historically located in different geographic regions of the Sacramento and San Joaquin River drainages (Yoshiyama et al. 1998; Lindley et al. 2004). Spring chinook salmon spawned earliest in the year in higher elevations, while late-fall and fall chinook salmon spawned later in lower elevation areas. Winter-run chinook salmon were found in streams with unique hydrogeographic properties as water originated from springs fed by snowmelt from lava beds on Mt. Lassen and Mt. Shasta in the Upper Sacramento River Basin (above Shasta Dam). These streams possess very stable, cool temperatures yearround. In turn, winter-run fish possess unique life history traits as compared with other chinook salmon: adults return to the Sacramento River in winter (as opposed to spring–summer–fall) and spawn in spring–summer (as opposed to summer–fall–winter) (Healey 1994; Yoshiyama et al. 1998; Lindley et al. 2004).

Descriptions of smolting in winter-run chinook salmon are vague, as most are based on the observation of downstream-migrating chinook salmon juveniles without any reference to specific population-level markers (physical tags, morphological attributes, genetic identity) or physiological status (hypoosmoregulatory ability) (Myers et al. 1998). A large proportion of the winter-run population appears to move downstream past Red Bluff Diversion Dam (located below the major spawning sites for winter-run fish) during September–October at relatively small sizes (~50 mm) (Gard 1995, cited in Myers et al. 1998; Gaines and Martin 2002). It is quite common for juvenile chinook salmon to display seasonal downstream movement prior to, and distinct from, smolting that occurs at a later time (Taylor and Larkin 1986; Bradford and Taylor 1997). To our knowledge, fish migrating past Red Bluff Diversion Dam have not been specifically assessed for physiological characters of smolting (ability to survive and grow in seawater). Juvenile chinook salmon found lower down in the Sacramento River or Delta or San Francisco Bay might come from any one of the four distinct population groups, so it has been difficult to identify winter-run smolts among the total population of juvenile salmonids (Brandes and McLain 2001). Descriptions published to date suggest that smolting occurs in October–April at sizes >70 mm (Myers et al. 1998). In contrast, Sacramento River spring and fall chinook salmon (the most abundant population groups in the Sacramento Basin) generally smolt within 1–4 months postemergence, in the spring – early summer, at sizes of 50–70 mm (Myers et al. 1998; Yoshiyama et al. 1998; Lindley et al. 2004).

The current paradigm organizing life history variability (including smolting) between chinook salmon populations is based on a dichotomy proposed by Healey (1991). In this classification, Healey suggested that that there are two "races" of chinook salmon (ocean-type and stream-type), each having distinct geographic distributions and life history characteristics (juvenile and adult). Smolting pattern is suggested to fall into two main categories: ocean-type (enter seawater in spring or summer, weeks to months after emergence, at 40–70 mm in length) and stream-type (enter seawater in the spring at an age of >1 year after spending the winter in fresh water, >70 mm in length). Healey (1991) suggested that ocean-type fish are found in the southern geographic range of chinook salmon from coastal British Columbia to California. It is not clear how, or if, the smolting pattern of Sacramento River winter-run chinook salmon relates to the ocean-type – stream-type dichotomy. Thus, we will use the term "underyearling" (fish smolt before spending a winter in fresh water) or "yearling" (smolt after spending a winter in freshwater) to describe smolting pattern for results in this paper, as these terms do not imply associated genetic population structure or intertwined juvenile and adult life history traits.

Potential smolting patterns are presumably genetically set; however, the environment modulates the endocrine and physiological status of a fish to produce a specific smolting phenotype for a given individual. The results of Clarke et al. (1992, 1994) suggest that smolting in stream-type chinook salmon may be plastic, occurring either as yearlings in the spring or as underyearlings in the preceding year. Further studies have shown that this plasticity may depend on size and growth rate of individual fish (Ewing et al. 1980; Beckman and Dickhoff 1998; Connor et al. 2005). Larger, faster growing fish have been found to smolt in the fall, while smaller, slower growing fish do not smolt until the following spring for fish exposed to normal seasonal photoperiodic schedules. Beckman et al. (2003) suggested that smolting in the autumn as an underyearling fish might be considered distinct from prototypical ocean-type smolting, as the fish were larger and older than characteristic ocean-type fish and these same fish, as a group, appeared to be able to smolt either in the autumn (as underyearlings) or in the spring (as yearlings). Smolting may thus be variable both between populations (ocean-type versus stream-type) and between individuals within populations (underyearling versus yearling). This variability and the interactions between genetic and environmental sources of this variability make it very difficult to predict either smolting pattern or the environmental control of smolting pattern in Sacramento River winter-run chinook salmon.

Juvenile male salmonids may directly mature rather than smolt. This has been termed "early male maturation", as these fish mature at a young age (1 or 2 years old) and a small size (as small as 10 g) as compared with full-size anadromous males (Healey 1991; Unwin et al. 1999). This alternative developmental pathway has been of both theoretical and practical interest and has received a great deal of attention, especially with Atlantic salmon (*Salmo salar*) (Thorpe 1986; Fleming 1998; Garant et al. 2003). Studies of Atlantic salmon have revealed that early male maturation is a conditional event occurring or not depending on seasonal growth rate and (or) fat stores. Larger, faster growing parr initiate male maturation as opposed to smaller, slower growing fish that smolt instead (Thorpe 1986, 1989). Similarly, juvenile

© 2007 NRC Canada

chinook salmon males may undertake early maturation dependent on growth and adiposity (Clarke and Blackburn 1994; Silverstein et al. 1998; Shearer and Swanson 2000). Depending on conditions (temperature and feed), up to 90% of males in an experimental population of chinook salmon may mature (Foote et al. 1991; Shearer et al. 2006). Thus, variation in the juvenile life history of chinook salmon not only includes age, size, and season of smolting but also an alternative for males to either mature or smolt.

There are specific conservation and management concerns that stimulate investigating life history in Sacramento River winter-run chinook salmon. These fish were listed under the US Endangered Species Act as threatened in 1989 and subsequently as endangered in 1994 (Yoshiyama et al. 2000). Based on this situation, hatchery and captive broodstock programs were initiated to supplement the natural winter-run population (U.S. Fish and Wildlife Service 2000). These programs might be better managed if there were a basic understanding of the range of juvenile life history variation possible within winter-run fish and the factors controlling this variation were known.

We thus designed an experiment to investigate variability of smolting and early male maturation in winter-run chinook salmon. Based on the findings of Healey (1991) and Clarke et al. (1992, 1994), we can offer several predictions: (*i*) if winter-run fish have an ocean-type life history pattern, smolting will be size dependent and photoperiod independent, (*ii*) if winter-run fish have a stream-type life history pattern, smolting will be photoperiod dependent and occur in the spring, and (*iii*) if winter-run fish have a variable smolting pattern, smolting might occur in either the autumn or the spring dependent on individual fish growth rate and photoperiod.

Accordingly, fish were reared under two feeding regimes (HiFeed and LoFeed) and three different photoperiod regimes. Eggs were obtained from crosses of captively reared adults at Bodega Marine Laboratory. Fry were ponded (first exposure to light and when feeding was initiated) on the same day but under different photoperiods matching the natural range of emergence (first-feeding) for winter-run fish (June–October). The objective was to assess life history variability among fish of the same size and age (and of the same genetic composition) emerging at different points of a seasonal photoperiod cycle.

Materials and methods

Fish and rearing

Eyed eggs from five male × female crosses (spawned on 23 July 2002) were obtained from the Sacramento River winter-run chinook salmon captive broodstock program at Bodega Marine Laboratory, Bodega, California (see Arkush et al. (2004) for a description of spawning protocols). Eggs were shipped to the Northwest Fisheries Science Center experimental hatchery in Seattle, Washington, and arrived on 23 August 2002. Egg lots were incubated separately in Heath trays, in the dark, in a recirculating-water egg incubation system maintained at 11 °C. Permits allowing these eggs to be used for research purposes were granted from both the National Marine Fisheries Service and the California Department of Fish and Game, as the eggs were in excess of broodstock program demands and considered surplus. Total egg hatch for all crosses was achieved by 4 September. Differential mortality between crosses occurred owing to incomplete hatch (fry became stuck in the egg membrane as they emerged and subsequently died). One to two hundred fry per cross (depending on availability) were placed into each of six 1.3 m diameter fiberglass tanks on 9 October for a total of 690 fry per tank. Water was supplied from a recirculating system with biofiltration, ozonation, and ultraviolet sterilization and maintained at 12 °C (±1 °C). Average fry weight at ponding varied from 0.210 to 0.265 g between crosses (n = 15 per cross). Each tank was illuminated with an incandescent light with a photoperiod set to match that of Sacramento, California (38°N), adjusted weekly. Photoperiod varied among tanks as described below. Fry were fed Biodiet Starter ad libitum through 15 November for 6 days per week, after which rations were set as described below and fed Biodiet Grower 5 days per week. Fish were maintained in their respective tanks through July of 2003 (9 months of rearing).

Experimental design

At ponding (no egg sac visible, ventral body wall nearly or completely fused), fish were placed into three separate photoperiods (two tanks per photoperiod): early (matching emergence early in the summer, 27 June, 104-day shift from the actual date), middle (matching emergence in the middle of summer, 15 August, 55-day shift), and late (matching emergence late in the summer, 27 September, 13-day shift) (Fig. 1). Photoperiod followed a normal seasonal trajectory from each respective starting date.

After a robust feeding response was established, fish from each photoperiod were fed at two different rates to cleanly establish fish with different growth histories within each photoperiod. Thus, a high- or low-feeding treatment was given to each pair of tanks for each photoperiod (two feeding treatments × three photoperiods) designed to yield fish of 10 and 25 g by a calendar date of 1 February using the delta-I method of Piper et al. (1982). Subsequently, during the experiment, fish appetite was found to decrease strongly with winter solstice photoperiods and ration was determined every 2 weeks by feeding the HiFeed tank in the photoperiod closest to solstice (displayed the poorest feeding response) to satiation. Feeding for the subsequent days for HiFeed fish was set at 80% of satiation. LoFeed tanks were fed 50% of the HiFeed ration. This feeding strategy allowed us to maintain equivalent sizes and growth rates among HiFeed or LoFeed fish, respectively, in the different photoperiod treatments and subsequently allowed us to directly assess the effects of photoperiod on smolting and maturation while removing any photoperiod-influenced difference in appetite and subsequently growth that might have compounded a direct photoperiod effect. Actual amounts fed correspond to 3.5% of body weight per day in November dropping to 1.7% of body weight per day in May for the HiFeed groups.

Fish sampling

Batch weights (three 25-fish composite samples per tank) were taken approximately monthly to facilitate ration calculations. Twelve fish per tank were sampled about every 3 weeks for gill tissue starting on 13 November. By 18 De-

© 2007 NRC Canada

Fig. 1. Experimental shift of seasonal photoperiod as compared with that found at Sacramento, California (38°N). Spawning dates of broodstock for experimental fish and actual ponding date (first exposure to light) are shown by arrows on the *x*-axis. The natural ranges of spawning date and emergence timing displayed by winter-run chinook salmon (*Oncorhynchus tshawytscha*) in the Sacramento River are shown by light- and dark-shaded bars under the *x*-axis (Yoshiyama et al. 1998).

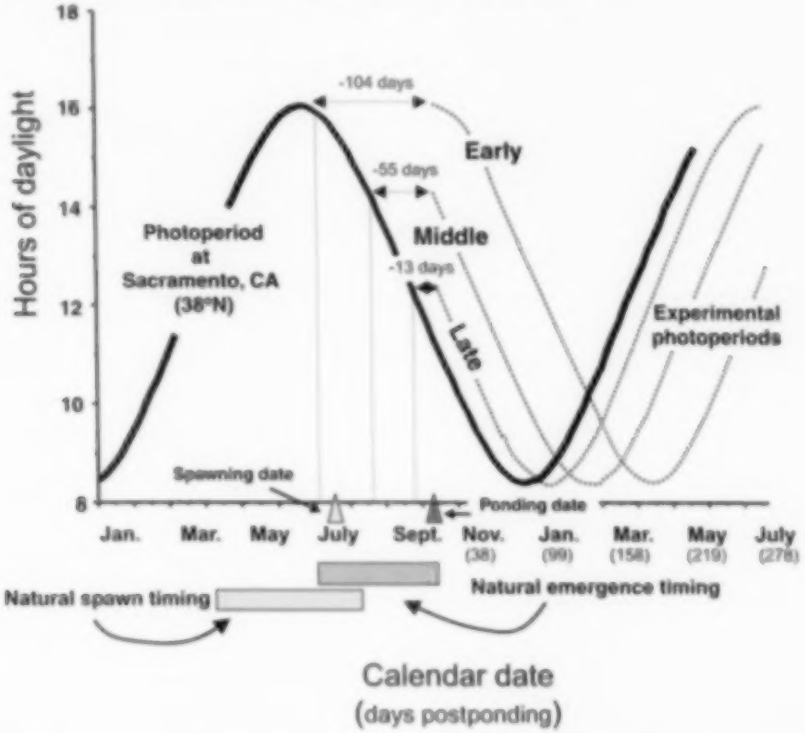

cember, fish were large enough to make blood sampling practical. Blood samples were pooled (two fish per pool) for samples obtained 18 December – 7 February; single-fish samples were obtained thereafter. Fish were sampled on a total of 11 occasions, with the last sample taken on 15 July. Sampling started with fish first netted and counted into a bucket and then netted singly into a lethal dose of tricaine methanesulfonate. Fish were then blotted dry, fork length (millimetres) and weight (grams) were measured, the caudal peduncle was severed, and blood was obtained in a heparinized capillary tube. The blood was subsequently transferred to a microfuge tube and stored on ice until all samples were obtained (<2 h). Microfuge tubes were spun at 3000*g*, plasma obtained, and samples stored at –80 °C until hormone analysis was undertaken. Gill tissue was snipped from arches, placed in a buffered solution of sucrose, EDTA, and imidazole according to McCormick (1993), and frozen at –80 °C until assayed for gill Na^+,K^+-ATPase activity.

Also, on an approximately 3-week schedule, 15 fish per treatment were placed into a 0.65 m^2 tank filled with 35 g artificial seawater·L^{-1} (Instant Ocean) aerated and maintained at 12 °C (Clarke and Blackburn 1977). Survival was monitored for 72 h after transfer to seawater. Testis size was visually assessed in all sampled fish to monitor for early male maturation. Differences in testis size between maturing and nonmaturing males may be ascertained up to 6 months prior to final maturation (spermiation) (Campbell et al. 2003; Larsen et al. 2004). Maturing males were excluded from subsequent analysis of smolting characters. At the end of the experiment, all remaining fish were sacrificed to assess gender and testis development, determined as above. In addition, up to 10 immature and 10 mature testes from male fish from each treatment were weighed as the experiment was terminated to determine gonadal somatic index (GSI).

Laboratory methods

Plasma insulin-like growth factor-I (IGF-I) levels were determined by radioimmunoassay (RIA) using components obtained from GroPep Ltd. (Adelaide, Australia) as described in Shimizu et al. (2000). Briefly, 10 µL of plasma was thoroughly mixed with acid–ethanol (87.5% ethanol and 12.5% 2 mol HCl·L^{-1} by volume) at a ratio of 1:4 and then incubated at room temperature for 30 min. The tubes were centrifuged at 3000*g* for 20 min at 4 °C. The supernatant was decanted into a new set of tubes, neutralized with 0.855 mol·L^{-1} Tris base at a ratio of 5:2, and assayed for IGF-I. Gill Na^+,K^+-ATPase activity was assessed using the method of McCormick (1993). All gill Na^+,K^+-ATPase activities are reported in units of µmol PO_4·mg $protein^{-1}$·h^{-1}.

Analytical methods

Neither of our experimental variables was fixed: daylength progressed through a natural seasonal cycle for each photoperiod treatment, and while feeding rates were consistently set at either HiFeed or LoFeed levels between photoperiod treatments, actual feeding rates changed temporally

© 2007 NRC Canada

with appetite and fish size. Thus, within this experiment, photoperiod, feeding rate, and fish age all varied and differences in feeding rate resulted in variation in fish size and fish growth. The experiment was purposely designed, as we expected developmental decisions for individual fish to be dependent on interactions between photoperiod, fish size, fish growth, and fish age. There are two frames of reference for this experiment: (*i*) calendar day, which refers to the actual day on which experimental events occurred, and (*ii*) photoperiod day, which corresponds to the day of the year in which a respective experimental photoperiod could be found. Thus, for each calendar day during the experiment, there were three different photoperiod days corresponding to the date 104, 55, and 13 days previous (early, middle, and late) (Fig. 1). Both frames of reference are valid and both might be considered to appreciate the results. To reduce confusion between these frames of reference, we have transformed calendar dates to days postponding for use in figures, tables, and statistical analysis. Thus, the experiment ranged from day 1 postponding (9 October 2002) to day 277 postponding (15 July 2003).

We most formally examined results by comparing fish of the same age, sampled at the same number of days postponding, using a three-way analysis of variance (ANOVA) with date, ration (HiFeed and LoFeed), and photoperiod (Early, Middle, and Late) the effects examined. If significant effects were found, a one-way ANOVA followed by Scheffé's multiple range test was conducted to assess differences between individual means. Overall, significant effects and interactions were found for all main factors for the three parameters examined (length, plasma IGF-I, gill Na^+,K^+-ATPase activities; results not shown).

Within this statistical framework, photoperiod affects were apparent as consistent differences between photoperiod treatments within a feed treatment (e.g., EarlyEmergeHiFeed different from LateEmergeHiFeed). State-dependent effects (size or growth) were apparent as differences between HiFeed and LoFeed treatments within a photoperiod (e.g., EarlyEmergeHiFeed different from EarlyEmergeLoFeed). Interactions between photoperiod and feed treatment are indicated when HiFeed and LoFeed differences are not consistent between photoperiod treatments (e.g., EarlyEmergeHiFeed different from EarlyEmergeLoFeed, while LateEmergeHiFeed not different from LateEmergeLoFeed). Significant differences between treatments for a given number of days postponding are shown in the figures. Significant differences between sampling dates within a treatment are discussed in the text. The significance level was set at $p < 0.05$.

The metric for seawater challenges was percent survival; for each treatment, for any one date, there was only one trial, so $n = 1$ for each date. On a calendar date scale, we assessed mean seawater survival for each treatment over trials conducted between days 439 and 553 postponding (five trials, $n = 5$ per treatment). The square root of the proportion of fish surviving (0–1) was arcsine transformed prior to analysis with ANOVA (Zar 1984). All subsequent percentage data were similarly transformed (percentage of males maturing, GSI). Differences in transformed means were determined by one-way ANOVA followed by Scheffé's multiple range test.

Percent early male maturation (summed over samples taken from the whole experiment) was compared simply between HiFeed and LoFeed treatments with ANOVA (two treatments, three replicates). Simple regression was used to assess percent early male maturation in all treatments with respect to photoperiod day at emergence after values were standardized to a common mean for each feed treatment (HiFeed or LoFeed): standardized mean = % maturation for a treatment – (mean % maturation for a feed group – overall mean % maturation). GSI was determined as GSI = gonad weight × body weight^{-1} × 100.

Seasonal framework for analytical analysis

Simple regression was used to assess the relations among length and gill Na^+,K^+-ATPase activity for fish grouped into seasonal stanzas (August–September, October–November, December–January, February–March, April–May, June–July) by photoperiod date. A simple size versus gill Na^+,K^+-ATPase activity relation consistent over all dates would be indicative of an underyearling smolting pattern. A significant size versus gill Na^+,K^+-ATPase activity relation only found in the spring would be indicative of a yearling smolting pattern. Seasonal changes in the size versus gill Na^+,K^+-ATPase activity relation would indicate a variable smolting pattern. Differences in mean seasonal gill Na^+,K^+-ATPase activities were also assessed by one-way ANOVA as discussed previously, with fish binned into the same seasonal stanzas as described above. Finally, mean seawater tolerance of each treatment was also assessed on a photoperiodic scale over the photoperiod dates of 15 November – 15 January ($n = 3$ or 4 per treatment) to demarcate potential autumnal smolting.

Assessing size, growth, maturation, and smolting

Size and growth were examined, as they represent physiological pathways through which environment influences development (smolting and maturation). More directly, size and growth rate may influence the decision of individual fish to either smolt or mature. As such, we are not so much interested in the effects of feeding rate and photoperiod on size and growth; instead, we are interested in how size and growth relate to environment and the subsequent expression of smolting and early male maturation. We measured size of fish in each treatment at each sampling date and assessed differences between treatments with ANOVA (described above). We could not estimate growth rate of fish over each sampling interval, as we neither tagged individual fish nor included robust replication of tanks within our experiment; however, we did measure plasma levels of the hormone IGF-I at each sampling interval, as it has been established as an effective index of fish growth (Beckman et al. 2004). Overall, we assessed IGF-I not to ascertain growth differences between individual treatments; rather, we wished to test whether we produced two different growth trajectories (HiFeed and LoFeed). We could again assess differences in mean IGF-I between treatments with ANOVA.

Maturation represents a binary response (yes or no) and male maturation may be easily assessed visually as a thickening of the testis (Campbell et al. 2003; Larsen et al. 2004). The number of males in each treatment that initiated maturation was simply counted cumulatively over the course of

© 2007 NRC Canada

Fig. 2. Mean (±SE) length of Sacramento River winter-run chinook salmon (*Oncorhynchus tshawytscha*) reared under three differing photoperiods (EarlyEmerge (squares), MiddleEmerge (triangles), and LateEmerge (circles)) and two feeding levels (HiFeed (solid lines) and LoFeed (broken lines)). Symbols with similar superscripted letters are not significantly different frpm each other for a given date. The order of letters (top to bottom) corresponds to the order of symbols (top to bottom) on a given date.

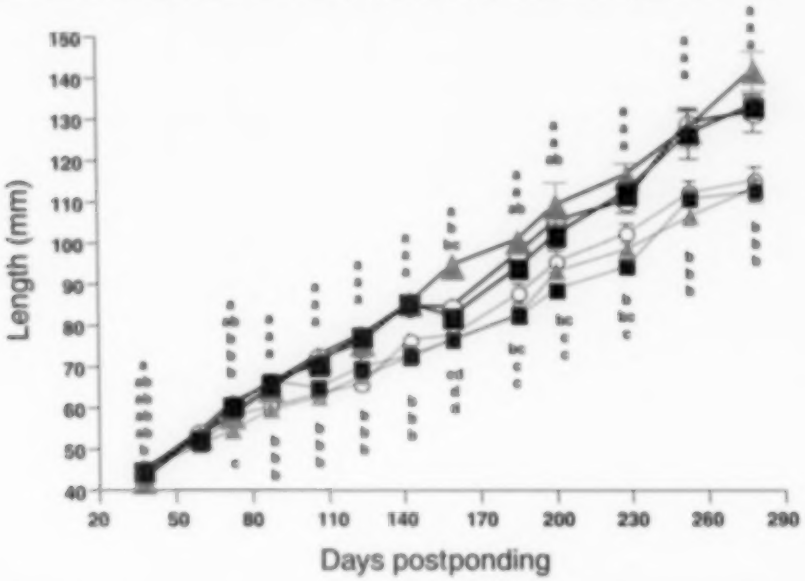

sampling and added to the count made by terminally sampling all of the remaining fish at the end of the experiment.

Ecologically, smolting is a binary response that is represented by whether or not fish migrate downstream to the ocean (yes or no) and whether the individual can adapt to seawater when they reach that destination (live or die). Functionally, smolting thus includes both behavioral (migration) and physiological (seawater tolerance) traits that are seasonally correlated but represent distinct organismal responses. Assessing smolting in an experimental context is difficult, as there is no one character that represents the overall biological response. Investigators have used behavioral, morphological, endocrine, and physiological traits to index smolting (Hoar 1976; Folmar and Dickhoff 1980; McCormick and Saunders 1987). All of these traits display gradual quantitative changes that occur over a period of weeks to months within both individuals and populations that are difficult to transform into a simple binary smolt index (smolt or nonsmolt). In addition, smolting is reversible (Shrimpton et al. 2000). Thus, any one sample of a population may include individuals that are initiating smolting, fish fully within the smolting process, and fish readapting to fresh water. Thus, we cannot simply count individual smolts within a treatment over the course of time.

We assessed smolting by marking the development of seawater tolerance, a key characteristic for animals successfully making a freshwater to seawater transition. Two measures of seawater tolerance were conducted: measuring the activity of the enzyme Na^+,K^+-ATPase found in the gill (Zaugg and Wagner 1973) and survival in a seawater challenge (Clarke and Blackburn 1977). It is tempting to interpret the results of seawater challenge (live or die) as a binary indicator of smolting (yes or no). However, again, smolting is reversible, so a given seawater challenge can not determine whether a fish has not yet smolted (dies) or has smolted and subsequently readapted to fresh water (dies). We interpret differences in the mean value of either gill Na^+,K^+-ATPase activity or proportion of individuals surviving a seawater challenge as differences in the tendency of individuals within an experimental population to smolt during a given period. Given that smolting is a temporally extended process (weeks to months), we expect diagnostic differences in seawater tolerance to extend through at least two sampling periods. Furthermore, note that changes in the results of seawater challenges tend to lag changes in gill Na^+,K^+-ATPase activity in captive populations and these indicators are thus not expected to display exact temporal equivalence (Beckman et al. 1999).

Results

Length and growth

Consistent, significant differences in length were found between feeding treatments by 90 days postponding and these continued throughout the experiment, with fish from HiFeed treatments being larger than fish from LoFeed treatments (Fig. 2). Samples obtained from day 160 to day 230 postponding diverged somewhat both within and between feeding treatments, with fish from the EarlyEmergeHiFeed and the LateEmergeLoFeed groups not significantly different from each other on several sampling occasions. Subsequently, all HiFeed groups were significantly different from all LoFeed groups day 230 through day 277.

Significant differences in plasma IGF-I levels for fish in different feeding treatments (HiFeed versus LoFeed) were found on nine of the 11 dates that blood was obtained, dem-

© 2007 NRC Canada

Fig. 3. Mean (±SE) plasma IGF-I level of Sacramento River winter-run chinook salmon (*Oncorhynchus tshawytscha*) reared under three differing photoperiods (EarlyEmerge (squares), MiddleEmerge (triangles), and LateEmerge (circles)) and either (*a*) HiFeed (solid lines) or (*b*) LoFeed (broken lines) level. Symbols with similar superscripted letters are not significantly different from each other for a given date for each panel. The order of letters (top to bottom) corresponds to the order of symbols (top to bottom) on a given date.

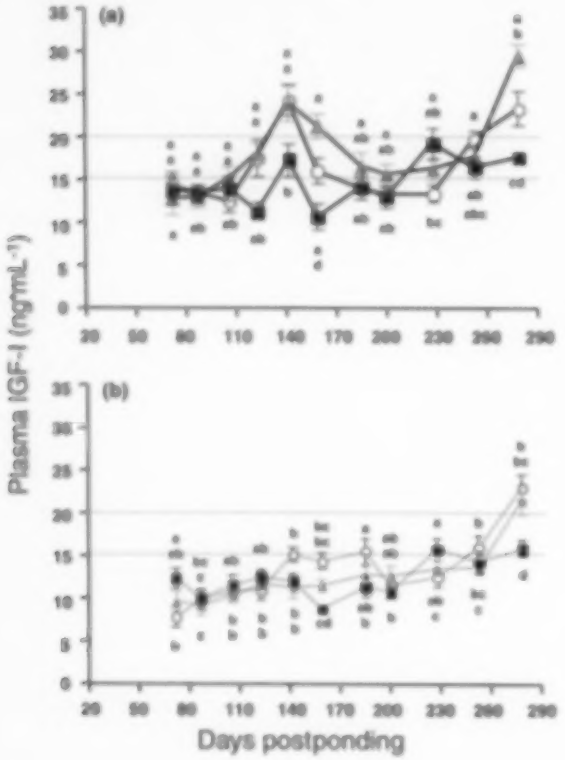

onstrating a strong effect of ration on plasma IGF-I level (statistical analysis not shown) (Fig. 3). Photoperiod effects were also found within feeding treatments. Plasma IGF-I levels in MiddleEmergeHighFeed and LateEmergeHiFeed fish increased from ~12 ng·mL^{-1} to a peak of ~25 ng·mL^{-1} before declining to ~15 ng·mL^{-1} between days 110 and 200 postponding (Fig. 3*a*). Plasma IGF-I levels in the EarlyEmergeHiFeed group were significantly less than found in the other two HiFeed groups during this period (days 110–200). Similarly, IGF-I levels found in fish from the EarlyEmergeLoFeed group were significantly less than found in fish from the LateEmergeLoFeed group days 140–185 postponding (Fig. 3*b*). Photoperiod for the EarlyEmerge fish matched that of the winter solstice at approximately day 188 postponding (Fig. 1); thus, the period of relatively low IGF-I levels in EarlyEmerge fish matches the period during which the fish received the least photoperiodic stimulation.

Smolting

Gill Na$^+$,K$^+$-ATPase activities increased significantly from day 170 to day 260 postponding in all treatments (Figs. 4*a* and 4*b*). Gill Na$^+$,K$^+$-ATPase activity increases occurred later in both EarlyEmerge groups (HiFeed and LoFeed) as compared with the other photoperiod groups. This difference corresponds to the 100-day delay in the spring increase in daylight as defined by differences between the EarlyEmerge and LateEmerge photoperiod treatments and directly translates into a photoperiod effect on the increase in gill Na$^+$,K$^+$-ATPase activities. There were no significant differences between feeding groups within a photoperiod treatment from day 170 to day 260 postponding, suggesting that there was no effect of size or growth on smolting during this period.

Differences between both feeding and photoperiod treatments were found from day 50 to day 110 postponding. LateEmergeHiFeed fish had lower gill Na$^+$,K$^+$-ATPase activities than found in other HiFeed groups between day 50 and day 110. In addition, fish from both EarlyEmergeHighFeed and MidEmergeHiFeed groups had significantly higher gill Na$^+$,K$^+$-ATPase activities than fish from EarlyEmergeLowFeed and MidEmergeLoFeed groups for at least three sampling dates from day 50 to day 110 (Figs. 4*a* and 4*b*), suggesting a state-dependent effect (size or growth) on smolting in the EarlyEmerge and MiddleEmerge photoperiod treatments during this time period.

Seawater survival increased from 0% day 36 through day 110 postponding to 100% in all groups by day 285 (Fig. 5). Photoperiod at emergence had a stronger effect than feeding rate on seawater survival (two-way ANOVA: photoperiod, $F = 7.2$, $p = 0.005$; feeding rate, $F = 2.2$, $p = 0.16$; interaction, $F = 0.3$, $p = 0.77$, $n = 30$) over days 143–248 postponding.

Seasonal size–smolting relations

In general, bigger fish had high gill Na$^+$,K$^+$-ATPase activity (Fig. 6*a*), with only fish >80 mm possessing gill Na$^+$,K$^+$-ATPase activities >6. However, fish of this size were not found until February–March (photoperiod dates), with bigger fish and higher gill Na$^+$,K$^+$-ATPase activities found at even later dates (April–July, photoperiod dates, gill Na$^+$,K$^+$-ATPase activities 6–10). Physiological condition of fish altered the general size – gill Na$^+$,K$^+$-ATPase activity relation, as maturing males (visibly enlarged testis) had gill Na$^+$,K$^+$-ATPase activities significantly less than found in fish of a similar size (for fish >100 mm, mature male gill Na$^+$,K$^+$-ATPase = 3.8, not mature male gill Na$^+$,K$^+$-ATPase = 6.0; $F = 69$, $p < 0.0001$). Seasonal photoperiod also appeared to influence the size – gill Na$^+$,K$^+$-ATPase activity relation, as some fish of a size of ~60 mm had gill Na$^+$,K$^+$-ATPase activities >4.25; these fish were sampled in the autumn period (August–November, photoperiod date).

Size–smolting relations were not consistent through season. Simple regression showed significant, positive relations in August–September, February–March, and April–May. No relation was found in October–November and a negative relation was found in December–January. This later finding may be due to some relatively large males (90–100 mm) that had physiologically initiated maturation prior to the beginning of visually discernable enlargement of the testis. Nevertheless, there was no sign of increased gill Na$^+$,K$^+$-ATPase activities during the December–January period. Finally, a seasonal comparison of mean gill Na$^+$,K$^+$-ATPase activities was made (Fig. 6*b*). Average gill Na$^+$,K$^+$-ATPase values

© 2007 NRC Canada

Fig. 4. Mean (±SE) gill Na^+,K^+-ATPase activity of Sacramento River winter-run chinook salmon (*Oncorhynchus tshawytscha*) reared under three differing photoperiods (EarlyEmerge (squares), MiddleEmerge (triangles), and LateEmerge (circles)) and either (*a*) HiFeed (solid lines) or (*b*) LoFeed (broken lines) level. Symbols with similar superscripted letters are not significantly different from each other for a given date. The order of letters (top to bottom) corresponds to the order of symbols on a given date (top to bottom).

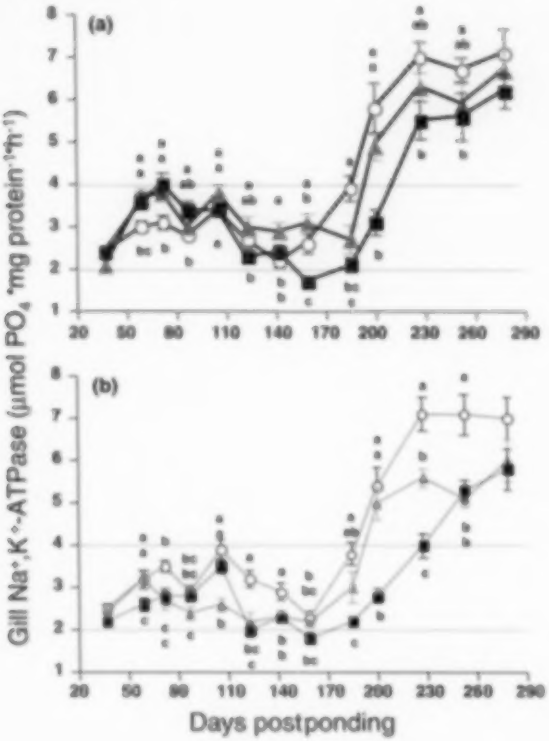

found in December–January were significantly lower than found during any other period, while strong increases were found from February through July. These analyses demonstrate a seasonally variable smolting pattern in winter-run chinook salmon.

When examined with regard to photoperiod date, increases in seawater tolerance were tightly coupled to photoperiod, with date of achieving 50% survival in seawater spanning less than 6 weeks between treatments (mid-February to late March), regardless of size or age (Fig. 7). All fish survived the 72-h seawater challenge in May (photoperiod date). In contrast, date of achieving 50% seawater survival spanned 3 months (early March – late June) when examined by calendar date (fish of the same age) (Fig. 5).

Early male maturation

Male maturation was significantly higher in HiFeed groups (31.5%) as compared with LoFeed groups (9.3%) ($F = 28.7$, $p = 0.006$, $n = 6$) (Fig. 8*a*). In addition, a significant linear relation was found between photoperiod at emergence and feed treatment standardized percent male maturation ($F = 1184$, $p = 0.02$, $r^2 = 0.96$, $n = 6$) (Fig. 8*b*).

Fig. 5. Percent survival of Sacramento River winter-run chinook salmon (*Oncorhynchus tshawytscha*) reared under three differing photoperiods (EarlyEmerge (squares), MiddleEmerge (triangles), and LateEmerge (circles)) and two feeding levels (HiFeed (solid lines) and LoFeed (broken lines)) subjected to a 72-h 35 ppt seawater challenge plotted versus days postponding. Broken-lined arrows indicate the period over which different treatment groups first achieved 50% survival.

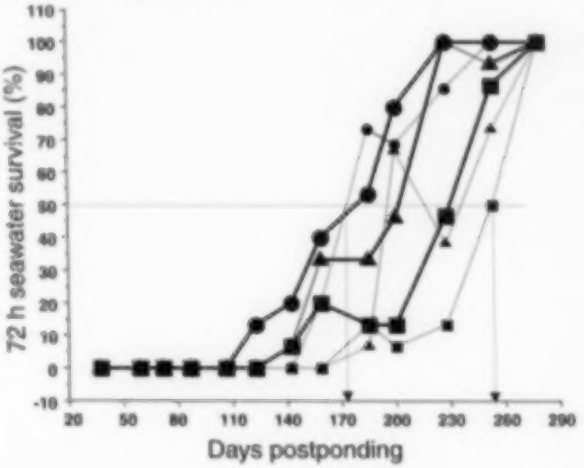

There were no differences in GSI among immature males at the termination of the experiment in July ($F = 1.5$, $p = 0.19$) (Fig. 9*a*). In contrast, GSI of maturing males was significantly higher in LateEmerge and MiddleEmerge fish than in EarlyEmerge fish ($F = 26.1$, $p < 0.0001$) (Fig. 9*b*). Spermiating males were found in both the MiddleEmerge and LateEmerge groups.

Discussion

Sacramento River winter-run chinook salmon displayed a variable juvenile life history dependent on photoperiod at emergence and subsequent growth rate. Two different smolting patterns were found: the first, a distinct seasonally defined, photoperiod-driven, spring smolting pattern typical of chinook salmon that smolt as yearlings (Beckman et al. 1998, 1999, 2000); in addition, autumnal smolting occurred (Ewing et al. 1980; Beckman and Dickhoff 1998; Beckman et al. 2003). Autumnal smolting appeared to be both size (growth) and photoperiod dependent, as (*i*) EarlyEmerge-HiFeed fish appeared to smolt, while EarlyEmergeLoFeed fish did not and (*ii*) LateEmergeHiFeed fish did not smolt when they were the same age and size as EarlyEmerge-HiFeed fish but were experiencing a different photoperiodic signal. Both smolting patterns were clearly seasonal (photoperiod driven), as spring smolting and autumnal smolting were separated by the December–January period (photoperiod date) during which there was little evidence of smolting regardless of fish size or growth rate.

Precocious male maturation was growth dependent, as has been demonstrated previously in chinook salmon (Clarke and Blackburn 1994; Silverstein et al. 1998; Larsen et al. 2006), as HiFeed groups had higher maturation rates than photoperiod-matched LoFeed groups. In addition, there was

© 2007 NRC Canada

Fig. 6. (*a*) Scatterplot of length and gill Na^+,K^+-ATPase activity for individual Sacramento River winter-run chinook salmon (*Oncorhynchus tshawytscha*). Different symbols indicate season (photoperiod) under which fish were sampled. Maturing males are depicted by separate discrete symbol regardless of season. Regression relations between length and gill Na^+,K^+-ATPase activity are plotted for each season; the length of each line encompasses the range of fish length for each season (August–September: $p < 0.0001$, $r^2 = 0.34$, $n = 119$; October–November: $p = 0.6$, r^2 not significant, $n = 215$; December–January: $p < 0.0001$, $r^2 = 0.22$, $n = 118$; February–March: $p < 0.0001$, $r^2 = 0.37$, $n = 283$; April–May: $p = 0.008$, $r^2 = 0.07$, $n = 102$; June–July: $p = 0.28$, r^2 not significant, $n = 45$). (*b*) Mean seasonal gill Na^+,K^+-ATPase activity (regardless of treatment); columns with similar superscripted letters are not significantly different from each other ($p > 0.05$).

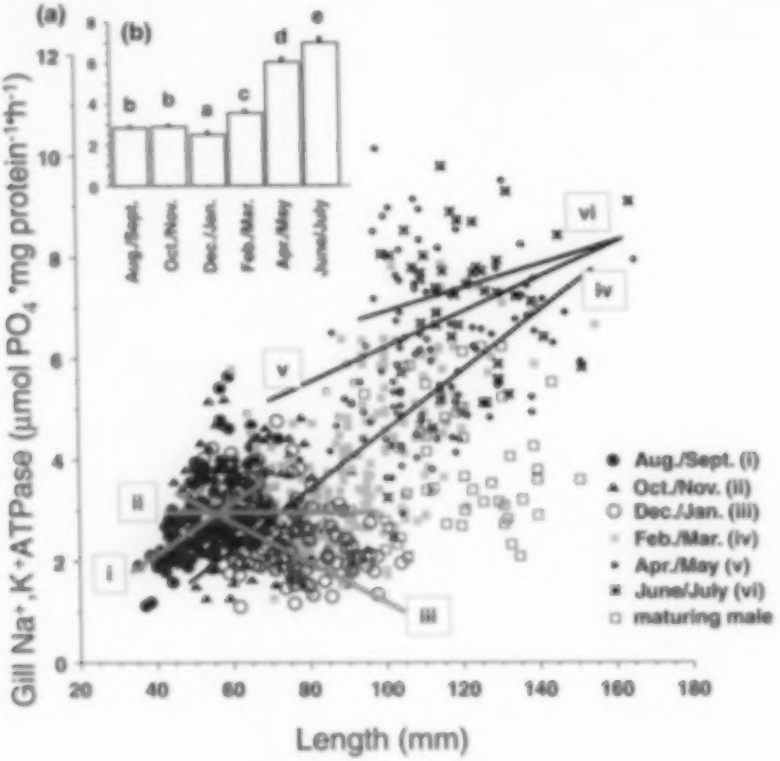

a linear relation between emergence date and maturation, as EarlyEmerge fish matured at a higher rate than LateEmerge fish. This photoperiod effect suggests that there is a growth × photoperiod interaction involved in the early maturation "decision" (see below).

Photoperiod, seasonal windows, emergence timing, and quantitative threshold traits

Key to this experimental design was the exposure of first-emerging fry to different photoperiods. Exposing salmonids to altered experimental photoperiods is not novel. In many cases, investigators have used a constant short-day photoperiod (simulating emergence during the winter or early spring) in an effort to produce "zero-age" coho (*Oncorhynchus kisutch*), Atlantic, or chinook salmon smolts that might be transferred to seawater at a younger age, thus increasing the efficiency of aquaculture operations (Clarke et al. 1989; Duston and Saunders 1995; Duncan and Bromage 1998). For chinook salmon, Clarke et al. (1989, 1992, 1994) compared the smolting response of individuals from ocean-type and stream-type populations from British Columbia exposed to constant short-day (9.5 h, photoperiod equivalent to emerging prior to the spring equinox) and long-day (14.5 h, photoperiod equivalent to emerging after the spring equinox) photoperiods for 2 months postemergence prior to placing them on the same natural photoperiod. He found that fish from ocean-type populations smolted as underyearlings regardless of photoperiod. In contrast, fish from stream-type populations smolted as underyearlings when exposed to a short-day photoperiod at emergence but did not when exposed to a long-day photoperiod. These experiments demonstrated both that there were genetic differences between chinook salmon populations with regard to the photoperiod dependence of smolting and the physiological fact that smolt timing was sensitive to the photoperiod during early development. Placed into an ecological context, these data suggest that fry that emerge relatively late in a growing season (long-day photoperiod) suppress the initiation of smolting until the following spring regardless of their growth rate.

Similarly, Clarke and Blackburn (1994) exposed fry from a stream-type chinook salmon population to short-day (10 h of light) and long-day (14 h of light) photoperiods for 2 months postemergence and then examined the effect of this photoperiod treatment on early male maturation. They

© 2007 NRC Canada

Fig. 7. Percent survival of Sacramento River winter-run chinook salmon (*Oncorhynchus tshawytscha*) reared under three differing photoperiods (EarlyEmerge (squares), MiddleEmerge (triangles), and LateEmerge (circles)) and two feeding levels (HiFeed (solid lines) and LoFeed (broken lines)) levels subjected to a 72-h 35 ppt seawater challenge plotted versus photoperiod date. Broken-lined arrows indicate the period over which different treatment groups first achieved 50% survival.

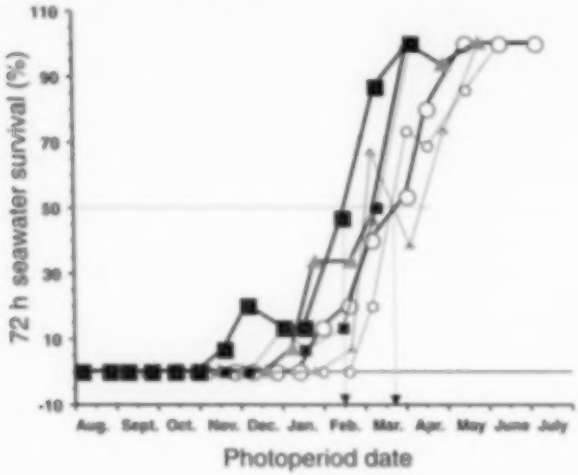

found no maturing males in the long-day group but 7.8% of the short-day males were mature at age 1. Subsequently, at age 2, 83% of the short-day males were found to be mature, while only 40% of the long-day males matured. Berrill et al. (2003, 2006) have developed additional evidence for the effect of photoperiod on early male maturation in Atlantic salmon. Fish were placed into several different compressed photoperiod schedules with first-emergent fry first placed into a constant 24-h light environment for 6 or 8 weeks (simulated summer) followed by 8 or 12 weeks of short-day photoperiod (simulated winter) and then returned to constant 24-h light (simulated summer) in an attempt to provide fish the proper seasonal sequence of photoperiod changes to promote smolting (normally in the second spring of life) at an early age. Male maturation at age 1 ranged from 4.3% to 20.9% varying by photoperiod treatment, again demonstrating a physiological interaction between photoperiod and development. Once again, placing these data on the photoperiod effect on early male maturation into an ecological context suggests that fry that emerge early (short-day photoperiod) in a growing season are more likely to mature at age 1 than fry that emerge later. This strongly suggests that individual developmental decisions are made with reference to season as delineated by photoperiod.

Relations among emergence timing and life history variation have also been examined using a correlational approach. Several investigators have found positive relations among emergence timing, metabolic rates, behavioral dominance, growth rate, and tendency to either smolt or mature at a relatively early age (Metcalfe and Thorpe 1992; Metcalfe et al. 1995; Cutts et al. 1999). However, these experiments do not strictly test for an effect of photoperiod at emergence; rather, they really demonstrate an overall correlation between developmental rate and metabolic rate, as photoperiod was not directly manipulated. Instead, the traits of naturally early-emerging fish were compared with fish naturally emerging later. Moreover, the differences in emergence timing in these experiments ranged from a few days to several weeks, and thus, the differences in photoperiod experienced by fry emerging at different times did not approach the 4-month difference in photoperiod experienced by fish in the present experiment.

Fig. 8. (*a*) Percentage of male Sacramento River winter-run chinook salmon (*Oncorhynchus tshawytscha*) reared under three differing photoperiods (EarlyEmerge, MiddleEmerge, and LateEmerge) and either HiFeed or LoFeed conditions determined to be maturing at age 1 based on visual assessment of testis size. (*b*) Scatterplot of standardized (to the mean maturation rate) arcsine square root transformed percent maturation data plotted against day of the year for photoperiod at emergence ($F = 107.8$, $p < 0.001$, $r^2 = 0.96$, $n = 6$). Shaded diamonds represent HiFeed and open diamonds represent LoFeed treatments.

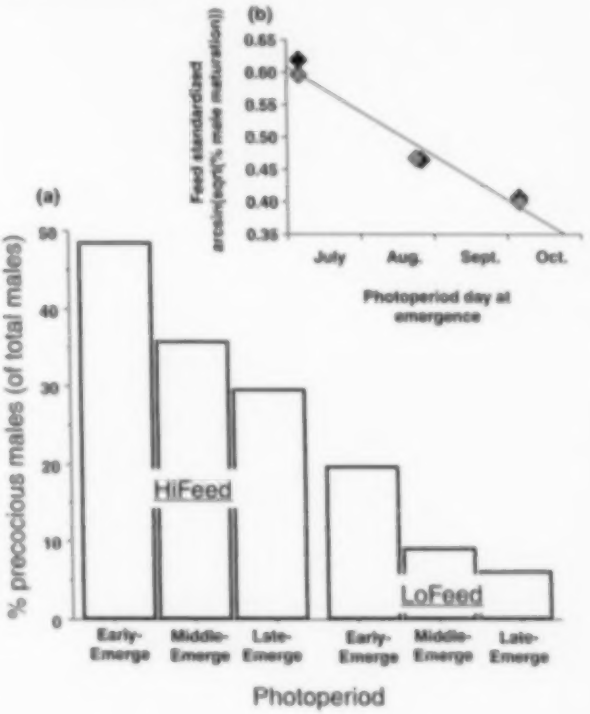

The experiment detailed herein differed from these other approaches. All fish were exposed to the same seasonal photoperiod; fish just entered the seasonal photoperiod cycle (emergence) at different points. Thus, fish from different photoperiod treatments received seasonal photoperiod signals at different ages (i.e., autumnal equinox occurred at 86 days postemergence for EarlyEmerge fish, 37 days postemergence for MiddleEmerge fish, and 5 days preemergence for LateEmerge fish) but they received exactly the same photoperiod signal. Thus, we were not testing for an effect of photoperiod, but rather, we were testing for the effect of emergence at seasonally different dates as defined

© 2007 NRC Canada

Fig. 9. Average arcsine square root transformed GSI of (*a*) immature male and (*b*) maturing male Sacramento River winter-run chinook salmon (*Oncorhynchus tshawytscha*) reared under three differing photoperiods (EarlyEmerge, MiddleEmerge, and LateEmerge) and either HiFeed (shaded bars) or LoFeed (open bars) conditions and sampled at termination of the experiment. Bars with similar superscripted letters are not significantly different. The horizontal line indicates the 0.05 level for both panels.

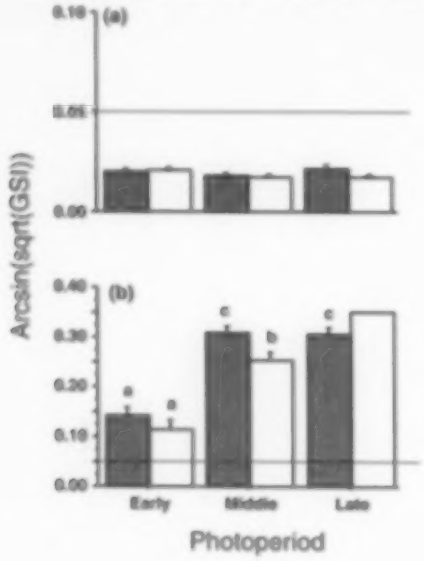

by photoperiod. We directly compared fish of the same age and size and inferred a photoperiod effect by differences between treatments. However, our primary objective was to infer how a range of seasonal emergence timings, coupled to different growth rates, would alter life history patterns in these fish as they progressed through seasonal periods with differing conditions.

HiFeed fish were the same age and size throughout the experiment (days postponding), but some EarlyEmerge fish smolted in the autumn and a greater percentage of EarlyEmerge males matured as compared with LateEmerge fish, suggesting that photoperiod at emergence did alter life history pattern. It is an important point to note the GSI differences in maturing males from EarlyEmerge and LateEmerge treatments at the termination of the experiment. While maturing, the EarlyEmerge fish were not yet mature (as indicated by the lower GSI and the lack of spermiating fish) and the seasonal photoperiod cue had not yet advanced to the point that stimulates Sacramento River winter-run chinook salmon to spawn, while photoperiod had passed this point for the LateEmerge fish (as indicated by the higher GSI and the presence of spermiating fish). Again, because these fish were the same age, seasonally changing photoperiod was synchronizing maturation. In addition, fish from the MiddleEmerge and LateEmerge treatments were mature (spermiating) at the "correct" seasonal time, in synchrony with naturally breeding winter-run chinook salmon (Myers et al. 1998; Yoshiyama et al. 1998). This suggests that fish in this experiment were "correctly" interpreting the photoperiod signals given to them.

McNamara and Houston (1996) developed the concept that life history variation may be "state dependent". This formalized the observation that an animal's reproductive decisions (to reproduce (yes or no), fecundity (how many), and offspring size (big or little)) were dependent on the actual physiological status of the animal (size or energy reserves), not just on an animal's age. Among salmonids, this concept has been explored most thoroughly in Atlantic salmon. A series of studies has demonstrated that the "decisions" on early maturation (yes or no) and smolting (yes or no) are dependent on growth rate and (or) adiposity, with bigger, faster growing, fatter fish initiating development and smaller, slower growing, leaner fish delaying development (Thorpe 1986, 1989; Metcalfe 1998). Based on these studies, theoretical models predicting life history trajectory for Atlantic salmon have been developed (Metcalfe 1998; Thorpe et al. 1998). These models explicitly recognize that development is dependent on an individual salmon's condition.

A number of experiments in salmon have suggested that there is a period of initiation and commitment to male maturation that occurs in the autumn–winter, up to a year prior to spawning (Thorpe 1994; Silverstein et al. 1998; Campbell et al. 2003). This work underlies models of Atlantic salmon life history variability (Metcalfe 1998; Thorpe et al. 1998), which recognize that developmental decisions are made within photoperiod-circumscribed seasonal periods. Thus, development is dependent on condition surpassing a threshold during a certain seasonal period. Recent work by Aubin-Horth and Dodson (2004) and Baum et al. (2004) supports the theoretical construct of this model by demonstrating variable size- and growth-dependent thresholds for maturation. Together, this work on Atlantic salmon provided the basis for our experimental design. There was good reason to believe that juvenile life history of winter-run chinook salmon was variable, but because of the unique run and spawn timing of these fish, it was hard to predict when seasonal periods for commitment to developmental decisions might occur. Thus, we needed to produce cohorts of juvenile fish of different condition progressing through different, photoperiod-defined seasonal periods.

Ecologically, the best way to view these data is size (growth) plotted against season in association with photoperiod (photoperiod date) (Fig. 10). Based on this, one can infer the interactions between photoperiod, size, and age. Two important points are illustrated by this approach. (*i*) LateEmergeHiFeed fish emerged after EarlyEmergeHiFeed fish had already developed elevated gill Na^+,K^+-ATPase activities, suggesting that LateEmergeHiFeed fish had missed the seasonal period for autumnal smolting by emerging near the autumn equinox. It is not clear whether these recently emerged fry were not old enough or not large enough to respond to the photoperiod at emergence, whether they were not growing fast enough to trigger development, or whether the fish emerged late enough in the season that the photoperiod cuing autumn smolting had already passed. Regardless of whether the fish did not receive the "correct" cue or whether the fish were not developed enough to perceive the cue, LateEmerge fish did not smolt in the autumn. (*ii*) LateEmergeHiFeed fish were smaller than EarlyEmergeLoFeed in late December and January (photoperiod date). Enlarged testes were first observed during this same winter

© 2007 NRC Canada

Fig. 10. Mean length of juvenile Sacramento River winter-run chinook salmon (*Oncorhynchus tshawytscha*) reared under three differing photoperiods (EarlyEmerge (squares), MiddleEmerge (triangles), and LateEmerge (circles)) and two feeding levels (HiFeed (solid lines) and LoFeed (broken lines)) plotted versus photoperiod date. Dates when enlarged testis and spermiation first observed are indicated by arrows. Dates over which Sacramento River winter-run chinook salmon naturally spawn are indicated by a shaded bar on the *x*-axis. The broken line and shaded area indicate the timing of autumn gill Na^+,K^+-ATPase activity increase in the EalyEmergeHiFeed treatment.

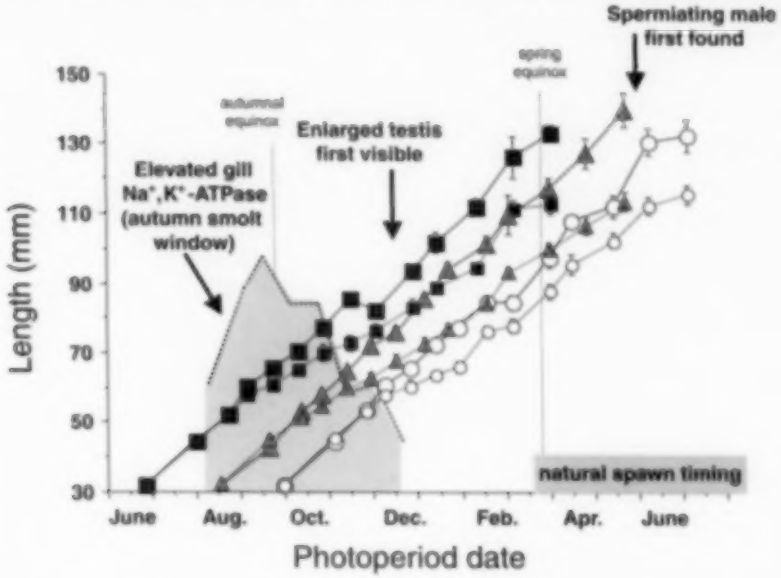

Fig. 11. Seasonal timing of selected life history events (spawning, emergence, smolting, and early male maturation) comparing (*a*) Columbia River spring-run and (*b*) Sacramento River winter-run chinook salmon (*Oncorhynchus tshawytscha*). The solid line depicts seasonal photoperiod change on an arbitrary scale. Vertical broken lines indicate spring and autumn equinoxes.

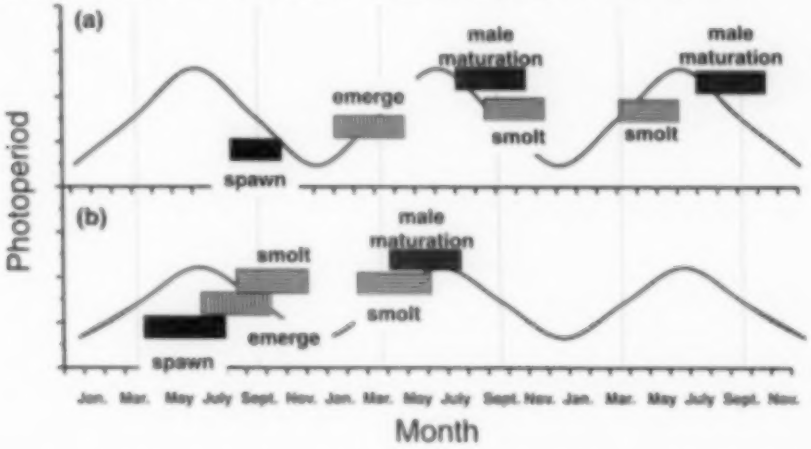

solstice period. Clearly, fish must have initiated maturation sometime prior to this point to allow testis development to visibly occur in December. Given that the size of EarlyEmergeLoFeed fish was greater than that of LateEmergeHiFeed fish through December, size was unlikely to be the factor determining male maturation, given that the rate of maturation was greater in LateEmergeHiFeed fish than in EarlyEmergeLoFeed fish. Instead, we suspect that differences in growth rate within seasonal period may have triggered the maturational decision (Rowe and Thorpe 1990; Larsen et al. 2006; Morita and Fukuwaka 2006).

The data presented herein suggest that emergence timing may play a role in life history variability of chinook salmon. Emergence timing is dependent on adult spawn timing, incubation temperature, maternal effects (egg size), genetic effects (individual differences in development rate), and interactions among all of these (Beacham and Murray 1990; Robison et al. 1999; Berg et al. 2001). Variation in emergence timing has been a little-explored axis promoting life history variation in salmon, as there is a general dogma that there is very strong stabilizing selection for emergence timing in a local area (Brannon 1987; Brannas 1995; Letcher et

© 2007 NRC Canada

al. 2004) owing to interactions between seasonal flooding and predation (selection against early emergence; Jensen and Johnsen 1999) and territorial dominance and rapid growth by first-colonizing fry (selection against late emergence; Einum and Fleming 2000). Whether this dogma is operational on a basin scale (such as the Sacramento River) is unknown. Certainly, there may be enough environmental variability in this region to result in variations in emergence timing. Moreover, it is uncertain if a dogma generated for territorial juvenile salmonids applies to winter-run chinook salmon, as they presently spawn in mainstem habitats and may rear in the mainstem or even delta habitats that may not be conducive to establishing and maintaining individual feeding territories. Thus, it is possible that significant differences in emergence timing may occur in the Sacramento River Basin (or other large river systems) that may result in ecologically relevant life history variation among chinook salmon.

Comparative juvenile chinook salmon life history

The life history of Sacramento River winter-run chinook salmon is apparently unique among chinook salmon populations (Healey 1994). However, this uniqueness is most readily apparent through the seasonal timing of life history events (adult migration and spawn timing); individual variation in life history pattern within the population and the photoperiodic regulation of these patterns appear to have been maintained. Among chinook salmon populations, smolting and early maturation of spring-run fish from the Fraser and Columbia rivers have been relatively well studied (Healey 1991; Myers et al. 1998). Three differences stand out between Fraser and Columbia River spring-run and Sacramento River winter-run chinook salmon juvenile life histories (Fig. 11). First, the juvenile period is temporally compressed in winter-run fish. Only weeks separate spawning and emergence instead of a 3- to 6-month period found in spring-run fish. In addition, the period between emergence and smolting is also compressed, with at most 1 year separating the two events in winter-run fish. A minimum of 12 months separates these events in naturally rearing Columbia River spring-run fish and 18–20 months is standard. One might speculate that this is simply the consequence of water temperature. Winter-run fish emerge relatively quickly after spawning, as water temperature is relatively warm; in contrast, spring-run eggs and alevins experience a rapidly decreasing water temperature as eggs are deposited in the fall as winter approaches. Nevertheless, fish from each population appear to be sensitive to and respond to photoperiodic signals that occur at emergence, even though these signals may be different (see below). Thus, salmon are capable of maintaining a photoperiodic cuing for developmental events, even though the temporal duration of life history expression is compressed.

Second, the temporal order in which developmental decisions are manifested is switched. Winter-run fish may smolt either in the autumn or in the succeeding spring before any male maturation is apparent. In contrast, spring-run males have an opportunity to mature in the late summer or fall prior to or simultaneous with the first autumnal smolting period. Note that just because smolting was apparent before early male maturation in Sacramento River winter-run chinook salmon, this does not necessarily imply either that (*i*) the smolting "decision" was made prior to the early maturation "decision" or that (*ii*) there are two distinct "decisions" (smolt (yes or no) or mature (yes or no) during two distinctly different occasions) or (*iii*) there is one decision with three "choices" (mature, smolt, wait). We did not directly determine whether there were large, fast-growing males in the fall, which we would predict might have smolted, that instead had "made the decision" to mature the following spring–summer and thus did not smolt. These observations on the timing of smolting and early male maturation imply some plasticity in the interactions between age, photoperiod, and developmental decisions in the evolutionary history of chinook salmon.

Third, smolting and maturation decisions in both populations appeared to occur during equinoxes; however, the direction of photoperiod change stimulating development appears to be reversed between the populations, early male maturation occurring at the spring equinox (increasing photoperiod) for winter-run fish and at the autumnal equinox (decreasing photoperiod) for spring-run fish. Fish from either population appear to be capable of smolting in either the autumn or the spring, synchronized by either increasing or decreasing photoperiods.

Together, these differences suggest that chinook salmon have a great deal of flexibility (at least in an evolutionary sense) with regard to the photoperiodic signals that key development and the order in which developmental events occur. Given the great variability in chinook salmon life history, this last statement might seem simplistic; however, the statement does point out the comparative opportunities available to investigate the mechanism(s) that allow this plasticity to occur.

Acknowledgements

This research was conducted in collaboration with the US Fish and Wildlife Service and the California Department of Fish and Game under permits from the National Marine Fisheries Service and the California Department of Fish and Game and was supported by funds from the US Bureau of Reclamation and the California Department of Water Resources (contract 4600001540). We thank Anne McBride and Holly Mendonca for assistance with fish spawning and shipment of eggs and Correigh Greene, Joe Cech, Scott Foott, Steve Lindley, and two anonymous reviewers for providing constructive critical comments that improved the manuscript. Finally, we thank Penny Swanson for making the introductions that initiated this work. Reference to trade names does not imply endorsement by the National Marine Fisheries Service or the National Oceanic and Atmospheric Administration.

References

Arkush, K.D., Mendonca, H.L., McBride, A.M., and Hedrick R.P. 2004. Susceptibility of captive adult winter-run chinook salmon *Oncorhynchus tshawytscha* to waterborne exposures with infectious hematopoietic necrosis virus (IHNV). Dis. Aquat. Org. **59**: 211–216.

© 2007 NRC Canada

Aubin-Horth, N., and Dodson, J.J. 2004. Influence of individual body size and variable thresholds on the incidence of a sneaker male reproductive tactic in Atlantic salmon. Evolution, **58**: 136–144.

Banks, M.A., Rashbrook, V.K., Calavetta, M.J., Dean, C.A., and Hedgecock, D. 2000. Analysis of microsatellite DNA resolves genetic structure and diversity of chinook salmon (*Oncorhynchus tshawytscha*) in California's Central Valley. Can. J. Fish. Aquat. Sci. **57**: 915–927.

Bartley, D., Bentley, B., Brodziak, J., Gomulkiewicz, R., Mangel, M., and Gall, G.A.E. 1992. Geographic variation in population genetic structure of chinook salmon from California and Oregon. Fish. Bull. **90**: 77–100.

Baum, D., Laughton, R., Armstrong, J.D., and Metcalfe, N.B. 2004. Altitudinal variation in the relationship between growth and maturation rate in salmon parr. J. Anim. Ecol. **73**: 253–260.

Beacham, T.D., and Murray, C.B. 1990. Temperature, egg size, and development of embryos and alevins of 5 species of Pacific salmon — a comparative analysis. Trans. Am. Fish. Soc. **119**: 927–945.

Beckman, B.R., and Dickhoff, W.W. 1998. Plasticity of smoltification in spring chinook salmon (*Oncorhynchus tshawytscha*): relation to growth and insulin-like growth factor-I. J. Fish Biol. **53**: 808–826.

Beckman, B.R., Larsen, D.A., Lee-Pawlak, B., Moriyama, S., and Dickhoff, W.W. 1998. Insulin-like growth factor-I and environmental modulation of growth during smoltification of spring chinook salmon (*Oncorhynchus tshawytscha*). Gen. Comp. Endocrinol. **109**: 325–335.

Beckman, B.R., Dickhoff, W.W., Zaugg, W.S., Sharpe, C., Hirtzel, S., Schrock, R., Larsen, D.A., Ewing, R.D., Palmisano, A., Schreck, C.B., and Mahnken, C.V.W. 1999. Growth, smoltification, and smolt-to-adult return of spring chinook salmon (*Oncorhynchus tshawytscha*) from hatcheries on the Deschutes River, Oregon. Trans. Am. Fish. Soc. **128**: 1125–1150.

Beckman, B.R., Larsen, D.A., Sharpe, C., Lee-Pawlak, B., and Dickhoff, W.W. 2000. Physiological status of naturally-rearing juvenile chinook salmon in the Yakima River: seasonal dynamics and changes associated with the parr–smolt transformation. Trans. Am. Fish. Soc. **129**: 727–753.

Beckman, B.R., Larsen, D.A., and Dickhoff, W.W. 2003. Life history plasticity in chinook salmon: relation of size and growth rate to autumnal smolting. Aquaculture, **222**: 149–165.

Beckman, B.R., Fairgrieve, W., Cooper, K.A., Mahnken, C.V.W., and Beamish, R.J. 2004. Evaluation of endocrine indices of growth in post-smolt coho salmon (*Oncorhynchus kisutch*). Trans. Am. Fish. Soc. **133**: 1057–1067.

Berg, K.O., Hendry, P.A., Svendsen, B., Bech, C., Arnekleiv, V.J., and Lohrmann, A. 2001. Maternal provisioning of offspring and the use of those resources during ontogeny: variation within and between Atlantic salmon families. Funct. Ecol. **15**: 13–23.

Berrill, I.K., Porter, M.J.R., Smart, A., Mitchell, D., and Bromage, N.R. 2003. Photoperiodic effects on precocious maturation, growth and smoltification in Atlantic salmon, *Salmo salar*. Aquaculture, **222**: 239–252.

Berrill, I.K., Smart, A., Porter, M.J.R., and Bromage, N.R. 2006. A decrease in photoperiod shortly after first feeding influences the development of Atlantic salmon (*Salmo salar*). Aquaculture, **254**: 625–636.

Bradford, M.J., and Taylor, G.C. 1997. Individual variation in dispersal behaviour of newly emerged chinook salmon (*Oncorhynchus tshawytscha*) from the upper Fraser River, British Columbia. Can. J. Fish. Aquat. Sci **54**: 1585–1592.

Brandes, P.L., and McLain, J.S. 2001. Juvenile chinook salmon abundance, distribution, and survival in the Sacramento – San Joaquin Estuary. *In* Fish. Bull. 179. Contributions to the biology of Central Valley salmonids. Vol. 2. *Edited by* R.L. Brown. California Department of Fish and Game. pp. 39–138. (Available from http://www.dfg.ca.gov/nafwb/bulletins.html)

Brannas, E. 1995. First access to territorial space and exposure to strong predation pressure — a conflict in early emerging Atlantic salmon (*Salmo salar* L.) fry. Evol. Ecol. **9**: 411–420.

Brannon, E.L. 1987. Mechanisms stabilizing salmonid fry emergence timing. *In* Sockeye salmon (*Oncorhynchus nerka*) population biology and future management. Can. Spec. Publ. Fish. Aquat. Sci. No. 96. pp. 120–124.

Campbell, B., Dickey, J.T., and Swanson, P. 2003. Endocrine changes during onset of puberty in male spring chinook salmon, *Oncorhynchus tshawytscha*. Biol. Reprod. **69**: 2109–2117.

Clarke, W.C., and Blackburn, J. 1977. A seawater challenge test to measure smolting of juvenile salmon. Can. Fish. Mar. Serv. Tech. Rep. 705.

Clarke, W.C., and Blackburn, J. 1994. Effect of growth on early sexual maturation in stream-type chinook salmon (*Oncorhynchus tshawytscha*). Aquaculture, **121**: 95–103.

Clarke, W.C., and Shelbourn, J.E. 1985. Growth and development of seawater adaptability by juvenile fall chinook salmon (*Oncorhynchus tshawytscha*) in relation to temperature. Aquaculture, **45**: 21–31.

Clarke, W.C., Shelbourn, J.E., Ogasawara, T., and Hirano, T. 1989. Effect of initial daylength on growth, seawater adaptability and plasma growth hormone levels in underyearling coho, chinook, and chum salmon. Aquaculture, **82**: 51–62.

Clarke, W.C., Withler, R.E., and Shelbourn, J.E. 1992. Genetic control of juvenile life history pattern in chinook salmon (*Oncorhynchus tshawytscha*). Can. J. Fish. Aquat. Sci. **49**: 2300–2306.

Clarke, W.C., Withler, R.E., and Shelbourn, J.E. 1994. Inheritance of smolting phenotypes in backcrosses of hybrid stream-type × ocean-type chinook salmon (*Oncorhynchus tshawytscha*). Estuaries, **17**: 13–25.

Connor, W.P., Sneva, J.G., Tiffan, K.F., Steinhorst, R.K., and Ross, D. 2005. Two alternative juvenile life history types for fall chinook salmon in the Snake River basin. Trans. Am. Fish. Soc. **134**: 291–304.

Cutts, C.J., Brembs, B., Metcalfe, N.B., and Taylor, A.C. 1999. Prior residence, territory quality and life-history strategies in juvenile Atlantic salmon (*Salmo salar* L.) J. Fish Biol. **55**: 784–794.

Duncan, N.J., and Bromage, N. 1998. The effect of different periods of constant short days on smoltification in juvenile Atlantic salmon (*Salmo salar*). Aquaculture, **168**: 369–386.

Duston, J., and Saunders, R.L. 1995. Advancing smolting to autumn in age 0+ Atlantic salmon by photoperiod, and long-term performance in sea water. Aquaculture, **135**: 295–309.

Einum, S., and Fleming, I.A. 2000. Selection against late emergence and small offspring in Atlantic salmon (*Salmo salar*). Evolution, **54**: 628–639.

Ewing, R.D., Pribble, H.J., Johnson, S.L., Fustish, C.S., Diamond, J., and Lichatowich, J.A. 1980. Influence of size, growth rate, and photoperiod on cyclic changes in gill (Na^+ K^+)-ATPase activity in chinook salmon (*Oncorhynchus tshawytscha*). Can. J. Fish. Aquat. Sci. **37**: 600–605.

Fleming, I.A. 1998. Pattern and variability in the breeding system of Atlantic salmon (*Salmo salar*), with comparisons to other salmonids. Can. J. Fish. Aquat. Sci. **55**(Suppl. 1): 59–76.

Folmar, L.C., and Dickhoff, W.W. 1980. The parr–smolt transformation (smoltification) and seawater adaptation in salmonids. Aquaculture, **21**: 1–37.

© 2007 NRC Canada

Foote, C.J., Clarke, W.C., and Blackburn, J. 1991. Inhibition of smolting in precocious male chinook salmon, *Oncorhynchus tshawytscha*. Can. J. Zool. **69**: 1848–1852.

Gaines, P.D., and Martin, C.D. 2002. Abundance and seasonal, spatial and diel distribution patterns of juvenile salmonids passing the Red Bluff Diversion Dam, Sacramento River. Red Bluff Research Pumping Plant Report Series. Vol. 14. U.S. Fish and Wildlife Service, Red Bluff, Calif.

Garant, D., Fleming, I.A., Einum, S., and Bernatchez, L. 2003. Alternative male life-history tactics as potential vehicles for speeding introgression of farm salmon traits into wild populations. Ecol. Lett. **6**: 541–549.

Gross, M.R. 1987. Evolution of diadromy in fishes. *In* Am. Fish. Soc. Symp. 1. Common strategies of anadromous and catadromous fishes. *Edited by* M.J. Dadswell, R.J. Klauda, C.M. Moffitt, R.L. Saunders, R.A. Rulifson, and J.E. Cooper. American Fisheries Society, Bethesda, Md. pp. 14–25.

Healey, M.C. 1991. Life history of chinook salmon (*Oncorhynchus tshawytscha*). *In* Pacific salmon life histories. *Edited by* C. Groot and L. Margolis. University of British Columbia Press, Vancouver, B.C. pp. 311–394.

Healey, M.C. 1994. Variation in the life-history characteristics of chinook salmon and its relevance to conservation of the Sacramento winter run on chinook salmon. Conserv. Biol. **8**: 876–877.

Hoar, W.S. 1976. Smolt transformation: evolution, behavior, and physiology. J. Fish. Res. Board Can. **33**: 1233–1252.

Jensen, A.J., and Johnsen, B.O. 1999. The functional relationship between peak spring floods and survival and growth of juvenile Atlantic Salmon (*Salmo salar*) and brown trout (*Salmo trutta*). Funct. Ecol. **13**: 778–785.

Larsen, D.A., Beckman, B.R., Cooper, K.A., Barrett, D., Johnston, M., Swanson, P., and Dickhoff, W.W. 2004. Assessment of high rates of precocious male maturation in a spring chinook salmon supplementation hatchery program. Trans. Am. Fish. Soc. **133**: 98–120.

Larsen, D.A., Beckman, B.R., Strom, C., Parkins, P., Cooper, K.A., Fast, D., and Dickhoff, W.W. 2006. Growth modulation alters the incidence of early male maturation and physiological development of hatchery reared spring chinook salmon: a comparison with wild fish. Trans. Am. Fish. Soc. **135**: 1017–1032.

Letcher, B.H., Dubreuil, T., O'Donnell, M.J., Obedzinski, M., Griswold, K., and Nislow, K.H. 2004. Long-term consequences of variation in timing and manner of fry introduction on juvenile Atlantic salmon (*Salmo salar*) growth, survival, and life-history expression. Can. J. Fish. Aquat. Sci. **61**: 2288–2301.

Lindley, S.T., Schick, R., May, B.P., Anderson, J.J., Greene, S., Hanson, C., Low, A., McEwan, D., MacFarlane, R.B., Swanson, C., and Williams, J.G. 2004. Population structure of threatened and endangered chinook salmon ESUs in California's Central Valley basin. NOAA Tech. Memo. NMFS-SWFSC-360. (Available from http://santacruz.nmfs.noaa.gov/publications)

McCormick, S.D. 1993. Methods for nonlethal gill biopsy and measurement of Na^+,K^+-ATPase activity. Can. J. Fish. Aquat. Sci. **50**: 656–658.

McCormick, S.D., and Saunders, R.L. 1987. Preparatory physiological adaptations for marine life of salmonids: osmoregulation, growth and metabolism. *In* Am. Fish. Soc. Symp. 1. Common strategies of anadromous and catadromous fishes. *Edited by* M.J. Dadswell, R.J. Klauda, C.M. Moffitt, R.L. Saunders, R.A. Rulifson, and J.E. Cooper. American Fisheries Society, Bethesda, Md. pp. 211–230.

McNamara, N.M., and Houston, A.I. 1996. State-dependent life histories. Nature, **380**: 215–221.

Metcalfe, N.A. 1998. The interaction between behavior and physiology in determining life history patterns in Atlantic salmon (*Salmo salar*). Can. J. Fish. Aquat. Sci. **55**(Suppl. 1): 93–103.

Metcalfe, N.B., and Thorpe, J.E. 1992. Early predictors of life-history events: the link between first feeding date, dominance and seaward migration in Atlantic salmon, *Salmo salar* L. J. Fish Biol. **41B**: 93–99.

Metcalfe, N.B., Taylor, A.C., and Thorpe, J.E. 1995. Metabolic rate, social status and life-history strategies in Atlantic salmon. Anim. Behav. **49**: 431–436.

Morita, K., and Fukuwaka, M. 2006. Does size matter most? The effect of growth history on probabilistic reaction norm for salmon maturation. Evolution, **60**: 1516–1521.

Myers, J.M., Kope, R.G., Bryant, G.J., Teel, D., Lierheimer, L.J., Wainwright, T.C., Grant, W.S., Waknitz, F.W., Neely, K., Lindley, S.T., and Waples, R.S. 1998. Status review of chinook salmon from Washington, Idaho, Oregon, and California. NOAA Tech. Memo. NMFS-NWFSC-35. (Available from http://www.nwfsc.noaa.gov/pubs/tm/tm35/index.htm)

Piper, R.G., McElwain, I.B., Orme, L.E., McCraren, J.P., Fowler, L.G., and Leonard, J.R. 1982. Fish hatchery management. American Fisheries Society, Bethesda, Md.

Robison, B.D., Wheeler, P.A., and Thorgaard, G.H. 1999. Variation in development rate among clonal lines of rainbow trout (*Oncorhynchus mykiss*). Aquaculture, **173**: 131–141.

Rowe, D.K., and Thorpe, J.E. 1990. Suppression of maturation in male Atlantic salmon (*Salmo salar* L.) parr by reduction in feeding and growth during spring months. Aquaculture, **86**: 291–313.

Shearer, K.D., and Swanson, P. 2000. The effect of whole body lipid on early sexual maturation of 1+ age male chinook salmon (*Oncorhynchus tshawytscha*). Aquaculture, **190**: 343–367.

Shearer, K.D., Parkins, P., Gadberry, B., Beckman, B.R., and Swanson, P. 2006. The effects of growth rate/body size and a low lipid diet on the incidence of early sexual maturation in juvenile male spring chinook salmon (*Oncorhynchus tshawytscha*). Aquaculture, **252**: 545–556.

Shimizu, M., Swanson, P., Haruhisa, F., Hara, A., and Dickhoff, W.W. 2000. Comparison of extraction methods and assay validation for salmon insulin-like growth factor-I using commercially available components. Gen. Comp. Endocrinol. **119**: 26–36.

Shrimpton, J.M., Bjornsson, B.T., and McCormick, S.D. 2000. Can Atlantic salmon smolt twice? Endocrine and biochemical changes during smolting. Can. J. Fish. Aquat. Sci. **57**: 1969–1976.

Silverstein, J.T., Shearer, K.D., Dickhoff, W.W., and Plisetskaya, E.M. 1998. Effects of growth and fatness on sexual development of chinook salmon (*Oncorhynchus tshawytscha*) parr. Can. J. Fish. Aquat. Sci. **55**: 2376–2382.

Taylor, E.B., and Larkin, P.A. 1986. Current response and agonistic behavior in newly emerged fry of chinook salmon, *Oncorhynchus tshawytscha*, from ocean- and stream-type populations. Can. J. Fish. Aquat. Sci. **43**: 565–573.

Thorpe, J.E. 1986. Age at first maturity in Atlantic salmon, *Salmo salar*: freshwater period and influences and conflicts with smolting. Can. Spec. Publ. Fish. Aquat. Sci. No. 89. pp. 7–14.

Thorpe, J.E. 1989. Developmental variation in salmonid populations. J. Fish Biol. **35**(Suppl. A): 295–303.

Thorpe, J.E. 1994. Reproductive strategies in Atlantic salmon, *Salmo salar* L. Aquat. Fish. Manag. **25**: 77–87.

Thorpe, J.E., Mangel, M., Metcalfe, N.B., and Huntingford, F.A. 1998. Modeling the proximate basis of salmonid life-history variation, with application to Atlantic salmon, *Salmo salar* L. Evol. Ecol. **12**: 581–599.

Unwin, M.J., Kinnison, M.T., and Quinn, T.P. 1999. Exceptions to semelparity: postmaturation survival, morphology, and energetics

© 2007 NRC Canada

of male chinook salmon (*Oncorhynchus tshawytscha*). Can. J. Fish. Aquat. Sci. **56**: 1172–1181.

U.S. Fish and Wildlife Service. 2000. Biological assessment of artificial propagation at Coleman National Fish Hatchery and Livingston Stone National Fish Hatchery: program description and incidental take of chinook salmon and steelhead trout. U.S. Fish and Wildlife Service, Red Bluff, Calif.

Yoshiyama, R.M., Fisher, F.W., and Moyle, P.B. 1998. Historical abundance and decline of chinook salmon in the Central Valley region of California. N. Am. J. Fish. Manage. **18**: 487–521.

Yoshiyama, R.M., Gerstung, E.R., Fisher, F.W., and Moyle, P.B. 2000. Fisheries management — chinook salmon in the California Central Valley: an assessment. Fisheries, **25**: 6–20.

Zar, J.H. 1984. Biostatistical analysis. Prentice-Hall, Englewood Cliffs, N.J.

Zaugg, W.S., and Wagner, H.H. 1973. Gill ATPase activity related to parr–smolt transformation in steelhead trout (*Salmo gairdneri*): influence of photoperiod and temperature. Comp. Biochem. Physiol. **45**: 955–965.

© 2007 NRC Canada

Biological identifications through DNA barcodes: the case of the Crustacea

Filipe O. Costa, Jeremy R. deWaard, James Boutillier, Sujeevan Ratnasingham, Robert T. Dooh, Mehrdad Hajibabaei, and Paul D.N. Hebert

Abstract: The ability of a 650 base pair section of the mitochondrial cytochrome *c* oxidase I (COI) gene to provide species-level identifications has been demonstrated for large taxonomic assemblages of animals such as insects, birds, and fishes, but not for the subphylum Crustacea, one of the most diverse groups of arthropods. In this study, we test the ability of COI to provide identifications in this group, examining two disparate levels in the taxonomic hierarchy — orders and species. The first phase of our study involved the development of a sequence profile for 23 dominant crustacean orders, based upon the analysis of 150 species, each belonging to a different family. The COI amino acid data placed these taxa into cohesive assemblages whose membership coincided with currently accepted boundaries at the order, superorder, and subclass levels. Species-level resolution was subsequently examined in an assemblage of Decapoda and in representatives of the genera *Daphnia* (Cladocera) and *Gammarus* (Amphipoda). These studies revealed that levels of nucleotide sequence divergence were from 19 to 48 times greater between congeneric species than between individuals of a species. We conclude that sequence variation in the COI barcode region will be very effective for discriminating species of Crustacea.

Résumé : Il a été démontré que l'utilisation d'une section de 650 paires de bases du gène mitochondrial de la cytochrome *c* oxydase I (COI) permet de faire des identifications au niveau spécifique de grands ensembles taxonomiques d'animaux tels que les insectes, les oiseaux et les poissons, mais pas encore dans le sous-phylum des crustacés, l'un des groupes les plus diversifiés d'arthropodes. Nous testons dans notre étude le potentiel de l'utilisation de COI pour faire des identifications dans ce groupe en examinant deux niveaux disparates de la hiérarchie taxonomique — les ordres et les espèces. La première phase de notre recherche consiste en l'établissement de profils de séquences pour 23 des ordres principaux de crustacés, d'après l'analyse de 150 espèces, appartenant chacune à une famille différente. Les données sur les acides aminés de COI permettent de placer ces taxons en ensembles cohésifs dont la composition coïncide avec les frontières couramment acceptées aux niveaux de l'ordre, du super-ordre et de la sous-classe. Nous avons ensuite étudié la détermination au niveau spécifique chez un ensemble de décapodes et chez des représentants des genres *Daphnia* (Cladocera) et *Gammarus* (Amphipoda). Ces études révèlent que les niveaux de divergence des séquences de nucléotides sont de 19 à 48 fois plus importants entre les espèces d'un même genre qu'entre les individus d'une même espèce. Nous concluons que la variation des séquences dans la région du code-barre de COI devrait permettre de séparer de façon très efficace les espèces de crustacés.

[Traduit par la Rédaction]

Introduction

The ideal DNA-based identification system would employ a single gene for the placement of any organism in the full taxonomic hierarchy from kingdom to species. The ability of a ~658 base pair (bp) section of the mitochondrial cytochrome *c* oxidase I (COI) gene to provide this resolution has now been demonstrated for many animal lineages, including lepidopterans (Hebert et al. 2003; Janzen et al. 2005; Hajibabaei et al. 2006), birds (Hebert et al. 2004), spiders (Barrett and Hebert 2005), ants (Smith et al. 2005), and fishes (Ward et al. 2005) (but see Dasmahapatra and Mallet 2006 for a discussion of success rates). Although COI appears to have high potential as the foundation for an identification system, it is critical to verify that it can deliver similar taxonomic resolution in other groups. The present study addresses this issue by examining the patterning of COI diversity in the subphylum Crustacea, the most ancient and structurally diverse group of arthropods. The diversity of modern crustaceans, in addition to their remarkable vari-

Received 20 January 2006. Accepted 26 October 2006. Published on the NRC Research Press Web site at http://cjfas.nrc.ca on 24 February 2007.
J19120

F.O. Costa.[1,2] Instituto do Mar (IMAR), Universidade Nova de Lisboa, 2829-516 Caparica, Portugal.
J.R. deWaard, S. Ratnasingham, R.T. Dooh, M. Hajibabaei, and P.D.N. Hebert. Biodiversity Institute of Ontario, University of Guelph, ON N1G 2W1, Canada.
J. Boutillier. Pacific Biological Station, Fisheries and Oceans Canada, 3190 Hammond Bay Road, Nanaimo, BC V9T 6N7, Canada.

[1]Corresponding author (e-mail: f.o.costa@bangor.ac.uk).
[2]Present address: School of Biological Sciences, University of Wales, Bangor, Bangor, Gwynedd, LL57 2UW, United Kingdom.

 doi:10.1139/F07-008 © 2007 NRC Canada

ety in morphologies, habitats, and ecologies, is reflected by their assignment to six classes, 48 orders, 849 different families, and about 52 000 species (Martin and Davis 2001). By comparison, the more than one million described species of insects are assigned to about 1000 families, but just 30 orders and a single class (Borror et al. 1989; Nielsen 1995).

While the higher level systematics (i.e., class, subclass) of the Crustacea are not fully stabilized (Martin and Davis 2001), ordinal boundaries have been nearly constant for more than 20 years despite ongoing morphological and molecular studies. As such, this taxonomic rank represents a useful criterion to judge the ability of a DNA-based identification system to deliver coarse taxonomic placement of an unknown taxon. However, as the primary task of taxonomy lies in identification of species, it is also critical to test the effectiveness of DNA barcodes at this level. The present study examines the effectiveness of a 658 bp section near the 5′ end of COI (hereafter referred to as the COI barcode) as an identification tool at these two disparate levels in the taxonomic hierarchy — orders and species. Its effectiveness at the ordinal level was tested in a two-step process: 150 species, each in a different family and including representatives from 23 of the 48 crustacean orders, were sequenced to establish a COI ordinal profile. The effectiveness of this profile in ordinal-level placements was subsequently evaluated by determining its success in the assignment of 100 new taxa to the proper order. The present study also sought to determine if the COI barcode region can enable species-level assignments within the Crustacea; this issue was examined in representatives of nine genera of Decapoda and in single genera of Cladocera and Amphipoda.

Materials and methods

Taxon sampling

COI ordinal profile

One hundred and fifty species, each belonging to a different family and including representatives from 23 of 48 crustacean orders, were sequenced to establish a COI ordinal profile (sequences for 75 of these families were acquired from GenBank, see below). More than 10 families were examined from each of four orders (Amphipoda, Calanoida, Decapoda, Isopoda), between four and nine families from eight other orders (Anostraca, Cladocera, Cumacea, Diplostraca, Harpacticoida, Podocopida, Sessilia, Stomatopoda), while one to two families were examined from the other 11 orders. Sequences were also obtained for 100 additional species (53 were acquired from GenBank, see below) in families included in the profile, but belonging to different genera to provide a group of test taxa (details on specimens are provided in Appendix A, Tables A1 and A2).

Decapod case study

Family- and species-level resolution was analyzed in a data set that comprised members of the order Decapoda. Most newly analyzed decapods were collected on research cruises led by Fisheries and Oceans Canada (DFO) off the Pacific coast of Canada in 2002 and 2004, but a few species were collected in Resolute Bay, Nunavut; in the Gulf of Gdansk, Poland; and off Lizard Island, Australia. These specimens were identified to the species level after collection and were subsequently preserved in 100% ethanol. In total, sequences were newly gathered for 146 specimens, representing 57 species, and these results were merged with 173 sequences from GenBank, representing 71 species (complete list of decapods in Appendix A, Tables A3 and A4).

Selected crustacean genera

To obtain detailed information on the patterning of COI diversity among closely related Crustacea, additional data were assembled on two genera to enable a comparison of congeneric versus conspecific divergences. This analysis was performed for 13 species in the cladoceran genus *Daphnia* (Adamowicz et al. 2004) and for 12 species in the amphipod genus *Gammarus* (F.O. Costa and P.D.N. Hebert, unpublished data). A complete list of species used in these analyses is provided in Appendix A, Tables A5 and A6.

GenBank data

With more than 5000 entries, COI is the most intensively studied crustacean gene, representing nearly 50% of the GenBank mitochondrial DNA data for this subphylum (GenBank search, 30 June 2005). Although these entries provide COI sequences for over 600 species, very few include a complete sequence for the gene. Because the partial sequences were acquired with varied primers, the opportunities for sequence comparisons are limited. From sequences available in GenBank (September 2004), 1585 providing coverage for the COI barcode region were extracted. Use of these data was further limited by the short lengths of some sequences. Only those with a minimum of 500 bp of the COI barcode were used, with a single exception to accommodate a small group of 498 bp sequences for the crab *Carcinus* (Roman and Palumbi 2004). The data from GenBank do provide valuable information for analyses that require a broad taxonomic coverage, such as an examination of shifts in guanine–cytosine (GC) usage among crustacean lineages. For this purpose, a total of 617 sequences were extracted and analyzed at various taxonomic levels.

DNA extraction, amplification, and sequencing

In the case of newly analyzed specimens for the ordinal study, DNA was extracted using the proteinase K protocol (Schwenk et al. 1998) or Isoquick (Orca Research Inc., Bothell, Washington). A 658 bp fragment from the 5′ end of COI was amplified using the primer pair LCO1490 (5′-GGTCAACAAATCATAAAGATATTGG-3′) and HCO2198 (5′-TAAACTTCAGGGTGACCAAAAAATCA-3′) (Folmer et al. 1994). Each polymerase chain reaction (PCR) had a total volume of 50 µL and contained 5 µL of 10× PCR buffer, 1.5 mmol·L^{-1} of $MgCl_2$, 50 µmol·L^{-1} of each dNTP, 1 unit (U) of *Taq* polymerase (1 U ≈ 16.67 nkat), 0.3 µmol·L^{-1} of each primer, and 2–4 µL of DNA template. The PCR thermal regime consisted of 60 s at 94 °C; five cycles of 30 s at 94 °C, 90 s at 45 °C, and 60 s at 72 °C; 35 cycles of 30 s at 94 °C, 90 s at 51 °C, and 60 s at 72 °C; followed by a final extension of 5 min at 72 °C. The PCR product was subsequently gel-purified with Qiaex II kit (Qiagen Inc., Valencia, California.) and sequenced in one direction on an ABI 377

© 2007 NRC Canada

automated sequencer (Applied Biosystems, Inc., Foster City, California).

A slightly different protocol was used in the decapod case study; DNA was isolated using either the GenElute kit (Sigma Inc., St. Louis, Missouri) or the Chelex dry release method (Hajibabaei et al. 2005). The COI barcode was amplified using HCO2198 as reverse primer combined with one of three forward primers: LCO1490, CrustF1 (5′-TTTTCTACAAATCATAAAGACATTGG-3′), or CrustF2 (5′-GGTTCTTCTCCACCAACCACAARGAYATHGG-3′). Each polymerase chain reaction had a total volume of 50 µL and contained 5 µL of 10× PCR buffer, 2.2 mmol·L^{-1} of $MgCl_2$, 50 µmol·L^{-1} of each dNTP, 1.5 U of *Taq* polymerase, 0.2 µmol·L^{-1} of each primer, and 1 µL of DNA template. The PCR thermal regime was identical to the one described above except for the CrustF2 primer, which was as follows: 1 cycle of 60 s at 94 °C; 35 cycles of 30 s at 94 °C, 90 s at 42 °C, and 60 s at 72 °C; followed by a final cycle of 5 min at 72 °C. The PCR product was subsequently gel-purified with UltraClean™15 DNA purification kit (MoBio Laboratories, Inc., Solana Beach, California) and sequenced in one or both directions using an ABI 377 or ABI 3730. For sequencing reactions we used BigDye® Terminator v3.1 cycle sequencing kit (Applied Biosystems, Inc., Foster City, California).

Data analysis

Sequence data, electropherograms, and primer details for each newly analyzed specimen are available in the completed project file entitled "Crustacean Barcodes" on the Barcode of Life Data Systems (BOLD) website (http://www.barcodinglife.org). COI sequences were edited using SeqApp 1.9 sequence editor (http://iubio.bio.indiana.edu/soft/molbio/seqapp/) and Sequencher (Gene codes Corporation, Ann Arbor, Michigan) and aligned using CLUSTAL W (Thompson et al. 1994) implemented in MEGA3 (Kumar et al. 2004). To accommodate GenBank data, all sequences were subsequently pruned to 658 bp.

Neighbor-joining (NJ) analysis, implemented in MEGA3 (Kumar et al. 2004), was employed for graphical representation of the patterns of COI divergences among crustacean species. The Kimura two-parameter (K2P) distance model was used to calculate nucleotide divergences (Kimura 1980), while Poisson correction (Nei and Kumar 2000) was used to compute amino acid divergences for the ordinal profile. Both the ordinal amino acid NJ tree and the Decapod nucleotide NJ tree were subjected to 10 000 bootstraps.

The first phase of the ordinal analysis involved the generation of an NJ tree for the 150 profile taxa. This profile was subsequently used as a classification engine by rerunning the NJ analysis following repeated addition of a single test taxon to the data set. After each analysis, the test species was assigned membership in the same taxonomic group as its nearest neighboring taxon. For example, a test taxon was identified as a member of the order Anostraca if it grouped most closely with any one of the seven anostracan families included in the profile. The success of the classification was quantified by determining the proportion of test taxa assigned to their proper order.

Levels of COI nucleotide divergences among conspecific and congeneric individuals were compared in *Daphnia*, *Gammarus*, and in those genera from the decapod data set that included at least three species and two specimens of each species. For this purpose, the "Distance Summary" implemented in BOLD (Ratnasingham and Hebert 2007) was used. This feature performs an automated computation of pairwise divergences at the species, genus, and family level for all possible specimen combinations in the data set. The average values obtained for conspecific and congeneric divergences were applied in the calculation of the taxonomic resolution ratio, which is defined as the quotient between congeneric divergences and conspecific divergences.

Results

Ordinal profile

The amino acid NJ tree for representatives of 150 crustacean families showed high cohesion of taxonomic groups. Most allied species formed assemblages that mirrored established higher-taxonomic categories — orders, superorders, or subclasses (Fig. 1; a detailed tree can be found in Supplemental Appendix S1).[1] For example, members of the orders Sessilia and Pedunculata formed a cohesive group as superorder Thoracica, while members of the subclasses Copepoda and Phyllopoda formed distinctive assemblages. Members of the orders Amphipoda, Anostraca, Isopoda, Mysida, and Stomatopoda were also joined in cohesive clusters. There were, however, a few deviations from this pattern; members of the order Decapoda split into two groups, with Stomatopoda embedded within. As well, two species in the orders Cumacea and Amphipoda (*Pseudocuma similis* and *Themisto gaudichaudii*, respectively) were genetically divergent from allied taxa, grouping instead with species from orders represented by a single family. A few other species, such as the parasitic isopods, (*Bopyroides hippolytes*, *Olenciru praegustator*, *Rocinela angustata*), occupied isolated positions in the tree.

The ordinal profile was subsequently used to classify 100 newly analyzed species. In 95 of these cases, the test taxon was assigned to the correct order. In three cases, the test taxa were assigned only at a rank above the order level, namely *Drepanopus* sp., *Eurycercus longirostris*, and *Mytilocypris ambiguosa*, which were assigned to subclasses Copepoda and Phyllopoda and class Ostracoda, respectively. Two misassignments involved taxa in the order Mysidacea, namely *Paramesopodopsis rufa* and *Tenagomysis australis*.

Decapod study

Members of most (13 of 17) decapod families represented by more than one species formed a cohesive cluster. However, species in the families Palaemonidae, Portunidae, and Oplophoridae were each split into two separate clusters, while Paguridae clustered with Lithodidae. The NJ tree for 127 species of Decapoda did, however, reveal the regular

[1] Supplementary data for this article are available on the journal Web site (http://cjfas.nrc.ca) or may be purchased from the Depository of Unpublished Data, Document Delivery, CISTI, National Research Council Canada, Building M-55, 1200 Montreal Road, Ottawa, ON K1A 0R6, Canada. DUD 5134. For more information on obtaining material refer to http://cisti-icist.nrc-cnrc.gc.ca/irm/unpub_e.shtml.

© 2007 NRC Canada

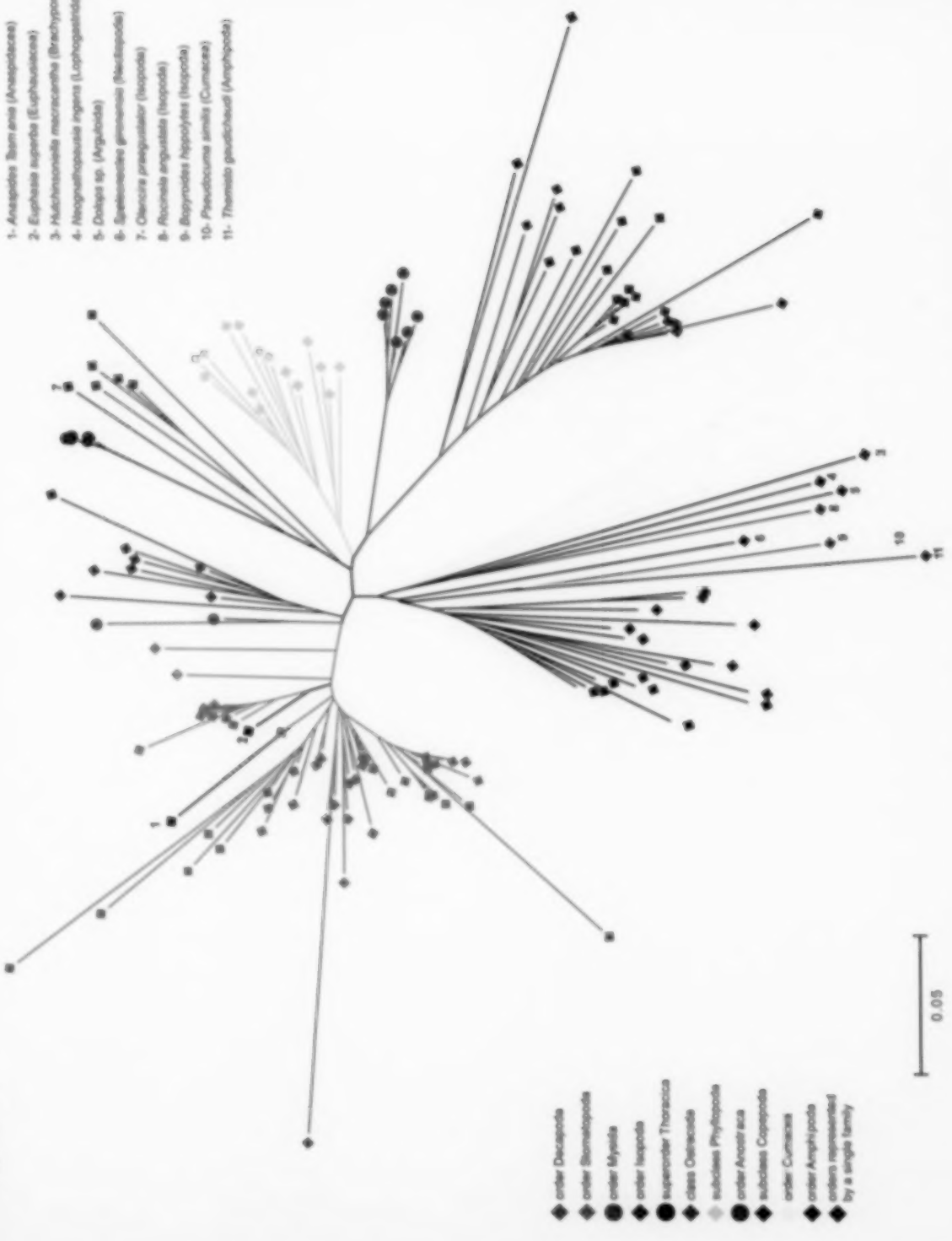

Fig. 1. Neighbor-joining radiation tree showing mitochondrial cytochrome *c* oxidase 1 (COI) barcode amino acid profile for 150 crustacean species, each belonging to a different family. Numbers 1–11 indicate species from orders represented here by a single family, as well as species divergent from allied taxa. The detailed tree is displayed in Supplemental Appendix S1.[3]

© 2007 NRC Canada

Fig. 2. Three illustrative branches of the neighbor-joining tree based on mitochondrial cytochrome *c* oxidase I (COI) barcode nucleotide distances (K2P) for 127 decapod species representing 30 families. Bootstrap values for 10 000 replicates are shown near the respective branches. The complete tree is displayed in Supplemental Appendix S2.[3]

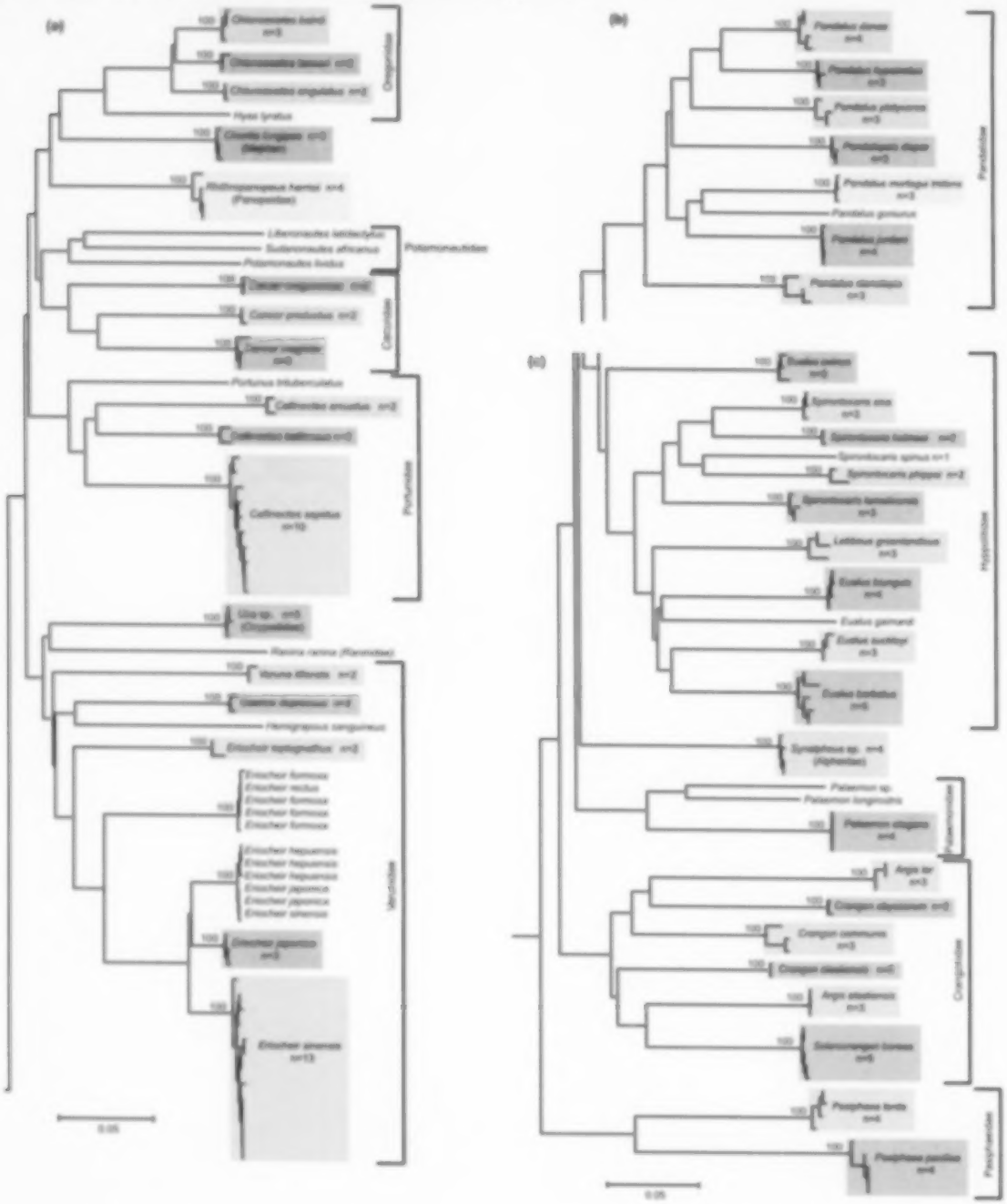
(a)
Oregoniidae
Hyas lyratus
Chionoecetes bairdi n=3
Chionoecetes tanneri n=2
Chionoecetes angulatus n=2
Chionoecetes opilio n=3
(Majidae)
Rhithropanopeus harrisii n=4
(Panopeidae)
Lithodidae
Lithodes maja n=3
(Lithodidae)
Paralithodes camtschaticus n=3
(Lithodidae)
Paralithodes platypus n=3
(Lithodidae)
Paralithodes brevipes n=3
(Lithodidae)
Lithodes couesi n=3
(Lithodidae)
Lithodes aequispinus n=3
(Lithodidae)
Lithodes confundens n=3
(Lithodidae)
Lithodes santolla n=3
(Lithodidae)
Lithodes turkayi n=3
(Lithodidae)
Lithodes longispina n=3
(Lithodidae)
Lithodes murrayi n=3
(Lithodidae)
Lithodes nintokuae n=3
(Lithodidae)
Lithodes wiracocha n=3
(Lithodidae)
Lithodes ferox n=3
(Lithodidae)
Lithodes manningi n=3
(Lithodidae)
Lithodes aotearoa n=3
(Lithodidae)
Lithodes n. sp. n=3
(Lithodidae)
Lithodes n. sp. n=3
(Lithodidae)
Lithodes n. sp.

Table 1. Pairwise mitochondrial cytochrome *c* oxidase I (COI) barcode nucleotide divergences for Decapoda and selected crustacean genera, using K2P distances (%).

Taxon[a]	Pairwise divergences	No. of comparisons	Min. distance	Mean distance[b]	Max. distance	TRR[c]	Reference
Order Decapoda	Within a species	144	0.00	0.46±0.05	2.57	37.6	This study
(54 species, 31 genera,	Within a genus	409	4.92	17.16±0.18	23.66		
138 sequences)	Within a family	459	11.27	19.75±0.17	49.93		
	Within a order	8441	15.30	27.65±0.05	49.00		
Genus *Cancer*	Within a species	5	0.16	0.50±0.15	0.97	34.6	This study
(3 species, 7 sequences)	Within a genus	16	14.97	17.24±0.45	20.01		
Genus *Chionoecetes*	Within a species	5	0.00	0.26±0.08	0.47	21.5	This study
(3 species, 7 sequences)	Within a genus	16	4.92	5.67±0.09	6.28		
Genus *Crangon*	Within a species	5	0.00	0.94±0.41	2.13	20.1	This study
(3 species, 7 sequences)	Within a genus	16	17.31	18.91±0.41	21.74		
Genus *Eualus*	Within a species	22	0.00	0.59±0.14	2.57	32.5	This study
(5 species, 16 sequences)	Within a genus	98	15.17	19.24±0.23	23.64		
Genus *Pandalus*	Within a species	24	0.00	0.48±0.11	1.86	34.4	This study
(6 species, 21 sequences)	Within a genus	186	9.85	16.49±0.18	20.82		
Genus *Spirontocaris*	Within a species	8	0.15	0.47±0.11	1.20	32.9	This study
(5 species, 11 sequences)	Within a genus	47	10.80	15.40±0.29	18.74		
GenBank Decapoda							
Genus *Callinectes*	Within a species	47	0.11	0.57±0.03	1.08	29.9	Pfeiler et al. 2005
(3 species, 14 sequences)	Within a genus	44	15.86	17.03±0.10	18.09		Darden et al., unpublished data[d]
Genus *Cherax*	Within a species	22	0.17	2.81±0.52	9.12	5.7	Munasinghe et al. 2003
(3 species, 14 sequences)	Within a genus	69	10.43	15.95±0.42	22.63		Miller et al. 2004
Genus *Raymunida*	Within a species	26	0.00	0.25±0.08	2.17	48.3	Macpherson and Machordom 2001
(4 species, 17 sequences)	Within a genus	110	7.6	12.08±0.21	16.41		
Other crustaceans							
Order Cladocera							
Genus *Daphnia*	Within a species	472	0.00	1.32±0.05	4.30	19.2	Adamowicz et al. 2004
(13 species, 80 sequences)	Within a genus	2688	13.18	25.28±0.05	30.65		
Order Amphipoda							
Genus *Gammarus*	Within a species	284	0	0.74±0.05	3.09	26.1	Costa and Hebert, unpublished data[e]
(12 species, 69 sequences)	Within a genus	2062	5.58	25.33±0.06	31.39		

[a]Number of species with more than one sequence and number of sequences analysed are shown in parentheses.
[b]Data reported as K2P distance (%) ± SE.
[c]Taxonomic resolution ratio (see Data analysis in Materials and methods).
[d]R.L. Darden, B.R. Kreiser, and A. Place, Biological Sciences, University of Southern Mississippi, 118 College Drive #5018, Hattiesburg, MS 39406, USA.
[e]F.O. Costa and P.D.N. Hebert, School of Biological Sciences, University of Wales, Bangor, Bangor, Gwynedd, LL57 2UW, United Kingdom.

(Chu et al. 2003), and its members show incomplete resolution in the NJ tree with *E. formosa* and *E. rectus* in one cluster and *E. hepuensis*, *E. sinensis*, and *E. japonica* in a second cluster.

COI divergences among members of a species versus congeners

For members of the order Decapoda, the average K2P distance within species averaged 0.46%, while congeneric divergences averaged 17.16%, but ranged from a low 4.92% in the crab genus *Chionoecetes* to a high of 31.39% in the amphipod genus *Gammarus* (Table 1). Within-species divergences were below 1% for 86% of the within-species comparisons in decapods. The equivalent value in *Gammarus* was only 75%, while in *Daphnia* it was 59%. Athough the *Daphnia* data set showed higher within-species distances, the congeneric distances were are also high, averaging 25.28%, so even in this genus there was a clear separation of conspecific and congeneric distances (Fig. 3). The distribution of K2P distances within different taxonomic categories (species, genus) for the Decapoda and as well for the genera *Pandalus*, *Daphnia*, and *Gammarus* is shown (Fig. 3).

Variation of GC content in crustacean COI genes

The availability of 25 complete mitochondrial sequences enabled examination of the relationship between GC content of the COI barcode region and that in the whole mitochondrial genome. This analysis revealed that the GC content of the barcode region was a very strong predictor ($r^2 = 0.81$, $p < 0.001$) of genomic shifts in nucleotide usage, motivating an examination of GC content in all crustaceans where 5′-COI information was available. The GC content of the

© 2007 NRC Canada

Fig. 3. Frequency distribution of conspecific (solid bars) and congeneric (shaded bars) mitochondrial cytochrome *c* oxidase I (COI) barcode distances (K2P) from pairwise comparisons among members of the order Decapoda and selected crustacean genera: (*a*) order Decapoda, (*b*) genus *Pandalus*, (*c*) genus *Daphnia*, and (*d*) genus *Gammarus*. Values below 0.1% are not displayed.

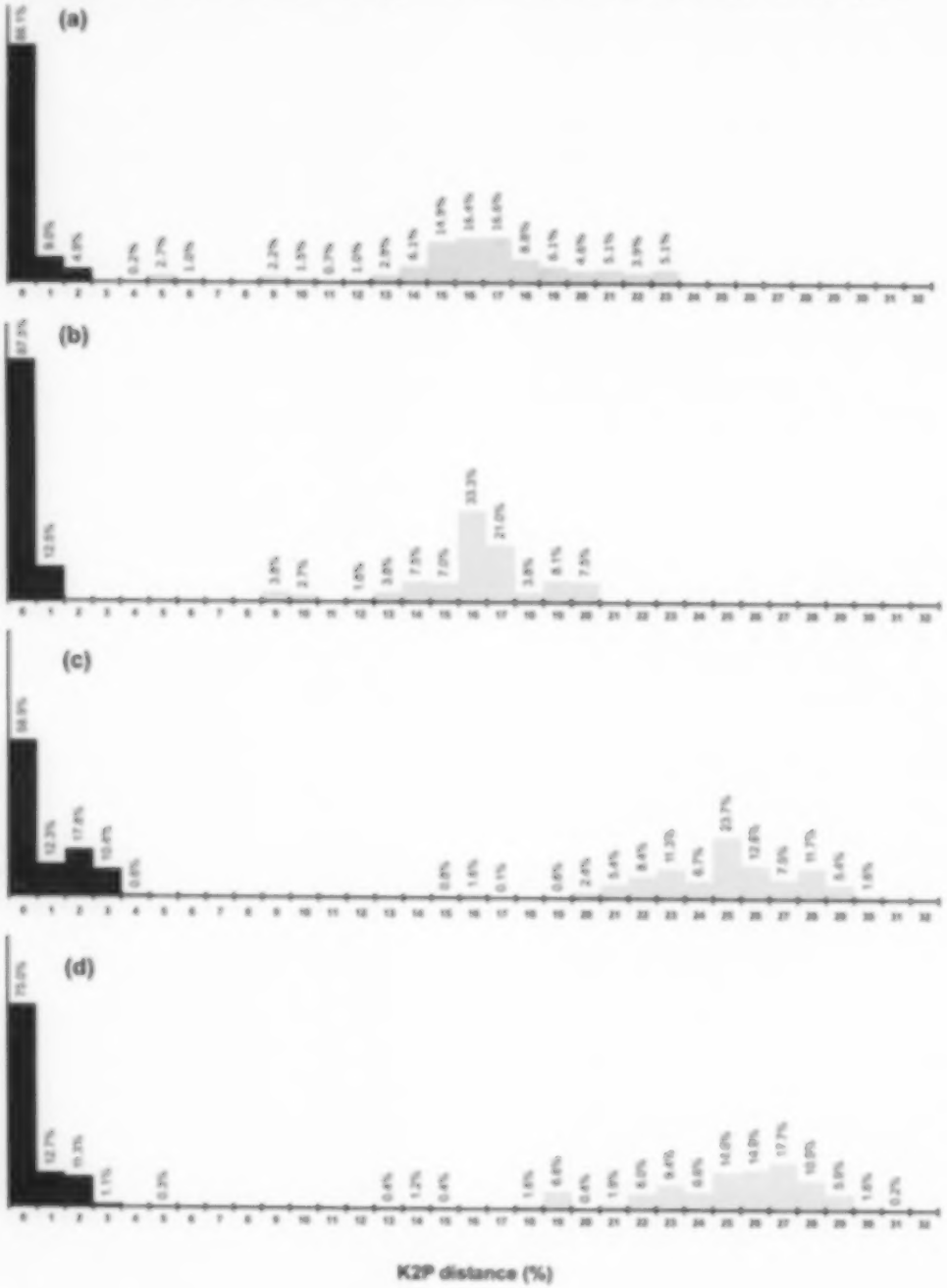

barcode region varied among the 617 species of crustaceans from 29.9% to 49.6% (Table 2). The highest GC content was observed in *Parartemia longicaudata* from saline lakes in Australia, while the lowest GC content was found in the amphipod *Hyperia galba*, a parasite of jellyfish. Members of the orders Amphipoda and Isopoda possessed the highest and lowest average GC content, respectively (41.2% vs. 38.7%). In all cases, the GC content decreased from the first

© 2007 NRC Canada

Table 2. Variation in GC content in the mitochondrial cytochrome *c* oxidase I (COI) barcode region among crustacean taxa.

				Codon position		
Taxon[a]	Min.	Mean	Max.	1st	2nd	3rd
Subphylum Crustacea (617)	29.86	38.98±0.14	49.62	49.35±0.14	43.05±0.06	24.21±0.33
Order Amphipoda (48)	35.02	40.39±0.53	49.39	47.54±0.42	43.61±0.17	29.82±1.34
Order Anostraca (35)	35.81	39.46±0.53	49.62	51.07±0.35	44.27±0.19	23.03±1.38
Subclass Copepoda (61)	33.50	38.69±0.38	44.73	48.34±0.28	42.02±0.12	25.71±0.97
Order Decapoda (138)	32.62	39.29±0.27	47.04	50.82±0.25	42.96±0.10	23.92±0.64
Order Isopoda (36)	33.17	38.93±0.54	45.69	47.95±0.55	44.00±0.33	24.83±1.23
Subclass Phyllopoda (55)	34.48	40.10±0.36	46.35	51.42±0.33	43.93±0.08	24.81±0.89

[a]Number of species analyzed are shown in parentheses.

to the third codon position, ranging from 48% to 52% in the former, but only from 23% to 31.6% in the latter. Variation in GC content was consistently higher in the third codon base, while the second base showed the least variation.

Discussion

This study establishes that the barcode region of COI has considerable potential as the foundation for a DNA barcoding identification system for crustaceans. A COI profile based on single representatives of 150 crustacean families proved 95% effective in placing newly encountered species to the right order. This high success makes it clear that a profile based on even a few thousand species will provide a highly effective tool for taxonomic assignments at this level. Further parameterization of the ordinal profile should begin by adding sequence records for each of the 849 crustacean families. Higher sampling intensity should be directed to families with accelerated rates of molecular evolution, and the present results provide some directions in this regard. Parasitic lineages often show rate acceleration (Hassanin 2006; J.R. deWaard and P.D.N. Hebert, unpublished data), and this pattern was apparent in the current study, as evidenced by the isolated positions of parasitic isopods in the NJ tree. As a result, particular sampling intensity should be directed to crustacean lineages with parasitic lifestyles to subdivide the misleading long branches and to create an effective system for placements deep in the taxonomic hierarchy.

The present study suggests that a COI-based system will regularly deliver species-level resolution for crustacean lineages. In fact, levels of sequence divergence among congeneric species of crustaceans averaged 17.16%, the highest value yet reported for any animal group. By comparison, congeneric species of lepidopterans show just 6.1% variation (Hebert et al. 2003), birds show 7.93% variation (Hebert et al. 2004), and fishes possess 9.93% divergence (Ward et al. 2005). Of course, the actual level of divergence among congeners is less critical than the ratio of the genetic divergence between species to that within species. Levels of intraspecific variation in crustaceans averaged 0.46%, values slightly higher than those reported in other groups (most range from 0.25% to 0.30%), but the interspecific to intraspecific ratios of sequence divergence were very large, ranging from 19.2 to 48.3. As a consequence, species recognition was straightforward in most cases (~95%). Based on these observations, we conclude that a COI barcoding system will deliver levels of species resolution comparable with those seen in tropical lepidopterans (98%, Hajibabaei et al. 2006), marine gastropods (96%, Meyer and Paulay 2005), fishes (100%, Ward et al. 2005), and birds (95%, Hebert et al. 2004).

We emphasize the need for a critical assessment of both barcode results and current taxonomic systems in cases of discordance. For example, the lack of barcode divergence between members of the mitten crab genus *Eriocheir* reflects a case where there is a growing consensus that some recognized species do not merit this status (discussed in detail in Chu et al. 2003 and Tang et al. 2003). In other cases, levels of barcode variation within species have surely been inflated by a failure of current taxonomic systems to recognize valid species. For example, the presence of two genetically divergent groups in the hermit crabs *Pagurus longicarpus* and *Pagurus pollicaris* is thought to reflect overlooked species (Young et al. 2002). Similarly, the freshwater shrimp *Paratya australiensis* includes several highly divergent mitochondrial lineages that are now thought to represent species that diversified in the Pliocene (Baker et al. 2004). Finally, both morphological and biogeographic data suggest the possibility of overlooked species within *Cherax tenuimanus* and *Cherax preissi* (Munasinghe et al. 2003).

No single approach can provide a definitive conclusion on species boundaries (but see Lee 2003). We emphasize that DNA barcoding is not a substitute for conventional taxonomic approaches. It seeks instead to flag cases of deep genetic divergence among individuals grouped as a single species that may indicate overlooked species. For example, we noted particularly high intraspecific divergences (3.1%) in *Gammarus oceanicus*, but individuals from the Baltic Sea, Iceland, and Hudson Bay showed an average within-species K2P divergence of only 0.43%. The extreme divergence values all reflected samples of this species from the St. Lawrence estuary, perhaps reflecting an overlooked species endemic to this region. In contrast with these cases, there are other cases where species recognized through past taxonomic work show little or no barcode divergence. Some of these cases may represent instances where current taxonomic systems inappropriately recognize variation as reflecting species status. However, other cases may reflect very young species. We emphasize that the recognition of taxo-

© 2007 NRC Canada

nomic boundaries in such cases is always demanding, often subjective, and best pursued through a weight of evidence approach that employs molecular, morphological, and ecological traits to reach a decision.

As the creation of a comprehensive COI barcode database for crustaceans will be a substantial undertaking, we stress that benefits will be diverse. COI can, for example, serve as a sentinel gene enabling the detection of lineages with unusual patterns of nucleotide usage or exceptional rates of evolution. The analysis of GC content in the present study demonstrates that the COI barcode region can be a predictor of the nucleotide usage of the entire mitochondrial genome. Similarly, the molecular rate acceleration of parasitic lineages revealed previously using other gene regions (Hassanin 2006; J.R. deWaard and P.D.N. Hebert, unpublished data) was evident in the current data set. As such, it will aid multigene systematics by allowing such studies to target taxa showing unusual attributes of nucleotide usage or evolutionary rates. The benefits of a barcode system will also extend into ecological work. For example, an estimated one-third of marine arthropods (thus mainly crustaceans) in 138 studies from the North Atlantic could not be identified to a species level (Schander and Willassen 2005). Schander and Willassen (2005) pointed out several relevant means by which improved ability to recognize marine species will benefit marine biological and ecological sciences in a number of ways (see also Böttger-Schnack et al. 2004). A particular gain could arise through species-level identification of larvae, enabling studies of larval dispersal and ecology, and benthic adult connectivity, all critical for management of crustacean fisheries (Tully et al. 2003). DNA barcoding will also allow the identification of crustacean prey items in stomach contents of fishes, birds, and other predators, aiding parameterization of food web models. For example, morphological approaches did not allow the species identification of several crustacean prey in the stomach contents of fulmars (*Fulmarus glacialis*) (Phillips et al. 1999). Other potential benefits of a COI barcode identification system for crustaceans include the identification of parasitic crustaceans at any developmental stage (e.g., Øines and Heuch 2005), as well as the detection of invasive crustacean species (Armstrong and Ball 2005). In summary, the present study reveals that a large-scale effort to assemble DNA barcode records for crustaceans will deliver a highly effective identification system with impacts on a broad range of research themes.

Acknowledgements

The "Fundação para a Ciência e a Tecnologia" (Portugal) provided a postdoctoral fellowship (BPD/11588/2002) to F.O. Costa. This work was supported by grants to PDNH from the Natural Sciences and Engineering Research Council of Canada (NSERC) and from the Gordon and Betty Moore Foundation. We thank Monika Normant for decapod samples from the Baltic Sea.

References

Adamowicz, S.J., Hebert, P.D.N., and Marinone, M.C. 2004. Species diversity and endemism in the *Daphnia* of Argentina: a genetic investigation. Zool. J. Linn. Soc. **140**: 171–205.

Armstrong, K.F., and Ball, S.L. 2005. DNA barcodes for biosecurity: invasive species identification. Philos. Trans. R. Soc. Lond. B Biol. Sci. **360**: 1813–1823.

Baker, A.M., Hurwood, D.A., Krogh, M., and Hughes, J.M. 2004. Mitochondrial DNA signatures of restricted gene flow within divergent lineages of an atyid shrimp (*Paratya australiensis*). Heredity, **93**: 196–207.

Barrett, R.D.H., and Hebert, P.D.N. 2005. Identifying spiders through DNA barcodes. Can. J. Zool. **83**: 481–491.

Borror, D.J., Triplehorn, C.A., and Johnson, N.F. 1989. An introduction to the study of insects. 6th ed. Saunders College Publishing, Philadelphia, Pa.

Böttger-Schnack, R., Lenz, J., and Weikert, H. 2004. Are taxonomic details of relevance to ecologists? An example from oncaeid microcopepods of the Red Sea. Mar. Biol. **144**: 1127–1140.

Chu, K.H., Ho, H.Y., Li, C.P., and Chan, T.Y. 2003. Molecular phylogenetics of the mitten crab species in *Eriocheir, sensu lato* (Brachyura: Grapsidae). J. Crustac. Biol. **23**: 738–746.

Dasmahapatra, K.K., and Mallet, J. 2006. DNA barcodes: recent successes and future prospects. Heredity, **97**: 254–255.

Folmer, O., Black, M., Hoeh, W., Lutz, R., and Vrijenhoek, R. 1994. DNA primers for amplification of mitochondrial cytochrome *c* oxidase subunit I from diverse metazoan invertebrates. Mol. Mar. Biol. Biotechnol. **3**: 294–297.

Hajibabaei, M., deWaard, J.R., Ivanova, N.V., Ratnasingham, S., Dooh, R.T., Kirk, S.L., Mackie, P.M., and Hebert, P.D.N. 2005. Critical factors for assembling a high volume of DNA barcodes. Philos. Trans. R. Soc. Lond. B Biol. Sci. **360**: 1959–1967.

Hajibabaei, M., Janzen, D.H., Burns, J.M., Hallwachs, W., and Hebert, P.D.N. 2006. DNA barcodes distinguish species of tropical Lepidoptera. Proc. Natl. Acad. Sci. U.S.A. **103**: 968–971.

Hassanin, A. 2006. Phylogeny of Arthropoda inferred from mitochondrial sequences: strategies for limiting the misleading effects of multiple changes in pattern and rates of substitution. Mol. Phylogenet. Evol. **38**: 100–116.

Hebert, P.D.N., Cywinska, A., Ball, S.L., and deWaard, J.R. 2003. Biological identifications through DNA barcodes. Proc. R. Soc. Lond. B Biol. Sci. **270**: 313–322.

Hebert, P.D.N., Stoeckle, M.Y., Zemlak, T.S., and Francis, C.M. 2004. Identification of birds through DNA barcodes. PLoS Biol. **2**: 1657–1663.

Janzen, D.H., Hajibabaei, M., Burns, J.M., Hallwachs, W., Remigio, E., and Hebert, P.D.N. 2005. Wedding biodiversity inventory of a large complex Lepidoptera fauna with DNA barcoding. Philos. Trans. R. Soc. Lond. B Biol. Sci. **360**: 1835–1845.

Kimura, M. 1980. A simple method of estimating evolutionary rate of base substitutions through comparative studies of nucleotide sequences. J. Mol. Evol. **16**: 111–120.

Kumar, S., Tamura, K., and Nei, M. 2004. MEGA3: integrated software for molecular evolutionary genetics analysis and sequence alignment. Brief. Bioinform. **5**: 150–163.

Lee, M.S.Y. 2003. Species concepts and species reality: salvaging a Linnaean rank. J. Evol. Biol. **16**: 179–188.

Macpherson, E., and Machordom, A. 2001. Phylogenetic relationships of species of *Raymunida* (Decapoda: Galatheidae) based on morphology and mitochondrial cytochrome oxidase sequences, with the recognition of four new species. J. Crustac. Biol. **21**: 696–714.

Martin, J.W., and Davis, G.E. 2001. An updated classification of the recent Crustacea. Natural History Museum, Los Angeles, Calif. Contrib. Sci. Ser. 39.

Meyer, C.P., and Paulay, G. 2005. DNA barcoding: error rates based on comprehensive sampling. PLoS Biol. **3**: 2229–2238.

© 2007 NRC Canada

Miller, A.D., Nguyen, T.T., Burridge, C.P., and Austin, C.M. 2004. Complete mitochondrial DNA sequence of the Australian freshwater crayfish, *Cherax destructor* (Crustacea: Decapoda: Parastacidae): a novel gene order revealed. Gene, **331**: 65–72.

Munasinghe, D.H.N., Murphy, N.P., and Austin, C.M. 2003. Utility of mitochondrial DNA sequences from four gene regions for systematic studies of Australian freshwater crayfish of the genus *Cherax* (Decapoda: Parastacidae). J. Crustac. Biol. **23**: 402–417.

Nei, M., and Kumar, S. 2000. Molecular evolution and phylogenetics. Oxford University Press, New York.

Nielsen, C. 1995. Animal evolution: interrelationships of the living phyla. Oxford University Press, Oxford, UK.

Øines, Ø., and Heuch, P.A. 2005. Identification of sea louse species of the genus *Caligus* using mtDNA. J. Mar. Biol. Assoc. U.K. **85**: 73–79.

Pfeiler, E., Hurtado, L.A., Knowles, L.L., Torre-Cosío, J., Bourillón-Moreno, L., Márquez-Farías, J.F., and Montemayor-López, G. 2005. Population genetics of the swimming crab *Callinectes bellicosus* (Brachyura: Portunidae) from the eastern Pacific Ocean. Mar. Biol. **146**: 559–569.

Phillips, R.A., Petersen, M.K., Lilliendahl, K., Solmundsson, J., Hamer, K.C., Camphuysen, C.J., and Zonfrillo, B. 1999. Diet of the northern fulmar *Fulmarus glacialis*: reliance on commercial fisheries? Mar. Biol. **135**: 159–170.

Ratnasingham, S., and Hebert, P.D.N. 2007. BOLD: The Barcode of Life Data System (www.barcodinglife.org). Mol. Ecol. Notes, doi:10.1111/j.1471-8286.2006.01678.x.

Roman, J., and Palumbi, S.R. 2004. A global invader at home: population structure of the green crab, *Carcinus maenas*, in Europe. Mol. Ecol. **13**: 2891–2898.

Schander, C., and Willassen, E. 2005. What can biological barcoding do for marine biology? Mar. Biol. Res. **1**: 79–83.

Schwenk, K., Sand, A., Boersma, M., Brehm, M., Mader, E., Offerhaus, D., and Spaak, P. 1998. Genetic markers, genealogies and biogeographic patterns in the Cladocera. Aquat. Ecol. **32**: 37–51.

Smith, M.A., Fisher, B., and Hebert, P.D.N. 2005. DNA barcoding for effective biodiversity assessment of a hyperdiverse arthropod group: the ants of Madagascar. Philos. Trans. R. Soc. Lond. B Biol. Sci. **360**: 1825–1834.

Tang, B., Zhou, K., Song, D., Yang, G., and Dai, A. 2003. Molecular systematics of the Asian mitten crabs, genus *Eriocheir* (Crustacea: Brachyura). Mol. Phylogenet. Evol. **29**: 309–316.

Thompson, J.D., Higgins, D.G., and Gibson, T.J. 1994. CLUSTAL W: improving the sensitivity of progressive multiple sequence alignment through sequence weighting, position-specific gap penalties and weight matrix choice. Nucleic Acids Res. **22**: 4673–4680.

Tully, O., Freire, J., and Addison, J. 2003. Crustacean fisheries. Fish. Res. **65**: 1–2.

Ward, R.D., Zemlak, T.S., Innes, B.H., Last, P.R., and Hebert, P.D.N. 2005. DNA barcoding Australia's fish species. Philos. Trans. R. Soc. Lond. B Biol. Sci. **360**: 1847–1957.

Young, A.M., Torres, C., Mack, J.E., and Cunningham, C.W. 2002. Morphological and genetic evidence for vicariance and refugium in Atlantic and Gulf of Mexico populations of the hermit crab *Pagurus longicarpus*. Mar. Biol. **140**: 1059–1066.

Appendix A

Table A1. List of specimens used in the profile of 150 crustacea families, sorted by family name.

GenBank accession No.	Class	Order	Family	Species	Length
AY145426	Maxillopoda	Calanoida	Acartiidae	*Acartia omorii*	624
EF432739	Malacostraca	Isopoda	Aegidae	*Rocinela angustata*	654
AF436034	Malacostraca	Decapoda	Aeglidae	*Aegla uruguayana*	657
AF531742	Maxillopoda	Calanoida	Aetideidae	*Gaetanus tenuispinus*	627
AF436036	Malacostraca	Decapoda	Albuneidae	*Blepharipoda occidentalis*	657
DQ889084	Malacostraca	Amphipoda	Ampeliscidae	*Byblis gaimardi*	623
DQ889076	Malacostraca	Anaspidacea	Anaspididae	*Anaspides tasmaniae*	657
DQ889126	Malacostraca	Amphipoda	Anisogammaridae	*Ramellogammarus* sp.	654
DQ889078	Malacostraca	Isopoda	Arcturidae	*Arcturus baffini*	644
DQ889096	Maxillopoda	Arguloida	Argulidae	*Dolops* sp.	624
DQ889079	Malacostraca	Isopoda	Armadillidiidae	*Armadillidium* sp.	657
NC_001620	Branchiopoda	Anostraca	Artemiidae	*Artemia franciscana*	624
DQ889085	Malacostraca	Isopoda	Asellidae	*Caecidotea* sp.	652
DQ889120	Malacostraca	Decapoda	Atyidae	*Paratya australiensis*	657
AF242660	Maxillopoda	Sessilia	Balanidae	*Semibalanus balanoides*	642
DQ889092	Malacostraca	Cumacea	Bodotriidae	*Cyclaspis caprella*	633
DQ889082	Malacostraca	Isopoda	Bopyridae	*Bopyroides hippolytes*	629
DQ889083	Branchiopoda	Cladocera	Bosminidae	*Bosmina* sp.	639
AF209064	Branchiopoda	Anostraca	Branchinectidae	*Branchinecta paludosa*	639
AF209059	Branchiopoda	Anostraca	Branchipodidae	*Parartemia contracta*	639
AF044057	Malacostraca	Decapoda	Bresiliidae	*Rimicaris exoculata*	605
DQ889086	Branchiopoda	Diplostraca	Caenestheriidae	*Carnestheriella setosa*	639
DQ889087	Maxillopoda	Calanoida	Calanidae	*Calanus glacialis*	624
AF436025	Malacostraca	Decapoda	Callianassidae	*Callichirus major*	649
DQ882037	Malacostraca	Decapoda	Calocarididae	*Calocaris investigatoris*	658

© 2007 NRC Canada

Table A1 (*continued*).

GenBank accession No.	Class	Order	Family	Species	Length
DQ889125	Malacostraca	Decapoda	Cambaridae	*Procambarus clarkii*	654
DQ882040	Malacostraca	Decapoda	Cancridae	*Cancer magister*	655
AY145434	Maxillopoda	Calanoida	Candaciidae	*Candacia ethiopica*	624
AF315015	Maxillopoda	Harpacticoida	Canuellidae	*Coullana* sp.	657
DQ889075	Malacostraca	Amphipoda	Caprellidae	*Aeginina longicornis*	644
AY428048	Maxillopoda	Sessilia	Catophragmidae	*Catomerus polymerus*	643
DQ356555	Maxillopoda	Calanoida	Centropagidae	*Boeckella gracilis*	636
DQ889088	Branchiopoda	Diplostraca	Cercopagididae	*Cercopagis pengoi*	639
AF209062	Branchiopoda	Anostraca	Chirocephalidae	*Artemiopsis stefanssoni*	639
DQ889089	Maxillopoda	Sessilia	Chthamalidae	*Chamaesipho* sp.	657
DQ889090	Branchiopoda	Cladocera	Chydoridae	*Chydorus* sp.	639
AF513651	Maxillopoda	Calanoida	Clausocalanidae	*Pseudocalanus mimus*	639
AF315009	Maxillopoda	Harpacticoida	Cletodidae	*Cletocamptus deitersi*	657
AY327387	Maxillopoda	Harpacticoida	Cletopsyllidae	*Bathycletopsyllus* sp.	603
AF205247	Malacostraca	Stomatopoda	Coronididae	*Parvisquilla multituberculata*	648
AY174366	Maxillopoda	Sessilia	Coronulidae	*Chelonibia testudinaria*	586
DQ889128	Malacostraca	Decapoda	Crangonidae	*Sclerocrangon boreas*	657
DQ889090	Malacostraca	Amphipoda	Crangonyctidae	*Crangonyx* sp.	637
DQ889093	Branchiopoda	Diplostraca	Cyclestheriidae	*Cyclestheria hislopi*	639
AF255791	Malacostraca	Isopoda	Cymothoidae	*Olencira praegustator*	583
DQ889094	Ostracoda	Podocopida	Cypridiidae	*Cypridopsis vidua*	624
NC_000844	Branchiopoda	Diplostraca	Daphniidae	*Daphnia pulex*	624
AJ534411	Ostracoda	Podocopida	Darwinulidae	*Vestalenula molopoensis*	534
DQ889095	Maxillopoda	Calanoida	Diaptomidae	*Diaptomus* sp.	608
AF520442	Malacostraca	Cumacea	Diastylidae	*Diastylopsis thilenuisi*	657
DQ882097	Malacostraca	Decapoda	Diogenidae	*Paguristes turgidus*	658
DQ889097	Malacostraca	Decapoda	Dromiidae	—	644
DQ889118	Malacostraca	Amphipoda	Epimeriidae	*Paramphithoe hystrix*	644
AB091772	Maxillopoda	Calanoida	Eucalanidae	*Eucalanus bungii*	900
AF531749	Maxillopoda	Calanoida	Euchaetidae	*Paraeuchaeta biloba*	618
DQ889098	Malacostraca	Euphausiacea	Euphausiidae	*Euphausia superba*	633
DQ889127	Malacostraca	Amphipoda	Eusiridae	*Rhachotropis aculeata*	641
DQ882090	Malacostraca	Decapoda	Galatheidae	*Munida quadrispina*	658
DQ889100	Malacostraca	Amphipoda	Gammaridae	*Gammarus lacustris*	654
DQ889101	Malacostraca	Decapoda	Gnathophyllidae	*Gnathophyllum americanus*	657
AF048822	Malacostraca	Stomatopoda	Gonodactylidae	*Gonodactylus graphurus*	645
AF317338	Malacostraca	Decapoda	Grapsidae	*Grapsus albolineratus*	573
AF520447	Malacostraca	Cumacea	Gymodiastylidae	*Gymodiastylis* sp.	657
L43049	Maxillopoda	Harpacticoida	Harpactidae	*Tigriopus californicus*	606
AF205252	Malacostraca	Stomatopoda	Hemisquillidae	*Hemisquilla ensigera*	645
AF531745	Maxillopoda	Calanoida	Heterorhabdidae	*Heterorhabdus farrani*	642
AF048823	Malacostraca	Stomatopoda	Heterosquillidae	*Heterosquilla tricarinata*	655
DQ882084	Malacostraca	Decapoda	Hippolytidae	*Lebbeus groenlandicus*	505
DQ889102	Branchiopoda	Cladocera	Holopedidae	*Holopedium gibberum*	639
AF370852	Cephalocarida	Brachypoda	Hutchinsoniellidae	*Hutchinsoniella macracantha*	634
AY152752	Malacostraca	Amphipoda	Hyalellidae	*Hyalella* sp.	637
AY639937	Malacostraca	Amphipoda	Hyalidae	*Parhyale hawaiiensis*	900
DQ889133	Malacostraca	Amphipoda	Hyperiidae	*Themisto gaudichaudii*	657
DQ889111	Malacostraca	Isopoda	Idoteidae	*Mesidotea entomon*	657
AF451354	Malacostraca	Amphipoda	Iphimediidae	*Gnathiphimedia sexdentata*	624
DQ889106	Malacostraca	Amphipoda	Ischyroceridae	*Ischyrocerus latipes*	643
AF352297	Malacostraca	Cumacea	Lampropidae	*Lampropis quadriplicata*	626
AF436030	Malacostraca	Decapoda	Laomediidae	*Jaxea nocturna*	593
DQ889131	Malacostraca	Mysidacea	Lepidomysidae	*Tasmanomysis oculata*	633
DQ889107	Branchiopoda	Cladocera	Leptodoridae	*Leptodora kindtii*	638
AF137516	Malacostraca	Cumacea	Leuconidae	*Eudorella pusilla*	657
DQ889130	Maxillopoda	Cyclopoida	Lichomolgidae	*Stellicola* sp.	654

© 2007 NRC Canada

Table A1 (*continued*).

GenBank accession No.	Class	Order	Family	Species	Length
AF255780	Malacostraca	Isopoda	Ligiidae	*Ligia occidentalis*	583
AJ534412	Ostracoda	Podocopida	Limnocytheridae	*Limnocythere inopinata*	533
DQ882086	Malacostraca	Decapoda	Lithodidae	*Lithodes couesi*	639
DQ889115	Malacostraca	Lophogastrida	Lophogastridae	*Neognathophausia ingens*	630
DQ889108	Malacostraca	Decapoda	Luciferidae	*Lucifer* sp.	656
DQ889109	Branchiopoda	Diplostraca	Lynceidae	*Lynceus* sp.	639
DQ889077	Malacostraca	Amphipoda	Lysianassidae	*Anonyx nugax*	643
DQ889117	Branchiopoda	Cladocera	Macrothricidae	*Ophryoxus gracilis*	639
DQ889114	Malacostraca	Decapoda	Majidae	*Naxia* sp.	657
AF474106	Maxillopoda	Calanoida	Metridinidae	*Metridia lucens*	648
DQ889112	Branchiopoda	Cladocera	Moinidae	*Moina* sp.	639
DQ889119	Malacostraca	Mysidacea	Mysidae	*Paramysis intermedia*	618
AF520450	Malacostraca	Cumacea	Nannastacidae	*Campylaspis* sp.	657
AF125435	Malacostraca	Decapoda	Nematocarcinidae	*Nematocarcinus ensifer*	600
DQ889104	Malacostraca	Decapoda	Nephropidae	*Homarus americanus*	654
DQ889116	Ostracoda	Podocopida	Notodromadidae	*Notodromas monacha*	523
AF205234	Malacostraca	Stomatopoda	Odontodactylidae	*Odontodactylus scyllarus*	644
EF432738	Malacostraca	Amphipoda	Oedicerotidae	*Monoculodes borealis*	644
DQ882168	Malacostraca	Decapoda	Oplophoridae	*Systellaspis braueri*	654
DQ882047	Malacostraca	Decapoda	Oregoniidae	*Chionoecetes bairdi*	658
NC_003058	Malacostraca	Decapoda	Paguridae	*Pagurus longicarpus*	657
DQ889110	Malacostraca	Decapoda	Palaemonidae	*Macrobrachium* sp.	656
NC_004251	Malacostraca	Decapoda	Palinuridae	*Panulirus japonicus*	657
DQ882111	Malacostraca	Decapoda	Pandalidae	*Pandalus danae*	658
DQ882143	Malacostraca	Decapoda	Panopeidae	*Rhithropanopeus harrisii*	658
AF474110	Maxillopoda	Calanoida	Paracalanidae	*Paracalanus parvus*	648
AF493624	Malacostraca	Decapoda	Parastacidae	*Cherax crassimanus*	600
DQ882133	Malacostraca	Decapoda	Pasiphaeidae	*Pasiphaea pacifica*	658
AF217843	Malacostraca	Decapoda	Penaeidae	*Penaeus monodon*	657
AF255775	Malacostraca	Isopoda	Phreatoicidae	*Colubotelson thomsoni*	583
AF317341	Malacostraca	Decapoda	Plagusiidae	*Plagusia immaculata*	573
DQ889099	Branchiopoda	Cladocera	Podonidae	*Evadne spinifera*	639
AF209063	Branchiopoda	Anostraca	Polyartemiidae	*Polyartemiella hazeni*	639
DQ889121	Branchiopoda	Cladocera	Polyphemidae	*Polyphemus pediculus*	639
AY145429	Maxillopoda	Calanoida	Pontellidae	*Calanopia thompsoni*	624
AY189478	Malacostraca	Amphipoda	Pontogammaridae	*Obesogammarus crassus*	654
DQ889122	Malacostraca	Amphipoda	Pontoporeiidae	*Pontoporeia femorata*	653
DQ889123	Malacostraca	Isopoda	Porcellionidae	*Porcellio spinicornis*	654
DQ889124	Malacostraca	Decapoda	Portunidae	*Portunus pelagicus*	657
AF399980	Malacostraca	Decapoda	Potamidae	*Potamon fluviatilis*	539
AF205253	Malacostraca	Stomatopoda	Protosquillidae	*Chorisquilla excavata*	644
AF137514	Malacostraca	Cumacea	Pseudocumatidae	*Pseudocuma similis*	657
AY145436	Maxillopoda	Calanoida	Pseudodiaptomidae	*Pseudodiaptomus marinus*	624
AF205245	Malacostraca	Stomatopoda	Pseudosquillidae	*Pseudosquilla ciliata*	646
AF346400	Malacostraca	Decapoda	Raninidae	*Ranina ranina*	632
AY456188	Maxillopoda	Pedunculata	Scalpellidae	*Pollicipes polymerus*	658
DQ889105	Malacostraca	Decapoda	Scyllaridae	*Ibacus peronii*	654
DQ882149	Malacostraca	Decapoda	Sergestidae	*Sergestes similis*	658
DQ889129	Branchiopoda	Diplostraca	Sididae	*Sida crystallina*	639
AF370851	Remipedia	Nectiopoda	Speleonectidae	*Speleonectes gironesis*	613
AF255785	Malacostraca	Isopoda	Sphaeromatidae	*Sphaeroma quadridentatum*	544
AF531751	Maxillopoda	Calanoida	Spinocalanidae	*Spinocalanus abyssalis*	507
NC_006081	Malacostraca	Stomatopoda	Squillidae	*Squilla mantis*	658
AF125441	Malacostraca	Decapoda	Stenopodidae	*Stenopus hispidus*	600
AF531752	Maxillopoda	Calanoida	Stephidae	*Stephos longipes*	621
AF209065	Branchiopoda	Anostraca	Streptocephalidae	*Streptocephalus dorothae*	639
DQ889103	Malacostraca	Decapoda	Sundathelphusidae	*Holthuisana transversa*	653

© 2007 NRC Canada

Table A1 (*concluded*).

GenBank accession No.	Class	Order	Family	Species	Length
AF205257	Malacostraca	Stomatopoda	Takuidae	*Taku spinosocarinatus*	647
AY152751	Malacostraca	Amphipoda	Talitridae	*Orchestia uhleri*	637
DQ889132	Maxillopoda	Calanoida	Temoridae	*Temora stylifera*	636
AB126701	Maxillopoda	Sessilia	Tetraclitidae	*Tetraclita japonica*	658
AF209066	Branchiopoda	Anostraca	Thamnocephalidae	*Thamnocephalus platyurus*	639
AF474112	Maxillopoda	Calanoida	Tortanidae	*Tortanus derjugini*	617
DQ889134	Malacostraca	Decapoda	Trapeziidae	*Trapezia rufopunctata*	644
DQ889135	Branchiopoda	Notostraca	Triopsidae	*Triops australiensis*	639
DQ882062	Malacostraca	Decapoda	Varunidae	*Eriocheir sinensis*	623
DQ889081	Malacostraca	Decapoda	Xanthidae	*Atergatis floridus*	656
DQ889113	Ostracoda	Myodocopida	—	—	655

Table A2. List of 100 specimens used as test taxa in the amino acid profile of the crustacea.

GenBank accession No.	Class	Order	Family	Species	Length
DQ889136	Branchiopoda	Cladocera	Macrothricidae	*Acantholeberis curvirostris*	639
DQ889137	Branchiopoda	Cladocera	Chydoridae	*Acroperus harpae*	639
DQ889138	Branchiopoda	Cladocera	Chydoridae	*Alona setulosa*	639
DQ889139	Branchiopoda	Cladocera	Chydoridae	*Alonella exigua*	639
DQ882032	Malacostraca	Decapoda	Crangonidae	*Argis lar*	658
AY456187	Maxillopoda	Arguloida	Argulidae	*Argulus americanus*	658
AY531772	Malacostraca	Isopoda	Asellidae	*Asellus aquaticus*	651
AF308940	Branchiopoda	Anostraca	Thamnocephalidae	*Branchinella pinnata*	639
DQ889140	Branchiopoda	Diplostraca	Cercopagididae	*Bythotrephes* sp.	639
AF332791	Maxillopoda	Calanoida	Calanidae	*Calanoides acutus*	639
AY428047	Maxillopoda	Pedunculata	Scalpellidae	*Calantica spinosa*	677
DQ889141	Malacostraca	Amphipoda	Caprellidae	*Caprella unica*	641
AY616445	Malacostraca	Decapoda	Portunidae	*Carcinus aestuarii*	498
DQ889142	Maxillopoda	Calanoida	Centropagidae	*Centropages furcatus*	636
AY188999	Branchiopoda	Anostraca	Chirocephalidae	*Chirocephalus ruffoi*	654
DQ882053	Malacostraca	Decapoda	Majidae	*Chorilia longipes*	655
AF234819	Maxillopoda	Sessilia	Chthamalidae	*Chthamalus anisopoma*	656
AF462313	Maxillopoda	Calanoida	Clausocalanidae	*Clausocalanus minor*	648
AF520446	Malacostraca	Cumacea	Diastylidae	*Colurostylis longicaudata*	658
DQ882057	Malacostraca	Decapoda	Crangonidae	*Crangon alaskensis*	658
AF255776	Malacostraca	Isopoda	Phreatoicidae	*Crenoicus buntiae*	580
AF332789	Maxillopoda	Calanoida	Calanidae	*Ctenocalanus citer*	639
AF520449	Malacostraca	Cumacea	Nannastacidae	*Cumella* sp.	658
DQ889143	Branchiopoda	Diplostraca	Sididae	*Diaphanosoma* sp.	639
AF137510	Malacostraca	Cumacea	Diastylidae	*Diastylis sculpta*	658
DQ889144	Malacostraca	Amphipoda	Pontoporeiidae	*Diporeia hoyi*	649
DQ889145	Maxillopoda	Calanoida	Clausocalanidae	*Drepanopus* sp.	621
DQ889146	Branchiopoda	Cladocera	Macrothricidae	*Drepanothrix dentata*	639
AF451352	Malacostraca	Amphipoda	Iphimediidae	*Echiniphimedia echinata*	624
DQ889147	Malacostraca	Amphipoda	Gammaridae	*Echinogammarus ischnus*	640
AF493633	Malacostraca	Decapoda	Parastacidae	*Engaeus strictifrons*	600
AF520445	Malacostraca	Cumacea	Bodotriidae	*Eocuma longicorne*	657
AF451342	Malacostraca	Amphipoda	Epimeriidae	*Epimeria rezoevi*	644
DQ889148	Malacostraca	Amphipoda	Ischyroceridae	*Ericthonius* sp.	644
DQ882073	Malacostraca	Decapoda	Hippolytidae	*Eualus biunguis*	624
AF209061	Branchiopoda	Anostraca	Chirocephalidae	*Eubranchipus* sp.	639
AF234820	Maxillopoda	Sessilia	Chthamalidae	*Euraphia eastropacensis*	598
DQ889149	Branchiopoda	Cladocera	Chydoridae	*Eurycercus longirostris*	639
AY145427	Maxillopoda	Calanoida	Temoridae	*Eurytemora pacifica*	624

© 2007 NRC Canada

Table A2 (*continued*).

GenBank accession No.	Class	Order	Family	Species	Length
DQ889150	Malacostraca	Amphipoda	Eusiridae	*Eusirus cuspidatus*	644
DQ889151	Malacostraca	Isopoda	Sphaeromatidae	*Exosphaeroma* sp.	654
AF395115	Malacostraca	Decapoda	Penaeidae	*Fenneropenaeus* sp.	657
AF255781	Malacostraca	Isopoda	Idoteidae	*Glyptidotea lichtensteini*	574
AF205231	Malacostraca	Stomatopoda	Gonodactylidae	*Gonodactylellus hendersoni*	648
AF205224	Malacostraca	Stomatopoda	Gonodactylidae	*Gonodactylinus viridis*	627
AF205242	Malacostraca	Stomatopoda	Gonodactylidae	*Gonodactylopsis komodoensis*	645
DQ889152	Branchiopoda	Cladocera	Chydoridae	*Graptoleberis testudinaria*	639
AF205239	Malacostraca	Stomatopoda	Protosquillidae	*Haptosquilla glyptocercus*	646
AF317340	Malacostraca	Decapoda	Varunidae	*Hemigrapsus sanguineus*	573
AF061781	Malacostraca	Cumacea	Lampropidae	*Hemilamprops californicus*	658
DQ882079	Malacostraca	Decapoda	Oregoniidae	*Hyas lyratus*	658
DQ889153	Malacostraca	Amphipoda	Hyperiidae	*Hyperia galba*	643
DQ889154	Malacostraca	Amphipoda	Lysianassidae	*Ichnopus spinicornis*	626
DQ889155	Malacostraca	Isopoda	Idoteidae	*Idotea granulosa*	636
AF451347	Malacostraca	Amphipoda	Iphimediidae	*Iphimediella rigida*	618
AF339473	Malacostraca	Decapoda	Palinuridae	*Jasus edwardsii*	639
AY145428	Maxillopoda	Calanoida	Pontellidae	*Labidocera rotunda*	624
DQ889156	Branchiopoda	Notostraca	Triopsidae	*Lepidurus* sp.	639
AF520444	Malacostraca	Cumacea	Bodotriidae	*Leptocuma* sp.	633
DQ889157	Branchiopoda	Diplostraca	Limnadiidae	*Limnadia* sp.	639
DQ889158	Maxillopoda	Calanoida	Centropagidae	*Limnocalanus macrurus*	631
DQ889159	Malacostraca	Mysidacea	Mysidae	*Limnomysis benedeni*	634
AF260843	Malacostraca	Isopoda	Cymothoidae	*Livoneca vulgaris*	617
DQ882088	Malacostraca	Decapoda	Lithodidae	*Lopholithodes foraminatus*	658
DQ889160	Branchiopoda	Cladocera	Macrothricidae	*Macrothrix* sp.	639
AF137520	Malacostraca	Cumacea	Bodotriidae	*Mancocuma stellifera*	675
AJ319742	Ostracoda	Podocopida	Cyprididae	*Mesocyprideis irsacae*	462
DQ889161	Malacostraca	Mysidacea	Mysidae	*Mysis americana*	654
DQ889162	Ostracoda	Podocopida	Cyprididae	*Mytilocypris ambiguosa*	656
AF332793	Maxillopoda	Calanoida	Calanidae	*Nannocalanus minor*	613
AF513650	Maxillopoda	Calanoida	Calanidae	*Neocalanus robustior*	639
AF205235	Malacostraca	Stomatopoda	Gonodactylidae	*Neogonodactylus bredini*	648
DQ882094	Malacostraca	Decapoda	Oplophoridae	*Notostomus japonicus*	647
DQ889163	Malacostraca	Euphausiacea	Euphausiidae	*Nyctiphanes australis*	633
AY428049	Maxillopoda	Sessilia	Chthamalidae	*Octomeris angulosa*	639
DQ889164	Malacostraca	Amphipoda	Lysianassidae	*Onisimus glacialis*	639
DQ889165	Malacostraca	Decapoda	Cambaridae	*Orconectes propinquus*	653
DQ889166	Maxillopoda	Calanoida	Centropagidae	*Osphranticum labronectum*	636
AF137512	Malacostraca	Cumacea	Diastylidae	*Oxyurostylis smithi*	658
DQ882103	Malacostraca	Decapoda	Palaemonidae	*Palaemon elegans*	658
DQ882106	Malacostraca	Decapoda	Pandalidae	*Pandalopsis dispar*	657
DQ356574	Maxillopoda	Calanoida	Centropagidae	*Parabroteas sarsia*	636
AF052393	Malacostraca	Mysidacea	Mysidae	*Paramesopodopsis rufa*	651
AF255783	Malacostraca	Isopoda	Idoteidae	*Paridotea ungulata*	564
DQ889167	Branchiopoda	Cladocera	Podonidae	*Pleopis* sp.	639
DQ889168	Branchiopoda	Cladocera	Chydoridae	*Pleuroxus denticulatus*	639
DQ889169	Branchiopoda	Cladocera	Podonidae	*Podon leuckarti*	639
AF352302	Malacostraca	Cumacea	Bodotriidae	*Pomocuma australiae*	675
DQ889170	Malacostraca	Amphipoda	Gammaridae	*Pontogammarus maeoticus*	657
AF283874	Malacostraca	Decapoda	Galatheidae	*Raymunida dextralis*	657
AF531746	Maxillopoda	Calanoida	Eucalanidae	*Rhincalanus gigas*	633
DQ889171	Branchiopoda	Diplostraca	Daphniidae	*Scapholeberis rammneri*	639
DQ889172	Branchiopoda	Diplostraca	Daphniidae	*Simocephalus vetulus*	639
AF260846	Malacostraca	Isopoda	Sphaeromatidae	*Sphaeromene polytylotus*	579
DQ882157	Malacostraca	Decapoda	Hippolytidae	*Spirontocaris lamellicornis*	658
AF052394	Malacostraca	Mysidacea	Mysidae	*Tenagomysis australis*	645

© 2007 NRC Canada

Table A2 (*concluded*).

GenBank accession No.	Class	Order	Family	Species	Length
AY430813	Maxillopoda	Sessilia	Chthamalidae	*Tetrachthamalus oblitteratus*	603
DQ889173	Malacostraca	Decapoda	Scyllaridae	*Thenus orientalis*	657
AF352301	Malacostraca	Cumacea	Bodotriidae	*Vaunthompsonia cristata*	658
DQ889174	Malacostraca	Amphipoda	Gammaridae	*Weirpechtia pinguis*	644

© 2007 NRC Canada

Table A3. List of decapod specimens for which COI barcodes were acquired in this study, together with their country of collection, type of archive at the Biodiversity Institute of Ontario, primer pair used, and sequence length.

GenBank accession No.	Process ID	Species	Family	Country	Archive type	Primer pair[a]	Length
DQ882026	FCDPA135-04	*Acantholithodes hispidus*	Lithodidae	Canada	Specimen	FolA–FolB	658
DQ882029	FCDPA020-04	*Argis alaskensis*	Crangonidae	Canada	Specimen	FolA–FolB	658
DQ882028	FCDPA021-04	*Argis alaskensis*	Crangonidae	Canada	Specimen	FolA–FolB	654
DQ882027	FCDPA106-04	*Argis alaskensis*	Crangonidae	Canada	Specimen	FolA–FolB	658
DQ882032	FCDPA022-04	*Argis lar*	Crangonidae	Canada	Specimen	CrustF1–FolB	658
DQ882031	FCDPA023-04	*Argis lar*	Crangonidae	Canada	Specimen	CrustF1–FolB	658
DQ882030	FCDPA107-04	*Argis lar*	Crangonidae	Canada	Specimen	FolA–FolB	650
DQ882033	FCDPA050-04	*Bentheogennema borealis*	Benthesicymidae	Canada	Tissue	FolA–FolB	618
DQ882034	FCDPA051-04	*Bentheogennema borealis*	Benthesicymidae	Canada	Tissue	FolA–FolB	616
DQ882035	FCDPA111-04	*Calocarides spinulicauda*	Axiidae	Canada	Specimen	FolA–FolB	638
DQ882037	FCDPA052-04	*Calocaris investigatoris*	Calocarididae	Canada	Tissue	FolA–FolB	658
DQ882036	FCDPA053-04	*Calocaris investigatoris*	Calocarididae	Canada	Tissue	FolA–FolB	614
DQ882040	FCDPA061-04	*Cancer magister*	Cancridae	Canada	Tissue	CrustF1–FolB	655
DQ882038	FCDPA150-04	*Cancer magister*	Cancridae	Canada	Tissue	FolA–FolB	624
DQ882039	FCDPA151-04	*Cancer magister*	Cancridae	Canada	Tissue	FolA–FolB	638
DQ882041	FCDPA062-04	*Cancer oregonensis*	Cancridae	Canada	Tissue	CrustF1–FolB	616
DQ882042	FCDPA063-04	*Cancer oregonensis*	Cancridae	Canada	Tissue	CrustF1–FolB	511
DQ882044	FCDPA166-05	*Cancer productus*	Cancridae	Canada	Tissue	FolA–FolB	658
DQ882043	FCDPA064-04	*Cancer productus*	Cancridae	Canada	Tissue	FolA–FolB	605
DQ882045	FCDPA065-04	*Chionoecetes angulatus*	Oregoniidae	Canada	Tissue	FolA–FolB	620
DQ882046	FCDPA066-04	*Chionoecetes angulatus*	Oregoniidae	Canada	Tissue	FolA–FolB	520
DQ882049	FCDPA067-04	*Chionoecetes bairdi*	Oregoniidae	Canada	Tissue	FolA–FolB	652
DQ882048	FCDPA068-04	*Chionoecetes bairdi*	Oregoniidae	Canada	Tissue	CrustF1–FolB	643
DQ882047	FCDPA138-04	*Chionoecetes bairdi*	Oregoniidae	Canada	Specimen	FolA–FolB	658
DQ882051	FCDPA069-04	*Chionoecetes tanneri*	Oregoniidae	Canada	Tissue	FolA–FolB	523
DQ882050	FCDPA070-04	*Chionoecetes tanneri*	Oregoniidae	Canada	Tissue	FolA–FolB	656
DQ882054	FCDPA072-04	*Chorilia longipes*	Majidae	Canada	Specimen	CrustF1–FolB	552
DQ882053	FCDPA073-04	*Chorilia longipes*	Majidae	Canada	Tissue	FolA–FolB	655
DQ882052	FCDPA139-04	*Chorilia longipes*	Majidae	Canada	Specimen	FolA–FolB	656
DQ882055	FCDPA024-04	*Crangon abyssorum*	Crangonidae	Canada	Tissue	FolA–FolB	653
DQ882056	FCDPA025-04	*Crangon abyssorum*	Crangonidae	Canada	Tissue	FolA–FolB	645
DQ882057	FCDPA116-04	*Crangon alaskensis*	Crangonidae	Canada	Specimen	CrustF1–FolB	658
DQ882058	FCDPA117-04	*Crangon alaskensis*	Crangonidae	Canada	Specimen	FolA–FolB	655
DQ882060	FCDPA026-04	*Crangon communis*	Crangonidae	Canada	Specimen	CrustF1–FolB	574
DQ882061	FCDPA027-04	*Crangon communis*	Crangonidae	Canada	Specimen	CrustF1–FolB	658
DQ882059	FCDPA154-04	*Crangon communis*	Crangonidae	Canada	Specimen	CrustF1–FolB	630
DQ882062	FCDPA074-04	*Eriocheir sinensis*	Varunidae	Poland	Tissue	CrustF1–FolB	623
DQ882065	FCDPA123-04	*Eualus avinus*	Hippolytidae	Canada	Specimen	FolA–FolB	658
DQ882064	FCDPA124-04	*Eualus avinus*	Hippolytidae	Canada	Specimen	FolA–FolB	658
DQ882063	FCDPA125-04	*Eualus avinus*	Hippolytidae	Canada	Specimen	FolA–FolB	658
DQ882069	FCDPA034-04	*Eualus barbatus*	Hippolytidae	Canada	Specimen	FolA–FolB	651
DQ882070	FCDPA035-04	*Eualus barbatus*	Hippolytidae	Canada	Specimen	FolA–FolB	658

© 2007 NRC Canada

Table A3 (*continued*).

GenBank accession No.	Process ID	Species	Family	Country	Archive type	Primer pair[a]	Length
DQ882066	FCDPA109-04	*Eualus barbatus*	Hippolytidae	Canada	Specimen	FolA–FolB	645
DQ882067	FCDPA110-04	*Eualus barbatus*	Hippolytidae	Canada	Specimen	FolA–FolB	639
DQ882068	FCDPA140-04	*Eualus barbatus*	Hippolytidae	Canada	Specimen	FolA–FolB	643
DQ882074	FCDPA036-04	*Eualus biunguis*	Hippolytidae	Canada	Tissue	FolA–FolB	658
DQ882073	FCDPA037-04	*Eualus biunguis*	Hippolytidae	Canada	Tissue	FolA–FolB	624
DQ882072	FCDPA038-04	*Eualus biunguis*	Hippolytidae	Canada	Tissue	FolA–FolB	615
DQ882071	FCDPA039-04	*Eualus biunguis*	Hippolytidae	Canada	Tissue	FolA–FolB	624
DQ882075	FCDPA087-04	*Eualus gaimardi*	Hippolytidae	Canada	Specimen	FolA–FolB	659
DQ882078	FCDPA040-04	*Eualus suckleyi*	Hippolytidae	Canada	Tissue	FolA–FolB	624
DQ882076	FCDPA126-04	*Eualus suckleyi*	Hippolytidae	Canada	Specimen	FolA–FolB	656
DQ882077	FCDPA127-04	*Eualus suckleyi*	Hippolytidae	Canada	Specimen	FolA–FolB	657
DQ882079	FCDPA071-04	*Hyas lyratus*	Oregoniidae	Canada	Tissue	FolA–FolB	658
DQ882080	FCDPA130-04	*Hymenodora frontalis*	Oplophoridae	Canada	Tissue	FolA–FolB	658
DQ882081	FCDPA141-04	*Hymenodora frontalis*	Oplophoridae	Canada	Tissue	FolA–FolB	608
DQ882084	FCDPA081-04	*Lebbeus groenlandicus*	Hippolytidae	Canada	Specimen	FolA–FolB	639
DQ882083	FCDPA032-04	*Lebbeus groenlandicus*	Hippolytidae	Canada	Tissue	FolA–FolB	505
DQ882082	FCDPA033-04	*Lebbeus groenlandicus*	Hippolytidae	Canada	Tissue	FolA–FolB	614
DQ882086	FCDPA054-04	*Lithodes couesi*	Lithodidae	Canada	Tissue	FolA–FolB	639
DQ882085	FCDPA055-04	*Lithodes couesi*	Lithodidae	Canada	Tissue	FolA–FolB	619
DQ882089	FCDPA056-04	*Lopholithodes foraminatus*	Lithodidae	Canada	Tissue	CrustF1–FolB	638
DQ882088	FCDPA136-04	*Lopholithodes foraminatus*	Lithodidae	Canada	Tissue	FolA–FolB	658
DQ882087	FCDPA148-04	*Lopholithodes foraminatus*	Lithodidae	Canada	Tissue	CrustF1–FolB	642
DQ882090	FCDPA058-04	*Munida quadrispina*	Galatheidae	Canada	Tissue	FolA–FolB	658
DQ882092	FCDPA059-04	*Munida quadrispina*	Galatheidae	Canada	Specimen	FolA–FolB	658
DQ882091	FCDPA060-04	*Munida quadrispina*	Galatheidae	Canada	Tissue	FolA–FolB	603
DQ882093	FCDPA137-04	*Munidopsis quadrata*	Galatheidae	Canada	Tissue	FolA–FolB	658
DQ882094	FCDPA131-04	*Notostomus japonicus*	Oplophoridae	Canada	Tissue	FolA–FolB	647
DQ882095	FCDPA089-04	*Orconectes immunis*	Cambaridae	Canada	Specimen	FolA–FolB	632
DQ882096	FCDPA075-04	*Orconectes limosus*	Cambaridae	Canada	Tissue	CrustF1–FolB	632
DQ882097	FCDPA134-04	*Paguristes turgidus*	Diogenidae	Canada	Specimen	FolA–FolB	658
DQ882100	FCDPA145-04	*Paguristes turgidus*	Diogenidae	Canada	Specimen	FolA–FolB	614
DQ882099	FCDPA146-04	*Paguristes turgidus*	Diogenidae	Canada	Specimen	FolA–FolB	645
DQ882098	FCDPA147-04	*Paguristes turgidus*	Diogenidae	Canada	Specimen	FolA–FolB	643
DQ882101	FCDPA160-05	*Palaemon* sp.	Palaemonidae	Poland	Specimen	FolA–FolB	658
DQ882103	FCDPA157-05	*Palaemon elegans*	Palaemonidae	Poland	Specimen	FolA–FolB	658
DQ882104	FCDPA158-05	*Palaemon elegans*	Palaemonidae	Poland	Specimen	FolA–FolB	658
DQ882102	FCDPA159-05	*Palaemon elegans*	Palaemonidae	Poland	Specimen	FolA–FolB	658
DQ882105	FCDPA161-05	*Palaemon elegans*	Palaemonidae	Poland	Specimen	FolA–FolB	658
DQ882107	FCDPA018-04	*Pandalopsis dispar*	Pandalidae	Canada	Specimen	FolA–FolB	654
DQ882108	FCDPA019-04	*Pandalopsis dispar*	Pandalidae	Canada	Specimen	FolA–FolB	653
DQ882106	FCDPA105-04	*Pandalopsis dispar*	Pandalidae	Canada	Specimen	FolA–FolB	657
DQ882112	FCDPA001-04	*Pandalus danae*	Pandalidae	Canada	Tissue	FolA–FolB	626
DQ882111	FCDPA113-04	*Pandalus danae*	Pandalidae	Canada	Specimen	FolA–FolB	658

© 2007 NRC Canada

Table A3 (*continued*).

GenBank accession No.	Process ID	Species	Family	Country	Archive type	Primer pair[a]	Length
DQ882110	FCDPA114-04	*Pandalus danae*	Pandalidae	Canada	Specimen	FolA–FolB	654
DQ882109	FCDPA115-04	*Pandalus danae*	Pandalidae	Canada	Specimen	FolA–FolB	654
DQ882113	FCDPA002-04	*Pandalus goniurus*	Pandalidae	Canada	Tissue	FolA–FolB	614
DQ882116	FCDPA003-04	*Pandalus hypsinotus*	Pandalidae	Canada	Tissue	FolA–FolB	604
DQ882115	FCDPA004-04	*Pandalus hypsinotus*	Pandalidae	Canada	Tissue	FolA–FolB	656
DQ882114	FCDPA005-04	*Pandalus hypsinotus*	Pandalidae	Canada	Tissue	FolA–FolB	658
DQ882118	FCDPA006-04	*Pandalus jordani*	Pandalidae	Canada	Specimen	CrustF1–FolB	652
DQ882117	FCDPA007-04	*Pandalus jordani*	Pandalidae	Canada	Specimen	CrustF1–FolB	613
DQ882120	FCDPA008-04	*Pandalus jordani*	Pandalidae	Canada	Specimen	CrustF1–FolB	658
DQ882119	FCDPA009-04	*Pandalus jordani*	Pandalidae	Canada	Specimen	CrustF1–FolB	658
DQ882121	FCDPA010-04	*Pandalus mortagui tridens*	Pandalidae	Canada	Tissue	CrustF1–FolB	616
DQ882123	FCDPA011-04	*Pandalus mortagui tridens*	Pandalidae	Canada	Tissue	CrustF1–FolB	618
DQ882122	FCDPA012-04	*Pandalus mortagui tridens*	Pandalidae	Canada	Tissue	CrustF1–FolB	615
DQ882126	FCDPA013-04	*Pandalus platyceros*	Pandalidae	Canada	Specimen	CrustF1–FolB	538
DQ882125	FCDPA014-04	*Pandalus platyceros*	Pandalidae	Canada	Specimen	CrustF1–FolB	658
DQ882124	FCDPA153-04	*Pandalus platyceros*	Pandalidae	Canada	Specimen	CrustF1–FolB	643
DQ882129	FCDPA015-04	*Pandalus stenolepis*	Pandalidae	Canada	Specimen	FolA–FolB	602
DQ882128	FCDPA016-04	*Pandalus stenolepis*	Pandalidae	Canada	Specimen	CrustF2–FolB	653
DQ882127	FCDPA017-04	*Pandalus stenolepis*	Pandalidae	Canada	Specimen	FolA–FolB	617
DQ882130	FCDPA057-04	*Paralomis multispina*	Lithodidae	Canada	Tissue	FolA–FolB	615
DQ882133	FCDPA041-04	*Pasiphaea pacifica*	Pasiphaeidae	Canada	Specimen	CrustF1–FolB	658
DQ882134	FCDPA042-04	*Pasiphaea pacifica*	Pasiphaeidae	Canada	Specimen	CrustF1–FolB	648
DQ882135	FCDPA043-04	*Pasiphaea pacifica*	Pasiphaeidae	Canada	Specimen	CrustF1–FolB	657
DQ882132	FCDPA128-04	*Pasiphaea pacifica*	Pasiphaeidae	Canada	Specimen	FolA–FolB	659
DQ882131	FCDPA129-04	*Pasiphaea pacifica*	Pasiphaeidae	Canada	Specimen	FolA–FolB	658
DQ882137	FCDPA044-04	*Pasiphaea tarda*	Pasiphaeidae	Canada	Tissue	FolA–FolB	616
DQ882136	FCDPA045-04	*Pasiphaea tarda*	Pasiphaeidae	Canada	Tissue	CrustF2–FolB	656
DQ882139	FCDPA047-04	*Pasiphaea tarda*	Pasiphaeidae	Canada	Specimen	CrustF2–FolB	658
DQ882138	FCDPA048-04	*Pasiphaea tarda*	Pasiphaeidae	Canada	Specimen	CrustF2–FolB	641
DQ882143	FCDPA162-05	*Rhithropanopeus harrisii*	Panopeidae	Poland	Specimen	FolA–FolB	658
DQ882142	FCDPA163-05	*Rhithropanopeus harrisii*	Panopeidae	Poland	Specimen	FolA–FolB	658
DQ882140	FCDPA164-05	*Rhithropanopeus harrisii*	Panopeidae	Poland	Specimen	FolA–FolB	658
DQ882141	FCDPA165-05	*Rhithropanopeus harrisii*	Panopeidae	Poland	Specimen	FolA–FolB	658
DQ882144	FCDPA079-04	*Sclerocrangon boreas*	Crangonidae	Canada	Specimen	FolA–FolB	659
DQ882145	FCDPA080-04	*Sclerocrangon boreas*	Crangonidae	Canada	Specimen	FolA–FolB	659
DQ882146	FCDPA082-04	*Sclerocrangon boreas*	Crangonidae	Canada	Specimen	FolA–FolB	564
DQ882148	FCDPA086-04	*Sclerocrangon boreas*	Crangonidae	Canada	Specimen	FolA–FolB	658
DQ882147	FCDPA088-04	*Sclerocrangon boreas*	Crangonidae	Canada	Specimen	FolA–FolB	659
DQ882150	FCDPA142-04	*Sergestes similis*	Sergestidae	Canada	Specimen	FolA–FolB	646
DQ882152	FCDPA143-04	*Sergestes similis*	Sergestidae	Canada	Specimen	FolA–FolB	648
DQ882151	FCDPA144-04	*Sergestes similis*	Sergestidae	Canada	Specimen	FolA–FolB	647
DQ882149	FCDPA133-04	*Sergestes similis*	Sergestidae	Canada	Specimen	FolA–FolB	658
DQ882154	FCDPA028-04	*Spirontocaris holmesi*	Hippolytidae	Canada	Specimen	CrustF1–FolB	657

© 2007 NRC Canada

Table A3 *(concluded).*

GenBank accession No.	Process ID	Species	Family	Country	Archive type	Primer pair[a]	Length
DQ882153	FCDPA119-04	*Spinontocaris holmesi*	Hippolytidae	Canada	Specimen	FolA–FolB	658
DQ882156	FCDPA029-04	*Spinontocaris lamellicornis*	Hippolytidae	Canada	Specimen	CrustF1–FolB	626
DQ882155	FCDPA030-04	*Spinontocaris lamellicornis*	Hippolytidae	Canada	Specimen	CrustF1–FolB	621
DQ882157	FCDPA031-04	*Spinontocaris lamellicornis*	Hippolytidae	Canada	Specimen	CrustF1–FolB	658
DQ882158	FCDPA077-04	*Spinontocaris phippsi*	Hippolytidae	Canada	Specimen	FolA–FolB	589
DQ882159	FCDPA084-04	*Spinontocaris phippsi*	Hippolytidae	Canada	Specimen	FolA–FolB	659
DQ882162	FCDPA120-04	*Spinontocaris sica*	Hippolytidae	Canada	Specimen	FolA–FolB	657
DQ882161	FCDPA121-04	*Spinontocaris sica*	Hippolytidae	Canada	Specimen	FolA–FolB	658
DQ882160	FCDPA122-04	*Spinontocaris sica*	Hippolytidae	Canada	Specimen	FolA–FolB	658
DQ882163	FCDPA085-04	*Spinontocaris spinus*	Hippolytidae	Canada	Specimen	FolA–FolB	659
DQ882164	FCDPA099-04	*Synalpheus* sp.	Alpheidae	Australia	Specimen	FolA–FolB	653
DQ882166	FCDPA100-04	*Synalpheus* sp.	Alpheidae	Australia	Specimen	FolA–FolB	658
DQ882165	FCDPA101-04	*Synalpheus* sp.	Alpheidae	Australia	Specimen	FolA–FolB	659
DQ882167	FCDPA103-04	*Synalpheus* sp.	Alpheidae	Australia	Specimen	FolA–FolB	658
DQ882168	FCDPA049-04	*Systellaspis braueri*	Oplophoridae	Canada	Tissue	FolA–FolB	654
DQ882171	FCDPA091-04	*Uca* sp.	Ocypodidae	Australia	Specimen	FolA–FolB	659
DQ882169	FCDPA104-04	*Uca* sp.	Ocypodidae	Australia	Specimen	FolA–FolB	658
DQ882170	FCDPA152-04	*Uca* sp.	Ocypodidae	Australia	Specimen	CrustF1–FolB	632

[a]Primer FolA corresponds to LCO1490; FolB corresponds to HCO2198.

© 2007 NRC Canada

Table A4. List of decapod specimens for which COI barcodes were acquired from GenBank, together with their family and sequence length.

GenBank accession No.	Species	Family	Length
AF283888	*Agomonida incerta*	Galatheidae	657
AF283889	*Agomonida incerta*	Galatheidae	657
AB128829	*Alvinocaris* sp.	Bresiliidae	657
AY465911	*Callinectes arcuatus*	Portunidae	657
AY465913	*Callinectes arcuatus*	Portunidae	657
AY465907	*Callinectes bellicosus*	Portunidae	657
AY465909	*Callinectes bellicosus*	Portunidae	657
AY363392	*Callinectes sapidus*	Portunidae	658
AY465915	*Callinectes sapidus*	Portunidae	657
AY682072	*Callinectes sapidus*	Portunidae	658
AY682073	*Callinectes sapidus*	Portunidae	658
AY682074	*Callinectes sapidus*	Portunidae	658
AY682075	*Callinectes sapidus*	Portunidae	658
AY682076	*Callinectes sapidus*	Portunidae	658
AY682077	*Callinectes sapidus*	Portunidae	658
AY682078	*Callinectes sapidus*	Portunidae	658
AY682079	*Callinectes sapidus*	Portunidae	658
AY616445	*Carcinus aestuarii*	Portunidae	498
AY616437	*Carcinus maenas*	Portunidae	498
AY616438	*Carcinus maenas*	Portunidae	498
AY616439	*Carcinus maenas*	Portunidae	498
AY616440	*Carcinus maenas*	Portunidae	498
AY616441	*Carcinus maenas*	Portunidae	498
AY616442	*Carcinus maenas*	Portunidae	498
AY616443	*Carcinus maenas*	Portunidae	498
AY616444	*Carcinus maenas*	Portunidae	498
AF493625	*Cherax crassimanus*	Parastacidae	600
NC_011243	*Cherax destructor*	Parastacidae	658
AF493622	*Cherax preissii*	Parastacidae	600
AF493623	*Cherax preissii*	Parastacidae	600
AF493618	*Cherax quinquecarinatus*	Parastacidae	600
AF493619	*Cherax quinquecarinatus*	Parastacidae	600
AF493620	*Cherax quinquecarinatus*	Parastacidae	600
AF493621	*Cherax quinquecarinatus*	Parastacidae	600
AF493626	*Cherax tenuimanus*	Parastacidae	600
AF493627	*Cherax tenuimanus*	Parastacidae	600
AF493628	*Cherax tenuimanus*	Parastacidae	600
AF493629	*Cherax tenuimanus*	Parastacidae	600
AF493630	*Cherax tenuimanus*	Parastacidae	600
AF493631	*Cherax tenuimanus*	Parastacidae	600
AF493633	*Engaeus strictifrons*	Parastacidae	600
AF105249	*Eriocheir formosa*	Varunidae	658
AF105250	*Eriocheir formosa*	Varunidae	658
AF516698	*Eriocheir formosa*	Varunidae	558
AF317326	*Eriocheir formosa*	Varunidae	576
AF516699	*Eriocheir hepuensis*	Varunidae	558
AF317327	*Eriocheir hepuensis*	Varunidae	576
AF317328	*Eriocheir hepuensis*	Varunidae	576
AF105245	*Eriocheir japonica*	Varunidae	658
AF105246	*Eriocheir japonica*	Varunidae	658
AF516700	*Eriocheir japonica*	Varunidae	558
AF317330	*Eriocheir japonica*	Varunidae	576
AF317331	*Eriocheir japonica*	Varunidae	576
AF516701	*Eriocheir leptognathus*	Varunidae	558
AF316537	*Eriocheir leptognathus*	Varunidae	576
AF317332	*Eriocheir rectus*	Varunidae	576
AF105247	*Eriocheir sinensis*	Varunidae	658

© 2007 NRC Canada

Table A4 (*continued*).

GenBank accession No.	Species	Family	Length
AF105248	*Eriocheir sinensis*	Varunidae	658
AF435113	*Eriocheir sinensis*	Varunidae	588
AF435114	*Eriocheir sinensis*	Varunidae	588
AF435115	*Eriocheir sinensis*	Varunidae	588
AF435116	*Eriocheir sinensis*	Varunidae	588
AF435117	*Eriocheir sinensis*	Varunidae	588
AF435118	*Eriocheir sinensis*	Varunidae	588
AF435119	*Eriocheir sinensis*	Varunidae	588
AF516702	*Eriocheir sinensis*	Varunidae	558
AF317333	*Eriocheir sinensis*	Varunidae	576
AF317335	*Eriocheir sinensis*	Varunidae	576
AF317336	*Eriocheir sinensis*	Varunidae	576
AF493634	*Enastacus bispinosus*	Parastacidae	600
AF516703	*Gaetice depressus*	Varunidae	555
AF317339	*Gaetice depressus*	Varunidae	573
AF493632	*Geocharax falcata*	Parastacidae	600
AF317340	*Hemigrapsus sanguineus*	Varunidae	573
AF192875	*Jasus edwardsii*	Palinuridae	513
AF192877	*Jasus edwardsii*	Palinuridae	507
AF339473	*Jasus edwardsii*	Palinuridae	642
AF192882	*Jasus lalandii*	Palinuridae	513
AF192883	*Jasus verreauxi*	Palinuridae	518
AF399976	*Liberomastes latidactylus*	Potamonautidae	540
AF510695	*Macrobrachium australiense*	Palaemonidae	608
AF510696	*Macrobrachium australiense*	Palaemonidae	609
AF510697	*Macrobrachium australiense*	Palaemonidae	609
AF510699	*Macrobrachium australiense*	Palaemonidae	609
AF510702	*Macrobrachium australiense*	Palaemonidae	609
AF510704	*Macrobrachium australiense*	Palaemonidae	606
AF510705	*Macrobrachium australiense*	Palaemonidae	609
AF510706	*Macrobrachium australiense*	Palaemonidae	608
AF510708	*Macrobrachium australiense*	Palaemonidae	608
AF510709	*Macrobrachium australiense*	Palaemonidae	609
AF283885	*Munida rhodonia*	Galatheidae	657
AF283886	*Munida rhodonia*	Galatheidae	639
AF283887	*Munida rubrodigitalis*	Galatheidae	657
AF483156	*Pagurus acadianus*	Paguridae	525
AF483159	*Pagurus armatus*	Paguridae	521
AF483157	*Pagurus bernhardus*	Paguridae	525
AF483118	*Pagurus longicarpus*	Paguridae	642
AF483122	*Pagurus longicarpus*	Paguridae	642
AF483124	*Pagurus longicarpus*	Paguridae	642
AF483127	*Pagurus longicarpus*	Paguridae	642
AF483140	*Pagurus longicarpus*	Paguridae	642
AF483142	*Pagurus longicarpus*	Paguridae	642
AF483143	*Pagurus longicarpus*	Paguridae	642
AF483144	*Pagurus longicarpus*	Paguridae	642
AF483151	*Pagurus longicarpus*	Paguridae	642
AF483153	*Pagurus longicarpus*	Paguridae	642
AF483158	*Pagurus ochotensis*	Paguridae	525
AF483160	*Pagurus pollicaris*	Paguridae	525
AF483161	*Pagurus pollicaris*	Paguridae	525
AF483163	*Pagurus pollicaris*	Paguridae	525
AF483164	*Pagurus pollicaris*	Paguridae	525
AF483165	*Pagurus pollicaris*	Paguridae	525
AF483166	*Pagurus pollicaris*	Paguridae	525
AF483167	*Pagurus pollicaris*	Paguridae	525
AF483169	*Pagurus pollicaris*	Paguridae	525

© 2007 NRC Canada

Table A4 (*concluded*).

GenBank accession No.	Species	Family	Length
AF483170	*Pagurus pollicaris*	Paguridae	525
AF483171	*Pagurus pollicaris*	Paguridae	525
AJ640116	*Palaemon longirostris*	Palaemonidae	658
AF339452	*Panulirus argus*	Palinuridae	642
AF339453	*Panulirus cygnus*	Palinuridae	642
AF339454	*Panulirus echinatus*	Palinuridae	642
AF339456	*Panulirus guttatus*	Palinuridae	642
AF339457	*Panulirus homarus homarus*	Palinuridae	642
AF339458	*Panulirus homarus megasculpta*	Palinuridae	642
AF339459	*Panulirus inflatus*	Palinuridae	642
AF339461	*Panulirus japonicus*	Palinuridae	641
AB071201	*Panulirus japonicus*	Palinuridae	658
AF339462	*Panulirus laevicauda*	Palinuridae	642
AF339463	*Panulirus longipes femoristriga*	Palinuridae	642
AF339464	*Panulirus longipes longipes*	Palinuridae	642
AF339465	*Panulirus marginatus*	Palinuridae	641
AF339467	*Panulirus ornatus*	Palinuridae	636
AF339466	*Panulirus pascuensis*	Palinuridae	642
AF339468	*Panulirus penicillatus*	Palinuridae	642
AF339469	*Panulirus polyphagus*	Palinuridae	642
AF339470	*Panulirus regius*	Palinuridae	642
AF339471	*Panulirus stimpsoni*	Palinuridae	642
AF339472	*Panulirus versicolor*	Palinuridae	642
AF534894	*Paratya australiensis*	Atyidae	633
AF534898	*Paratya australiensis*	Atyidae	633
AF534901	*Paratya australiensis*	Atyidae	633
AF534902	*Paratya australiensis*	Atyidae	633
AY308079	*Paratya australiensis*	Atyidae	561
AY308080	*Paratya australiensis*	Atyidae	561
AY308085	*Paratya australiensis*	Atyidae	561
AY308086	*Paratya australiensis*	Atyidae	561
AY308101	*Paratya australiensis*	Atyidae	561
AY308104	*Paratya australiensis*	Atyidae	561
NC_002184	*Penaeus monodon*	Penaeidae	658
NC_005037	*Portunus trituberculatus*	Portunidae	658
AF399979	*Potamonautes lividus*	Potamonautidae	538
AF474366	*Procambarus acutus*	Cambaridae	658
AF346400	*Ranina ranina*	Raninidae	642
AF283869	*Raymunida cuvieri*	Galatheidae	657
AF283870	*Raymunida cuvieri*	Galatheidae	657
AF283871	*Raymunida cuvieri*	Galatheidae	657
AF283872	*Raymunida confundens*	Galatheidae	657
AF283873	*Raymunida confundens*	Galatheidae	657
AF283874	*Raymunida dextralis*	Galatheidae	657
AF283875	*Raymunida elegantissima*	Galatheidae	657
AF283876	*Raymunida elegantissima*	Galatheidae	657
AF283877	*Raymunida elegantissima*	Galatheidae	657
AF283878	*Raymunida elegantissima*	Galatheidae	657
AF283879	*Raymunida elegantissima*	Galatheidae	657
AF283880	*Raymunida elegantissima*	Galatheidae	657
AF283881	*Raymunida elegantissima*	Galatheidae	656
AF283882	*Raymunida erythrina*	Galatheidae	657
AF283883	*Raymunida erythrina*	Galatheidae	657
AY288292	*Raymunida formosanus*	Galatheidae	654
AF283884	*Raymunida insulata*	Galatheidae	657
AF399974	*Sudanonautes africanus*	Potamonautidae	528
AF516704	*Varuna litterata*	Varunidae	558
AF317343	*Varuna litterata*	Varunidae	573

© 2007 NRC Canada

Table A5. List of specimens of the genus *Gammarus* (Amphipoda) used for calculation of within- and among-species distances displayed in Table 1.

Process ID	Species	Country
FCGA011-04	*Gammarus aequicauda*	Italy
FCGA012-04	*Gammarus aequicauda*	Italy
FCGA041-04	*Gammarus chevreuxi*	Portugal
FCGA042-04	*Gammarus chevreuxi*	Portugal
FCGA043-04	*Gammarus chevreuxi*	Portugal
FCGA044-04	*Gammarus chevreuxi*	Portugal
FCGA027-04	*Gammarus crinicornis*	Belgium
FCGA029-04	*Gammarus crinicornis*	Belgium
FCGA045-04	*Gammarus crinicornis*	Portugal
FCGA054-04	*Gammarus duebeni*	Iceland
FCGA059-04	*Gammarus duebeni*	Iceland
FCGA072-05	*Gammarus duebeni*	Iceland
FCGA073-05	*Gammarus duebeni*	Iceland
FCGA074-05	*Gammarus duebeni*	Iceland
FCGA034-04	*Gammarus insensibilis*	Portugal
FCGA035-04	*Gammarus insensibilis*	Portugal
FCGA036-04	*Gammarus insensibilis*	Portugal
FCGA033-04	*Gammarus insensibilis*	Portugal
FCGA028-04	*Gammarus locusta*	Belgium
FCGA030-04	*Gammarus locusta*	Belgium
FCGA031-04	*Gammarus locusta*	Belgium
FCGA032-04	*Gammarus locusta*	Belgium
FCGA001-04	*Gammarus locusta*	Portugal
FCGA037-04	*Gammarus locusta*	Portugal
FCGA038-04	*Gammarus locusta*	Portugal
FCGA039-04	*Gammarus locusta*	Portugal
FCGA040-04	*Gammarus locusta*	Portugal
FCGA048-04	*Gammarus oceanicus*	Iceland
FCGA049-04	*Gammarus oceanicus*	Iceland
FCGA050-04	*Gammarus oceanicus*	Iceland
FCGA051-04	*Gammarus oceanicus*	Iceland
FCGA067-05	*Gammarus oceanicus*	Iceland
FCGA068-05	*Gammarus oceanicus*	Iceland
FCGA070-05	*Gammarus oceanicus*	Iceland
FCGA071-05	*Gammarus oceanicus*	Iceland
FCGA016-04	*Gammarus oceanicus*	Poland
FCGA017-04	*Gammarus oceanicus*	Poland
FCGA018-04	*Gammarus oceanicus*	Poland
FCGA019-04	*Gammarus oceanicus*	Poland
FCGA056-04	*Gammarus oceanicus*	Canada, Churchill
FCGA047-04	*Gammarus oceanicus*	Canada, Churchill
FCGA062-05	*Gammarus oceanicus*	Canada, Churchill
FCGA063-05	*Gammarus oceanicus*	Canada, Churchill
FCGA023-04	*Gammarus oceanicus*	Canada, Rimouski
FCGA025-04	*Gammarus oceanicus*	Canada, Rimouski
FCGA026-04	*Gammarus oceanicus*	Canada, Rimouski
FCGA002-04	*Gammarus* PS 1	Bulgaria
FCGA003-04	*Gammarus* PS 1	Bulgaria
FCGA004-04	*Gammarus* PS 1	Bulgaria
FCGA005-04	*Gammarus* PS 1	Bulgaria
FCGA006-04	*Gammarus* PS 1	Bulgaria
FCGA007-04	*Gammarus* PS 2	Bulgaria
FCGA008-04	*Gammarus* PS 2	Bulgaria
FCGA009-04	*Gammarus* PS 2	Bulgaria
FCGA010-04	*Gammarus* PS 2	Bulgaria
FCGA013-04	*Gammarus salinus*	Poland
FCGA014-04	*Gammarus salinus*	Poland
FCGA015-04	*Gammarus salinus*	Poland
FCGA076-05	*Gammarus salinus*	Poland
FCGA077-05	*Gammarus salinus*	Poland
FCGA078-05	*Gammarus salinus*	Poland
FCGA079-05	*Gammarus salinus*	Poland
FCGA080-05	*Gammarus salinus*	Poland
FCGA081-05	*Gammarus tigrinus*	Poland
FCGA082-05	*Gammarus tigrinus*	Poland
FCGA083-05	*Gammarus tigrinus*	Poland
FCGA084-05	*Gammarus tigrinus*	Poland
FCGA020-04	*Gammarus zaddachi*	Poland
FCGA021-04	*Gammarus zaddachi*	Poland

Table A5 (*concluded*).

Note: Data from F.O. Costa and P.D.N. Hebert, unpublished data.
PS, provisional species.

© 2007 NRC Canada

Table A6. List of specimens of the genus *Daphnia* (Cladocera) used for calculation of within- and among-species distances displayed in Table 1.

GenBank accession No.	Species	Length
AY323083	*Daphnia dadayana*	630
AY323084	*Daphnia dadayana*	630
AY323085	*Daphnia dadayana*	630
AY323086	*Daphnia dadayana*	630
AY323087	*Daphnia dadayana*	630
AY323088	*Daphnia dadayana*	630
AY323089	*Daphnia dadayana*	630
AY323090	*Daphnia dadayana*	630
AY323091	*Daphnia dadayana*	630
AY323092	*Daphnia dadayana*	630
AY323093	*Daphnia dadayana*	630
AY323094	*Daphnia dadayana*	629
AY323095	*Daphnia dadayana*	619
AY323096	*Daphnia dadayana*	630
AY323097	*Daphnia dadayana*	630
AY323098	*Daphnia dadayana*	630
AY323071	*Daphnia gessneri*	630
AY323072	*Daphnia laevis*	630
AY323073	*Daphnia laevis*	630
AY323074	*Daphnia menucoensis*	630
AY323075	*Daphnia menucoensis*	630
AY323076	*Daphnia menucoensis*	630
AY323077	*Daphnia menucoensis*	629
AY323078	*Daphnia menucoensis*	630
AY323079	*Daphnia menucoensis*	630
AY323080	*Daphnia menucoensis*	630
AY323081	*Daphnia menucoensis*	630
AY323082	*Daphnia menucoensis*	630
AY323123	*Daphnia ornithocephala*	629
AY323124	*Daphnia ornithocephala*	629
AY323125	*Daphnia ornithocephala*	629
AY323126	*Daphnia parvula*	630
AY323070	*Daphnia peruviana*	630
AF308971	*Daphnia similis*	645
AY323121	*Daphnia similis*	630
AY323048	*Daphnia* sp. 1 SA-2003	630
AY323049	*Daphnia* sp. 1 SA-2003	630
AY323050	*Daphnia* sp. 1 SA-2003	630
AY323051	*Daphnia* sp. 1 SA-2003	628
AY323052	*Daphnia* sp. 1 SA-2003	630
AY323053	*Daphnia* sp. 1 SA-2003	630
AY323054	*Daphnia* sp. 1 SA-2003	630
AY323055	*Daphnia* sp. 1 SA-2003	630
AY323056	*Daphnia* sp. 1 SA-2003	630
AY323057	*Daphnia* sp. 1 SA-2003	630
AY323058	*Daphnia* sp. 1 SA-2003	630
AY323059	*Daphnia* sp. 2 SA-2003	630
AY323060	*Daphnia* sp. 2 SA-2003	630
AY323061	*Daphnia* sp. 2 SA-2003	630
AY323062	*Daphnia* sp. 2 SA-2003	630
AY323063	*Daphnia* sp. 2 SA-2003	630
AY323064	*Daphnia* sp. 2 SA-2003	630
AY323065	*Daphnia* sp. 3 SA-2003	630
AY323066	*Daphnia* sp. 3 SA-2003	629
AY323067	*Daphnia* sp. 3 SA-2003	630
AY323068	*Daphnia* sp. 3 SA-2003	630
AY323069	*Daphnia* sp. 3 SA-2003	630
AY323122	*Daphnia* sp. 4 SA-2003	628
AY323099	*Daphnia spinulata*	630
AY323100	*Daphnia spinulata*	630
AY323101	*Daphnia spinulata*	630
AY323102	*Daphnia spinulata*	630
AY323103	*Daphnia spinulata*	630
AY323104	*Daphnia spinulata*	630
AY323105	*Daphnia spinulata*	630
AY323106	*Daphnia spinulata*	630
AY323107	*Daphnia spinulata*	630
AY323108	*Daphnia spinulata*	630
AY323109	*Daphnia spinulata*	630
AY323110	*Daphnia spinulata*	630
AY323111	*Daphnia spinulata*	630
AY323112	*Daphnia spinulata*	630
AY323113	*Daphnia spinulata*	630
AY323114	*Daphnia spinulata*	628
AY323115	*Daphnia spinulata*	630
AY323116	*Daphnia spinulata*	630
AY323117	*Daphnia spinulata*	630
AY323118	*Daphnia spinulata*	630
AY323119	*Daphnia spinulata*	630
AY323120	*Daphnia spinulata*	630

Table A6 (*concluded*).

Note: Data adapted from Adamowicz et al. (2004).

© 2007 NRC Canada

Three-dimensional photogrammetry as a tool for estimating morphometrics and body mass of Steller sea lions (*Eumetopias jubatus*)

Jason N. Waite, Wendy J. Schrader, Jo-Ann E. Mellish, and Markus Horning

Abstract: A technique was developed to estimate morphometrics and body mass of Steller sea lions (*Eumetopias jubatus*) using three-dimensional (3D) photogrammetry. 3D photogrammetry reduces many of the problems associated with camera and body position encountered with two-dimensional photogrammetric techniques, allowing body mass estimation of free-ranging, active sea lions, without sedation, heavy weighing equipment, and disturbance. 3D computer wireframes of 53 Steller sea lions of various age classes were generated from multiple time-synchronous digital photos and used to estimate length, girth, and volume. Average estimates of standard length and axillary girth were within ±2.5% and ±4.0% of physically measured dimensions, respectively. Average estimates of standard length and axillary girth using only wireframes based on ideal body postures were within ±1.7% and ±3.1% of physically measured dimensions, respectively. Regressions of physically measured mass on photogrammetrically estimated body volume yielded a predictive model. Body mass estimates using this model were on average within 9.0% (95% confidence interval = ±1.7%) of the physically measured mass. This technique was also successfully applied to reptiles and fish.

Résumé : Nous avons mis au point une technique pour estimer les données morphométriques et la masse corporelle chez des lions de mer de Steller (*Eumetopias jubatus*) à l'aide de la photogrammétrie tridimensionnelle (3D). La photogrammétrie 3D réduit plusieurs des problèmes associés à la position de la caméra et du corps dans les techniques de photogrammétrie à deux dimensions; cela permet l'estimation de la masse corporelle de lions de mer actifs et libres, sans recours à la sédation ni à un lourd appareillage de pesée et sans produire de perturbation. Nous avons généré à l'ordinateur des modèles 3D en fil de fer de 53 lions de mer de Steller appartenant à diverses classes d'âge à partir de photographies digitales multiples synchronisées et nous les avons utilisés pour estimer la longueur, le tour de poitrine et le volume. Les estimations moyennes de la longueur standard et du tour de poitrine au niveau des aisselles sont respectivement à ±2,5 % et ±4,0 % des dimensions mesurées directement sur l'animal. Les estimations moyennes de la longueur standard et du tour de poitrine au niveau des aisselles d'après les seuls modèles en fil de fer basés sur des postures corporelles idéales sont respectivement à ±1,7 % et ±3,1 % des mesures faites sur l'animal. Les régressions de la masse mesurée sur l'animal et du volume corporel estimé par photogrammétrie fournissent un modèle prédictif. Les estimations de masse corporelle faites par ce modèle sont en moyenne à moins de 9,0 % (intervalle de confiance de 95 % = ±1,7 %) de la masse déterminée directement sur l'animal. Nous avons aussi utilisé cette technique avec succès chez les reptiles et les poissons.

[Traduit par la Rédaction]

Introduction

Body mass is an important variable for the accurate and integrated interpretation of most types of biological studies in animals (Peters 1983; Schmidt-Nielsen 1984). Body mass data have been used to study many aspects of life histories in conjunction with not only reproductive strategies and sexual selection, but also with foraging ecology, as well as the evolution of diversity and complexity of fauna. Preseason body mass and condition have been identified as good predictors of reproductive effort and offspring survival in terrestrial and marine mammals and have been analyzed as determinants of timing of reproductive events, including implantation and pupping time (McElligott et al. 2003; Harding et al. 2005; Ferguson et al. 2006). From reproductive timing in relation to mass changes in a marsupial, Isaac et al. (2005) concluded that multiple adaptive sex-ratio models (Trivers–Willard and Local Resource Competition) best described offspring sex allocation. Similarly, Holand et al. (2006) showed bet-hedging (manipulation of offspring qual-

Received 16 June 2006. Accepted 14 December 2006. Published on the NRC Research Press Web site at http://cjfas.nrc.ca on 27 February 2007.
J19370

J.N. Waite,[1] W.J. Schrader, J.-A.E. Mellish,[1] and M. Horning.[2,3] Department of Marine Biology, Texas A&M University, 5007 Avenue U, Galveston, TX 77551, USA.

[1]Present address: Alaska SeaLife Center, 301 Railway Avenue, P.O. Box 1329, Seward, AK 99664, USA.
[2]Present address: Hatfield Marine Science Center, Oregon State University, Newport, OR 97365, USA.
[3]Corresponding author (e-mail: markus.horning@oregonstate.edu).

 doi:10.1139/F07-014 © 2007 NRC Canada

ity) as a likely reproductive strategy for reindeer (*Rangifer tarandus*).

The absence of relationships to body mass has been equally important in rejecting prevalent life history hypotheses. Terminal investment and mating-strategy effort hypotheses were rejected for ungulates (McElligott et al. 2003), and Ferguson et al. (2006) refuted delayed implantation as a hypothesized by-product of evolution of small sizes, both based on absence of mass-driven effects.

Spatial scaling of body size distributions in mammals has highlighted the role of habitat complexity in driving latitudinal gradients in faunal diversity (Bakker and Kelt 2000; Allen et al. 2006). In single-species studies, mass appears as a suitable predictor of day range, in particular for faunivores (Jetz et al. 2004; Carbone et al. 2005), but absence of mass effects on range area in some studies highlights the importance of density-related population effects (Makarieva et al. 2005; Benson et al. 2006).

Physiological performance (Kooyman 1989), ontogeny (Horning and Trillmich 1997), foraging ecology (Horning and Trillmich 1999), parental investment patterns (Clutton-Brock 1988), and population trends (Calkins et al. 1998) of marine mammals all have been studied through body mass data. Body size and mass trends are good indicators of general body condition in marine mammals (Eberhardt and Siniff 1977). Previous assessments of body condition of free-ranging Steller sea lions (*Eumetopias jubatus*) have been limited to cross-sectional comparisons of average body conditions of populations at different time periods (e.g., Castellini and Calkins 1993; Calkins et al. 1998). Body condition trend assessments of individuals were not possible, as these animals were typically assessed by lethal means. Longitudinal growth trend data in individual animals across a geographic range and time sequence are lacking, primarily because of the logistical difficulties and hazards of working with this species.

Current methods to assess mass typically require physical contact with or manipulation of animals. For many large, shy, remote, endangered, or aquatic animals, such manipulations are frequently disruptive, dangerous, or logistically impossible, especially when repeated values are required. Here we present a novel technique to remotely estimate body mass of Steller sea lions, an endangered and difficult to access marine mammal species, using close-range convergent 3D photogrammetry.

Photogrammetry

Photogrammetry is the science of making measurements on photographs (Baker 1960). This technique was first used in the field of marine mammal science by Laws (1953) to measure body length of southern elephant seals (*Mirounga leonina*). Close-range two-dimensional photogrammetry has been used to estimate morphometric and body mass measurements of northern elephant seals (*Mirounga angustirostris*), southern elephant seals, and Hawaiian monk seals (*Monachus schauinslandi*) (Haley et al. 1991; Bell et al. 1997; McFadden 1999). Axillary and maximum girth measurements were made from two photos by tracing the outline of the animal in the front view photos. Body length was measured from the side view photos.

Photogrammetrically derived measurements were then regressed against known body masses to create predictive models to estimate body mass based solely on photographic information. The accuracy of these measurements depended greatly on the position of the animal (Bell et al. 1997) and on the position of the camera. Since the measurements were made on a two-dimensional plane, the camera had to be positioned exactly orthogonal to the animal with a scaling object of known length. Mass estimates based solely on photogrammetric models varied from ±4.7% (Southern elephant seals, Bell et al. 1997) to ±12.0%–25.0% (Northern elephant seals, Haley et al. 1991). Aerial stereophotogrammetry was used to measure morphometrics of bowhead whales (*Balaena mysticetus*) and fin whales (*Balaenoptera physalus*) (Cubbage and Calambokidis 1987; Ratnaswamy and Winn 1993). With a known camera focal length and data from a radar altimeter, photographs were accurately scaled for measurement of whale size with a total error of 10.0% for fin whales (Ratnaswamy and Winn 1993) and 1.7% for bowhead whales (Cubbage and Calambokidis 1987).

3D photogrammetry is a new computer-based application that can eliminate or reduce the traditionally constraining need for specific animal postures, camera orientations, and specific scaling objects. Multiple images taken at various angles are used to recreate the subject as a spatially accurate 3D computer model.

Materials and methods

Equipment

Images were taken with Nikon D100, Kodak Digital Science DC260, and Kodak DC120 digital still cameras. Two yardsticks (1 yard = 0.9144 m) as scaling objects were used to validate measurement accuracy. Photogrammetric calculations were performed with PhotoModeler Pro® Version 3.1b (EOS Systems, Inc., Vancouver, British Columbia) 3D photogrammetry software and Triangulated Mesh Volume Calculator (Scientific Software Solutions, Seward, Alaska). Statistical analyses were performed with SPSS® for Windows 10.0 (SPSS, Inc., Chicago, Illinois). Cameras were individually calibrated using the procedure and test pattern provided by PhotoModeler Pro®.

The subjects

A total of 53 Steller sea lions were photographed. Captive juvenile sea lions were photographed at the Vancouver Aquarium in Vancouver, British Columbia (n = 4) and the Alaska SeaLife Center (ASLC), Alaska (n = 3). Free-ranging juveniles (n = 46) were captured under permit in the Gulf of Alaska using an underwater SCUBA technique (Curgus et al. 2001) by the Alaska Department of Fish and Game (ADF&G) and the ASLC for a variety of other research projects. Ages of the sea lions ranged from 6 months to 7 years, with 31 female and 22 male individuals. Captive sea lions at the ASLC were photographed on 10 separate occasions between June and December 1999. The captive sea lions at the Vancouver Aquarium were photographed on three separate occasions (approximately every 4 months) from May 1999 to March 2000. Free-ranging sea lions were sampled only once.

© 2007 NRC Canada

Physical measurements of the animals

Morphometric measurements to the nearest 0.5 cm were taken prior to image collection. These measurements included standard dorsal length (the straight-line distance from the nose to the tip of the tail on a prone animal; see Jefferson et al. 1993), girth measurements of the head, neck, body immediately in front of fore flipper insertion, axillary (immediately after fore flipper insertion), midtrunk, and ankles. Captive sea lions were weighed on a large platform scale, whereas free-ranging sea lions were placed in cages or nets and suspended from an electronic load-cell scale. Animal masses (to the nearest 0.5 kg) were corrected for mass of the net and (or) cage.

Taking the pictures

Free-ranging sea lions were under full gas anesthesia when photographed. The three ASLC animals were photographed both under anesthesia and awake under behavioral control. The Vancouver Aquarium animals were only photographed awake under behavioral control.

Multiple sets of four time-synchronous pictures were taken by four photographers positioned around the subject under behavioral control. Both the animals and the photographers were repositioned after each set. The animal initially laid on its ventral surface with its midline straight and both sets of flippers extended outward from the body. The photographers were positioned around the animal at ~3 m distance and were aimed at roughly 45 degrees to the animal's midline (Fig. 1). Successive picture sets included more natural postures, such as laying with flippers tucked up against or under its body, laying on its side or with its midline curved, or in various "sitting" postures.

Pictures of anesthetized animals were taken sequentially by a single operator. The animals were positioned on their ventral sides with both sets of flippers either fully extended or laying against the body in a natural position. The dorsal midline was made as straight as possible while taking care not to stretch the animal. A minimum of two complete sets of pictures were taken of each animal, each set taken with a different camera at different angles.

Because cameras were hand-held and their exact positions were not known, the 3D modeling software required the use of scaling objects. A minimum of two yardstick scaling objects was used during each photo session. Care was taken so that at least one of these objects was visible in each photograph.

Creating 3D wireframes

The scaling objects in each image were also used as orientation points, which were marked and referenced across images and used by the software to orient the photographs in 3D space and to calculate the coordinates of each camera location. The images were scaled by selecting the ends of one of the yardsticks and defining the distance between those points as 0.9144 m. Accuracy of the scaling was confirmed by then using the software's measuring tool to measure the secondary scaling object and other objects of known size in the images. In a well-calibrated and oriented set of photographs, the measurements of these known objects were accurate to ±1.0%.

Sea lion models were created in a similar fashion as the orientation marks, except points on the animal were marked and referenced across images. The first points marked on the animal represented the end points of the morphometric standard length that had been physically measured. Points on the animal representing the remaining morphometric measurements were marked and referenced. Additional points on the animal were marked, referenced, and linked to create a final 3D wireframe (Fig. 2). The open wireframe was then converted to a surfaced object to create a completely enclosed virtual sea lion suitable for volume measurements for use in predicting body mass without the need for specific animal postures or camera locations. For this purpose, the flippers were not included in the final wireframe. The fore-flippers were truncated at their point of insertion, and hind-flippers were truncated at the ankles.

Fig. 1. Diagram of relative camera positions used to photograph the subjects. Actual distances between cameras and subject were greater and depended on size of subject.

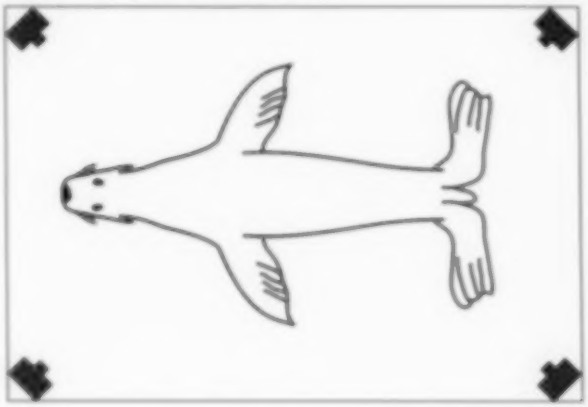

Photogrammetric measurements and data analysis

The PhotoModeler Pro® software calculates the distance between any two selected points of a 3D wireframe. Standard dorsal length was measured between the tips of the nose and tail. For axillary girth measurements, multiple points were marked along the axillary of the animal. This series of points was joined together by line segments and summed to estimate curvilinear length. The accuracy of this measurement could be increased with more points placed closer together, but there was a threshold where the addition of more points changed the length estimation by only a few millimetres.

The percent error of each standard length and axillary girth measurement was determined by the following equation:

$$(1) \qquad \%\,\text{Error} = [1 - (\text{Value}_{\text{photo}} / \text{Value}_{\text{physical}})] \times 100$$

The error values were log-transformed to meet assumptions of normality that were required for statistical testing; however, means and ranges are presented in the nontransformed format.

The standard dorsal length and the axillary girth measured from the wireframe were used to predict body mass based on the following regression equation derived from 390 animals by Castellini and Calkins (1993):

© 2007 NRC Canada

Fig. 2. Example of multiple time-synchronous images (*a*–*c*) and the completed 3D wireframe generated from these images (*d*).

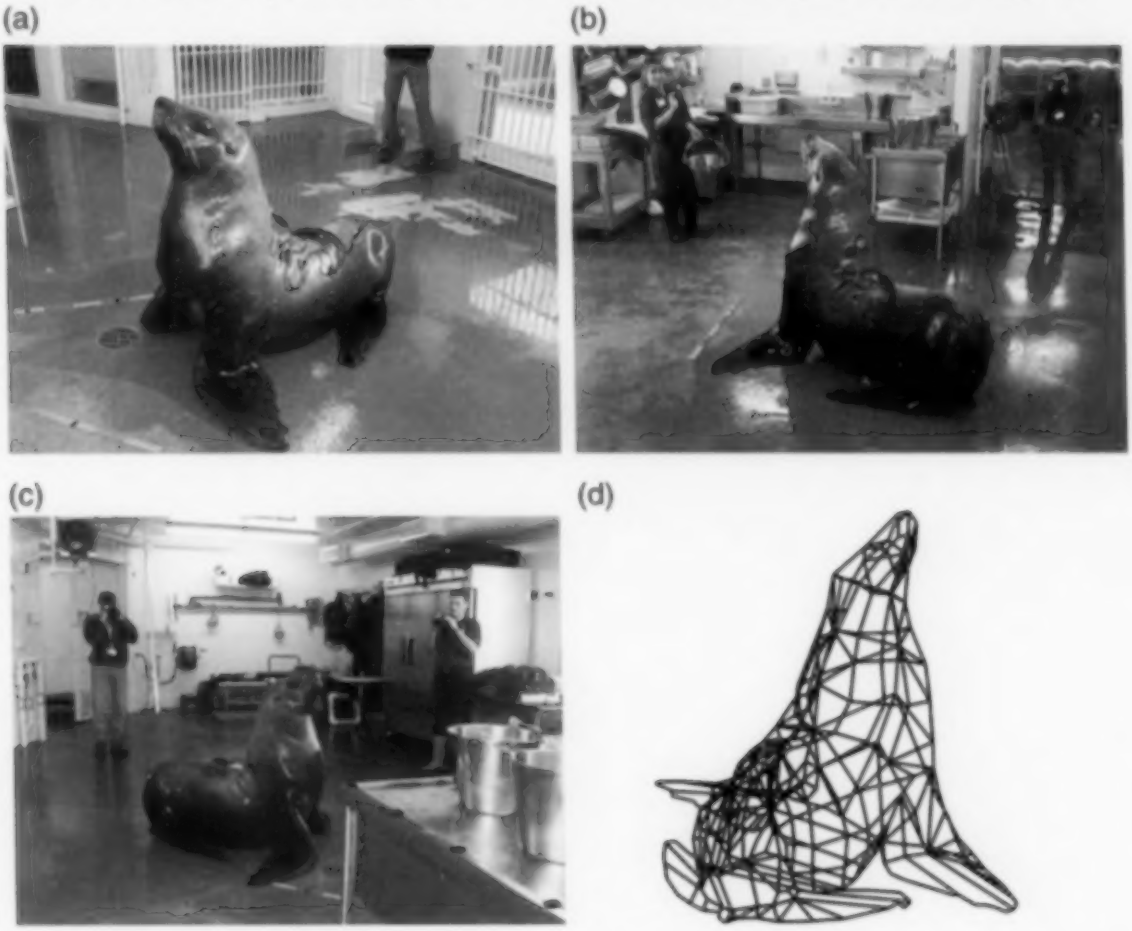

$$\text{Mass} = 4.96 \times 10^{-5} (\text{Length} \times \text{Girth}^2) \quad (2)$$

This relationship had a high correlation coefficient (r = 0.993), was significant ($P < 0.0001$), and had a predictive accuracy of ±0.98% (Castellini and Calkins 1993). Masses predicted using this equation were compared with the physically measured (PM) mass and predicted mass from PM morphometrics per eq. 2.

Triangulated Mesh Volume Calculator software was used to calculate the volume contained within each of the surfaced wireframes defined by 3D coordinates of the triangular surface planes to the nearest millilitre. While a commercially listed accuracy value was not available for this software, volume calculations of photogrammetrically created wireframes of simple geometric objects, such as cubes and pyramids of known volume, were accurate to ±1.0%. Volume calculations of photogrammetric wireframes of more complex objects were accurate to within ±4.3% (J.N. Waite, unpublished data). The reduced accuracy of volume calculations of rounded objects is likely an effect of the flat-faceted approximation of curved surfaces, which was a software limitation.

Paired *t* tests were used to evaluate the difference between photogrammetrically calculated (PC) morphometrics and PM morphometrics, the effect of flipper position on the accuracy of PC axillary girths, and the effect of body posture on the accuracy of PC standard lengths. A one-way analysis of variance (ANOVA) test and LSD multiple comparison tests were used to evaluate the effects of the level of fur wetness on the accuracy of PC axillary girths.

Linear regression analyses were performed on half of the free-ranging volume measurements and a single volume measurement from six of the captive animals, all randomly selected, to determine the best-fitting model for estimated PC body volume vs. PM body mass. Regressions were forced through the origin because of the expected relationship between an object with no volume and its mass. The final predictive equation was tested for accuracy by applying it to the remaining volume measurements.

Results

Accuracy of morphometrics

There was a significant difference between the PC and PM standard lengths (n = 138, $t_{[137]} = -6.054$, $P < 0.0005$) and axillary girths (n = 137, $t_{[136]} = 5.191$, $P < 0.0005$). PC

© 2007 NRC Canada

Table 1. Summary of average accuracy of morphometric measurements and mass estimations.

		% Error			
Measurement	*n*	Mean	Minimum	Maximum	95% CI
Standard length	138	2.5	0.0	16.2	±0.4
Axillary girth					
Overall	137	4.0	0.1	12.9	±0.5
Completely dry	25	7.4	1.0	12.9	±1.3
Damp	15	3.8	0.4	7.2	±1.1
Completely wet	14	3.1	0.1	8.4	±1.2
Morphometric-based mass					
Physically measured	137	6.5	0.2	19.4	±0.8
3D photogrammetrically measured	137	10.0	0.1	41.7	±1.3
Volume-based mass	50	10.0	0.1	33.2	±1.7

Note: CI, confidence interval.

standard lengths and axillary girths were within 2.5% and 4.0%, respectively, of PM dimensions (Table 1). Overall, PC standard lengths were shorter, whereas axillary girths were larger, than PM dimensions. Several length and girth measurements were repeated on the same animals using different sets of photographs to analyze the effect of body position on the accuracy of PC measurements.

Effect of posture

An independent researcher reviewed each of the photo sets and categorized the body posture of the sea lion as either ideal or poor. Ideal postures were those in which the sea lion was laying straight and still. Subjects with poor body posture were those lying in a position from which an accurate standard length could not be physically measured nor would such a measurement normally be attempted. Some examples are curved midlines, turned heads, and tucked-under hind ends. The mean standard length errors for wireframes with ideal and poor body postures differed significantly at 1.9% and 3.8%, respectively ($t_{[136]} = -4.348$, $P = 0.002$).

The position of the front flippers was analyzed for possible effects on axillary girth errors. The mean axillary girth error was 4.6% ± 3.4% ($n = 94$) for sea lions with their flippers positioned away from their body and 2.8% ± 2.3% ($n = 43$) for sea lions with their front flippers tucked up against their body. This difference was also significant ($t_{[135]} = 3.277$, $P = 0.001$).

Effect of fur wetness

A random subset of sea lion image sets ($n = 52$) were subjectively classified by an independent researcher as being completely wet, completely dry, or damp. Fur wetness had no effect on PC standard length measurements, but there was a significant difference in mean PC axillary girth percent errors between different levels of fur wetness ($F_{[2,51]} = 9.107$, $P < 0.0005$; Table 1). Further multiple comparison testing indicated a significant difference in mean percent error between completely wet animals and completely dry animals (LSD, $P < 0.0005$) and between completely dry animals and damp animals (LSD, $P = 0.007$). There was no significant difference between completely wet and damp animals.

Accuracy of mass estimates

Body mass was predicted based on both PC and PM morphometrics using eq. 2. Masses predicted using PC morphometrics were within 10.0% ± 7.9% (95% confidence interval (CI): ±1.3%) of PM mass. Masses predicted using PM dimensions were accurate to 6.5% ± 5.0% (95% CI: ±0.8%) of the PM masses.

Photogrammetrically predicted mass per eq. 2 and PC mass ($n = 137$, $t_{[136]} = 6.983$, $P < 0.0005$) and photogrammetrically predicted mass and physically predicted mass per using eq. 2 ($n = 137$, $t_{[136]} = 5.310$, $P < 0.0005$) differed consistently by small amounts.

The volumes for each of the wild sea lions were calculated once, and the volumes for the captive sea lions were calculated multiple times from image sets taken several weeks to several months apart for a total of 68 unique volume measurements. A linear regression with half of the free-ranging volume measurements and a single volume measurement from six of the captive animals, all randomly selected ($n = 29$), resulted in the following predictive equation:

(3) Mass (kg) = 1.3 × Volume (L)

This relationship had a high coefficient of determination (adjusted $r^2 = 0.996$) and was significant ($P < 0.0001$) (Fig. 3). Body masses predicted using eq. 3 on the remaining volume measurements were accurate to within an average of 9.0% ± 7.2% (95% CI: ±1.7%) of PM mass.

Captive ASLC sea lions were measured multiple times over a 6-month period during which they participated in an unrelated study with a diet change every 6 weeks that affected their body fat content and body density. Such forced changes in body composition should introduce more variability in body density within the captive animal replicates than between wild animals sampled once at the same time of the year. The goal of this project is the assessment of the suitability of body mass estimation based on 3D photogrammetry and specifically body volume, not to make inferences on a sampled population. Each set of photogrammetric measurements are based on a newly collected set of pictures, and we are therefore treating the replicate samples as independent samples during validation of the predictive equation.

Discussion

The use of 3D photogrammetry to estimate morphometrics and predict body mass is an improvement over current two-dimensional techniques by reducing the requirements for specific animal postures and camera locations. 3D

© 2007 NRC Canada

Fig. 3. Fitted line plot of mass vs. volume (n = 29, adjusted r^2 = 0.996, slope = 1.3, intercept = 0).

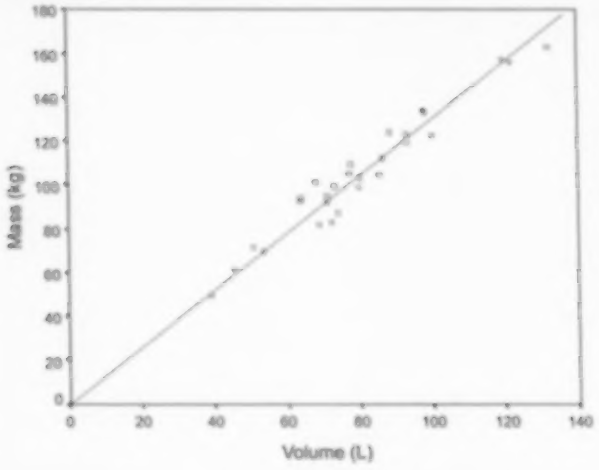

photogrammetry is an accurate way to measure standard lengths of Steller sea lions that are lying perfectly straight and flat, comparable with the level of accuracy that can be achieved with physical measurements. 3D photogrammetry is also an accurate way to measure the axillary girths of Steller sea lions. Mass predictions based on PC morphometrics are comparable with mass predictions based on PM morphometrics, but have the desirable advantage of being nondisturbing.

Body posture

Body posture was the primary factor affecting the calculated accuracy (% error) of PC standard length measurements. To accurately measure the standard length of a sea lion, it must be laying perfectly flat and straight, which was achieved with anesthetized animals. However, the captive, alert sea lions often were not as cooperative and usually had some degree of curvature to their midline. PC standard lengths could not be accurately obtained from animals in sitting postures. Accuracy of PC axillary girth measurements was not affected by midline curvature; however, measurement accuracy was affected by the position of the front flippers (i.e., either tucked up against or extended away from their body).

Fur wetness

Calculated accuracy of PC axillary girth measurements was most influenced by the dryness of the fur. When physical measurements are made, dry fur is compressed by the measuring tape such that the measurement is being made flush with the body. Photogrammetric girth measurements could not recreate this accurately, thus substantially inflating the measurement. As little as 0.5 cm of dry fur could increase the girth measurement by up to 3.5%, and fur depth ranged from 0.5 to 1.5 cm. Fur wetness had no effect on the accuracy of PC standard length measurements.

Physical measurements

Calculated accuracy of photogrammetric measurements in general was most influenced by the methods and accuracy of the physical measurements themselves. ASLC and the Vancouver Aquarium staff measured the standard length of their sea lions by asking them to target to an object while their tails were manually extended horizontally. The tails in the photographs were hanging naturally. Therefore, depending on the length of the tail and angle at which it hangs, the photogrammetrically measured length would be shorter than the physical measurement. Overall, standard length measurements were underestimated by an average of 3.8 cm using the 3D photogrammetric method.

While targeting, the captive animals often stretched their necks out to touch the target with their nose. This behavior had been encouraged at the ASLC, and measurements were taken while the animal was fully extended. Vancouver animals had been trained against this behavior; however, some neck stretching did occur. This behavior may have affected the calculated percent error of photogrammetric measurements only slightly because the same neck stretching behavior occurred while the animals were being held at a target during the photo sessions.

Measurements on the captive sea lions were made by several different members of the staff and not by the same person each time, which introduces the possibility of error due to variations in measurement techniques (up to 6.5 cm; J.N. Waite and J.-A.E. Mellish, unpublished data). Length measurements of the free-ranging sea lions were made by holding a measuring tape over the top of the animal instead of on the table next to it and then estimating where the tip of the tail was located, which could be up to 25 cm below the tape.

The calculated accuracy of the PC axillary girth measurements could also be affected by how tight the measuring tape was pulled around the animal while physically measuring axillary girth. The tighter the tape is pulled, the more the soft belly tissue is compressed, resulting in a girth measurement up to several centimetres smaller than the actual girth. Respiration stage, both during physical measurement and image acquisition, would also affect the girth measurements (i.e., measurements would be larger during inhalation).

Predicting body mass from morphometrics

The accuracy of predicted body mass using eq. 2 depended on the accuracy of the standard length and axillary girth measurements and on the accuracy of the actual equation. The body mass of each sea lion was predicted by eq. 2 using both PC and PM dimensions. Mass predicted from the PC measurements were within 10.2% of the actual mass; however, the mass predicted using PM measurements was only accurate to within 9.0% of the actual mass on average. Since using PC measurements adds only 3.5% to the average error and only 0.5% to the 95% CI, eq. 2 would be a suitable way to estimate body mass in conjunction with 3D photogrammetry techniques if the sea lion is laying in an ideal body posture with wet fur. The masses of sea lions in sitting postures cannot be determined using this method.

Predicting body mass from volume

The accuracy of the body masses predicted from body volume was comparable with the masses predicted using eq. 2. The 95% CI for the mean difference between predicted and actual body mass (±1.7%) was also comparable

© 2007 NRC Canada

with the 95% CI from eq. 2. The 95% CI was narrower using this method than with current two-dimensional techniques, which ranged from ±4.7% to ±25.0% (Haley et al. 1991; Bell et al. 1997). Since these mass estimates are not dependent on standard length and axillary girth measurements, the mass of sea lions in any posture could be calculated, potentially eliminating one of the largest hurdles of photogrammetric mass estimation.

Some of the factors that may have contributed to the error are similar to those that affected the accuracy of PC morphological measurements. It was shown that the PC axillary girths were significantly larger for dry animals than for wet animals. As a consequence, PC body volumes would also be larger for dry animals than for wet animals. This could not be adequately analyzed because of the small sample size of wet and dry animal volumes. An additional study should be conducted wherein the volume of individual sea lions are calculated when each animal is wet and then when dry to examine this relationship.

Variations in health and diet (stage of weaning) caused the body composition of the free-ranging pups to vary widely. Measurements of blubber depths ranged from 5 to 21mm between animals of the same age (J.N. Waite, personal observation). Many of the possible effects listed above might be factored out in the regression analysis if a large enough sample size is used.

The factor that may have affected the mass estimates the most is the accuracy of the PC volume measurements themselves. Since the actual volume of the individual sea lions were not known, it was not possible to calculate the accuracy of the PC volumes. Objects of known volume were modeled, and it was found that the volume estimates were accurate to within 4.3% of the actual volume. However, the shape of these objects were not as complex as a sea lion's body, and the wireframes were much more detailed than the wireframes used to estimate the sea lion volumes.

The average accuracy of the volume-based mass predictions in this project was within 9.0% of PM mass, comparable with PC and PM morphometrics-based mass predictions. Volume-based mass predictions are subject to fewer restrictions with respect to body posture than mass predictions based on other morphometric measurements. Since mass estimates based on these two photogrammetric methods are comparable, it is recommended that researchers use the morphometric-based prediction equation when their study sea lions are lying in a position that facilitates accurate PC standard length and axillary girth measurements. However, when such conditions cannot be met, mass prediction using volume-based calculations would be more appropriate.

If animals are captured and tranquilized and equipment is not available to directly weigh them, 3D photogrammetry using hand-held cameras and scaling objects could be used to estimate body mass. For long-term monitoring and trend analysis, remotely controlled, fixed-location cameras should be used to eliminate the need for scaling objects. Fixed installations of remote controlled cameras are being developed for long-term monitoring and body mass trend analyses in many inaccessible regions (Plankis et al. 2007). The use of fixed camera installations also eliminates the need for scaling objects.

Potential applications

Morphometrics and mass estimation using 3D photogrammetry is potentially a very valuable tool in the study of not only Steller sea lions, but also other endangered, shy, fragile, or otherwise inaccessible species or when direct handling would be undesirable. This technique has the potential for use in an underwater setting on aquatic species where traditional mass measurements cannot be made. For example, we successfully applied this method to two species of fish, sand seatrout (*Cynoscion arenarius*) and Gulf menhaden (*Brevoortia patronus*), as well as one specie of reptile, Chinese alligator (*Alligator sinensis*). Accuracies of the resulting predictive equations were ±5.6% (n = 30), ±3.4% (n = 32), and ±4.8% (n = 18), respectively.

3D photogrammetry systems would allow researchers to remotely monitor large numbers of sea lions over a long period of time to establish growth trends of individuals and populations from the rapidly disappearing western stock that could be compared with populations from the stable eastern stock. Growth trends of individuals, especially pups and young juveniles, could be compared with other remotely observed behaviors, such as measures of maternal investment and foraging trip durations. Growth trends of entire populations could be analyzed for a correlation with commercial fishing harvests, man-made or natural disasters, or climate-related events, contributing to our understanding of the decline of these rapidly disappearing marine mammals.

Acknowledgements

This project was supported by grant No. 1998-0244-009 from the National Fish and Wildlife Foundation to M.H., as well as through equipment, animal access, and husbandry support by the National Marine Mammal Laboratory (NMFS), the ASLC, the Marine Mammal Research Unit at The University of British Columbia, and the Vancouver Aquarium. We thank T. Loughlin (NMFS), as well as husbandry and veterinary staff at the ASLC and Vancouver Aquarium. Work was conducted under permits 881-1443 and 881-1668 issued to the ASLC under the US Marine Mammal Protection Act (MMPA) and the US Endangered Species Act (ESA) and was permitted by both ASLC's and Texas A&M University's Institutional Animal Care and Use Committees.

References

Allen, C.R., Garmestani, A.S., Havlicek, T.D., Marquet, P.A., Peterson, G.D., Restrepo, C., Stow, C.A., and Weeks, B.E. 2006. Patterns in body mass distributions: sifting among alternative hypotheses. Ecol. Lett. **9**(5): 630–643.

Baker, J.R. 1960. Elements of photogrammetry. The Ronald Press Company, New York.

Bakker, V.J., and Kelt, D.A. 2000. Scale dependent patterns in body size distributions of neotropical mammals. Ecology, **81**(12): 3530–3547.

Bell, C.M., Hindell, M.A., and Burton, H.R. 1997. Estimation of body mass in the southern elephant seal, *Mirounga leonina*, by photogrammetry and morphometrics. Mar. Mamm. Sci. **13**: 669–682.

Benson, J.F, Chamberlain, M.J., and Leopold, B.D. 2006. Regulation of space use in a solitary felid: population density or prey availability? Anim. Behav. **71**: 685–693.

© 2007 NRC Canada

Calkins, D.G., Becker, E.F., and Pitcher, K.W. 1998. Reduced body size of female Steller sea lions from a declining population in the Gulf of Alaska. Mar. Mamm. Sci. **14**: 232–244.

Carbone, C., Cowlishaw, G., Isaac, N., and Rowcliffe, J. 2005. How far do animals go? Determinants of day range in mammals. Am. Nat. **165**(2): 290–297.

Castellini, M.A., and Calkins, D.G. 1993. Mass estimates using body morphology in Steller sea lions. Mar. Mamm. Sci. **9**: 48–54.

Clutton-Brock, T.H. (*Editor*). 1988. Reproductive success. Studies of individual variation in contrasting breeding systems. The University of Chicago Press, Chicago, Ill.

Cubbage, J.C., and Calambokidis, J. 1987. Size-class segregation of bowhead whales discerned through aerial stereophotogrammetry. Mar. Mamm. Sci. **3**: 179–185.

Curgus, C.S., McAllister, D., Raum-Suryan, K., Pitcher, K., and Cunningham, W. 2001. Live capture method for Steller sea lions using SCUBA. *In* Abstracts of the 14th Biennial Conference on the Biology of Marine Mammals, Vancouver, Canada, 20 November – 3 December 2001. Society for Marine Mammalogy, San Francisco, Calif. p. 51.

Eberhardt, L.L., and Siniff, D.B. 1977. Population dynamics and marine mammal management policies. J. Fish. Res. Board Can. **34**: 183–190.

Ferguson, S.H., Higdon, J.W., and Lariviere, S. 2006. Does seasonality explain evolution and maintenance of delayed implantation in the family Mustelidae (Mammalia: Carnivora)? Oikos, **114**(2): 249–256.

Haley, M.P., Deutsch, C.J., and LeBoeuf, B.J. 1991. A method for estimating mass of large pinnipeds. Mar. Mamm. Sci. **7**: 157–164.

Harding, K.C., Fujiwara, M., Axberg, Y., and Harkonen, T. 2005. Mass-dependent energetics and survival in harbour seal pups. Funct. Ecol. **19**(1):129–135.

Holand, Ø., Mysterud A., Røed, K.H., Coulson, T., Gjøstein, H., Weladji, R.B., and Nieminen, M. 2006. Adaptive adjustment of offspring sex ratio and maternal reproductive effort in an iteroparous mammal. Proc. R. Soc. Lond. B Biol. Sci. **273**(1584): 293–299.

Horning, M., and Trillmich, F. 1997. Ontogeny of diving behaviour in the Galápagos fur seal. Behaviour, **134**: 1211–1257.

Horning, M., and Trillmich, F. 1999. Lunar cycles in diel prey migrations exert stronger effect on diving of juveniles than adult Galápagos fur seals. Proc. R. Soc. Lond. B. Biol. Sci. **266**: 1127–1132.

Isaac, J.L., Krockenberger, A.K., and Johnson, C.N. 2005. Adaptive sex allocation in relation to life-history in the common brushtail possum, *Trichosurus vulpecula*. J. Anim. Ecol. **74**: 552–558.

Jefferson, T.A., Leatherwood, S., and Webber, M.A. 1993. Marine mammals of the world. FAO Species Identification Guide. Food and Agriculture Organization (FAO), Rome, Italy.

Jetz, W., Carbone, C., Fulford, J., and Brown, J.H. 2004. The scaling of animal space use. Science (Washington, D.C.), **306**(5694): 266–268.

Kooyman, G.L. 1989. Diverse divers. Springer Verlag, Heidelberg, Germany.

Laws, R.M. 1953. The elephant seal (*Mirounga leonina* Linn.). I. Growth and age. Falkl. Isl. Depend. Surv. Sci. Rep. **8**: 1–61.

Makarieva, A.M., Gorshkov, V.G., and Li, B.-L. 2005. Why do population density and inverse home range scale differently with body size? Implications for ecosystem stability. Ecological Complexity, **2**(3): 259–271.

McElligott, A.G., Naulty, F., Clarke, W.V., and Hayden, T.J. 2003. The somatic cost of reproduction: what determines reproductive effort in prime-aged fallow bucks? Evol. Ecol. Res. **5**(8): 1239–1250.

McFadden, K. 1999. Photogrammetry as a tool for estimating size and condition in the Hawaiian monk seal (*Monachus schauinslandi*), the harbor seal (*Phoca vitulina*), and the northern elephant seal (*Mirounga angustirostis*). M.Sc. thesis, Department of Wildife and Fisheries Science, Texas A&M University, College Station, Tex.

Peters, R.H. 1983. The ecological implications of body size. Cambridge University Press, Cambridge, UK.

Plankis, B.J, Horning, M., Ponto, N., and Brown, L.K. 2007. Designing a dependable and fault-tolerant semiautonomous distributed control data collection network with opportunistic hierarchy. IEEE J. Oceanic Eng. **32**(2). doi:10.1109/JOE.2006.880390.

Ratnaswamy, M.J., and Winn, H.E. 1993. Photogrammetric estimates of allometry and calf production in fin whales, *Balaenoptera physalus*. J. Mammal. **74**: 323–330.

Schmidt-Nielsen, K. 1984. Scaling: Why is animal size so important? Cambridge University Press, Cambridge, UK.

© 2007 NRC Canada

An "experiment" on effort allocation of fishing vessels: the role of interference competition and area specialization

Jan-Jaap Poos and Adriaan D. Rijnsdorp

Abstract: A temporarily closed area established to protect spawning Atlantic cod (*Gadus morhua*) in the North Sea allowed us to study the response of the Dutch beam trawl fleet exploiting common sole (*Solea solea*) and plaice (*Pleuronectes platessa*). A number of vessels left the North Sea 1 month earlier than the normal seasonal pattern. The vessels that continued fishing in the North Sea were concentrated in the remaining open areas. In the first week after the closure, the catch rate decreased by 14%, coinciding with an increase in crowding of 28%. Area specialisation affected the response of individual vessels because vessels without prior experience in the open areas showed a larger decline in catch rate compared with vessels that previously fished in these open areas and were more likely to stop fishing during the closed period. The decrease in catch rate in response to the increase in competitor density allowed us to estimate the strength of the interference competition.

Résumé : Une zone fermée temporaire établie dans la mer du Nord pour protéger les morues franches (*Gadus morhua*) durant la fraye nous a permis d'étudier la réaction de la flotte hollandaise de chalutiers à perche qui pêchent la sole (*Solea solea*) et la plie (*Pleuronectes platessa*). Plusieurs navires ont quitté la mer du Nord un mois avant le calendrier saisonnier normal. Les navires qui ont poursuivi la pêche dans la mer du Nord se sont concentrés dans les zones ouvertes restantes. Dans la première semaine après la fermeture, le taux de capture a diminué de 14 %, ce qui coïncidait avec une augmentation de 28 % du taux d'encombrement. La spécialisation pour une zone particulière a affecté l'effet sur les différents navires, car les navires sans expérience préalable des zones ouvertes ont connu un déclin plus important de leur taux de capture par comparaison aux navires ayant déjà pêché dans ces zones ouvertes; les navires sans expérience préalable étaient aussi plus susceptibles de cesser la pêche durant la fermeture. Le déclin du taux de capture en réaction à l'augmentation de la densité des compétiteurs nous permet d'estimer la force de la compétition d'interférence.

[Traduit par la Rédaction]

Introduction

Fisheries management generally does not take into account the response of the fisheries to management measures (Holden 1994), which may lead to unforeseen changes in the exploitation pattern, reducing the effectiveness of the management of the target species, and unexpected implications for the sustainable use of the marine resources (Dinmore et al. 2003). To be able to include the response of fisheries to management, knowledge about the processes underlying spatial and temporal allocation of fishing effort is required. This is of paramount importance as a scientific basis for effective fisheries management (Gordon 1954; Palohеimo and Dickie 1964; Gillis 2003).

The dynamics of the spatial distribution of fishing vessels may be studied using the behavioural ecological theory of optimal foraging (Abrahams and Healey 1993), which has been successfully applied to fisheries problems (Gillis et al. 1993; Rijnsdorp et al. 2000*b*; Gillis 2003). One of the optimal foraging theories regarding spatial allocation of foragers is known as the ideal free distribution (IFD; Fretwell and Lucas 1970), which predicts how foragers will distribute themselves in relation to their food resources. The IFD assumes that individual foragers (*i*) are "ideal", meaning that they are able to choose the area that maximizes fitness rewards, and (*ii*) are "free", meaning that they experience no cost of moving between feeding areas. Also, all foragers are assumed equal. In its simplest form where no interactions occur among foragers, all foragers will aggregate in the best feeding area. However, if the intake rate is affected by the presence of other foragers by interference competition (Hassell and Varley 1969; van der Meer and Ens 1997), for instance, owing to interactions among foragers (Goss-Custard 1977) or a response of the prey to the density of foragers (Ruxton 1995; Stillman et al. 2000), foragers will distribute themselves over the resources. Hence, the occurrence

Received 9 December 2005. Accepted 25 July 2006. Published on the NRC Research Press Web site at http://cjfas.nrc.ca on 27 February 2007.
J19039

J.-J. Poos[1] and A.D. Rijnsdorp. Wageningen Institute for Marine Research and Ecological Studies (IMARES), P.O. Box 68, 1970 AB IJmuiden, the Netherlands.

[1]Corresponding author (e-mail: janjaap.poos@wur.nl).

 doi:10.1139/F06-177 © 2007 NRC Canada

of interference competition has the potential to strongly affect the spatial distribution of foragers (Sutherland 1983; van der Meer and Ens 1997).

In contrast to animal studies in which the interference interactions among foraging individuals can be observed directly (Goss-Custard 1980), interference competition among fishing vessels is more difficult to study quantitatively. Although the direct interactions among vessels can potentially be quantified (Gillis 1999), the interaction between fishing vessels and their fish resources is difficult to estimate. A decrease in the catch rate of fishing vessels with increasing number of vessels is insufficient evidence as it may reflect interference competition; however, it may also be due to the local depletion of the fisheries resource (exploitation competition).

The evidence for interference competition among fishing vessels is mainly inferred from observational studies: from equal catch rates among vessels exploiting different fishing grounds or from a change in catch rate following a change in vessel density (Hilborn and Ledbetter 1979; Healey and Morris 1992; Gillis et al. 1993) To our knowledge, only two studies provided "experimental" evidence for interference competition. Abrahams and Healey (1993) showed that vessel density had a significant influence on the catch rate of Chinook salmon (*Oncorhynchus tshawytscha*) and spiny dogfish (*Squalus acanthias*), but not on coho salmon (*Oncorhynchus kisutch*). Rijnsdorp et al. (2000*b*) showed that the catch rate of flatfish (order Pleuronectiformes) significantly increased during a week when part of the fleet remained in harbor for religious reasons.

The IFD offers a robust starting point for the analysis (Milinski and Parker 1991; Gillis 2003), although the assumptions of the IFD of perfect knowledge, equality among fishing vessels, and no cost of movement among fishing areas will certainly be violated in the real world. Fishers will differ in their knowledge about the location of trawlable grounds and the distribution of the prey (Hilborn and Ledbetter 1979; van Densen 2001). Bottom trawl fisheries, especially, are restricted to areas with soft sediment where the chances of gear loss are small (Rijnsdorp et al. 1998; Piet et al. 2000). Also, fishing effort allocation will be related to the distance to the home port (Sampson 1991).

The process underlying the spatial dynamics of fishing vessels is generally inferred from the observed dynamics of the system. These observational studies, however, do not allow us to draw unequivocal conclusions on the processes involved. Although experimental research on effort allocation is generally not feasible (but see Abrahams and Healey (1993)), changes in the management regime may provide an opportunistic experiment. Thus the response of fishermen with respect to catch rates and effort distribution following an area closure may provide answers to the mechanisms involved in effort distribution and their strength.

In this paper, we analyse the response of the Dutch beam trawl fleet to a temporarily closed area focussing on the effect of interference competition and providing an empirical estimate of the strength of the interference competition in a fisheries context. Further, we address the null hypothesis that fishers who lack knowledge of fishing in the remaining open areas will experience lower catch rates than fishers with local knowledge. Insight into these factors will allow us to better predict the response of fishing fleets to management measures.

Materials and methods

Fishing fleet

The Dutch beam trawl fleet targets common sole (*Solea solea*) and plaice (*Pleuronectes platessa*) (Daan 1997), towing demersal gears fitted with chains at speeds between 5 and 7 nautical miles per hour. Bycatches are comprised of other flatfish species such as turbot (*Scophthalmus maximus*), brill (*Scophthalmus rhombus*), and dab (*Limanda limanda*) and roundfish species such as Atlantic cod (*Gadus morhua*) and whiting (*Merlangius merlangus*). The fishing effort of the fleet shows a patchy distribution owing to the distribution of the target species and the physical characteristics of the sea bed (Rijnsdorp et al. 1998). Trips typically start on Monday and end on Friday, during which there is almost continuous fishing. The fleet is comprised of two components: small (≤300 horsepower (hp)) and large (>300 hp) beamers. The small vessels are allowed to fish in the coastal zone, from which the large beam trawlers with higher engine power are banned. Vessels in the northern harbours utilise beam trawls rigged with tickler chains and generally have engine powers up to 2000 hp. In the southern harbours, the large beamers typically use chain mats to fish the rough grounds in the southern North Sea, requiring engine powers up to 4500 hp.

Area closure in 2001

To reduce the fishing impact during the spawning period of the heavily depleted North Sea cod stock, two areas in the North Sea were closed for trawling ("closed north" and "closed south"; Fig. 1) between 15 February (Thursday, week 7) and 30 April (Monday, week 18) 2001. In this paper, the closed period is defined as weeks 8 to 17. With 43% of the fishing effort in the reference years, the two closed areas encompass the main fishing grounds of the Dutch beam trawl fleet. The remaining two areas open for fishing during the closure are referred to as "open north" and "open south". In addition to the area closure, an effort reduction program was set up by the Dutch Ministry of Agriculture, Nature Conservation and Food Safety (LNV). This program encompassed a voluntary reduction in fishing effort by staying in port for 3 weeks in April. The majority of the large beam trawl vessels participated in the program.

The management measures in 2001 mainly affected the fleet of large beam trawlers, because the small beamers were allowed to fish in the coastal waters (12-mile zone and plaice box). Hence, our study was restricted to the fleet of large beam trawlers representing approximately 50% of the fleet.

Analysis

The analysis is based on the EU logbook data of individual vessels available from the Dutch national catch and effort database. This database comprises data per trip on landings (kg) by commercial fish species, fishing effort (days at sea), ICES rectangle fished (boxes of 30′ latitude × 1° longitude), engine power, and fishing gear. The patterns in effort allocation and catch rates before (1 January –

© 2007 NRC Canada

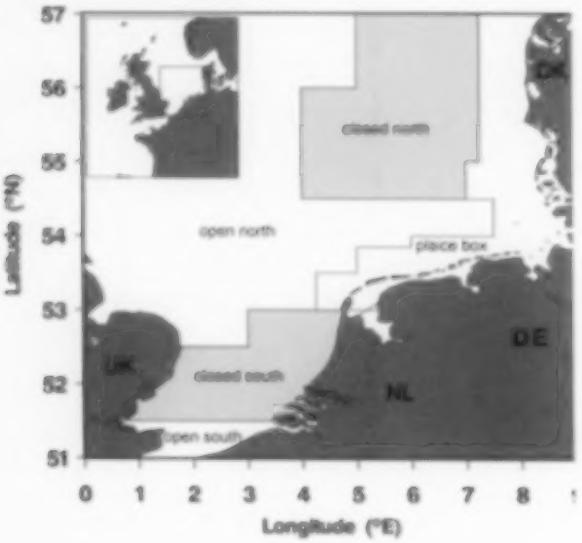

Fig. 1. Overview of the open and closed areas in the North Sea. The closed areas, indicated by shading, were closed between 15 February and 30 April 2001 to protect spawning Atlantic cod (*Gadus morhua*). The plaice box is permanently closed for demersal trawl fisheries such as beam trawling for vessels with engine power exceeding 300 hp.

15 February 2001), during (15 February – 30 April 2001), and after (1 May – 15 June 2001) the closure were compared with the average patterns in the reference years 1999, 2000, 2002, and 2003. The area closure in 2001 started in week 7, preceded by the annual week of prayer, during which part of the fleet stays in port for religious reasons.

Fishing effort was expressed as the number of days at sea and was spatially allocated per ICES rectangle. In addition, the number of fishing trips per week allocated in the different open and closed areas was calculated. The average competition that an individual fishing vessel experiences was quantified by calculating using Lloyd's index of mean crowding (m^*) (Lloyd 1967; Pielou 1969):

$$m^* = \frac{\sum f_j^2}{\sum f_j} - 1$$

where f_j is the number of vessels in the jth ICES rectangle. This index expresses the number of vessels with which a vessel shares a fishing area (ICES rectangle) and depends on the total effort. A high m^* value indicates a high level of co-occupation experienced by the individual vessels. The weekly mean crowding indices were calculated for the four study areas, including all recorded fishing trips (Fig. 1).

For the analysis of the effects of fishing effort on catch rates in the open areas, catch rates from vessels that were not present throughout the entire period were excluded to prevent a possible effect of a change in the composition of the fleet on the catch rate.

In both open areas, different selection criteria were set to the engine power of vessels to increase the homogeneity of the sample. For the open north area, only vessels with engine powers up to 2500 hp were included, whereas for the open south area, only vessels ranging from 2400 to 4500 hp were used, representing the chain-mat beamers that generally fish in this area. These selections result in a study fleet consisting of 124 vessels present throughout the study period, of which 93 vessels have fished in the areas open north versus 13 vessels in the open south during the closure. Based on the number of days at sea recorded in the open areas in the 3 years prior to the area closure, the fleet was further segregated into immigrant vessels (<50 days at sea), intermediate vessels (50–200 days at sea), and resident vessels (>200 days at sea; Fig. 2). Resident vessels thus have spent more time in the respective open areas in previous years and may therefore be more specialized in fishing its grounds. Using this classification, in the open north area, 10 vessels are classified as immigrant in comparison with 70 residents. In the open south area, six vessels were immigrant and seven were residents.

The effect of management measures on the effort allocation is likely to be mediated by the skipper's response to changes in revenue rather than weight of the catch of individual species. The catch rate was therefore expressed in monetary units (euros) combining the target species to a value per unit effort (VPUE):

$$\text{VPUE} = \frac{\sum C_s P_s}{f}$$

where C_s is the catch (kg) of species s, being sole, plaice, or cod, and P_s is the corresponding price (euros per kg). The fishing effort, denoted by f, is expressed in days at sea. Because the VPUE of beam trawl vessels is strongly affected by the engine power (hp) of the vessel (Rijnsdorp et al. 2000*a*), standardization was applied using a general linear model (GLM) to fit the following regression model:

$$\log_{10}(\text{VPUE}) = \alpha + \beta \log_{10}(\text{hp}) + \varepsilon$$

Normal distribution of the model was checked using visual inspection of the residuals.

Interference and exploitation competition

The catch rate on a fishing ground is determined by the density of fish and the interference among fishing vessels. The density of fish on a fishing ground will depend on the local biomass and change in time due to (*i*) immigration and emigration, (*ii*) removals by fishing, (*iii*) body growth, and (*iv*) natural mortality. Over short time periods, e.g., weeks, the changes in local biomass will be mainly determined by the combined effects of immigration and emigration and removals by fishing as natural mortality and body growth will be negligible.

Because interference will act immediately whereas exploitation will act gradually, interference and exploitation competition can be disentangled if a sudden change in vessel density occurs. In a situation without interference, but with exploitation competition, an increase in vessel density will result in a steeper slope of the catch rate. In a situation with interference and exploitation competition, an increase in vessel density results in a sudden decrease in catch rate owing to the lower efficiency resulting from the increased interfer-

© 2007 NRC Canada

Fig. 2. The distribution of previous fishing effort (1998 to 2000) allocated by individual vessels fishing in the two open areas during the closure in 2001. The vertical broken lines indicate the separation between the vessels categorized as immigrants, intermediate, and residents. The intermediate group is not used for further analysis.

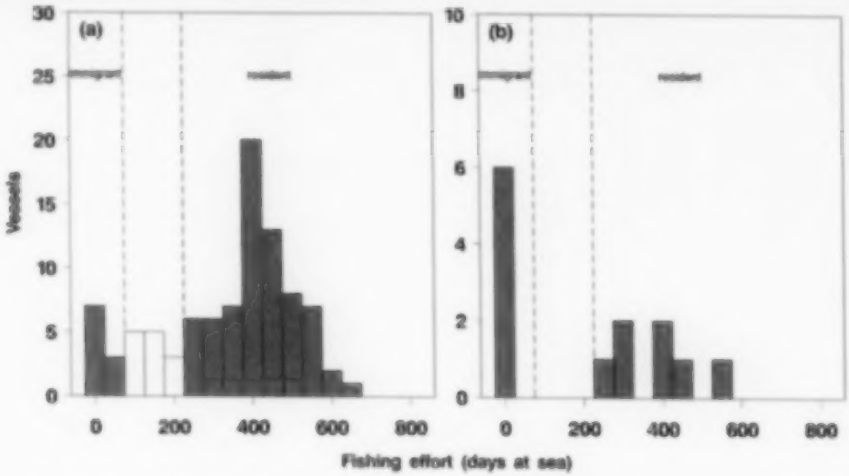

ence and an increase in the slope of the catch rate owing to the higher exploitation rate.

The sudden change in catch rate due to interference at the time of area closure and the change in the slope of the catch rate with time reflecting the net result of fisheries removals (exploitation) and the immigration–emigration from the study area was estimated with the following GLM:

$$\log_{10}(\text{VPUE}) = \mu + \alpha\,\text{week} + \beta\,\text{week closure} + \text{closure} + \log_{10}(\text{engine power}) + \varepsilon$$

where the closure parameter is a class variable that is set to 1 for those weeks when the area closure was in effect and set to 0 otherwise. The regression coefficients α and β estimate the slope in catch rate over a number of weeks. The interaction between the slope and the closure allows for a change in the slope during the closure. The effect of the class variable closure on the catch rate allows estimation of a change in the catch rates resulting from the area closure. The engine power of the vessel is added to the model to account for its effect on catch rates. Finally, ε is the error term of the model. The model was fitted to the data for each year separately from weeks 1 to 13. To exclude effects of area specialization owing to, for instance, differences in local knowledge, only resident vessels were included in the analysis.

Fig. 3. Number of fishing trips by Dutch beam trawl vessels (>300 hp) by week: number of trips in the North Sea in 2001, □; average number of trips in the reference years, ■; number of trips outside the North Sea in 2001, ○; average number of trips in the reference years, ●. The vertical bars indicate the range of the observations within the reference years. The shaded horizontal bar indicates the period of the area closure.

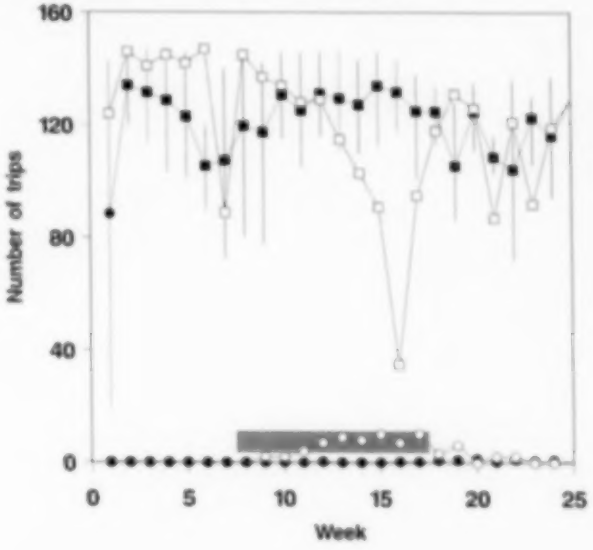

Results

Fishing effort

Following area closure in 2001, the fishing effort in the North Sea shows a decline coinciding with an increase in fishing effort outside the North Sea (e.g., Irish Sea). The low level of fishing effort in week 7 is related to the "bid week" during which a part of the Dutch fleet stayed in the harbour for religious reasons. The increase in fishing effort outside the North Sea starts in the second week of the closed period, much earlier than in the reference years (Fig. 3). The maximum of 7–10 trips, reached between weeks 12 and 17, is much higher than the maximum of three vessels in week 20 observed in the reference years.

Within the North Sea, the area closure on 15 February 2001 halts fishing in the closed areas. The few trips reported in the closed areas during this period are probably owing to misreporting. The beam trawl effort is mainly redistributed to the open north area (Fig. 4) in which the number of fish-

© 2007 NRC Canada

Fig. 4. Number of fishing trips by Dutch beam trawl vessels (>300 hp) by week in the four areas in 2001 (○) and the average number of trips in the reference years (●). The vertical bars indicate the range of the observations. The shaded horizontal bar indicates the period of the area closure.

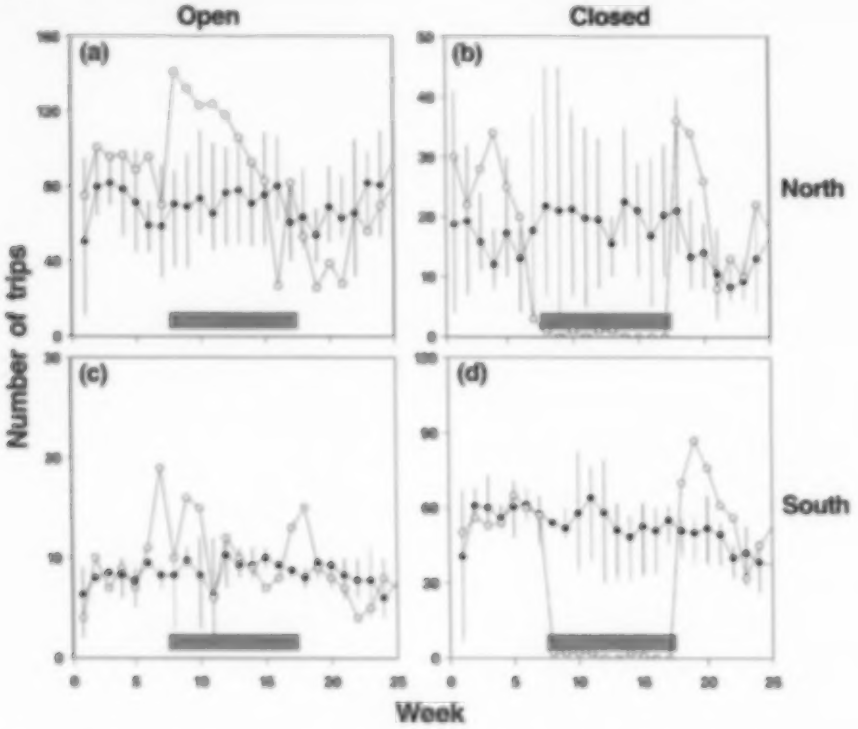

ing trips increased from 100 in weeks 1 to 6 to 140 trips in week 8. In the following weeks, the number of trips gradually decreased to reach the preclosure level around week 14. Fishing effort in the open south area only increased for two weeks following the closure, after which it fell back to the average level of the reference years. This may be owing to the rough grounds in this area that require specialised beam trawls (chain mats). To test whether resident and immigrant vessels differed in their response to the closure by staying in port, the average weekly probability of making a fishing trip was estimated. Resident vessels have a higher probability (p) of making a fishing trip during a week ($p = 0.76$) than immigrant vessels ($p = 0.59$) during the closure ($\chi^2 = 17.17$, df = 1, $p < 0.001$).

After the closure was lifted, the beam trawl fleet moved into the previously closed areas. The number of fishing trips in the closed south and closed north areas was higher than in any of the weeks prior to the closure, whereas the number of trips in the open north area was lower than in the weeks before the closure. In the open south area, no decrease in the number of trips was apparent after the closure was lifted.

Mean crowding index

The changes in the index of competition among vessels are show in relation to the area closure (Fig. 5). The trends in mean crowding generally corresponded to the trends in the number of fishing trips. Mean crowding among vessels in the open areas reached a peak value just before and during the first half of the closed period, whereas during the second half of the closed period, the mean crowding fluctuated around the level that was observed in the reference years. For about 3 weeks following the end of the closed period, the mean crowding index in the closed north and closed south areas reached peak values that were substantially higher than the reference levels. In correspondence to this, the mean crowding reached low values in the open south and open north areas. The high levels of mean crowding observed during the closed period in 2001, however, fall within the range of values observed in the reference periods, indicating that a strong aggregation of fishing effort is possible under normal conditions unrelated to the area closure.

Mean crowding in the individual areas deviated in minor detail from the general pattern described above. In the open north area, the increase in mean crowding was approximately 28% during the first week of the closure. In the open south area, the index of mean crowding was more variable among weeks, as well as among years. However, there is a distinct peak in the week just before the closure followed by a drop at the onset of the closure and a second peak during the subsequent two weeks.

Revenue rate

Revenue rates (VPUE) were standardised to a vessel of 2000 hp. The regression model used explained 16.5% of the total variance in VPUE ($F = 9063$, df = 1,45967, $p < 0.001$).

© 2007 NRC Canada

Fig. 5. Mean crowding index by week in the four areas in 2001 (○) and the average mean crowding index in the reference years (●). The vertical bars indicate the range of the observations. The shaded horizontal bar indicates the period of the area closure.

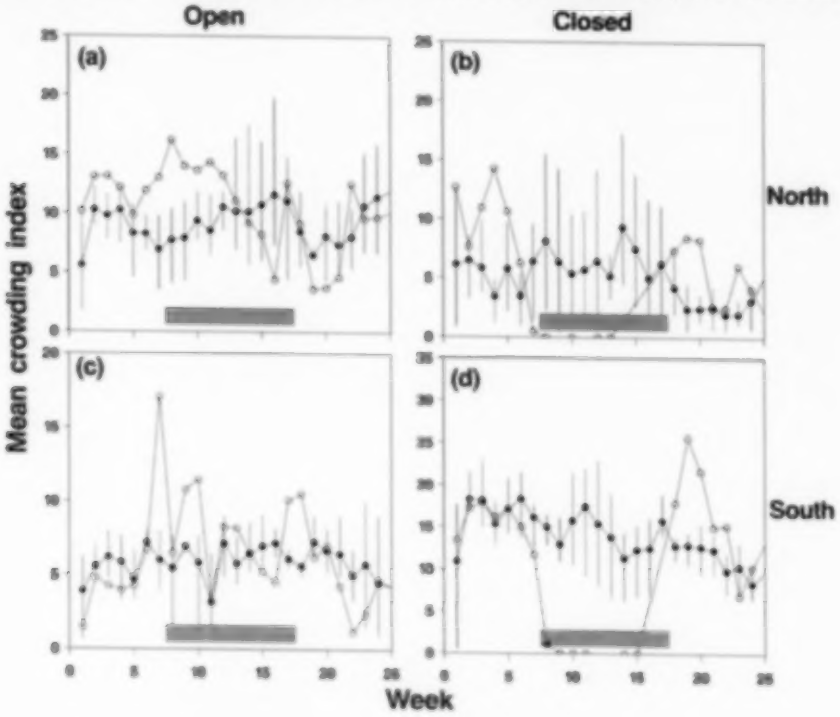

No apparent relation was found between model predictions and residuals or between engine powers and residuals.

In the reference years, the standardised VPUE showed a gradual decline from winter to spring in all four areas (Fig. 6). In January and early February, the $\log_{10}$(VPUE) varied around a level of about 3.85, corresponding to a revenue of 7.1×10^3 euros per day. VPUE decreased to a level of about 3.6×10^3 euros per day between April and June. In 2001, however, the results were different. In the weeks prior to the closure, VPUE was at a level similar to that of the reference years, but then dropped in the first week of the closure (week 8) to a level well below that of the reference years. In the subsequent weeks, the catch rates remained below the level of the reference years and reached a minimum in weeks 13 to 15. Only at the end of the closed period did the VPUE reached values comparable to the level in the reference years. In the open south area, VPUE started to decline in the week prior to the closure, coinciding with a peak in fishing effort. The drop in VPUE in the open north area coincided with an increase in the number of trips (from 70 in week 7 to 141 in week 8) and an increase in the mean crowding index. In the open south area, the number of trips increased from 11 in week 6 to 19 in week 7 and 17 and 16 in weeks 9 and 10, respectively.

After the closure was lifted in week 18, the revenue showed distinct peaks of 5.8×10^3 and 4.7×10^3 euros per day in the previously closed areas, which is a 100% and 48% increase compared with reference years, respectively. The catch rate decreased sharply in the second week and reached a level typical for the season in the fifth or sixth week after the areas were re-opened. Revenue rates in both open areas increased simultaneously, coinciding with a 30% decrease in the number of trips in the open north area, whereas in the open south area, the number of trips increased 15% to 15.

Area specialization

Comparison of the VPUE between residents and immigrants indicated that residents performed significantly better than immigrants in the open north area, but not in the open south. The first immigrant vessels enter the open areas in week 7, obtaining catch rates equal to the residents. In the open north area, the average VPUE drops in the subsequent week, when the number of competitors increases. The decline of immigrant VPUE at levels below those of the residents continues throughout the closure, with a maximum difference of 43% in week 15.

Interference and exploitation competition

The drop in VPUE of resident vessels in the first week of the area closure reflects the increased interference among the fishing vessels resulting from the increased competitor density. This $\log_{10}$(VPUE) difference of 0.065 reflects a drop in VPUE of 14% (Table 1). No significant difference was found in the reference years. A difference in the slope of resident VPUE reflects an increase in the exploitation competition combined with migration effects. The difference in $\log_{10}$(VPUE) slopes before and during the 2001 closure is

© 2007 NRC Canada

Fig. 6. Standardized $\log_{10}$(revenue rate) by week in the four areas for residents (●) and immigrants (○) in 2001 and residents during the reference years (■). Vertical bars indicate 2 standard deviations. The shaded horizontal bar indicates the time period of the closure in 2001.

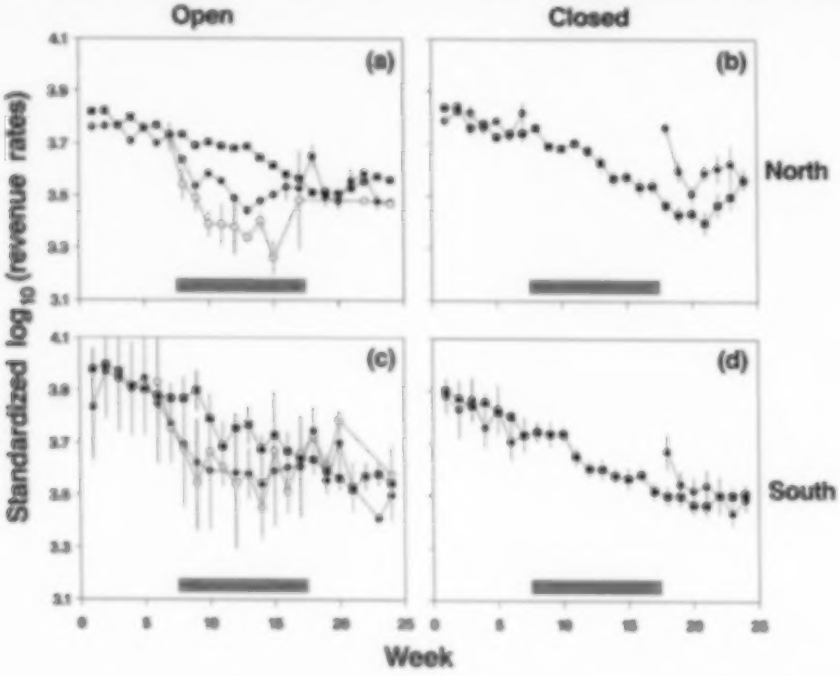

Table 1. Results of the general linear model of the decrease in $\log_{10}$(VPUE) in the open north area in different years.

	Δclosure			Δslope		
Year	Estimate	SE	$p > \chi^2$	Estimate	SE	$p > \chi^2$
1999	0.002	0.011	0.86	0.013	0.003	<0.01
2000	–0.003	0.013	0.79	0.002	0.003	0.51
2001	–0.065	0.010	0.01	–0.017	0.003	<0.01
2002	–0.024	0.016	0.14	–0.009	0.004	0.02
2003	0.013	0.014	0.36	–0.012	0.004	<0.01

Note: Parameter estimates are given for the difference in $\log_{10}$(VPUE) at the onset of the closure (Δclosure) and the difference in slope of $\log_{10}$(VPUE) before and after the onset of the closure (Δslope). Δclosure reflects the interference competition owing to the increase in vessels and Δslope reflects the combined effect of the exploitation of the resources and the immigration and emigration in the area. SE, standard error.

estimated to be –0.017, which is the largest difference found. However, significant differences are also found in the reference years, both positive and negative.

Discussion

Effort re-allocation

The area closure of 2001 resulted in a re-allocation of fishing effort by the Dutch large beam trawl fleet. Compared with the reference years, fishing effort shifted towards the open areas and areas outside the North Sea. In the first weeks after the closure, the number of competitors on the fishing grounds increased at the scale of the ICES rectangles.

During the closure, the total number of trips in the North Sea decreased. The decrease in fishing effort, which is especially noticeable after week 13, is related to the national cod recovery plan between the fishing industry and the government that started in week 13 (Anonymous 2001). The national recovery plan comprised of a vessel lay-up of 3 weeks in combination with the use of more selective fishing gear (large-mesh panel in upper net, lowering of the head rope).

The reallocation of fishing effort within the North Sea resulted in a mixing of vessels with different levels of experience on the open fishing grounds. Vessels with little experience in the open areas showed a lower level of fishing activity during the closure compared with the "resident" vessels that continued fishing on the grounds on which they fished in previous years. After the closure was lifted, the fishing effort peaked in the previously closed areas, coinciding with a VPUE that was well above the seasonal value in the reference years.

The number of vessels re-allocating their activities to fishing grounds outside the North Sea was relatively small compared with the total size of the fleet, reflecting the shortage of fishing rights (quota) in areas other than the North Sea. The vessels that temporarily fished outside the North Sea appeared to respond to the area closure and left the North Sea 1–2 months earlier than in the reference years.

Area specialization

In the open north area, the decrease in catch rate during the closure is stronger for immigrant vessels than for resident vessels, which indicates area specialization, i.e., vessels doing well in one area but not in the other. Such differences with regard to revenue rates concur with results found in the

© 2007 NRC Canada

British Columbia salmon purse seine fleet (Hilborn 1985). The area specialization may be caused by differences in (*i*) (personal) knowledge of skippers on the resource distribution and the optimal rigging of the gear for the fishing ground (sea bed characteristics, currents), (*ii*) vessel and gear design, or (*iii*) possession of individual transferable quota (ITQ) for the various target species. Lacking data about the skipper, the design and the ITQ of vessels hinders disentangling these effects.

Whatever the mechanism behind the area specialization, it does not seem to act in the open south area. A possible explanation may be that its surface area is far smaller than that of the open north area and the sample size (number of vessels) is much smaller.

If differences in personal information are the reason behind differences in fishing success between residents and immigrants, then learning could progressively reduce these differences. However, no decrease in the difference between the two categories is found, implying that either the period of the closure is too short for immigrants to gain sufficient knowledge or that difference in information is not the key issue explaining the difference in fishing success.

Interference and exploitation competition

The analysis showed an immediate decrease in catch rate of resident vessels at the start of the 2001 cod closure that is not seen during the same period in the reference years. This decrease of 14% in the open north area coincides with an almost doubling in the fishing effort and a substantial increase in the mean crowding index in this area. This result provides evidence for the occurrence of interference competition among beam trawlers. It corroborates the conclusion of an earlier study, which documented a 10% increase in catch rate in the week of prayer when the vessel density was substantially reduced (Rijnsdorp et al. 2000*b*).

It is likely that interference competition is the result of the targeted flatfish species response to the fishing vessels, known as interference competition through prey depression (Ruxton 1995; Stillman et al. 2000). Rijnsdorp et al. (2000*a*) showed that the catch rate of beam trawlers fishing with a slightly lower fishing speed decreased much faster that that of larger vessels fishing at higher speeds. This suggests that flatfish may increase their capability to escape from an approaching gear towed at low speeds. This is supported by differences in observation rates of Greenland halibut during bottom trawls (Albert et al. 2003).

We hypothesize that the spatial scale at which the interference competition occurs will substantially exceed the surface area covered during an individual tow. Because the beam trawl fleet concentrates its fishing effort on local hot spots (Rijnsdorp et al. 2000*a*, 2000*b*) and has tow lengths of about 12 nautical miles, the spatial scale of the ICES rectangles (~30 × 30 nautical miles) at which we could estimate the mean crowding index will be an acceptable proxy for the competitive interaction between vessels.

Ruxton (1995) has formulated a model for describing the relation between intake rates and competitor densities in prey depression situations. The functional response of this model approximates Beddington's equation (Beddington 1975), which, assuming handling time is negligible (Gillis et al. 1995), may be simplified to

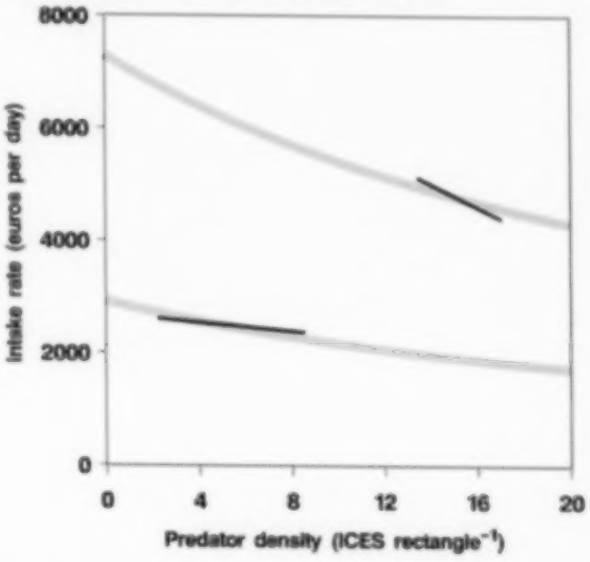

Fig. 7. Effects of predator density on intake rate for two studies of the North Sea beam trawl fleet combined. Black lines depict the results from the current study (upper line) and the study by Rijnsdorp et al. (2000*b*) (lower line). Shaded lines are model outcomes of a Ruxton-type interference competition model with $h = 0$ and $q = 0.035$ fitted through the observations.

$$I = \frac{an}{1 + qp}$$

where I is the intake rate, a is the search efficiency, n is the prey density, q is a parameter expressing the interference, and p is the predator density. For the beam trawl fishery, we can now estimate the interference parameter using the results of the present study and a previous study of Rijnsdorp et al. (2000*b*). To combine these studies, the catch rate data in that study are transformed to euros per day, and the mean crowding index for the fishing effort is calculated, showing that it decreased from 7.5 to 1.95 during the bid week, whereas the catch rate increased by 10%. The predator density is calculated using $m^* + 1$, which adds the predator itself to the competitors with which it shares the ICES rectangle. Fitting the Beddington equation to the combined results of both studies using nonlinear sums of squares approximation yields a q estimate of approximately 0.035, with 95% confidence limits –0.007 and 0.077 (Fig. 7). This method estimates the combined response of the three species. However, because sole is the higher-valued species, it probably affects the interference estimate more strongly than plaice and cod.

Upcoming techniques may allow us to gain insight in the processes of interference through prey depression at the individual-species level for flatfish. Tagging adult female plaice using data storage tags has proven to record geographical location and depth for individual fish (Hunter et al. 2004). Combining these data with the high resolution data of fishing effort allocation provided by vessel monitoring systems (VMS; Rijnsdorp et al. 1998; Dinmore et al. 2003) may reveal the effect of fishing activity on fish behavior. At pres-

© 2007 NRC Canada

ent, these data are not available for the total beam trawl fleet, which prevents a more detailed analysis.

The significant increase in the steepness of the slope of VPUE over time during the 2001 closure may indicate a faster rate of depletion of the local prey species (exploitation competition). It should be noted, however, that the slope shows substantial interannual variation, which may be due to the interannual variations in the combined effect of depletion and immigration–emigration.

The high catch rate experienced in the weeks directly following the re-opening of the closed areas may be the result of high survival during the closed period resulting in higher abundance of the resource. Also, the target species may have built up a high density on their preferred feeding grounds in absence of fishing disturbance. The steep decrease in catch rate after the re-opening of the fishery in the two areas may be due to a combined effect of the interference among vessels and the fishing-up of local concentrations.

The presence of interference competition and area specialization has important implications for our understanding of fisheries and fisheries management. Interference competition affects the relation between CPUE and fish stock biomass (Gillis and Peterman 1998) and plays an important role in fishing effort allocation (Abrahams and Healey 1990; Gillis et al. 1993). Area specialization affects the choice of fishing grounds by individual fishermen, because their catch rates are negatively affected by moving to areas that they have not fished. This may be the reason for the importance of previous fishing effort on selection of fishing grounds found in studies using random utility models (RUMs; Holland and Sutinen 2000; Hutton et al. 2004). Studies on the processes behind both interference competition and area specialization help to understand the spatial allocation of fishing effort.

Acknowledgements

This study was funded by NWO grant ALW88510104. Comments on a previous draft by Dr. Gerjan Piet and two anonymous reviewers are gratefully acknowledged.

References

Abrahams, M.V., and Healey, M.C. 1990. Variation in the competitive abilities of fishermen and its influence on the spatial distribution of the British Columbia Salmon troll fleet. Can. J. Fish. Aquat. Sci. **47**: 1116–1121.

Abrahams, M.V., and Healey, M.C. 1993. Some consequences of variation in vessel density: a manipulative field experiment. Fish. Res. **15**: 315–322.

Albert, O.T., Harbitz, A., and Hoines, A.S. 2003. Greenland halibut observed by video in front of survey trawl: behaviour, escapement, and spatial pattern. J. Sea Res. **50**: 117–127.

Anonymous. 2001. Regeling herstelmaatregelen kabeljauwbestand. Staatscourant nr. 83. p. 18.

Beddington, J.R. 1975. Mutual interference between parasites or predators and its effect on searching efficiency. J. Anim. Ecol. **44**: 331–340.

Dann, N. 1997. TAC management in North Sea flatfish fisheries. J. Sea Res. **37**: 321–341.

Dinmore, T.A., Duplisea, D.E., Rackham, B.D., Maxwell, D., and Jennings, S. 2003. Impact of a large-scale area closure on patterns of fishing disturbance and the consequences for benthic communities. ICES J. Mar. Sci. **60**: 371–380.

Fretwell, S.D., and Lucas, H.L. 1970. On territorial behavior and other factors influencing habitat distribution in birds. Acta Biotheor. **19**: 16–36.

Gillis, D.M. 1999. Behavioral inferences from regulatory observer data: catch rate variation in the Scotian Shelf silver hake (*Merluccius bilinearis*) fishery. Can. J. Fish. Aquat. Sci. **56**: 288–296.

Gillis, D.M. 2003. Ideal free distributions in fleet dynamics: a behavioral perspective on vessel movement in fisheries analysis. Can. J. Zool. **81**: 177–187.

Gillis, D.M., and Peterman, R.M. 1998. Implications of interference among fishing vessels and the ideal free distribution to the interpretation of CPUE. Can. J. Fish. Aquat. Sci. **55**: 37–46.

Gillis, D.M., Peterman, R.M., and Tyler, A.V. 1993. Movement dynamics in a fishery: application of the ideal free distribution to spatial allocation of effort. Can. J. Fish. Aquat. Sci. **50**: 323–333.

Gillis, D.M., Pikitch, E.K., and Peterman, R.M. 1995. Dynamic discarding decisions: foraging theory for high-grading in a trawl fishery. Behav. Ecol. **6**: 146–154.

Gordon, H.S. 1954. The economic theory of a common-property resource: the fishery. J. Political Econ. **62**: 124–142.

Goss-Custard, J.D. 1977. The ecology of the Wash. III. Density-related behaviour and the possible effects of a loss of feeding grounds on wading birds (Charadrii). J. Appl. Ecol. **14**: 721–739.

Goss-Custard, J.D. 1980. Competition for food and interference among waders. Ardea, **68**: 31–52.

Hassell, M.P., and Varley, G.C. 1969. New inductive population model for insect parasites and its bearing on biological control. Nature (London), **223**: 1133–1137.

Healey, M.C., and Morris, J.F.T. 1992. The relationship between the dispersion of salmon fishing vessels and their catch. Fish. Res. **15**: 135–145.

Hilborn, R. 1985. Fleet dynamics and individual variation: why some people catch more fish than others. Can. J. Fish. Aquat. Sci. **42**: 2–13.

Hilborn, R., and Ledbetter, M. 1979. Analysis of the British Columbia salmon purse seine fleet: dynamics of movement. J. Fish. Res. Board Can. **36**: 384–391.

Holden, M.J. 1994. The common fisheries policy. Fishing News Books, Oxford, UK.

Holland, D.S., and Sutinen, J.G. 2000. Location choice in New England trawl fisheries: old habits die hard. Land Econ. **76**: 133–149.

Hunter, E., Metcalfe, J.D., O'Brien, C.M., Arnold, G.P., and Reynolds, J.D. 2004. Vertical activity patterns of free-swimming adult plaice in the southern North Sea. Mar. Ecol. Prog. Ser. **279**: 261–273.

Hutton, T., Mardle, S., Pascoe, S., and Clark, R.A. 2004. Modelling fishing location choice within mixed fisheries: English North Sea beam trawlers in 2000 and 2001. ICES J. Mar. Sci. **61**: 1443–1452.

Lloyd, M. 1967. Mean crowding. J. Anim. Ecol. **36**: 1–30.

Milinski, M., and Parker, G.A. 1991. Competition for resources. *In* Behavioural ecology: an evolutionary approach. Blackwell Scientific Publications, Oxford, UK. pp. 137–168.

Palohcimo, J.E., and Dickie, L.M. 1964. Abundance and fishing success. Rapp. P.-V. Reun. Cons. Int. Explor. Mer, **155**: 152–163.

Pielou, E.C. 1969. An introduction to mathematical ecology. John Wiley & Sons, New York.

Piet, G., Rijnsdorp, A.D., Bergman, M.J.N., Santbrink, J.W.v., Craeymeersch, J.A., and Buijs, J. 2000. A quantitative evalua-

© 2007 NRC Canada

tion of the impact of beam trawling on benthic fauna in the southern North Sea. ICES J. Mar. Sci. **57**: 1332–1339.

Rijnsdorp, A.D., Buys, A.M., Storbeck, F., and Visser, E.G. 1998. Micro-scale distribution of beam trawl effort in the southern North Sea between 1993 and 1996 in relation to the trawling frequency of the sea bed and the impact on benthic organisms. ICES J. Mar. Sci. **55**: 403–419.

Rijnsdorp, A.D., van Maurik Broekman, P.L., and Visser, E.G. 2000*a*. Competitive interactions among beam trawlers exploiting local patches of flatfish in the North Sea. ICES J. Mar. Sci. **57**: 894–902.

Rijnsdorp, A.D., Dol, W., Hooyer, M., and Pastoors, M.A. 2000*b*. Effects of fishing power and competitive interactions among vessels on the effort allocation on the trip level of the Dutch beam trawl fleet. ICES J. Mar. Sci. **57**: 927–937.

Ruxton, G.D. 1995. Short term refuge use and stability of predator–prey models. Theor. Popul. Biol. **47**: 1–17.

Sampson, D.B. 1991. Fishing tactics and fish abundance, and their influence on catch rates. ICES J. Mar. Sci. **48**: 291–301.

Stillman, R.A., Goss-Custard, J.D., and Alexander, M.J. 2000. Predator search pattern and the strength of interference through prey depression. Behav. Ecol. **11**: 597–605.

Sutherland, W.J. 1983. Aggregation and the 'ideal free' distribution. J. Anim. Ecol. **52**: 821–828.

van Densen, W.L.T. 2001. On the perception of time trends in resource outcome. Its importance in fisheries co-management agriculture and whaling. Ph.D. thesis, Twente University, Enschede, the Netherlands.

van der Meer, J., and Ens, B.J. 1997. Models of interference and their consequences for the spatial distribution of ideal and free predators. J. Anim. Ecol. **66**: 846–858.

© 2007 NRC Canada

Disease dynamics and the potential role of thermal stress in the sea urchin, *Strongylocentrotus purpuratus*

Sarah E. Lester, Elizabeth D. Tobin, and Michael D. Behrens

Abstract: Evidence from field and laboratory data indicates that warmer ocean temperatures likely play a critical role in the disease dynamics of intertidal populations of the sea urchin, *Strongylocentrotus purpuratus*. Urchin populations along the west coast of North America have experienced numerous disease epidemics in the past several decades, and yet little is known about disease transmission, the geographic extent, or contributing factors to these outbreaks. In this study, we examine disease in Pacific *Strongylocentrotus* urchins over a broad geographic range with repeated sampling. We suggest that what has been assumed to be a single disease might be two distinct diseases presenting two disparate pathologies. Both potential pathologies were extremely rare or absent north of Point Conception, California, in a region associated with strong upwelling and cooler water temperatures but were common at warmer sites in southern California and northern Baja California, Mexico. Furthermore, during the survey period, disease prevalence at some of the study sites was positively correlated with sea surface temperatures as estimated from satellite data, leading us to hypothesize that heat stress may increase urchin susceptibility to disease. In experimentally elevated water temperatures, diseased individuals had significantly larger lesions and a significantly lower gonadal index, which could have important implications for urchin population dynamics.

Résumé : Des informations provenant de données de terrain et de laboratoire indiquent que les températures plus chaudes de l'océan jouent vraisemblablement un rôle primordial dans la dynamique de la maladie chez les oursins de mer, *Strongylocentrotus purpuratus*. Les populations d'oursins de la côte occidentale de l'Amérique du Nord ont connu de nombreuses épidémies au cours de plusieurs des dernières décennies; néanmoins, la transmission de la maladie, sa répartition géographique et les facteurs explicatifs des épidémies restent peu connus. Dans notre étude, nous examinons la maladie chez les oursins *Strongylocentrotus* du Pacifique sur une grande échelle géographique par des échantillonnages répétés. Nous croyons que ce qu'on a présumé être une seule maladie peut en fait en représenter deux qui présentent des pathologies distinctes. Les deux pathologies potentielles sont extrêmement rares ou absentes au nord de Point Conception, Californie, dans une région caractérisée par d'importants affleurements et des températures de l'eau plus fraîches; en revanche, elles sont communes aux sites plus chauds du sud de la Californie et du nord de la Basse-Californie, Mexique. De plus, durant l'inventaire, la prévalence de la maladie à certains sites d'étude était en corrélation positive avec la température de surface de la mer estimée d'après des données provenant des satellites, ce qui nous amène à émettre l'hypothèse selon laquelle le stress thermique peut accroître la vulnérabilité des oursins à la maladie. Dans de l'eau réchauffée expérimentalement, les individus malades ont des lésions significativement plus importantes et un indice gonadique significativement réduit, ce qui pourrait avoir des conséquences sérieuses sur la dynamique de population des oursins.

[Traduit par la Rédaction]

Introduction

Infectious diseases are a significant threat to marine ecosystems, particularly given the evidence of increased frequency of epidemics and an increase in emerging diseases (Harvell et al. 1999). Ward and Lafferty (2004) documented an increased rate of disease outbreaks since 1970 for five out of nine marine taxonomic groups. Disease agents can have devastating effects on marine populations, causing mass mortalities in cetaceans, mollusks, seagrasses, and corals (Harvell et al. 1999). The effects of epidemics can cascade through an ecosystem, particularly when disease infects

Received 16 June 2006. Accepted 25 January 2007. Published on the NRC Research Press Web site at http://cjfas.nrc.ca on 27 February 2007.
J19369

S.E. Lester,[1] E.D. Tobin,[2] and M.D. Behrens.[3] Department of Ecology, Evolution and Marine Biology, University of California, Santa Barbara, CA 93106, USA.

[1]Corresponding author (e-mail: lester@lifesci.ucsb.edu).
[2]Present address: School of Oceanography, University of Washington, Seattle, WA 98195, USA.
[3]Present address: Biology Department, Pacific Lutheran University, Tacoma, WA 98447, USA.

 doi:10.1139/F07-010 © 2007 NRC Canada

a species that either provides essential habitat (e.g., corals: McClanahan and Muthiga 1998), represents an important food source, (e.g., seagrasses: Robblee et al. 1991), or is a dominant consumer/predator (e.g., sea urchins: Liddell and Ohlhorst 1986; Hughes 1994; Behrens and Lafferty 2004). Additionally, recent research suggests that marine pathogens can spread much faster than terrestrial pathogens, possibly owing to fewer dispersal barriers, transport by ocean currents, and the potential to survive outside host organisms for longer time periods in the marine environment (McCallum et al. 2003).

Despite the importance of understanding the causes and consequences of marine diseases, they are understudied, particularly in comparison with terrestrial diseases (Harvell et al. 1999). Thus, there is limited information about etiological agents, modes of transmission, spatial and temporal dynamics of epidemics, and impacts on marine populations and communities. For many taxa, we lack the baseline data to even assess current incidence levels (Ward and Lafferty 2004). This is problematic given increasing human-facilitated introductions of novel pathogens to marine systems (Daszak et al. 2000) and impending climate change. Global warming is likely to be positively associated with disease in many systems owing to increased pathogen growth rates at higher temperatures, climate-related pathogen range expansions, and increased susceptibility of heat-stressed hosts (Holmes 1996; Harvell et al. 2002).

Numerous urchin species worldwide have experienced major epidemics (Maes and Jangoux 1984; Tajima and Lawrence 2001), and disease appears to have increased in this group in the past several decades (Ward and Lafferty 2004). Additionally, urchin mass mortalities can have widespread effects throughout a community, demonstrated by the near elimination of *Diadema antillarum* from the Caribbean in the 1980s (Lessios et al. 1984), which caused a shift from coral- to algal-dominated reefs (Liddell and Ohlhorst 1986; Hughes 1994; and see Behrens and Lafferty 2004 for a temperate example). Moreover, disease in Pacific *Strongylocentrotus* urchins may have economic consequences. There is a valuable red urchin fishery in Mexico and in the United States (Final California Commercial Landings 2004, http://www.dfg.ca.gov/mrd/landings04.html) and a potential purple urchin fishery in Mexico (e.g., a fishery for purple urchins recently started in the San Quintín region of Baja California (L. Rodriguez, Section of Evolution and Ecology, University of California, Davis, CA 95616, USA, personal communication)).

Disease in *Strongylocentrotus* spp.

Disease has been documented in multiple species of *Strongylocentrotus*, including Atlantic populations of *Strongylocentrotus droebachiensis* (e.g., Scheibling and Stephenson 1984), *Strongylocentrotus intermedius* in Japan (e.g., Tajima et al. 1997), and *Strongylocentrotus franciscanus* and *Strongylocentrotus purpuratus* along the Pacific coast of North America (e.g., Pearse et al. 1977). Maes and Janjoux (1984) grouped the diseases affecting *S. droebachiensis*, *S. franciscanus*, and *S. purpuratus* into a single lesion-causing disease infecting several urchin species in the Mediterranean and North Atlantic (genera: *Arbacia*, *Cidaris*, *Echinus*, *Paracentrotus*, *Psammechinus*, and *Sphaerechinus*). However, their assumption of a cosmopolitan "bald-sea-urchin disease" seems unlikely. Given the differing environments, suspected etiological agents, and reported signs, there are likely multiple diseases infecting the urchin species included in their review.

Studies investigating disease in *Strongylocentrotus* spp. indicate that there are multiple diseases affecting this genus. *Strongylocentrotus droebachiensis* populations in the Atlantic experienced widespread mortality events during the 1980s and 1990s (Scheibling 1986; Scheibling and Hennigar 1997). The disease was characterized by failure of spine and tube foot function and spine loss (Miller and Colodey 1983; Jones et al. 1985), with death occurring in several days to a month, depending on conditions such as temperature (Miller and Colodey 1983; Scheibling and Stephenson 1984). Through field and laboratory studies, the responsible pathogen was identified as an ameba, *Paramoeba invadens* (Jones 1985; Jones and Scheibling 1985). Two diseases (summer and spring) have impacted *S. intermedius* in aquaculture facilities in Japan, both of which have caused significant die-offs (Tajima and Lawrence 2001). The signs of "summer disease", which occur during warmer water temperatures, included blackish-red spotting lesions followed by spine loss and failure of tube foot function and was caused by a *Flexibacter* bacterium (Tajima et al. 1997). "Spring disease" had less conspicuous signs; it was typified by color change of the peristome, first to red and then to blue–black, and was caused by a *Vibrio* bacterium (Tajima and Lawrence 2001).

Localized, periodic disease outbreaks in *S. franciscanus* and *S. purpuratus* were reported for southern and central California in the 1970s and 1980s (Johnson 1971; Pearse et al. 1977; Gilles and Pearse 1986), and epidemics were linked to kelp forest expansion at some sites (Pearse et al. 1977; Pearse and Hines 1979). Diseased individuals were characterized by a green appearance of the epithelial tissue, lesions, and spine loss (Johnson 1971). The mode of transmission and etiological agent are poorly understood; multiple bacterial strains (*Vibrio* spp. and *Aeromonas* spp.) have been shown to induce lesion formation in the laboratory when urchins are mechanically abraded (Gilles and Pearse 1986). Regardless, this disease is likely different from that in *S. droebachiensis*, as the reported lesions are not indicative of the pathology described for the Atlantic epidemics (Scheibling and Stephenson 1984).

Since 1992, diseased *S. purpuratus* and *S. franciscanus* populations have been observed subtidally at the Channel Islands (Lafferty and Kushner 2000; Lafferty 2004). The urchin disease at the Channel Islands may be different from that reported in earlier studies (e.g., Johnson 1971; Pearse et al. 1977). The pathology described for recent outbreaks at the Channel Islands (Lafferty 2004), in which there is an overall shortening of the spines with large portions of the test lacking spines, does not match the description of disease signs in earlier studies. In particular, the disease documented in the 1970s and 1980s was characterized by lesions, with dark friable material in the lesion center, surrounded by swollen tissue (Johnson 1971; Gilles and Pearse 1986). Such lesions have not been noted in the more recent studies.

© 2007 NRC Canada

Confusion regarding the etiology of disease in *Strongylocentrotus* highlights the need for additional study. Field data collected previously on disease in *Strongylocentrotus* spanned a limited geographic area (southern and central California) relative to the geographic ranges of *S. purpuratus* and *S. franciscanus* (Alaska through Baja California Norte, Mexico). Disease outbreaks can be positively correlated with abundance (Anderson and May 1986; Lafferty 2004), and prior work indicates that the local abundance of *S. purpuratus* is highest at the southern extent of its range (Sagarin and Gaines 2002). Thus, it is crucial to better document patterns of disease in Mexico, where the potential for epidemics is high. We focus our disease surveys on *S. purpuratus* because this species has higher population densities and thus may influence disease dynamics in *S. franciscanus* (Lafferty 2004). This also allowed us to conduct intertidal surveys, as *S. purpuratus* is common both intertidally and subtidally, while *S. franciscanus* is only common subtidally. By circumventing the logistical difficulties of subtidal research, we could sample a much larger geographic area, with higher temporal frequency. The primary goals of this study were to (*i*) examine natural geographic and seasonal patterns of disease in purple urchins and (*ii*) examine the effect of elevated temperature on the progression and impact of disease on urchins in the laboratory. These data help to provide a more complete understanding of disease in *Strongylocentrotus*.

Materials and methods

Field surveys

We conducted disease surveys at 11 rocky intertidal sites spanning approximately 1600 km from central California to northern Baja California, Mexico (Table 1; Fig. 1), from February through December 2004. For each survey, 100–200 *S. purpuratus* individuals were randomly examined (100 was the minimum, but for most surveys we examined ~200+ urchins). Urchins were selected for examination based on random points along a transect line (15–30 m long) through the zone of highest urchin abundance. The closest urchin to each random point was examined, except when that urchin had already been examined for a previous point, in which case the second closest urchin was chosen, and so on. Individuals were examined across a minimum of 15 m of rocky intertidal urchin habitat (in case disease was patchily distributed) and were not biased towards a particular size class (e.g., the largest individuals). For repeated surveys at a site, we surveyed the same approximate area to investigate how disease prevalence at a location changes seasonally. We noted details of disease appearance, namely whether diseased individuals had shortened spines and spine loss and (or) lesions. During most transect surveys, density data were also collected by counting the number of individuals in 0.25 m^2 quadrats at every metre along the transect.

Sea surface temperature data were taken from satellite sea surface temperature images (day-and-night, 5 day composite, Pathfinder 5 AVHRR 4 km data; NOAA National Oceanographic Data Center: http://www.nodc.noaa.gov). Temperature values for our sites were calculated by averaging the three by three pixel square (12 km^2) centered on each site. These values were then used to calculate monthly mean temperatures over the sampling period for each site. A 17-year time series (January 1985 – December 2001) of these data was used to calculate the long-term summer mean sea surface temperature (the average of the June, July, and August long-term monthly means).

Laboratory experiments

Healthy *S. purpuratus* individuals were collected at low tide from Vandenberg Air Force Base for experiment 1 and from Montaña de Oro for experiment 2; both sites are in central California where no disease was found during our field surveys. For both experiments, diseased urchins with obvious lesions were collected from White's Point, a site in southern California where prevalence of the disease was high. All urchins were immediately transported to the laboratory and maintained in running seawater at 13–15 °C. Healthy urchins were acclimated to laboratory conditions for 2 weeks and fed weekly giant kelp, *Macrocystis pyrifera*. We recorded the wet weights of all experimental urchins immediately prior to the start of the experiments, and at the end of the experiments, we recorded the final wet weights and dissected and weighed gonadal tissues to calculate gonad indices (gonad wet weight/total body wet weight).

Experiment 1 investigated the mode of disease transmission. The methodology of Gilles and Pearse (1986) was used to infect healthy urchins with disease: we mechanically abraded 32 healthy experimental urchins, making 1 cm^2 abrasions on the aboral surface of the test using a sterile scalpel blade. We then transferred lesion material from black ring diseased urchins to the abraded surface of 16 healthy, abraded individuals by using sterile swab applicators. The experiment had three treatments, abraded and swabbed (AS), abraded only (A), and healthy, nonabraded (H) urchins, with 16 individuals each. Urchins were placed into individual plastic containers on a seawater table and each container was individually supplied with running seawater at ambient temperature (13–15 °C). Urchins were monitored daily for 2 weeks and twice per week thereafter for 55 days recording the presence of disease, lesion size, and mortality.

Experiment 2 tested the effect of water temperature on disease progression. We infected 22 healthy urchins with the black-ring pathology using the same methodology as in experiment 1 (AS). Twenty-two healthy control urchins (H) were not abraded or swabbed with lesion material. The experiment was a full factorial, two-factor (AS versus H and temperature) experiment with the following treatments, AS in ambient water temperature (~13 °C), H in ambient water temperature, AS in elevated water temperature (~19 °C), and H in elevated water temperature, with 11 individuals each, maintained as in experiment 1. We did not include abraded only (A) individuals in this experiment because the results from experiment 1 indicated that abrasion and swabbing was the most effective way to experimentally induce disease in the laboratory. For the elevated water temperature treatments, filtered seawater was heated to ~19 °C, controlled by a thermostat, and distributed to the individual containers in a flow-through system. The temperature of both ambient and elevated water supplies was continuously recorded using a

© 2007 NRC Canada

Table 1. *Strongylocentrotus purpuratus* disease survey sites.

Site	Location	GPS coordinates
Pied	Piedras Blancas Lighthouse, San Simeon, California	35.666°N, 121.287°W
MdO	Montaña de Oro State Park, San Luis Obispo, California	35.272°N, 120.596°W
VAFB	Vandenberg Air Force Base, Lompoc, California	34.719°N, 120.609°W
WP	Whites Point, Palos Verdes, California	33.715°N, 118.319°W
NLB	Shaws Cove, Laguna Beach, California	33.545°N, 117.799°W
SLB	Montage Resort, South Laguna Beach, California	33.514°N, 117.760°W
SM	San Miguel, Baja California Norte, Mexico	31.901°N, 116.729°W
SI	San Isidro, Eréndira, Baja California Norte, Mexico	31.293°N, 116.414°W
Vol	Volcanoes, San Quintín, Baja California Norte, Mexico	30.468°N, 116.045°W
Baja	Punta Baja, El Rosario, Baja California Norte, Mexico	29.952°N, 115.813°W
PSC	Punta San Carlos, Baja California Norte, Mexico	29.617°N, 115.492°W

Fig. 1. Map of study sites in California, USA, and Baja, Mexico. See Table 1 for location names and GPS coordinates.

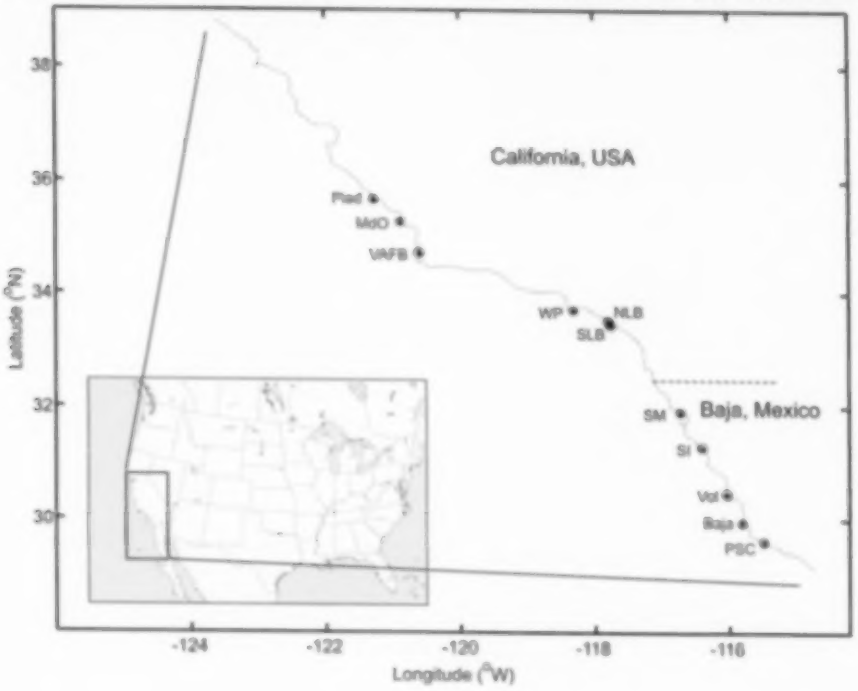

temperature probe. Urchins were monitored daily for 2 weeks and once a week thereafter for 70 days recording the presence of disease, lesion size, and cause of mortality.

Statistical analyses

The analyses of field survey data utilized logistic regression to determine factors significantly associated with disease prevalence. To evaluate whether temporal disease patterns at the study sites were correlated with water temperatures during the sampling period, we used logistic regression of mean sea surface temperature during the sampling month predicting disease prevalence (for black-ring, redspot, and both pathologies combined) for each site. To investigate the relationship between water temperature and disease prevalence across all study sites, we used logistic regression of mean August–September 2004 sea surface temperature, mean density, and the density × temperature interaction predicting August–September 2004 prevalence of both diseases combined. We included urchin density in the model because host density has been know to influence disease prevalence (Anderson and May 1986; Lafferty 2004). To verify that the results of the above analysis were not an artifact of atypical temperature conditions when satellite images were obtained, we also examined the relationship between long-term mean summer temperature and August–September 2004 disease prevalence or mean disease prevalence during the entire study period using logistic regression. To examine the effect of geographic variation in urchin density on disease prevalence patterns, controlling for the effect of temperature, we used a logistic regression model of

© 2007 NRC Canada

mean density, mean August–September 2004 sea surface temperature, and the density × temperature interaction predicting mean disease prevalence over the study period.

To determine if the various laboratory treatments in experiment 1 influenced rates of new infections, we used a χ^2 test (Zar 1999). We utilized t tests to determine differences in mean lesion size and days to maximum lesion size among treatments in experiments 1 and 2 (Zar 1999). To investigate differences in gonadal index at the end of an experiment among treatments, we used ANOVA. In experiment 1, we utilized a one-way ANOVA to determine if treatment (AS, A, H) influenced the gonadal index. In experiment 2, a two-way ANOVA with temperature (elevated, ambient) and treatment (AS, H) and the interaction term was used to determine how temperature and disease influenced the gonadal index. Differences between individual treatments were determined using sequential Bonferroni-corrected individual contrasts (Rice 1989). After confirming that the data met the assumptions of the statistical models (normality and homogeneity of variances), we performed all analyses on nontransformed data using JMP 6.0 (SAS Institute Inc., Cary, North Carolina).

Results

Field surveys

We documented two distinct pathologies in the field surveys: "red-spot" pathology, in which there is an overall shortening of the spines with large portions of the test lacking spines, and "black-ring" pathology, characterized by lesions with an outer black ring and lighter inner area of exposed test lacking spines and epithelial tissue, with lesion areas exhibiting test erosion and eventually perforation. Disease prevalence values for these two pathologies are reported both separately and combined because there is a possibility that the pathologies represent two distinct diseases, but this requires additional study to confirm.

Disease prevalence was lowest at the three northernmost sites north of Point Conception, California (Pied, MdO, VAFB) (Fig. 2). In fact, maximum disease prevalence over the course of our study was zero or near zero at these sites and was highest at the three southern California sites and two sites in Baja (WP, NLB, SLB, SM, Vol) (Fig. 3*a*). There were significant positive relationships between temperature and disease prevalence during the course of our sampling period for the black-ring pathology at five sites (NLB, SLB, SM, Baja, PSC) and for the red-spot pathology and both pathologies combined at four sites (NLB, SLB, Baja, PSC) (Table 2). There was only a significant negative relationship between disease prevalence and temperature over the study period at one site for the red-spot pathology (SM).

We also investigated the relationship between water temperature and disease prevalence across sites. Because host density can influence disease prevalence, we controlled for the effect of mean urchin density by using a logistic regression model of mean August–September 2004 sea surface temperature, mean density, and the density × temperature interaction predicting August–September 2004 prevalence of both diseases combined across all study sites. A highly significant relationship exists between temperature and disease prevalence (logistic regression: $\chi^2_1 = 71.94$, $p < 0.001$) (Fig. 3*b*), but this may be driven by the near absence of disease north of Point Conception, where temperatures also drop dramatically. However, when the two northernmost sites are excluded from the regression, thus reducing the variation in the dependent and independent variables, there is still a significant positive relationship for August–September temperature predicting prevalence of both pathologies combined (logistic regression: $\chi^2_1 = 31.64$, $p < 0.001$). This result further indicates that temperature stress may be associated with increased disease prevalence. Because the temperatures recorded in a few satellite images could reflect atypical conditions, we also examined the relationship between long-term mean summer temperature and August–September 2004 disease prevalence or mean disease prevalence during the entire study period and found highly significant positive relationships (logistic regression August–September disease prevalence: $\chi^2_1 = 58.40$, $p < 0.001$; logistic regression mean disease prevalence: $\chi^2_1 = 71.57$, $p < 0.001$) (Fig. 3*b*).

Contrary to expectations of a positive relationship between urchin density and disease prevalence, there was a significant negative relationship between urchin density and mean black ring prevalence (logistic regression: $\chi^2_1 = 7.72$, $p = 0.006$) and no relationships between urchin density and mean red-spot prevalence (logistic regression: $\chi^2_1 = 0.44$, $p = 0.507$) and mean prevalence of both pathologies combined (logistic regression: $\chi^2_1 = 0.07$, $p = 0.790$).

Laboratory experiments

For experiment 1, 100% of AS individuals developed a black-ring lesion compared with 56% and 0% for A and H individuals, respectively (Table 3). Individuals that were abraded but not swabbed were significantly less likely to develop disease than those that were also swabbed (Pearson $\chi^2_{10} = 8.96$, $p = 0.003$). No urchins died from disease during the experimental period and none developed the red-spot pathology. Of those individuals that developed initial disease symptoms (lesions), 6% of AS and 78% of A urchins recovered (the lesion healed and disappeared over the course of the experiment), a statistically significant difference (Pearson $\chi^2_{23} = 13.54$, $p = 0.0002$). Urchins that were abraded and swabbed with lesion material (AS) developed significantly larger lesions (t test: $t_{23} = -4.31$, $p = 0.0003$) (Table 3) after significantly fewer days (t test: $t_{123} = 3.62$, $p = 0.006$) compared with urchins that were only abraded (A). The three treatments did not have significantly different mean gonadal indices at the conclusion of the experiment (ANOVA: $F_{[2,45]} = 2.07$, $p = 0.138$).

For experiment 2, 100% of AS individuals developed the black-ring pathology (in both temperature treatments) compared with only one individual in the healthy ambient temperature treatment and two individuals in the healthy elevated temperature treatment (Table 3). Of the 25 total individuals that developed disease during experiment 2, only three (12%) recovered. Four individuals died from disease during the experiment, all in the elevated temperature treatment (Table 3). When considering only the AS treatments, individuals in the elevated temperature treatment had, on average, larger disease lesions than the urchins in the ambient temperature treatment, and this pattern was maintained

© 2007 NRC Canada

Fig. 2. Time series prevalence plots for black-ring pathology (dotted line with circles) and red-spot pathology (dashed line with triangles) and monthly mean sea surface temperature (solid line with plus signs) for 2004. Sites are arranged from north (top) to south (bottom). When black-ring or red-spot pathology was found at the site, but was not present in any individuals sampled using our transect survey method, the survey is indicated by a zero prevalence value but with a *BR or *RS, respectively.

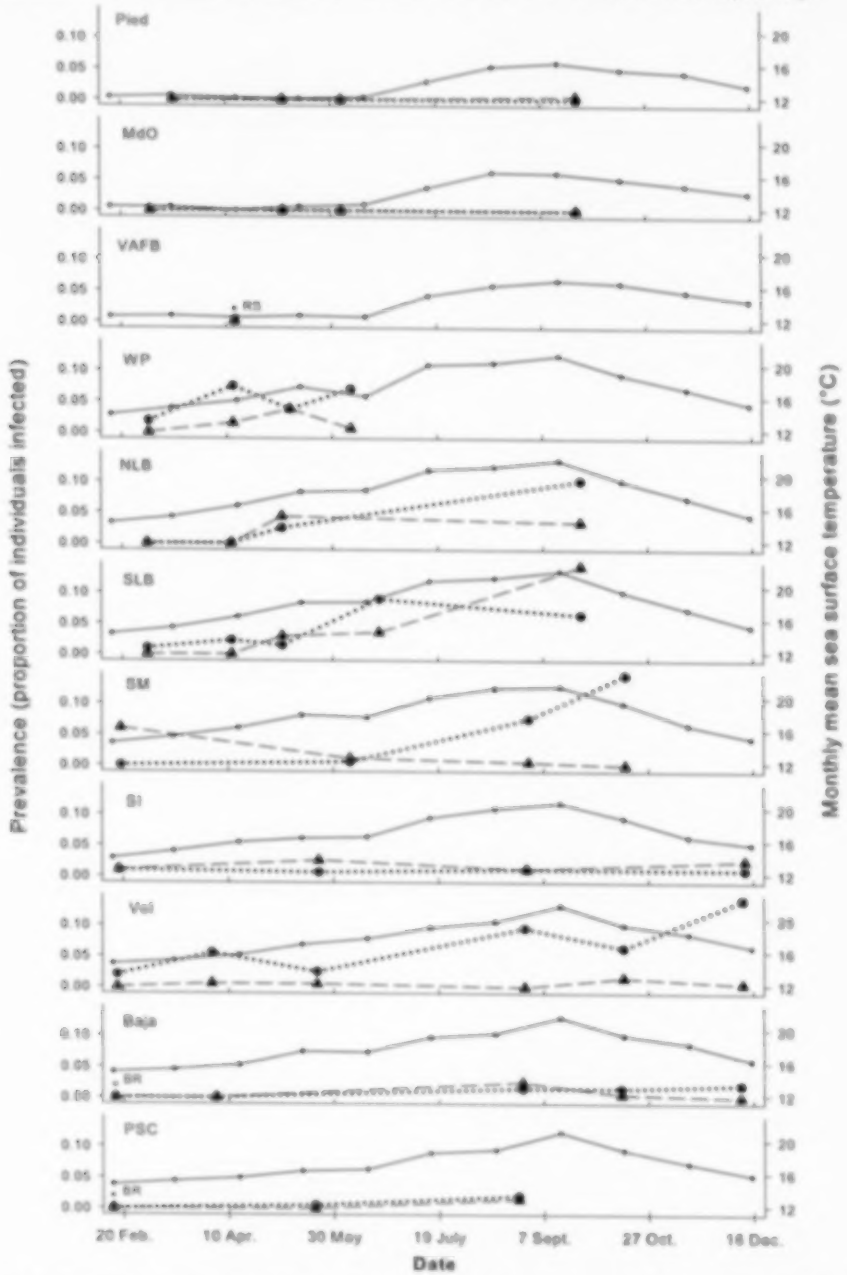

throughout the entire experimental period (Fig. 4). The average maximum lesion size reached by all AS individuals was significantly higher in the elevated temperature treatment (*t* test: $t_{[20]} = -4.10$, $p = 0.001$) (Table 3).

At the end of experiment 2, the gonadal index, and therefore reproductive potential, was significantly influenced by both temperature and disease (ANOVA effect tests: temperature, $F_{[1,35]} = 8.42$, $p = 0.006$; AS versus H, $F_{[1,35]} = 4.52$, $p = 0.041$; interaction term, $F_{[1,35]} = 0.94$, $p = 0.340$). Thus, AS individuals in the elevated temperature treatment had the lowest gonadal indices, significantly lower than both H and AS individuals in ambient water and H individuals in ele-

© 2007 NRC Canada

Fig. 3. (*a*) Maximum recorded disease prevalence for the two pathologies, black-ring (solid bars) and red-spot (hatched bars). (*b*) Late-summer (August or September survey, depending on the site) prevalence for both pathologies combined (shaded bars), mean August or September 2004 sea surface temperature (solid circles), and long-term mean summer sea surface temperature (open circles). Sites are arranged from north (left) to south (right). The 2004 temperature and disease data for Pied, MdO, NLB, and SLB are from September 2004 and for SM, SI, Vol, Baja, and PSC are from August 2004. ND, no disease survey data for August or September.

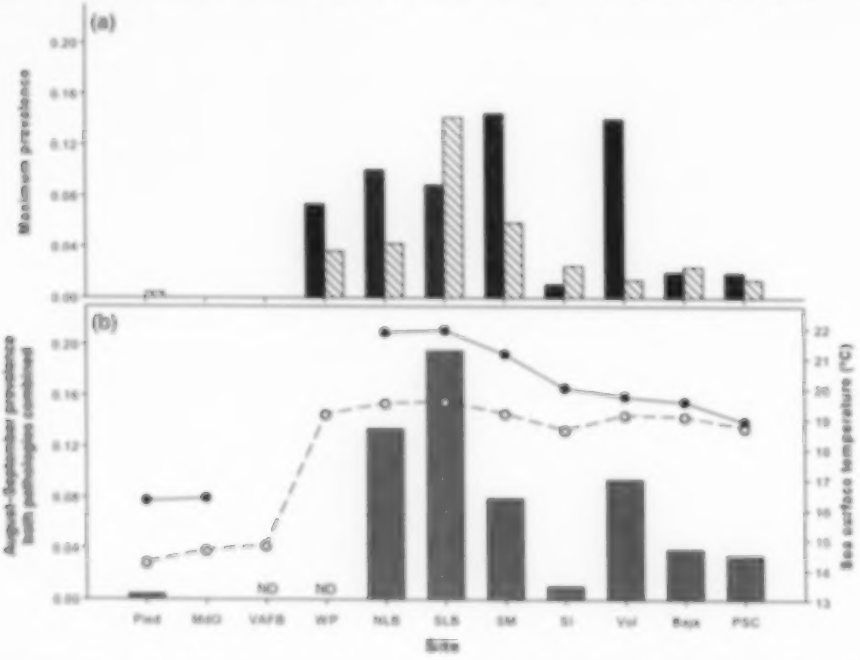

Table 2. Logistic regression results of mean sea surface temperature during the sampling month predicting disease prevalence of black-ring, red-spot, and both pathologies combined by site.

Site	Black-ring	Red-spot	Both pathologies combined
Pied	ns	ns	ns
MdO	ns	ns	ns
WP	ns	ns	ns
NLB	+ (<0.0001)	+ (0.052)	+ (<0.0001)
SLB	+ (0.003)	+ (<0.0001)	+ (<0.0001)
SM	+ (0.002)	– (0.0004)	ns
SI	ns	ns	ns
Vol	ns	ns	ns
Baja	ns	+ (0.0006)	+ (0.002)
PSC	ns, + (0.064)	+ (0.021)	+ (0.005)

Note: ns, no significant relationship; +, positive relationship between mean sea surface temperature and disease prevalence; –, negative relationship. The p values are given in parentheses; if no value is given, $p > 0.1$.

vated temperature water (AS-elevated versus H-ambient, $F_{[1,35]} = 11.48$, $p = 0.005$; AS-elevated versus AS-ambient, $F_{[1,35]} = 6.80$, $p = 0.027$; AS-elevated versus H-elevated, $F_{[1,35]} = 4.18$, $p = 0.048$).

Discussion

In field surveys from central California to northern Baja California, Mexico, we documented what appear to be two distinct pathologies affecting the sea urchin, *S. purpuratus*. We assert that the red-spot pathology may be the one recently recorded at the Channel Islands (e.g., Lafferty and Kushner 2000; Lafferty 2004), while the black-ring pathology may correspond to the lesions documented in earlier studies (e.g., Johnson 1971; Pearse et al. 1977). It is unlikely that these two pathologies represent different stages of a single disease given that red-spot epidemics at the Channel Islands are not preceded or followed by signs of black-ring (D. Kushner, Channel Islands National Park, 1901 Spinnaker Drive, Ventura, CA 93001, USA, personal communication). Furthermore, individuals with signs of red-spot die with an intact test, whereas test erosion and perforation appear to be a characteristic feature of black-ring individuals that suffer disease-induced mortality (Gilles and Pearse 1986; S.E. Lester and M.D. Behrens, unpublished data).

Our laboratory experiments corroborate that the two pathologies are probably not separate stages of a single disease. When lesion material from urchins with signs of black-ring collected in the field is swabbed on abrasions on healthy urchins, these previously healthy individuals only develop signs associated with black-ring pathology, not those associated with the red-spot pathology. Our laboratory studies also indicate that the black-ring pathology is likely not a generalized response to stressful conditions or secondary infections. Mechanically abraded urchins in our experiments often demonstrated repair to the abrasion area and recovered from any initial lesion signs, while those that were abraded and then swabbed with lesion material from field-collected diseased urchins rarely recovered. Additionally, the average maximum lesion size in abraded individuals was

© 2007 NRC Canada

Table 3. Summary results from the two laboratory experiments including the number of individuals that developed lesions, the number that recovered from disease, the number that died from disease, the mean maximum lesion size, and the mean gonadal index for each experimental treatment.

Treatment	Developed lesion (no.)	Recovered (no.)	Died from disease (no.)	Mean maximum lesion size (cm)[a]	Mean gonadal index (%)[a]
Experiment 1 (n = 16 urchins per treatment)					
AS	16	1	0	1.43 (0.080)	4.8 (0.539)
A	9	7	0	1.0 (0.060)	5.4 (0.577)
H	0	—	0	— (n = 0)	6.3 (0.453)
Experiment 2 (n = 11 urchins per treatment)					
AS, 13 °C	11	2	0	0.88 (0.046)	2.7 (0.448)
AS, 19 °C	11	1	3	1.45 (0.132)	0.6 (0.232)
H, 13 °C	1	0	0	— (n = 1)	3.3 (0.701)
H, 19 °C	2	0	1	— (n = 2)	2.3 (0.472)

Note: —, not applicable (e.g., number recovered is not applicable if no urchins developed disease lesions; mean lesion size is not applicable if the sample size of diseased individuals is too low).

[a]Standard errors are given in parentheses.

Fig. 4. Mean lesion size time series during experiment 2 for abraded and swabbed (AS) urchins in the two temperature treatments: ~13 °C (shaded circles) and ~19 °C (solid circles).

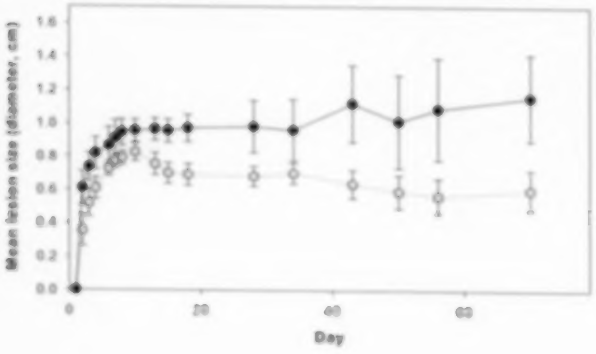

1 cm^2, the size of the original abrasion, whereas lesions on abraded and swabbed individuals grew beyond the size of the abrasion to an average size of 1.43 cm^2, demonstrating that direct contact with lesion material greatly increases the transmission of disease. Additional study is required to confirm whether these two presumed pathologies represent separate diseases.

Despite previous findings at the Channel Islands (Lafferty and Kushner 2000; Lafferty 2004) and theoretical work demonstrating that disease establishment and persistence often require a host density threshold (Anderson and May 1986), we did not find a positive correlation between mean urchin density and mean disease prevalence at a site. Because the disease transects were placed through high urchin density areas (see Materials and methods), in all cases the host density threshold may have been exceeded. A lack of a positive relationship in addition to the relatively low prevalence levels that we measured (20% or less, in contrast with the subtidal epidemics at the Channel Islands that can exceed 75% of individuals infected) could alternatively suggest that urchin densities at our sites may actually be too low to allow for prolonged disease persistence and spread, although this would require additional research to substantiate.

Although previous work has not found an association between prevalence and monthly mean temperature (Lafferty and Kushner 2000), our data suggest that disease in *S. purpuratus* may be at least partially driven by temperature through its effect on either host stress or infection rates. We found only a single diseased individual at the three northernmost sites, all north of Point Conception, around which there is a distinct thermal gradient owing to the proximity to the shore of the south-flowing California Current and stronger and more consistent upwelling north of the point (Mendelssohn and Schwing 2002). Our sites in southern California (WP, NLB, SLB; matched by Vol in Baja) are among those with the highest disease prevalence rates while also experiencing the warmest summer temperatures. Many of our Baja sites were characterized by strong, persistent upwelling (Zaytsev et al. 2003) and thus do not experience warmer summer or annual temperatures than southern California sites, despite being more than three degrees of latitude farther south.

An alternative explanation for our field data is that the two ocean current systems that collide at Point Conception create a barrier to flow around the point that impedes transport of either a waterborne pathogen or infected individuals (Gaylord and Gaines 2000). If disease is spreading northward from the southern end of the urchins' range, it may not have had sufficient time to expand beyond the point (or has been hindered by an oceanographic barrier). However, the black-ring pathology has been observed in central California in the past (Pearse et al. 1977) and recently in the Olympic Peninsula, Washington (M.D. Behrens, unpublished data). If these disease events were caused by the same pathogen(s) studied here, it appears that the responsible pathogen or diseased individuals can travel north of Point Conception. Furthermore, the occurrence of the pathology in more northern locations does not necessarily contradict our temperature hypothesis. Intertidal temperatures do not exhibit a latitudinal gradient along the west coast of North America, as maximum temperatures are strongly influenced by the timing of low tides (Helmuth et al. 2002). Summer low tides in central and southern California are in the middle of the night compared with during the middle of the day in Washington, and thus, urchins in Washington may experience maximum tem-

© 2007 NRC Canada

peratures similar to those experienced by urchins in southern California.

The positive relationships that we found between ocean temperatures and disease prevalence at sites over time could also be confounded by temperature covarying with elapsed time, since our surveys only spanned from winter to late fall at most sites. Furthermore, the lack of a relationship between temperature and disease at some sites could result from rather limited temperature variation at these sites. Thus, to better test the hypothesis that temperature facilitates disease progression, we experimentally manipulated temperature conditions in the laboratory. Higher than normal temperature conditions (~19 °C) resulted in urchins with faster growing, larger disease lesions compared with diseased urchins maintained in cooler water (~13 °C), suggesting that higher temperatures lead to faster pathogen growth rates. Urchins with larger lesions are unlikely to recover, thus impacting urchin survival (as lesions grow larger, they are more likely to perforate the test, making the individual extremely vulnerable to secondary infection and unlikely to survive). Even diseased individuals that do survive may have reduced fitness, as indicated by their lower mean gonadal index, an effect that is mediated not only by disease but also by the elevated temperature conditions. Thus, increased temperatures appear to facilitate disease progression while also lowering the fecundity of diseased individuals. Urchin populations in habitats near their upper thermal tolerance could therefore be seriously impacted by disease epidemics.

This study is consistent with studies of temperature effects on disease epidemics affecting black abalone (*Haliotis cracherodii*) populations in southern and central California (Friedman et al. 1997). Withering foot syndrome has caused mass mortality of black abalone populations in California since the mid-1980s. Die-offs have been correlated with warmer than average periods (e.g., strong El Niño years) and appear to proceed more rapidly in these warm periods (Lafferty and Kuris 1993; Raimondi et al. 2002). Additionally, withering foot syndrome appears to have propagated from south to north, with an interesting exception: it appeared in Diablo Cove, a site with unusually warm water because of discharge from a power plant, years before it became common at neighboring sites (Altstatt et al. 1996; Raimondi et al. 2002), supporting the role of temperature in the onset of disease epidemics.

This study represents the first attempt to determine the natural geographic and seasonal disease dynamics in purple urchins. Whether the spatial patterns we document are static through time will require continued field surveys. Our field and laboratory studies indicate that high temperatures may exacerbate the effects of disease. If thermal stress does increase host susceptibility, disease in *Strongylocentrotus* species could increase with global warming and increased human impacts along the coast. Studies like this are critical for more informed management of valuable urchin fisheries and of kelp forest ecosystems, which can be heavily modified by urchin grazing.

Acknowledgements

We thank E. Bomkamp, A. Haupt, K. Kunkel, E. Lowry, E. Madin, and R. Pelc for assistance with field surveys, K. Lafferty for helpful comments, and B. Kinlan and K. Casey for assistance with acquiring the satellite temperature data. Comments from two anonymous reviewers improved this manuscript. This work was supported by a National Science Foundation graduate fellowship and a National Oceanic and Atmospheric Administration Nancy Foster scholarship to S.E.L., a Fletcher Jones Foundation fellowship to M.D.B., the Partnership for Interdisciplinary Studies of Coastal Oceans, funded by the David and Lucile Packard Foundation and the Betty and Gordon Moore Foundation (contribution No. 240), and the Marine Ecosystems Dynamics Consortium, funded by the Andrew W. Mellon Foundation.

References

Altstatt, J.M., Ambrose, R.F., Engle, J.M., Haaker, P.L., Lafferty, K.D., and Raimondi, P.T. 1996. Recent declines of black abalone *Haliotis cracherodii* on the mainland coast of central California. Mar. Ecol. Prog. Ser. **142**: 185–192.

Anderson, R.M., and May, R.M. 1986. The invasion, persistence and spread of infectious diseases within animal and plant communities. Philos. Trans. R. Soc. Lond. B Biol. Sci. **314**: 533–570.

Behrens, M.D., and Lafferty, K.D. 2004. Effects of marine reserves and urchin disease on southern California rocky reef communities. Mar. Ecol. Prog. Ser. **279**: 129–139.

Daszak, P., Cunningham, A.A., and Hyatt, A.D. 2000. Emerging infectious diseases of wildlife — threats to biodiversity and human health. Science (Washington, D.C.), **287**: 443–449.

Friedman, C.S., Thomson, M., Chun, C., Haaker, P.L., and Hedrick, R.P. 1997. Withering syndrome of the black abalone, *Haliotis cracherodii* (Leach): water temperature, food availability, and parasites as possible causes. J. Shellfish Res. **16**: 403–411.

Gaylord, B., and Gaines, S.D. 2000. Temperature or transport? Range limits in marine species mediated solely by flow. Am. Nat. **155**: 769–789.

Gilles, K.W., and Pearse, J.S. 1986. Disease in sea urchins *Strongylocentrotus purpuratus*: experimental infection and bacterial virulence. Dis. Aquat. Org. **1**: 105–114.

Harvell, C.D., Kim, K., Burkholder, J.M., Colwell, R.R., Epstein, P.R., Grimes, D.J., Hofmann, E.E., Lipp, E.K., Osterhaus, A.D.M.E., Overstreet, R.M., Porter, J.W., Smith, G.W., and Vasta, G.R. 1999. Emerging marine diseases: climate links and anthropogenic factors. Science (Washington, D.C.), **285**: 1505–1510.

Harvell, C.D., Mitchell, C.E., Ward, J.R., Altizer, S., Dobson, A.P., Ostfeld, R.S., and Samuel, M.D. 2002. Climate warming and disease risks for terrestrial and marine biota. Science (Washington, D.C.), **296**: 2158–2162.

Helmuth, B., Harley, C.D.G., Halpin, P.M., O'Donnell, M., Hofmann, G.E., and Blanchette, C.A. 2002. Climate change and latitudinal patterns of intertidal thermal stress. Science (Washington, D.C.), **298**: 1015–1017.

Holmes, J.C. 1996. Parasites as threats to biodiversity in shrinking ecosystems. Biodivers. Conserv. **5**: 975–983.

Hughes, T.P. 1994. Catastrophes, phase shifts, and large-scale degradation of a Caribbean coral reef. Science (Washington, D.C.), **265**: 1547–1551.

Johnson, P.T. 1971. Studies on diseased urchins from Point Loma. *In* Kelp habitat improvement project, annual report 1970–1971. *Edited by* W.J. North. California Institute of Technology, Pasadena. pp. 82–90.

Jones, G.M. 1985. *Paramoeba invadens* n. sp. (Amebida, Paramoebidae), a pathogenic amoeba from the sea urchin *Strongy-*

© 2007 NRC Canada

franciscanus, near Santa Cruz, California. Fish. Bull. **75**: 647–648.

Raimondi, P.T., Wilson, C.M., Ambrose, R.F., Engle, J.M., and Minchinton, T.E. 2002. Continued declines of black abalone along the coast of California: are mass mortalities related to El Nino events? Mar. Ecol. Prog. Ser. **242**: 143–152.

Rice, W.R. 1989. Analyzing tables of statistical tests. Evolution, **43**: 223–225.

Robblee, M.B., Barber, T.R., Carlson, P.R., Durako, M.J., Fourqurean, J.W., Muehlstein, L.K., Porter, D., Yarbro, L.A., Zieman, R.T., and Zieman, J.C. 1991. Mass mortality of the tropical seagrass *Thalassia testudinum* in Florida Bay (USA). Mar. Ecol. Prog. Ser. **71**: 297–299.

Sagarin, R.D., and Gaines, S.D. 2002. Geographical abundance distributions of coastal invertebrates: using one-dimensional ranges to test biogeographic hypotheses. J. Biogeogr. **29**: 985–997.

Scheibling, R. 1986. Increased macroalgal abundance following mass mortalities of sea urchins (*Strongylocentrotus droebachiensis*) along the Atlantic coast of Nova Scotia. Oecologia, **68**: 186–198.

Scheibling, R.E., and Hennigar, A.W. 1997. Recurrent outbreaks of disease in sea urchins *Strongylocentrotus droebachiensis* in Nova Scotia: evidence for a link with large-scale meteorologic and oceanographic events. Mar. Ecol. Prog. Ser. **152**: 155–165.

Scheibling, R.E., and Stephenson, R.L. 1984. Mass mortality of *Strongylocentrotus droebachiensis* (Echinodermata: Echinoidea) off Nova Scotia, Canada. Mar. Biol. **78**: 153–164.

Tajima, K., and Lawrence, J.M. 2001. Disease in edible sea urchins. *In* Edible sea urchins: biology and ecology. *Edited by* J.M. Lawrence. Elsevier, Amsterdam, Netherlands. pp. 103–113.

Tajima, K., Hirano, T., Shimizu, M., and Ezura, Y. 1997. Isolation and pathogenicity of the causative bacterium of spotting disease of sea urchin *Strongylocentrotus intermedius*. Fish. Sci. **63**: 249–252.

Ward, J.R., and Lafferty, K.D. 2004. The elusive baseline of marine disease: are diseases in ocean ecosystems increasing? PLoS Biol. **2**: 542–547.

Zar, J.H. 1999. Biostatiscal analysis. Prentice Hall, Englewood Cliffs, N.J.

Zaytsev, O., Cervantes-Duarte, R., Montante, O., and Gallegos-Garcia, A. 2003. Coastal upwelling activity on the Pacific shelf of the Baja California Peninsula. J. Oceanogr. **59**: 489–502.

© 2007 NRC Canada

Juvenile coho salmon (*Oncorhynchus kisutch*) responses to salmon carcasses and in-stream wood manipulations during winter and spring

Guillermo R. Giannico and Scott G. Hinch

Abstract: We investigated the growth rate, winter survival, presmolt size, and emigration timing of juvenile coho salmon (*Oncorhynchus kisutch*) in response to salmon carcasses and in-stream wood. Experimental trials were conducted during two consecutive years and pre-winter fish size and densities differed between years. Sixteen pens with emigration traps were built in a side-channel of the Mamquam River, British Columbia. Pens were randomly assigned salmon carcasses, in-stream wood, both carcasses and in-stream wood, or neither (control). Our first trial was conducted between December 1996 and August 1997 and the second between December 1997 and August 1998. Initial rearing densities and average individual body mass were 3.1 fish·m^{-2} and 2.4 g, respectively, in the first trial and were 1.6 fish·m^{-2} and 6.6 g, respectively, in the second trial. Results were influenced by both fish initial size and density. During the first trial (smaller-sized fish at high densities), salmon carcasses increased fish growth rates and presmolt size. Winter survival did not increase in response to any treatment; however, a pre-winter size-related survival pattern was observed during the first trial. During the second trial, (larger-sized fish at low densities), no treatment influenced fish growth rates or presmolt size but all treatments augmented fish survival.

Résumé : Nous avons étudié le taux de croissance, la survie à l'hiver, la taille avant la transformation en saumoneau et le calendrier de l'émigration chez de jeunes saumons coho (*Oncorhynchus kisutch*) en réaction à la présence de carcasses de saumons et de débris ligneux dans le cours d'eau. Nous avons fait des essais expérimentaux au cours de 2 années consécutives : les tailles des poissons avant l'hiver et leurs densités différaient d'une année à l'autre. Nous avons construit 16 enclos munis de pièges d'émigration dans un chenal latéral de la Mamquam, Colombie-Britannique. Nous avons placé dans les enclos de manière aléatoire des carcasses de saumons, des débris ligneux, à la fois des carcasses et du bois ou alors aucun ajout (témoins). Notre premier essai a eu lieu de décembre 1996 à août 1997 et le second de décembre 1997 à août 1998. La densité initiale d'élevage était de 3,1 poissons·m^{-2} et la masse individuelle moyenne du corps de 2,4 g dans le premier essai et respectivement de 1,6 poisson·m^{-2} et de 6,6 g dans le second essai. Les résultats sont influencés à la fois par la taille initiale et la densité des poissons. Durant le premier essai (poissons plus petits à forte densité), les carcasses de saumons augmentent les taux de croissance des poissons et leur taille avant la transformation en saumoneaux. La survie à l'hiver n'augmente dans aucune des situations expérimentales : on observe cependant dans le premier essai un patron de survie relié à la taille des poissons avant l'hiver. Durant le second essai (poissons plus grands à densité faible), aucune des conditions expérimentales n'influence les taux de croissance des poissons, ni leur taille avant la transformation en saumoneaux, mais toutes les conditions augmentent la survie des poissons.

[Traduit par la Rédaction]

Introduction

Juvenile coho salmon (*Oncorhynchus kisutch*) smolt output is largely dependent on winter nursery habitat. The availability of this type of habitat can constitute a "bottleneck" to coho salmon smolt production (Mason 1976; Nickelson et al. 1992*a*; Solazzi et al. 2000). Slow-flowing waters, deep pools, off-channel areas (i.e., side-channels, backwaters, and ponds), and in-stream structures such as fallen logs, root wads, and boulders appear to be critical to the young of this species (Bustard and Narver 1975; Peterson 1982; Swales and Levings 1989).

In many watersheds of the Pacific Northwest, reduced spawning by anadromous fish seems to have affected aquatic,

Received 2 February 2006. Accepted 17 November 2006. Published on the NRC Research Press Web site at http://cjfas.nrc.ca on 6 March 2007.
J19148

G.R. Giannico.[1,2] Institute for Resources, Environment and Sustainability, University of British Columbia, Vancouver, BC V6T 1Z4, Canada.
S.G. Hinch. Institute for Resources, Environment and Sustainability, and Department of Forest Sciences, University of British Columbia, Vancouver, BC V6T 1Z4 Canada.

[1]Corresponding author (e-mail: giannico@oregonstate.edu).
[2]Present address: Department of Fisheries and Wildlife, Nash Hall 104, Oregon State University, Corvallis, OR 97331-3803, USA.

 doi:10.1139/F07-011 © 2007 NRC Canada

and even terrestrial, productivity (Cederholm et al. 1999; Gresh et al. 2000). The delivery of nutrients by spawning salmon to Washington, Oregon, Idaho, and California watersheds is presently at about 6%–7% of historical levels (Gresh et al. 2000). Even in southern British Columbia, large reductions in nutrient delivery by salmon have occurred (Larkin and Slaney 1997). Such important losses of subsidies of marine-derived nutrients (i.e., nitrogen and carbon) are deemed to decrease the capacity of many freshwater habitats to support juvenile salmon and other aquatic biota (Bilby et al. 1998). Therefore, stream salmon carcass placement is promoted by stream restoration organizations based on the assumption that it should help compensate for the effects of declining postspawning salmon carcass availability.

Most studies on the fate of salmon carcasses in streams have focused on the incorporation pathways of marine-derived nutrients by primary producers and benthic macroinvertebrates (Wipfli et al. 1998; Chaloner and Wipfli 2002). However, the response of juvenile salmonids to indirect nutrient uptake or direct carcass consumption has received limited attention. Bilby et al. (2001) looked at the indirect uptake of marine-derived nitrogen and found that this element increases in juvenile coho salmon muscle tissue in direct proportion to the abundance of salmon carcasses and reaches a peak at densities of approximately 0.15 kg of carcass per square metre of streambed. More recently, Heintz et al. (2004) found that salmon carcass availability led to increased lipid reserves in juvenile coho salmon.

The effects of direct consumption of salmon eggs and (or) carcasses on juvenile salmonids have been examined in only three studies. The earliest, by Bilby et al. (1998), found that carcass availability caused a significant boost in juvenile coho salmon densities, body weight, and condition factor. The two more recent studies, those of Wipfli et al. (2003, 2004), reported that salmon carcass addition caused a significant boost in the growth rates, body mass, and production of cutthroat trout (*Oncorhynchus clarkii*) and juvenile coho salmon. Increased growth rates and large late-fall body mass in juvenile salmonids can significantly raise their odds of surviving winter (Holtby 1988; Quinn and Peterson 1996). Considering that juvenile coho salmon continue feeding at low water temperatures (Bustard and Narver 1975; Giannico and Healey 1998) and can even gain weight under winter conditions (Peterson 1982), it is possible that salmon carcasses and eggs contribute to increasing fish winter survival and smolt output as long as the winter carrying capacity of the system is not limited by availability of refuge (Armstrong and Griffiths 2001).

Juvenile salmon body size and growth rates have a strong influence on smolting rates and emigration timing. Thorpe (1986) reported that juvenile Atlantic salmon (*Salmo salar*) need to reach a minimum critical size by winter to "afford" smolting the following spring and that smaller individuals remained in freshwater for an additional year. In turn, among smolting individuals, body size is one of the factors determining emigration timing. Larger coho salmon have been observed to emigrate up to several weeks before peak dates for smolt output in the Keogh River (Irvine and Ward 1989). Thus, salmon carcass availability may potentially increase the proportion of juvenile coho salmon that smolt at age 1+ and affect their emigration timing by increasing winter growth rates and fish body size.

In late fall and winter, when freshet intensity and frequency increase in coastal streams, in-stream wood (often termed large woody debris) becomes particularly important to the young fish by offering not only predation refuge (Dolloff 1993) but also protection from elevated water velocities (Nickelson et al. 1992*b*; Cederholm et al. 1997). Thus, winter refuge availability and the tendency to avoid sharing it with other individuals observed in some wild juvenile salmonids (Cunjak 1988; Armstrong and Griffiths 2001) may help define the winter carrying capacity of a stream reach because fish that fail to find shelter are likely to emigrate or be removed by predators (Gregory and Griffith 1996). This explains the frequently observed lower densities of juvenile salmonids in pools with scarce in-stream wood than in wood-rich pools (Nickelson et al. 1992*b*; Cederholm et al. 1997; Roni and Quinn 2001). During the spawning season, in-stream wood also contributes to retaining salmon carcasses and preventing stream currents from flushing them downstream (Cederholm et al. 1989), thus increasing the influence of carcasses on the food web.

This study examined whether salmon carcass availability, when in-stream wood is abundant, affects juvenile coho salmon winter growth, winter survival, presmolt size, and emigration timing. It also looked at the relationship between early-winter fish body size and emigration. Our predictions (hypotheses) were as follows: (1) salmon carcasses cause a longer-lasting increase in winter daily growth rates of coho salmon parr when in-stream wood is present than when it is absent, (2) the combination of carcasses and in-stream wood significantly increases coho salmon parr winter survival, (3) the combination of carcasses and in-stream wood significantly increases coho salmon presmolt size, (4) the early-winter body size of survivors to spring is larger than that of nonsurvivors, (5) the early-winter body size of coho salmon parr that emigrate in spring (presmolts) is larger than that of individuals that remain in the channel through the summer (residual fish), and (6) carcasses and in-stream wood significantly augment the proportion of early emigrants (by increasing fish body size).

Materials and methods

Study site

We carried out experiments in an artificial side-channel of the lower reaches of the Mamquam River, a tributary to the Squamish River, draining into Howe Sound in southwestern British Columbia (Fig. 1). The Upper Mamquam side-channel is 360 m long and runs parallel to the river. It was constructed in the 1980s as a spawning area for adult coho and chum salmon (*Oncorhynchus keta*); however, juveniles of both species occupy it for very different periods of time. Chum salmon fry are only present in the side-channel during a few days in late February and early March, whereas juvenile coho salmon are found in it throughout the year. Steelhead/rainbow trout (*Oncorhynchus mykiss*), cutthroat trout, Dolly Varden (*Salvelinus malma*), sculpins (*Cottus* spp.), and suckers (*Catostomus* spp.) are also present but in very low abundance (e.g., only one to four individuals of each species were captured while surveying the channel).

© 2007 NRC Canada

Fig. 1. Location of the study side-channel. The inset map provides a regional reference. The main map represents an enlarged view of area within the rectangle in the inset map. The Upper Mamquam side-channel is shown as a short tributary to the lower reach of the Mamquam River, British Columbia, Canada.

The Upper Mamquam side-channel has little or no gradient (0.005), and the fluvial deposits that were exposed during its excavation constitute its gravel substrate (average grain size 0.042 m). The channel's banks are armored with boulders (i.e., rip-rap), 0.30–0.50 m in diameter, to approximately 0.50 m above the water level. The channel has an average width of 6.2 m and depth of 0.53 m. It only connects to the river through its downstream end, while its upstream end is closed and has a circular pond 12.5 m in diameter and a maximum depth of 1.75 m. A mix of groundwater and river water reaches the Upper Mamquam side-channel as subsurface flow and raises its winter water temperatures slightly above those in the adjacent river (Upper Mamquam December–March water temperature: mean = 3.36 °C, SD = 0.79 °C, and range = 2.33–3.88 °C in 1996–1997 and mean = 3.92 °C, SD = 0.63 °C, and range = 3.00–4.71 °C in 1997–1998; adjacent mainstem river December–March water temperature: mean = 2.31 °C, SD = 1.01 °C, and range = 1.56–4.02 °C in 1996–1997 and mean = 2.75 °C, SD = 0.93 °C, and range = 2.10–5.82 °C in 1997–1998). Water discharge in the Upper Mamquam side-channel was constant and ranged from 0.07 $m^3 \cdot s^{-1}$ in summer to 0.11 $m^3 \cdot s^{-1}$ in winter between 1996 and 1998. Water samples (three replicates each time) were taken in December, March, and June of each year. Nitrate concentrations averaged 0.466 ppm (SE = 0.005) and orthophosphate concentrations averaged 0.054 ppm (SE = 0.001).

We selected the top 100 m of the side-channel, downstream from the pond, for our experimental manipulations and closed it off with a transverse fence at the upstream end to prevent any fish in the pond from entering this section. The fence, which spanned the width of the channel, consisted of three 1 m × 3 m panels of galvanized hardware-cloth (2 mm mesh) framed with 0.05 m × 0.10 m × 3 m wooden boards. A 0.4 m wide clear plastic "skirt" was stapled along the bottom board of each fence panel. The panels were placed vertically with their bottom edges buried 0.20 m deep in the substrate, and their plastic skirts were spread underneath the gravel to prevent fish movement. All fish found in the experimental section were removed by means of a combination of repeated pole seining and electrofishing.

The pens were built with the same type of fence panels described above and arranged in eight pairs (n = 16) along the side-channel's experimental section. Each pair of pens

© 2007 NRC Canada

was delimited by an upper and a lower fence running perpendicular to the banks of the channel parallel to each other and 6 m apart. These fences, which spanned the entire channel width, enclosed an area that was subsequently divided into two equal 3 m wide halves by means of a longitudinal midchannel fence. Thus, seen from above, the resulting fence configuration for each pair of pens resembled a letter "H" (Fig. 2). Each pair of pens was separated from the next one immediately downstream by a 6 m long "buffer" zone. As in the upstream fence, the pen panels were placed with their bottom edges buried 0.20 m deep in the substrate, and their 0.40 m wide clear plastic skirts were spread underneath the gravel in a downstream direction. Any spaces between the end of the cross-channel fences and the channel banks were sealed using hardware-cloth and geotextile material (Amoco® 1199).

Each pen had one downstream passageway that allowed fish to leave the pen and reach an "emigration" trap (Rubbermaid® container: 0.84 m long × 0.40 m wide × 0.45 m high). The mouth of this passageway was a clear plastic funnel glued with silicone by its broadest end (0.20 m diameter) to a similar-sized opening in the mesh of the fence. In turn, the funnel was connected to a 2 m long plastic pipe (0.08 m inner diameter), which led fish into the emigration trap. The end of the pipe, inside the trap, was fitted with a "one-way exit door" shaped like a cone made of three triangular clear acetate sheets (Fig. 2). This kind of conical fixture operated like a one-way valve that let fish into the trap but, once in the trap, did not allow them to return to the pen. To minimize the attractiveness of the outlet structures as predation shelters, both the funnel and the plastic pipe were of translucent plastic. The emigration traps were placed in the buffer zones between pen pairs (Fig. 2).

Fig. 2. Top view of several experimental pens located near the dead upper end of the Upper Mamquam side-channel. Emigration traps are located within the buffer zone left between pairs of pens. The enlarged trap view shows details of a one-way valve. "A" indicates a stop fence on the upper end of the experimental reach.

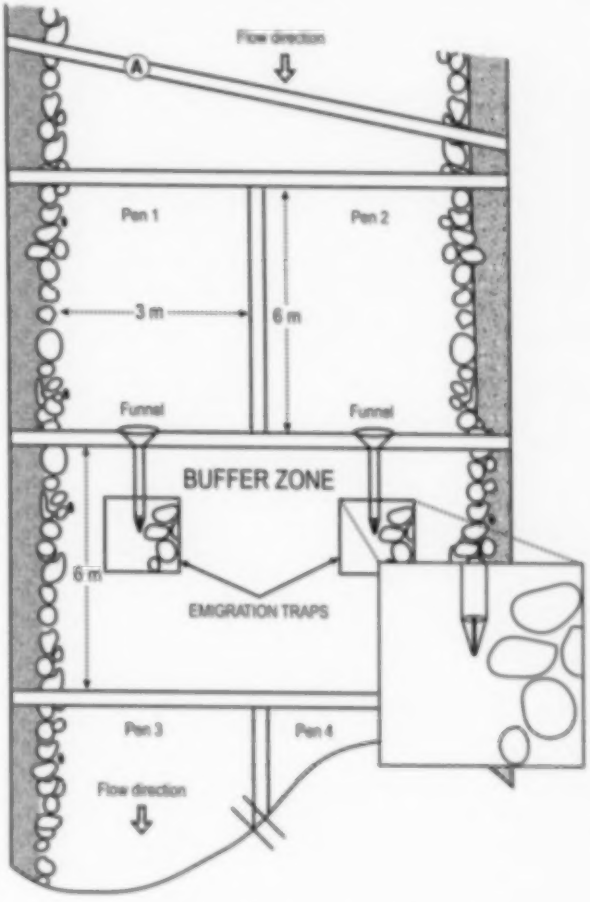

Experimental manipulations

We randomly assigned salmon carcasses or in-stream wood to four pens each (for a total of eight). The combination treatment (carcasses and in-stream wood) was randomly assigned to another four pens, and the remaining four pens did not receive any treatment and served as control. Pens treated with in-stream wood received a bundle made of a single red alder (*Alnus rubra*) log (0.30 m in diameter and 3.0 m long) covered with 40 alder twigs (0.03–0.06 m thick and 2.0–3.0 m long) and 10 western redcedar (*Thuja plicata*) branches (0.02–0.04 m thick and 1.5 m long). Those treated with carcasses received one chum salmon carcass per pen. Carcasses were cut into 0.10 m × 0.20 m pieces to keep bald eagles (*Haliaeetus leucocephalus*) from taking them and prevent juvenile coho salmon from using them as cover. All carcasses were collected from the lower portion of the side-channel, where wild chum salmon spawned between late November and early January and coho salmon between December and late January. The day before beginning the experiment, one large chum carcass (mean wet mass = 10 kg, SE = 019 kg) was placed into the appropriate pens. This represented a carcass wet mass of approximately 0.56 kg·m^{-2} per pen, which is equivalent to that used by Bilby et al. (1998) in one of their experimental streams and mimics the average carcass mass per streambed area observed elsewhere in the side-channel. Additional carcasses were stored in a freezer for later use. Carcasses were available for approximately 8 weeks in the side-channel; this was in part due to the relatively slow decomposition of carcasses under low temperatures but also to the arrival of late spawners whose carcasses lasted in some cases until early March. To match the natural availability of carcass remnants elsewhere in the channel, half a chum salmon carcass was added to the appropriate pens 1 month after the trials had begun.

Although not tested in a direct manner, we assessed the influence of early-winter average fish size and rearing densities on fish response to our treatments by running our trials over two consecutive years. During the first year, juvenile coho salmon were relatively small and reared at high densities, whereas in the second year, they were approximately three times larger and almost half as abundant.

Juvenile coho salmon captured with a pole seine in the lower section of the side-channel were used in this study. Once captured, fish were kept overnight in a holding pen that was partially submerged in the channel. The following day, captured fish were transported to a nearby hatchery for

© 2007 NRC Canada

individual marking. Fish were rendered unconscious with CO_2 (dissolving one teaspoon of Bromoseltzer® in 4 L of water), weighed to the nearest 0.01 g, measured to the nearest 0.1 mm fork length, and individually marked using a modified high-pressure inoculation gun (Biomark Ltd.) that injected dye into the fins. The combination of four different fluorescent colours of dye and three fins (i.e., dorsal, caudal, and anal) made individual marking of fish possible. Fish were randomly assigned to the experimental pens before receiving their unique marks. Once marked, fish were held overnight in 16 small holding tanks (one for each pen) at the hatchery. The following day, they were examined to make sure marks were still visible and re-marked if necessary. Only 2%–3% of the fish needed to be re-marked. Afterwards, fish were transported in separate buckets to the side-channel and released into the pens.

The mark–recapture method and Petersen's mark–recapture equation (Krebs 1989) were used to estimate juvenile coho salmon densities (and their 95% confidence limits) 50 m downstream of the pen locations. The area was blocked off with a pair of nets, and then, 10 minnow traps (6 mm mesh) baited with salmon roe were soaked overnight for two consecutive nights for the capture and recapture, respectively. Fish trapped during the first session had half of one pelvic fin clipped. Juvenile coho densities in the side-channel were 3.10 fish·m^{-2} (95% confidence limits = 2.51 and 3.69) in December 1996 and 1.56 fish·m^{-2} (95% confidence limits = 1.42 and 1.70) in December 1997. These natural densities were replicated in our experiments by releasing 55 fish in each pen on 23 December 1996 and 28 fish in each pen on 24 December 1997. Initial fish biomass per unit of area was lower at the beginning of the "high-density" 1996–1997 trial (7.41 g·m^{-2}) than at the beginning of the "lower-density" 1997–1998 trial (10.35 g·m^{-2}). This was due to the smaller initial size of coho in December 1996 (mean mass = 2.39 g, SE = 0.05 g, mean fork length = 5.1 cm, SE = 0.07 cm) than in December 1997 (mean mass = 6.64 g, SE = 0.15 g, mean fork length = 7.6 cm, SE = 0.05 cm).

After being released in the pens, fish were given 1 week to acclimatize to the conditions of the pens before the outlets were opened to allow "emigration". General fish activity level and movement were recorded during 32 min long morning and afternoon observations (2 min per pen) carried out from the channel banks on the days the emigration traps were examined. We made the following three assumptions: (*i*) the persistence of high levels of fish activity and exploratory behaviour at low winter temperatures after 1 week of acclimatization was an indicator of unfavourable conditions in the experimental pens, (*ii*) individuals that were active and explored their surroundings could find the passageways to the emigration traps relatively easily, and (*iii*) the 2 m long emigration pipes, made of translucent plastic, did not offer fish protection from predation and constituted unsuitable zones for residency. Thus, one would expect that only true emigrants would be enticed to explore such areas and reach exits with one-way valves leading them into traps (Matter et al. 1989). Therefore, more fish should "emigrate" from pens lacking adequate cover and food than from those with in-stream wood and (or) salmon carcasses.

The downstream movement of juvenile coho salmon into the emigration traps was monitored three times a week from January to June. These fish were removed from the traps, identified by their marks, weighed to the nearest 0.01 g, measured to the nearest 0.1 mm fork length, and released in the side-channel downstream of our experimental section. Fish that entered the emigration traps between January and March were considered winter emigrants and those trapped between April and June spring emigrants. Fish that had not moved into the emigration traps by the end of June were considered summer residual individuals and were removed from the pens using minnow traps and electrofishing between July and mid-August. This allowed us to account for all surviving coho salmon that had not left the pens by the end of June, when movement into the traps ceased. Fish mortality of those individuals not accounted for was attributed to predation because the pens did not exclude avian or mammalian predators.

Growth of juvenile coho during the trials was examined in terms of changes in weight (mass gain) and in fork length. We calculated the percent daily (or instantaneous) growth rate for each fish as

$$(1) \qquad (\log_e W_2 - \log_e W_1) / t_2 - t_1 \times 100$$

$$(2) \qquad (\log_e L_2 - \log_e L_1) / t_2 - t_1 \times 100$$

where W_1 is the initial weight (g) and L_1 is the initial fork length (cm) when released into the experimental pens and W_2 is the final weight and L_2 is the final fork length at time of entering the emigration traps or when removed from the pens at the end of trials. The formulas' denominators, $t_2 - t_1$, are the numbers of days between the releases and recaptures of fish (Ricker 1975).

Statistical analyses

Because fish size, fish stocking densities, and side-channel water temperatures differed between the winter of 1996–1997 and the winter of 1997–1998, data for these two trials were analyzed separately. We used an α value of 0.05 in all tests and SAS systems software (SAS Institute Inc. 1988) for all of our analyses. We utilized normal probability plots of the residuals (also known as q-q-norm plots) (Kuehl 2000) derived from ANOVAs to examine departures from normality. Residual versus fit plots were used to determine whether our data met the assumption of homogeneity of variance. Before testing our various hypotheses, we investigated possible differences in the initial body mass and length of fish among the 16 pens using one-way ANOVAs with the 16 pens as the factor.

The first prediction was tested using three-way mixed-model ANOVAs, with pens also randomly nested within treatments, and season as the third factor. The response variable in this case was daily growth rate. When using mixed models, the expectations of the mean squares may show that the F statistics cannot be formed directly with the use of mean squares; in such cases, approximate F statistics were calculated. This caused the degrees of freedom associated with each mean square to be approximate and thus took on fractional values. The term "approximate F" is used because under these conditions, the underlying F_0 distribution is approximated (Kuehl 2000).

One-way general linear model ANOVAs, with the treatments carcass, wood, carcass plus wood, and control as four levels of a single factor, were used to test our second predic-

© 2007 NRC Canada

tion. In this case, the response variable was total number of survivors. To test our third prediction, we used two-way mixed-model ANOVAs, with pens nested as a random effect within treatments, and final size (body mass or fork length) of presmolts as the response variable. Two-way general linear model ANOVAs were used to test our fourth prediction (factors survival status and pen, and response variable initial mass or fork length). Pen was used as the second factor in these two-way analyses to detect potential effects of individual pens on fish responses. Two-way general linear model ANOVAs were also used to test our fifth prediction (factors season of emigration and pen, and response variable initial mass or fork length), with pen as the second factor. Finally, three-way mixed-model ANOVAs, with repeated measures for winter, spring, and summer, were used to test our sixth prediction. The four factors were carcass (fixed), wood (fixed), season (fixed), and pen (random and nested within carcass and wood). The response variable was number of emigrants per season.

Results

The normal probability plots of the residuals indicated that our fork length data were normally distributed and did not need to be transformed. However, the fish mass data showed a positively skewed distribution and were logarithmically transformed before being used in any of our statistical analyses. The residual versus fit plots revealed that our data met the homogeneity of variance assumption. No significant differences were observed among the 16 experimental pens in either of the trials with regard to initial fish body mass (1996–1997 trial: $F_{[15]} = 1.23$, $p = 0.239$; 1997–1998 trial: $F_{[15]} = 1.57$, $p = 0.084$) or initial fish fork length (1996–1997 trial: $F_{[15]} = 1.50$, $p = 0.100$; 1997–1998 trial: $F_{[15]} = 1.45$, $p = 0.122$), thus confirming that all pens received groups of fish with equivalent initial mean sizes.

First prediction

A statistically significant "treatment and season" interaction effect was detected on fish daily growth rates during the first trial (Table 1). Specific contrasts showed that treatment effects on fish daily growth rates changed from one season to the next. For example, winter daily gain in body mass increased in response to both wood and carcasses combined and salmon carcasses alone ($t_{[474]} = 2.22$, $p = 0.027$ and $t_{[474]} = 2.35$, $p = 0.019$, respectively). In the spring, only the combination of wood and carcasses increased growth rates in body mass in a significant manner ($t_{[474]} = -2.56$, $p = 0.011$). The results for daily growth rates in fork length showed the same patterns. In contrast, the daily growth rates of residual fish were not influenced by any of our treatments. During the second-year trial, which involved relatively larger fish, we failed to reject the null hypothesis regarding treatment effect on daily growth rates (Table 1). Only "season" had a statistically significant effect on fish growth rates (body mass: $F_{[2]} = 38.22$, $p < 0.001$; fork length: $F_{[2]} = 17.82$, $p < 0.001$), and specific contrasts revealed that growth rates increased between winter and spring regardless of treatment (body mass: $F_{[1]} = 59.07$, $p < 0.001$; fork length: $F_{[1]} = 26.07$, $p < 0.001$).

Second prediction

In the first trial, none of the treatments had a significant effect on fish survival, although fish had low body masses and occurred at high densities (Table 1). The percentage of fish that survived during this first trial ranged from a minimum average of 51% in control pens to a maximum average of 62% in pens with wood plus carcasses (Fig. 3*a*). However, in the second trial, when fish had high body masses and were at low densities, statistically significant differences among treatments were found (Table 1). Specific contrasts of the ANOVA showed that the availability of salmon carcasses ($t_{[1]} = -2.50$, $p = 0.028$), wood ($t_{[1]} = -2.40$, $p = 0.033$) or the combination of carcasses and wood ($t_{[1]} = -3.55$, $p = 0.004$) significantly increased fish survival during the second-year trial. Percent fish survival in pens receiving these two treatments combined was 59%, in those receiving only carcasses was 50%, and in those with only wood was 49%, while in control pens, it was 27% (Fig. 3*b*).

Third prediction

When early-winter juvenile coho salmon size was relatively small, during the first trial, we found a statistically significant treatment effect on both the final body mass and the length of presmolts (Table 1). The specific contrasts of least square means revealed that the combination of carcasses and in-stream wood was responsible for these differences (body mass: $t_{[12]} = -3.88$, $p = 0.002$; fork length: $t_{[12]} = -3.46$, $p = 0.005$) (Fig. 4*a*). However, during the second trial, there were no statistically significant differences in the final body size of fish among treatments (Table 1) (Fig. 4*b*).

Fourth prediction

In the first trial, statistically significant differences in early-winter body size were detected between fish that survived winter and those that were presumed dead (Table 1). Winter survivors were heavier in December than fish that were not recaptured again and presumed dead (mean body mass = 2.65 g, SE = 0.07 g, mean fork length = 6.24 cm, SE = 0.05 cm and mean body mass = 2.06 g, SE = 0.04 g, mean fork length = 5.71 cm, SE = 0.07 cm, respectively). In the second trial, juvenile coho salmon were in general heavier at the start of the experiment than those tested the previous year (survivors mean body mass = 6.65 g, SE = 0.213 g, mean fork length = 7.58 cm, SE = 0.077 cm; dead or missing fish mean body mass = 6.64 g, SE = 0.216 g, mean fork length = 7.62 cm, SE = 0.068 cm), and in this case, no significant size differences were found in December between survivors and nonsurvivors (Table 1).

Fifth prediction

The early-winter size of emigrating presmolts was significantly larger than that of residual individuals in the first trial (Table 1). The December mean body mass of spring emigrants was 2.74 g (SE = 0.083 g) and their mean fork length was 6.34 cm (SE = 0.059 cm), whereas the December mean body mass and fork length of the residual fish were 1.72 g (SE = 0.125 g) and 5.46 cm (SE = 0.106 cm), respectively. Because by the end of the second trial, residual fish remained only in a few pens, a *t* test on the December weight of spring emigrants versus residual fish was used to test the

© 2007 NRC Canada

Table 1. Results of ANOVA and *t* tests.

Prediction	Variable	Trial	df	*F*	*t*	*p* (power of test)
1	Growth (mass)	1	6	2.20	—	0.042
	Growth (length)	1	6	2.58	—	0.018
	Growth (mass)	2	3	0.22*	—	0.881 (0.05)
	Growth (length)	2	3	0.28*	—	0.838 (0.05)
2	No. of survivors	1	3	0.37	—	0.777 (0.05)
	No. of survivors	2	3	4.51	—	0.024
3	Final size (mass)	1	3	8.25*	—	0.003
	Final size (length)	1	3	7.49*	—	0.004
	Final size (mass)	2	3	0.40*	—	0.759 (0.05)
	Final size (length)	2	3	0.51*	—	0.685 (0.05)
4	Initial mass	1	1	46.37	—	<0.001
	Initial length	1	1	44.59	—	<0.001
	Initial mass	2	1	0.15	—	0.702 (0.05)
	Initial length	2	1	0.01	—	0.923 (0.05)
5	Initial mass	1	1	43.92	—	<0.001
	Initial length	1	1	41.40	—	<0.001
	Initial mass	2	185	—	0.36	0.717 (0.05)
	Initial length	2	185	—	0.45	0.652 (0.05)
6	Emigrants per season	1	2	28.94	—	<0.001
	Emigrants per season	2	2	38.07	—	<0.001

Note: Trial 1, 1996–1997; trial 2, 1997–1998. An asterisk indicates an approximate *F* value. The power of tests is provided only for tests that failed to reject the null hypothesis.

Fig. 3. Percentage of juvenile coho salmon in experimental pens that survived winter. The total percentage of survivors includes both spring emigrants and summer residual fish. (*a*) First trial; (*b*) second trial. Vertical error bars represent 2 SE. W + C, pens with wood plus carcass treatment.

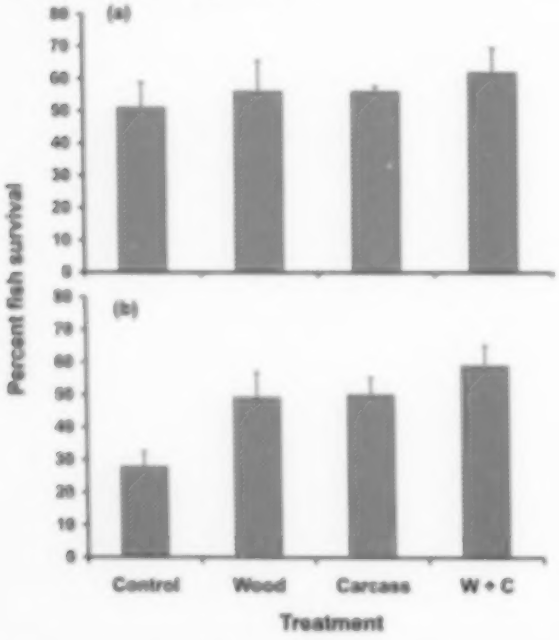

Fig. 4. Final weight of spring emigrant and residual juvenile coho salmon from experimental pens. (*a*) First trial; (*b*) second trial. Vertical error bars represent 2 SE. W + C, pens with wood plus carcass treatment. Dissimilar scales on the vertical axes reflect interannual differences in fish size.

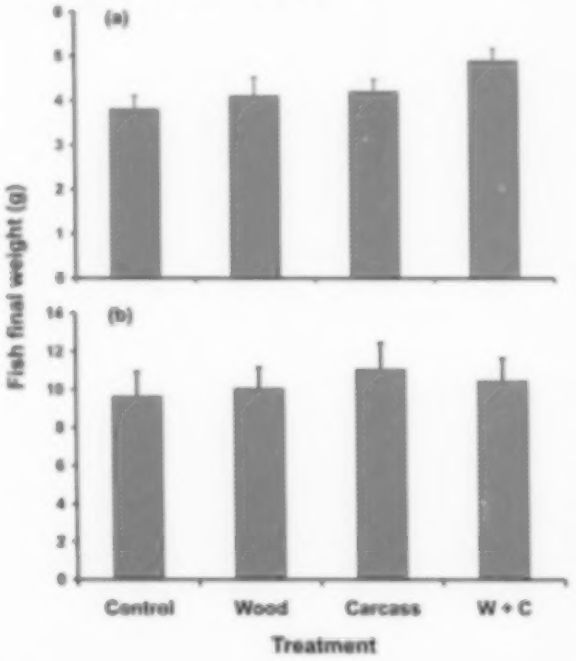

fifth hypothesis instead of a two-way ANOVA. This test showed that during the second year, the slight difference in December size between emigrating presmolts and summer residual fish was not statistically significant (Table 1). The mean December body mass of presmolts was 6.46 g (SE = 0.231 g) and their mean fork length was 7.55 cm (SE = 0.080 cm), while the mean December body mass of residual

© 2007 NRC Canada

fish was 5.90 g (SE = 0.773 g) and their mean fork length was 7.40 cm (SE = 0.304 cm).

Sixth prediction

We found a statistically significant difference in the number of emigrants per season among treatments in the first trial (Table 1). This corroborates the obvious effect of the factor "season" on number of emigrants (Fig. 5) and shows that these numbers were not affected by any of the pen treatments. Fish movement was limited during winter – early spring (January–April), and few juvenile coho salmon entered the emigration traps during that period (Fig. 5*a*). Emigration peaked between May and June (spring). No fish left the pens during July and August. The summer "residual" fish, which had to be removed by the end of August, represented approximately 8% of the initial number of fish that were released in the pens at the beginning of the trial. This was the only case in which the results of the second trial did not differ from those in the previous year. However, although season had a significant effect on number of emigrants in the second trial (Table 1), it also interacted with the wood treatment (wood × season: $F_{[2]} = 3.84$, $p = 0.036$). In this trial, with fish with higher initial body mass, residual individuals were only 4% of the initial number of fish released in the pens (Fig. 5*b*).

Discussion

Our most important finding is that the initial size and density of juvenile coho salmon, which differed between years, had noticeable effects on our overall results. Only the results of the first trial (1996–1997) showed that salmon carcasses increase juvenile coho salmon growth rates and body mass, which is consistent with what Wipfli et al. (2003) reported for the species in Alaska. Therefore, our first prediction was supported only when the early-winter size of experimental fish was small and their densities high. Under those circumstances, salmon carcasses had longer-lasting effects on juvenile coho salmon daily growth rates when in-stream wood was present than when it was not. The growth rate boosting effect of in-stream wood lasted well into spring, weeks after the carcasses had totally disintegrated. In contrast, in pens that only received salmon carcasses, fish daily growth rates, although initially high, dropped once the carcasses were no longer available. The greater growth observed in pens that received the combined wood and carcass treatment suggests that the presence of in-stream cover somehow reduces fish energetic costs and thus enhances growth rates during late winter and early spring. This could be due to reductions in either predation pressure (Reinhardt and Healey 1999) or aggressive interactions among the young fish (Giannico and Healey 1999; Vøllestad and Quinn 2003) or both. In-stream wood could not have played an important velocity shelter role in this study because water flow in the side-channel was very low.

None of our results support the second prediction that the combination of carcasses and in-stream wood would increase over-winter fish survival. However, there were important inter-annual differences in our findings. While during the 1996–1997 trial, none of the treatments (i.e., carcasses, in-stream wood, and carcasses and wood combined) had an effect on coho salmon parr over-winter survival rates, all of the treatments, not just carcasses plus wood, increased fish overwinter survival during the 1997–1998 trial. Having dissimilar fish sizes and densities between trials caused different responses to our treatments, and the combination of both small body mass and high densities in early winter seemed to have an overriding effect over other factors in terms of survival rates.

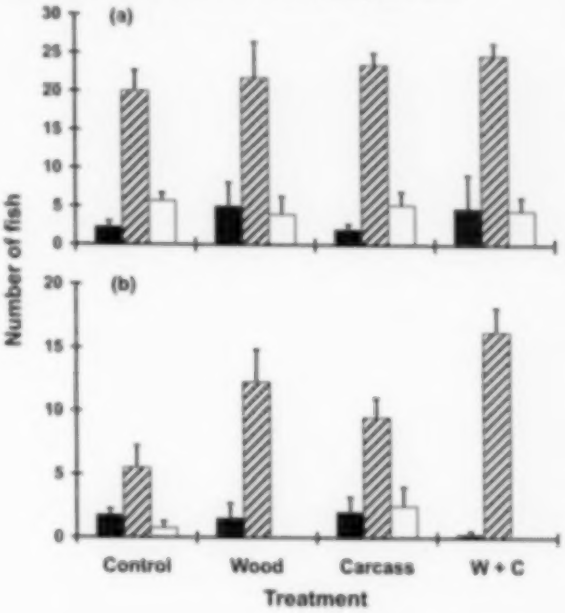

Fig. 5. Number of juvenile coho salmon emigrating each season from experimental pens. (*a*) First trial; (*b*) second trial. Solid bars, winter emigrants; hatched bars, spring emigrants; open bars, residual fish. Vertical error bars represent 2 SE. W + C, pens with wood plus carcass treatment. Dissimilar scales on the vertical axes reflect interannual differences in fish rearing densities.

Our third prediction regarding salmon carcasses and in-stream wood increasing coho salmon presmolt size was also only confirmed during our first year trial, when fish were relatively small and densities high. However, the results of our second trial show that the final-size response of juvenile coho salmon to treatments was influenced by their early-winter size and rearing densities. Hence, when the average fish size was relatively large and densities high, none of the treatments affected presmolt size. Treatment effect may have been more difficult to detect in this trial because any spring growth spurt (percent mass gained per day) that took place was proportionately smaller in these large fish than in the small fish of the first trial.

We had anticipated, in our fourth prediction, a positive relationship between early-winter fish body size and survival, and this was observed during the first trial, in which the smallest individuals in that relatively small body size-class died in greater proportion than their larger counterparts regardless of treatment. Interference competition (Sutherland 1983) for resources (including space) under the crowded condition of the first trial may have exacerbated size-related mortality in all pens to a point where no treatment effect

© 2007 NRC Canada

could be detected. Conversely, during the second trial, with large coho salmon parr at low densities, no size-related mortality was detected, as all treatments increased the percentage of fish that survived winter.

Relationships between juvenile salmonid pre-winter size and winter survival are complex in nature and therefore not simple to predict. Results not only change with fish rearing densities but also respond to a range of other factors (both biotic and abiotic) that influence the intensity of selection pressures during the least favourable of all seasons. For example, Quinn and Peterson (1996) found that during a low-survival year, juvenile coho salmon that were larger than average by October had greater probability of surviving to smolt stage, and this was independent of habitat quality. This result contrasted sharply with the independence that they observed between fish fall size and winter survival during a subsequent high-survival year, when even fish from the smallest size-classes fared well. Quinn and Peterson (1996) did not mention differences in fish rearing densities and suggested that the higher winter discharge during the first year of their study may have accounted for some of the interannual variation they observed. Water temperature seems to have been similar during both years in their study creek, and they considered it too mild (consistently above 4 °C) to have induced thermal stress on the fish.

In our experimental reach, however, average water temperatures were well below 4 °C during both years and were particularly lower during the first year, with temperatures in January dropping to 2.33 °C and remaining low well into mid-February. Under these conditions, it is feasible that size-related fish survival, particularly for our experimental group with the smallest body size, could be attributed to the increase in metabolic efficiency that occurs with greater body mass at low water temperatures (Hunt 1969). The physiological advantages that relatively large early-winter body mass may give some individuals under crowded rearing conditions (i.e., high competitive pressure) could override some of the effects that cover and food have on their survival. Our smaller than average fish may have starved to death (Hunt 1969; Meyer and Griffith 1997), and the fact that salmon carcass availability, especially when combined with submerged wood, had no effect on their survival suggests that the growth path that they were on from before the experiments began could not be reversed by food availability later on in winter. Morgan and Metcalfe (2001) explained this as the result of "deferred costs of fall food shortages". In their study, juvenile Atlantic salmon that had faced a food shortage during summer underwent delayed compensatory or "catch up" growth in late fall or early winter, but despite this spurt in growth, they remained at a physiological disadvantage compared with other fish in the long term. The salmon that were undernourished before winter suffered a persistent decline in body lipids, and their growth rates fell below those of the well-fed individuals between December and March (Morgan and Metcalfe 2001). It is possible that the size-dependent winter survival that we observed was the belated outcome of previous restrictions in food access caused by, among other things, differences in the social status of fish (Metcalfe et al. 1990). The absence of such a size-dependent survival pattern during our second trial suggests that most fish in it may have been larger than a minimum threshold size at which low-temperature-induced physiological stress causes mortality. Furthermore, the good initial condition of these relatively large fish may have allowed them to use more efficiently any benefits derived from having access to food and cover in winter (Morgan and Metcalfe 2001).

Size-dependent shelter use also deserves consideration in the interpretation of our results, particularly because the proportion of individuals with access to shelter should have been lower under the crowded conditions of the first trial than in the second trial. It has been well established that juvenile salmonids consistently show a clear tendency to avoid sharing shelter with conspecifics (Cunjak 1988; Gregory and Griffith 1996; Armstrong and Griffiths 2001). Under high-density rearing conditions, one would expect the smallest fish to be displaced from shelters by the largest fish (Harwood et al. 2002; Orpwood et al. 2003), which could explain the observed size-related mortality if, for example, predators consistently captured fish that were not able to occupy shelters (Dolloff 1993). Like in Quinn and Peterson's (1996) study, size-selective predation may have had an influence on our results because pens were not designed to exclude predators (except for large fish that were removed from the experimental section). American dippers (*Cinclus mexicanus*) and minks (*Mustela vison*) were observed in or near the pens, whereas river otters (*Lutra canadensis*) and belted kingfishers (*Ceryle alcion*) were known to be present in the area. Nevertheless, because fish survival was relatively the same across all pens regardless of treatment during the first trial and differed between the control and treatment pens during the second trial, it seems unlikely that access to predation shelter may have been a major factor in our results. Instead, thermal stress induced by the lower temperatures of the first trial on the smaller than average individuals within a cohort of small-bodied fish provides a better explanation for the observed size-related over-winter fish survival. Temperature-related physiological stress accounted for the lower winter survival rates Smith and Griffith (1994) reported for small Snake River rainbow trout compared with large ones, and this was the case even when protected from predators.

Results from the first trial confirmed our fifth prediction that early-winter body size of spring emigrants is larger than that of residual fish. This size difference at the beginning of the winter between regular 1-year-old smolts and residual coho suggests that there may be a minimum size for a successful smolt (Holtby et al. 1990), and unless fish reach such a threshold during a critical time window, they tend to remain in freshwater for an additional year (Thorpe 1986). The idea of such a threshold size may help explain the observed differences in percentage of residual fish between our two trials. Residual fish were twice as abundant at the end of our first trial, with relatively small fish, than at the end of the second trial, in which the average size of fish was larger.

Contrary to our sixth prediction, the timing of presmolt emigration was not affected by any of our treatments and was likely a response to season-related factors such as temperature and photoperiod (Saunders and Henderson 1970). Fish in our study showed emigration patterns and timing similar to those reported by Giannico and Hinch (2003) for this same side-channel and another one in a nearby system. Although during the first trial, there was a tendency for

© 2007 NRC Canada

some of the largest individuals to emigrate in mid- to late winter, emigration in earnest started in April and peaked in May in both of our trials. This tendency for the larger, and likely older, juvenile coho salmon to move downstream earlier than their smaller conspecifics was also observed by Irvine and Ward (1989) in the Keogh River, northern Vancouver Island. Giannico and Hinch (2003) concluded that the large-sized early emigrants were generally 2-year-old individuals that had probably been too small at the start of their first winter to afford the physiological costs of smolting (Thorpe 1986) and needed an additional year to reach a size that would improve their odds of ocean survival (Holtby et al. 1990). It is likely that in the present study, the 2-year-old coho salmon were the few that emigrated several weeks prior to most of the fish, which were 1 year old. Emigration only peaked after water temperatures rose above 4.5 °C in the springs of both 1997 and 1998. This observation was consistent with other studies of juvenile coho salmon winter activity (Bustard and Narver 1975; Giannico and Healey 1998).

Unlike other studies that reported effects of experimental-unit position (e.g., Spalding et al. 1995), we did not find evidence that any potential difference among pens, which were included as one of the factors in the analyses, biased our results. Although salmon carcass derived nutrients might have induced an increase in invertebrate numbers in our entire experimental reach (Wipfli et al. 1998; Chaloner and Wipfli 2002), this did not mask the strong positive effect that direct access to salmon flesh had on fish growth rates during the first trial. Fish were observed feeding on the available pieces of salmon carcass, and this significantly boosted the growth rates of most individuals. Bilby et al. (1998) showed that the salmon flesh and eggs consumed by young salmonids are readily assimilated. They calculated that the ratio of marine-derived nitrogen in muscle tissue ranged from 44.1% in coho salmon to 71.9% in age-1 steelhead that had access to carcasses compared to 16.6% and 36.3% in coho salmon and steelhead, respectively, from reaches without carcasses.

Densities of juvenile coho salmon in streams vary from year to year depending on adult escapement, early-life survival, and availability of nursery habitat. Likewise, the average body size of coho salmon parr will change on an annual basis in response to not only their rearing densities but also water temperature and food availability. In our study, the interannual differences in initial juvenile coho salmon densities and body size, which reflect that natural variation, have had marked effects on the results. Had the study been performed during only one of the two years, its findings would have been very different. A simple interpretation of a single year's worth of data could have been that there was either a strong treatment effect or none at all. However, our results imply that the extent of the benefit that young coho salmon can derive from salmon carcasses varies with both their physiological and their rearing conditions.

Our mesocosm experiment allowed us to test specific factors in a setup that had many natural conditions (e.g., water temperature, photoperiod, and predation) while improving statistical power through replication. Although our results contribute to our understanding of coho salmon ecology, caution is required when they are extrapolated to natural systems (Warren and Davis 1971). However, it is important to highlight that our findings agree with those of earlier field- and enclosure-based studies (Bilby et al. 1998; Wipfli et al. 2003) regarding the important role that salmon carcasses play in increasing juvenile coho salmon winter growth and body mass. Furthermore, they reveal that wood availability may play an important role in extending over time the beneficial effects that carcasses have on fish daily growth rates.

When evaluating the role of salmon carcasses in feeding another generation of salmonids, it is important to consider not only the influence that in-stream habitat complexity may have on the final outcome but also that the effect of carcasses will differ from year to year depending on juvenile fish pre-winter body size and over-wintering densities. Under the experimental conditions of this study, small-sized juvenile coho salmon rearing at high densities derive benefits from salmon carcasses (in terms of both winter growth and presmolt size) that large-sized individuals at low densities do not. Historically, juvenile coho salmon were likely to occupy nursery habitats at higher densities than they do at present in the countless basins that have low adult escapement (Gresh et al. 2000). The prevailing rearing conditions of the past mean that summer feeding competition among salmon fry must have been intense, and as a result, the average prewinter salmon parr size should have been relatively small. Consequently, one may hypothesize that the influence of salmon carcasses on the next generation of salmon may have been greater in the past than it is today in many underseeded streams where large-sized salmon parr occur at low rearing densities. Although additional research is needed to investigate such a proposition, the potential benefits of salmon carcass placement projects should be considered within the ecological context of each individual watershed and cannot be regarded as the "silver bullet" of stream restoration.

Acknowledgments

This experimental work could not have been completed without the invaluable assistance and dedication of Andrew Lotto. Statistical advice was provided by Lisa Ganio and Brandt Balgooyen. The comments of Phil Roni, David Noakes, Hiram Li, Tom Quinn, and Sean Mitchell have substantially improved the manuscript, and we want to thank them for that. Financial support for this project was provided by a Forest Renewal BC grant to G.R. Giannico and S.G. Hinch.

References

Armstrong, J.D., and Griffiths, S.W. 2001. Density-dependent refuge use among over-wintering wild Atlantic salmon juveniles. J. Fish Biol. **58**: 1524–1530.

Bilby, R.E., Fransen, B.R., Bisson, P.A., and Walter, J.K. 1998. Response of juvenile coho salmon (*Oncorhynchus kisutch*) and steelhead (*Oncorhynchus mykiss*) to the addition of salmon carcasses to two streams in southwestern Washington, U.S.A. Can. J. Fish. Aquat. Sci. **55**: 1909–1918.

Bilby, R.E., Fransen, B.R., Walter, J.K., Cederholm, C.J., and Scarlett, W.J. 2001. Preliminary evaluation of the use of nitrogen stable isotope ratios to establish escapement levels for Pacific salmon. Fisheries (Bethesda), **26**: 6–14.

© 2007 NRC Canada

Bustard, D.R., and Narver, D.W. 1975. Aspects of the winter ecology of juvenile coho salmon (*Oncorhynchus kisutch*) and steelhead trout (*Salmo gairdneri*). J. Fish. Res. Board Can. **32**: 667–680.

Cederholm, C.J., Houston, D.B., Cole, D.L., and Scarlett, W.J. 1989. Fate of coho salmon (*Oncorhynchus kisutch*) carcasses in spawning streams. Can. J. Fish. Aquat. Sci. **46**: 1347–1355.

Cederholm, C.J., Bilby, R.E., Bisson, P.A., Bumstead, T.W., Fransen, B.R., Scarlett, W.J., and Ward, J.W. 1997. Response of juvenile coho salmon and steelhead to placement of large woody debris in a coastal Washington stream. N. Am. J. Fish. Manag. **17**: 947–963.

Cederholm, C.J., Kunze, M.D., Murota, T., and Sibatani, A. 1999. Pacific salmon carcasses: essential contributions of nutrients and energy for aquatic and terrestrial systems. Fisheries (Bethesda), **24**: 6–15.

Chaloner, D.T., and Wipfli, M.S. 2002. Influence of decomposing Pacific salmon carcasses on macroinvertebrate growth and standing stock in southeastern Alaska streams. J. North Am. Benthol. Soc. **21**: 430–442.

Cunjak, R.A. 1988. Behaviour and microhabitat of young Atlantic salmon (*Salmo salar*) during winter. Can. J. Fish. Aquat. Sci. **45**: 2156–2160.

Dolloff, C.A. 1993. Predation by river otters (*Lutra canadensis*) on juvenile coho salmon (*Oncorhynchus kisutch*) and Dolly Varden (*Salvelinus malma*) in Southeast Alaska. Can. J. Fish. Aquat. Sci. **50**: 312–315.

Giannico, G.R., and Healey, M.C. 1998. Effects of flow and food on winter movements of juvenile coho salmon. Trans. Am. Fish. Soc. **127**: 645–651.

Giannico, G.R., and Healey, M.C. 1999. Ideal free distribution theory as a tool to examine juvenile coho salmon habitat choice under different conditions of food abundance and cover. Can. J. Fish. Aquat. Sci. **56**: 1–12.

Giannico, G.R., and Hinch, S.G. 2003. The effect of wood and temperature on juvenile coho salmon winter movement, growth, density and survival in side-channels. River Res. Appl. **19**: 219–231.

Gregory, J.S., and Griffith, J.S. 1996. Aggressive behaviour of underyearling rainbow trout in simulated winter concealment habitat. J. Fish Biol. **49**: 237–245.

Gresh, T., Lichatowich, J., and Schoonmaker, P. 2000. An estimation of historic, and current levels of salmon production in the northeast Pacific ecosystem: evidence of a nutrient deficit in freshwater systems of the Pacific Northwest. Fisheries (Bethesda), **25**: 15–21.

Harwood, A.J., Metcalfe, N.B., Griffiths, S.W., and Armstrong, J.C. 2002. Intra- and inter-specific competition for winter concealment in juvenile salmonids. Can. J. Fish. Aquat. Sci. **59**: 1515–1523.

Heintz, R.A., Nelson, B.D., Hudson, J., Larsen, M., Holland, L., and Wipfli, M. 2004. Marine subsidies in freshwater: effects of salmon carcasses on lipid class and fatty acid composition of juvenile coho salmon. Trans. Am. Fish. Soc. **133**: 559–567.

Holtby, L.B. 1988. The effects of logging on stream temperatures at Carnation Creek. *In* Proceedings of the Workshop: Applying 15 Years of Carnation Creek Results. *Edited by* T.W. Chamberlin. Pacific Biological Station, Nanaimo, B.C. pp. 118–122.

Holtby, L.B., Andersen, B.C., and Kadowaki, R.K. 1990. Importance of smolt size and early ocean growth to interannual variability in marine survival of coho salmon (*Oncorhynchus kisutch*). Can. J. Fish. Aquat. Sci. **47**: 2181–2194.

Hunt, R.L. 1969. Overwinter survival of wild fingerling Brook trout in Lawrence Creek, Wisconsin. J. Fish. Res. Board Can. **26**: 1473–1483.

Irvine, J.R., and Ward, B.R. 1989. Patterns of timing and size of wild coho salmon (*Oncorhynchus kisutch*) smolts migrating from the Keogh River watershed on northern Vancouver Island. Can. J. Fish. Aquat. Sci. **46**: 1086–1094.

Krebs, C.J. 1989. Ecological methodology. Harper and Row, New York.

Kuehl, R.O. 2000. Design of experiments: statistical principles of research design and analysis. 2nd ed. Duxbury Press, Pacific Grove, Calif.

Larkin, G., and Slaney, P.A. 1997. Implications of trends in marine-derived nutrient influx to south coastal British Columbia salmonid production. Fisheries (Bethesda), **22**: 16–24.

Mason, J.C. 1976. Response of underyearling coho salmon to supplemental feeding in a natural stream. J. Wildl. Manag. **40**: 775–788.

Matter, W.J., Mannan, R.W., Bianchi, E.W., McMahon, T.E., Menke, J.H., and Tash, J.C. 1989. A laboratory approach for studying emigration. Ecology, **70**: 1543–1546.

Metcalfe, N.B., Huntingford, F.A., Thorpe, J.E., and Adams, C.E. 1990. The effects of social status on life-history variation in juvenile salmon. Can. J. Zool. **68**: 2630–2636.

Meyer, K.A., and Griffith, J.S. 1997. First-winter survival of rainbow trout and brook trout in the Henrys Fork of the Snake River, Idaho. Can. J. Zool. **75**: 59–63.

Morgan, I.J., and Metcalfe, N.B. 2001. Deferred costs of compensatory growth after autumnal food shortage in juvenile salmon. Proc. R. Soc. Lond. B Biol. Sci. **268**: 295–301.

Nickelson, T.E., Rodgers, J.D., Johnson, S.L., and Solazzi, M.F. 1992*a*. Seasonal changes in habitat use by juvenile coho salmon (*Oncorhynchus kisutch*) in Oregon coastal streams. Can. J. Fish. Aquat. Sci. **49**: 783–789.

Nickelson, T.E., Solazzi, M.F., Johnson, S.L., and Rodgers, J.D. 1992*b*. Effectiveness of selected stream improvement techniques to create suitable summer and winter rearing habitat for juvenile coho salmon (*Oncorhynchus kisutch*) in Oregon coastal streams. Can. J. Fish. Aquat. Sci. **49**: 790–794.

Orpwood, J.E., Griffiths, S.W., and Armstrong, J.D. 2003. Effects of body size on sympatric shelter use in over-wintering juvenile salmonids. J. Fish Biol. **63**: 166–173.

Peterson, N.P. 1982. Population characteristics of juvenile coho salmon (*Oncorhynchus kisutch*) overwintering in riverine ponds. Can. J. Fish. Aquat. Sci. **39**: 1303–1307.

Quinn, T.P., and Peterson, N.P. 1996. The influence of habitat complexity and fish size on over-winter survival and growth of individually marked juvenile coho salmon (*Oncorhynchus kisutch*) in Big Beef Creek, Washington. Can. J. Fish. Aquat. Sci. **53**: 1555–1564.

Reinhardt, U.G., and Healey, M.C. 1999. Season- and size-dependent risk taking in juvenile coho salmon: experimental evaluation of asset protection. Anim. Behav. **57**: 923–933.

Ricker, W.E. 1975. Computation and interpretation of biological statistics of fish populations. Bull. Fish. Res. Board Can. No. 191.

Roni, P. and Quinn, T.P. 2001. Density and size of juvenile salmonids in response to placement of large woody debris in western Oregon and Washington streams. Can. J. Fish. Aquat. Sci. **58**: 282–292.

SAS Institute Inc. 1988. SAS/STAT user's guide. Release 6.03 ed. SAS Institute Inc., Cary, N.C.

Saunders, R.L., and Henderson, E.B. 1970. Influence of photoperiod on smolt development and growth in Atlantic salmon *Salmo salar*. J. Fish. Res. Board Can. **27**: 1295–1311.

Smith, R.W., and Griffith, J.S. 1994. Survival of rainbow trout during their first winter in the Henrys Fork of the Snake River, Idaho. Trans. Am. Fish. Soc. **123**: 747–756.

Solazzi, M.F., Nickelson, T.E., Johnson, S.L., and Rodgers, J.D. 2000. Effects of increasing winter rearing habitat on abundance

© 2007 NRC Canada

of salmonids in two coastal Oregon streams. Can. J. Fish. Aquat. Sci. **57**: 906–914.

Spalding, S., Peterson, N.P., and Quinn, T.P. 1995. Summer distribution, survival and growth of juvenile coho salmon *Oncorhynchus kisutch* under varying experimental conditions of brushy instream cover. Trans. Am. Fish. Soc. **124**: 124–130.

Sutherland, W.J. 1983. Aggregation and the 'ideal free' distribution. J. Anim. Ecol. **52**: 821–828.

Swales, S., and Levings, C.D. 1989. Role of off-channel ponds in the life cycle of coho salmon (*Oncorhynchus kisutch*) and other juvenile salmonids in the Coldwater River, British Columbia. Can. J. Fish. Aquat. Sci. **46**: 232–242.

Thorpe, J.E. 1986. Age at first maturity in Atlantic salmon, *Salmo salar*: freshwater period influences and conflicts with smolting. Can. Spec. Publ. Fish. Aquat. Sci. No. 89. pp. 7–14.

Vøllestad, L.A., and Quinn, T.P. 2003. Trade-off between growth rate and aggression in juvenile coho salmon, *Oncorhynchus kisutch*. Anim. Behav. **66**: 561–568.

Warren, C.E., and Davis, G.E. 1971. Laboratory stream research: objectives, possibilities, and constraints. Annu. Rev. Ecol. Syst. **2**: 111–144.

Wipfli, M.S., Hudson, J., and Caouette, J. 1998. Influence of salmon carcasses on stream productivity: response of biofilm and benthic macroinvertebrates in southeastern Alaska, U.S.A. Can. J. Fish. Aquat. Sci. **55**: 1503–1511.

Wipfli, M.S, Hudson, J.P., Caouette, J.P., and Chaloner, D.T. 2003. Marine subsidies in freshwater ecosystems: salmon carcasses increase the growth rates of stream-resident salmonids. Trans. Am. Fish. Soc. **132**: 371–381.

Wipfli, M.S., Hudson, J.P., and Caouette, J.P. 2004. Restoring productivity of salmon-based food webs: contrasting effects of salmon carcass and salmon carcass analog additions on stream-resident salmonids. Trans. Am. Fish Soc. **133**: 1440–1454.

© 2007 NRC Canada

Multiple determinants of welfare in farmed fish: stocking density, disturbance, and aggression in Atlantic salmon (*Salmo salar*)

C.E. Adams, J.F. Turnbull, A. Bell, J.E. Bron, and F.A. Huntingford

Abstract: Adult Atlantic salmon (*Salmo salar*) were held in seawater tanks at stocking densities of 15, 25, and 35 kg·m^{-3} (with five replicates). After 51 days, four measures of welfare (body condition, fin condition, plasma glucose, and cortisol) were collected and combined by principal components analysis into an integrated welfare score for each fish. Fish with high and low welfare scores were found in all conditions, but overall welfare was best at the intermediate density, supporting the view that low densities as well as high densities can compromise welfare in salmon. The effect of stocking density interacted with the stronger effect of disturbance, creating a complex pattern of variation in welfare among the experimental tanks. Counter-intuitively, welfare scores were higher in tanks with a high level of disturbance, while welfare scores were strikingly low at the lowest density. Aggression in all tanks was low, but rose after feeding, when aggression was negatively related to both disturbance and stocking density. These data highlight the complex determinants of welfare in fish in production systems and, taken together, suggest that negative effects of husbandry practice and density on welfare in Atlantic salmon might be mediated by their influence on social interactions.

Résumé : Nous avons gardé des saumons atlantiques (*Salmo salar*) adultes dans des bassins d'eau de mer à des densités d'empoissonnement de 15, 25 et 35 kg·m^{-3} (cinq séries de chaque expérience). Après 51 jours, nous avons déterminé quatre indices de bien-être (condition corporelle, état des nageoires, glucose et cortisol du plasma) et les avons combinés par analyse des composantes principales pour obtenir un indice intégré du bien-être chez chaque poissons. On trouve des poissons avec des indices de bien-être hauts et bas dans toutes les conditions expérimentales, mais en général le bien-être est meilleur aux densités intermédiaires, ce qui appuie l'idée que tant les basses que les fortes densités peuvent réduire le bien-être des saumons. L'effet de la densité d'empoissonnement interagit avec l'effet plus important de la perturbation, ce qui crée un patron complexe de variation du bien-être dans les bassins expérimentaux. Contrairement à ce qu'on pourrait attendre intuitivement, les indices de bien-être sont plus élevés dans les bassins ayant un fort niveau de perturbation et les scores de bien-être sont remarquablement bas à la densité la plus faible. Il y a peu d'agressivité dans les bassins, mais elle s'accroît après l'alimentation et l'agressivité est alors en relation négative tant avec la perturbation qu'avec la densité d'empoissonnement. Ces données mettent en lumière la complexité des facteurs déterminants du bien-être dans les systèmes de production des poissons; dans leur ensemble, elles laissent croire que les effets négatifs des pratiques et de la densité d'élevage sur le bien-être du saumon atlantique s'expliquent par leur influence sur les interactions sociales.

[Traduit par la Rédaction]

Introduction

The question of whether and to what extent fish have the capacity to experience pain and other forms of suffering is a matter of considerable current debate (e.g., Chandroo et al. 2004*a*, 2004*b*). Suffering is defined (sensu Dawkins 1998) as the conscious experience of something very unpleasant, based on awareness of internal and external stimuli. If they do not have such a capacity, then arguably it does not matter what humans do to them (Bermond 1997). In the context of whether fish suffer pain, Rose (2002) has argued robustly that their behavioural capacities are simple, that their responses to noxious stimuli are reflex-like, with no emotional correlates, and that fish lack the brain region (the neocortex) that mediates suffering in humans. An alternative view (e.g., Braithwaite and Huntingford 2004; Chandroo et al. 2004*a*, 2004*b*) stresses the fact that fish are capable of complex behaviour and display complex cognitive processes. In addition, similar functions are served by different brain regions in different vertebrate groups, and there is more homology

Received 7 April 2006. Accepted 26 October 2006. Published on the NRC Research Press Web site at http://cjfas.nrc.ca on 7 March 2007.
J19263

C.E. Adams[1] and F.A. Huntingford. Fish Biology Group, Scottish Centre for Ecology and the Natural Environment, Division of Environmental and Evolutionary Biology, University of Glasgow, Rowardennan, Glasgow G63 0AW, United Kingdom.
J.F. Turnbull, A. Bell, and J.E. Bron. Institute of Aquaculture, University of Stirling, Stirling FK9 4LA, United Kingdom.

[1]Corresponding author (e-mail: C.Adams@bio.gla.ac.uk).

 doi:10.1139/F07-018 © 2007 NRC Canada

between the brains of fish and mammals than was previously thought. According to this view, to which the authors of this paper subscribe, fish probably do experience some of the adverse states that humans associate with pain and emotional distress, even if they do not have the capacity for self-awareness necessary for conscious suffering in the full human sense. This puts the welfare of fish firmly on the political and scientific agenda.

Various human activities potentially compromise the welfare of fish (FSBI 2002; Huntingford et al. 2006), including both unintentional effects (e.g., through environmental degradation) and intentional effects (e.g., through scientific research). In some respects, more problematic are activities such as angling and keeping ornamental fish, where fish welfare may be compromised in the interests of human sport and enjoyment, and activities such as commercial fisheries and aquaculture, where fish welfare may be compromised in the interests of providing high-quality food for humans. Public concern and the actions of legislators and regulators has concentrated on the last of these, and scientific research has shown that various husbandry systems can impact negatively on the welfare of fish held in aquaculture systems (FSBI 2002; Huntingford et al. 2006). A proper understanding of how such negative effects come about is a necessary first step towards developing husbandry practices in aquaculture that promote fish welfare. This issue is addressed in the present paper, in the context of the effects of stocking density on welfare in farmed Atlantic salmon (*Salmo salar*).

Intensive farming inevitably involves holding animals at densities that are substantially greater than they routinely experience in the wild, although the fact that many species of fish form dense schools in the wild (Trevorrow and Clayton 1998) is important when assessing the welfare of such species when held in captivity. For this reason, public and scientific attention to fish, as for other farmed animals (see e.g., McLean et al. 2002; Dawkins et al. 2004; Kim et al. 2004), has focused on stocking density as one of the main factors that may impair welfare in agriculture systems. Several studies have examined the effects of stocking density on welfare in farmed fish species (Wedemeyer 1997), with varying results depending on the species concerned. For example, in Arctic charr (*Salvelinus alpinus*), increased fin damage, lower growth, and a higher incidence of agonistic interactions have all been reported in fish held in farm conditions at low density compared with high density (Brown et al. 1992; Jørgensen et al. 1993; Adams and Huntingford 1996). Mortality and plasma glucose and cortisol levels are significantly higher in tambaqui (*Colossoma macropomum*) following a short period at high density (Gomes et al. 2003), but no effect was reported for similar experiments in the red porgy (*Pagrus pagrus*, Pavlidis et al. 2003).

As well as such between-species diversity, the observed relationship between stocking density and welfare is often variable among different studies of the same species. For example, Ellis et al. (2002) reviewed 43 studies of the effect of stocking density on 30 measures of welfare in farmed rainbow trout (*Oncorhynchus mykiss*). The proportion of studies that found a negative effect of stocking density depended, partly, on the welfare measure being used. For example, 70% of the 40 studies reviewed showed adverse effects of density on growth, whereas 42% of 23 studies reported significant adverse effects on mortality rate. This review concluded that where density effects were evident, the impact on welfare was mostly mediated through the effects of reduced water quality rather than through increased levels of aggression at high stocking densities (Ellis et al. 2002). This is in spite of the fact that aggressive encounters between individuals have a clear effect on widely used indicators on welfare (see for example Höglund et al. 2001 on Arctic charr).

The review by Ellis et al. (2002) highlighted the need to incorporate data from different biological systems in estimates of welfare and the possibility of complex interactions among the various husbandry variables that impact on fish welfare. The same points emerged in a study of the effects of stocking density on the welfare of salmon in production cages by Turnbull et al. (2005). In that study, four commonly used measures of fish welfare (condition of body and fins and plasma concentrations of glucose and cortisol) were collected from Atlantic salmon in cages on a commercial marine farm exposed to densities ranging from 9.7 to 34 $kg \cdot m^{-3}$. Principal components analysis (PCA) was used to combine the four variables into a single welfare score, which was consistent with the evaluation of welfare by experienced farmers on the study site. Regression analysis showed that at densities above an inflection point at about 22 $kg \cdot m^{-3}$, welfare was predicted by stocking density; above this point increasing stocking density was associated with lower welfare scores. Welfare was also related to location of the cage (possibly depending upon the amount of disturbance by tidal currents) and time since stocking.

The Turnbull et al. (2005) study was under production conditions. Thus, the welfare score developed could be calibrated against information from experienced fish farmers. However, the use of working farms placed inevitable logistic constraints on the study. In particular, controlled, replicated manipulation of stocking density was not feasible (so statistical inferences had to be drawn from regression analysis, making cause and effect hard to unravel), and direct observation of the behaviour of the fish was impossible (so the role of behaviour in generating the observed results could not be determined). The study described in this paper is a companion to that of Turnbull et al. (2005), in which we manipulated stocking density in Atlantic salmon held in large experimental tanks in a replicated controlled experiment to determine its effects on welfare of the fish. During the course of this study, it transpired that exposure to disturbance during routine husbandry (controlled for by a randomized, replicated experimental design) had a substantial effect on experimental outcome. As a result, this variable was incorporated retrospectively into the analysis. Thus, we addressed the following questions: (*i*) How is the welfare of Atlantic salmon held in tanks influenced by stocking density across a range exceeding that commonly used in aquaculture? (*ii*) What is the impact of routine husbandry disturbance on salmon welfare? (*iii*) Do disturbance and stocking density interact to influence fish welfare? (*iv*) Can any effects of density or husbandry on welfare be explained by differences in frequency of aggressive interactions among the fish?

© 2007 NRC Canada

Materials and methods

Establishing and maintaining experimental groups

Atlantic salmon of 24 months old were selected from a stock of Strathaird S½ fish that had been held in seawater for one winter at the Marine Research Laboratory at Machrihanish, Argyllshire, Scotland. In March 2000, they were anaesthetized, weighed, and measured, and 16 fish from each tank were tagged in the postocular tissue with visible implant (VI) tags (Hughes et al. 2000). Fish were then distributed among 15 experimental tanks, 2 m diameter, 1.2 m deep, in five replicates of three stocking densities.

Tanks were randomly arranged within a block of 3 × 5, and the block was screened from the rest of the farm unit by blinds to reduce disturbance. The stocking density at the beginning of the experiment was calculated to give experimental densities of 15, 25, and 35 kg·m^{-3} at the midpoint of the experiment, using a predicted growth rate of 0.5% of body weight per day. These densities were chosen to extend beyond the range used at that time in the UK salmon mariculture industry (a survey of commercial producers in 2000 showed a range of 9–21 kg·m^{-3} (J.F. Turnbull, unpublished data). In establishing these experimental groups, fish were drawn from across the full weight range of the stock available (weight: mean 0.98 ± 0.24 kg; fork length 441.1 ± 36.5 mm (mean ± standard deviation (SD)) to create a similar (normal) weight distribution in each tank. Retrospectively, tanks were given a rank of between 1 and 3 for the level of disturbance they were likely to receive during routine husbandry, based on tank position. If the only disturbance to tanks was a once-daily cleaning, the lowest husbandry disturbance rank of 1 was assigned (i.e., when access around this tank was not needed to gain access to other tanks); if tank position in the experimental block would subject fish to the additional disturbance of staff passing to conduct routine husbandry in tanks deeper in the block, a disturbance rank of 3 was assigned. The intermediate rank of 2 was assigned to tanks with lower but moderately high frequencies of such disturbance.

The fish were fed 5 mm pellets of a salmon diet supplied by Trouw (Northwich, UK) by automatic feeders, at a rate allowing for maximum growth for that temperature (according to manufacturer's feeding tables) in two periods each day, between 0900 and 0930 and again between 1400 and 1430, local time. The flow rate in each tank was maintained at ~25 L·min^{-1}. Temperature was monitored twice daily and ranged from 8 to 10 °C during the period of the experiment.

Behavioural screening

Screening for aggressive interactions commenced 2 weeks after the establishment of the experimental groups. Cameras were installed above the centre of tanks 24 h before filming. On each day of filming, three tanks were filmed; the video cameras capturing an image of the entire surface of the tank. Each of the 15 tanks was filmed from first light until dusk on 3 randomly allocated days. To provide a relative (between-tank) measure of baseline aggression rates for each tank, a previously used successful technique was adopted (Adams et al. 2000). One 5 min period when the fish were not being fed was selected randomly for observation from each hour of film for each tank. In addition, to determine aggression rates for each tank immediately after feeding, a further 5 min period was randomly selected for observation from the 10 min periods immediately following the end of a feeding period (i.e., after 0930 and 1430). Aggression was quantified by the pooled frequency of all aggressive actions (chasing, charging, displacement, and fin-nipping; see descriptions of behaviour in Adams et al. 1998). The fish were not marked externally, so no attempt was made to assign aggressive actions to individual fish; data are therefore presented for the whole group. Fish were visible throughout the water column in each tank, but at times some fish were obscured by others. Thus, to standardize between tanks, aggression rate was adjusted to the number of interactions per 10 fish per 5 min observation period.

Postexperimental assessment of welfare status

After 51 days, the experiment was terminated, all fish were removed from the tanks, killed with a blow to the head (followed by brain destruction), weighed, and measured. Weights and fork lengths were used to calculate condition factor (K) (Jobling 1995), where

$$K = (\text{mass (g)} \cdot 100)/\text{fork length}^3\ \text{(cm)}$$

Those fish with VI tags were used to determine the specific growth rate (SGR) for each tank as

$$\text{SGR} = [\ln(w_{t_2}) - (\ln(w_{t_1})]/(t_2 - t_1)$$

where w_{t_2} and w_{t_1} are the weights at the end and beginning of the experiment, respectively, and $t_2 - t_1$ is the growth period.

Fin damage was scored for the dorsal, caudal, and pectoral fins (the fins known to show the most damage, (Turnbull et al. 1998) according to the percentage of fin intact and the degree of splitting and postdamage scarring (thickening, sensu Turnbull et al. 1998) of these fins according to Table 1*a*. Following Turnbull et al. (2005), PCA was used to combine the 12 measures of fin condition into a single measure of fin condition (based on the first principal component and accounting for 19.5% of the total variance in this data set), which gave high scores to fish with little fin erosion, splitting, or scar tissue formation (thickening) of the four fins (Table 1*b*).

Blood samples for glucose and cortisol analysis were taken by caudal venipuncture using a heparinised 2 mL syringe and then transferred into a 1.5 ml Epindorf containing heparin and 0.85% NaCl and stored on ice. Blood plasma was separated by centrifuge (5 min at 1000*g*; Force 10® portable microcentrifuge) (Denver Instrument Co., Arvada, Colorado) and stored at –20 °C until transferred in dry ice to the Institute of Aquaculture, Stirling, where samples were stored at –70 °C. Plasma glucose concentration was subsequently quantified spectrophotometrically by the Trinder enzymatic reaction (Trinder 1969; Sigma kit No. 3150). Plasma cortisol was analysed by radioimmunoassay using Amerlex™ kits. Although neither of these assays was originally designed for use in fish, they have been widely used in aquatic species, including Atlantic salmon (e.g., cortisol — Wiik et al. 1989; Espelid et al. 1996; glucose — Pottinger and Carrick 1999;

© 2007 NRC Canada

Table 1. (*a*) Criteria for the assessment of fin damage (from Turnbull et al. 1998) and (*b*) loadings on the first principal component (PC) used to generate a single fin condition score (after Turnbull et al. 2005).

(*a*) Fin damage assessment criteria.

Assessment criteria	Score
% Fin remaining	
>90	0
60–90	1
30–60	2
10–30	3
<10	4
Degree of splitting	
None	0
Moderate	1
Severe	2
Degree of thickening	
None	0
Moderate	1
Severe	2

(*b*) Loadings of first PC.

Variable	PC coefficient
Dorsal loss	0.080
Dorsal splitting	0.165
Dorsal thickening	0.182
Caudal loss	0.156
Caudal splitting	0.184
Caudal thickening	0.233
Left pelvic loss	0.011
Left pelvic splitting	0.178
Left pelvic thickening	0.335
Right pelvic loss	0.127
Right pelvic splitting	0.107
Right pelvic thickening	0.314

Ackerman et al. 2000). There was no detectable effect of storage on the samples (Bell 2003).

Blood sampling of fish was completed in less than half an hour for all tanks. Breakpoint (piecewise) regression analysis (see Tom and Lesperance 2003; Boylan and Adams 2006 for an example of its use) of cortisol levels from all groups on time since sampling showed a significant rise in cortisol, with a break point at 11.7 min and with no significant time effect on cortisol level before this point. Therefore, to avoid any confounding effect of time, only fish sampled in the first 5 min were used in further analysis; this resulted in a minimum sample size of 15 fish per tank.

Again following the techniques of Turnbull et al. (2005), PCA was used to examine the relationships among the four measures of welfare and to combine these into a single welfare score that was used in subsequent analysis. This is reported in the Results section, since we found it striking that the compound welfare score derived from the present data set collected from fish held in very different conditions should be so similar to that found by Turnbull et al. (2005).

Table 2. Loadings on the first principal component (PC) used to generate a single welfare score (after Turnbull et al. 2005).

Variable	PC loading
Condition factor	0.354
Fin condition	0.349
Plasma glucose	–0.453
Plasma cortisol	–0.547

Statistical analysis of effects of stocking density and disturbance

The effects of stocking density and level of disturbance on welfare score (and interactions between them) were examined using two-way analysis of variance (ANOVA, fixed effects). Model-derived residuals (a measure of welfare, independent of density, disturbance, and their interaction effects) showed no significant differences between tanks (ANOVA: $F_{[14,204]} = 1.25$; $P = 0.244$), indicating that there were no systematic tank effects on the welfare score other than those related to density and disturbance. Behavioural data were compared using nonparametric, Mann–Whitney sum rank and Kruskal–Wallis tests. The SPSS statistical package was used throughout (SPSS Inc., Chicago, Illinois).

Results

Deriving a multivariate score of welfare

The first derived component from the PCA (accounting for 33.3% of total variance) generated positive loadings for fin condition and condition factor coupled with negative loadings for plasma glucose and cortisol (Table 2). This component yielded high numerical values for fish with high condition factor and good fin condition coupled with low plasma glucose and cortisol levels, and the converse. It therefore combined physical condition and physiological status into a single, objectively determined welfare score for the present data set.

Growth

The mean fish growth (SGR) over the 51-day experimental period was 0.185 ± 0.001 (mean ± standard error (SE)). Growth rate did not differ significantly between tanks ($F_{[1,14]} = 1.30$, $P = 0.21$), and two-way ANOVA showed no significant effect of density ($F_{[2,209]} = 1.42$, $P = 0.25$), although the effect of disturbance was almost significant ($F_{[2,209]} = 2.97$, $P = 0.054$)

Effects of stocking density and of disturbance on welfare

Two-way ANOVA showed that stocking density and husbandry disturbance both had a highly significant effect on the welfare score (the latter effect being the stronger), but there was also a significant interaction effect between these two variables (Table 3). Overall, the density–disturbance interaction model explained 23% of variation in the PCA-derived welfare score, suggesting that other factors not controlled for in this experiment caused considerable variation in this index. The interaction effects were complex, and to

© 2007 NRC Canada

Table 3. Two-way analysis of variance (ANOVA) of the effects of density and disturbance on the welfare score.

	df	F	P
All effects	8	9.32	<0.001
Disturbance	2	15.0	<0.001
Density	2	3.94	0.021
Interaction	4	11.2	<0.001

pick our way through the results, we present the results of stocking density and disturbance separately and then look at the interactions between them.

Individual fish with a low welfare score were found at all three stocking densities. Forty-four percent of fish in the lowest quartile of the distribution of welfare scores were found in the 15 kg·m^{-3} tanks, 27% in the 25 kg·m^{-3} tanks, and 29% in the 35 kg·m^{-3} tanks. Two-way ANOVA showed that stocking density had a highly significant effect on the welfare score (Table 3). Overall, the highest mean welfare score was recorded at the intermediate density, with lower scores at both the higher and particularly at the lower density (Fig. 1*a*).

Individual fish with a low welfare score were also found at all three disturbance levels. Forty-seven percent, 26%, and 27% of fish within the lowest quartile of welfare scores were found in tanks exposed to low, intermediate, and high levels of disturbance, respectively. Two-way ANOVA showed that husbandry disturbance had a highly significant effect on the welfare score (stronger than the effect of stocking density; Table 3). Overall, the mean welfare score increased with the degree of husbandry disturbance (Fig. 1*b*).

Interactions between stocking density and disturbance

ANOVA with post hoc analysis revealed complex density effects within disturbance level (Table 3; Fig. 2*a*). At the lowest disturbance level, where the welfare scores were generally well below the average for all conditions combined (i.e., a welfare score of 0), the welfare score was strikingly lower at 35 kg·m^{-3} compared with lower densities. At intermediate disturbance levels, the welfare score showed a highly significant increase from a very low level at 15 kg·m^{-3} to average levels at 25 kg·m^{-3} and above average levels at 35 kg·m^{-3}. At the highest level of disturbance, no density effect was detectable, all welfare scores being above average.

ANOVA with post hoc analysis also revealed complex disturbance effects within density levels (Table 3; Fig. 2*b*). At densities of 15 and 35 kg·m^{-3}, the welfare score increased with disturbance, the significant step effect from very low to well above average welfare coming between intermediate and high levels of disturbance at 15 kg·m^{-3} density and between low and intermediate levels of disturbance at 35 kg·m^{-3}. At 25 kg·m^{-3}, there was no significant effect of disturbance on the welfare score, all fish have close to average welfare scores.

Aggressive behaviour of fish held at different densities

The baseline level of aggression was low in all tanks, with a mean of 0.06 interactions per 10 fish per 5 min observation period. During the period immediately after feeding, the number of aggressive actions increased significantly over

Fig. 1. Mean and standard error of the welfare score of fish exposed to (*a*) three density (D) regimes (15, 25, and 35 kg·m^{-3}) at three disturbance levels (combined) and (*b*) three levels of husbandry disturbance (low, intermediate, and high frequency) at the three stocking density levels (combined).

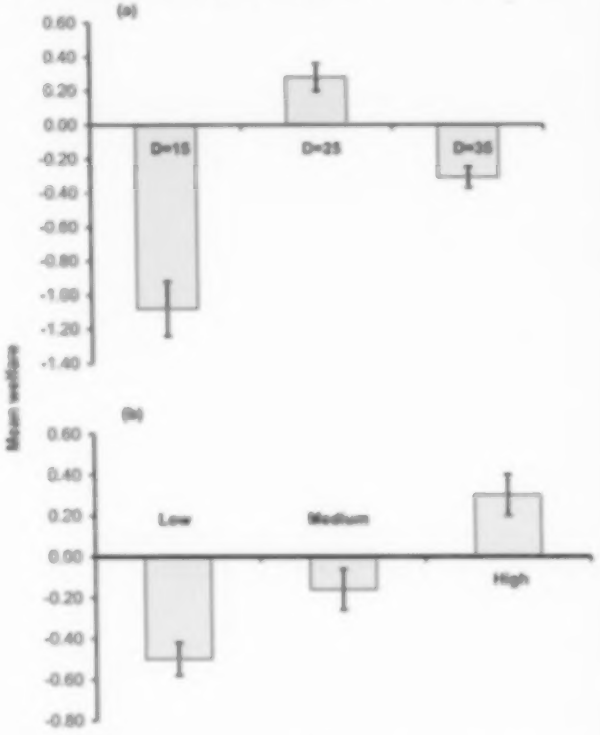

baseline levels (to 0.20 interactions per 10 fish per 5 min observation period; Mann–Whitney U = 18 555, P < 0.0001).

There were no significant effects of either density (Kruskal–Wallis: H = 1.39, 595 df, P = 0.50) or husbandry disturbance on baseline aggression (outside feeding period) (Kruskal–Wallis: H = 2.37, 595 df, P = 0.31) However, there were significant differences in postfeeding aggression rate between tanks exposed to different densities, with the highest level of postfeeding aggression being recorded at lowest density (Fig 3*a*; Kruskal–Wallis: H = 13.1, 862 df, P = 0.002). In addition, level of disturbance had a significant effect on postfeeding aggression, with highest levels being recorded within tanks that were exposed to the lowest frequency of disturbance (Kruskal–Wallis: H = 7.85, 862 df, P < 0.02; Fig. 3*b*).

Discussion

Previous attempts to measure welfare impairment in animals have generally focussed upon single functional systems (behavioural, physical, health, physiological) to identify change (see e.g., Etscheidt 1995). PCA allows trends in multivariate data to be reduced to scores that can then be used as dependent variables in subsequent analysis, without requiring a priori judgements of the relative value of individual variables. Such scores offer the possibility of providing an integrated and objective reflection of diverse, measured

© 2007 NRC Canada

Fig. 2. Mean and standard error of the welfare score of fish. (*a*) Fish exposed to three density regimes (15, 25, and 35 kg·m^{-3}) at three levels of husbandry disturbance (low (level 1), intermediate (level 2), and high (level 3) frequency). Open bars represent 15 kg·m^{-3}, shaded bars represent 25 kg·m^{-3}, and solid bars represent 35 kg·m^{-3}. (*b*) Fish exposed to three levels of husbandry disturbance at three density regimes (15, 25, and 35 kg·m^{-3}). Open bars represent low disturbance, shaded bars represent intermediate disturbance, and solid bars represent high disturbance. ↔ indicates *P* values for the ANOVA across densities or disturbance levels. Identical column letters indicate no post hoc significant differences between densities within disturbance levels. N.S., not significant.

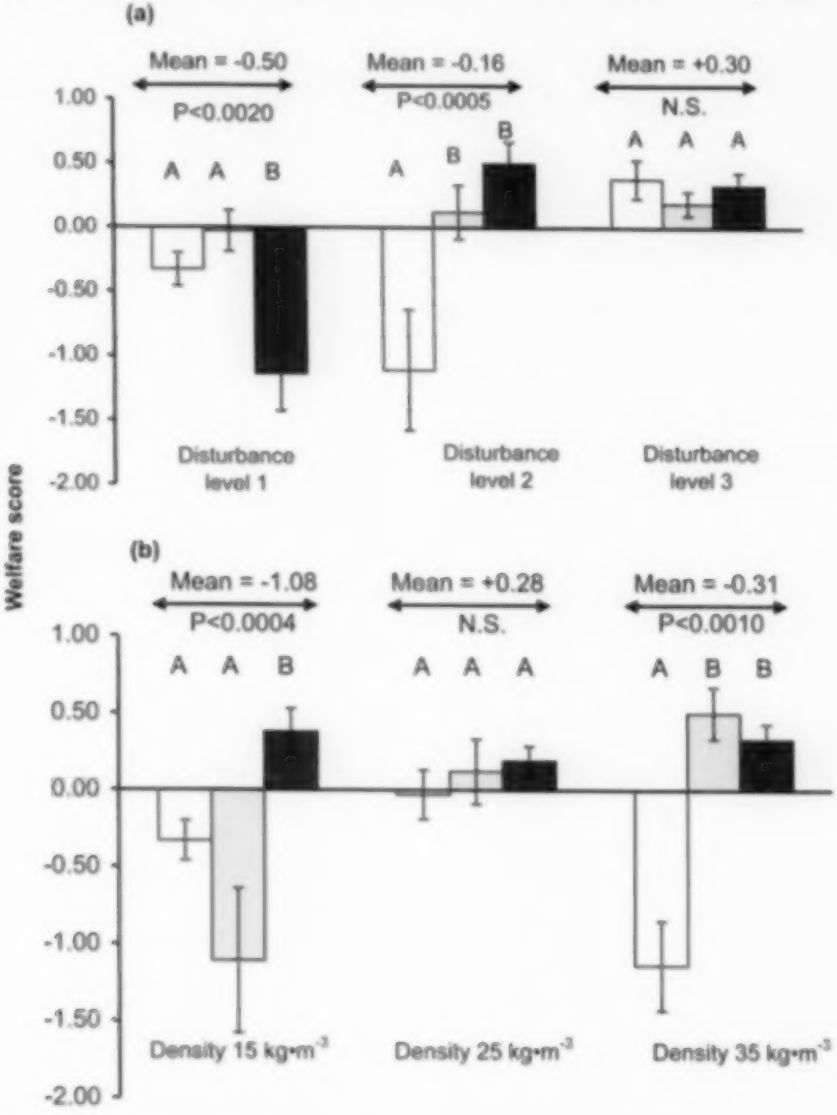

welfare indicators. Here we use this multivariate statistical approach to combine data derived from four distinct measures of welfare for three distinct functional systems (physical damage, body condition, and physiological change) into a single, usable index of welfare. Thus fin condition, a measure of physical damage; condition factor, a measure of size-corrected body mass; and plasma glucose and cortisol levels, measures of physiological state, are combined into a single welfare score. Each of the individual components is influenced by factors other than welfare, and thus they are often imprecise or noisy indicators. The approach adopted here provides a more robust measure of welfare than univariate measures could provide individually, partly through the composite effects of the multivariate combination and partly because it brings together measures from very different biological systems, which may well not covary during a welfare-compromising event.

The PCA-derived welfare score for this study was similar to that in Turnbull et al. (2005), both in amount of variance explained (30% in Turnbull et al. 2005) and in pattern of loadings (0.46 and 0.26 for fin condition and condition factor, respectively, and –0.72 and –0.44 for glucose and

© 2007 NRC Canada

Fig. 3. Mean (and standard error) frequency of aggressive interactions observed (number per 10 fish per 5 min) during the 10 min postfeeding period in tanks at (*a*) three density conditions (15, 25, and 35 kg·m^{-3}) ($P = 0.002$) and (*b*) three levels of husbandry disturbance (1, low; 2, medium; 3, high) ($P < 0.02$). Identical column letters indicate no post hoc significant differences between disturbance levels or densities.

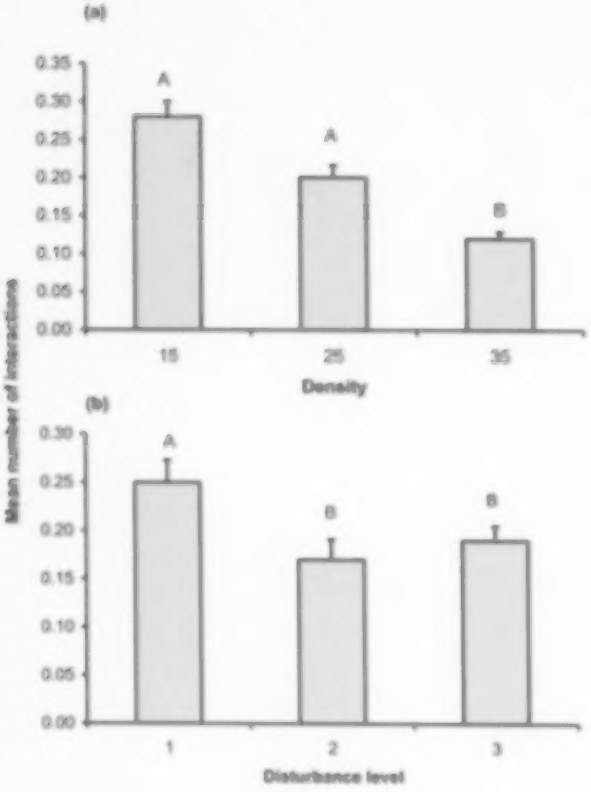

cortisol, respectively, in Turnbull et al. 2005). This suggests that while the loading should be derived anew for each new data set, the welfare score does capture a general aspect of welfare in Atlantic salmon held in very different conditions. Our study therefore supports the general approach of using multivariate analysis to integrate different measures into a single score that can be used to detect subtle and complex influences on fish welfare. In both the present study and that described by Turnbull et al. (2005), the salmon were captive, held at unnatural densities, fed artificially, and not breeding, so there is no reason to think that such an approach to measuring welfare would similarly apply to fish in more natural conditions, where individuals can, to some extent, elect the conditions to which they are exposed.

This study demonstrates effects of manipulated stocking density and of disturbance during husbandry on welfare at the level of the population. Over a density range of 15–35 kg·m^{-3}, which exceeds that found within the UK Atlantic salmon farming industry at the time this study was conducted, welfare was significantly affected by density. The relationship was dome-shaped, with highest welfare at intermediate stocking density (25 kg·m^{-3}) and with welfare declining significantly at both higher and lower densities, particularly with low welfare scores being recorded at the lowest density used in this study (15 kg·m^{-3}). This is an important result given a recent recommendation of 15 kg·m^{-3} as the maximum stocking density for Atlantic salmon (FAWC 1996). A similar effect of low density on welfare has been shown in another salmonid fish, the Arctic charr, where fish held at low densities (15–30 kg·m^{-3}) showed significant reductions in growth performance coupled with poor fin condition and higher mortality rates compared with charr held at higher densities (60–150 kg·m^{-3}) (Jørgensen et al. 1993; Siikavuopio and Jobling 1995).

The sharply rising arm of the dome-shaped relationship between density and welfare found in the present study could be explained by higher levels of direct aggression (relatively infrequent overall, but increasing significantly after feeding) at low densities. Elevated aggression at low densities has also been found in juvenile Atlantic salmon by Wedemeyer (1997) and in Arctic charr by Brown et al. (1992). Aggressive encounters between individuals have been shown to have a clear negative affect on widely used indicators on welfare in Arctic charr (Hoglund et al. 2001). The weaker decline in welfare at the highest density could potentially be due to falling water quality (as found in rainbow trout in the meta-analysis of Ellis et al. 2002), although water quality was generally high in all tanks. Alternatively, and more likely, it might be due to some other consequence of high densities, for example increased rates of collision with other fish or with the tank wall. Such a two-process mechanism would explain the fact that welfare was highest in fish at the intermediate density.

Although the choice of stocking densities used here was designed to yield compromised welfare in some conditions, an unexpected finding was that the observed variation in welfare depended much more importantly on exposure to disturbance during routine fish farm husbandry. Overall, and counter-intuitively, welfare increased with increasing exposure to husbandry disturbance. In practice, all tanks in this experiment were subject to some disturbance, being cleaned once daily by scouring with a brush and by flushing water to remove excess food. For those tanks that were disturbed least, there was rarely any additional disturbance of fish. For those that were disturbed most, the inevitable passage of husbandry staff to gain access to neighbouring tanks resulted in a much higher frequency of low-level disturbance. The results of this study suggest that low-frequency but intrusive disturbance (the daily husbandry procedures of tank cleaning, feeding, etc.) carries a higher welfare cost than more frequent disturbance. This can also be explained by the behavioural data, as the relative frequency of aggressive actions was significantly higher in fish at the lowest level of disturbance. It is possible that regular disturbance during routine husbandry has a suppressive effect on aggression (and thus a beneficial effect on welfare) similar to that of a predator (Ukegbu and Huntingford 1988) or of a larger conspecific (Adams et al. 2000).

The relationship between disturbance and density demonstrated in this experiment is complex. A positive relationship between disturbance and welfare is found at the two extreme densities, though with a lower transition point at high densi-

© 2007 NRC Canada

ties. No such effect was found at the intermediate density, though welfare does increase nonsignificantly as level of disturbance increases. Thus, when looking at disturbance regardless of density, we were picking up a robust beneficial effect of disturbance on welfare, albeit more apparent at extreme densities.

The effect of density on welfare at different disturbance levels is more complex, because the effects of density reverse depending on the level of disturbance. Here we suggest that this pattern of welfare score variation could be (in part, at least) best explained by the effects of aggression. Thus, we suggest that at intermediate disturbance, the overall effect of density on aggression (causing aggression to decline) mediates an increase in welfare score with increasing density. In contrast, at low disturbance levels the effects of density on welfare score are reversed, suggesting either that at low disturbance, the effect of increasing density is increasing aggression or that density effects are mediated through an alternative route. Other possible mechanisms include density effects on water quality or physical effects with tank and conspecifics. These seem much less likely, as their effect would have to also be modified by disturbance level. At high disturbance level, there was no observed effect of density.

Overall, the density–disturbance interaction model explained only 23% of variation in the welfare score, suggesting that other factors not controlled for in this experiment caused major variation in the welfare score. Individual fish with a low welfare score were found across all tanks and disturbance levels, so other influential factors not measured in this study must be involved. In addition, although density and disturbance may influence the average welfare status of fish in the population, not all individuals in a group exposed to conditions that promote high welfare will achieve high welfare status. Similar conclusions were reached in a companion study of salmon in sea cages (Turnbull et al. 2005). Aggression-mediated effects on welfare may contribute to the very high variation in welfare score between individual fish, since within groups of Atlantic salmon some are attacked frequently and some rarely (Adams et al. 1998). One limitation of this study is that it was only possible to examine group means for both the behavioural data and the welfare condition. More detailed studies to assess the role of aggression on the welfare status at the level of individual fish would allow for a greater understanding of the role of aggression in mediating welfare of individuals and the variation within groups of fish.

In conclusion, this study has shown that although there is an effect of stocking density on welfare, the effect is relatively small and dependent in complex ways on other aspects of husbandry practice, namely disturbance, over which farmers may have little control (some tanks and cages will always be exposed to more disturbance than others). The general conclusion is that the welfare of farmed species has multiple determinants, and these interact in complex ways. This underlies a developing consensus among welfare scientists, veterinarians, and regulators alike that rather than trying to identify conditions that will guarantee welfare, the best way to try to promote the welfare of farmed fish is to develop simple welfare indicators that can be used on working farms to monitor easily but reliably and transparently the current welfare status of any group of fish (FSBI 2002; Huntingford et al. 2006).

Acknowledgements

We thank Link Aquaculture (Project SAL 18), the Natural Environment Research Council (NERC), and Scottish Quality Salmon who funded this project.

References

Ackerman, P.A., Forsyth, R.B., Mazur, C.F., and Iwama, G.K. 2000. Stress hormones and the cellular stress response in salmonids. Fish Physiol. Biochem. **23**: 327–336.

Adams, C.E., and Huntingford, F.A. 1996. What is a successful fish? Determinants of competitive success in Arctic char (*Salvelinus alpinus*) in different social contexts. Can. J. Fish. Aquat. Sci. **53**: 2446–2450.

Adams, C.E., Huntingford, F.A., Turnbull, J.F., and Beattie, C. 1998. Alternative competitive strategies and the cost of food acquisition in juvenile Atlantic salmon. Aquaculture, **167**: 17–27.

Adams, C.E., Huntingford, F.A., Turnbull, J.F., Arnott, S., and Bell, A. 2000. Size heterogeneity can reduce aggression and promote growth in Atlantic salmon parr. Aquac. Int. **8**: 543–549.

Bell, A. 2003. The effects of some management practices on the behaviour and welfare of farmed Atlantic salmon (*Salmo salar*) in marine cages. Ph.D. thesis, University of Stirling, Scotland.

Bermond, B. 1997. The myth of animal suffering. *In* Animal consciousness and animal ethics. *Edited by* M. Dol, S. Kasanmoentalib, S. Lijmbach, E. Rivas, and R. van den Bos. Van Gorcum, Assen, the Netherlands. pp. 125–143.

Boylan, P., and Adams, C.E. 2006. The influence of broad scale climatic phenomena on long term trends in Atlantic salmon population size: an example from the River Foyle, Ireland. J. Fish Biol. **68**: 276–283.

Braithwaite, V.A., and Huntingford, F.A. 2004. Fish and welfare: do fish have the capacity for pain perception and suffering? Anim. Welf. **13**: S87–S92.

Brown, G.E., Brown, J.A., and Srivasta, R.K. 1992. The effects of stocking density on the behaviour of Arctic charr (*Salvelinus alpinus*). J. Fish Biol. **41**: 955–963.

Chandroo, K.P., Duncan, I.J.H., and Moccia, R.D. 2004*a*. Can fish suffer? Perspectives on sentience, pain, fear and stress. Appl. Anim. Behav. Sci. **86**: 225–250.

Chandroo, K.P., Yue, S., and Moccia., R.D. 2004*b*. An evaluation of current perspectives on consciousness and pain in fishes. J. Fish Fisheries, **5**: 281–295.

Dawkins, M.S. 1998. Evolution and animal welfare. Q. Rev. Biol. **73**: 305–328.

Dawkins, M.S., Connelly, C.A., and Jones, J.A. 2004. Chicken welfare is influenced more by housing conditions than by stocking density. Nature (London), **427**: 342–344.

Ellis, T., North, B., Scott, A.P., Bromage, N.R., Porter, M., and Gadd, D. 2002. The relationship between stocking density and welfare in farmed rainbow trout. J. Fish Biol. **61**: 493–531.

Espelid, S., Løkken, G.B., Steiro, K., and Bøgwald, J. 1996. Effects of cortisol and stress on the immune system in Atlantic Salmon (*Salmo salar* L.). Fish Shellfish Immunol. **6**: 95–110.

Etscheidt, J. 1995. Kriterien zur Beurteilung der Haltung von Susswasseraquarienfichen im Zoohandel. Tierarztl Prax, **50**: 196–199.

FAWC. 1996. Report on the welfare of farmed fish. The Farm Animal Welfare Council, Surbiton, Surrey, UK.

© 2007 NRC Canada

FSBI. 2002. Fish welfare. Fisheries Society of the British Isles Briefing Paper 2. Granta Information Systems, Sawston, Cambridge, UK.

Gomes, L.C., Araujo-Lima, C.A.R.M., Roubach, R., Chippari-Gomes, A.R., Lopes, N.P., and Urbinati, E.C. 2003. Effect of fish density during transportation on stress and mortality of juvenile tambaqui *Colossoma macropomum*. J. World Aquac. Soc. **34**: 76–84.

Hegfund, E., Kolm, N., and Winberg, S. 2001. Stress-induced changes in brain serotonic activity, plasma cortisol and aggressive behaviour in Arctic charr (*Salvelinus alpinus*) is counteracted by L-DOPA. Physiol. Behav. **74**: 381–389.

Huntingford, F.A., Adams, C.E., Braithwaite, V., Kadri, S., Pottinger, T., Sandoe, P., and Turnbull, J. 2006. Current issues in fish welfare. J. Fish Biol. **68**: 332–372.

Hughes, T.C., Josephson, D.C., Krueger, C.C., and Sullivan, P.J. 2000. Comparison of large and small visible implant tags: retention and readability in hatchery brook trout. N. Am. J. Aquac. **62**: 273–278.

Jobling, M. 1995. Environmental biology of fishes. Chapman and Hall, London, UK.

Jørgensen, E.H., Christiansen, J.S., and Jobling, M. 1993. The effects of stocking density on food intake, growth performance and oxygen consumption in Arctic charr (*Salvelinus alpinus*). Aquaculture, **110**: 191–204.

Kim, D.H., Woo, J.H., and Lee, C.Y. 2004. Effects of stocking density and transportation time of market pigs on their behaviour, plasma concentrations of glucose and stress-associated enzymes and carcass quality. Asian Austral. J. Anim. Sci. **17**: 116–121.

McLean, J.A., Savory, C.J., and Sparks, N.H.C. 2002. Welfare of male and female broiler chickens in relation to stocking density, as indicated by performance, health and behaviour. Anim. Behav. **11**: 55–73.

Pavlidis, M., Angellotti, L., Papandroulakis, N., and Divanach, P. 2003. Evaluation of transportation procedures on water quality and fry performance in red porgy (*Pagrus pagrus*) fry. Aquaculture, **218**: 187–202.

Pottinger, T.G., and Carrick, T.R. 1999. A comparison of plasma glucose and plasma cortisol as selection markers for high and low stress-responsiveness in female rainbow trout. Aquaculture, **175**: 351–363.

Rose, J.D. 2002. The neurobehavioral nature of fishes and the question of awareness and pain. Rev. Fish. Sci. **10**: 1–38.

Siikavuopio, S.I., and Jobling, M. 1995. The effects of stocking density on survival and growth of wild-caught Arctic char. Nord. J. Freshw. Res. **71**: 419–423.

Tom, J.D., and Lesperance, M.L. 2003. Piecewise regression: a tool for identifying ecological thresholds. Ecology, **84**: 2034–2041.

Trevorrow, M.V., and Clayton, R.R. 1998. Detection of Atlantic herring (*Clupea harengus*) schools in shallow waters using high-frequency sidescan sonars. Can. J. Fish. Aquat. Sci. **55**: 1419–1429.

Trinder, P. 1969. Determination of blood glucose using an oxidase–peroxidase system with a non-carcinogenic chromogen. J. Clin. Pathol. **22**: 158–161.

Turnbull, J.F., Adams, C.E., and Robertson, D.A. 1998. Attack site and resultant damage during aggressive encounters in Atlantic salmon (*Salmo salar* L.) parr. Aquaculture, **159**: 345–353.

Turnbull, J.F., Bell, A., Adams, C.E., Bron, J., and Huntingford, F.A. 2005. Stocking density and welfare of cage farmed Atlantic salmon: application of a multivariate analysis. Aquaculture, **243**: 121–132.

Ukegbu, A.A., and Huntingford, F.A. 1988. Brood value and life expectancy as determinants of parental investment in male three-spined sticklebacks, *Gasterosteus aculeatus*. Ethology, **78**: 72–82.

Wedemeyer, G.A. 1997. Effects of rearing conditions on the health and physiological quality of fish in intensive culture. *In* Fish stress and health in aquaculture. *Edited by* J.K. Iwama, A.D. Pickering, J.P. Sumpter, and C.B. Schrek. Cambridge University Press, Cambridge, UK. pp. 35–72.

Witk, R., Andersen, K., Uglenes, I., and Egidius, E. 1989. Cortisol-induced increase in susceptibility of Atlantic salmon, *Salmo salar*, to *Vibrio salmonicida*, together with effects on the blood cell pattern. Aquaculture, **83**: 201–215.

© 2007 NRC Canada

Effects of hypoxia on scope-for-activity and power capacity of lake trout (*Salvelinus namaycush*)

David O. Evans

Abstract: This study develops a quantitative model of the combined effects of temperature and ambient dissolved oxygen on metabolic scope-for-activity and power capacity of juvenile lake trout (*Salvelinus namaycush*). The model provides a framework for evaluating the effects of hypoxia on the capacity of lake trout to perform critical daily life support activities. Maximum power output for sustained swimming of yearling lake trout occurred at 12–20 °C and a dissolved oxygen concentration of >7 mg·L^{-1}. At 4–8 °C, temperatures typical of the hypolimnetic summer habitat of juvenile lake trout, maximum power capacity was reduced by 33%, 67%, and 100% at ambient dissolved oxygen concentrations of 7, 5, and 3 mg·L^{-1}, respectively. Analysis of power outputs, growth impairment, and recruitment success indicated that attainment of 3/4 power capacity would accommodate most daily life support activities of juvenile lake trout. At 4–14 °C, the threshold dissolved oxygen concentration for attainment of 3/4 scope-for-activity varied from 7.5 to 6.6 mg·L^{-1}, respectively, with a mean and standard deviation of 7.04 ± 0.33 mg·L^{-1}. A dissolved oxygen criterion of 7 mg·L^{-1} is recommended for protection of the hypolimnetic habitat of juvenile lake trout.

Résumé : On trouvera ici un modèle quantitatif des effets combinés de la température et de l'oxygène dissous du milieu sur le profil métabolique et le potentiel de puissance des jeunes touladis (*Salvelinus namaycush*). Le modèle fournit un cadre pour évaluer les effets de l'hypoxie sur la capacité des touladis de remplir les activités quotidiennes essentielles à leur survie. La puissance maximale pour la nage soutenue de jeunes touladis d'un an est produite à 12–20 °C et à une concentation d'oxygène dissous de >7 mg·L^{-1}. À 4–8 °C, des températures typiques de l'habitat d'été des jeunes touladis dans l'hypolimnion, le potentiel maximum de puissance est réduit de 33 %, 67 % et 100 % aux concentrations respectives d'oxygène dissous du milieu de 7, 5 et 3 mg·L^{-1}. L'analyse des puissances produites, de la réduction de la croissance et du succès du recrutement indique que l'atteinte de 3/4 du potentiel de puissance suffit pour permettre la plupart des activités essentielles à la survie chez les jeunes touladis. À 4–14 °C, le seuil de la concentration d'oxygène dissous qui permet d'atteindre les 3/4 du profil métabolique varie de 7,5 à 6,6 mg·L^{-1}, avec une moyenne et un écart type de 7,04 ± 0,33 mg·L^{-1}. Le seuil recommandé de 7 mg·L^{-1} assurerait la protection de l'habitat hypolimnétique des jeunes touladis.

[Traduit par la Rédaction]

Introduction

Throughout their geographic range, lake trout (*Salvelinus namaycush*) are routinely affected by hypoxia, both naturally occurring and associated with watershed disturbances caused by human activities (Dillon et al. 1994, 2003; Ryan and Marshall 1994). Phosphorus is the limiting nutrient that controls primary production in lake trout lakes of the boreal forest ecozone (Dillon and Rigler 1974; Dillon et al. 1986; Molot and Dillon 1991). Phosphorus loading causes increased algal production (Schindler et al. 1971) and depletion of late-summer dissolved oxygen levels in the hypolimnion of lakes (Molot et al. 1992; Evans et al. 1996; Lienesch et al. 2005). Recreational and urban development of watersheds and associated impacts on natural shorelines are significant contributors to phosphorus loads and to oxygen depletion in thermally stratified lakes (Evans et al. 1996; Dillon et al. 2004). In the broader context of global climate change, lake trout have been identified as highly vulnerable because of effects on thermal stratification and water chemistry of lakes and associated loss of summer habitat and productive capacity (Magnuson et al. 1990; Schindler 1998; Schindler and Gunn 2004). These factors are now poised to affect lake trout distribution and production across the species' range (Magnuson et al. 1997; Stefan et al. 2001; Shuter and Lester 2004). Concerns about climatic change and local impacts of human activity on the future sustainability of lake trout are driving the need for improved quantitative models of the habitat requirements of this species.

Lake trout is a stenothermal species that inhabits relatively deep, cold lakes spanning the North American continent from Alaska to Labrador (Lindsey 1964), with the southern limits of the primary range extending into Minnesota, Wisconsin, Michigan, New York, Vermont, New Hampshire, and Maine. Across this range, lake trout seek thermal refuge in the cooler waters of the hypolimnion of

Received 14 August 2006. Accepted 28 October 2006. Published on the NRC Research Press Web site at http://cjfas.nrc.ca on 7 March 2007.
J19019

D.O. Evans. Ontario Ministry of Natural Resources, Trent University, 2140 East Bank Drive, Peterborough, ON K9J 7B8, Canada (e-mail: david.evans@ontario.ca).

 doi:10.1139/F07-007 © 2007 NRC Canada

thermally stratified lakes during summer (Evans et al. 1991, 1996). During this time, an adequate supply of dissolved oxygen is essential to meet the metabolic demands of life support activities, including swimming, feeding, avoidance of predators, growth, and reproduction. Adult lake trout inhabit temperatures of 4–18 °C (Martin and Olver 1980) but during summer are most often found at 8–12 °C (Christie and Regier 1988), although Sellers et al. (1998) have reported that warmer temperatures up to 20 °C are frequented during the night in small boreal forest lakes. During early summer, lake trout move to deeper water and are found near the base of the thermocline during the day. Lake trout continue to occupy this habitat during summer, gradually moving to greater depths as the thermocline deepens (Martin and Olver 1980). Young-of-the-year and older juvenile lake trout inhabit greater depths and cooler temperatures than adults (Elrod and Schneider 1987; Evans et al. 1991; Davis et al. 1997). As surface waters cool during early fall, adult lake trout again move shoreward and are widely dispersed prior to spawning, which occurs on shallow rocky shorelines during September and October (Martin and Olver 1980; Sly and Evans 1996).

Dissolved oxygen also directs the vertical movements of lake trout, but field observations of responses to low dissolved oxygen are relatively rare. The dissolved oxygen avoidance threshold in Lac la Ronge was about 3.6–4.3 mg·L^{-1} (Martin and Olver 1980). In Lake Simcoe, a general upward movement of lake trout occurred in response to dissolved oxygen <4 mg·L^{-1} (Evans et al. 1996). In small lakes in northwestern Ontario, 75%–90% of lake trout were found at >6 mg·L^{-1} and the daytime avoidance threshold appeared to be 2–4 mg·L^{-1} (Sellers et al. 1998). Dissolved oxygen concentrations of 1.4–2.9 mg·L^{-1} were observed to be lethal in Swan Lake, Alberta (Martin and Olver 1980). The laboratory response threshold to reduced dissolved oxygen for salmonids, measured as increased random swimming, occurs at about 6 mg·L^{-1} and the avoidance threshold is about 4 mg·L^{-1} (Davis 1975; Spoor 1990).

The energetic consequences of temperature and oxygen variation for lake trout can be defined within the metabolic framework of scope-for-activity and quantified in terms of power output or energy flow required to support critical daily life support activities. On balance, adequate power output must be maintained to support the necessary daily work load. Temperature and oxygen operate as directive, controlling, and limiting factors (Fry 1971; Brett and Groves 1979; Evans and Neill 1990) that ultimately affect survival, growth, abundance, and sustainability at the population level (Ricker 1975; Shuter et al. 1998).

This study develops a quantitative model of the combined effects of temperature and ambient dissolved oxygen on metabolic scope-for-activity and power capacity of juvenile lake trout and links these to requirements for critical life support activities including routine and maximal swimming activity and energy costs for maintenance and maximum feeding rates. The purpose is to provide a quantitative metabolic model that can effectively inform management decisions concerning temperature and dissolved oxygen requirements for the protection of lake trout habitat under the emerging pressures of climate change, water regulation, forest harvesting, shoreline development, and nutrient loading in lakes across the species' range (Steedman et al. 2004).

Materials and methods

Metabolic scope-for-activity and response to hypoxia

This paper provides a new and extended analysis of data originally published in Gibson and Fry (1954) and integration of more recent metabolism data for lake trout, with emphasis on scope-for-activity and power outputs for critical daily activities under the influence of hypoxia. Scope-for-activity is defined as the difference between standard (resting, postabsorptive) metabolic rate and the maximum sustained metabolic rate (Fry 1947, 1971), the latter being measured during laboratory swimming trials (e.g., Brett 1964; Beamish 1978). Scope-for-activity therefore defines the range of metabolic energy that is potentially available for capture of prey, avoidance of predators, diurnal vertical movements, spawning migration, aggressive behaviour, and all other types of volitional activity, including the increased energy demands of the heart, respiratory muscles, and kidneys during exercise (Jones and Randall 1978). Scope-for-activity offers an effective measure of the aerobic capacity to perform work and provides a quantitative, physiological construct for characterizing the effects of hypoxia on fish activity.

The general analytical construct for the limiting effect of dissolved oxygen on active metabolic rate of aquatic species (Fig. 1) was described by Fry (1947) and Hughes (1964) and later elaborated by Davis (1975). The limiting effects of reduced dissolved oxygen occur within the zone of respiratory dependence (Fig. 1), which is bounded at its upper limit by the partial pressure of dissolved oxygen at which the transport of oxygen across the gill membrane first begins to be dependent on ambient dissolved oxygen. The zone of respiratory dependence is intersected by the incipient lethal dissolved oxygen level, which corresponds to the postabsorptive oxygen consumption rate that is required to maintain the basic integrity of the organism (referred to as standard metabolic rate; Fry 1971). This threshold also corresponds to the level of no-excess-activity, meaning that there is no surplus energy available for volitional activities (Fry 1971). The incipient lethal level therefore marks the boundary between the zone of tolerance and the zone of resistance, death being a simple function of exposure time within the latter. Lake trout and other species can enter their zone of resistance, but only temporarily and at high risk (Priede 1977).

Standard and active metabolic rates

Published information on the metabolism of lake trout has been used to derive the effects of reduced ambient dissolved oxygen on scope-for-activity and power capacity. The only published study on the effects of hypoxia on the metabolism of lake trout is Gibson and Fry (1954). The initial step in my analysis was to compare the metabolic data in Gibson and Fry (1954) with those from more recent studies (Stewart et al. 1983; Beamish et al. 1989; Rottiers 1993) to establish the consistency of the data. The latter studies provided independent measures of standard and active metabolic rates of juvenile lake trout under normoxic conditions.

© 2007 NRC Canada

Fig. 1. Metabolic response of fish to reduced partial pressure of dissolved oxygen showing the zones of respiratory regulation and dependence and the zones of tolerance and resistance. The standard metabolic rate intersects the response curve at the incipient lethal threshold for dissolved oxygen (modified after Davis 1975).

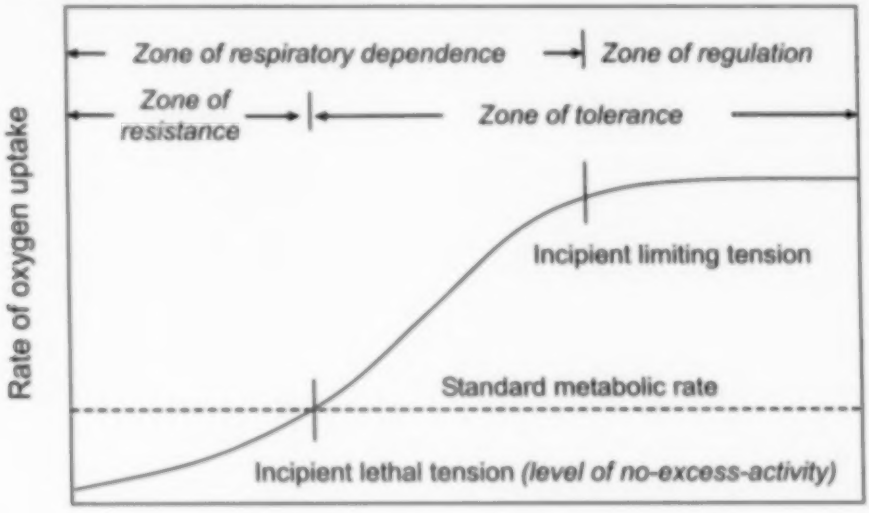

Standard and active metabolic rates of yearling and 2-year-old lake trout were determined in laboratory trials by Gibson and Fry (1954). They used Erlenmeyer flask respirometers to determine standard rates of quiescent fish and a rotating annular swimming chamber to determine active rates (Smit 1965; Beamish 1978). Figure 2 in Gibson and Fry (1954) was digitized to recapture the original standard and active metabolic rates. Data for yearling and 2-year-old lake trout were included in comparisons of standard and active metabolic rates with more recent published data. The hypoxia data for yearlings were analyzed here but the data for 2-year-olds were too incomplete for further analysis.

Metabolic rates were converted from $mL \cdot L^{-1}$ in the original study (Gibson and Fry 1954) to $mg \cdot L^{-1}$, and for comparison with other studies, oxygen consumption was adjusted to $mg \cdot kg^{-1} \cdot h^{-1}$ for a 100 g lake trout using a weight exponent of 0.85 based on Job (1955) and Beamish et al. (1989). The body weights of the yearlings and 2-year-olds were 16.4–37.9 g (mean = 27.7 g) and 57.6–120.6 g (mean = 82.8 g) and their estimated mean total lengths, based on length–weight relationships for Ontario hatchery stock (Haliburton strain) at the same ages, were 14.8 and 20.9 cm, respectively (D.O. Evans, unpublished data). These mean body weights were used to correct the standard metabolic rate data in Gibson and Fry (1954) to a body weight of 100 g. A weight exponent of 0.85 was also applied to adjust the metabolic data in Beamish et al. (1989) and Rottiers (1993) to correspond to a 100 g fish.

The respiration model of Stewart et al. (1983), which included weight, temperature, and swim speed coefficients, was used to calculate standard and active metabolic rates for that study. Swimming speed is strongly influenced by fish size (Brett 1965; Beamish 1978). Small fish swim at higher relative speed ($L \cdot s^{-1}$) but attain lower absolute speed than larger fish. The actual maximum swimming speed of a 100 g lake trout at each of the five test temperatures, 3.5, 5, 7, 10, and 15 °C, reported in Stewart et al. (1983) was much lower than the maximum speed (50–60 $cm \cdot s^{-1}$) reported by those authors for fish of larger average size. Mean body weight of fish in their study was 486 g (range 20–1835 g). The original data set, provided by D.V. Rottiers (7540 Dexter Pickney Road, Dexter, MI 48130-9608, USA), was used to estimate the maximum swim speed of fish of various lengths by fitting a regression model of maximum $L \cdot s^{-1}$ versus total length at each temperature and estimating speed for a 100 g fish with total length of 22.8 cm. The relationship between temperature and estimated maximum speed for a 100 g fish was then fitted and speeds were calculated at 4, 6, 8, 10, 12, and 14 °C. These speeds, 44.0, 45.6, 47.3, 49.0, 50.7, and 52.4 $cm \cdot s^{-1}$, respectively, were used in the Stewart et al. (1983) model to calculate the active metabolic rates for a 100 g lake trout (Fig. 2). Standard metabolic rates at temperatures from 4 to 20 °C were estimated for all studies by fitting exponential regression functions. Brett and Groves (1979) concluded that this transformation effectively characterizes the relationship between standard metabolic rate and temperature for fish. The ascending and descending limbs of the active metabolic rate versus temperature relationships were also fitted using exponential functions.

Response to hypoxia

Metabolic rates at 1/4, 1/2, and 3/4 scope-for-activity levels were obtained for yearling lake trout at 4, 6, 8, 10, 12, 14, 16, 18, 20, and 22 °C by partitioning the scope-for-activity envelope (Fig. 3) derived from equations fitted to the original data in Gibson and Fry (1954). These arbitrary scope-for-activity horizons were selected to provide a structured metabolic framework to relate energy costs for various

© 2007 NRC Canada

Fig. 2. Active and standard metabolic rates of lake trout (*Salvelinus namaycush*) derived from the published literature as indicated. Rates from Gibson and Fry (1954) are for yearlings and 2-year-olds and have been adjusted to a body weight of 100 g using a weight exponent of 0.85 as were the rates from Beamish et al. (1989). Data from Stewart et al. (1983) and Rottiers (1993) have been adjusted to 100 g body weight using their weight exponents. Active rates for Gibson and Fry (1954) at 4 and 6 °C are based on their estimated swim speeds using the respiration model in Stewart et al. (1983). The vertical line connecting the standard and active metabolic rates at 23.5 °C is the upper incipient lethal temperature level, i.e., the level that causes 50% mortality of a sample of thermally acclimated fish.

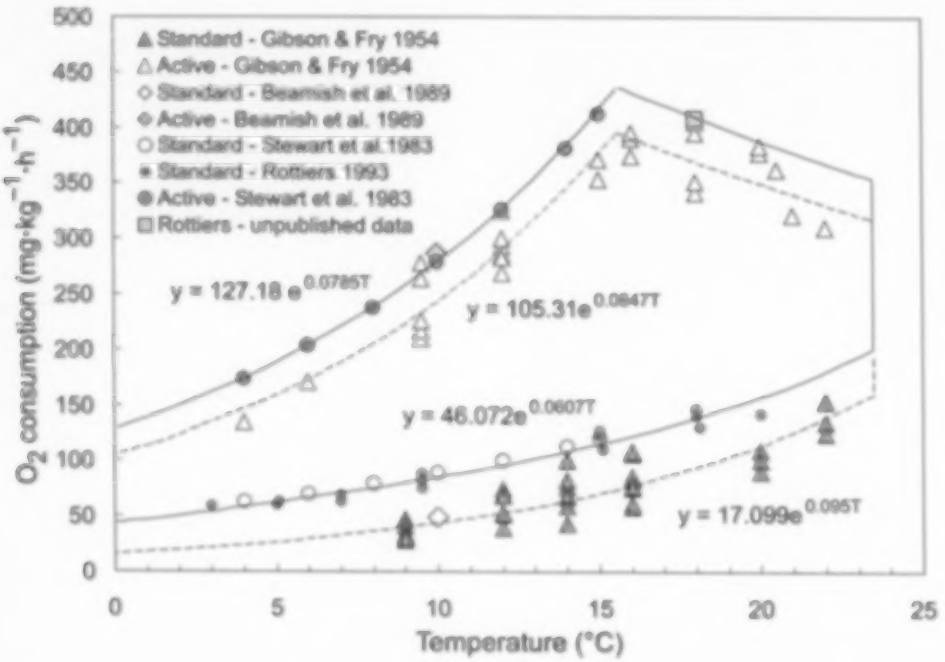

activities to the limiting effects of hypoxia on oxygen consumption. The framework required the following steps and calculations: (*i*) determination of the active rate of oxygen uptake over a wide range of temperatures and limiting ambient dissolved oxygen conditions from Gibson and Fry (1954), (*ii*) determination of oxygen consumption over a range of temperatures for each scope-for-activity horizon, (*iii*) determination of the ambient dissolved oxygen levels on each temperature response curve that correspond to oxygen consumption rates of 1/4, 1/2, and 3/4 scope-for-activity, and (*iv*) compilation of the metabolic costs for various daily life support activities including maintenance, routine and maximum feeding, aggressive behaviour, and excitability that would occur during predator avoidance to determine critical thresholds of ambient dissolved oxygen.

Limiting effect of dissolved oxygen on active metabolic rate

Gibson and Fry (1954) determined the effect of low dissolved oxygen on juvenile lake trout. I have digitized and replotted their fig. 3, active metabolic rate versus oxygen pressure, at 9.5–18 °C for yearling lake trout. Analyses of metabolic rates and responses of yearling lake trout to hypoxia were completed using the original data unadjusted for body weight because the individual weights of fish in each experiment were not reported. Also, given the variation in the oxygen consumption – body size exponent reported among species and studies (Fry 1971; Brett and Glass 1973; Clarke and Johnston 1999), it was deemed best to minimize adjustments of the original data used in the hypoxia analyses. Therefore, I used the original values for normoxic standard and active metabolic rates. Similarly, the active metabolic rate response to hypoxia for yearling lake trout was adjusted directly to $mg \cdot kg^{-1} \cdot h^{-1}$. Partial pressures of atmospheric oxygen, reported in the original paper, were converted to dissolved oxygen concentrations in $mg \cdot L^{-1}$ using standard solubility tables (e.g., Davis 1975) for atmospheric pressure at 243.8 m above sea level at Maple, Ontario, where the original experiments were performed. Oxygen partial pressures reported in the original paper (Gibson and Fry 1954, their fig. 3) were adjusted from measured concentrations to fractions of 100% air saturation. I have used the same approach in converting partial pressures reported in the paper back to concentrations, except to adjust the concentration at full saturation for elevation as noted.

The detailed derivation of ambient dissolved oxygen concentrations that limit lake trout yearlings to 1/4, 1/2, and 3/4 scope-for-activity is illustrated for experiments conducted at 12 °C (Fig. 4). I used the derived values for 1/4, 1/2, and 3/4 scope from Fig. 3 to utilize the strength of the whole data set to obtain the best estimates rather than simply using the individual response curves to identify the cut points. The curves

© 2007 NRC Canada

Fig. 3. Active and standard metabolic rate of yearling lake trout at a body weight of 27.7 g. Scope-for-activity is defined by the active and standard metabolic rate boundaries. Intermediate boundaries are shown at 1/4, 1/2, and 3/4 scope-for-activity defining progressively increasing potential power available for life support activities. The standard and metabolic rates are derived from fitted exponential functions based on the original data and the intermediate scope-for-activity values were calculated at each temperature based on the fitted equations for standard and active rates. Active rates at 4, 6, and 8 °C were modeled using Stewart et al. (1983) and swim speeds estimated from Gibson and Fry (1954).

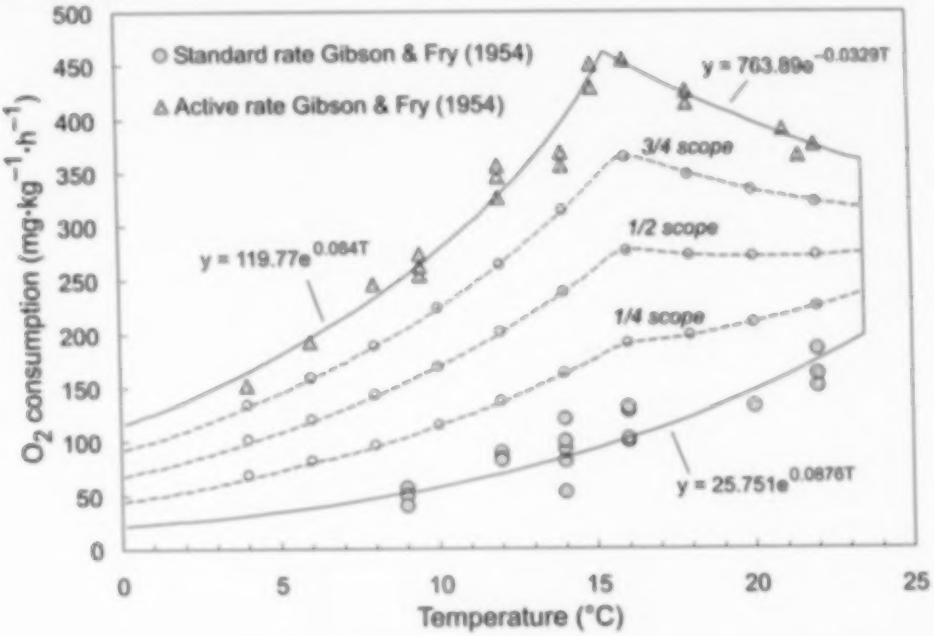

Fig. 4. Response of active metabolic rate of yearling lake trout to declining partial pressure of oxygen at 12 °C to illustrate the derivation of dissolved oxygen thresholds for scope-for-activity. Oxygen pressures and dissolved oxygen consumption rates corresponding to the level of no-excess-activity, 1/4, 1/2, and 3/4 scope for activity (from Fig. 3), and the incipient response threshold at 95% oxygen saturation are indicated by arrows on each response curve. The symbols are observed values reported by Gibson and Fry (1954). Oxygen consumption rates at 1/4, 1/2, and 3/4 scope-for-activity were taken from Table 2 to establish the associated ambient oxygen pressures.

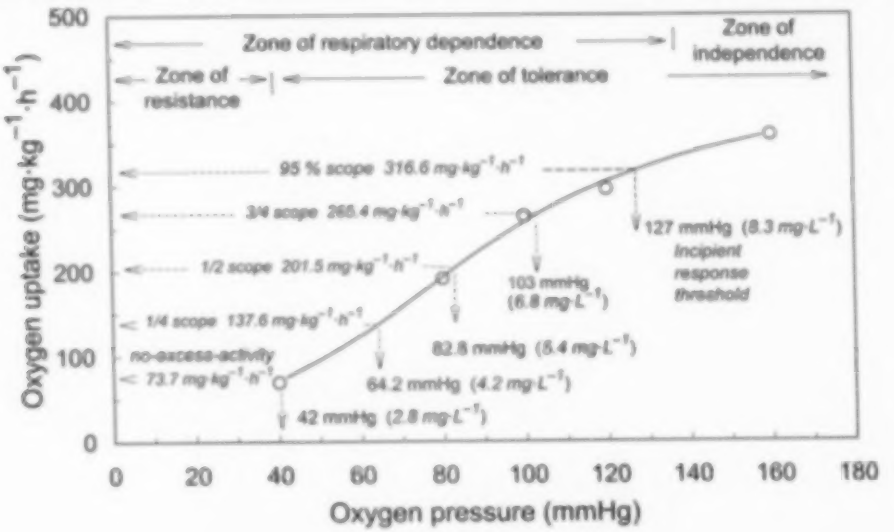

© 2007 NRC Canada

Fig. 5. Response of active metabolic rate of yearling lake trout to reduced partial pressure of dissolved oxygen at 4, 6, 8, 10, 12, 14, and 18 °C. The incipient response thresholds of respiratory dependence are indicated by the vertical tick marks at the upper right of each curve. Tick marks on each curve also indicate 1/4, 1/2, and 3/4 scope-for-activity thresholds. The symbols are observed data from Gibson and Fry (1954). The curves at 4, 6, and 8 °C were drawn by eye between the estimated standard and active metabolic rates shown in Fig. 3 and Table 1.

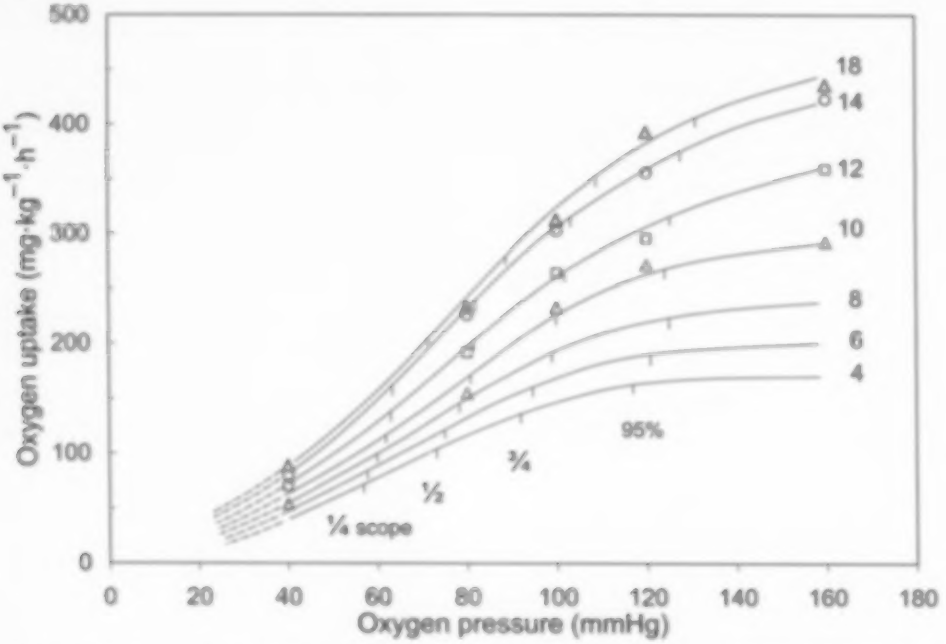

for 10, 12, and 14 °C were fitted by eye and the response curves at 4, 6, and 8 °C were interpolated using the standard and active rates from Fig. 1 to fix the upper and lower ends of the curves (Fig. 5). For each temperature curve, the intercept is shown for the oxygen consumption rates that correspond to 1/4, 1/2, and 3/4 scope-for-activity (as in Fig. 4). The threshold of respiratory dependence is also indicated on each curve as is the point of significant initial respiratory decline set arbitrarily at the 95% scope-for-activity response level. It should be noted that the analyses are based on the original data of Gibson and Fry (1954) and that any potential limitations of the original data remain. The integrity of the original data set has been maintained with the added benefit that the standard and active metabolic rate versus temperature curves are now based on fitted regressions that make no specific assumptions about the data. The data have also been integrated with the more recent published literature to test for any inconsistencies that might potentially introduce bias into the present analyses.

Power capacity

Power capacity was calculated at 1/4, 1/2, 3/4, and full scope-for-activity at temperatures from 4 to 23.5 °C. Power is defined as the rate of energy flow per unit time in watts (1 W = 1 J·s^{-1}). Scope-for-activity expressed as mg O_2·kg^{-1}·h^{-1} for yearling lake trout was converted to energy units using an oxycalorific equivalent of 3.241 cal·mg oxygen^{-1} (Elliott and Davison 1975; Brett and Groves 1979) or 13.6 J·mg oxygen^{-1} (Priede 1985). Power capacity was calculated for temperatures from 4 to 23.5 °C and partial pressures of oxygen from 30 to 160 mmHg at 20 mmHg intervals by interpolation of the metabolic rate – oxygen partial pressure response curves at 4, 6, 8, 10, 12, 14, and 18 °C (Fig. 5) and converting oxygen consumption to milliwatts. Power capacity at each oxygen saturation level was then plotted versus temperature. These curves were fitted by eye and interpolated to construct a response surface of power capacity over the temperature range 4–23.5 °C and 30–160 mmHg partial pressure of oxygen.

Results

There is general consistency among the published studies of lake trout metabolism (Fig. 2), but the standard and active metabolic rates in Stewart et al. (1983) are higher than reported by Gibson and Fry (1954) and Beamish et al. (1989). The higher standard rates reported by Stewart et al. (1983) are consistent with those of Rottiers (1993), the latter two studies being based on the same experimental data. Their standard rates were for 1-, 2-, and 3-year-old lake trout tested in a tunnel respirometer. In those experiments, lake trout were forced to swim at initial speeds of 10–20 cm·s^{-1} up to maxima of 50–60 cm·s^{-1} and swimming speed was increased in increments of 10 cm·s^{-1} after 90 min swimming intervals. Standard metabolic rates were estimated for individual fish or groups of small fish using the intercept of the oxygen consumption versus swimming speed relationships. Typically, in tunnel respirometers, fish express spontaneous swimming at lower speeds especially when tested in groups (Brett and Sutherland 1965; Fry 1971; Beamish 1978).

© 2007 NRC Canada

Table 1. Standard and active metabolic rates, scope-for-activity, the level of no-excess-activity corresponding to standard metabolic rate, and the threshold of respiratory dependence corresponding to 95% of full scope-for-activity for yearling lake trout (*Salvelinus namaycush*) at 4–18 °C based on data in Gibson and Fry (1954).

	Metabolic rate			Level of no-excess-activity (incipient lethal threshold)		Threshold of respiratory dependence (95% scope-for-activity)	
Temperature (°C)	Standard ($mg \cdot kg^{-1} \cdot h^{-1}$)	Active ($mg \cdot kg^{-1} \cdot h^{-1}$)	Scope-for-activity at 100% O_2 saturation ($mg \cdot kg^{-1} \cdot h^{-1}$)	O_2 partial pressure (mmHg)	O_2 concentration ($mg \cdot L^{-1}$)	O_2 partial pressure (mmHg)	O_2 concentration ($mg \cdot L^{-1}$)
4	36.6	167.8	131.2	39.5	3.2	118.0	9.4
6	43.6	198.6	155.0	40.0	3.1	122.0	9.2
8	51.9	235.1	183.2	41.0	3.0	126.3	9.1
10	61.8	278.3	216.5	41.5	2.9	124.8	8.6
12	73.7	329.4	255.7	42.0	2.8	126.8	8.3
14	87.8	389.9	302.1	42.5	2.7	129.2	8.1
18	124.6	422.5	297.9	52.0	3.0	132.7	7.7

Spontaneous activity at slow speeds might explain the elevated standard metabolic rates in Stewart et al. (1983). The standard rate reported by Beamish et al. (1989) at 10 °C was identical to that of Gibson and Fry (1954) and the latter authors provide the best estimates of standard metabolic rate for this species over a wide range of temperatures.

The higher active metabolic rates in Stewart et al. (1983) might be due to higher swimming speeds being attained in the tunnel-type respirometer versus the rotating annular chamber used by Gibson and Fry (1954). Direct comparison of fish of the same size, however, revealed that swimming speeds attained in the annular chamber and tunnel respirometer were similar. At 10 °C, fish averaging 14.9 cm total length attained a maximum mean speed of 38.1 $cm \cdot s^{-1}$ in the rotating annular respirometer (Gibson and Fry 1954) compared with 10 fish of 15.0 cm mean total length that attained a sustained maximum speed of 36.7 $cm \cdot s^{-1}$ in the tunnel respirometer. Similarly, at 18 °C, lake trout of 20.7 cm total length swam at 63.8 $cm \cdot s^{-1}$ in the annular chamber versus 50.1 $cm \cdot s^{-1}$ for 10 fish of mean length 24.7 cm in the tunnel respirometer. Juvenile lake trout, therefore, swam as fast or faster in the Gibson and Fry (1954) annular chamber compared with the tunnel respirometer of Stewart et al. (1983). The active metabolic rate at 10 °C measured by Beamish et al. (1989) was 17% higher than that estimated by Gibson and Fry (1954). Similarly, the estimated active rate at 10 °C from Stewart et al. (1983) was 13.5% higher than that from Gibson and Fry (1954), but scope-for-activity at 10 °C was estimated as 201.4 $mg \cdot L^{-1}$ by Gibson and Fry (1954) versus 189.4 $mg \cdot L^{-1}$ by Stewart et al. (1983) and 237.9 $mg \cdot L^{-1}$ at 10 °C by Beamish et al. (1989). The active metabolic rates in the annular chamber were slightly lower than those in the tunnel respirometers but well within the range of variation normally seen among studies (Beamish 1978, 1980). The overall similarity of scope-for-activity for lake trout among these studies validates use of the data from Gibson and Fry (1954) in the present study.

Standard metabolic rates of yearling lake trout increased monotonically with temperature, whereas active metabolism peaked at 15–16 °C, as did scope-for-activity (Fig. 2). The level of no-excess-activity varied from about 2.7 to 3.2 $mg \cdot L^{-1}$ over the range 4–18 °C (Table 1). The incipient response threshold, indicating the boundary of the zone of respiratory dependence, defined herein as the 95% scope-for-activity threshold, varied from 9.4 to 8.1 $mg \cdot L^{-1}$ at temperatures of 4–18 °C, respectively (Fig. 5; Table 1). Above these thresholds, full scope-for-activity is attainable. Full scope-for-activity was 3.5 times standard at 4–14 °C but decreased to 2.4 times standard at 18 °C. These ratios define the upper limit for the costs of activity in lake trout.

The selected scope-for-activity thresholds (1/4, 1/2, and 3/4 scope) partitioned the scope into four equal segments (Fig. 3). The active metabolic rate at various ambient partial pressures of oxygen is illustrated in detail for tests at 12 °C (Fig. 4). The selected thresholds, i.e., 1/4, 1/2, and 3/4 scope-for-activity, the level of no-excess-activity, and the incipient response threshold are indicated on the dissolved oxygen response curves for all test temperatures (Fig. 5). These curves revealed the limiting effect of hypoxia on active metabolic rate at various temperatures. As a general rule, hypoxia caused a more precipitous decline in active metabolic rate at the higher temperatures, 14–18 °C.

The ambient dissolved oxygen concentrations that limited performance to 1/4, 1/2, and 3/4 scope-for-activity varied from 4.1 to 4.6, from 5.2 to 5.9, and from 6.3 to 7.5 $mg \cdot L^{-1}$, respectively (Table 2). The mean dissolved oxygen thresholds for 1/4 and 3/4 scope-for-activity at 10 °C, 4.4 and 7.0 $mg \cdot L^{-1}$, were separated by only 2.6 mg ambient dissolved $oxygen \cdot L^{-1}$, revealing that relatively small changes in oxygen content of the natural environment can have major implications for metabolism and activity of yearling lake trout. This range defines the scale from avoidance and maintenance feeding at about 4.3 $mg \cdot L^{-1}$ to a relatively high level of metabolic performance at 7.0 $mg \cdot L^{-1}$. At 4–14 °C and 1/4, 1/2, and 3/4 scope, the activity component of the total metabolic rate averaged 0.89 ± 0.01, 1.76 ± 0.03, and 2.63 ± 0.04 times standard metabolic rate, respectively. These ratios, i.e., multipliers of standard metabolic rate, define the maximum upper limits for activity at the corresponding ambient dissolved oxygen levels shown in Table 2.

Effect of hypoxia on power capacity

Hypoxia and temperature had a dramatic effect on net power capacity, i.e., the power available for all volitional activities. The net power capacity is illustrated per kilogram of yearling lake trout at various partial pressures of oxygen

© 2007 NRC Canada

Table 2. Scope-for-activity of juvenile lake trout at 1/4, 1/2, and 3/4 scope-for-activity.

	1/4 scope			1/2 scope			3/4 scope		
Temperature (°C)	O_2 uptake ($mg \cdot kg^{-1} \cdot h^{-1}$)	O_2 partial pressure (mmHg)	Ambient O_2 ($mg \cdot L^{-1}$)	O_2 uptake ($mg \cdot kg^{-1} \cdot h^{-1}$)	O_2 partial pressure (mmHg)	Ambient O_2 ($mg \cdot L^{-1}$)	O_2 uptake ($mg \cdot kg^{-1} \cdot h^{-1}$)	O_2 partial pressure (mmHg)	Ambient O_2 ($mg \cdot L^{-1}$)
4	69.4	58.0	4.62	102.2	74.5	5.94	135.0	93.6	7.46
6	82.3	59.0	4.47	121.1	76.3	5.78	159.9	96.0	7.27
8	97.7	61.0	4.40	143.5	79.5	5.73	189.3	100.2	7.22
10	115.9	63.2	4.35	170.1	82.0	5.64	224.2	101.0	6.95
12	137.6	64.2	4.22	201.5	82.8	5.44	265.4	103.0	6.77
14	163.3	64.5	4.06	238.8	83.0	5.23	314.3	104.5	6.58
16	199.1	71.3	4.13	273.6	88.7	5.13	348.0	108.6	6.29

Notes: Scope values at each temperature were derived from Fig. 3 for yearling lake trout at a mean body weight of 27.7 g.

(Fig. 6). Power capacity is maximal at 14–18 °C and declines to zero as ambient partial pressure of oxygen declines to 40 mmHg. At 66 mmHg, which is equivalent to about 4.0 mg dissolved oxygen·L^{-1} at 16 °C, power capacity fell to about 25% of full power. Hence, there is a dramatic decline in power available for various work activities as dissolved oxygen falls from air saturation to the avoidance threshold near 4.0 mg·L^{-1}. At temperatures >16 °C, lake trout were operating at an aerobic power deficit at 40 mmHg partial pressure of oxygen and at 30 mmHg were in a deficit position at all temperatures. The chronic lethal threshold for lake trout survival would therefore be expected to be about 40 mmHg partial pressure (Fig. 6). The mean ± SD incipient lethal threshold corresponding to the level of no-excess-activity was estimated to be 40.8 ± 3.5 mmHg at 4–18 °C (Table 1). Interpolation of Fig. 6 provided a rectangular matrix of power capacity across the range of temperatures and oxygen pressures normally experienced by lake trout in the natural environment. This matrix was used to generate a two-dimensional response surface of power capacity (Fig. 7; the points are the interpolated values from Fig. 6). The temperature range exploited by lake trout during summer, 4–20 °C, provides for a potential power capacity of about 500–1300 mW·kg^{-1} at 100% oxygen saturation, declining to zero near 40 mmHg (Fig. 7). The response surface has been partitioned to include the habitats associated with juveniles and adults (Fig. 8). The maximum power capacity of lake trout occurred at oxygen concentrations exceeding 7 mg·L^{-1} and temperatures of 12–20 °C (Fig. 8, shaded area). Juvenile lake trout that inhabit the hypolimnion and frequent temperatures of about 4–8 °C during the summer months (Davis 1997) clearly have greatly reduced power capacity (500–700 mW) compared with 700–1300 mW·kg^{-1} at temperatures of 8–20 °C, i.e., the thermal habitat routinely frequented by adult lake trout. Within the thermal zone occupied by juvenile lake trout, it is also clear that a decline in oxygen pressure from air saturation to 120 mmHg would have relatively little impact on power capacity of the juveniles. A further decline in oxygen pressure to 86–96 mmHg corresponding to a concentration of about 7 mg·L^{-1} at 4–8 °C, however, would reduce net power capacity by about 33%, and further declines in oxygen pressure to 66 mmHg (5 mg·L^{-1}) and 40 mmHg (3 mg·L^{-1}) would result in dramatic declines in net power capacity of 67% and 100%, respectively (Fig. 8).

Discussion

Habitat, life history, and dissolved oxygen

Using a remotely operated vehicle, Davis (1997) and Davis et al. (1997) directly observed juvenile lake trout in the hypolimnion of four study lakes at temperatures of 4–8 °C. The deep distribution of juvenile lake trout at physiologically suboptimal temperatures (McCauley and Tait 1970; Edsall and Cleland 2000) is probably maintained by the predation pressure of cannibalistic adults, which inhabit shallower depths (Evans and Willox 1991; Evans et al. 1991). The juveniles are confined to the hypolimnion during the summer months, making this habitat a potential bottleneck for lake trout recruitment because of the limiting effect of low dissolved oxygen that commonly occurs in stratified lakes. A recent whole-lake fertilization experiment in a

© 2007 NRC Canada

Fig. 6. Net power capacity of yearling lake trout per kilogram of fish at various oxygen pressures and ambient temperatures. Power was derived from oxygen consumption at each oxygen pressure taken directly from Fig. 5 minus standard metabolic rate at each temperature. The broken horizontal line corresponds to the level of no-excess-activity or lethal threshold below which lake trout would be in a deficit energy state.

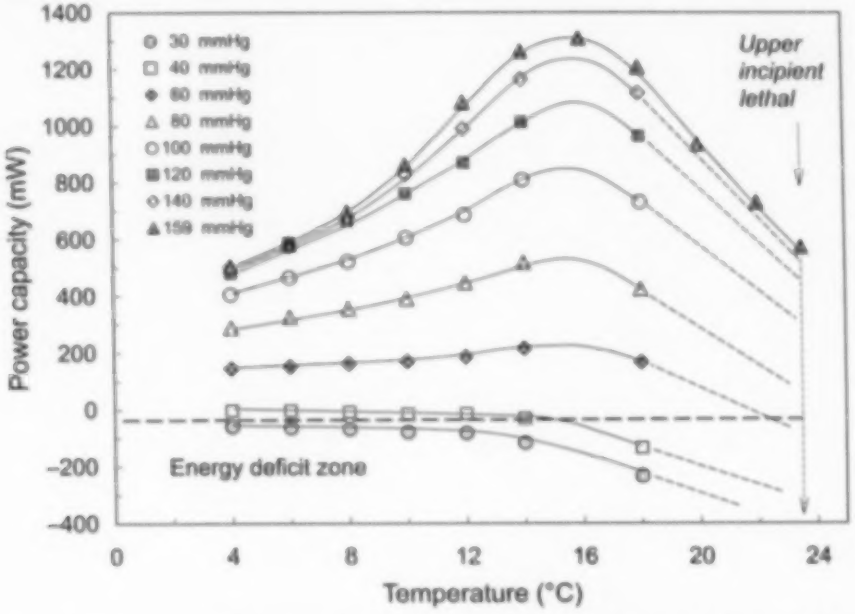

Fig. 7. Response surface of net power capacity for yearling lake trout per kilogram of fish derived from Fig. 6. The points indicate the interpolated values. The vertical broken lines at 4 and 20 °C represent the potential operational temperature range for all life stages of lake trout.

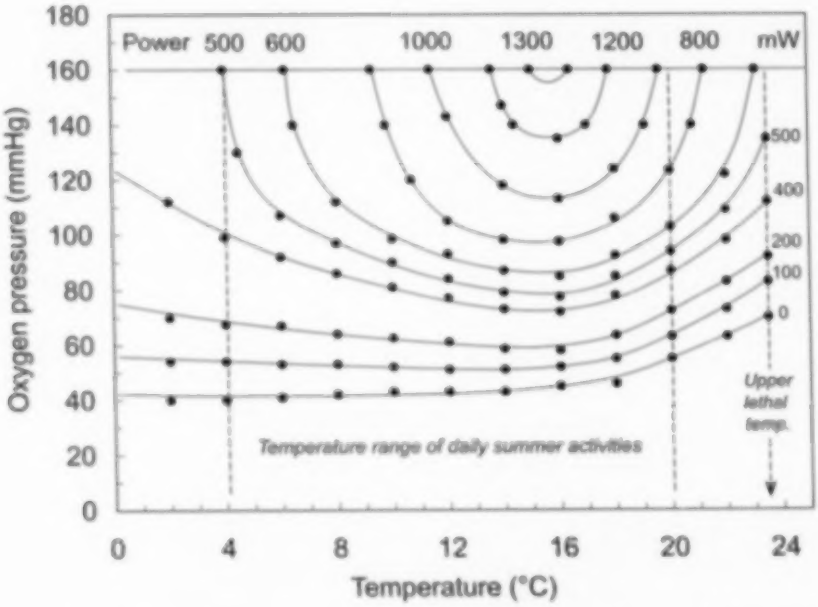

small Arctic lake has clearly demonstrated the linkages between phosphorus loading, primary production, hypolimnetic dissolved oxygen depletion, and lake trout recruitment (Lienesch et al. 2005).

Standard and active metabolic rates of lake trout

Standard metabolic rates are difficult to obtain because of the effects of handling stress (Fry 1971) and the need to account for spontaneous activity (Evans 1972, 1984, 1990). In

© 2007 NRC Canada

Fig. 8. Net power capacity of yearling lake trout illustrating the zone of optimal performance (shaded area) and selected dissolved oxygen thresholds at 3, 5, and 7 mg·L^{-1}. The primary temperature ranges frequented by juvenile (4–8 °C) and adult lake trout during summer (8–20 °C) are indicated by vertical broken lines. The solid curves indicate the power capacity for yearling lake trout of 27.7 g mean body weight expressed per kilogram. The sloping broken lines are the dissolved oxygen concentrations at 3, 5, and 7 mg·L^{-1} corresponding to temperatures and oxygen partial pressures across the surface. The percentages shown in the juvenile zone indicate approximate power losses of 33%, 67%, and 100% at the dissolved oxygen boundaries of 7, 5, and 3 mg·L^{-1}, respectively.

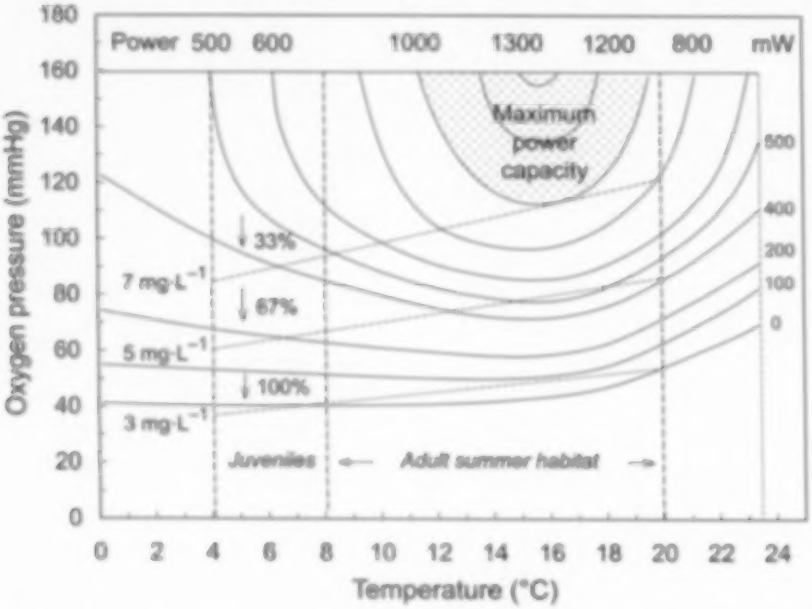

this study, standard metabolic rates adjusted to a 100 g fish varied from 25.5 to 114.3 mg·kg^{-1}·h^{-1} for yearling lake trout at 4–20 °C, which are similar to standard rates reported for sockeye salmon (*Oncorhynchus nerka*) (Brett 1964), Atlantic salmon (*Salmo salar*) (Peterson and Anderson 1969), and rainbow trout (*Oncorhynchus mykiss*) (Dickson and Kramer 1971) over the same temperature range. Beamish et al. (1989) reported a standard metabolic rate of 50.7 mg·kg^{-1}·h^{-1} at 10 °C for yearling lake trout adjusted to a body weight of 100 g that was essentially identical to the rate 51.0 mg·kg^{-1}·h^{-1} determined for yearling lake trout at 10 °C by Gibson and Fry (1954).

Standard metabolic rates estimated for lake trout by Rottiers (1993) and Stewart et al. (1983), however, were consistently higher than those reported by Gibson and Fry (1954). Webb (1997) suggested that a change in swimming gait at slower speeds results in J-shaped speed–cost curves, oxygen consumption rising at lower speeds. Extrapolation of this type of relationship to zero activity would tend to overestimate standard metabolic rate. Brett and Sutherland (1965) first noted the marked effect of spontaneous activity at slow speeds on oxygen consumption in tunnel respirometers. Beamish et al. (1989) observed similar behaviour in lake trout and omitted measurements of oxygen consumption for fish swimming at 20 cm·s^{-1} when extrapolating to zero activity. Spontaneous start-and-stop swimming compared with swimming at a constant speed has also been shown to have dramatically increased costs (Smit 1965). Variation in swimming gait or mode at low speeds might in part explain the higher standard rates reported by Rottiers (1980, 1993) and Stewart et al. (1983) compared with Gibson and Fry (1954) and Beamish et al. (1989). Gibson and Fry (1954) used the lowest measured rates of quiescent fish over a 24 h cycle to characterize standard metabolic rate, which also explains their lower estimates.

The active metabolic rate of lake trout at 10 °C from Gibson and Fry (1954) was 14.5% lower than that from Beamish et al. (1989) and 11.9% lower than that from Stewart et al. (1983). Differences of this magnitude can easily be accounted for by variation in study-specific oxygen consumption – body weight exponents used to adjust to a common fish size (Fry 1971). In contrast, the scope-for-activity for lake trout from Gibson and Fry (1954) is 4–10% higher than scope-for-activity values from Stewart et al. (1983) at 4–15 °C and within 2% of values calculated for brown trout (*Salmo trutta*) at 15 °C (Priede 1985), indicating consistency between metabolic scope reported by Gibson and Fry (1954) and the more recent literature.

Response to hypoxia

The response of lake trout to hypoxia was similar to that observed for brook trout (*Salvelinus fontinalis*), active metabolic rate declining from the highest oxygen partial pressures to the level of no-excess-activity with little or no zone of oxygen independence (Graham 1949; Job 1955; Basu 1959). For brook trout at 10 and 15 °C, 1/2 scope occurred at about 87 and 95 mmHg (Basu 1959) compared with 82 and 86 mmHg, respectively, for lake trout. Similarly, 3/4 scope for brook trout at 10 and 15 °C occurred at 120 and 125 mmHg (Basu 1959) compared with 101 and 105 mmHg,

© 2007 NRC Canada

respectively, for lake trout. The acute lethal threshold for brook trout fry was 1.58 $mg \cdot L^{-1}$ (Sheppard 1955), but a comparable value is not available for lake trout. Carlson and Seifert (1974) did find that all lake trout larvae incubated at 1.9–3.2 $mg \cdot L^{-1}$ at 7 °C and 3.0–4.2 $mg \cdot L^{-1}$ at 10 °C died at or prior to first-feeding.

An important question with reference to the ability to compensate for the effects of hypoxia on metabolic scope is whether exposure to low oxygen results in acclimation with the benefit of improved survival and swimming performance. Bushnell et al. (1984) found that acclimation of rainbow trout to hypoxia (oxygen partial pressure = 40 and 60 mmHg at 15 °C) did not increase maximum swimming speeds in normoxic or hypoxic swim trails. Similarly, Kutty (1968) found no evidence of enhanced swimming capacity in hypoxia-acclimated goldfish (*Carassius auratus*).

Standard metabolic rates of rainbow trout were not significantly affected by acclimation to hypoxia when tested under normoxic or hypoxic conditions, oxygen partial pressure of 40 mmHg (Bushnell et al. 1984), although control fish tended to have higher standard rates under hypoxia. The latter observation is consistent with Beamish (1964) who reported elevated standard metabolic rate of brook trout at 80 mmHg when tested at 10 and 15 °C. In contrast with Bushnell et al. (1984), Beamish (1964) also found that hypoxia-acclimated brook trout showed a noticeable, but smaller, increase at 80 mmHg than the normoxic controls. This suggested that acclimation to low oxygen reduced the cost of ventilation at low ambient dissolved oxygen. Beamish (1964) attributed the 40%–50% increase in standard metabolic rate of normoxic control fish at 80 mmHg to the cost of increased respiratory volume needed to meet standard metabolic costs. Standard oxygen consumption did not rise to the level of active metabolic rate and swimming continued until the oxygen partial pressure reached 30–40 mmHg. Beamish (1964) speculated that anaerobiosis might be engaged to help meet the metabolic demands at low oxygen partial pressure. If a similar mechanism occurs in lake trout, the current values of scope-for-activity would be overestimated at ambient oxygen levels near 80 mm Hg, i.e., near the level of 1/2 power capacity. In effect, an aerobic power reduction would appear at the 1/2 scope threshold when costs of elevated heart rate and increased respiratory volume become engaged, thereby increasing standard costs and reducing metabolic scope (Saunders 1962). There would be an apparent slight recovery of scope when second-stage biochemical mechanisms and anaerobic pathways come on line (Heath et al. 1980; Dunn and Hochachka 1986). This possible increase in standard metabolic rate and associated decline in scope at about 60–80 mmHg oxygen partial pressure would have no effect on the ambient oxygen required to attain 3/4 scope-for-activity because this would be well above the oxygen partial pressure that causes elevation of the standard rate.

Scope-for-activity and net power capacity

Scope-for-activity defines the amount of energy available for activity, whereas power is the flow of energy per unit time in $J \cdot s^{-1}$. While these measures can be converted from one to the other, they have distinctive meanings. Scope is the range of aerobic metabolism available for volitional activities and power is the output of energy associated with a specific workload. The limiting effect of hypoxia on oxygen uptake directly constrains scope-for-activity and the power output that can be achieved during performance of various activities. Maintenance of power outputs comfortably within the boundaries set by standard and active metabolic rates (Fry 1971; Priede 1977, 1985), while at the same time providing surplus energy for somatic growth, requires a balancing of energy intake and the metabolic costs of capturing prey and avoiding predators (Brett 1979; Brett and Groves 1979). The latter activities of lake trout would be severely constrained by hypoxia because of the limits imposed on oxygen uptake (Jones 1971; Davis 1975). There would also be elevated foraging risks associated with reduced quality and availability of summer nursery habitat (Molot et al. 1992; Evans et al. 1996; Dillon et al. 2003).

Feeding metabolism at levels from maintenance to maximum ration includes the cost of standard metabolism, swimming activity, and heat increment associated with handling and processing ingested food, all of which can be expressed as a fraction of the available scope-for-activity (Table 3). These activities are additive and their relative contributions to total metabolism are continually under adjustment during the activity trade-offs of a normal day (Brett and Groves 1979; Priede 1985). Hypoxia has the potential to limit or completely interdict some or all of these activities, which in the latter case could cause an energy deficit with metabolic power falling below the level of no-excess-activity. If persistent, this would result in mortality.

Cost of daily life support activities with reference to hypoxia

Knowledge of the actual daily costs of critical activities would allow the significance of hypoxia on scope-for-activity to be quantified for wild fish. Energy intake (prey) minus energy expenditures for standard metabolism, locomotory activity, heat increment, and excretion determines the energy available for growth and production (Brett and Groves 1979). Hence, quantification of the actual level of swimming activity and associated energy expenditure of free-ranging fish has been the subject of much scientific enquiry (Boisclair and Leggett 1989; Rowan and Rasmussen 1996; Rennie et al. 2005). Metabolic costs of daily activities have not been published for free-ranging lake trout, but costs for various activities are available from laboratory studies for lake trout and other salmonids, including sockeye salmon (Brett 1964, 1965) and brown trout (Elliott 1976; Priede 1985). Sockeye salmon attain sustained active metabolic rates that are 10 times the standard metabolic rate compared with lake trout at five times and brown trout at 4.3 times standard (Table 3). Sockeye salmon, brown trout, and lake trout, however, have similar standard metabolic baselines.

Standard metabolism for lake trout in Table 3 is from Gibson and Fry (1954), active metabolism is from Stewart et al. (1983), maintenance, routine, and maximum feeding metabolism were derived from Rottiers (1993) and maximum aggression or excitability metabolism was estimated as one-half active metabolic rate (Fry 1971). The oxygen consumption – feeding ration relationship at 15 °C derived from Rottiers (1993) was used to estimate metabolic rates of lake trout at maximum and maintenance feeding levels. The maximum

© 2007 NRC Canada

Table 3. Comparison of metabolic rates (mg·kg^{-1}·h^{-1}) of sockeye salmon (*Oncorhynchus nerka*), brown trout (*Salmo trutta*), and lake trout (*Salvelinus namaycush*) and costs of various activities adjusted to a body weight of 100 g at 15 °C.

Species	Standard rate, R_s	Active rate, R_{act}	Scope-for-activity, $R_{act} - R_s$	Feeding maintenance, R_{fmm}	Feeding routine, R_{fr}	Feeding maximum, R_{fmax}	Aggression or excitability	Migration maximum
Sockeye salmon	75	790	715	140	250	360	310–420	640
			100	*9*	*24*	*40*	*32–48*	*79*
Brown trout	98	421	323	175	229	368	210	na
			100	*24*	*41*	*84*	*35*	
Lake trout	71	413	342	116	253	370	207	na
			100	*13*	*53*	*87*	*40*	

Note: Standard and active metabolic rates of brown trout and lake trout were adjusted using a weight exponent of 0.85. The data for sockeye salmon are from Brett and Groves (1979) and for brown trout are from Elliott (1976) and Priede (1985). Lake trout data: standard from Gibson and Fry (1954), active rate from Stewart et al. (1983), and maintenance and maximum feeding from Rottiers (1993). Aggression or excitability for brown trout and lake trout was calculated as 0.5 of the active metabolic rate (Fry 1971). The percentage of scope-for-activity required by each activity is shown in italics. The cost of standard metabolism is included in all values except scope-for-activity. na, not available.

feeding rate (78.1 cal·g^{-1}·day^{-1}) was the mean at the observed maximum ration at 15 °C (Rottiers 1993). Maintenance ration (22.03 cal·g^{-1}·day^{-1}) was the intercept of the growth–ration curve at 15 °C ($y = 22.026e^{0.0528x}$, where y is ration (cal·g^{-1}·day^{-1}) and x is growth (cal·g^{-1}·day^{-1})). Elliott (1976) reported similar maximum (65.5 cal·g^{-1}·day^{-1}) and maintenance (18.6 cal·g^{-1}·day^{-1}) feeding rations for brown trout at 15 °C. Routine field metabolism of lake trout was based on observed field growth of juvenile lake trout at 7.25 °C (Rottiers 1993). The estimated routine ration in the field, 2.0% body weight·day^{-1} (Rottiers 1993), was adjusted to an expected ration at 15 °C of 4.39% body weight·day^{-1} using the slope ($b = 0.308$) of the optimal ration–temperature curve in Brett (1979, their fig. 10A). Using Rottiers' (1993) relationship between oxygen consumption and ration expressed as % body weight·day^{-1}, the routine field metabolic rate was 252.7 mg·kg^{-1}·h^{-1} for a 100 g fish, which was equivalent to 53% of full scope-for-activity. Priede (1985) provided a power estimate of 340 mW for a 500 g randomly feeding, free-ranging brown trout in a Scottish loch. This equates to oxygen consumption of 229 mg·kg^{-1}·h^{-1} or 41% of full scope-for-activity for a 100 g fish (Table 3). Lake migration of juvenile sockeye in Babine Lake, British Columbia (Johnson and Groot 1963; Groot and Wiley 1965), required 380–640 mg O_2·kg^{-1}·h^{-1} or 53%–79% of the available scope-for-activity (Brett and Groves 1979).

Under laboratory conditions at 15 °C, maintenance, routine, and maximum feeding and excitability of sockeye consumed 9%, 24%, 40%, and 34%–48%, respectively, of the maximum scope-for-activity (Brett and Groves 1979) (Table 3). Brown trout utilized 24%, 41%, 84%, and 35% of available scope for maintenance, routine, and maximum feeding and excitability, respectively (Elliott 1976; Priede 1985), compared with lake trout at 13%, 53%, 87%, and 40% for the same activities (Table 3). Similar daily activity costs of lake trout and brown trout reflect their well-matched lacustrine life histories and corresponding low power capacities. Sockeye power capacity is much higher, reflecting a more demanding life history that includes extensive ocean and freshwater migrations. Somatic energy reserves are accumulated in ocean-feeding sockeye in proportion to the distance and difficulty of migration routes of various stocks (Hendry and Berg 1999). These and similar observations (e.g., Rand and Hinch 1998; Cooke et al. 2006) suggest that physiological mechanisms are well adapted to satisfy but not greatly exceed the functional requirements of the whole organism (Lindstedt and Jones 1987). Accordingly, lake trout have limited physiological capacity to compensate for hypoxia, and because of the tight coupling between oxygen uptake, power capacity, swimming activity, and feeding, both acquisition and consumption of energy are directly affected.

The present laboratory estimates of costs (Table 3), with the exception of excitement, must be minimal estimates of the normoxic energy expenditures of wild fish because of the additional costs of searching for and capturing living prey, competition for resources, and avoiding and escaping predators in the natural environment (e.g., Pazzia et al. 2002; Rennie et al. 2005). Nevertheless, routine feeding by lake trout at 53% of available scope means that the routine metabolic rate would be 1.88 times standard (Table 3). This compares with mean activity multipliers of 1.51 ± 0.54 (SD) times resting metabolic rate for immature lake trout from Great Slave Lake and 2.27 for Lake Michigan based on analysis of mass balances of growth and ^{137}Cs (Rowan and Rasmussen 1996). These independent estimates of mean activity expenditures are similar and consistent with the idea that the probability of mortality is minimized when an organism operates well within its maximal metabolic range with a mean power output near 1/2 scope (Priede 1977, 1985).

A quantitative model for protection of lake trout summer habitat

Viable habitats for lake trout must provide adequate oxygen to meet the energy demands of standard and active metabolism. Based on telemetry studies, Priede (1985) concluded that for most of the time, brown trout operated conservatively at about 1/2 power capacity and that maximum power capacity occurred only about 1% of the time. Half scope of lake trout can be attained at oxygen partial pressures of 74.5–88.7 mmHg or 5.1–5.9 mg·L^{-1} at 4–18 °C. Half scope would not be an effective threshold for protection of brown trout or lake trout, however, considering that daily activity levels would routinely vary between 1/4 and 3/4 scope and occasionally approach 100%. Maximal feeding of lake trout and brown trout requires about 84%–87% of full scope. The upper range of normal power output correspond-

© 2007 NRC Canada

Fig. 9. Net power capacity response surface showing the spatial distribution of juvenile and adult lake trout segregated by temperature and dissolved oxygen and the physiological and population consequences of exposure to hypoxia by life stage. Juvenile and adult ovals are shown within their usual daytime summer thermal distributions, 4–8 and 8–20 °C, respectively.

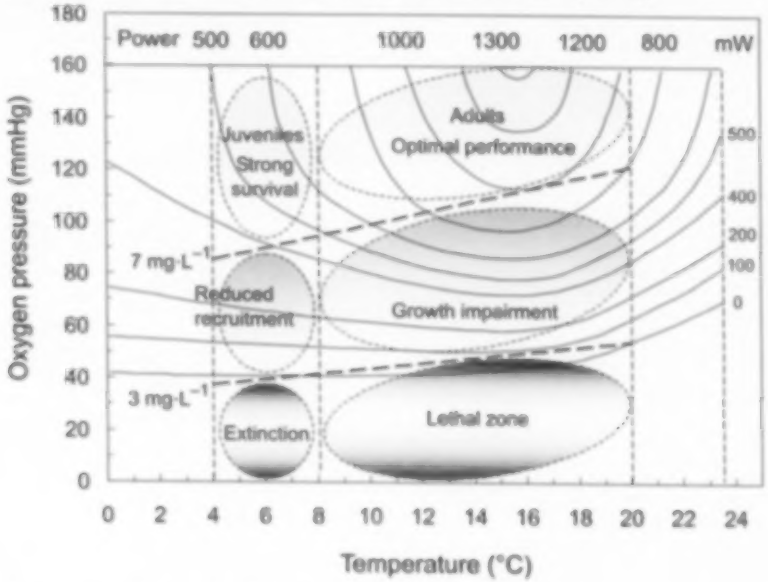

ing to 3/4 scope-for-activity, which is attainable by lake trout at an ambient dissolved oxygen concentration of about 7 mg·L^{-1}, would be a better criterion for protection of their summer habitat.

Effects of hypoxia on growth are especially relevant because of the high aerobic energy demands of capturing and processing prey (Brett and Groves 1979). The total metabolic costs will determine the amount of energy available for growth after accounting for the costs of activity, heat increment, and losses in feces and urine. The limiting effect of hypoxia on oxygen uptake will constrain activity that is required for searching for and capturing prey and escaping capture by predators. Processing of the prey that is captured will in turn impose a feedback limit on further activity. In the case of extreme hypoxia at 40 mmHg, there is zero capacity for capture of prey or avoidance of predators. Growth would cease at a somewhat higher oxygen concentration set by power requirements for activities needed to sustain basic maintenance. A conservative estimate of this threshold corresponds to 1/4 scope-for-activity or an ambient dissolved oxygen concentration of about 4.4 mg·L^{-1}.

The response threshold for growth impairment in laboratory experiments at high feeding rates for six species of salmonid was 7–8 mg·L^{-1} (British Columbia Ministry of Environment, Lands and Parks 1997) and growth impairment increased exponentially at oxygen concentrations below 7 mg·L^{-1}, reaching 20%–30% at 4 mg·L^{-1}. Complete impairment of growth at this level of hypoxia would be expected in the natural environment where searching and capturing prey would be energetically much more costly than in laboratory tanks.

A recent compilation of recruitment success in 81 lake trout lakes in south-central Ontario (D.O. Evans, unpublished data) revealed good to excellent recruitment in lakes with late-summer (15 August – 15 September) mean hypolimnetic oxygen concentrations exceeding 7 mg·L^{-1}. Lakes with average to poor recruitment had hypolimnetic oxygen concentrations of 5–6 mg·L^{-1} and lakes with very poor recruitment were at 4 mg·L^{-1} or lower. These results showed that prolonged exposure to ambient dissolved oxygen of <7 mg·L^{-1} during late summer had a negative effect on lake trout recruitment. This is consistent with the effects of hypoxia on power capacity and the published effects of hypoxia on growth of salmonids (Davis 1975; Jensen et al. 1993; Barton and Taylor 1996).

Most daily life support activities of lake trout appear to be accommodated within bounds set by 3/4 scope-for-activity. Ambient dissolved oxygen of 7.13 ± 0.27 mg·L^{-1} corresponding to oxygen partial pressures of 95–105 mmHg enabled juvenile lake trout to attain 3/4 power capacity at 4–12 °C, temperatures that conservatively span their summer habitat. Population responses of lake trout to combinations of temperature and oxygen partial pressures are illustrated in Fig. 9. No negative effects would be expected at dissolved oxygen concentrations above 7 mg·L^{-1}. Growth and recruitment impairment would be expected at ambient dissolved oxygen concentrations between 7 and 3 mg·L^{-1} and mortality and local extinctions would be expected at conditions below 40 mmHg or 3 mg·L^{-1}.

Davis (1975) identified three levels of dissolved oxygen protection for freshwater and marine fishes in Canada corresponding to low, medium, and high risk thresholds. He recommended a low risk criterion of 7.75 mg·L^{-1} for the protection of freshwater salmonids (rainbow trout, brown trout, brook trout, including steelhead) and a moderate risk level for this group of 6.0 mg·L^{-1}. The moderate risk category was defined as "the oxygen value where the average member of a population would begin to exhibit symptoms of

© 2007 NRC Canada

oxygen distress". At the moderate risk level, he further noted that "some degree of risk to a portion of fish populations exists at this level if the oxygen minimum period is prolonged beyond a few hours". In the context of the no-net-loss concept (Department of Fisheries and Oceans 1986; Minns 1997), it is obvious that a short-term response threshold would not meet the requirements for long-term maintenance of productive capacity and that a moderate risk criterion that accepts some distress to a portion of a fish population is not acceptable. Davis (1975) set the low risk levels at 1 SD above the mean dissolved oxygen response threshold. The responses that he considered for postlarval life stages included the effect of hypoxia on respiratory dependence of metabolic processes and swimming ability, respiratory functions (breathing amplitude, buccal pressures, oxygen saturation of the blood), circulatory functions (heart rate, stroke volume), growth rate, and avoidance. I have shown that a decline of only 1 $mg \cdot L^{-1}$ from 7 to 6 $mg \cdot L^{-1}$ can have significant negative effects on power capacity, growth, and recruitment success of lake trout and that a minimum of 7.0 $mg \cdot L^{-1}$ is required for the protection of lake trout summer habitat. Davis' (1975) level B protection at 6.0 $mg \cdot L^{-1}$ for freshwater salmonids is definitely not adequate for protection of lake trout summer habitat, while his level A protection at 7.75 $mg \cdot L^{-1}$ appears to be more conservative than required for this purpose.

Resource management implications

Long-term sustainability of lake trout populations requires regulatory measures to ensure healthy aquatic ecosystems for this species. In small inland lakes, dissolved oxygen is critically important from a regulatory perspective because of the influence of land-use activities on phosphorus loading and lake trophic state (Evans et al. 1996; Hutchinson 2002; Steedman et al. 2004). Municipal sewage, cottage septic systems, and surface runoff from developed landscapes are potential sources of phosphorus. The linkage between phosphorus and lake trout habitat is mediated by the annual cycle of algae production and decomposition (Schindler et al. 1971; Dillon and Rigler 1974), the latter process placing a significant demand on the fixed supply of dissolved oxygen in the hypolimnion (Molot et al. 1992; Clark et al. 2004; Lienesch et al. 2005). Quantitative models are now available to predict the consequences of shoreline development and associated phosphorus loading for algal production and hypolimnetic oxygen depletion in Precambrian Shield lakes (Hutchinson et al. 1991; Dillon et al. 1994; Paterson et al. 2006).

Given that juvenile lake trout inhabit the hypolimnion during the summer months (Davis 1997; Davis et al. 1997), the recommended 7 $mg \cdot L^{-1}$ criterion should be applied to the hypolimnetic volume. Evans et al. (1996) characterized the mean volume-weighted hypolimnetic dissolved oxygen concentration (MVWHDO) to provide a measure specific to the summer habitat utilized by coldwater species. Correction of MVWHDO to a fixed date, 15 September, using estimated or observed oxygen depletion rates provides consistent estimates for interannual and interlake comparisons. Lake trout lakes having late-summer MVWHDO at or below the 7.0 $mg \cdot L^{-1}$ criterion would have no further capacity for anthropogenic phosphorus loading without negatively affecting lake trout habitat. Lake trout populations in lakes below the threshold would also be more susceptible to other stressors (Evans and Willox 1991) and should be identified as requiring a high level of stock protection. The data requirements for application of this criterion are described in Quinlan et al. (2005) and standard calculations in Evans et al. (1996) and Clark et al. (2002).

Acknowledgements

I would like to acknowledge and thank my colleagues Dr. Tim Johnson, Glenora Fishery Station, Picton, Ontario, Dr. John Casselman, Queens University, Kingston, Ontario, and Cheryl Lewis Ontario Ministry of Natural Resources, Peterborough, Ontario, for helpful and encouraging comments on the manuscript. Technical support provided by Audie Skinner, Ontario Ministry of Natural Resources, Peterborough, for various aspects of our lake trout research is also gratefully acknowledged. I would like to acknowledge and thank Donald V. Rottiers, Dexter, Michigan, for making available his original lake trout data set, which proved to be very helpful. I also extend thanks to two anonymous reviewers whose comments helped to improve the manuscript. Research funding to D.O.E. in support of this work has been generously provided by the Ontario Ministry of Natural Resources.

References

Barton, B.A., and Taylor, B.R. 1996. Oxygen requirements of fishes in northern Alberta rivers with a general review of the adverse effects of low dissolved oxygen. Water Qual. Res. J. Can. **31**: 361–409.

Basu, S.P. 1959. Active respiration of fish in relation to ambient concentrations of oxygen and carbon dioxide. J. Fish. Res. Board Can. **16**: 175–212.

Beamish, F.W.H. 1964. Respiration of fishes with special emphasis on standard oxygen consumption. III. Influence of oxygen. Can. J. Zool. **42**: 355–366.

Beamish, F.W.H. 1978. Swimming capacity. *In* Fish physiology. Vol. 7. *Edited by* W.S. Hoar and D.J. Randall. Academic Press, New York. pp. 101–187.

Beamish, F.W.H. 1980. Swimming performance and oxygen consumption in charrs. *In* Charrs: salmonid fishes of the genus *Salvelinus*. *Edited by* E.K. Balon. Dr. W. Junk bv Publishers, The Hague, Netherlands.

Beamish, F.W.H., Howlett, J.C., and Medland, T.E. 1989. Impact of diet on metabolism and swimming performance in juvenile lake trout, *Salvelinus namaycush*. Can. J. Fish. Aquat. Sci. **46**: 384–388.

Boisclair, D., and Leggett, W.C. 1989. The importance of activity in bioenergetics models applied to actively foraging fishes. Can. J. Fish. Aquat. Sci. **46**: 1859–1867.

Brett, J.R. 1964. The respiratory metabolism and swimming performance of young sockeye salmon. J. Fish. Res. Board Can. **21**: 1183–1226.

Brett, J.R. 1965. The relation of size to rate of oxygen consumption and sustained swimming speed of sockeye salmon (*Oncorhynchus nerka*). J. Fish Res. Board Can. **22**: 1491–1501.

Brett, J.R. 1979. Environmental factors and growth. *In* Fish physiology. Vol. VIII. Bioenergetics and growth. *Edited by* W.S. Hoar, D.J. Randall, and J.R. Brett. Academic Press, New York. pp. 599–675.

© 2007 NRC Canada

Brett, J.R., and Glass, N.J. 1973. Metabolic rates and critical swimming speeds of sockeye salmon (*Oncorhynchus nerka*) in relation to size and temperature. J. Fish. Res. Board Can. **30**: 379–387.

Brett, J.R., and Groves, T.D.D. 1979. Physiological energetics. *In* Fish physiology. Vol. VIII. Bioenergetics and growth. *Edited by* W.S. Hoar, D.J. Randall, and J.R. Brett. Academic Press, New York. pp. 279–352.

Brett, J.R., and Sutherland, D.B. 1965. Respiratory metabolism of pumpkinseed (*Lepomis gibbosus*) in relation to swimming speed. J. Fish. Res. Board Can. **22**: 405–409.

British Columbia Ministry of Environment, Lands and Parks. 1997. Ambient water quality criteria for dissolved oxygen. Water Management Branch, Environment and Lands Headquarters Division, British Columbia Ministry of Environment, Lands and Parks, Victoria, B.C. (Available from http://wlapwww.gov.bc.ca/wat/wq/BCguidelines/do/index.html)

Bushnell, P.G., Steffenson, J.P., and Johansen, K. 1984. Oxygen consumption and swimming performance in hypoxia-acclimated rainbow trout, *Salmo gairdneri*. J. Exp. Biol. **113**: 225–235.

Carlson, A.R., and Seifert, R.E. 1974. Effects of reduced oxygen on the embryos and larvae of lake trout (*Salvelinus namaycush*) and largemouth bass (*Micropterus salmoides*). J. Fish. Res. Board Can. **31**: 1393–1396.

Christie, G.C., and Regier, H.A. 1988. Measures of optimal thermal habitat and their relationship to commercial yield for four commercial fish species. Can. J. Fish. Aquat. Sci. **45**: 301–314.

Clark, B.J., Dillon, P.J., Molot, L.A., and Evans, H.E. 2002. Application of a hypolimnetic oxygen profile model to lakes in Ontario. Lake Reservoir Manag. **18**: 32–43.

Clark, B.J., Dillon, P.J., and Molot, L.A. 2004. Lake trout (*Salvelinus namaycush*) habitat volumes and boundaries in Canadian Shield lakes. *In* Boreal Shield waters: lake ecosystems in a changing environment. *Edited by* J.M. Gunn, R.J. Steedman, and R.A. Ryder. Lewis Publishers, New York. pp. 111–117.

Clarke, A., and Johnston, N.M. 1999. Scaling of metabolic rate with fish body mass and temperature in teleost fish. J. Anim. Ecol. **68**: 893–905.

Cooke, S.J., Hinch, S.G., Crossin, G.T., Patterson, D.A., English, K.K., Shrimpton, J.M., Van Der Kraak, G., and Farrell, A.P. 2006. Physiology of individual late-run Fraser River sockeye salmon (*Oncorhynchus nerka*) sampled in the ocean correlates with fate during spawning migration. Can. J. Fish. Aquat. Sci. **63**: 1469–1480.

Davis, C.L. 1997. Habitat, distribution and abundance of juvenile lake trout, sculpin and burbot in four small Precambrian Shield lakes in Ontario. M.Sc. thesis, York University, Toronto, Ont. Natl. Libr. Can. Theses Microfilm No. LJ-27344.

Davis, C.L., Carl, L.M., and Evans, D.O. 1997. Use of a remotely operated vehicle to study habitat and population density of juvenile lake trout. Trans. Am. Fish. Soc. **126**: 871–875.

Davis, J.C. 1975. Minimum dissolved oxygen requirements of aquatic life with emphasis on Canadian species: a review. J. Fish. Res. Board Can. **32**: 2295–2332.

Department of Fisheries and Oceans. 1986. Policy for the management of fish habitat. Department of Fisheries and Oceans, Ottawa, Ont.

Dickson, I.W., and Kramer, R.H. 1971. Factors influencing scope for activity and active and standard metabolism of rainbow trout (*Salmo gairdneri*). J. Fish. Res. Board Can. **28**: 587–596.

Dillon, P.J., and Rigler, F.H. 1974. The phosphorus–chlorophyll relationship in lakes. Limnol. Oceanogr. **19**: 767–773.

Dillon, P.J., Scheider, W.A., Reid, R.A., and Jefferies, D.S. 1986. Lakeshore capacity study, trophic status. Ontario Ministry of Municipal Affairs and Housing, Toronto, Ont.

Dillon, P.J., Scheider, W.A., Reid, R.A., and Jeffries, D.S. 1994. Lakeshore Capacity Study. Part I. Tests of effects of shoreline development on the trophic status of lakes. Lake Reservoir Manag. **8**: 121–129.

Dillon, P.J., Clark, B.J., Molot, L.A., and Evans, H.E. 2003. Predicting the location of optimal habitat boundaries for lake trout (*Salvelinus namaycush*) in Canadian Shield lakes. Can. J. Fish. Aquat. Sci. **60**: 959–970.

Dillon, P.J., Clark, B.J., and Evans, H.E. 2004. The effects of phosphorus and nitrogen on lake trout (*Salvelinus namaycush*) production and habitat. *In* Boreal Shield waters: lake ecosystems in a changing environment. *Edited by* J.M. Gunn, R.J. Steedman, and R.A. Ryder. Lewis Publishers, New York. pp. 119–131.

Dunn, J.E., and Hochachka, P.W. 1986. Metabolic responses of trout (*Salmo gairdneri*) to acute environmental hypoxia. J. Exp. Biol. **123**: 1144–1148.

Edsall, T.A., and Cleland, J. 2000. Optimal temperature for growth and preferred temperatures of age-0 lake trout. N. Am. J. Fish. Manag. **20**: 804–809.

Elliott, J.M. 1976. The energetics of feeding, metabolism, and growth of brown trout (*Salmo trutta*) in relation to body weight, water temperature and ration size. J. Anim. Ecol. **45**: 923–948.

Elliott, J.M., and Davison, W. 1975. Energy equivalents of oxygen consumption in animal energetics. Oecologia, **19**: 195–201.

Elrod, J.H., and Schneider, C.P. 1987. Seasonal bathythermal distribution of juvenile lake trout in Lake Ontario. J. Gt. Lakes Res. **13**: 121–134.

Evans, D.O. 1972. Correction for lag in continuous flow respirometry. J. Fish. Res. Board Can. **29**: 1214–1216.

Evans, D.O. 1984. Temperature independence of the annual cycle of standard metabolism in the pumpkinseed. Trans. Am. Fish Soc. **113**: 494–512.

Evans D.O. 1990. Metabolic thermal compensation in the rainbow trout: effects on standard metabolic rate and potential usable power. Trans. Am. Fish. Soc. **119**: 585–600.

Evans, D.O., and Neill, W.H. 1990. Introduction to the proceedings of the symposium From Environment to Fish to Fisheries: A Tribute to F.E.J. Fry. Trans. Am. Fish. Soc. **119**: 567–570.

Evans, D.O., and Willox, C.C. 1991. Loss of exploited, indigenous populations of lake trout, *Salvelinus namaycush*, by stocking of non-native stocks. Can. J. Fish. Aquat. Sci. **48**(Suppl. 1): 134–147.

Evans, D.O., Casselman, J.M., and Willox, C.C. 1991. Effects of exploitation, loss of nursery habitat, and stocking on the dynamics and productivity of lake trout populations in Ontario lakes. Lake trout synthesis. Ontario Ministry of Natural Resources, Toronto, Ont.

Evans, D.O., Nicholls, K.H., Allen, Y.C., and McMurtry, M.J. 1996. Historical land use, phosphorus loading and loss of fish habitat in Lake Simcoe, Canada. Can. J. Fish. Aquat. Sci. **53**(Suppl. 1): 194–218.

Fry, F.E.J. 1947. Effects of the environment on animal activity. Univ. Toronto Stud. Biol. Ser. **55**: 1–62.

Fry, F.E.J. 1971. The effect of environmental factors on the physiology of fish. *In* Fish physiology. Vol. VI. *Edited by* W.S. Hoar and D.J. Randall. Academic Press, New York. pp. 1–98.

Gibson, E.S., and Fry, F.E.J. 1954. The performance of the lake trout, *Salvelinus namaycush*, at various levels of temperature and oxygen pressure. Can. J. Zool. **32**: 252–260.

Graham, J.M. 1949. Some effects of temperature and oxygen pressure on the metabolism and activity of the speckled trout, *Salvelinus namaycush*. Can. J. Res. Sect. D Zool. Sci. **27**: 270–288.

Groot, C., and Wiley, W.L. 1965. Time lapse photography of an ASDIC echo-sounder PPI-scope as a technique for recording

© 2007 NRC Canada

fish movements during migration. J. Fish. Res. Board Can. **22**: 1025–1034.

Heath, A.J., Burton, D.T., and Smith, M.J. 1980. Anaerobic metabolism in fishes: environmental thresholds and time dependence. Rev. Can. Biol. **39**: 123–128.

Hendry, A.P., and Berg, O.K. 1999. Secondary sexual characteristics, energy use, senescence, and the cost of reproduction in sockeye salmon. Can. J. Zool. **77**: 1663–1675.

Hughes, G.M. 1964. Fish respiratory homeostasis. Soc. Exp. Biol. Symp. **18**: 81–107.

Hutchinson, N.J. 2002. Limnology, plumbing and planning: evaluation of nutrient-based limits to shoreline development in Precambrian Shield watersheds. *In* Handbook of water sensitive planning and design. *Edited by* R.L. France. Lewis Publishers, New York. pp. 647–680.

Hutchinson, N.J., Neary, B.P., and Dillon, P.J. 1991. Validation and use of Ontario's trophic status model in establishing development guidelines. Lake Reservoir Manag. **7**: 13–23.

Jensen, F.B., Nikinmaa, M., and Weber, R.E. 1993. Environmental perturbations of oxygen transport in teleost fishes: causes, consequences and compensations. *In* Fish ecophysiology. *Edited by* J.C. Rankin and F.B. Jensen. Fish and Fisheries Series 9. Chapman and Hall, London, U.K. pp. 161–179.

Job, S.V. 1955. The oxygen consumption of *Salvelinus namaycush*. Univ. Toronto Stud. Biol. Ser. No. 61. Publ. Ont. Fish. Res. Lab. No. 73.

Johnson, W.E., and Groot, C. 1963. Observations on the migration of young sockeye salmon (*Oncorhynchus nerka*) through a large complex lake system. J. Fish. Res. Board Can. **20**: 919–938.

Jones, D.R. 1971.The effect of hypoxia and anemia on the swimming performance of rainbow trout (*Salmo gairdneri*). J. Exp. Biol. **55**: 541–551.

Jones, D.R., and Randall, D.J. 1978. The respiratory and circulatory systems during exercise. *In* Fish physiology. Vol. VII. Locomotion. *Edited by* W.S. Hoar and D.J. Randall. Academic Press, New York. pp. 279–352.

Kutty, M.N. 1968. Influence of ambient oxygen on swimming performance of goldfish and rainbow trout. Can. J. Zool. **46**: 647–653.

Lienesch, P.W., McDonald, M.E., Hershey, A.E., O'Brien, W.J., and Bettez, N.D. 2005. Effects of a whole-lake, experimental fertilization on lake trout in an oligotrophic arctic lake. Hydrobiologia, **548**: 51–66.

Lindsey, C.C. 1964. Problems in the zoogeography of the lake trout, *Salvelinus namaycush*. J. Fish. Res. Board Can. **21**: 977–994.

Lindstedt, S.L., and Jones, J.H. 1987. Symmorphosis: the concept of optimal design. *In* New directions in ecological physiology. *Edited by* M.E. Feder, A.F. Bennett, W.W. Burggren, and R.B. Huey. Cambridge University Press, Cambridge, U.K. pp. 109–289.

Magnuson, J.J., Meisner, J.D., and Hill, D.K. 1990. Potential change in thermal habitat of Great Lakes fish after global climate warming. Trans. Am. Fish. Soc. **119**: 254–264.

Magnuson, J.J., Webster, K.E., Assel, R.A., Bowser, C.J., Dillon, P.J., Eaton, J.G., Evans, H.E., Fee, E.J., Hall, R.I., Mortsch, L.R., Schindler, D.W., and Quinn, N.F.H. 1997. Potential effects of climate changes on aquatic systems: Laurentian Great Lakes and Precambrian Shield region. Hydrol. Process. **11**: 828–871.

Martin, N.V., and Olver, C.H. 1980. The lake charr, *Salvelinus namaycush*. *In* Charrs: salmonid fishes of the genus *Salvelinus*. *Edited by* E.K. Balon. Dr. W. Junk bv Publishers, The Hague, Netherlands.

McCauley, R.W., and Tait, J.S. 1970. Preferred temperature of yearling lake trout, *Salvelinus namaycush*. J. Fish. Res. Board Can. **27**: 1729–1733.

Minns, C.K. 1997. Quantifying "no net loss" of productivity of fish habitats. Can. J. Fish. Aquat. Sci. **54**: 2463–2473.

Molot, L.A., and Dillon, P.J. 1991. Nitrogen/phosphorus ratios and the prediction of chlorophyll in phosphorus-limited lakes in central Ontario. Can. J. Fish. Aquat. Sci. **48**: 140–145.

Molot, L.A., Dillon, P.J., Clark, B.J., and Neary, B.P. 1992. Predicting end-of-summer oxygen profiles in stratified lakes. Can. J. Fish. Aquat. Sci. **49**: 2363–2372.

Paterson, A.M., Dillon, P.J., Hutchinson, M.N., Futter, M.N., Clark, B.J., Mills, R.B., Reid, R.A., and Scheider, W.A. 2006. A review of the components, coefficients and technical assumptions of Ontario's Lakeshore capacity Model. Lake Reservoir Manag. **22**: 7–18.

Pazzia, I., Trudel, M., Ridgway, M., and Rasmussen, J.B. 2002. Influence of food web structure on the growth and bioenergetics of lake trout (*Salvelinus namaycush*). Can. J. Fish. Aquat. Sci. **59**: 1593–1605.

Peterson, R.H., and Anderson, J.M. 1969. Influence of spontaneous locomotory activity and oxygen consumption of Atlantic salmon, *Salmo salar*, acclimated to two temperatures. J. Fish. Res. Board Can. **26**: 93–109.

Priede, I.G. 1977. Natural selection for energetic efficiency and relationship between activity level and mortality. Nature (Lond.), **267**: 610–611.

Priede, I.G. 1985. Metabolic scope in fishes. *In* Fish energetics: new perspectives. *Edited by* P. Tytler and P. Calow. The John Hopkins University Press, Baltimore Md. pp. 33–64.

Quinlan, R., Paterson, A.M., Smol, J.P., Douglas, M.S.V., and Clark, B.J. 2005. Comparing different methods of calculating volume-weighted hypolimnetic oxygen (VWHO) in lakes. Aquat. Sci. **67**: 97–103.

Rand, P.S., and Hinch, S.G. 1998. Swim speeds and energy use of upriver migrating sockeye salmon (*Oncorhynchus nerka*): simulating metabolic power and assessing risk of energy depletion. Can. J. Fish. Aquat. Sci. **55**: 1832–1841.

Rennie, M.D., Collins, N.C., Shuter, B.J., Rajotte, J.W., and Couture, P. 2005. A comparison of methods for estimating activity costs of wild fish populations: more active fish observed to grow slower. Can. J. Fish. Aquat. Sci. **62**: 767–780.

Ricker, W.E. 1975. Computation and interpretation of biological statistics of fish populations. Bull. Fish. Res. Board Can. No. 191.

Rottiers, D.V. 1980. Energy budget for yearling lake trout. Admin. Rep. No. 80-11. U.S. Fish Wildl. Serv. GLFL/AR-80-11.

Rottiers, D.V. 1993. Energy budget for yearling lake trout, *Salvelinus namaycush*. J. Freshw. Ecol. **8**: 319–327.

Rowan, D.J., and Rasmussen, J.B. 1996. Measuring the bioenergetic cost of fish activity in situ using a globally dispersed radiotracer (^{137}Cs). Can. J. Fish. Aquat. Sci. **53**: 734–745.

Ryan, P.A., and Marshall, T.R. 1994. A niche definition for lake trout (*Salvelinus namaycush*) and its use to identify populations at risk. Can. J. Fish. Aquat. Sci. **51**: 2513–2519.

Saunders, R.L. 1962. The irrigation of the gills in fishes. II. Efficiency of oxygen uptake in relation to respiratory flow, activity and concentration of oxygen and carbon dioxide. Can. J. Zool. **40**: 817–862.

Schindler, D.W. 1998. A dim future for boreal waters and landscapes: cumulative effects of climatic warming, stratospheric ozone depletion, acid precipitation and other human activities. Bioscience, **48**: 157–164.

Schindler, D.W., and Gunn, J.M. 2004. Dissolved organic carbon as a controlling variable in lake trout and other Boreal Shield lakes. *In* Lake trout, the Boreal Shield, and factors that shape lake trout ecosystems. *Edited by* J.M. Gunn, R.J. Steedman, and R.A. Ryder. Lewis Publishers, New York. pp. 133–145.

© 2007 NRC Canada

Schindler, D.W., Armstrong, F.A.J., Holmgren, S.K., and Brunskill, G.J. 1971. Eutrophication of Lake 227, Experimental Lakes Area, northwestern Ontario, by addition of phosphate and nitrate. J. Fish. Res. Board Can. **28**: 1763–1782.

Sellers, T.J., Parker, B.R., Schindler, D.W., and Tonn, W.M. 1998. Pelagic distribution of lake trout (*Salvelinus namaycush*) in small Canadian Shield lakes with respect to temperature, dissolved oxygen, and light. Can. J. Fish. Aquat. Sci. **55**: 170–179.

Sheppard, M.P. 1955. Resistance and tolerance of young speckled trout (*Salvelinus fontinalis*) to oxygen lack, with special reference to low oxygen acclimation. J. Fish. Res. Board Can. **12**: 387–446.

Shuter, B.J., Jones, M.L., Korver, R.M., and Lester, N.P. 1998. A general, life history based model for regional management of fish stocks: the inland lake trout (*Salvelinus namaycush*) fisheries of Ontario. Can. J. Fish. Aquat. Sci. **55**: 2161–2177.

Shuter, B.S., and Lester, N.P. 2004. Climate change and sustainable lake trout exploitation: predictions from a regional life history model. *In* Boreal Shield waters: lake ecosystems in a changing environment. *Edited by* J.M. Gunn, R.J. Steedman, and R.A. Ryder. Lewis Publishers, New York. pp. 281–291.

Sly, P.G., and Evans, D.O. 1996. Suitability of habitat for spawning lake trout. J. Aquat. Ecosyst. Health, **5**: 153–175.

Smit, H. 1965. Some experiments on the oxygen consumption of goldfish (*Carassius auratus* L.) in relation to swimming speed. Can. J. Zool. **43**: 623–633.

Spoor, W.A. 1990. Distribution of fingerling brook trout, *Salvelinus fontinalis* (Mitchill), in dissolved oxygen concentration gradients. J. Fish Biol. **36**: 363–373.

Steedman, R.J., Allan, C.J., France, R.L., and Kushneriuk, R.S. 2004. Land, water, and human activities on Boreal watersheds. *In* Boreal Shield waters: lake ecosystems in a changing environment. *Edited by* J.M. Gunn, R.J. Steedman, and R.A. Ryder. Lewis Publishers, New York. pp. 59–85.

Stefan, H.F., Fang, X., and Eaton, J.F. 2001. Simulated fish habitat changes in North American lakes in response to projected climate warming. Trans. Am. Fish. Soc. **130**: 459–477.

Stewart, D.J., Weininger, D., Rottiers, D.V., and Edsall, T.A. 1983. An energetics model for lake trout, *Salvelinus namaycush*: application to the Lake Michigan population. Can. J. Fish. Aquat. Sci. **40**: 681–698.

Webb, P.W. 1997. Swimming. *In* The physiology of fishes. *Edited by* D.H. Evans. CRC Press, New York. pp. 3–24.

© 2007 NRC Canada

Multifrequency backscattering properties of Atlantic herring (*Clupea harengus*) and Norway pout (*Trisopterus esmarkii*)

Sascha M.M. Fässler, Rita Santos, Norma García-Núñez, and Paul G. Fernandes

Abstract: The multifrequency backscattering characteristics of echotraces of Atlantic herring (*Clupea harengus*) and Norway pout (*Trisopterus esmarkii*) are described. These fish cohabit similar areas of the North Sea in summer and echotraces of their schools are difficult to distinguish. Mean volume backscattering strengths at 18, 38, 120, and 200 kHz were taken from the International North Sea Herring Acoustic Surveys along with coincident pelagic trawl samples. The results indicate that echotraces of these fish species cannot be distinguished on the basis of differences in backscattering at discrete frequencies typically used in fish surveys and on fishing vessels. However, some discrimination between herring size-classes was evident. The empirical data for herring were then compared with a backscattering model for herring combining fish flesh, the swimbladder, and the effect of increased pressure at depth. Both the empirical data and model data indicate that, compared with large herring, progressively smaller herring generally have higher backscattering at the lowest frequency (18 kHz), although variability was high. According to the model, this frequency-specific signature is due to the progressively more significant contribution made by the fish body compared with the swimbladder, as the latter diminishes owing to an increase in ambient pressure in deeper water.

Résumé : Nous décrivons les caractéristiques de rétrodiffusion à fréquences multiples des échotraces du hareng atlantique (*Clupea harengus*) et du tacaud norvégien (*Trisopterus esmarkii*). Ces poissons cohabitent dans des régions semblables de la mer du Nord en été et les échotraces de leurs bancs sont difficiles à distinguer. Nous avons tiré les forces moyennes des volumes de rétrodiffusion à 18, 38, 120 et 200 kHz des Inventaires acoustiques internationaux des harengs de la mer du Nord ainsi que d'échantillons simultanés au chalut pélagique. Les résultats indiquent que les échotraces de ces espèces de poissons ne peuvent se distinguer à partir de différences de rétrodiffusion aux fréquences discrètes généralement utilisées dans les inventaires de poissons et sur les navires de pêche. Néanmoins, il y a une certaine discrimination évidente entre les classes de taille des harengs. Nous avons ensuite comparé les données empiriques sur le hareng avec un modèle de rétrodiffusion pour le hareng qui tient compte de la chair des poissons, de la vessie natatoire et de l'effet de l'accroissement de la pression en fonction de la profondeur. Tant les données empiriques que les données de la modélisation indiquent que, par comparaison aux harengs de grande taille, les harengs progressivement plus petits produisent une rétrodiffusion de plus en plus forte à la fréquence la plus basse (18 Hz), bien que la variabilité soit élevée. D'après le modèle, cette signature spécifique à la fréquence s'explique par la contribution progressivement plus importante du corps du poisson par rapport à la vessie natatoire, puisque cette dernière diminue en volume à cause de l'augmentation de la pression ambiante dans les eaux plus profondes.

[Traduit par la Rédaction]

Introduction

Acoustic techniques are important in many surveys aiming to determine the abundance and distribution of fish and other marine resources (Simmonds and MacLennan 2005). This is especially true for abundant pelagic species such as Atlantic herring (*Clupea harengus*), which usually form large schools in midwater and can be detected effectively by echosounders, providing information that is vital to stock assessments (Simmonds 2003). As a means to estimate abundance, acoustic surveys are an efficient tool because they offer almost continuous detection of objects in the whole water column at a very high resolution (typically 20 cm in the vertical) over large distances. This has distinct advantages over point sampling techniques such as trawls. However, the objects detected still require identification and this

Received 17 February 2006. Accepted 16 November 2006. Published on the NRC Research Press Web site at http://cjfas.nrc.ca on 7 March 2007.
J19179

S.M.M. Fässler[1] and P.G. Fernandes. FRS Marine Laboratory, P.O. Box 101, 375 Victoria Road, Torry, Aberdeen, AB11 9DB, Scotland, UK.
R. Santos. Fundação para a Ciência e a Tecnologia (FCT), Avenida Dom Carlos I, 126, 2° andar, 1249-074, Lisboa, Portugal.
N. García-Núñez. Departamento de Acuerdos Globales, La Secretaría de Medio Ambiente y Recursos Naturales, Mexico City, Mexico.

[1]Corresponding author (e-mail: s.faessler@marlab.ac.uk).

 doi:10.1139/F07-013 © 2007 NRC Canada

verification is usually carried out by what McClatchie et al. (2000) termed "ground truthing" using other sampling devices such as trawls.

Acoustic data are visualized as two-dimensional slices of the water column known as echograms. Individual fish schools are detected as echotraces and these provide a variety of descriptive features. A number of studies have considered echotrace classification (see Reid (2000) for a review). Coetzee (2000) used a shoal analysis and estimation system (SHAPES) to characterize sardine schools. Lawson et al. (2001) combined the SHAPES system with discriminant function analysis to classify and assign morphometric attributes of fish schools, such as school height, depth, or width, which differed between schools of different species. Although these methods can obtain a classification success of up to 96% in monospecific situations, it is generally thought that the information available at a single frequency is rarely sufficient to deal with more complex situations (MacLennan and Holliday 1996). The use of more than one frequency in an acoustic survey can give more acoustic information, which may improve the accuracy of the scrutinizing process, especially if the acoustic properties of individual species vary with the frequency in use (Madureira et al. 1993). Such techniques have been used to discriminate between groups of fish, micronekton, and zooplankton and also for discrimination between biological targets and physical phenomena such as bubbles (see Horne 2000). Korneliussen and Ona (2002) used multifrequency processing techniques to distinguish various targets such as mackerel, swimbladdered fish, and zooplankton. A similar approach was used by Kloser et al. (2002) to identify and distinguish three dominant deep-sea fish groups. The difference in mean volume backscattering strength between frequencies was described by Kang et al. (2002) as one of the most promising methods for acoustic species identification. If nothing else, the technique has been recommended for not being as subjective as visual classification (Watkins and Brierley 2002).

Despite these advances, the practice in acoustic surveys with regard to target identification is still based on visual interpretation or scrutiny (Reid et al. 1998) aided by trawling (McClatchie et al. 2000). The International North Sea Herring Acoustic Survey is one such example (Bailey et al. 1998). The northwest component of this survey, which accounts for over 90% of the adult biomass (International Council for the Exploration of the Sea 2004), encounters few major identification problems. One problem that is encountered is distinguishing echotraces of herring schools from those of Norway pout (*Trisopterus esmarkii*). These fish have similar acoustic properties based on the fact that their physiology and behaviour are also quite similar. Both species occur close to the seabed in densely packed schools, which are similar in shape and size. In addition, both species possess swimbladders. Nevertheless, the nature of their swimbladder is essentially different, since Norway pout are physoclists and herring are physostomes.

In recent years, multifrequency data have been collected during these surveys. The aim of this paper is to compare the multifrequency backscattering properties of echotraces from herring and Norway pout schools in the North Sea. Significant effort was applied to ensure that the data were comparable between frequencies. Echotraces of both species were divided according to fish size-class to compare backscattering levels. The results were compared with a numerical model of whole-fish backscatter. Many of the previous studies that have modelled backscatter from swimbladdered fish have been restricted to a model that considers only the swimbladder (Love 1978; McClatchie et al. 1996; Kloser et al. 2002). This was primarily due to the perception that the backscatter was dominated by the swimbladder component. More recent attempts were aimed at combining the swimbladder and fish body, such as the model used by Gorska and Ona (2003*a*, 2003*b*) for herring and the more elaborate Kirchhoff-ray mode (KRM) approach for a variety of fish species (Clay and Horne 1994; Jech et al. 2000; Gauthier and Horne 2004*b*).

The goal of the current work was to determine the different backscattering properties at the frequencies commonly used in fisheries acoustics and establish if the two species could be distinguished on the basis of their backscattering profiles. We also attempted to understand these properties with reference to a comprehensive backscattering model that not only included the fish flesh and swimbladder but also considered the realistic shapes of each and the effect of increased pressure (depth). Ultimately, this information could be used to differentiate echotraces of the two species, or of the size-classes of the two species, using frequencies that are commonly deployed on fisheries research vessels and commercial fishing boats.

Materials and methods

Data collection

Data were taken from the Scottish component of the International North Sea Herring Acoustic Survey in the summers of 2000, 2001, and 2002 carried out on the Fisheries Research Vessel *Scotia*. The Fisheries Research Vessel *Scotia* is responsible for the northwestern part of the area, which covers International Council for the Exploration of the Sea Division IVa. Further details of survey procedures can be found in individual survey reports (e.g., International Council for the Exploration of the Sea 2004).

Acoustic data were collected using a Simrad EK500 scientific echosounder (Bodholt et al. 1989) operating three transducers at frequencies of 38, 120, and 200 kHz and a Simrad EA500 echosounder operating at 18 kHz. The EA500 was adapted to use EK500 software by replacing firmware on the signal and main processor boards in consultation with the manufacturer. Transducers connected to the EK500 were located adjacent to one another (within 0.5 m) on the drop-keel of the vessel and were deployed approximately 3 m below the hull. The 18 kHz transducer was hull-mounted just over 5 m directly forward of the other transducers. The echosounders were configured to ping simultaneously at each frequency every second with pulse lengths of 0.7, 1.0, 1.0, and 0.6 ms at 18, 38, 120, and 200 kHz, respectively. The performance of both echosounders was monitored using similar standard target calibration techniques (Fernandes and Simmonds 1996). Acoustic data were collected from 0300 to 2300.

Data were logged from the echosounder to a personal computer with SonarData's Echolog software (SonarData Pty Ltd., G.P.O. Box 1387 Hobart, Tasmania, Australia). The

© 2007 NRC Canada

raw data were collected as echogram (Q) telegrams consisting of time-stamped digitized mean volume backscattering strengths ($\hat{S}_v$). Each pixel on the echogram therefore corresponds to a volume backscattering strength (S_v, dB re 1 m^{-1}). Other telegrams collected include detected seabed depth and geographic location (latitude and longitude).

Major echotrace concentrations were sampled with a pelagic trawl with a net of 20 mm mesh in the cod-end. When trawling at a speed of approximately 4 kn, the trawl's vertical opening was 12 m and the horizontal opening was 20 m. Trawl data provided information on catch composition in numbers, latitude and longitude, and time of start and end of the haul as well as other parameters such as trawl depth and a description of the fished echotraces. Data from a total of 124 trawl hauls were examined from the three surveys: 34 trawl hauls were composed exclusively of Atlantic herring and two trawls exclusively of Norway pout. These numbers, particularly the latter, were quite small, so other trawl hauls that contained a mixture of these and other species were used: trawl hauls that comprised >85% of Norway pout numbers in the catch and >90% of herring numbers were considered as comprising that species. This resulted in the sample sizes given in Table 1.

Acoustic data analysis and corrections

SonarData Echoview was used for the analysis of the echosounder data. Using the positional information from the trawl haul, polygons were constructed to delimit the areas on the echograms sampled by the trawl: these sample polygons were designated as "sampols". Echoview's school module, based on Barange's (1994) SHAPES algorithm, was then used to detect schools and make measurements of school descriptors. Only the "identified" echotraces contained inside the sampols were considered. These detected and identified echotraces were then divided into two categories according to the species caught: herring and Norway pout.

The characteristics of the 18 kHz transducer (specifically its 11° beam) and, more significantly, its position on the hull of the vessel 5 m ahead of the other transducers required positional corrections so that data from the four frequencies were comparable. The general philosophy adopted was to attempt to align isolated distinctive echotraces in the two data sets (hereafter referred to as EA data for the 18 kHz frequency and EK data for the 38, 120, and 200 kHz frequencies).

A vertical offset of approximately 3 m was applied to the EA data in order to match the vertical position of echotraces. The seabed on the EA data was then adjusted to be equivalent to that detected by the 38 kHz frequency in the EK data. In some cases, the border that defined the detected echotrace on the EK data did not match with a whole ping on the EA data. This was presumably due to a drift in clock times between the two systems. Echoview's Match Ping Time operator was applied to correct this. This operator selects pings from the first operand in such a way as to match the times of the pings in the second operand. The EA data echotraces had an additional horizontal displacement compared with the EK data (owing to the alongship displacement and occasional significant time mismatches). Echoview's Ping Time Shift operator was applied, shifting the time on each ping to the time of either the prior or the following ping. The procedure was repeated until the position of the echotrace on the EA data matched the position of the equivalent echotrace on the EK data.

To account for the different beamwidths in the two systems, two types of corrections were attempted, which resulted in two separate sets of data. (*i*) School parameters were corrected using Echoview's echotrace statistics, which applies a beam angle correction algorithm according to Diner (2001). (*ii*) A different type of correction used image analysis techniques to isolate the "kernel" of the school as recommended by Korneliussen et al. (2004). This was done by applying an erosion filter (Reid and Simmonds 1993) to replace each data point with the minimum value of the data points in the surrounding cells. Effectively, this erosion process reduced all echotrace boundaries by one pixel. Schools were then redetected on the eroded data and the new "eroded" borders were used to create an alternative data set (see Fig. 1 for details).

Backscattering levels

Energetic parameters of the detected echotraces from the herring and Norway pout categories (Table 1) were extracted in linear units (i.e., mean volume backscattering coefficients $\hat{s}_v$, m^{-1}) using Echoview's export facility. The $\hat{s}_v$ were then transformed into the log measure (i.e., mean volume backscattering strength $\hat{S}_v$ (=10 $\log_{10}[\hat{s}_v]$), dB re 1 m^{-1}). Backscatter levels at the four frequencies were compared by examining $\hat{S}_v$ of the beam angle corrected echotraces (hereafter referred to as "corrected $\hat{S}_v$") and the $\hat{S}_v$ of the eroded echotraces (hereafter referred to as "eroded $\hat{S}_v$") of both species. Differences between the mean values of these variables at each frequency were tested for both species using a Mann–Whitney test (Zar 1984).

The frequency-specific characteristics of each echotrace were then compared using two measures, the dB difference ΔdB and the frequency response $r(f)$ (Korneliussen and Ona 2003):

$$(1) \qquad \Delta\text{dB} = \hat{S}_v(f) - \hat{S}_v(38)$$

$$(2) \qquad r(f) = \hat{s}_v(f) / \hat{s}_v(38)$$

where $\hat{S}_v(f)$ is the mean volume backscattering strength of the echotrace at a frequency (f) and $\hat{s}_v(f)$ is the mean volume backscattering coefficient of the echotrace at a frequency (f). These measures are actually equivalent, since $S_v = 10 \log_{10}(s_v)$ (MacLennan et al. 2002) such that $r(f) = 10^{\Delta dB/10}$. Naturally, comparative backscattering profiles using one or the other can look quite different according to the scales used.

Size-classes

The frequency-specific backscattering levels of both species were also considered for different size-classes of fish. Based on the mean length of fish in each haul, echotrace data were collated into groups corresponding to fish in 5 cm size-classes ranging from the smallest size-class of 5–10 cm to the largest of 30–35 cm. Similar to the species-specific backscattering levels, both the corrected $\hat{S}_v$ and the eroded $\hat{S}_v$ data were examined for the echotraces corresponding to the different size-classes of both species. Likewise, frequency-

© 2007 NRC Canada

Table 1. Number of echotraces used for the analyses of eroded and noneroded Atlantic herring and Norway pout echotraces as indicated with a breakdown of numbers by size (length-class).

	Length-class (cm):						
Echotrace	5–10	10–15	15–20	20–25	25–30	30–35	Σn
Atlantic herring	—	—	31	112	526	35	704
Atlantic herring eroded	—	—	13	47	226	13	299
Norway pout	31	25	6	—	—	—	62
Norway pout eroded	18	7	4	—	—	—	29

Fig. 1. Processing steps to produce eroded echotraces that define the "kernel" of the school. (*a*) Original echotraces of two fish schools; (*b*) same fish echotraces after applying a 3 × 3 erosion shown inside the borders of the original detected echotraces; (*c*) eroded schools with new detected borders; (*d*) original echotraces with borders of the eroded kernel shown. Broken lines indicate how the borders of the echotraces line up ping to ping. Note that the erosion only redefines the borders of the schools to define a kernel: the actual S_v values used are in this inner "Eroded herring" kernel area of Fig. 1*d*, which are the same as the equivalent pixels in Fig. 1*a*.

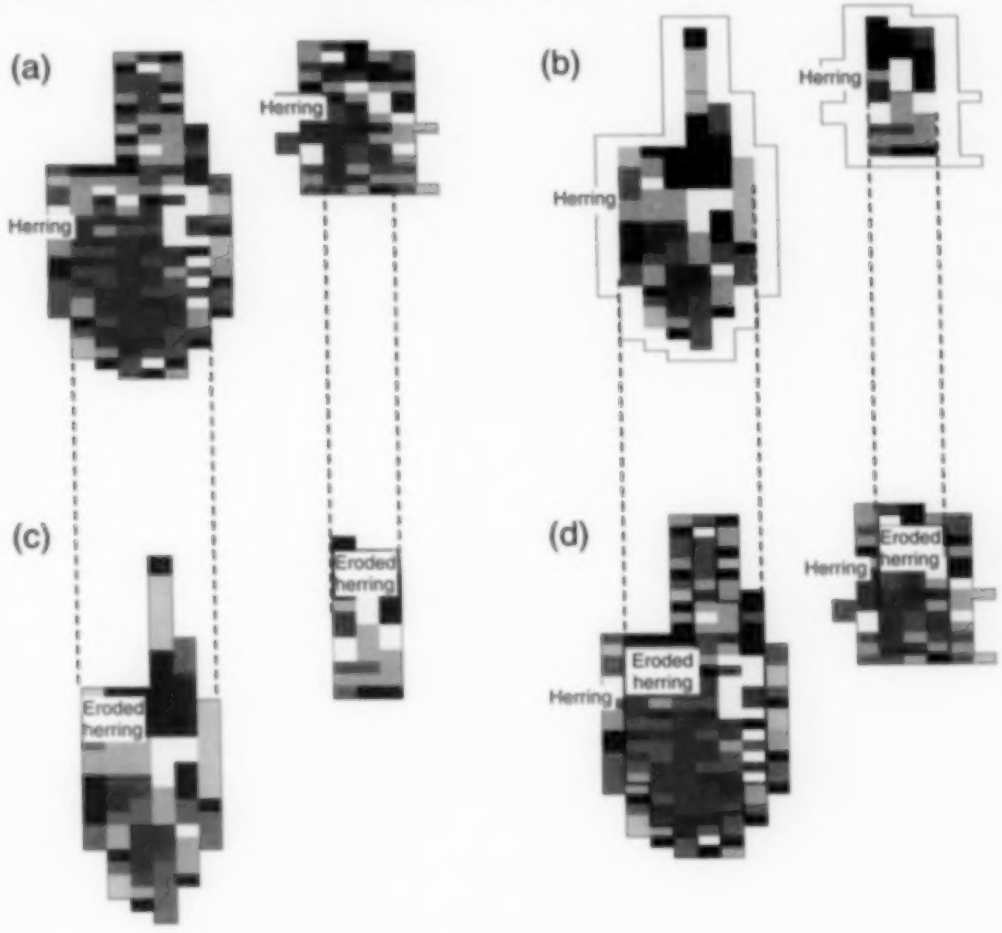

specific characteristics were compared using ΔdB and *r*(*f*) (see eqs. 1 and 2).

Herring backscattering model

A backscattering model for swimbladdered fish was developed to help explain the results from examination of the empirical size-class data. The output of the model was the backscattering cross section (σ_{bs}, m^2) for an individual fish, which was converted to target strength (TS, dB re 1 m^2) according to MacLennan et al. (2002) as

$$(3) \qquad TS = 10 \log_{10}(\sigma_{bs})$$

The *r*(*f*) and ΔdB were calculated from σ_{bs} using eqs. 1 and 2 (replacing $\hat{s}_v$ with σ_{bs} and $\hat{S}_v$ with TS).

© 2007 NRC Canada

The model consisted of three separate components that were combined to give a total for the whole-fish backscatter: a low-frequency model for the swimbladder at 18 and 38 kHz, a high-frequency model for the swimbladder at 120 and 200 kHz, and one model for the fish body over the entire frequency range. The total backscattering cross section was then expressed according to Gorska and Ona (2003*b*) by

$$\sigma_{bs}^{f} = \sigma_{bs}^{sb}(z) + \sigma_{bs}^{b} \quad (4)$$

where σ_{bs}^{f} is the backscatter of the whole fish and σ_{bs}^{sb} and σ_{bs}^{b} denote the backscattering cross section of the swimbladder at a depth z (m) and of the fish body, respectively.

The low frequency swimbladder component was based on a gas-filled prolate spheroid model modified from Kloser et al. (2002). This model was first developed for spheres by Andreeva (1964) and was later adapted for prolate spheroids by Weston (1967) before being applied by Holliday (1972) for swimbladders in schooling pelagic fish. It was then used, with slight changes in notations, by Ye (1997) and then by Kloser et al. (2002) to model backscatter from dominant deepwater fish species. Backscattering by the swimbladder, where normal dorsal incidence was assumed, was

$$\sigma_{bs}^{sb}(z) = a_{es}^{2}(z)\left\{\left[\left(\frac{f_p}{f}\right)^2 - 1\right]^2 + \frac{1}{Q^2}\right\}^{-1} \quad (5)$$

where f_p represents the prolate resonant frequency, f describes the incident acoustic frequency, Q is the resonant quality factor, and $a_{es}(z)$ is the radius of an equivalent sphere at a depth z whose volume is the same as that of the swimbladder. This volume is depth dependent, as it was assumed that the swimbladder volume decreases with increasing ambient pressure (Ona 1990; Nero et al. 2004). Parameter $a_{es}(z)$ was defined by

$$a_{es}(z) = \sqrt{\frac{3}{4\pi}V(z)} \quad (6)$$

where

$$V(z) = \frac{P(0)V(0)}{P(z)} \quad (7)$$

The gas-filled swimbladder was therefore assumed to compress below the sea surface according to Boyle's Law where $P(0)V(0) = P(z)V(z)$ (Boyle 1662). Ambient pressure was calculated according to

$$P = (1 + 0.103z) \times 10^5 \quad (8)$$

The volume of the swimbladder at the surface, $V(0)$, is a function of fish weight and ultimately fish size. The conversion from herring length to weight is given by $W = 0.0033 \times L^{3.3078}$, where W is the fish weight (g) and L is the fish length (cm). This was based on the lengths and weights of 3290 herring caught during the 2002 North Sea acoustic survey. According to Brawn (1969), fish density for surface herring was assumed to be 1.026 g·cm^{-3}. Herring swimbladder volume was assumed to be 5% of the total fish volume at the surface. This represents the upper limit as suggested by Ona (1990) and is considered a general value for marine fish according to MacLennan and Simmonds (1992). However, according to Nero et al. (2004), herring are naturally positively buoyant at the sea surface and therefore contain up to three times greater a volume of gas than neutrally buoyant fish. Consequently, $V(0) = 0.15 \times W/1.026$. Parameter f_p is a function of the spherical resonant frequency f_0 and the prolate spheroid roundness e at an ambient hydrostatic pressure P:

$$f_p = f_0\, 2^{\frac{1}{2}} e^{-\frac{1}{3}}(1-e^2)^{\frac{1}{4}}\left\{\ln\left[\frac{1+(1-e^2)^{\frac{1}{2}}}{1-(1-e^2)^{\frac{1}{2}}}\right]\right\}^{-\frac{1}{2}} \quad (9)$$

The swimbladder was assumed to be 0.26 times the total length of the fish (Gorska and Ona 2003*a*). Parameter e describes the prolate spheroid roundness and is the ratio of the minor axis a_{ps} to the major axis b_{ps} of the spheroid. Parameter b_{ps} is the swimbladder length and a_{ps} can be calculated using the volume (V) equation for a prolate spheroid, where $a_{ps} = \sqrt{(6 \times V/b_{ps} \times \pi)}$. The major modifications applied to the model in this paper are concerned with depth-dependent contraction rates of the swimbladder dimensions according to Gorska and Ona (2003*a*). The axes are assumed to contract with depth at different rates:

$$a(z) = a(0)(1 + z/10)^{-\alpha} \quad (10)$$

$$b(z) = b(0)(1 + z/10)^{-\beta} \quad (11)$$

Boyle's Law requires that the different contraction rates behave according to $2\alpha + \beta = 1$. Gorska and Ona's (2003*a*) intermediate contraction rates (case *ii*) were used, where $\alpha = 2/5$ and $\beta = 1/5$. This results in the contraction of swimbladder length being relatively small compared with that of its width or height. Gorska and Ona (2003*a*) found that for any case where $0 < \beta < \alpha$, model values were similar to empirical measurements of swimbladder contraction.

The spherical resonant frequency was calculated according to Holliday (1972) as

$$f_0 = \frac{1}{2\pi a_{es}}\left(\frac{3\gamma P + 4\mu_1}{\rho}\right)^{\frac{1}{2}} \quad (12)$$

where ρ is the fish tissue density and γ is the ratio of specific heats for the swimbladder gas. To make the model specifically applicable to herring, constants were taken from studies on herring by Brawn (1969) and other similar pelagic species such as northern anchovy (*Engraulis mordax*) (Holliday 1972). The following values were used: $\mu_1 = 10^5$ Pa, $\gamma = 1.4$, $\rho = 1071$ kg·m^{-3}, and $Q = 5$. For the depth z, the mean depth of the echotraces in each size-class was taken (15–20 cm = 84 m, 20–25 cm = 112 m, 25–30 cm = 131 m, and 30–35 cm = 162 m).

To account for the directivity-dependent tilt angle distribution, a directivity pattern $D_{sb}(\theta,z)$ (Medwin and Clay 1998) was determined and applied to the backscattering length (square root of the backscattering cross section) of the swimbladder as

© 2007 NRC Canada

$$\sigma_{bs}^{sb}(\theta, z) = \left(D_{sb}(\theta, z) \sqrt{\sigma_{bs}^{sb}(90^\circ)} \right)^2 \quad (13)$$

$$D_{sb}(\theta, z) = \frac{\sin^2[kh_{ps}(z)\sin(\theta + \Delta\theta)]}{[kh_{ps}(z)\sin(\theta + \Delta\theta)]^2} \cos(\theta + \Delta\theta) \quad (14)$$

where θ refers to the fish tilt angle, $\Delta\theta$ is the offset of the swimbladder axis relative to the body axis, which was found to be 5.6°, k is the wave number ($k = 2\pi f/c$), and $b_{ps}(z)$ is the depth-dependent length of the prolate spheroid.

The high-frequency component (120 and 200 kHz) of the swimbladder model was based on the simple model developed by Love (1971) and also applied more recently by Nero et al. (2004). Complex high-frequency backscattering models for fish with swimbladders require detailed information on size and shape, which was not available in the present study. Love (1971) fitted a pair of regression lines to empirical TS measurements on various marine and freshwater fish. In the model, backscatter decreases as the ratio L/λ (fish length to wavelength) increases to about 14; for values of L/λ beyond 14, backscatter increases again: if $L/\lambda \leq 14$, then

$$\mathrm{TS} = 15.8 \log\left(\frac{L}{100}\right) + 7.5 \log(\lambda) - 22.9 \quad (15)$$

and if $L/\lambda > 14$, then

$$\mathrm{TS} = 27.5 \log\left(\frac{L}{100}\right) + 4.2 \log(\lambda) - 36.2 \quad (16)$$

where the wavelength $\lambda = c/f$ (MacLennan and Simmonds 1992) and c is the sound speed in seawater (1500 m·s^{-1}). The directivity was also applied to the high-frequency component of the model using the same parameters as for the low-frequency model.

The final component of the model was one used for the fish body over the entire frequency range. This was a distorted wave Born approximation (DWBA) fluid-filled ellipsoid model developed by Dezhang Chu (Woods Hole Oceanographic Institution, Woods Hole, MA 02543, USA, personal communication). For a plane incident wave, $p_{inc} = e^{ikr}$, where p_{inc} describes the sound pressure at a distance r from the source, backscattering by a fluid ellipsoid, whose acoustic impedance (the product of sound speed and density) is close to that of the surrounding medium, can be calculated using a DWBA. The quadratic surface of the ellipsoid in the Cartesian coordinates is

$$\frac{x^2}{a^2} + \frac{y^2}{b^2} + \frac{z^2}{c^2} = 1 \quad (17)$$

where a, b, and c are the lengths of the semi-axes. For the fish body, length $L = 2c$, width (dorsal view) $W = 2b$, and height (lateral view) $H = 2a$. In spherical coordinates, eq. 17 becomes

$$\frac{r^2 \sin^2\theta \cos^2\phi}{a^2} + \frac{r^2 \sin^2\theta \sin^2\phi}{b^2} + \frac{r^2 \cos^2\theta}{c^2} = 1 \quad (18)$$

where the azimuthal angle $\phi \in [0, 2\pi]$ and polar angle $\theta \in [0, \pi]$. A vector $\vec{\mu}$ is then defined whose x, y, and z components can be expressed by

$$\begin{cases} \mu_x = 2\sin\theta\cos\phi \\ \mu_y = 2\sin\theta\cos\phi \\ \mu_z = 2\cos\theta \end{cases} \quad (19)$$

The backscattering amplitude can be expressed as

$$f_{bs} = C_B k^2 abc \frac{j_1(k_f a \mu_\Theta)}{k_f a \mu_\Theta} \quad (20)$$

where $j_1(x)$ is the spherical Bessel function of order 1. Parameter k_f is the wave number in the fish and

$$C_B = \frac{1 - gh^2}{gh^2} - \frac{g - 1}{g} \quad (21)$$

$$\mu_\Theta = \sqrt{\mu_x^2 + \left(\frac{b}{a}\right)^2 \mu_y^2 + \left(\frac{c}{a}\right)^2 \mu_z^2} \quad (22)$$

where g and h are the density and sound speed contrasts, respectively, between the fish body and the surrounding water. According to Gorska and Ona (2003*a*), both were set to 1.04. The backscattering cross section for the fish body is then

$$\sigma_{bs}^{b} = \left| f_{bs}(\theta) \right|^2 \quad (23)$$

For a broadside backscatter of dorsal view, $\theta = \pi/2$. The model required specific relationships between the different dimensions of the ellipsoid. The ratio of fish length to half the height was 9.42. The ratio of fish length to half the width was 22.84. Values were determined from 40 measurements of North Sea herring.

The model component was evaluated as a mean value of distributions of fish length and tilt. The distributions of fish length were taken from those in the trawl data size-classes and the tilt was taken from a Gaussian distribution with a mean of –1° (0° = normal incidence) and standard deviation of 10° (Ona 2001).

Results

Species-specific backscattering levels

The results of the comparisons of backscattering levels indicate that both Atlantic herring and Norway pout have very similar trends in backscattering levels at the four frequencies studied (Fig. 2). Corrected $\hat{S}_v$ values in both species were highest at 18 kHz and lowest at 120 kHz (Fig. 2*a*). Herring had higher mean corrected $\hat{S}_v$ at all frequencies as well as the largest range of corrected $\hat{S}_v$ compared with Norway pout. However, this difference was only significant at 120 and 200 kHz (Mann–Whitney: $p < 0.05$) and not significant at 18 and 38 kHz (Mann–Whitney: $p_{18\,kHz} = 0.20$, $p_{38\,kHz} = 0.07$).

When considering the eroded echotraces, the trends according to frequency of herring and Norway pout $\hat{S}_v$ were also similar (Fig. 2*b*). However, at 18 and 200 kHz, values of herring and Norway pout were significantly different (Mann–Whitney: $p < 0.05$), with herring having lower mean values at 18 kHz and higher values at 200 kHz. Values at 38 and 120 kHz were not significantly different (Mann–Whitney: $p > 0.05$). The eroded herring echotraces exhibited

© 2007 NRC Canada

Fig. 2. Mean values of (*a*) corrected $\hat{S}_v$ and (*b*) eroded $\hat{S}_v$ echotraces. Solid symbols, Atlantic herring; open symbols, Norway pout; upright triangles, 95th percentile; inverted triangles, 5th percentile. The values for Norway pout have been shifted slightly along the *x*-axis for clarity.

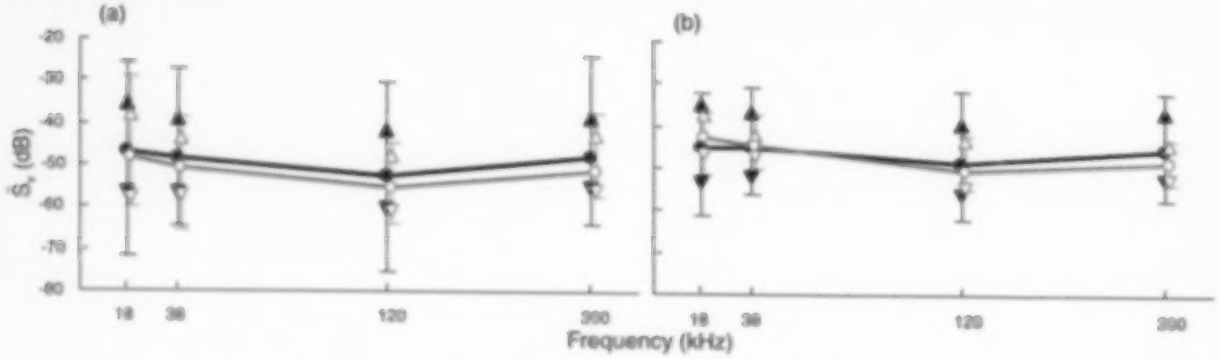

a smaller range of $\hat{S}_v$ at all frequencies compared with the range of corrected $\hat{S}_v$; those for Norway pout were similar. As the trends between corrected $\hat{S}_v$ and eroded $\hat{S}_v$ were similar regardless of subsequent analyses, further comments are restricted to the eroded data but could equally apply to corrected $\hat{S}_v$.

The decibel difference (ΔdB, eq. 1) of the mean $\hat{S}_v$ values relative to 38 kHz showed similar trends according to frequency for both species (Fig. 3*a*). Norway pout had positive values at 18 kHz and negative values at 120 and 200 kHz, whereas herring had a mean ΔdB close to 0 at 18 kHz and negative values at 120 and 200 kHz (Fig. 3*a*). The differences between the mean values at 18 and 38 kHz were +1.84 and –0.30 for Norway pout and herring, respectively. Another point to note is that, on average, herring had a ΔdB at 200 kHz that was close to 0 (–0.78), whereas the value for Norway pout was clearly negative (–4.16).

Examination of the relative frequency response (*r*(*f*), eq. 2) yielded identical patterns, as expected given that the measures are equivalent according to $r(f) = 10^{\Delta dB/10}$. However, the presentation of this parameter is different owing to the differences in scale at which they are plotted (Fig. 3*b*). This is particularly noticeable at low values of *r*(*f*) (negative ΔdB) where the scale makes it difficult to observe any significant changes. Another presentational difference concerns the variability of the mean value, which looks higher at 18 kHz where the ΔdB difference is positive. The highest *r*(*f*) values were observed at 18 kHz compared with the three other frequencies for both species. For the other two frequencies (120 and 200 kHz), the *r*(*f*) was rather flat, close to 1, and therefore very similar to that at 38 kHz.

Size-specific backscattering levels

Given the similarity between backscattering levels of the two species and the fact that Norway pout had very small sample sizes when broken down into size-classes (Table 1), only the results of the size-specific backscattering levels for herring are reported here.

One consistent trend was apparent in the backscattering levels of the different herring size-classes: the ΔdB between 18 and 38 kHz changed according to size-class, whereas the ΔdB at 120 and 200 kHz did not (Figs. 4*a*–4*d*). Generally, values of ΔdB at 18 kHz were high (and positive) for small fish, lower for progressively larger fish, and negative for the largest size-class of fish (Figs. 4*a*–4*d*). ΔdB values at 120 kHz were smallest for every size-class. The *r*(*f*) values for the eroded echotrace data for different herring size-classes behaved in a manner analogous to the ΔdB data (Figs. 4*e*–4*h*). A decrease in *r*(*f*) at 18 kHz from the smallest to the biggest size-class was detected, whereas *r*(*f*) levels at 120 and 200 kHz remained similar.

Model predictions

The predicted TS from the herring model is given in Fig. 5. The resonant peak derived from backscattering of the swimbladder occurs at approximately 1.8 kHz for a herring in the 20–25 cm size-class. The TS then declines and levels out at about –43 dB from 10 kHz. Backscattering from the body component rises at low frequencies to a peak at about 18 kHz of approximately –40 dB and then undergoes dampened oscillations to a level of about –43 dB at 120 kHz. The TS at 18 and 38 kHz, therefore, is influenced more by the fish body component than by the swimbladder when the fish is at a depth of, for example, 112 m (Fig. 5). At higher frequencies, backscattering from the two components is similar at normal incidence. Naturally, the TS changes according to the fish size, orientation, and body shape. The values described here were derived from an average over the range of sizes encountered, but tilt angle distributions were chosen according to Ona (2001): a Gaussian distribution with a mean of –1° and standard deviation of 10°. Including the directivity pattern in the swimbladder component reduces the backscattering level significantly at frequencies beyond resonance (4 kHz).

To compare the model output with the empirical data, model values at 18, 38, 120, and 200 kHz were converted to the ΔdB and *r*(*f*) metrics used previously for each size-class. Model values followed similar trends to the eroded herring echotraces and were similar to the empirical values (Fig. 4). In common with the empirical data, model output ΔdB and *r*(*f*) at 18 kHz decreased with increasing fish size. However, there were no negative values observed at 18 kHz for the model data in the biggest size-class. For all size-classes, the closest match in frequency response occurred at 120 and 200 kHz. Model outputs at 200 kHz were usually lower than

© 2007 NRC Canada

Fig. 3. Mean values of (*a*) decibel difference and (*b*) relative frequency response for Atlantic herring (solid symbols) and Norway pout (open symbols). Upright triangles, 95th percentile; inverted triangles, 5th percentile. Both decibel difference and relative frequency response are expressed in relation to 38 kHz.

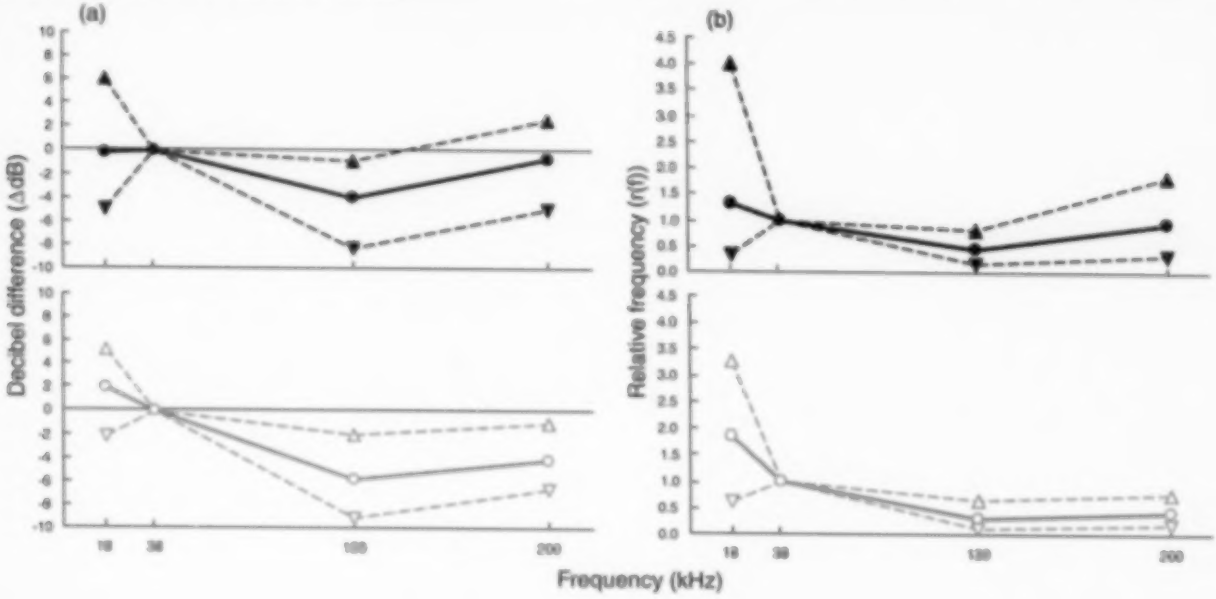

the empirical data, resulting in a rather flat response for model values at the higher frequencies (120 and 200 kHz).

Discussion

Based on energetic characteristics, Atlantic herring and Norway pout seem to have similar backscattering levels at frequencies of 18, 38, 120, and 200 kHz. This may allow these two species to be distinguishable from groups of other fish species, such as mackerel, which may be expected to have a different response at these frequencies. Korneliussen and Ona (2004) concentrated on multifrequency backscattering properties of the nonswimbladdered Atlantic mackerel (*Scomber scombrus*). They found that backscatter increased with higher frequencies for this species ($r(f)$ at 200 kHz was 4). Compared with nonswimbladdered fish, fish with swimbladders generally seem to have weaker backscatter at higher frequencies (e.g., 200 kHz) (Foote et al. 1993). Gauthier and Horne (2004*a*, 2004*b*) also found frequency-dependent differences in backscatter between swimbladdered and nonswimbladdered fish species in the Gulf of Alaska and Bering Sea. Their findings were based on KRM backscatter models. If discrimination algorithms, based on frequency-specific backscatter differences, are applied, distinction between swimbladdered fish (e.g., herring) and nonswimbladdered fish (e.g., mackerel) can be facilitated (Korneliussen and Ona 2004).

In the present study, echotraces were chosen where herring and Norway pout were believed to be the main source of backscattering based on biological samples taken with a pelagic trawl. Although Norway pout were caught in smaller numbers, and their length composition was, on average, smaller than that of herring, the echoes derived from the Norway pout schools were strong. Since there was not a big overlap in the size distribution of Norway pout and herring, it might be expected that a distinction between the two species could be obtained owing to the weaker reflecting properties of the smaller fish. Nakken and Olsen (1977) examined backscatter of different swimbladdered fish and found distinct differences between differently sized fish species at 38 and 120 kHz. Similarly, Gauthier and Horne (2004*b*) suggested potential differences in backscatter among swimbladdered forage fish species of different sizes and emphasized the importance of the specific frequency ratios used. Especially at higher frequencies (e.g., 200 kHz), the TS response becomes more variable with increasing fish length (Gauthier and Horne 2004*b*). However, the results of the present study showed that fish size alone was not a significant factor influencing the overall echo strength. Kloser et al. (2002) successfully managed to distinguish between three swimbladder-bearing fish species in deep waters using multifrequency acoustic methods. Nevertheless, the vast differences in terms of swimbladder type (e.g., one of the species studied, orange roughy (*Hoplostethus atlanticus*), has a wax ester filled swimbladder) and size of the observed species facilitated such an attempt.

Differences between $\hat{S}_v$ in herring and Norway pout may be influenced by erroneous allocation of species to the supposed ground-truthed echograms (Suuronen et al. 1997; Bethke et al. 1999; McClatchie et al. 2000). For instance, in some cases, information on the echograms might not have corresponded exactly to data on the matching trawl, by either not sampling the whole school or targeting a different school. As in every acoustic fish survey, the assumption made, that haul composition represented the echotrace composition, is uncertain. Nonetheless, during all of the North

© 2007 NRC Canada

Fig. 4. Mean values (circles) of (*a*–*d*) decibel difference and (*e*–*h*) relative frequency response with 95th percentile (upright triangles) and 5th percentile (inverted triangles) for eroded Atlantic herring echotraces. Panels correspond to different size-classes: (*a* and *e*) 15–20 cm, (*b* and *f*) 20–25 cm, (*c* and *g*) 25–30 cm, and (*d* and *h*) 30–35 cm. Both decibel difference and relative frequency response are expressed in relation to 38 kHz. The model output (diamonds) is superimposed.

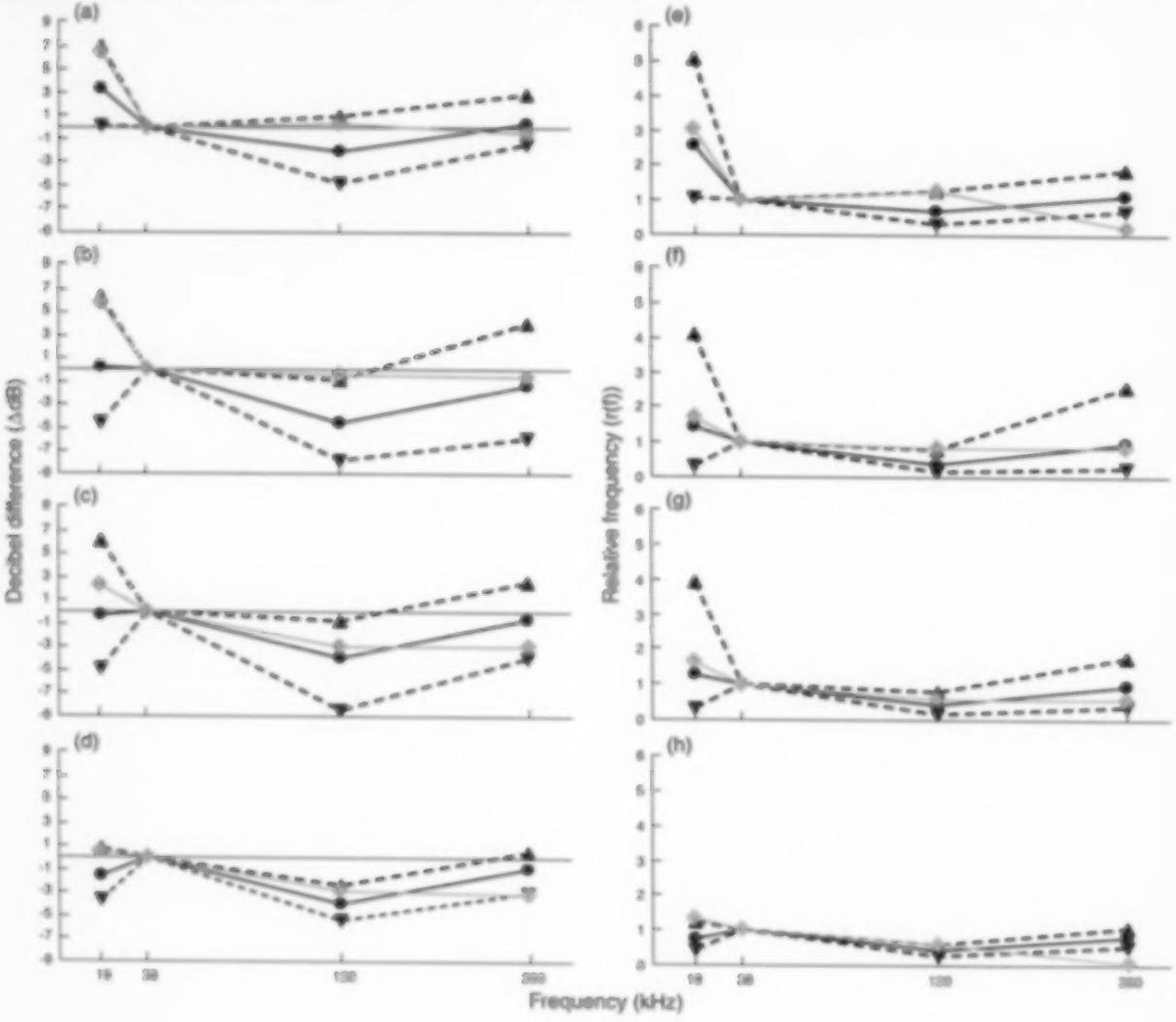

Sea herring acoustic surveys from which data were used, explicit care was taken while sampling. Trawling processes were constantly monitored using a net sonde (net-mounted echosounder displayed in real time), and echograms were compared during pretrawl and trawl phases to make sure that the correct schools were captured.

A decrease in variability of $\hat{S}_v$ between eroded and non-eroded echotraces was observed for both species at all frequencies. This is probably associated with the erosion process, which removes the smaller values at the edges of the schools and results in a much narrower range of data. The statistically significant differences in $\hat{S}_v$ values at 18 and 200 kHz between eroded Norway pout and eroded herring schools may be explained in part by the erosion process, which separates the mean values further, and in part by the amount of data, which led to small standard deviations. However, despite these differences being statistically significant, they are unlikely to be useful as a discriminator owing to the overlap that still exists. An algorithm that incorporated morphological and positional parameters, in addition to these subtle frequency differences, may, therefore, have some merit.

Nero et al. (2004) compared measured backscattering levels with values from theoretical backscattering models in herring at high (38–200 kHz) and low frequencies (1.5–5 kHz). A distinct resonant peak was observed at 2.5 kHz. At higher frequencies, backscattering values decreased, reaching a minimum level at 38 kHz for measured values

© 2007 NRC Canada

Fig. 5. Modelled predicted backscattering strength from Atlantic herring of the 20–25 cm size-class at 112 m depth. The thick solid line represents the combined model output. The swimbladder (broken line) was modelled using a prolate spheroid to represent the lower frequency range (0–40 kHz) and a simple regression model based on empirical measurements to represent the higher frequencies (40–200 kHz). The fish body model (thin solid line) was based on a DWBA fluid-filled ellipsoid backscattering model averaged, at each 1 kHz step, over 10 000 realizations of fish size (within the size-class) and tilt angle.

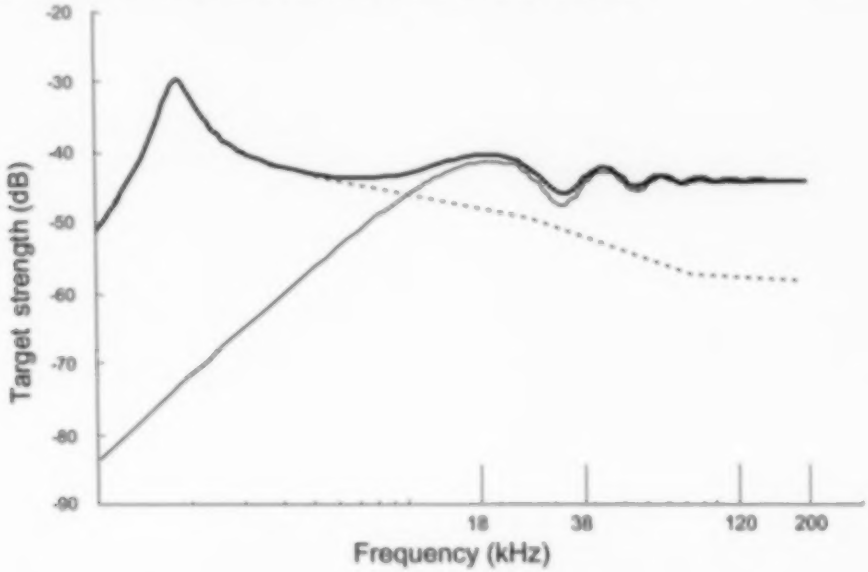

and 90 kHz for model values. In the present study, a similar trend was observed in the high-frequency domain. However, minimum values occurred at 120 kHz. From the output of the model used in the present study, backscatter from the swimbladder changes most dramatically around the resonant frequency domain. Beyond 10 kHz, it gradually flattens and is steadily decreasing at higher frequencies. The fish body component has negligible backscatter in the resonant frequency region (1–3 kHz) and only starts to have an influence on the total fish backscatter beyond 10 kHz. The dominant contributor in the resonant frequency range, independent of fish depth, is the swimbladder (Farquhar 1977). The relatively high amplitude of the resonant peak allows useful information to be derived from measurements of backscatter in that frequency region for the purposes of species identification (Nero and Huster 1996; Nero et al. 1998, 2004). However, as described by the latter authors, low operating frequencies require specialized hardware and large transducers, so their usage is rather limited. Additionally, previous studies that examined the enhanced backscatter at low frequencies found the resonance frequency also to differ with fish size, species, and depth (in the case of physostomes) (Love 1978; Feuillade and Nero 1998). Such implications might limit potential low frequency (<10 kHz) dependent species discrimination for swimbladdered fish. Furthermore, the range of frequencies used by commercial fishing vessels is similar to those examined here (12–200 kHz) and so these results will be of interest to that community.

Of the models used to date, which incorporate simple geometric shapes, the DWBA ellipsoid model is the one that most accurately reflects the shape of the herring body. Nero et al. (2004) concentrated on the resonant frequencies and therefore considered only the swimbladder component. Consequently, their model values were very low at 38 kHz. Gorska and Ona (2003*a*, 2003*b*) did consider the fish body, as well as the swimbladder, but used a prolate spheroid model for both. In contrast with the sausage-shaped prolate spheroid, the ellipsoid is a better representative of the herring's body shape because the herring body width is much smaller than its height (e.g., see Knorr 1974). Arguably, fully three-dimensional model techniques such as the KRM approximation or the boundary element method would provide more realistic outputs in terms of accuracy of fish body shapes, since they do not assume any symmetry and can therefore be applied to arbitrary shapes (Simmonds and MacLennan 2005). Nevertheless, the KRM is inaccurate at low frequencies, while the boundary element method involves many more calculations. Moreover, such models would have required precise mapping of the swimbladder surface into digital representation. Since the purpose of the model used in this paper was to explain the observed empirical data and concentrate on the body–swimbladder relationship in particular, a simpler model applying plain geometrical shapes was found to be sufficient.

Different shapes and dimensions of the fluid-filled ellipsoid were found to bring about large differences in frequency-dependent backscattering levels. The slightest change in ellipsoid dimensions resulted in the backscattering oscillating response being shifted quite dramatically in both signal strength and frequency. A general observation was, for example, that the narrower an ellipsoid was in its lateral direction (width), the higher was the modelled overall fish body backscatter. If a fluid-filled prolate spheroid model is chosen

© 2007 NRC Canada

to model the fish body (representing the fish body with equal lateral and dorsal dimensions), the results differ considerably from those of a fluid-filled ellipsoid model. Averaging the fish body model over tilt angle was found to have an amplitude-reducing effect.

Including the directivity associated with the tilt angle distribution into the swimbladder model resulted in decreasing backscattering levels with increasing frequency. The result was the fish body being the dominant contributor to the total backscatter at the observed depths. In that case, the frequency response at 18 kHz was emphasized, and therefore, it was higher than observed in the normal incidence case. Since no data were available, the tilt angle distribution was chosen as having a Gaussian distribution. Ona (2001) observed tilt angle distributions in herring having a mean of 88.9 and 86.9° (90° = normal incidence) with standard deviations of 10 and 14.2°, respectively. The former measurement was used in the current study and other authors have found similar results (Beltestad 1973). Gorska and Ona (2003*a*) did not take into account the shift of the swimbladder axis relative to the body axis in herring. However, this axis was found to be 5.6° after measuring 40 herring caught in the North Sea, and the measurement was implemented into the directivity calculation. Diurnal changes in tilt angle, as observed for Norwegian spring-spawning herring (Huse and Ona 1996), have profound implications on acoustic backscatter. Ideally, tilt angle distributions should be ascertained for the fish schools in question, as this may be affected by species, time of year, and time of day.

At 112 m depth, the model output for the fish body backscatter at 38 kHz exceeds that of the swimbladder. Herring are physostomes and the swimbladder is connected to the digestive tract by a pneumatic duct (Bone et al. 1995). There is no interior gas gland that allows the fish to inflate the swimbladder once its volume has decreased after the fish has descended (Nero et al. 2004). It is assumed, as discussed or suggested previously by various authors (Brawn 1962; Blaxter et al. 1979; Ona 1990), that herring are only able to inflate their swimbladder by "gulping" atmospheric air at the surface. This means that a herring could not increase the gas content of its swimbladder without access to the surface. The result is a decrease in swimbladder volume with depth and therefore a reduction in backscatter from this organ compared with other potentially important components (e.g., the body itself and the bone). At a certain depth, therefore, the fish body component becomes an even stronger scatterer than the swimbladder and contributes the most to the total backscatter of the fish. Owing to the oscillating feature of the body component backscatter, this was found to be strongly dependent on fish size. Gorska and Ona (2003*b*) modelled swimbladder contraction in a 32 cm herring using prolate spheroids to represent the swimbladder and fish body. They found the depth where the swimbladder and the fish body contributed equally to the total backscatter at 38 kHz to be at about 180 m.

Considering the oscillating shape of the predicted backscatter response of ellipsoid fluid-filled bodies of different sizes, responses varied considerably at certain frequencies. Smaller fish were found to have stronger backscatter at 18 kHz relative to 38 kHz compared with bigger fish. Assuming that the model is a good representation of the observed data, the gradual positional change of frequency response observed at 18 kHz relative to 38 kHz for different herring size-classes is solely due to the relative shape of the body backscatter. As for the two higher frequencies used (120 and 200 kHz), the model was primarily not thought to represent their backscattering response. Neither was it intended to explain frequency-specific backscatter at 120 and 200 kHz with the model, as the relative backscattering response at these frequencies did not change for different-sized fish. This is why a more simple model, based on empirical measurements (Love 1971), was used to at least approximate the observations at the two higher frequencies. The trend for a reduced frequency response at 18 kHz with increasing fish size does not support a potential discrimination between different herring size-classes, since the overlap was still considerable. However, the trend was most clearly marked for eroded herring data, possibly because of these data being less variable.

In conclusion, herring and Norway pout schools had similar backscattering levels at frequencies of 18, 38, 120, and 200 kHz. Backscattering was generally highest at 18 and 38 kHz and always lowest at 120 kHz for both species. Owing to this similarity, a distinction between Norway pout and herring, based solely on differences in backscattering values at the four distinct frequencies, was not possible in the data set used. Consequently, since herring and Norway pout inhabit a similar area in the northern North Sea, it will remain problematic to distinguish these two species on the basis of backscattering profiles using standard survey frequencies. A possible backscattering model for Norway pout, taking into account tilt angle, size, and physiology, such as swimbladder dimensions, may reveal potential means of discrimination.

Analyses of scattering in herring by size-class revealed a potential discrimination between small (15–20 cm) and large (30–35 cm) individuals based on differences in backscatter at 18 and 38 kHz: larger fish had progressively smaller backscattering values at 18 kHz relative to those at 38 kHz. Comparison of the backscatter data values of herring size-classes with a model insinuated similar differences at the lower frequencies used (18 and 38 kHz). This is due to the predicted backscatter curve of the body, which has an oscillating nature beyond 10 kHz. However, discrimination of herring size-classes based on this dual-frequency response is not reliable, since values are very variable and do overlap. Usage of additional frequencies in the low-frequency region (10–40 kHz) may allow for the differences to become more discrete.

An important aspect is that for the physostomous herring, backscatter from the fish body becomes more important with increasing depth. Furthermore, the model used in this study suggests that backscatter from the fish body can even exceed backscatter from the swimbladder when the fish is at depth and the swimbladder is compressed. Such findings have implications for acoustic surveys of herring or similar physostomous species where simple size-dependent TS equations are used to estimate biomass abundances. Ona (2003) argued that estimates of herring abundance would be about 50% less if the depth dependence of the TS were considered in the calculations. We postulate that precise measurements of the herring swimbladder at various depths should be incor-

© 2007 NRC Canada

porated into fully three-dimensional backscatter models using techniques such as the KRM approach or the boundary element method to reveal more precise depth-dependent TS estimates. In the meantime, the simple decibel difference approach, while useful for separating echotraces of organisms of vastly different physiology (Kang et al. 2002), falls short of being able to discriminate between echotraces of these two swimbladdered fish.

Acknowledgements

The authors would like to thank Dezhang Chu and Gareth Lawson from the Woods Hole Oceanographic Institution, Woods Hole, Massachusetts, for providing the MATLAB code for the fish body model. We are also grateful to our colleagues at the Marine Laboratory, Aberdeen, who provided assistance at various stages of the work and to the two anonymous reviewers for their comprehensive list of constructive comments. This document was made with support from the European Commission's Fifth Framework Programme (SIMFAMI project, grant No. Q5RS-2001-02054).

References

Andreeva, I.B. 1964. Scattering of sound by air bladders of fish in deep sound-scattering ocean layers. Sov. Phys. Acoust. **10**: 17–20.

Bailey, M.C., Maravelias, C.D., and Simmonds, E.J. 1998. Changes in the distribution of autumn spawning herring (*Clupea harengus* L.) derived from annual acoustic surveys during the period 1984–1996. ICES J. Mar. Sci. **55**: 545–555.

Barange, M. 1994. Acoustic identification, classification and structure of biological patchiness on the edge of the Agulhas Bank and its relationship to frontal features. S. Afr. J. Mar. Sci. **14**: 333–347.

Beltestad, A.K. 1973. Beiteadferd og vertical vandring hos 0-gruppe slid (*Clupea harengus* L.) i relasjon til lysintensitet. Fishery Biology Thesis, Norges Fiskerihøgskole, University of Bergen, Norway.

Bethke, E., Arrhenius, F., Cardinale, M., and Håkansson, N. 1999. Comparison of the selectivity of three pelagic sampling trawls in a hydroacoustic survey. Fish. Res. **44**: 15–23.

Blaxter, J.H.S., Denton, E.J., and Gray, J.A.B. 1979. The herring swimbladder as a gas reservoir for the acoustico-lateralis system. J. Mar. Biol. Assoc. U.K. **59**: 1–10.

Bodholt, H., Ness, H., and Solli, H. 1989. A new echo-sounder system. Proc. Inst. Acoust. **11**: 123–130.

Bone, Q., Marshall, N.B., and Blaxter, J.H.S. 1995. Biology of fishes. 2nd ed. Blackie, New York.

Boyle, R. 1662. New experiments physico-mechanical, touching the air: whereunto is added a defence of the author's explication of the experiments, against the objections of Franciscus Linus and Thomas Hobbes. Printed by H. Hall for T. Robinson, Oxford, UK.

Brawn, V.M. 1962. Physical properties and hydrostatic function of the swimbladder of herring (*Clupea harengus* L.). J. Fish. Res. Board Can. **19**: 635–656.

Brawn, V.M. 1969. Buoyancy of Atlantic and Pacific herring. J. Fish. Res. Board Can. **26**: 2077–2091.

Clay, C.S., and Horne, J.K. 1994. Acoustic models of fish: the Atlantic cod (*Gadus morhua*). J. Acoust. Soc. Am. **96**: 1661–1668.

Coetzee, J. 2000. Use of a shoal analysis and patch estimation system (SHAPES) to characterise sardine schools. Aquat. Living Resour. **13**: 1–10.

Diner, N. 2001. Correction on school geometry and density: approach based on acoustic image simulation. Aquat. Living Resour. **14**: 211–222.

Farquhar, G.B. 1977. Biological sound scattering in the ocean: a review. *In* Oceanic sound scattering prediction. *Edited by* N.R. Andersen and B.J. Zahuranec. Plenum, New York pp. 493–527.

Fernandes, P.G., and Simmonds, E.J. 1996. Practical approaches to account for receiver delay and the TVG start time in the calibration of the Simrad EK500. ICES CM 1996/B:17.

Feuillade, C., and Nero, R.W. 1998. A viscous-elastic swimbladder model for describing enhanced-frequency resonance scattering from fish. J. Acoust. Soc. Am. **103**: 3245–3255.

Foote, K.G., Hansen, K.A., and Ona, E. 1993. More on the frequency dependence of target strength of mature herring. ICES CM 1993/B:30.

Gauthier, S., and Horne, J.K. 2004*a*. Potential acoustic discrimination within boreal fish assemblages. ICES J. Mar. Sci. **61**: 836–845.

Gauthier, S., and Horne, J.K. 2004*b*. Acoustic characteristics of forage fish species in the Gulf of Alaska and Bering Sea based on Kirchhoff-approximation models. Can. J. Fish. Aquat. Sci. **61**: 1839–1850.

Gorska, N., and Ona, E. 2003*a*. Modelling the acoustic effect of swimbladder compression in herring. ICES J. Mar. Sci. **60**: 548–554.

Gorska, N., and Ona, E. 2003*b*. Modelling the effect of swimbladder compression on the acoustic backscattering from herring at normal or near-normal dorsal incidence. ICES J. Mar. Sci. **60**: 1381–1391.

Holliday, D.V. 1972. Resonance structure in echoes from schooled pelagic fish. J. Acoust. Soc. Am. **51**: 1322–1332.

Horne, J. 2000. Acoustic approaches to remote species identification: a review. Fish. Oceanogr. **9**: 356–371.

Huse, I., and Ona, E. 1996. Tilt angle distribution and swimming speed of overwintering Norwegian spring spawning herring. ICES J. Mar. Sci. **53**: 863–873.

International Council for the Exploration of the Sea. 2004. Report of the planning group for herring surveys. ICES CM 2004/G:05.

Jech, J.M., Reeder, D.B., Stanton, T.K., and Chu, D. 2000. Three-dimensional visualisation of acoustic backscattering and models by alewife. J. Acoust. Soc. Am. **108**: 2457–2458.

Kang, M., Furusawa, M., and Miyashita, K. 2002. Effective and accurate use of difference in mean volume backscattering strength to identify fish and plankton. ICES J. Mar. Sci. **59**: 794–804.

Kloser, R., Ryan, T., Sakov, P., Williams, A., and Koslow, J.A. 2002. Species identification in deep water using multiple acoustic frequencies. Can. J. Fish. Aquat. Sci. **59**: 1065–1077.

Knorr, G. 1974. *Clupea harengus*: Linnaeus, 1758. Atlas zur Anatomie und Morphologie der Nutzfische für den praktischen Gebrauch in Wissenschaft und Wirtschaft. No. 6. Verlag Paul Parey, Hamburg and Berlin, Germany.

Korneliussen, R.J., and Ona, E. 2002. An operational system for extraction of plankton and fish from mixed recordings. ICES J. Mar. Sci. **59**: 293–313.

Korneliussen, R.J., and Ona, E. 2003. Synthetic echograms generated from the relative frequency response. ICES J. Mar. Sci. **60**: 636–640.

Korneliussen, R.J., and Ona, E. 2004. Verified acoustic identification of Atlantic mackerel. ICES CM 2004/R:20.

Korneliussen, R.J., Diner, N., Ona, E., and Fernandes, P. 2004. Recommendations for the collection of multi-frequency acoustic data. ICES CM 2004/R:36.

© 2007 NRC Canada

Lawson, G.L., Barange, M., and Fréon, P. 2001. Species identification of pelagic fish schools on the South African continental shelf using acoustic descriptors and ancillary information. ICES J. Mar. Sci. **58**: 275–287.

Love, R.H. 1971. Dorsal-aspect target strength of an individual fish. J. Acoust. Soc. Am. **49**: 816–823.

Love, R.H. 1978. Resonant acoustic scattering by swimbladder-bearing fish. J. Acoust. Soc. Am. **64**: 571–580.

MacLennan, D.N., and Holliday, D.V. 1996. Fisheries and plankton acoustics: past, present, and future. ICES J. Mar. Sci. **53**: 513–516.

MacLennan, D.N., and Simmonds, E.J. 1992. Fisheries acoustics: theory and practice. 2nd ed. Chapman and Hall, London, U.K.

MacLennan, D.N., Fernandes, P.G., and Dalen, J. 2002. A consistent approach to definitions and symbols in fisheries acoustics. ICES J. Mar. Sci. **59**: 365–369.

Madureira, L.S.P., Everson, I., and Murphy, E.J. 1993. Interpretation of acoustic data at two frequencies to discriminate between Antarctic krill (*Euphausia superba* Dana) and other scatterers. J. Plankton Res. **15**: 787–802.

McClatchie, S., Alsop, J., and Coombs, R.F. 1996. A re-evaluation of relationships between fish size, acoustic frequency, and target strength. ICES J. Mar. Sci. **53**: 780–791.

McClatchie, S., Thorne, R.E., Grimes, P., and Hanchet, S. 2000. Ground truth and target identification for fisheries acoustics. Fish. Res. **47**: 173–191.

Medwin, H., and Clay, C.S. 1998. Fundamentals of acoustical oceanography. Academic Press, San Diego, Calif.

Nakken, O., and Olsen, K. 1977. Target strength measurements of fish. Rapp. P.-v. Réun. Cons. Int. Explor. Mer, **170**: 52–69.

Nero, R.W., and Huster, M.E. 1996. Low-frequency acoustic imaging of Pacific salmon on the high seas. Can. J. Fish. Aquat. Sci. **53**: 2513–2523.

Nero, R.W., Thompson, C.H., and Love, R.H. 1998. Low-frequency acoustic measurements of Pacific hake, *Merluccius productus*, off the west coast of the United States. Fish. Bull. **96**: 329–343.

Nero, R.W., Thompson, C.H., and Jech, J.M. 2004. In situ acoustic estimates of the swimbladder volume of Atlantic herring (*Clupea harengus*). ICES J. Mar. Sci. **61**: 323–337.

Ona, E. 1990. Physiological factors causing natural variations in acoustic target strength of fish. J. Mar. Biol. Assoc. U.K. **70**: 107–127.

Ona, E. 2001. Herring tilt angles measured through target tracking. *In* Herring: expectations for a new millennium. *Edited by* F. Funk, J. Blackburn, D. Hay, A.J. Paul, R. Stephenson, R. Toresen, and D. Witherell. Lowell Wakefield Fisheries Symposium Series. Alaska Sea Grant College Program, Fairbanks, Alaska. pp. 509–519.

Ona, E. 2003. An expanded target-strength relationship for herring. ICES J. Mar. Sci. **60**: 493–499.

Reid, D.G. (*Editor*). 2000. Echo trace classification: a comprehensive review of the state-of-the-art and directions for future research. ICES Coop. Res. Rep. No. 238.

Reid, D.G., and Simmonds, E.J. 1993. Image analysis techniques for the study of fish school structure from acoustic survey data. Can. J. Fish. Aquat. Sci. **50**: 886–893.

Reid, D.G., Fernandes, P.G., Bethke, E., Couperus, A., Goetze, E., Håkansson, N., Pedersen, J., Staehr, K.J., Simmonds, E.J., Toresen, R., and Tortensen, E. 1998. On visual scrutiny of echograms for acoustic stock estimation. ICES CM 1998/J:3.

Simmonds, E.J. 2003. Weighting of acoustic- and trawl-survey indices for the assessment of North Sea herring. ICES J. Mar. Sci. **60**: 463–471.

Simmonds, E.J., and MacLennan, D.N. 2005. Fisheries acoustics: theory and practice. 2nd ed. Blackwell Science, Oxford, U.K.

Suuronen, P., Lehtonen, E., and Wallace, J. 1997. Avoidance and escape behaviour of herring encountering midwater trawls. Fish. Res. **29**: 13–24.

Watkins, J.L., and Brierley, A.S. 2002. Verification of the acoustic techniques used to identify Antartic krill. ICES J. Mar. Sci. **59**: 1326–1336.

Weston, D.E. 1967. Sound propagation in the presence of bladder fish. *In* Underwater acoustics. *Edited by* V.A. Albers. Plenum, New York. pp. 56–88.

Ye, Z. 1997. Low-frequency acoustic scattering by gas-filled prolate spheroids in liquids. J. Acoust. Soc. Am. **101**: 1945–1952.

Zar, J.H. 1984. Biostatistical analysis. 2nd ed. Prentice-Hall, Inc., Englewood Cliffs, N.J.

© 2007 NRC Canada

PERSPECTIVE / PERSPECTIVE

The growing degree-day and fish size-at-age: the overlooked metric

Anna B. Neuheimer and Christopher T. Taggart

Abstract: Growth rate in ectotherms, including most fish, is a function of temperature. For decades, agriculturalists (270+ years) and entomologists (45+ years) have recognized the thermal integral, known as the growing degree-day (GDD, °C·day), to be a reliable predictor of growth and development. Fish and fisheries researchers have yet to widely acknowledge the power of the GDD in explaining growth and development among fishes. We demonstrate that fish length-at-day (LaD), in most cases prior to maturation, is a strong linear function of the GDD metric that can explain >92% of the variation in LaD among 41 data sets representing nine fish species drawn from marine and freshwater environments, temperate and tropical climes, constant and variable temperature regimes, and laboratory and field studies. The GDD demonstrates explanatory power across large spatial scales, e.g., 93% of the variation in LaD for age-2 to -4 Atlantic cod (*Gadus morhua*) across their entire range (17 stocks) is explained by one simple GDD function. Moreover, GDD can explain much of the variation in fish egg development time and in aquatic invertebrate (crab) size-at-age. Our analysis extends the well-established and physiologically relevant GDD metric to fish where, relative to conventional time-based methods, it provides greater explanatory power.

Résumé : Le taux de croissance des ectothermes, dont celui de la plupart des poissons, est fonction de la température. Depuis des décennies, les spécialistes l'agriculture (270+ ans) et de l'entomologie (45+ ans) reconnaissent que la sommation thermique, connue sous le nom de degré-jour de croissance (GDD, °C·jour), permet de prédire de façon fiable la croissance et le développement. Les chercheurs en ichtyologie et en pêcheries tardent à reconnaître à grande échelle la puissance de GDD pour expliquer la croissance et le développement chez les poissons. Nous démontrons que la longueur en fonction du jour (LaD), la plupart des cas avant la maturation, est une solide fonction linéaire de la métrique GDD qui peut expliquer >92 % de la variation de LaD dans 41 séries de données représentant neuf espèces de poissons et tirées de milieux marins et d'eau douce, de climats tempérés et tropicaux, de régimes thermiques constants et variables et d'études de laboratoire et de terrain. La métrique GDD possède une pouvoir d'explication qui s'étend sur de grandes échelles spatiales; par exemple, une simple fonction GDD rend compte de 93 % de la variation de LaD chez des morues franches (*Gadus morhua*) d'âges 2–4 sur l'ensemble de leur répartition (17 stocks). De plus, GDD peut expliquer une grande partie de la variation du temps de développement des oeufs de poissons et de la taille en fonction de l'âge chez les invertébrés aquatiques (crabes). Notre analyse étend aux poissons l'utilisation de la métrique GDD, déjà bien établie et d'intérêt physiologique; cette métrique possède d'ailleurs un pouvoir explicatif plus important que les autres méthodes basées sur le temps.

[Traduit par la Rédaction]

Introduction

The physiological processes that determine growth (e.g., metabolic rate, gas exchange, risk of desiccation in terrestrial organisms, and oxygen supply in aquatic animals) are directly influenced by temperature (Atkinson 1994; van der Have and de Jong 1996). Accordingly, time-dependent variations in temperature are reflected in time-dependent variations in development and in size-at-age where the latter is frequently used to infer growth rate. Within limits, and in general, higher temperatures result in higher enzymatic reaction rates that govern growth (Higley et al. 1986). Diffusion of substrates or enzymes or both increases, resulting in a greater number of enzyme–substrate complexes and more energy to meet reaction demands. This physiological response, greatly simplified in terms of the complex processes involved, is generally linear over a midrange of temperatures approaching the optimum and nonlinear at extreme tempera-

Received 17 April 2006. Accepted 15 January 2007. Published on the NRC Research Press Web site at http://cjfas.nrc.ca on 7 March 2007.
J19275

A.B. Neuheimer and C.T. Taggart.[1] Department of Oceanography, Dalhousie University, 1355 Oxford Street, Halifax, NS B3H 4J1, Canada.

[1]Corresponding author (e-mail: chris.taggart@dal.ca).

 doi:10.1139/F07-003 © 2007 NRC Canada

tures where control enzyme(s) are inactivated by conformational change (Sharpe and DeMichele 1977) or where enzymes or substrates are destroyed more rapidly than they are sequestered (Howe 1967). This appears to be true for all ectotherms including plants, insects, aquatic invertebrates, and most reptiles, amphibians, and fish.

In fish, variation in size influences predator–prey interactions, maturation, reproduction and recruitment potential, and vulnerability to size-selective fishing. Thus, explaining or predicting growth variation through size-at-age is often essential to population and ecosystem studies and nutrient/energy pathway explorations (food webs) as well as in determining fishing pressures suitable for sustainable fisheries. The greatest impediment to most fish growth models, including the pervasive von Bertalanffy growth function (VBGF) (von Bertalanffy 1938), is their dependence on calendar time to explain length variation (i.e., length-at-age). Such dependence explicitly ignores time-dependent and physiologically meaningful variables such as temperature. Some growth models do attempt to incorporate temperature, usually instantaneous measures of temperature (Francis 1994; Mallet et al. 1999; Dion and Hughes 2004). However, instantaneous local temperature estimates (e.g., daily mean) do not necessarily reflect the phenotypic expression of the growth integral (i.e., length-at-age) in an equally instantaneous manner. For over 270 years in agriculture and for at least 45 years in entomology, the time-based integral of the heat available for growth — heat transferred from the environment to the ectotherm — has been employed with remarkable success in explaining and predicting growth and development (e.g., Seamster 1950; Atkinson 1994; Bonhomme 2000). The most prevalent parameterization of the heat integral is the growing degree-day (GDD, °C·day), the time integral of the daily temperature measured above some temperature threshold (T_{Th}). The GDD method allows growth and development to be correctly scaled to the physiology that drives ectotherm growth and development. Simply stated, growth and development are proportional to the time spent at temperature (thermal time; Trudgill et al. 2005) within the range where metabolic reaction rates are near-linear functions of temperature. The thermal integral concept should be applicable to most fish simply because they are ectotherms; their metabolic rate is largely determined by the heat transferred from the environment during the period of growth and development (e.g., Leggett et al. 1984; Hamel et al. 1997; Kjellman et al. 2001). However, relative to agriculture and entomology, our examination of the primary literature (Fig. 1) demonstrates that only a handful (4.6%) of studies that address temperature and growth in fishes refer to the GDD metric (e.g., Mills 1988; Mills et al. 1989; Kjellman et al. 2001). Although several fish studies address the combination of time and temperature (e.g., Iwama and Tautz 1981; Brander 1995), none appear to follow through on the implications of the thermal integral or explore its generality. To paraphrase Reaumur (1735, cited in Bonhomme 2000): "The same [fish] are harvested in very different climates; it would be interesting to compare the sums of heat degrees over the months during which the [fish] does most of its growing and

Fig. 1. Histograms of (*a*) the number of articles listed by Web of Science® for the period 1980–2006 referring in title, keywords, or abstracts to temperature and growth (gray bars, key words: "temperature" AND ("development" OR "growth")) or GDD (open bars, key words: "degree day*" OR "thermal sum" OR "day degree*" OR "growing degree day*" OR "thermal time") in agriculture, entomology, and fish science and (*b*) the percent total number of articles listed by the Web of Science® for the period 1980–2006 referring in title, keywords, or abstracts to GDD (key words: "degree day*" OR "thermal sum" OR "day degree*" OR "growing degree day*" OR "thermal time") in agriculture, entomology, and fish science.

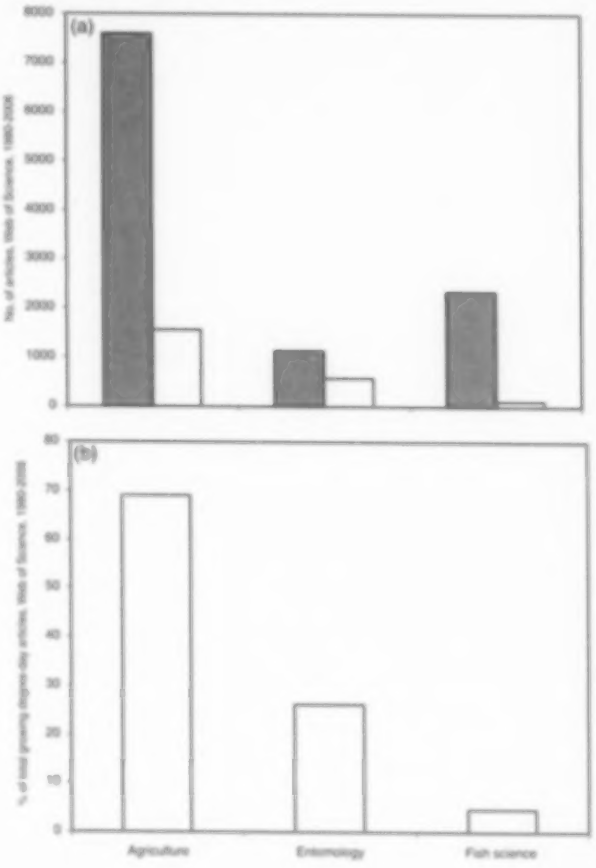

reaches complete maturity in hot countries, like Spain or Africa...in temperate countries like France and in the colder countries of the North."

Data mining and analyses

We examined 41 data sets (Supplemental Tables S1 and S2)[2] representing nine fish species and different life history stages (most prior to maturation) among subtropical, temperate, freshwater, and marine environments, including control experiments with constant and variable temperature and field

[2] Supplementary data for this article are available on our Web site (http://cjfas.nrc.ca) or may be purchased from the Depository of Unpublished Data, Document Delivery, CISTI, National Research Council Canada, Building M-55, 1200 Montreal Road, Ottawa, ON K1A 0R6, Canada. DUD 5139. For more information on obtaining material, refer to http://cisti-icist.nrc-cnrc.gc.ca/irm/unpub_e.shtml.

© 2007 NRC Canada

studies. Across these data, we are able to show that variation in length-at-day (LaD, mm) is a strong linear function ($r^2 \geq 0.92$, $P < 0.05$) of the variation in GDD. Further, our analyses show that GDD is able to explain variation in LaD within and among data sets, something that calendar time cannot do in environments where there are temporal variations in temperature within or among trials or field studies.

GDD in the laboratory

Among constant-temperature growth trials (Folkvord et al. 2004) with Atlantic herring (*Clupea harengus*), calendar time explains most of the variation in LaD within a given trial (Fig. 2*a*), but each trial requires a different parameterization (analysis of covariance (ANCOVA): different slopes, $P = 0.0003$). In contrast, the thermal integral (i.e., GDD) explains the LaD variation within and among trials (Fig. 2*b*) using a single parameterization (ANCOVA: similar slopes, $P = 0.74$; similar intercepts, $P = 0.59$; LaD = 0.033GDD + 10.4; $r^2 = 0.99$, $P < 0.0001$). Other growth trials with herring (Folkvord et al. 2004), now employing a time-varying temperature, show that although calendar time again explains much of the LaD variation within a given trial (Fig. 2*c*), the explanatory power is less than under constant temperature (Fig. 2*a*). Further, and more importantly, each trial requires a different parameterization (ANCOVA: different slopes, $P = 0.0032$). In contrast, GDD explains a greater degree of variation in LaD within and among trials (Fig. 2*d*) and a single parameterization is sufficient (ANCOVA: similar slopes, $P = 0.55$; similar intercepts, $P = 0.064$; *LaD* = 0.035GDD + 10.1; $r^2 = 0.98$, $P < 0.0001$). The strength of the GDD metric becomes readily apparent when one recognizes that there are no differences among the above parameterizations of LaD as a function of GDD in the constant-temperature (Fig. 2*b*) and in the time-varying temperature (Fig. 2*d*) growth trials (Fig. 2*f*) (ANCOVA: similar slopes, $P = 0.91$; similar intercepts, $P = 0.19$; LaD = 0.034GDD + 10.3; $r^2 = 0.98$, $P < 0.0001$). In summary, a single parameterization of LaD as a function of physiological time is sufficient to explain size-at-age variation, with considerable accuracy, among any of the above temperature growth trials that require four different parameterizations when LaD is expressed as a function of calendar time.

A further example of the strength of the GDD metric in assessing fish size-at-age can be demonstrated using the Malzahn et al. (2003) laboratory-rearing of larval houting (*Coregonus oxyrhynchus*). Here, two different parameterizations of LaD as a function of calendar time are required for each trial (Fig. 2*g*) (ANCOVA: different slopes, $P = 0.0001$), although they, like the herring above, collapse to a simpler parameterization when GDD is used (Fig. 2*h*) (ANCOVA: similar slopes, $P = 0.10$; different intercepts, $P < 0.0001$).

When GDD is unable to explain the variation in LaD among trials, it is an indication that other factors (e.g., food availability, genetic composition) are contributing to the size-at-age variation (or the thermal record is incorrect, see below). How much of that size-at-age variation is due to temperature versus other factors can only be teased apart once the trials are compared on the same physiological timescale, i.e., with GDD. When size-at-age is assessed in the same larval houting as above (Malzahn et al. 2003) but now under food limitation, there is no relation (i.e., no growth) between LaD and either calendar time or GDD. (Figs. 2*g* and 2*h*) (linear regression; $0.11 \leq P \leq 0.13$). However, when calendar time is used as the predictor, it is not clear how much of the variation in LaD is a function of temperature and how much is a function of food. As we have shown above, when the GDD metric is employed, the variation in size-at-age owing to temperature can be explained and more so than by calendar time. Consequently, with GDD, any variation related to food limitation (and presumably other variables independent of temperature-dependent physiology) becomes readily apparent. The GDD appears to explain the variation in size-at-age owing to variation in thermal histories of fish and thus can be used to identify the remaining size-at-age variation that can be explored (e.g., other factors). In addition, laboratory growth studies need not control for temperature (within limits) if GDD is employed in the analyses because the GDD can account for the temperature variation through integration as described above (Figs. 2*e* and 2*f*) and below (Figs. 2*i* and 2*j*).

GDD in the field

The strength of the GDD is also demonstrated among field studies (Dion and Hughes 2004) where, for example, the nonlinear evolution in GDD is able to explain the nonlinear evolution of LaD in two different year-classes of age-0+ Arctic grayling (*Thymallus thymallus*) in consecutive years in the same habitat (Fig. 3) and does so in a linear manner (Figs. 2*i* and 2*j*). The original study (Dion and Hughes 2004) used the growth model of Mallet et al. (1999) that was developed for grayling to incorporate seasonal size-at-age variation in the VBGF through a "coefficient of temperature", a coefficient requiring estimates of the minimum, maximum, and optimum growth temperatures for grayling based on "expert opinion". A comparison of the residuals resulting from the GDD metric applied to the grayling and those obtained using the modified VBGF (Dion and Hughes 2004) reveals that the residuals (Supplemental Fig. S1)[2] from the former are smaller, more uniform, and trend-free relative to the modified VBGF (although both are autocorrelated, as are most variables of this nature). Thus, consistent with all above, the GDD method provides a simpler metric with greater explanatory power and obviates the five parameters required by the modified VBGF (Dion and Hughes 2004) and by analogues used elsewhere that incorporate asymptotic length, growth coefficient, optimum temperatures, seasonal amplitudes and phases, etc.

The GDD not only explains the variation in LaD among different year-classes in different years (above), it can also explain size-at-age variation among year-classes across multiple years as shown (Figs. 2*k* and 2*l*) by the freshwater minnow in a north-temperate environment (Mills 1988). Here, calendar time explains much of the evolution of LaD with a similar slope among year-classes, but the intercepts are different (Fig. 2*k*) (ANCOVA: similar slopes, $P = 0.85$; different intercepts, $P = 0.0014$). The common slope result (Mills 1988) is most likely related to the fact that there were limited differences in the GDD among years (coefficient of variation (CV) = 16%), i.e., limited differences in the ther-

© 2007 NRC Canada

Fig. 2. Length-at-day as a function of calendar time (left panels) and as a function of GDD (right panels) for Atlantic herring (Folkvord et al. 2004) (*a*, *b*, *e*, and *f*) for 4 °C constant trial (solid circles) and 12 °C constant trial (crosses), (*c*, *d*, *e*, and *f*) for 4, 8, and 4 °C variable trial (open circles), and (*c*, *d*, *e*, and *f*) for 12, 8, and 12 °C variable trial (squares), houting (Malzahn et al. 2003) (*g* and *h*) for 8.4 °C constant and fed (open circles), 17.5 °C constant and fed (solid circles), 8.4 °C constant and starved (squares), and 17.5 °C constant and starved (crosses), Arctic grayling (Dion and Hughes 2004) (*i* and *j*) for 2000 year-class (solid circles) and 2001 year-class (open circles), and minnow (Mills 1988) (*k* and *l*) for 1978 year-class (solid circles), 1979 year-class (open circles), 1980 year-class (crosses), and 1981 year-class (squares). Also shown is carapace width in spider crab (Penha-Lopes et al. 2006) (*m* and *n*) for 25 °C constant (solid circles) and 28 °C constant (open circles). The linear regression (solid line) and 95% prediction intervals (broken lines) are provided for each relation (see Supplemental Table S2 for details)[2] except where not significant.

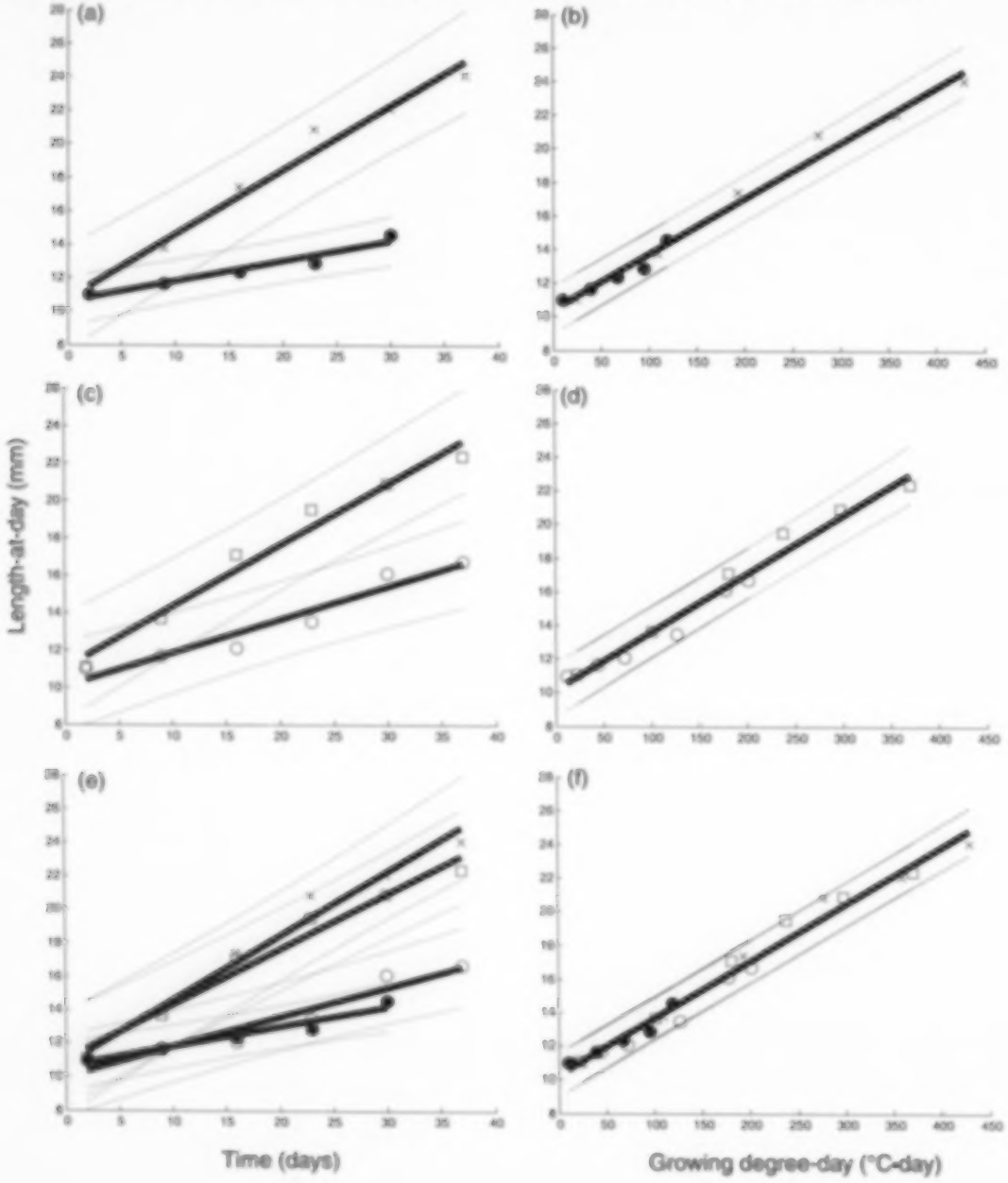

© 2007 NRC Canada

Fig. 2 (*continued*).

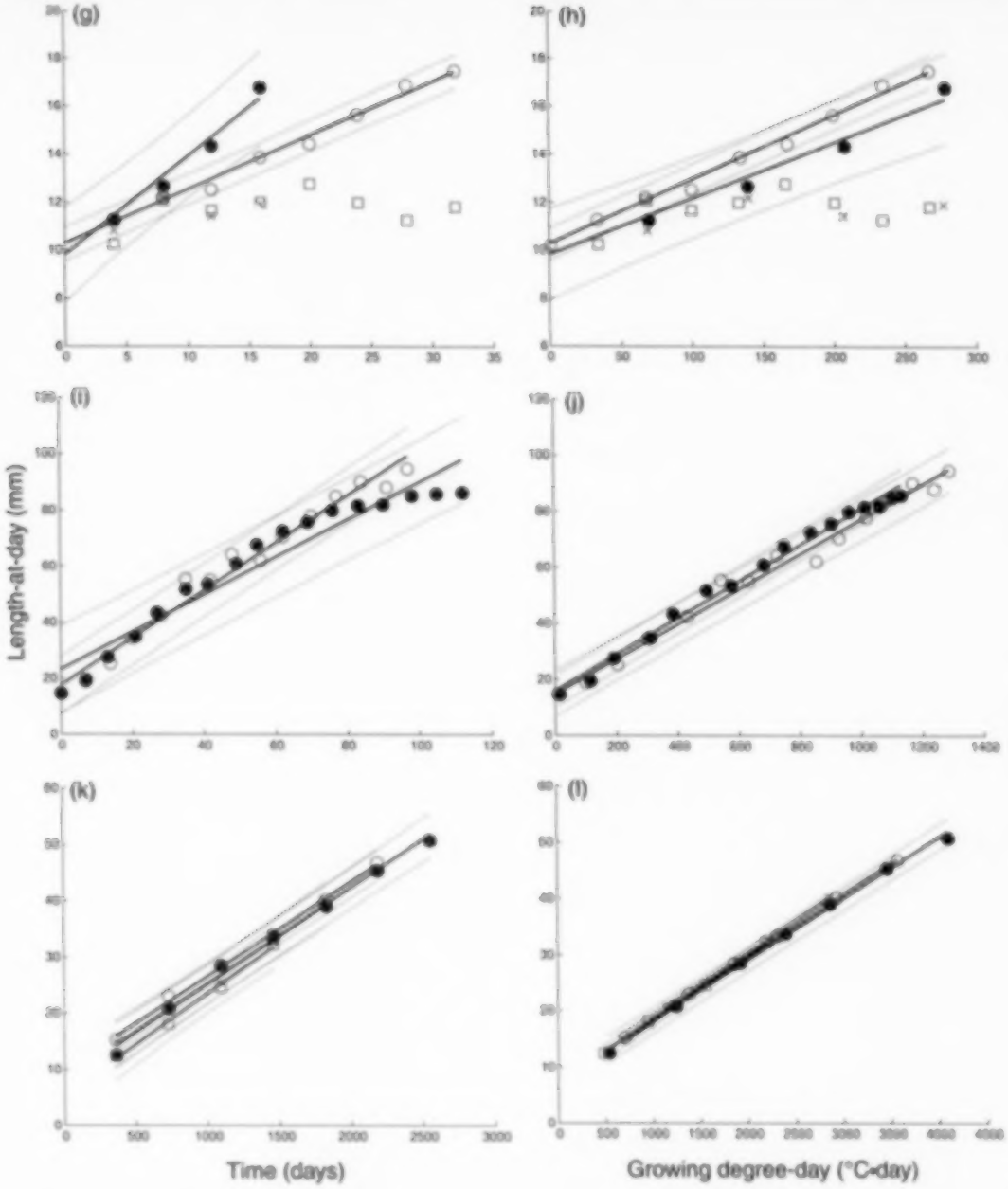

mal histories (thermal integrals) of the four year-classes over the 4- to 7-year-period. The disparate intercepts may be related to the first sampling dates among year-classes in relation to the thermal histories of the fish. When the same fish are assessed in terms of their year-class (cohort) and GDD, a single relation holds (Fig. 2*l*) (ANCOVA: similar slopes, $P = 0.19$; marginally similar intercepts, $P = 0.032$) (Supplemental Table S2).[2] In summary, where the thermal environment varies little from one year to the next, calendar time can be expected to explain much of the variation in LaD among year-classes, although in this case, the GDD metric delivers slightly better explanatory power.

GDD in general

The above demonstrations of the ability of the GDD method to explain LaD variation in fishes is mirrored among the other data sets that we examined (41 in all, including those detailed above and below; Supplemental Tables S1 and S2)[2] where the CV (51%) in slopes derived from LaD-at-GDD relations is

© 2007 NRC Canada

Fig. 2 (*concluded*).

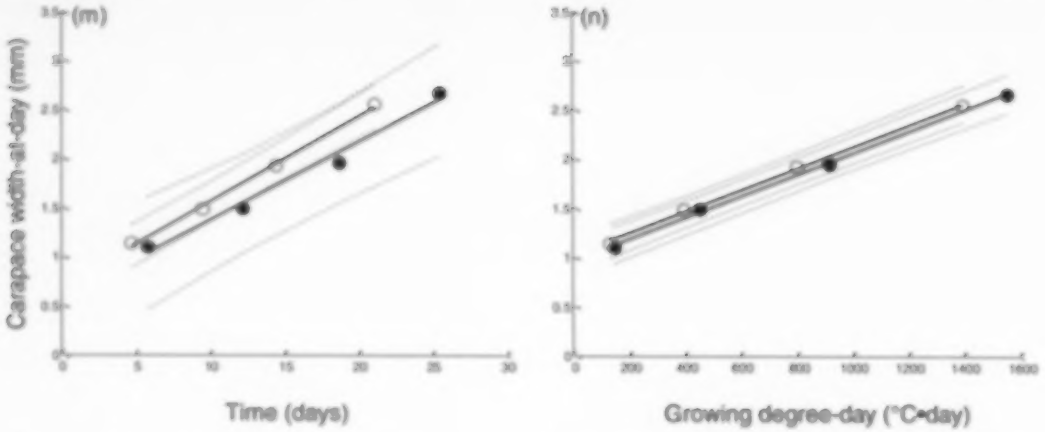

Fig. 3. Nonlinear evolution of length-at-day for (*a*) 2000 year-class (circles) and (*b*) 2001 year-class (circles) of age 0+ Arctic grayling (Dion and Hughes 2004) and the parallel and nonlinear evolution of growing degree-day (line) in time for each year and year-class.

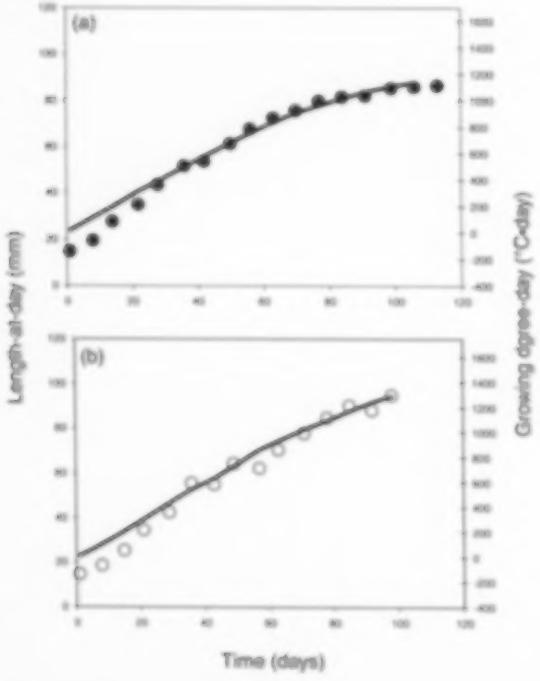

smaller than that derived from the LaD-at-calendar-time relations (63%), demonstrating that physiological time is able to explain more of the variation in size-at-age in fishes among studies (temperatures, year-classes, species, etc.) than does calendar time.

GDD in other aquatic ectotherms

The explanatory power of the GDD appears to hold for other aquatic ectotherms. For example, and as shown above for herring and houting, spider crab (*Mithraculus forceps*) constant-temperature (25 and 28 °C) growth trials (Penha-Lopes et al. 2006) demonstrate that calendar time explains much of the variation in carapace width (mm) within a given trial (Fig. 2*m*) but each trial requires a different parameterization, at least in the intercept (ANCOVA: similar slopes, $P = 0.41$; different intercepts, $P = 0.01$). However, when physiological time is employed, size-at-age relations between temperature trials are identical in slope and the intercepts are marginally the same (ANCOVA: similar slopes, $P = 0.86$; marginally similar intercepts, $P = 0.031$). The GDD method (Stevens 1990) also proves useful for assessing size-at-age in the red king crab (*Paralithodes camtschatics*) where 92% of the variation in carapace length-at-age is a simple linear function of GDD (linear regression, $P < 0.0001$) (Supplemental Fig. S2).[2]

GDD and development

A corollary to the GDD is the thermal constant — the degree-days achieved to advance a given developmental stage — routinely used in agriculture and entomology to determine developmental time to stages such as emergence or maturation (Trudgill et al. 2005). This concept is applicable to fish (Lange and Greve 1997) including, for example, the development and hatching of chinook salmon (*Oncorhynchus tshawytscha*) eggs (Alderdice and Velsen 1978) incubated across a 16 °C temperature range (Fig. 4*a*). Here, the GDD achieved for hatching to occur is 516 ± 40 °C·days regardless of incubation temperature (Fig. 4*b*; Supplemental Table S2),[2] thus reducing the CV in time-to-hatch from 65% (calendar time) to 7.8% (physiological time), although there are some outliers in the thermal constant estimates (see below). Time-to-hatch as a thermal constant is also noted in trout (*Salmo fario*) eggs (Gray 1928) (Fig. 4*a*) near 493 ± 48 °C·days (Fig. 4*b*) and yellowtail flounder (*Limanda ferruginea*, formerly *Pleuronectes ferrugineus*) eggs (Benoit and Pepin 1999) (Fig. 4*c*) near 52 ± 3 °C·days (Fig. 4*d*) where the CV in time-to-hatch is reduced from 44% to 9.7% and from 32% to 6.4%, respectively, when GDD is used instead of calendar time. Again, there are some outliers. The anomalously low thermal constants (outliers) generally appear at the extremes in the incubation temperature ranges, possibly

© 2007 NRC Canada

Fig. 4. Egg development in calendar time to hatch (left panels) and in GDD to hatch (right panels) for incubation at constant temperatures for (*a* and *b*) trout (solid circles) (Gray 1928) and chinook salmon (open circles) (Alderdice and Velsen 1978) and (*c* and *d*) Atlantic cod (squares) (Pepin et al. 1997) and yellowtail flounder (crosses) (Benoit and Pepin 1999).

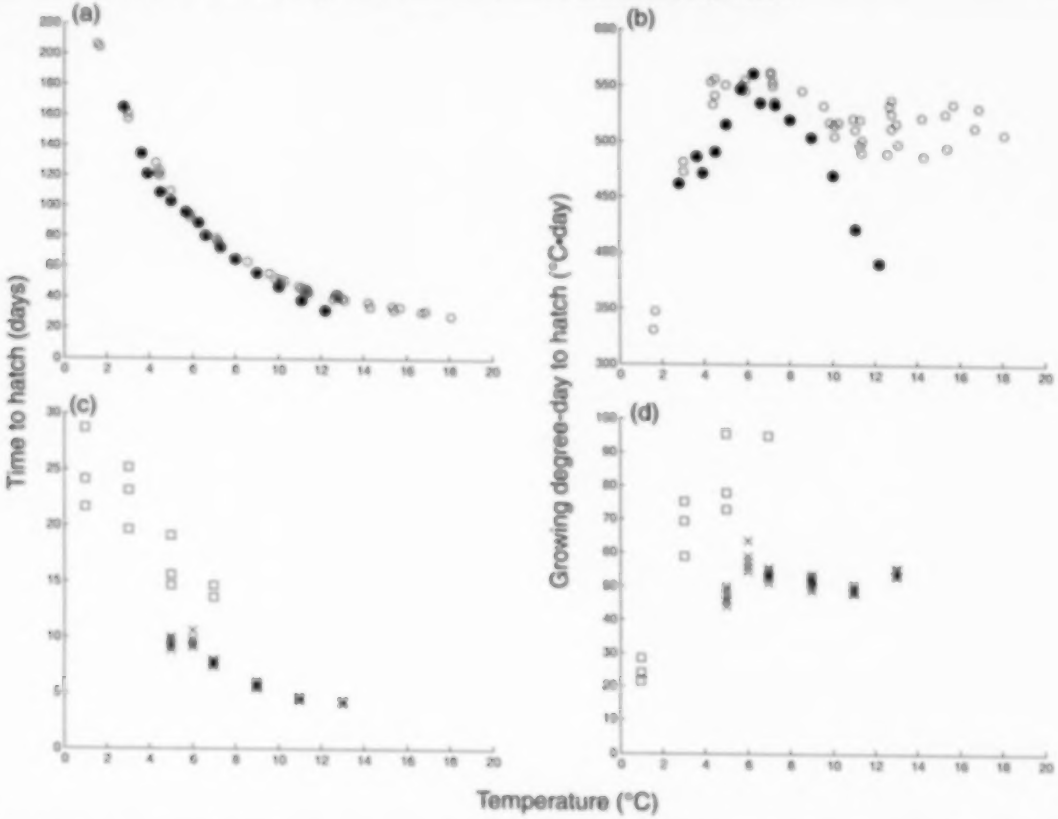

indicating that the eggs are being incubated outside of the temperature range normally experienced by the organism where the metabolic response to changing temperature is expected to be near-linear. This may explain our examination of Atlantic cod (*Gadus morhua*) eggs (Pepin et al. 1997) (Fig. 4*c*) reared between 1 and 7 °C where the thermal constant appears to be near 66 ± 29 °C·days with anomalously low estimates at the low end of the incubation temperature range (demonstrating an increase in CV from 25% to 44% for calendar time (Fig. 4*c*) and GDD (Fig. 4*d*), respectively), again suggesting incubation outside of temperature ranges within that that the organism has evolved or that some other low-temperature physiology is involved (Valerio et al. 1992). Nevertheless, these examples (Figs. 4*b* and 4*d*) illustrate that the GDD thermal constant may be useful in predicting the timing of life history development and transformation in fish. The substantial variation in thermal constants over large ranges in egg incubation temperatures for some species found in our study, and in that of Reibisch (1902), indicates that our greatly simplified assumptions regarding the physiological responses to temperature may not explain all of the variation stemming from the complex processes involved.

In fish, life history transformations (e.g., smoltification, maturation) are marked by changes in energy allocation from growth to other physiological demands and thus a discontinuity in LaD as a function of GDD is to be expected. Such discontinuities are observed in some of the multiyear data that we examined (e.g., Atlantic salmon (*Salmo salar*) and threespine stickleback (*Gasterosteus aculeatus*)) and they appear to identify thermal constants that define the physiological time for life history transformation. For example, a discontinuity at approximately 1600 °C·days is apparent (Supplemental Fig. S3)[2] in Atlantic salmon growth trials (based on data from Jones et al. 2002) corresponding to an average LaD of approximately 114 mm, well within the standard deviation of the average LaD (124 ± 14 mm; Hutchings and Jones 1998) reported for smoltification in the study area. Smoltification is associated with physiological changes involving salinity tolerance, hormone titre (thyroid activity), and olfaction (Specker et al. 2000), each presumably associated with a changing energy budget and thus a change in the LaD-at-GDD relation.

GDD at large spatial scales

To test the generality of the GDD measure in explaining size-at-age for fish over large spatial and temperature scales, we examined age-2 to -4 Atlantic cod and their associated long-term mean ocean temperature across their North Atlantic range using Brander's (1995) compilation. In doing so, we explicitly assume that the variation in temperature among

© 2007 NRC Canada

Fig. 5. Length-at-day (LaD) for 17 stocks of age-2 to -4 North Atlantic cod (Brander 1995) as a function of (*a*) calendar time (no significant relation among stocks, linear regression, $P = 0.097$) and (*b*) growing degree-day (GDD) (significant relation among stocks: LaD = 0.034GDD + 280; $r^2 = 0.93$, $P < 0.0001$ with 95% confidence intervals for the prediction (broken lines)). Data labels are stock identifiers (cf. Brander 1995): East and West Greenland (1), Northeast Arctic (2), Iceland (3), Faroe (4), West Scotland (5), North Sea (6), Celtic Sea (7), Irish Sea (8), Eastern Channel (9), Labrador/Grand Bank (10), Southern Grand Bank (11), Northern Gulf of St. Lawrence (12), St. Pierre Bank (13), Southern Gulf of St. Lawrence (14), Eastern Scotian Shelf (15), Western Scotian Shelf (16), and Georges Bank (17).

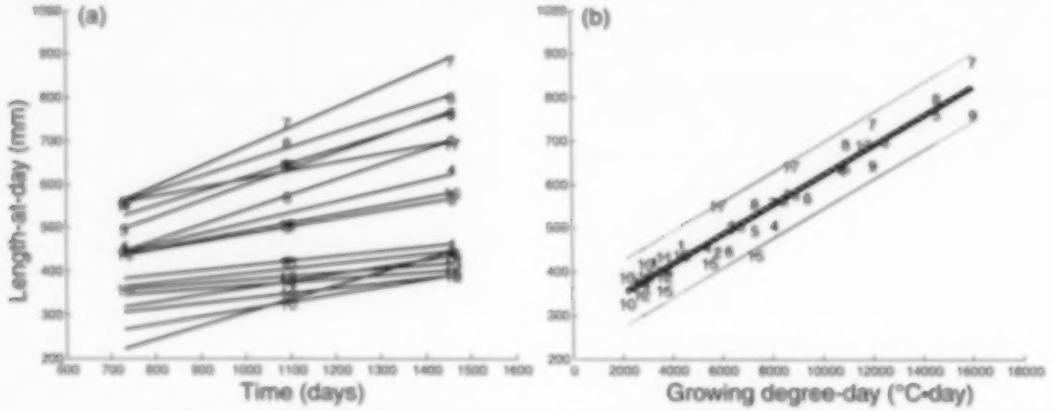

stocks is greater than that within. We are able to demonstrate that although there is a well known and nearly threefold range in length-at-age across the 17 stocks examined — a range attributable to differences in habitat temperature among the stocks (Brander 1995) — fully 93% of the variation in LaD is explained as a single linear function of GDD, i.e., the length of any cod, no matter its stock and habitat–temperature association, is very predictable (±19% being the 95% prediction interval; Fig. 5) from the GDD metric, despite the fact that each stock has its own size-at-age (calendar time) relation owing to differences in their thermally controlled growth rate. Such stock-specific length-at-age relations for many species abound in the literature.

Critical assumptions and unresolved questions

The temperature measures used to estimate GDD must be representative of that experienced by the organism. This ideally requires measurements at a sufficiently high frequency in the locale where the organism is growing. Much literature involving the application of the GDD metric to plant species has focused on microclimates near the plant (Wang 1960). Owing to the high heat capacity of the aquatic environment, the time and space decorrelation scales are typically large relative to terrestrial locales, allowing temperature to be less-frequently estimated and at a larger spatial scale. Further, the thermal acclimation limits of most aquatic ectotherms compromise their ability to move across thermal gradients. Nevertheless, evidence for the necessity of reliable local temperature estimates is found in a study (Kjellman et al. 2001) on European perch (*Perca fluviatilis*) and zander (*Sander lucioperca*, formerly *Stizostedion lucioperca*). There, differences in size-at-age among bay-specific populations disappear within species when a bay-specific GDD is used in place of bay-specific parameterizations based on local air temperature (Kjellman et al. 2001). Further, representative GDD must include the entire thermal history of the organism up to the point of interest (Trudgill et al. 2005), e.g., from hatch or spawning date to a given size or development stage. The more complete the temperature time series, the more the variation in LaD will be explained, as it is the complete (i.e., integrated) thermal history of the fish that contributes to the size-at-age. For example, the New Zealand snapper (*Pagrus auratus*) data (Francis 1994) begin with a hatch date (1 January) near the maximum spawning period and we are able to determine LaD as a strong function of GDD ($0.97 < r^2 < 0.98$) with statistically similar relations among year-classes (ANCOVA: similar slopes, $P = 0.26$; similar intercepts, $P = 0.78$). However, the burbot (*Lota lota*) data (Kjellman and Eloranta 2002) begin at arbitrary starting points in relation to the thermal history of the fish, and although the strength of the LaD-at-GDD relation is maintained ($0.98 < r^2 < 0.99$), the relations between the two year-classes are marginally different (ANCOVA: slopes, $P = 0.058$; intercepts, $P = 0.035$). It is difficult to know if the contrast between the snapper and the burbot examples is due simply to the choice of start date relative to the entire thermal history. It seems that the GDD method maintains strength in the face of temperature data that may be compromised by location, frequency, or completeness of measurement. However, when care is made to optimize these criteria, the GDD is frequently able to explain variation in LaD within as well as among different groups (e.g., locations, year-classes), something that calendar time cannot achieve unless the fish grow in a constant thermal environment. It is here that the increasing amount of archival tag data (e.g., Palsson and Thorsteinsson 2003) may provide unequivocal substantiation of the utility of the GDD measure owing to the relatively high-frequency temperature measures provided over the recorded thermal history of the tagged fish, although getting a comparable length-at-age series may be challenging; we offer microscale accelerometry as a possible avenue of exploration and such development is now underway (D. King, VEMCO Ltd., 77 Chain Lake Drive, Halifax, Nova Scotia, personal communication).

We stress the importance of measuring the length of the fish in studies where the intent is to use a thermal integral. Al-

© 2007 NRC Canada

Fig. 6. Normalized stomach fullness index (nSFI) as a function of (*a*) calendar time and (*b*) growing degree-hour (GDH, °C·h) for freshwater sculpin held at 2 °C (crosses), 7 °C (open circles), and 12 °C (solid circles). Stomach fullness index (SFI) was calculated by Miyasaka et al. (2005) with SFI = $\log_e$[{1000(dry mass of stomach contents)/(dry mass of fish body)} +1]. We have normalized the SFI within temperature trials where nSFI = SFI/(maximum SFI). The linear regression (solid line) and 95% prediction intervals (broken lines) are provided for each (see Supplemental Table S3 for details).[2]

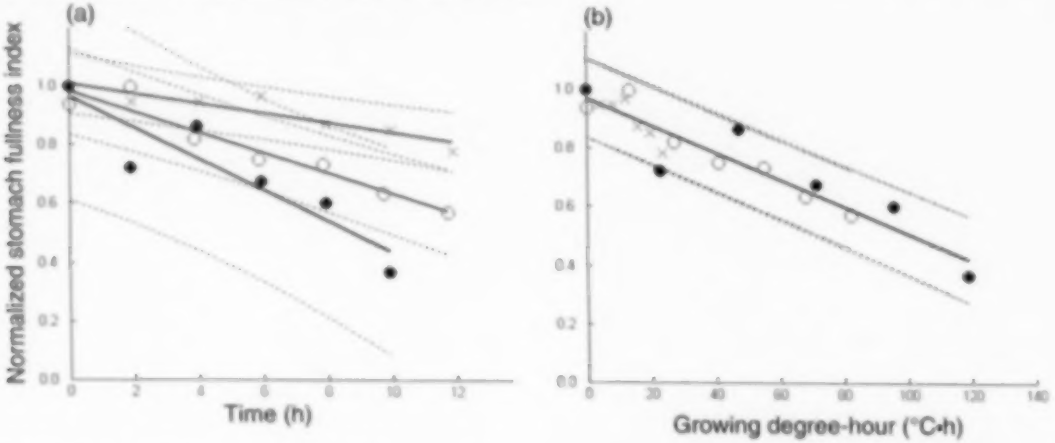

though weight, as a function of length, should, in general, be explained by GDD, seasonal variations in weight-at-age compromise the size measure in contrast with length-at-age that is relatively invariant on a seasonal basis. The latter case is the reason that we converted Brander's (1995) cod weight-at-age to length-at-age (see Supplementary Appendix).[2]

Summary and future directions

Each of the above examples demonstrates that, with basic information on variation in the thermal environment, the physiological time-scaling provided by the GDD explains most of the temperature-related variation in length-at-age (inferred growth) prior to maturation and perhaps beyond. This appears to apply within and among stocks and populations of a given fish species, something that cannot be achieved using calendar time unless the thermal histories are very similar. It appears that the GDD has similar utility in explaining variation in life history development and stage transitions through the thermal constant. Thus, the GDD appears as an essential metric to explain a large amount of variation that is observed in fish growth and development, variation that is frequently attributed to temperature, but often with limited success or in an overly complicated manner, simply because a physiologically scaled temperature measure was not used. Such physiological scaling via GDD could be incorporated into fish simulation models and likely advance such models by avoiding the complications that result from different responses to time-varying and time-constant temperature environments (e.g., Neill et al. 2004). Indeed, identifying a correct physiological timescale through the use of GDD may advance many aspects of aquatic ectotherm research from population-wide studies (e.g., timing of coral bleaching; Berkelmans 2002) to physiological timing within an individual. An example of the latter is the temperature-related variation in the rate of gastric evacuation associated with fish food consumption. In evacuation trials, the fish can be held at different trial-specific constant temperatures, and following the cessation of feeding, the reduction in stomach content (e.g., fullness index) over time is used as an estimate of evacuation. Miyasaka et al. (2005) used this method to determine gastric evacuation in freshwater sculpin (*Cottus nozawae*) held at constant temperatures of 2, 7, and 12 °C. As with our size-at-age analyses above, we show, in accord with Miyasaka et al. (2005), that calendar time requires three separate parameterizations, one for each trial (Fig. 6*a*) (ANCOVA: different slopes, $P = 0.0081$). When assessed using the thermal integral (here using growing - degree-hour (GDH)), we can explain the variation in the normalized stomach fullness index (nSFI) within and among trials using a single parameterization (ANCOVA: similar slopes, $P = 0.49$; similar intercepts, $P = 0.92$; nSFI = -0.0046GDH + 0.97; $r^2 = 0.88$, $P < 0.0001$). We offer this example simply to demonstrate that when the physiologically relevant and short timescale GDH is employed, it clearly explains the different rates in the physiological processes (digestion and evacuation) at the time and temperature scales at which they are occurring.

The implications of not using a physiologically scaled temperature become apparent when we examine the effect of a small increase in daily temperature on a predicted LaD. By example, when the daily temperatures for the 2000 year-class of age-0+ Arctic grayling (Figs. 2*i* and 2*j*) are uniformly raised by 0.6 °C or less, we cannot statistically detect a significant difference between the means of the original and elevated temperature series (neither normal, Wilcoxon rank sum, $P = 0.096$) (Fig. 7) because the variance within is greater than between. However, the GDD method predicts a significant ~5% increase (89–93 mm) in the length-at-day of the grayling at the end of their first growing season based on the elevated temperature record, a change in size that cannot be explained by the change (not significant) in the mean temperature. The LaD estimates from the two series diverge because original and adjusted temperature-based GDD series diverge as the heat transferred from the environment to the fish accumulates. The effect (expected LaD) will magnify

© 2007 NRC Canada

Fig. 7. Percent increase in predicted final length-at-age (mm) (squares and solid line) for the 2000 year-class of age 0+ Arctic grayling (Dion and Hughes 2004) as a function of growing degree-day when the daily temperature series is uniformly increased between 0.1 and 1.0 °C in 0.1 °C increments. The broken line defines the P value of a Wilcoxon rank sum test assessing the difference between the mean temperature of each elevated series relative to the original series. The boxed region indicates the predicted increase in length-at-age that cannot be predicted from differences (not significant) in the mean temperature (i.e., mean temperature of original and perturbed temperature series are statistically similar at a conservative $P > 0.09$).

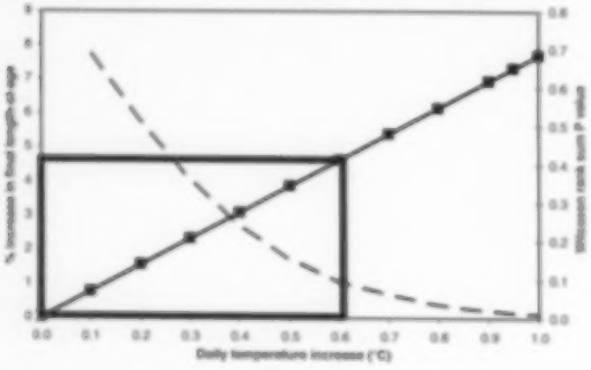

with time (age). Therefore, this physiologically relevant measure of temperature (heat integral) is essential in predicting the response of fish size-at-age to even small changes in temperature, simply because the changes are integrated by the fish over time. Thus, the GDD metric may prove relevant in resolving size-at-age changes in relation to small changes in ocean temperature (e.g., 0.3 °C increase in the 0–300 m ocean stratum from the 1950s to 1990s; Levitus et al. 2000) being reported as a result of global warming.

Although the GDD method has a proven record in explaining growth and development variation among ectotherms for some considerable time (decades to centuries), we know of no previous demonstrations that show GDD to be equally and generally applicable in explaining growth variation (size-at-age) in a variety of fish species and environments, in control and field studies, over large and small spatial and temporal scales.

The GDD appears to have greater explanatory power than contemporary fish growth models. Clearly, "If the life-table, or population model, is to predict the population dynamics correctly, it must work on the correct time-scale. In the case of homeotherms, the correct time-scale is, clearly, calendar time.... If we base [a fish] population model on calendar time, we must allow for the effect of temperature. But it is much simpler to base the model on the [fish's] own 'physiological' time-scale, which is a combination of calendar time and temperature." (Gilbert et al. 1976, pp. 15–16). Thus, we challenge others to test the GDD metric in all aspects of fish and aquatic invertebrate physiology, growth, and development. We set this challenge because most ectotherms use similar chemical constituents and thermally controlled reaction rates to create an amazing variety of forms across large time and temperature scales. The question has been asked: "Do biological phenomena obey underlying universal laws of life that can be [parameterized] so that biology can be formulated as a predictive, quantitative science?"(West and Brown 2004). Perhaps a convergence of fish physiology, growth, and development, under the scaling of physiological time as provided by the GDD, with that already established in agricultural and entomological research will provide a significant step toward such an underlying law for ectotherm growth and development.

Acknowledgements

We express many thanks to C.A. Dion and N.F. Hughes for their paper (Dion and Hughes 2004) that initiated this study and for graciously providing their temperature data. We are grateful to I. McLaren, B. Ruddick, K. Frank, W. Gentleman, M. Lewis, I. Suthers, D. Reed, J. Michaud, and A. Vanderlaan for comments and suggestions, E. Neuheimer for translation help, and C. Thiel for the graphic digitizer program. A Natural Sciences and Engineering Research Council of Canada PGS-D scholarship to A.B.N. and Discovery Grant to C.T.T. supported this research.

References

Alderdice, D.F., and Velsen, F.P.J. 1978. Relation between temperature and incubation time for eggs of chinook salmon (*Oncorhynchus tshawytscha*). J. Fish. Res. Board Can. **35**: 69–75.

Atkinson, D. 1994. Temperature and organism size — a biological law for ectotherms? Adv. Ecol. Res. **25**: 1–58.

Benoit, H.P., and Pepin, P. 1999. Interaction of rearing temperature and maternal influence on egg development rates and larval size at hatch in yellowtail flounder (*Pleuronectes ferrugineus*). Can. J. Fish. Aquat. Sci. **56**: 785–794.

Berkelmans, R. 2002. Time-integrated thermal bleaching thresholds of reefs and their variation on the Great Barrier Reef. Mar. Ecol. Prog. Ser. **229**: 73–82.

Bonhomme, R. 2000. Bases and limits to using 'degree.day' units. Eur. J. Agron. **13**: 1–10.

Brander, K.M. 1995. The effect of temperature on growth of Atlantic cod (*Gadus morhua* L.). ICES J. Mar. Sci **52**: 1–10.

Dion, C.A., and Hughes, N.F. 2004. Testing the ability of a temperature-based model to predict the growth of age-0 Arctic grayling. Trans. Am. Fish. Soc. **133**: 1047–1050.

Folkvord, A., Johannessen, A., and Moksness, E. 2004. Temperature-dependent otolith growth in Norwegian spring-spawning herring (*Clupea harengus* L.) larvae. Sarsia, **89**: 297–310.

Francis, M.P. 1994. Growth of juvenile snapper, *Pagrus auratus*. N.Z. J. Mar. Freshw. Res. **28**: 201–218.

Gilbert, N., Gutierrez, A.P., Frazer, B.D., and Jones, R.E. 1976. Ecological relationships. W.H. Freeman and Company, San Francisco, Calif.

Gray, J. 1928. The growth of fish. III. The effect of temperature on the development of the eggs of *Salmo fario*. J. Exp. Biol. **6**: 125–130.

Hamel, P., Magnan, P., East, P., Lapointe, M., and Laurendeau, P. 1997. Comparison of different models to predict the in situ embryonic developmental rate of fish with special reference to white sucker (*Catostomus commersoni*). Can. J. Fish. Aquat. Sci. **54**: 190–197.

Higley, L.G., Pedigo, L.P., and Ostlie, K.R. 1986. DEGDAY: a program for calculating degree-days, and assumptions behind the degree-day approach. Environ. Entomol. **15**: 999–1016.

© 2007 NRC Canada

Howe, R.W. 1967. Temperature effects on embryonic development in insects. Annu. Rev. Entomol. **12**: 15–42.

Hutchings, J.A., and Jones, M.E.B. 1998. Life history variation and growth rate thresholds for maturity in Atlantic salmon, *Salmo salar*. Can. J. Fish. Aquat. Sci. **55**(Suppl. 1): 22–47.

Iwama, G.K., and Tautz, A.F. 1981. A simple growth model for salmonids in hatcheries. Can. J. Fish. Aquat. Sci. **38**: 649–656.

Jones, W., Gurney, W.S.C., Speirs, D.C., Bacon, P.J., and Youngson, A.F. 2002. Seasonal patterns of growth, expenditure and assimilation in juvenile Atlantic salmon. J. Anim. Ecol. **71**: 916–924.

Kjellman, J., and Eloranta, A. 2002. Field estimations of temperature-dependent processes: case growth of young burbot. Hydrobiologia, **481**: 187–192.

Kjellman, J., Lappalainen, J., and Urho, L. 2001. Influence of temperature on size and abundance dynamics of age-0 perch and pikeperch. Fish. Res. **53**: 47–56.

Lange, U., and Greve, W. 1997. Does temperature influence the spawning time, recruitment and distribution of flatfish via its influence on the rate of gonadal maturation? Dtsch. Hydrogr. Z. **49**(2/3): 251–263.

Leggett, W.C., Frank, K.T., and Carscadden, J.E. 1984. Meteorological and hydrographic regulation of year-class strength in capelin (*Mallotus villosus*). Can. J. Fish. Aquat. Sci. **41**: 1193–1201.

Levitus, S., Antonov, J.I., Boyer, T.P., and Stephens, C. 2000. Warming of the world ocean. Science, **287**: 2225–2229.

Mallet, J.P., Charles, S., Persat, H., and Auger, P. 1999. Growth modelling in accordance with daily water temperature in European grayling (*Thymallus thymallus* L.). Can. J. Fish. Aquat. Sci. **56**: 994–1000.

Malzahn, A.M., Clemmesen, C., and Rosenthal, H. 2003. Temperature effects on growth and nucleic acids in laboratory-reared larval coregonid fish. Mar. Ecol. Prog. Ser. **259**: 285–293.

Mills, C.A. 1988. The effect of extreme northerly climatic conditions on the life history of the minnow, *Phoxinus phoxinus* (L.). J. Fish Biol. **33**: 545–561.

Mills, E.L., Sherman, R., and Robson, D. 1989. Effect of zooplankton abundance and body size on growth of age-0 yellow perch (*Perca flavescens*) in Oneida Lake, New York, 1975–86. Can. J. Fish. Aquat. Sci. **46**: 880–886.

Miyasaka, H., Kawaguchi, Y., Genkai-Kato, M., Yoshino, K., Ohnishi, H., Kuhara, N., Shibata, Y., Tamate, T., Taniguchi, Y., Urabe, H., and Nakano, S. 2005. Thermal changes in the gastric evacuation rate of the freshwater sculpin *Cottus nozawae* Snyder. Limnology, **6**: 169–172.

Neill, W.H., Brandes, T.S., Burke, B.J., Craig, S.R., Dimichele, L.V., Duchon, K., Edwards, R.E., Fontaine, L.P., Gatlin, D.M., III, Hutchings, C., Miller, J.M., Ponwith, B.J., Stahl, C.J., Tomasso, J.R., and Vega, R.R. 2004. Ecophys.Fish: a simulation model of fish growth in time-varying environmental regimes. Rev. Fish. Sci. **12**: 233–288.

Palsson, O.K., and Thorsteinsson, V. 2003. Migration patterns, ambient temperature, and growth of Icelandic cod (*Gadus morhua*): evidence from storage tag data. Can. J. Fish. Aquat. Sci. **60**: 1409–1423.

Penha-Lopes, G., Rhyne, A.L., Lin, J., and Narciso, L. 2006. Effects of temperature, stocking density and diet on the growth and survival of juvenile *Mithraculus forceps* (A. Milne Edwards, 1875) (Decapoda: Brachyura: Majidae). Aquac. Res. **37**: 398–408.

Pepin, P., Orr, D.C., and Anderson, J.T. 1997. Time to hatch and larval size in relation to temperature and egg size in Atlantic cod (*Gadus morhua*). Can. J. Fish. Aquat. Sci. **54**(Suppl. 1): 2–10.

Reibisch, J. 1902. Ueber den Einfluss de Temperatur auf die Entwicklung von Fisch-Eiern. Wiss. Meeresunters. Abt Kiel, **6**: 213–231.

Seamster, A.P. 1950. Developmental studies concerning the eggs of *Ascaris lumbricoides* var. suum. Am. Midl. Nat. **43**: 450–470.

Sharpe, P.J.H., and DeMichele, D.W. 1977. Reaction kinetics of poikilotherm development. J. Theor. Biol. **64**: 649–670.

Specker, J.L., Eales, J.G., Tagawa, M., and Tyler, W.A.I. 2000. Parr–smolt transformation in Atlantic salmon: thyroid hormone deiodination in liver and brain and endocrine correlates of change in rheotactic behavior. Can. J. Zool. **78**: 696–705.

Stevens, B.G. 1990. Temperature-dependent growth of juvenile red king crab (*Paralithodes camtschatica*) and its effects on size-at-age and subsequent recruitment in the Eastern Bering Sea. Can. J. Fish. Aquat. Sci. **47**: 1307–1317.

Trudgill, D.L., Honek, A., Li, D., and van Straalen, N.M. 2005. Thermal time — concepts and utility. Ann. Appl. Biol. **146**: 1–14.

Valerio, P.F., Goddard, S.V., Kao, M.H., and Fletcher, G.L. 1992. Survival of northern Atlantic cod (*Gadus morhua*) eggs and larvae when exposed to ice and low temperatures. Can. J. Fish. Aquat. Sci. **49**: 2588–2595.

van der Have, T.M., and de Jong, G. 1996. Adult size in ectotherms: temperature effects on growth and differentiation. J. Theor. Biol. **183**: 329–340.

von Bertalanffy, L. 1938. A quantitative theory of organic growth (inquiries on growth laws. II). Hum. Biol. **10**: 181–213.

Wang, J.Y. 1960. A critique of the heat unit approach to plant response studies. Ecology, **41**: 785–790.

West, G.B., and Brown, J.H. 2004. Life's universal scaling laws. Phys. Today, **57**: 36–42.

© 2007 NRC Canada

ERRATUM / ERRATUM

Erratum: A multifrequency method to classify and evaluate fisheries acoustics data

J. Michael Jech and William L. Michaels

Ref.: Can. J. Fish. Aquat. Sci. **63**: 2225–2235 (2006).

The order of the symbols for s_A(WC) and $s_A(AH_V)$ in the first sentence of the caption for Fig. 2 are incorrect. The sentence should read as follows: "Mean 38 kHz areal backscatter (s_A) integrated throughout the entire water column (s_A(WC), ◆), in visually selected herring regions ($s_A(AH_V)$, +), in cells where all three frequencies were present throughout the water column ($s_A(WC_{123})$, ●), and in cells where all three frequencies were present within visually selected herring regions ($s_A(AH_{123})$, ■) as a function of 38 kHz volume backscatter (S_v) threshold."

Received 11 January 2007. Accepted 25 January 2007. Published on the NRC Research Press Web site at http://cjfas.nrc.ca on 7 March 2007.
J19116E

J.M. Jech[1] and W.L. Michaels. Northeast Fisheries Science Center (NOAA/NMFS), 166 Water Street, Woods Hole, MA 02543, USA.

[1]Corresponding author (e-mail: michael.jech@noaa.gov).

 doi:10.1139/F07-009 © 2007 NRC Canada

Fisheries and Aquatic Sciences
Sciences halieutiques et aquatiques

Photographic Atlas of Fish Otoliths of the Northwest Atlantic Ocean
By / Par Stephen E. Campana

$54.95 CAN. Other countries $54.95 US
54,95 $CAN. À l'étranger 54,95 $US
Softcover / Édition brochée
(*Can. Spec. Publ. Fish. Aquat. Sci. / Publ. spéc. can. sci. halieut. aquat. 133*)
284 pages ISBN 0-660-19108-3 ISSN 0706-6481 NRC / CNRC 46328

Salmonine Introductions to the Laurentian Great Lakes:
An Historical Review and Evaluation of Ecological Effects
By / Par Stephen S. Crawford

$42.95 CAN. Other countries $42.95 US
42,95 $CAN. À l'étranger 42,95 $US
Softcover / Édition brochée
(*Can. Spec. Publ. Fish. Aquat. Sci. / Publ. spéc. can. sci. halieut. aquat. 132*)
215 pages ISBN 0-660-17639-4 ISSN 0706-6481 NRC / CNRC 42734

Marine Protected Areas and Fisheries Closures in British Columbia
By Glen S. Jamieson and Joanne Lessard

$69.95 CAN. Other countries $69.95 US
69,95 $CAN. À l'étranger 69,95 $US
Softcover / Édition brochée
(Can. Spec. Publ. Fish. Aquat. Sci. / Publ. spéc. can. sci. halieut. aquat. 131)
414 pages ISBN 0-660-17788-9 ISSN 0706-6481 NRC / CNRC 42846

Workshop on Rebuilding Abalone Stocks in British Columbia
By / Par Alan Campbell

$42.95 CAN. Other countries $42.95 US
42,95 $CAN. À l'étranger 42,95 $US
Softcover / Édition brochée
(*Can. Spec. Publ. Fish. Aquat. Sci. / Publ. spéc. can. sci. halieut. aquat. 130*)
158 pages ISBN 0-660-18292-0 ISSN 0706-6481 NRC / CNRC 42841

To order any of the above titles / Commandez n'importe quel titre ci-dessus à :

Telephone / Téléphone : (613) 990-2254
Fax / Télécopieur : (613) 952-7656
E-mail / Courriel : pubs@nrc-cnrc.gc.ca
Web site / Site web : http://pubs.nrc-cnrc.gc.ca

Order Office / Bureau des commandes
NRC Research Press / Presses scientifique du CNRC
National Research Council / Conseil national de recherches
Ottawa, ON K1A 0R6, Canada

Canadian customers add GST (6%). Prepayment required unless order is accompanied by a purchase order number. Cheques or money orders should be made payable to : "Receiver General for Canada, Credit NRC". For all orders outside Canada, rates are in U.S. Dollars. All sales are final.
Clients du Canada, ajoutez la TPS (6 %). Les commandes doivent être payées d'avance à moins qu'elles ne soient accompagnées d'un numéro de bon de commande. Les chèques ou mandats doivent être libellés au « Receveur général du Canada, crédit du CNRC ».
Pour les commandes hors-Canada, les tarifs sont en dollars américains. Toutes les ventes sont finales.

National Research Council Canada | Conseil national de recherches Canada

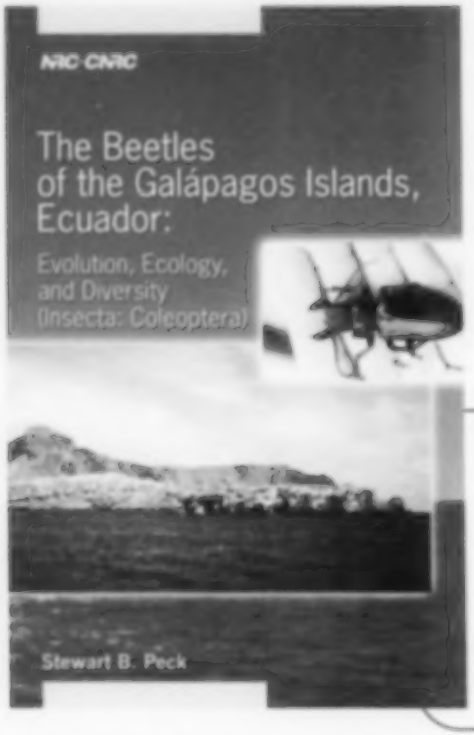
NRC·CNRC
The Beetles of the Galápagos Islands, Ecuador:
Evolution, Ecology, and Diversity (Insecta: Coleoptera)
Stewart B. Peck

The Beetles of the Galápagos Islands, Ecuador:

Evolution, Ecology, and Diversity (Insecta: Coleoptera)

By / Par
Stewart B. Peck

305 Pages 2006
Softcover / Édition brochée

ISBN 0-660-19421-X; NRC 46846
ISBN 0-660-19421-X; CNRC 46846

$45.95 CAN; Other countries: $45.95 US
45,95 $CAN; À l'étranger : 45,95 $US

Generalizations are presented on the dynamics and patterns of the evolution, ecology, and distribution of the entire beetle fauna. The core of the book is an account of the 486 species of beetles with detailed information on their distribution and bionomics. This work will be of interest to entomologists, island ecologists, evolutionary biologists, and conservation scientists as a framework for future study and protection of the fauna and flora of the islands. It is a contribution to a comparative global understanding of the origin, evolution, and ecological structuring of oceanic island insect faunas.

On y présente des généralisations sur la dynamique et les tendances de l'évolution, de l'écologie et de la répartitionde l'ensemble des populations de coléoptères. Le corps de l'ouvrage est un relevé des 486 espèces de coléoptères offrant de l'information détaillée sur leur répartition et leur bionomie. Les entomologistes, les spécialistes de l'écologie insulaire, les biologistes évolutionnistes et les scientifiques en conservation s'intéresseront à cet ouvrage qui constitue un cadre pour l'étude et la protection de la faune et de la flore des îles. Il contribue à une compréhension comparative de l'origine, de l'évolution et de la structuration écologique des populations d'insectes d'îles océaniques

To order books / Commandez des livres à :

Order Office / Bureau des commandes
NRC Research Press / Presses scientifique du CNRC National Research Council
Conseil national de recherches
Ottawa, ON K1A 0R6, Canada

Shipping and handling extra.
Canadian customers add GST (6%). Prepayment required unless order is accompanied by a purchase order number. Cheques or money orders should be made payable to: "Receiver General for Canada, Credit NRC". For all orders outside Canada, rates are in U.S. dollars. All sales are final.

Telephone / Téléphone : 613-990-2254
Fax / Télécopieur : 613-952-7656
E-mail / Courriel : pubs@nrc-cnrc.gc.ca
Order online / Commandez en ligne :
http://pubs.nrc-cnrc.gc.ca

Frais d'expédition et de manutention en plus.
Clients du Canada, ajoutez la TPS (6 %). Les commandes doivent être payées d'avance à moins qu'elles ne soient accompagnées d'un numéro de bon de commande. Les chèques ou mandats doivent être libellés au « Receveur général du Canada, crédit du CNRC ». Pour les commandes hors-Canada, les tarifs sont en dollars américains. Toutes les ventes sont finales.

National Research Council Canada | Conseil national de recherches Canada

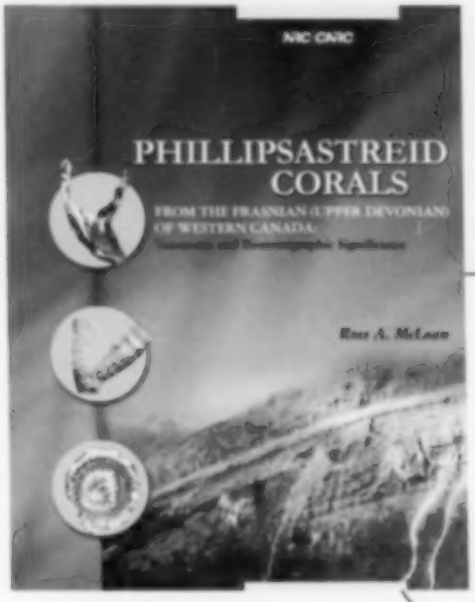

Phillipsastreid Corals

from the Frasnian (Upper Devonian) of Western Canada: Taxonomy and Biostratigraphic Significance

By / Par
Ross A. McLean

109 Pages 2005
Softcover / Édition brochée

ISBN 0-660-19364-7; NRC 46847
ISBN 0-660-19364-7; CNRC 46847

$49.95 CAN; Other countries: $49.95 US
49,95 $CAN; À l'étranger : 49,95 $US

Rugose corals of the Family Phillipsastreidae are abundant, diverse, and geographically widespread in the Frasnian (lower Upper Devonian) of western Canada. Species of the solitary genus Macgeea are described. Thamnophyllum and Peneckiella are branching forms. Biostratigraphic distribution of these species is reviewed, together with that of previously described Canadian massive phillipsastreid species belonging to the genera Phillipsastrea, Chuanbeiphyllum, Pachyphyllum, Smithicyathus, and Frechastraea. The coral biostratigraphy is expressed in terms of the Montagne Noire conodont zonation and modified western Canada rugose coral faunal assemblages.

Les coraux rugueux de la famille des Phillipsastreidae sont abondants, diversifiés et répandus sur le plan géographique dans le Frasnien (étage de base du Dévonien supérieur) de l'Ouest du Canada. L'ouvrage expose les espèces appartenant au genre solitaire Macgeea. Les genres Thamnophyllum et Peneckiella sont des formes branchues. La répartition biostratigraphique de ces espèces est examinée, ainsi que celle d'espèces massives de Phillipsastreidae canadiennes déjà décrites appartenant aux genres Phillipsastrea, Chuanbeiphyllum, Pachyphyllum, Smithicyathus et Frechastraea. La biostratigraphie des coraux est présentée suivant la zonation des conodontes de la Montagne Noire etles assemblages fauniques modifiés de coraux rugueux de l'Ouest du Canada.

To order books / Commandez des livres à :

Order Office / Bureau des commandes
NRC Research Press / Presses scientifique
du CNRC National Research Council
Conseil national de recherches
Ottawa, ON K1A 0R6, Canada

Telephone / Téléphone : 613-990-2254
Fax / Télécopieur : 613-952-7656
E-mail / Courriel : pubs@nrc-cnrc.gc.ca
Order online / Commandez en ligne :
http://pubs.nrc-cnrc.gc.ca

Shipping and handling extra.
Canadian customers add GST (6%). Prepayment required unless order is accompanied by a purchase order number. Cheques or money orders should be made payable to: "Receiver General for Canada, Credit NRC". For all orders outside Canada, rates are in U.S. dollars. All sales are final.

Frais d'expédition et de manutention en plus.
Clients du Canada, ajoutez la TPS (6 %). Les commandes doivent être payées d'avance à moins qu'elles ne soient accompagnées d'un numéro de bon de commande. Les chèques ou mandats doivent être libellés au « Receveur général du Canada, crédit du CNRC ». Pour les commandes hors-Canada, les tarifs sont en dollars américains. Toutes les ventes sont finales.

NRC·CNRC

Canada

POST-DOCTORAL RESEARCHER

US Northwest Fisheries Science Center, Seattle, Washington

The US National Research Council (US-NRC) of the National Academies will offer a postdoctoral research award tenable at the Northwest Fisheries Science Center in Seattle, WA, to study the feeding ecology of top predators—specifically marine mammals, such as killer whales and humpback whales.

The postdoctoral research Associate will use a variety of chemical tracers (e.g., persistent organic contaminant concentrations, patterns and ratios; stable isotopes of carbon and nitrogen; fatty acid profiles) in assessing both predator diet and foraging ranges. The study should be designed to provide further insight into the diet of cetacean species for which little dietary information is available.

The successful applicant should have expertise in the biology or physiology of marine mammals, as well as experience in conducting chemical and instrumental laboratory investigations.

Applications will be considered for the May 1 Review, with an application deadline of May 1 and a starting date of July 07 or later.

Further information and application instructions are at www.national-academies.org/rap. Applications must be submitted online directly to the US-NRC.

Prior to submitting a formal application to the US-NRC, contact:
Dr. Peggy Krahn,
Deputy Director,
Environmental Conservation Division,
Northwest Fisheries Science Center,
e-mail: peggy.krahn@noaa.gov. or telephone: 206-860-3326.

Jason N. Waite, Wendy J. Schrader, Jo-Ann E. Mellish, and Markus Horning	**296–303**	Three-dimensional photogrammetry as a tool for estimating morphometrics and body mass of Steller sea lions (*Eumetopias jubatus*)
Jan-Jaap Poos and Adriaan D. Rijnsdorp	**304–313**	An "experiment" on effort allocation of fishing vessels: the role of interference competition and area specialization
Sarah E. Lester, Elizabeth D. Tobin, and Michael D. Behrens	**314–323**	Disease dynamics and the potential role of thermal stress in the sea urchin, *Strongylocentrotus purpuratus*
Guillermo R. Giannico and Scott G. Hinch	**324–335**	Juvenile coho salmon (*Oncorhynchus kisutch*) responses to salmon carcasses and in-stream wood manipulations during winter and spring
C.E. Adams, J.F. Turnbull, A. Bell, J.E. Bron, and F.A. Huntingford	**336–344**	Multiple determinants of welfare in farmed fish: stocking density, disturbance, and aggression in Atlantic salmon (*Salmo salar*)
David O. Evans	**345–361**	Effects of hypoxia on scope-for-activity and power capacity of lake trout (*Salvelinus namaycush*)
Sascha M.M. Fässler, Rita Santos, Norma García-Núñez, and Paul G. Fernandes	**362–374**	Multifrequency backscattering properties of Atlantic herring (*Clupea harengus*) and Norway pout (*Trisopterus esmarkii*)
PERSPECTIVE		PERSPECTIVE
Anna B. Neuheimer and Christopher T. Taggart	**375–385**	The growing degree-day and fish size-at-age: the overlooked metric
ERRATAUM		ERRATAUM
J. Michael Jech and William L. Michaels	**386**	Erratum: A multifrequency method to classify and evaluate fisheries acoustics data

National Research Council Canada
Ottawa, Canada K1A 0R6

Conseil national de recherches Canada
Ottawa, Canada K1A 0R6

Postage paid at Ottawa
Publications mail
Registration No. 40062591

Port payé à Ottawa
Poste-publication
Enregistrement n° 40062591

USPS periodical postage paid at Plattsburgh, NY 12901, USA

Canadian Journal of Fisheries and Aquatic Sciences

Volume 64, Number 2, February 2007

Journal canadien des sciences halieutiques et aquatiques

Volume 64, numéro 2, février 2007

		RAPID COMMUNICATION / COMMUNICATION RAPIDE
Andrea Bertolo and Pierre Magnan	**181–186**	Logging-induced variations in dissolved organic carbon affect yellow perch (*Perca flavescens*) recruitment in Canadian Shield lakes
		ARTICLES / ARTICLES
Richard B. Deriso, Mark N. Maunder, and John R. Skalski	**187–197**	Variance estimation in integrated assessment models and its importance for hypothesis testing
Toby S. Daly-Engel, R. Dean Grubbs, Brian W. Bowen, and Robert J. Toonen	**198–204**	Frequency of multiple paternity in an unexploited tropical population of sandbar sharks (*Carcharhinus plumbeus*)
Jason M. Cope and André E. Punt	**205–218**	Admitting ageing error when fitting growth curves: an example using the von Bertalanffy growth function with random effects
Sherrylynn Rowe, Jeffrey A. Hutchings, and Jon Egil Skjæraasen	**219–226**	Nonrandom mating in a broadcast spawner: mate size influences reproductive success in Atlantic cod (*Gadus morhua*)
Michael J. Bowes, Jim T. Smith, John Hilton, Michael M. Sturt, and Patrick D. Armitage	**227–238**	Periphyton biomass response to changing phosphorus concentrations in a nutrient-impacted river: a new methodology for phosphorus target setting
Albert Kjartansson Imsland, Atle Foss, Thomas Alvseike, Arild Folkvord, Sigurd Olav Stefansson, and Thor Magne Jonassen	**239–248**	Interaction between temperature and photoperiod on growth and feeding of Atlantic cod (*Gadus morhua*): possible secondary effects
David Griffiths and Chris Harrod	**249–255**	Natural mortality, growth parameters, and environmental temperature in fishes revisited
Brian R. Beckman, Brad Gadberry, Paul Parkins, Kathleen A. Cooper, and Kristen D. Arkush	**256–271**	State-dependent life history plasticity in Sacramento River winter-run chinook salmon (*Oncorhynchus tshawytscha*): interactions among photoperiod and growth modulate smolting and early male maturation
Filipe O. Costa, Jeremy R. deWaard, James Boutillier, Sujeevan Ratnasingham, Robert T. Dooh, Mehrdad Hajibabaei, and Paul D.N. Hebert	**272–295**	Biological identifications through DNA barcodes: the case of the Crustacea

Continued on inside back cover / Suite au verso

Front cover: Iboko Saito/Toshiyuki Tajima/Dex Image/Getty Images.

Page couverture : Iboko Saito/Toshiyuki Tajima/Dex Image/Getty Images.

Canada

Printed in Canada by / Imprimé au Canada par
NRC Reprographic Services / Service de reprographie CNRC
Page production by / Mise en page par
NRC Research Press / Presses scientifiques du CNRC

0706-652X(200702)64:2;1-7